NUREG/CR–6513, No. 1
CNWRA 96–OIA

NRC High-Level Radioactive Waste Program Annual Progress Report: Fiscal Year 1996

Center for Nuclear Waste Regulatory Analyses
Southwest Research Institute

Prepared for
U.S. Nuclear Regulatory Commission

AVAILABILITY NOTICE

Availability of Reference Materials Cited in NRC Publications

Most documents cited in NRC publications will be available from one of the following sources:

1. The NRC Public Document Room, 2120 L Street, NW., Lower Level, Washington, DC 20555-0001

2. The Superintendent of Documents, U.S. Government Printing Office, P. O. Box 37082, Washington, DC 20402-9328

3. The National Technical Information Service, Springfield, VA 22161-0002

Although the listing that follows represents the majority of documents cited in NRC publications, it is not intended to be exhaustive.

Referenced documents available for inspection and copying for a fee from the NRC Public Document Room include NRC correspondence and internal NRC memoranda; NRC bulletins, circulars, information notices, inspection and investigation notices; licensee event reports; vendor reports and correspondence; Commission papers; and applicant and licensee documents and correspondence.

The following documents in the NUREG series are available for purchase from the Government Printing Office: formal NRC staff and contractor reports, NRC-sponsored conference proceedings, international agreement reports, grantee reports, and NRC booklets and brochures. Also available are regulatory guides, NRC regulations in the *Code of Federal Regulations*, and *Nuclear Regulatory Commission Issuances*.

Documents available from the National Technical Information Service include NUREG-series reports and technical reports prepared by other Federal agencies and reports prepared by the Atomic Energy Commission, forerunner agency to the Nuclear Regulatory Commission.

Documents available from public and special technical libraries include all open literature items, such as books, journal articles, and transactions. *Federal Register* notices, Federal and State legislation, and congressional reports can usually be obtained from these libraries.

Documents such as theses, dissertations, foreign reports and translations, and non-NRC conference proceedings are available for purchase from the organization sponsoring the publication cited.

Single copies of NRC draft reports are available free, to the extent of supply, upon written request to the Office of Administration, Distribution and Mail Services Section, U.S. Nuclear Regulatory Commission, Washington, DC 20555-0001.

Copies of industry codes and standards used in a substantive manner in the NRC regulatory process are maintained at the NRC Library, Two White Flint North, 11545 Rockville Pike, Rockville, MD 20852-2738, for use by the public. Codes and standards are usually copyrighted and may be purchased from the originating organization or, if they are American National Standards, from the American National Standards Institute, 1430 Broadway, New York, NY 10018-3308.

NUREG/CR-6513, No. 1
CNWRA 96-OIA

NRC High-Level Radioactive Waste Program Annual Progress Report: Fiscal Year 1996

Manuscript Completed: December 1996
Date Published: January 1997

Budhi Sagar, Editor

Center for Nuclear Waste Regulatory Analyses
Southwest Research Institute
6220 Culebra Road
San Antonio, TX 78228-0510

Prepared for
Division of Waste Management
Office of Nuclear Material Safety and Safeguards
U.S. Nuclear Regulatory Commission
Washington, DC 20555-0001
NRC Job Code D1035

ABSTRACT

This annual status report for fiscal year 1996 documents technical work performed on ten key technical issues (KTI) that are most important to performance of the proposed geologic repository at Yucca Mountain. This report has been prepared jointly by the staff of the Nuclear Regulatory Commission (NRC) Division of Waste Management and the Center for Nuclear Waste Regulatory Analyses. The programmatic aspects of restructuring the NRC repository program in terms of KTIs is discussed and a brief summary of work accomplished is provided in chapter 1. The other ten chapters provide a comprehensive summary of the work in each KTI. Discussions on probability of future volcanic activity and its consequences, impacts of structural deformation and seismicity, the nature of the near-field environment and its effects on container life and source term, flow and transport including effects of thermal loading, aspects of repository design, estimates of system performance, and activities related to the U.S. Environmental Protection Agency standard are provided.

CONTENTS

CONTENTS

CONTENTS

Section | Page

CONTENTS

CONTENTS

CONTENTS

Section | Page

FIGURES

Figure | Page

FIGURES

Figure | Page

FIGURES

FIGURES

Figure Page

TABLES

EXECUTIVE SUMMARY

ES.1 INTRODUCTION AND GENERAL PROGRAM ACCOMPLISHMENTS

Early in 1995, the Nuclear Regulatory Commission (NRC) staff recognized the need to refocus its prelicensing repository program on resolving issues most significant to repository performance. Since that time, three major events have driven a significant restructuring of the NRC repository program: (i) a reduction in Congressional appropriations for the repository program for both the NRC and the U.S. Department of Energy (DOE), (ii) a reorganization of the DOE high-level waste (HLW) work in what became known as the Program Approach in 1994 and its modification in 1995, and (iii) a report issued to the U.S. Environmental Protection Agency (EPA) by the National Academy of Sciences (NAS) that contained recommendations for setting a safety standard for a proposed HLW repository at Yucca Mountain (YM). The scope of the NRC prelicensing program was adjusted to focus on only those topics most critical to repository performance; these topics are called the key technical issues (KTIs). This was done with a recognition that items not on the current list of KTIs may be found to be important to repository performance in the future, carrying some risk of either (i) having to make overly conservative assumptions about such items or (ii) causing a delay in regulatory actions.

This report was jointly produced by the NRC and Center for Nuclear Waste Regulatory Analyses (CNWRA) staffs. The CNWRA, located in San Antonio, Texas, is a Federally Funded Research and Development Center sponsored by the NRC to provide technical assistance for the repository program. This report provides a status of NRC-HLW work conducted in fiscal year (FY) 96, as well as assessments of progress toward resolution of the KTIs. Chapter 1 describes the restructured NRC program and provides a programmatic context for the remaining ten chapters. Chapters 2 through 11 provide succinct summaries of work accomplished for each of the ten KTIs considered to be critical to repository performance. It should be noted that details of the activities summarized here are available in separate reports and technical papers, noted in the references at the end of each chapter. Highlights of program accomplishments for FY96 are given in the following pages.

The NRC revised approach focuses on resolving ten KTIs. Other activities necessary for licensing have been deferred as a result of FY96 budget reductions. The ten KTIs are as follows.

1) Igneous activity
2) Structural deformation and seismicity
3) Evolution of the near-field environment
4) Container life and source term
5) Thermal effects on flow
6) Repository design and thermal-mechanical effects
7) Total system performance assessment and integration
8) Activities related to development of the U.S. Environmental Protection Agency Yucca Mountain Standard
9) Unsaturated and saturated flow under isothermal conditions
10) Radionuclide transport

Because each of the ten KTIs encompasses a number of important subissues and resources are severely limited, the NRC staff is using a vertical slice or audit approach that has been successfully used in other areas of NRC responsibility, including reactor licensing. To further focus the work within each

KTI, the NRC staff will evaluate a few narrow slices or topics (focused, well-defined scope) in depth; while conclusions about resolution of the broader issue will be inferred from examining these topics in detail. Within a particular vertical slice, the NRC staff plans to conduct appropriate activities such as evaluating alternate conceptual models, including underlying data and assumptions; conducting independent modeling for use in sensitivity and importance analyses; performing limited technical investigations, including laboratory tests, to develop an independent understanding of relevant processes; reviewing the DOE data and independent literature; establishing acceptance criteria, to guide reviews and issue resolution; and establishing clear objectives for each interaction with the DOE and others to ensure progress toward issue resolution.

The NRC approach is to focus all activities on resolution of the ten KTIs at the staff level. Issue resolution is achieved when the NRC staff has no further questions or comments regarding how the DOE is addressing the issue in its program. However, it is recognized that there may be some cases where reaching a common understanding regarding differences in the NRC and the DOE points of view may be all that can be achieved. The NRC staff will prepare periodic issue resolution status reports to document significant progress and give the DOE timely feedback regarding specific issues or subissues. In addition, an annual report, such as this document, is intended to summarize the significant technical work completed for all KTIs during the preceding FY. To the extent that the NRC and the DOE can resolve issues before the Viability Assessment (VA), there would be greater confidence that the potential licensing vulnerabilities have been properly addressed by the DOE in its VA.

Numerous advantages are apparent in refocusing the NRC program on KTIs using the vertical slice approach. Scarce resources are keyed on those issues most significant to repository performance, thus enhancing attention to safety. Issue resolution is facilitated by acknowledging the appropriate bounding of less significant effects and aiming interactions with the DOE on those factual or interpretative differences with the greatest significance to performance. The audit nature of the vertical slice approach effectively evaluates a wide range of the DOE activities and identifies how well they are integrated. Integration of the NRC program is improved by coordinating necessary activities and technical disciplines in the review of each issue. Stressing issues that are potential licensing vulnerabilities is a robust approach that is not highly dependent on the DOE products and thus less likely to be seriously impacted by potential future changes in the DOE program. Finally, the approach is flexible enough to allow necessary changes to the issues or priority of activities based on new site information or new insights regarding repository performance.

As with any approach, there are some disadvantages. The audit nature of focusing only on the ten KTIs and selected vertical slices within each issue will result in areas of the DOE program not being examined in detail during prelicensing. Also, if some vulnerabilities are not recognized as KTIs and effectively addressed during prelicensing, the licensing review could be extended.

Significant progress has been made in developing paths to resolution for various subissues in the ten KTIs. The path to resolution takes into consideration the DOE data and analyses, non-DOE data and analyses available in the literature, the NRC independent data and analyses, future investigations proposed by the DOE, and an understanding of the impact of the subissue on the overall performance of the repository. It should be understood that the DOE is ultimately responsible for developing an integrated safety case for the repository, and the DOE may choose to adopt a different path to issue resolution than would be developed by the NRC.

For each individual KTI, the specific path to resolution is unique and reflects both the nature of the issue and progress of the DOE and the NRC technical work to date. Overall, for most of the KTIs, activities in FY96 concentrated on establishing a sound technical basis for future issue resolution during FY97. For a few KTIs, this involved data collection to improve the understanding of parameters or processes thought to be important to various analyses and for which data were not available. Activities also emphasized refining or in some cases completing development of models and associated computer codes representing various subsystems or processes of the repository. These models were then used to conduct sensitivity/importance analyses in FY96 at the repository subsystem or process level to help focus further resolution work on those factors having a dominant effect on the subsystem or specific processes. Subsystem or process models will provide additional value by either calculating parameter input for use in the total performance assessment (TPA) code or being abstracted as modules in the TPA code during FY97. The resulting updated TPA code will be used for sensitivity/importance analyses in FY97 that integrate the various subsystems and processes that can then be used to confirm the importance of various parameters and processes to the total system performance measure of dose. Such integrated analyses are necessary to support resolution of individual issues or subissues that cannot be resolved in isolation of the total system. These analyses will also help develop acceptance criteria during FY97. In FY96, various approaches were evaluated on how acceptance criteria could be identified and used to support the issue resolution process. Presently, they are envisioned to be part of the technical basis for issue resolution.

While the resolution of many KTIs is dependent on additional work in FY97, some important progress was made this past year. Interactions between the NRC and the DOE during FY96 were successful in achieving informal agreements to be documented in issue resolution status reports in FY97. Examples include narrowing the range of tectonic models, identifying an acceptable seismic design methodology, and resolving design control process concerns. Another major step toward issue resolution was made in the total system performance assessment (TSPA) area. An NRC and DOE interaction identified differences between the NRC and the DOE TSPAs, causes, and potential future resolution actions. Finally, the staff completed a Branch Technical Position (BTP) giving an acceptable methodology for the use of expert elicitation. This guidance resolved questions of when and how to use expert elicitations for areas of major uncertainty, and currently is being used by the DOE to conduct and plan future expert elicitations. Progress made in each KTI is described very briefly in the following. More detailed abstracts of KTI technical activities are included in chapter 1.

ES.2 IGNEOUS ACTIVITY

In this KTI, work focused on determining an upper bound for the probability of repository disruption by future volcanic eruptions. The probability estimates obtained from historical data were conditioned by knowledge about the geologic structure. The range of this probability was determined to be between 10^{-7} to 10^{-8} per year, similar to the range determined by the DOE through elicitation of an expert panel. Sensitivity analyses of consequences of such disruptions indicated that the number of waste packages (WPs) impacted in a volcanic event, the resulting fuel particle size, and the incorporation ratio of fuel into the volcanic ash were critical to determining dose to a postulated critical group.

ES.3 STRUCTURAL DEFORMATION AND SEISMICITY

Two subissues found to be most critical to performance in this KTI are: (i) potential impact of faulting and seismicity on WPs and (ii) effect of structure and tectonic stresses on groundwater flow. Understanding of the regional tectonic setting is required to resolve both subissues. Work in this KTI has

reduced the number of conceptual tectonic models to five and has shown that seismicity along the Bare Mountain fault is critical. Analyses of the effects of stress and deformation on groundwater flow indicate that discrete networks of fractures and faults may strongly influence both local and regional flow patterns. Further refinements of these models will lead to technically supported estimates of future faulting, seismicity, and structural influence on flow and their effect on repository performance.

ES.4 EVOLUTION OF THE NEAR-FIELD ENVIRONMENT

Rates of WP failures and waste dissolution are affected by evolution of the environment close to WPs. The work in this KTI was directly focused on investigating several components of the DOE Waste Containment and Isolation Strategy (WCIS)[1] (e.g., low water flux through the repository, slow corrosion of waste containers, and low waste dissolution rates). An equivalent porous medium model that coupled thermal, hydrological, and chemical processes was completed. Analyses using this model indicated a wide variation in pH and salinity, strong functions of the repository thermal loading. The effect of these changes on total repository system performance (i.e., on dose to a critical group) will be investigated in FY97. It was concluded that for bounding the near-field environment, approaches other than the equivalent porous medium may need to be considered.

ES.5 CONTAINER LIFE AND SOURCE TERM

An assessment tool called the Engineered Barrier System Performance Assessment Code (EBSPAC) was developed in this KTI. Through a sensitivity analysis using EBSPAC, it was concluded that galvanic coupling between the inner and outer overpacks was perhaps the most important factor in determining container life. Higher galvanic efficiency caused an increase in container life. In the absence of galvanic protection, intermediate heat loads tended to produce lower container lives than either the low or the high heat loads. Work on this KTI has been eliminated at the CNWRA in FY97 due to further reduction in appropriations.

ES.6 THERMAL EFFECTS ON FLOW

Work in this KTI focused on estimating the effect of thermal load on water and vapor flow through the repository. Results of sensitivity analyses showed that backfill initially lowered the WP temperature as thermal energy was consumed in evaporating pore water in the backfill. Once the backfill was dry, however, it acted as an insulator and increased WP temperature. Depending on heat load, the insulation effect may persist for hundreds of years. Another analysis indicated that ventilation during the preclosure phase can lower the drift wall temperature by tens of degrees. The effects of these and other thermal-hydrologic factors on total system performance will be evaluated in FY97.

ES.7 REPOSITORY DESIGN AND THERMAL-MECHANICAL EFFECTS

Thermal effects on design of the underground facility was the primary subissue considered for resolution in this KTI. Phase I of a sensitivity analysis was undertaken to bound the effects of key

---

[1] U.S. Department of Energy. 1996. *Highlights of the U.S. Department of Energy's Updated Waste Containment and Isolation Strategy for the Yucca Mountain Site*. DOE Concurrence Draft. July 1996. Washington, DC: U.S. Department of Energy.

parameters on drift stability. Thermal loading, and properties and patterns of rock joints were found to significantly influence drift stability. Efforts at developing a suitable rock-joint constitutive equation that will apply to the situation of multiple reversals of shear displacements resulting from seismic events is incomplete at this time. The NRC, however, was able to resolve several methodology subissues regarding seismic design of the repository. The NRC staff will continue to evaluate the DOE design control process but no further work on this KTI will be undertaken at the CNWRA in FY97 in response to budget reductions.

ES.8 TOTAL SYSTEM PERFORMANCE ASSESSMENT AND INTEGRATION

An audit and detailed review of the latest DOE iteration of TSPA-95 (TRW Environmental Safety Systems, Inc., 1995) was performed in this KTI. Based on the audit review, five topics were selected for detailed review: (i) water flux through the repository, (ii) dilution in the saturated zone, (iii) temperature and humidity in the near-field environment, (iv) WP failure modes, and (v) model abstraction. A comparison of the cumulative complementary distribution function in TSPA-95 (TRW Environmental Safety Systems, Inc., 1995) and the one obtained using the NRC/CNWRA code TPA together with TSPA-95 data indicated significant differences attributable to differences in model abstraction. These differences, their causes, and potential resolution were discussed with the DOE. Also included in this KTI was the completion of a BTP on expert elicitation. Finally, a licensing support system test bed accessible through the Internet was brought on line. The test bed allows for searching, retrieving, and downloading documents, and obtaining user feedback.

ES.9 ACTIVITIES RELATED TO DEVELOPMENT OF THE U.S. ENVIRONMENTAL PROTECTION AGENCY YUCCA MOUNTAIN STANDARD

With the goal of contributing to the development of reasonable and implementable standards for YM, activities in this KTI focused on analyses of critical components of the standard. These analyses can also be applied to future development of the NRC regulations to implement these standards. These critical components included (i) definition of the compliance period, (ii) determination of critical groups, (iii) establishment of methods to deal with human intrusion scenarios, and (iv) provision of details to which other disruptive scenarios would be specified. Comparing hazard assessment of a uranium ore body with a HLW repository indicated that hazards were comparable at 10,000 yr, providing a rationale for adopting 10,000 yr as the compliance period. Stylized analysis of human intrusion showed that exploratory drilling was an unlikely event and that its consequences were low. It was concluded that consequences of human intrusion should be analyzed separately from other scenarios and its consequences need not be incorporated into the overall risk assessment. In addition to the scoping calculations, numerous interactions conducted with EPA achieved the following: a consistent understanding of NAS recommendations and implementation complexities; general acceptance in many areas of appropriate approaches for the proposed standard; and clear identification of where significant differences remain, such as groundwater protection.

ES.10 UNSATURATED AND SATURATED FLOW UNDER ISOTHERMAL CONDITIONS

Based on analyses of paleoclimatic data in the YM region, this KTI concluded that an upper bound on future precipitation can be estimated at two to three times the present rate. Efforts were also

made to bound the rate of shallow infiltration under present day conditions. Considering space-time variability of climatic and subsoil conditions, the average shallow infiltration was estimated to lie between 10 to 20 mm per yr. This study will be extended to estimate bounds on deep percolation. In FY96, the preliminary modeling study of existing perched waters indicated a possible average rate of deep percolation of about 6 to 8 mm/yr.

ES.11 RADIONUCLIDE TRANSPORT

Radionuclide sorption was studied in this KTI. Although part of the DOE WCIS[2], the importance of geochemical sorption has been reduced in comparison to dilution in the saturated zone and retardation provided by matrix diffusion. The aim of this KTI was to determine the lower bounds for geochemical sorption of important radionuclides. Laboratory and natural analog studies combined with modeling indicate strong dependence of sorption on pH. For example, the sorption coefficient for uranium can vary between 0.1 to 1,000 as pH varies between 2 to 9. Similar results were also obtained for neptunium. Work on this KTI has been eliminated at both the NRC and the CNWRA in FY97 as a result of further budget reductions.

ES.12 REFERENCE

TRW Environmental Safety Systems, Inc. 1995. *Total System Performance Assessment—1995: An Evaluation of the Potential Yucca Mountain Repository*. B00000000-01717-2200-00136. Las Vegas, NV: TRW Environmental Safety Systems, Inc.

---

[2]U.S. Department of Energy. 1996. *Highlights of the U.S. Department of Energy's Updated Waste Containment and Isolation Strategy for the Yucca Mountain Site*. DOE Concurrence Draft. July 1996. Washington, DC: U.S. Department of Energy.

ACKNOWLEDGMENTS

The quality of the report was enhanced through editorial, technical, and programmatic reviews. Efforts of these Nuclear Regulatory Commission (NRC) and Center for Nuclear Waste Regulatory Analyses (CNWRA) reviewers are gratefully acknowledged. Skillful editorial review was provided by B. Long (CNWRA). Two technical reviews were obtained for each chapter. The CNWRA technical reviewers were R.G. Baca, A.C. Bagtzoglou, A.H. Chowdhury, R.T. Green, R.P. Manteufel, W.M. Murphy, W.C. Patrick, E.C. Pearcy, J.L. Russell, N. Sridhar, and J.A. Stamatakos; and the NRC reviewers were J.W. Bradbury, R.B. Codell, N.A. Eisenberg, B.W. Leslie, C.H. Lui, K.I. McConnell, T.J. McCartin, S.M. McDuffie, and J.A. Pohle. Each chapter was also reviewed for programmatic context. The programmatic reviews were provided by the High-Level Waste Management Review Board members: J.H. Austin, M.J. Bell, M.V. Federline, W.C. Patrick, and B. Sagar.

Finally, the help from L.F. Gutierrez in coordinating the production of this document and able secretarial support provided by E.F. Cantu, B.P. Caudle, B.L. Garcia, C. Garcia, L.G. Hearon, Y.C. Lozano, A. Ramos, R.A. Sanchez, and L. Selvey are appreciated. Quality Assurance (QA) oversight was provided by B. Mabrito. Obviously, this report would not be possible without the wholehearted cooperation from key technical issue teams who kept to the tight schedule of the editor. Names of primary authors, technical contributors, and principal investigators are given at the front of the report and are also included at the beginning of each chapter.

QUALITY OF DATA: Sources of data are referenced in each chapter. CNWRA-generated laboratory and field data contained in this report meet QA requirements described in the CNWRA QA Manual. Data from other sources, however, are freely used. Sources for other data should be consulted for determining the level of quality for those data.

ANALYSES AND CODES: Scientific/engineering computer software used in analyses contained in this report are: 3DStress, Version 1.2 (chapters 2, 3), controlled, release date 11/13/96; PVHVIEW, Version 1.0 (chapter 2), in development, not released; UDEC, Version 2.01 (chapter 3), leased commercial version under CNWRA configuration control; ABAQUS, Version 5.5 (chapter 3), leased commercial version under CNWRA configuration control; MULTIFLO, Version 1.0 (chapters 4, 6), in development, not yet released; EBSPAC, Version 1.0β (chapter 5), in development, not yet released; CTOUGH, Version 1.0 (chapter 6), controlled, release date 2/08/96; TPA, Version 2.0 (chapter 8), in development, not released; CHAINT, Version 2.3 (chapter 9), documentation in final stage, not released; MAGNUM, Version 3.2 (chapter 9), documentation in final stage, not released; BREATH 1.2 (chapter 10), in development, not released; SUFLAT, Version 1.0 (chapter 10), documentation in process, not released; and MINTEQA2, Version 3.10/3.11 (chapter 11), release date 8/02/96. These computer software are being configured under the CNWRA Technical Operating Procedure Development and Control of Scientific and Engineering Software (TOP-018, Revision 4, Change 1). The software SIMUL (chapter 4), created by the University of Waterloo and not under CNWRA control, was utilized for preliminary, nonquality affecting scoping analyses, although its use is described in a CNWRA scientific notebook.

Other software, ARCVIEW, Version 2.0β, and ARCINFO, Version 6.1, are commercial codes and only the object codes are available to the CNWRA.

FOREWORD

This is the first in a series of annual reports prepared jointly by the Nuclear Regulatory Commission (NRC) staff from the Division of Waste Management (DWM) and staff from the Center for Nuclear Waste Regulatory Analyses (CNWRA). Each Key Technical Issue team was headed by two principal investigators: one each from the DWM and the CNWRA. Primary authors of each chapter were responsible for writing the text that describes the work of many investigators. Names of the primary authors, technical contributors, and principal investigators are given below, and are also included at the beginning of each chapter. This report was edited by B. Sagar (CNWRA).

PRIMARY AUTHORS

NRC: T.M. Ahn, J.W. Bradbury, R.B. Codell, N.M. Coleman, B.N. Jagannath, R.L. Johnson, P.S. Justus, M.P. Lee, B.W. Leslie, T.J. McCartin, M.S. Nataraja, J.S. Trapp, and R.G. Wescott

CNWRA: P.J. Angell, R.G. Baca, A.C. Bagtzoglou, R. Chen, A.H. Chowdhury, C.B. Connor, G.A. Cragnolino, A.R. DeWispelare, D.S. Dunn, D.A. Ferrill, A. Ghosh, R.T. Green, B.E. Hill, S.M. Hsiung, M.S. Jarzemba, P.C. Lichtner, P.C. Mackin, H.K. Manaktala, R.D. Manteufel, S. Mohanty, W.M. Murphy, G.I. Ofoegbu, R.T. Pabalan, E.C. Pearcy, D.A. Pickett, B. Sagar, N. Sridhar, J.A. Stamatakos, S.A. Stothoff, D.R. Turner, and G.W. Wittmeyer

TECHNICAL CONTRIBUTORS

NRC: R. Abu-Eid, J.H. Austin, M.J. Bell, J.W. Bradbury, R.E. Cady, R.B. Codell, N.M. Coleman, B.J. Davis, M.V. Federline, J.R. Firth, B.N. Jagannath, J. Kotra, M.P. Lee, B.W. Leslie, T.J. McCartin, S.M. McDuffie, M.S. Nataraja, R.B. Neel, C.W. Reamer, J.S. Trapp, and R.G. Wescott

CNWRA: M.P. Ahola, M.G. Almendarez, P.J. Angell, R.G. Baca, A.C. Bagtzoglou, D.P. Cederquist, R. Chen, A.H. Chowdhury, C.B. Connor, F.M. Conway, A.R. DeWispelare, D.A. Ferrill, A. Ghosh, S.L. Greenan, D.B. Henderson, B.E. Hill, M.E. Hill, S.M. Hsiung, A.M. Hoh, K.M. James, R.W. Janetzke, M.S. Jarzemba, H. Karimi, R.V. Klar, P.L. LaFemina, P.A. LaPlante, P.C. Lichtner, H.L. McKague, P.C. Mackin, S.B. Magsino, R.D. Manteufel, R.H. Martin, S. Mohanty, M.A. Muller, W.M. Murphy, G.I. Ofoegbu, R.T. Pabalan, W.C. Patrick, E.C. Pearcy, D.A. Pickett, J.D. Prikryl, B.R. Rahe, K.J. Smart, N. Sridhar, J.A. Stamatakos, G.L. Stirewalt, S.A. Stothoff, T.L. Tolley, D.R. Turner, and G.W. Wittmeyer

CONSULTANTS: F.P. Bertetti, S. Larose, Y.-M. Pan, R.A. Rapp, G. Rice, and D.A. Woolhiser

KEY TECHNICAL ISSUE CO-LEADS

NRC: J.W. Bradbury, K.C. Chang, N.M. Coleman, B.N. Jagannath, P.S. Justus, B.W. Leslie, T.J. McCartin, J.A. Pohle, J.S. Trapp, and R.G. Wescott

CNWRA: R.G. Baca, A.H. Chowdhury, H.L. McKague, E.C. Pearcy, and N. Sridhar

1 DESCRIPTION OF THE NUCLEAR REGULATORY COMMISSION FY96 REPOSITORY PROGRAM AND ACCOMPLISHMENTS

1.1 INTRODUCTION

Early in 1995, the Nuclear Regulatory Commission (NRC) staff recognized the need to refocus its prelicensing repository program on resolving issues most significant to repository performance. Since that time, three major events have driven a significant restructuring of the NRC repository program: (i) a reduction in Congressional appropriations for the repository program for both the NRC and the U.S. Department of Energy (DOE), (ii) a reorganization of the DOE high-level waste (HLW) work in what became known as the Program Approach in 1994 and its modification in 1995, and (iii) a report issued to the U.S. Environmental Protection Agency (EPA) by the National Academy of Sciences (NAS) that contained recommendations for setting a safety standard for a proposed HLW repository at Yucca Mountain (YM). The scope of the NRC prelicensing program was adjusted to focus on only those topics most critical to repository performance; these topics are called the key technical issues (KTIs). This was done with a recognition that items not on the current list of KTIs may be found to be important to repository performance in the future, carrying some risk of either (i) having to make overly conservative assumptions about such items or (ii) causing a delay in regulatory actions.

This report was jointly produced by the NRC and Center for Nuclear Waste Regulatory Analyses (CNWRA) staffs. The CNWRA, located in San Antonio, Texas, is a Federally Funded Research and Development Center sponsored by the NRC to provide technical assistance for the repository program. This report provides a status of NRC-HLW work conducted in fiscal year (FY) 96, as well as assessments of progress toward resolution of the KTIs. Chapter 1 describes the restructured NRC program and provides a programmatic context for the remaining ten chapters. Further details and rationales for the NRC restructured program are available in SECY-96-120.[1] Chapters 2 through 11 provide succinct summaries of work accomplished for each of the ten KTIs considered to be critical to repository performance. It should be noted that details of the activities summarized here are available in separate reports and technical papers, noted in the references at the end of each chapter.

1.2 EVENTS IMPACTING THE NRC REPOSITORY PROGRAM

The first major event impacting the NRC program was the reduction of Congressional appropriations for the NRC HLW program in FY96—$22 million to $11 million (a 50 percent reduction). Use of previous year funds to supplement the FY96 appropriation resulted in a $17 million funding level for the overall HLW program.[2]

---

[1]Nuclear Regulatory Commission's Refocused Prelicensing High-Level Waste Repository Program, Division of Waste Management, Office of Nuclear Material Safety and Safeguards.

[2]The FY97 appropriation for the NRC HLW program remains at $11 million. Adding $3 million from previous year funds, the overall HLW program at the NRC for FY97 is funded at $14 million. This further reduction by $3 million led to the decision to defer a majority of work on three of the ten KTIs that were the focus of the FY96 program. Thus, the NRC will sponsor work at the CNWRA on only seven KTIs in FY97. The NRC staff, to the extent limited resources permit, will monitor the DOE program and address only the most urgent regulatory issues for the deferred KTIs.

Second, the DOE FY96 budget for the repository program at YM was reduced from $375 million in FY95 to $250 million in FY96 (a reduction of 33 percent). In 1994, the DOE issued a Program Approach for streamlining its HLW activities and demonstrating clear measurable progress. The cornerstone of the Program Approach was preparation of the Site Suitability Analysis in 1998. FY96 budget reductions, together with Congressional guidance, led the DOE to revise its Program Approach in early FY96 addressing the critical unanswered technical questions leading to an assessment (in late FY98) of the viability of licensing the proposed repository at YM. This Viability Assessment (VA) is intended to provide a better understanding of the repository design and its performance in the geologic setting, a better appreciation of the remaining work needed to prepare a license application, and a more accurate cost estimate for licensing and developing a repository. Completion of the VA by June 1998 is included as a milestone in the Energy and Water Appropriations Act of 1997 (H.R. 3816). The VA, which is not a regulatory document, is anticipated to be somewhat less rigorous technically than the Site Suitability Analysis originally incorporated in the Program Approach.

Congressional guidance and severe budget constraints resulted in the DOE reducing its site characterization activities to those core scientific activities necessary to determine suitability of the site and to complete conceptual designs for the repository and waste package (WP). These remaining activities will be further focused by the DOE Waste Containment and Isolation Strategy (WCIS)[3] that is currently being refined. Hypotheses making up this strategy comprise an integrated safety case for YM that the DOE intends to test, using existing data, together with additional data from limited future testing. In June 1996, the DOE released a revised program plan including a revised schedule. Although preparing the VA remains the major near-term mission, the DOE announced schedules for several additional activities that had been eliminated from earlier plans or were not previously scheduled. Of particular importance to the NRC program are a revision to the Siting Guidelines (10 CFR Part 960) in FY97, which requires Commission concurrence; a final Environmental Impact Statement (EIS) in FY99; a site recommendation report in FY2001 (including the NRC sufficiency comments); and a license application in FY2002. The DOE also described a phased approach to preparing the repository design and the project integrated safety assessment, which will integrate data, assumptions, designs, and assessments into one common document, to support the VA, site recommendation report, EIS, and the license application. DOE plans on preparing important sections of this document in FY97-98, including data synthesis and site process models that, together with the designs, will be the major input to the DOE total system performance assessment (TSPA). As the DOE continues to implement its revised program approach, more detailed information will become available.

A third event impacting the NRC program was the issuance of the August 1995 NAS report, containing findings and recommendations for YM standards. This was the first in a series of actions under the Energy Policy Act of 1992 (EnPA), which also requires EPA to develop YM specific standards and the NRC to amend its technical criteria consistent with these standards. Under EnPA, EPA and the NRC must establish standards and regulations consistent with NAS recommendations. Although the NAS provides thoughtful and studied recommendations, a number of areas will require additional efforts from EPA and the NRC to formulate reasonable and implementable regulations: definition of an appropriate level of risk, compliance period, exposure scenarios, reference biosphere, and composition of a critical

---

[3]U.S. Department of Energy. 1996. *Highlights of the U.S. Department of Energy's Updated Waste Containment and Isolation Strategy for the Yucca Mountain Site*. DOE Concurrence Draft. July 1996. Washington, DC: U.S. Department of Energy. For ease of reading, the reference to DOE WCIS is omitted from all subsequent citations.

group. EPA is expected to issue a proposed standard for public comment in late 1996 and a final standard in 1997.

1.3 THE NRC REFOCUSED PRELICENSING PROGRAM

1.3.1 Revised Prelicensing Objectives

Staff recognition of the need to refocus its prelicensing program, as well as the impacts described, resulted in a revised prelicensing schedule and objectives for the prelicensing period. Although new HLW authorizing legislation is being considered, enactment is uncertain.[4] Therefore, the refocused program is based on the NRC current statutory responsibilities under the Nuclear Waste Policy Act (NWPA) as amended and the EnPA.

- Cooperate with EPA to ensure development of reasonable and implementable HLW standards. Implement these standards through a simplified, risk-informed performance-based, regulation specific to YM.

- Review and advise the Commission on concurrence with the DOE Siting Guidelines in Part 960.

- Establish program priorities based on KTIs that are most important to repository performance. Achieve agreement with the DOE on KTIs. Make progress toward KTI resolution at the staff level.

- Provide timely feedback to the DOE on potentially significant site, design, or assessment vulnerabilities for the DOE consideration in preparing its 1998 VA. Review the DOE VA to identify licensing vulnerabilities.

- Develop and exercise independent technical assessment capability necessary to implement EPA Standards, evaluate significance of KTIs and develop paths to resolution, test hypotheses and assumptions of the DOE WCIS, provide feedback to the DOE for consideration in preparing the VA, provide sufficiency comments for incorporation into the DOE site recommendation report, and eventually review a license application.

- Improve program efficiency by streamlining integration of the NRC activities and simplifying procedures for the NRC interactions with the DOE and others.

- Review and provide comments on the DOE draft EIS so the NRC can adopt the final EIS to the extent practicable as provided in the NWPA.

- Prepare comments on sufficiency of at-depth site characterization and waste form for the DOE to include in its site recommendation report.

---

[4]S. 1936 — Nuclear Waste Policy Act was passed in the U.S. Senate on July 31, 1996. The House of Representatives failed to complete action on the bill in the 104th Congress. New bill(s) may be introduced in the 105th Congress

1.3.2 Refocused Approach

To achieve the revised objectives in a resource-constrained environment, NRC has also revised its approach during FY96 to focus on resolving ten KTIs the staff considers to be the most important to repository performance and, therefore, licensing. Other activities necessary for licensing have been deferred as a result of FY96 budget reductions.[5] The ten KTIs are as follows.

1) Igneous activity
2) Structural deformation and seismicity
3) Evolution of the near-field environment
4) Container life and source term
5) Thermal effects on flow
6) Repository design and thermal-mechanical effects
7) Total system performance assessment and integration
8) Activities related to development of the U.S. Environmental Protection Agency Yucca Mountain Standard
9) Unsaturated and saturated flow under isothermal conditions
10) Radionuclide transport

These issues were identified through the NRC iterative performance assessments, previously conducted exploratory and confirmatory research, a systematic analysis of 10 CFR Part 60, review of the DOE draft WCIS, and the NRC understanding of relevant processes and events at the YM site, based on independent studies, evaluations, reviews of the DOE work, and other experience. The NRC will periodically re-evaluate the significance of the KTIs considering new information and performance assessments. In a November 1995 technical exchange, the DOE and the NRC agreed on the potential significance to repository performance of eight of the ten KTIs. The DOE questioned the technical basis for two KTIs dealing with the significance of igneous activity and structural deformation and seismicity. The NRC staff is evaluating data, conducting analyses, and interacting with DOE and others to clarify differences on these issues.

Because each of the ten KTIs encompasses a number of important subissues and resources are severely limited, the NRC staff is using a vertical slice or audit approach that has been successfully used in other areas of NRC responsibility, including reactor licensing. To further focus the work within each KTI, the NRC staff will evaluate a few narrow slices or topics (focused, well-defined scope) in depth; while conclusions about resolution of the broader issue will be inferred from examining these topics in detail. Within a particular vertical slice, the NRC staff plans to conduct appropriate activities such as evaluating alternate conceptual models, including underlying data and assumptions; conducting independent modeling for use in sensitivity and importance analyses; performing limited technical investigations, including laboratory tests, to develop an independent understanding of relevant processes; reviewing the DOE data and independent literature; establishing acceptance criteria, to guide reviews and issue resolution; and establishing clear objectives for each interaction with the DOE and others to ensure progress toward issue resolution.

---

[5]Nuclear Regulatory Commission's Refocused Prelicensing High-Level Waste Repository Program, Division of Waste Management, Office of Nuclear Material Safety and Safeguards.

The NRC approach is to focus all activities on resolution of the ten KTIs at the staff level.[6] Issue resolution is achieved when the NRC staff has no further questions or comments regarding how the DOE is addressing the issue in its program. However, it is recognized that there may be some cases where reaching a common understanding regarding differences in the NRC and the DOE points of view may be all that can be achieved. The NRC staff will prepare periodic issue resolution status reports to document significant progress and give the DOE timely feedback regarding specific issues or subissues. In addition, an annual report, such as this document, is intended to summarize the significant technical work completed for all KTIs during the preceding FY. To the extent that the NRC and the DOE can resolve issues before the VA, there would be greater confidence that the potential licensing vulnerabilities have been properly addressed by the DOE in its VA.

1.3.3 Prioritized Activities

To focus its limited resources most effectively on issue resolution, the staff prioritized all the activities (i.e., technical assistance and research) believed necessary to resolve each of the KTIs before licensing. Priorities were established by considering significance of the work to repository performance and issue resolution; appropriate timing of feedback to the DOE; lead times necessary to conduct activities; likelihood of success; and efficiency. During the budget cycle, the NRC staff intends to revisit defined activities and prioritization each year and consider new information and results of performance assessments. Table 1-1 (located at the end of this chapter) provides an overview of funded and unfunded KTI activities for FY96.

Activities funded for resolving the Total System Performance Assessment and Integration KTI are particularly important to the NRC approach. Integrated assessments conducted as part of this KTI will provide the basis for continuing confirmation or revision of significance of the NRC KTIs to repository performance and identifying new issues that might need to be considered. It will also provide a systems perspective for evaluating the DOE WCIS, including the DOE performance assessment—the centerpiece of the DOE VA and ultimately the license application. Sensitivity and importance analyses will also facilitate an understanding of the relative significance of processes and events to repository performance and provide a basis for concluding that certain effects are appropriately bounded. This information is vitally important to issue resolution and compliance determination. Analyses will also indicate where additional detailed analyses or data may be necessary to narrow uncertainties. Finally, integration activities under this KTI are essential for ensuring that interfaces among the NRC activities are identified and consistent and appropriate information flows among these activities.

1.3.4 Reduced Staff, Restructured Organizations, and Responsibilities

Refocusing the HLW repository program within the $17 million funding level resulted in a 27 percent total staff reduction among over the Office of Nuclear Material Safety and Safeguards (NMSS), Office of Nuclear Regulatory Research (RES), Office of Information Resources Management (IRM), and

---

[6]The FY97 appropriation for the NRC HLW program remains at $11 million. Adding $3 million from previous year funds, the overall HLW program at the NRC for FY97 is funded at $14 million. This further reduction by $3 million led to the decision to defer a majority of work on three of the ten KTIs that were the focus of the FY96 program. Thus, the NRC will sponsor work at the CNWRA on only seven KTIs in FY97. The NRC staff, to the extent limited resources permit, will monitor the DOE program and address only the most urgent regulatory issues for the deferred KTIs.

the Advisory Committee on Nuclear Waste (ACNW). The direct sponsorship of work by RES was eliminated and the critical parts of various research projects were incorporated into the KTI plans. These reductions were accomplished through reassigning NRC staff to other programs. At the CNWRA, the funding level led to a 20 percent staff reduction accommodated by attrition as well as elimination of some temporary positions and subcontractors. Additional reductions resulted from the FY97 HLW $11 million appropriations.

Staff reductions, improved efficiency, and integration of staff activities led to restructuring organizations and responsibilities. In February 1996, the Division of Waste Management (DWM) reorganized, consolidating its HLW activities in two branches instead of three. This action was taken to improve coordination and to better direct management attention. Additional changes were made within DWM branches and at the CNWRA to redistribute supervisory responsibilities and facilitate multidisciplinary interaction. In addition, the HLW Management Review Board (Board) was established to support the DWM Director by providing direct management oversight of the refocused program. The Board is comprised of DWM management representatives and senior management representatives from the CNWRA. The intent of this Board is to improve the overall integration of the program by coordinating policy and implementation guidance and providing a focus for decisionmaking on recommendations to upper management.

The NRC and the CNWRA staffs were also reorganized into ten KTI teams with the necessary technical and regulatory expertise for resolving each KTI. With oversight from the Board, each KTI team is responsible for planning and conducting those activities needed to resolve its issue within the established schedule and budget. The ten multidisciplinary teams represent the core technical expertise needed for the refocused program under the $17 million funding level. Sustaining this expertise was a key consideration in management decisions regarding staff reductions. Reductions in NMSS, RES, and CNWRA staff expertise occurred in a broad range of skills including geology, hydrology, engineering, project management, quality assurance, and systems engineering. These areas of expertise were chosen to minimize the impact on the core technical expertise required to resolve the KTIs. Many of these areas, however, are unique disciplines with specialized experience regarding repository issues that will be difficult and time-consuming to replace.

1.3.5 Advantages and Disadvantages of Refocused Approach

Numerous advantages are apparent in refocusing the NRC program on KTIs using the vertical slice approach. Scarce resources are keyed on those issues most significant to repository performance, thus enhancing attention to safety. Issue resolution is facilitated by acknowledging the appropriate bounding of less significant effects and aiming interactions with the DOE on those factual or interpretative differences with the greatest significance to performance. The audit nature of the vertical slice approach effectively evaluates a wide range of the DOE activities and identifies how well they are integrated. Integration of the NRC program is improved by coordinating necessary activities and technical disciplines in the review of each issue. Stressing issues that are potential licensing vulnerabilities is a robust approach that is not highly dependent on the DOE products and thus less likely to be seriously impacted by potential future changes in the DOE program. Finally, the approach is flexible enough to allow necessary changes to the issues or priority of activities based on new site information or new insights regarding repository performance.

As with any approach, there are some disadvantages. The audit nature of focusing only on the ten KTIs and selected vertical slices within each issue will result in areas of the DOE program not being examined in detail during prelicensing. Also, if some vulnerabilities are not recognized as KTIs and effectively addressed during prelicensing, the licensing review could be extended.

1.3.6 Importance of Maintaining a Credible Prelicensing Program

A sustained and credible prelicensing program is important to the success of the national program for several reasons. First, the NRC must ensure that practical and implementable safety standards and regulations are developed. Second, the NRC must be prepared to comment on the DOE VA for YM. Although it is recognized that the DOE VA is not a regulatory document, it certainly will be the basis for decisions about the future of the national program for storage and disposal of HLW and spent fuel. The NRC comments on the potential vulnerabilities of the YM site from a licenseability viewpoint and the technical assumptions underlying the DOE cost estimates are essential input to what will undoubtedly be a complex and controversial decisionmaking process. Finally, a credible prelicensing program is essential for identifying potential licensing issues early in the repository development process, rather than later after substantial investments have been made. As the DOE prepares its WCIS and supporting program plan, critical decisions are being made to focus the program on issues important to repository performance. Although commendable, such decisions will be the basis for identifying those site characterization and design activities that can be eliminated, reduced, or delayed to stay within the budget. As the NRC, the DOE, and others work toward resolution of the KTIs, it will be essential for the NRC to advise the DOE if these reductions will pose a risk to licensing. If so, these resolutions might be the basis for comments on the sufficiency of the DOE at-depth site characterization and waste form proposal.

1.4 HIGHLIGHTS OF FY96 TECHNICAL ACCOMPLISHMENTS

As discussed in more detail in chapters 2 through 11, significant progress has been made in developing paths to resolution for various subissues in the ten KTIs. The path to resolution takes into consideration the DOE data and analyses, non-DOE data and analyses available in the literature, the NRC independent data and analyses, future investigations proposed by the DOE, and an understanding of the impact of the subissue on the overall performance of the repository. It should be understood that the DOE is ultimately responsible for developing an integrated safety case for the repository, and the DOE may choose to adopt a different path to issue resolution than would be developed by the NRC. In each chapter, general program accomplishments are summarized first, followed by specific accomplishments for each individual KTI.

General Program Accomplishments

As described in the previous sections of this chapter, a major accomplishment in FY96 was refocusing the entire NRC repository program after a thorough evaluation of important external events including the NRC budget reductions, the DOE program revisions, and NAS recommendations for YM standards. The program was refocused on resolving ten KTIs most important to repository performance. Activities were reprioritized and organizations were restructured to support issue resolution and improve integration of technical work. An initial step in this program was to discuss the ten KTIs and the issue resolution process with the DOE and others. As a result, agreement was achieved with the DOE on the potential significance to repository performance of eight of the ten KTIs. For the two remaining issues on

igneous activity and structural deformation and seismicity, the DOE has been responsive by revising its WCIS to include evaluations of these issues.

For each individual KTI, the specific path to resolution is unique and reflects both the nature of the issue and progress of the DOE and the NRC technical work to date. Overall, for most of the KTIs, activities in FY96 concentrated on establishing a sound technical basis for future issue resolution during FY97. For a few KTIs, this involved data collection to improve the understanding of parameters or processes thought to be important to various analyses and for which data were not available. For example, state-of-the-art ground magnetic surveys of buried igneous features in the YM region (YMR) and studies of an actively erupting basaltic volcano were conducted to help construct scenarios and conceptual models of potential volcanic processes.

Activities emphasized refining or in some cases completing development of models and associated computer codes representing various subsystems or processes of the repository such as engineered barriers; near-field coupled thermal, hydrological, and chemical processes; volcanic processes; and fault deformation. These models were used to conduct sensitivity/importance analyses in FY96 at the repository subsystem or process level. Examples include thermal effects on moisture flow, drift stability, and radionuclide transport. Results of these analyses help focus further resolution work on those factors having a dominant effect on the subsystem or on processes.

Subsystem or process models will provide additional value by either calculating parameter input for use in the total performance assessment (TPA) code or being abstracted as modules in the TPA code during FY97. The resulting updated TPA code will be used for sensitivity/importance analyses in FY97 that integrate the various subsystems and processes that can then be used to confirm the importance of various parameters and processes to the total system performance measure of dose. Such integrated analyses are necessary to support resolution of individual issues or subissues that cannot be resolved in isolation of the total system. These analyses will also help develop acceptance criteria during FY97. In FY96, various approaches were evaluated on how acceptance criteria could be identified and used to support the issue resolution process. Presently, they are envisioned to be part of the technical basis for issue resolution.

While the resolution of many KTIs is dependent on additional work in FY97, some important progress was made this past year. Interactions between the NRC and the DOE during FY96 were successful in achieving informal agreements to be documented in issue resolution status reports in FY97. Examples include narrowing the range of tectonic models, identifying an acceptable seismic design methodology, and resolving design control process concerns. Another major step toward issue resolution was made in the TSPA area. An NRC and DOE interaction identified differences between the NRC and the DOE TSPAs, causes, and potential future resolution actions. Finally, the staff completed a Branch Technical Position giving an acceptable methodology for the use of expert elicitation. This guidance resolved questions of when and how to use expert elicitations for areas of major uncertainty, and currently is being used by the DOE to conduct and plan future expert elicitations.

Igneous Activity KTI

The Igneous Activity (IA) KTI is directed toward evaluating the significance of IA to repository performance by reviewing and independently confirming the data, and evaluating and developing alternative conceptual models for the probability and consequences of IA at YM. Technical investigations conducted in FY96 provide quantitative information to assess the DOE WCIS for IA—that volcanic events

within the controlled area will be rare and consequences of volcanism will be acceptable. The CNWRA staff developed probability models that cast volcano distribution and structural models as continuous probability density functions. This approach results in a probability estimate for volcanic eruptions at the proposed repository that does not rely on subjectively defined source zones, a feature common to all previous probability estimates that attempt to incorporate structural models into the analysis. These new models show that the probability of future basaltic volcanic eruptions at the proposed repository site is 10^{-8} to 10^{-7} per year. This probability range will likely form the basis for issue resolution with the DOE as it is unlikely that new information, such as changes in volcano recurrence rate or structural setting of the proposed repository, will result in order of magnitude changes in this probability range.

Although not considered a significant hazard at this time, the character of approximately 6 Ma silica volcanic material is being re-evaluated because of evidence that silicic activity occurred in the YMR well after caldera-forming eruptions ceased.

Field data and modeling show that basaltic volcanic eruptions are capable of dispersing considerably more material over much greater areas than assumed in the DOE performance models. Based on observations of modern basaltic eruptions, current CNWRA models of volcanic dispersion may underestimate deposit thicknesses by up to 50 percent at distances of tens of kilometers from the source. Issue resolution on IA consequences will address the interpreted dispersal capabilities of YMR basaltic volcanoes, in addition to assumptions regarding incorporation and transport of waste material, which are key parameters for assessing dose to a critical group. Based on current technical investigations, the consequences of basaltic IA on proposed repository performance may be greater than indicated in the DOE WCIS.

Structural Deformation and Seismicity KTI

The primary objective of the Structural Deformation and Seismicity (SDS) KTI is to evaluate potential SDS hazards relevant to safe containment and isolation of HLW at the DOE proposed repository at YM. SDS KTI technical investigations were carried out in FY96 to evaluate four aspects of the overall YM SDS program: (i) hypotheses outlined in the DOE WCIS, (ii) conclusions regarding SDS in the DOE 1995 TSPA (TSPA-95) (TRW Environmental Safety Systems, Inc., 1995), (iii) the DOE probabilistic and deterministic seismic hazard analyses (PSHA and DSHA), and (iv) controlled design assumptions concerning faults and fractures. In this report, SDS KTI technical investigations in four areas are presented: (i) analyses and evaluations of viable tectonic models and present conditions of crustal-scale stresses and strains describing the structural setting of the YM, (ii) identification of faults in the YMR that pose significant seismic risk to repository performance (Type I Faults), (iii) numerical models that describe the attenuation of seismic energy from nearby (near-field) seismic sources such as Bare Mountain fault (BMF), and (iv) investigations of the potential effects of structural deformation on groundwater flow and infiltration. As a result of these technical investigations, the effects of SDS on repository performance appear to be greater and more complex than indicated in the DOE WCIS and TSPA-95 (TRW Environmental Safety Systems, Inc. 1995).

Based on detailed analysis of Basin and Range tectonism and discussions during an NRC and CNWRA hosted Appendix 7 Meeting on tectonic models with the DOE, U.S. Geological Survey (USGS), ACNW, Nuclear Waste Technical Review Board (NWTRB), Electric Power Research Institute (EPRI), and representatives of the State of Nevada, it was concluded that only 5 conceptual tectonic models of the more than 12 proposed for the YMR are presently supported by existing data. Of these five, two of the models (proposed by representatives of the State of Nevada and the USGS) envision Crater Flat (CF) as

part of a tectonic (pull-apart) basin that formed from regional strike-slip or transtensional deformation. These strike-slip dominated models appear to pose the greatest seismic risk because of the potential for significant blind or buried faults currently not accounted for in the DOE PSHA. The CNWRA investigations examined the development of pull-apart basins through a series of analog sandbox experiments. Results of the experiments confirm earlier suggestions that pull-apart basins evolve in four stages (incipient, early, early mature, and late mature). Of these four, the risk for large magnitude and damaging earthquakes is greatest in the late mature stage; a pull-apart stage that closely resembles the conceptualization of CF in the State of Nevada tectonic model.

Fifty-two faults that pose significant seismic risk to the proposed repository (Type I faults) were differentiated from the catalog of more than 400 mapped faults in the YMR using the deterministic approach established in NUREG-1415 (McConnell et al., 1992). In this approach, seismic risk is evaluated in terms of ground motion a given fault could potentially generate (gauged as a peak horizontal acceleration assuming the fault's maximum-magnitude earthquake (the largest earthquake a fault could generate because of its size). Maximum magnitude and peak acceleration derive from empirical scaling and attenuation functions based on fault length and source-to-site distance. Two important assumptions in this type of analysis are fault ruptures are confined to single fault segments and attenuation functions properly extrapolate the seismic energy of near-site earthquakes (i.e., earthquakes close enough to the site that they no longer behave as point sources). Numerical modeling of faulting and seismicity on a stylized cross section of CF and YM, consisting of a listric BMF and two antithetic YM faults, indicates that the single rupture assumption is reasonable (at least for this fault geometry). Only minimal displacement is triggered on the antithetic YM faults from an initial rupture on the BMF. The latter assumption, however, may not be valid. Empirical attenuation functions, like those used in current DOE PSHA, appear to underestimate ground motions (horizontal accelerations) at the YM site from slip on the BMF. The numerical models predict anisotropic seismic energy propagation from the rupture point on the BMF to the surface.

The potential influence of structural features on groundwater flow and infiltration was investigated at two scales of observation. Regional groundwater flow patterns in the fractured aquifer around YM were modeled based on results of dilation-tendency analyses. Results from this analysis suggest a convergence of groundwater flow paths near the eastern boundary of the proposed repository, which could potentially limit lateral spreading of contaminant plumes emanating from the repository and thereby reduce dilution. This effect needs to be considered in assessments of the DOE WCIS hypothesis regarding dilution as a favorable condition. Local variations in fracture and fault dilation were examined by numerical modeling of hangingwall deformation above a series of normal faults akin to the geometry of faults in the proposed repository block. Faults were steeply dipping and each faulting event consisted of 1 m of displacement parallel to the fault plane. The results suggest significant dilation of vertical fractures and joints in the hangingwall block (with concomitant increases in porosity and permeability) after each faulting episode. This observation is counter to the DOE hypothesis that future tectonic events are unlikely to significantly alter current hydrologic characteristics of the site.

Further investigation of the effects of alternate tectonic models on future faulting activity and structural control on flow provide the foundation for resolution of several aspects of this KTI in FY97.

Evolution of Near-Field Environment KTI

The DOE updated WCIS for the proposed repository at YM has the primary goals of near complete containment of radionuclides within WPs for several thousand years and acceptably low annual

doses to a member of the public living near the site. Among the system attributes recognized in this strategy to be most important in accomplishing these goals are the rate of seepage of water into the proposed repository, WP lifetime (containment), release rate of radionuclides from breached WPs, and radionuclide transport through engineered and natural barriers. Of potential importance to the WP lifetime and radionuclide release from the engineered barrier system is the chemical composition of groundwater in the near-field region that could come in contact with the WP. This includes environmental variables defining the oxidation state, pH, chloride concentration, and other compositional variables of ingressing fluid that may affect the waste container and waste form. Depending on composition of this fluid, the rate of corrosion and leaching of spent fuel could be either greatly accelerated or inhibited. Additionally, chemical changes in the near-field environment can affect radionuclide transport characteristics such as speciation, sorption, and permeability. The objective of the Evolution of the Near-Field Environment (ENFE) KTI is to evaluate these characteristics of the evolving near-field environment and provide input to the TSPA.

In the DOE TSPA-95 (TRW Environmental Safety Systems, Inc., 1995), effects of waste emplacement on the near-field temperature and relative humidity were considered. These considerations led to determination of the time the WPs got wet, considered to trigger the aqueous corrosion processes, radionuclide release from the waste form, and radionuclide transport out of the WPs. However, in studying corrosion and radionuclide release, the chemistry of the near-field environment was not considered. Rather, assumptions were made relating corrosion behavior of waste containers to corrosion in humid industrial atmosphere or river water. Similarly, parametric equations relating the dissolution of spent fuel to environmental species were used, but no explicit justification was made regarding concentrations of these environmental species. A similar approach may be adopted in the viability assessment. The tools developed in the ENFE KTI can be used to assess the validity of using these environmental parameters. While the evolution of the near-field environment can occur by a variety of processes, three effects were investigated this FY: (i) effect of evaporation and condensation, (ii) effect of interactions between cementitious materials and groundwater, and (iii) effect and viability of microbiological activity.

The MULTIFLO code was used to determine the range of possible near-field environments due to evaporation and condensation processes as a function of thermal loading of the proposed repository. Calculations show that significant changes in pH and salinity could occur with moderate thermal loading of the proposed repository. With increasing heat load, higher concentrations of dissolved solutes are expected. At the extreme case of complete dryout, salts are expected to precipitate during the heating regime and dissolve during the cooling phase as the proposed repository rewets. It is expected that for the higher heat loads where complete dryout occurs, an evaporite deposit will form in the near-field with the deposition of salts occurring throughout the dryout zone. The effect of evaporite deposition on fluid composition during the rewetting stage is being investigated.

A primary limitation of the present calculation is use of the equivalent continuum model (ECM). In this model, fractured porous medium is represented as a single average continuum. Capillary equilibrium is assumed to be maintained between the fracture and matrix. As a consequence of this assumption, it is not possible for flow to take place in the fracture network without the matrix becoming fully saturated at the same time. This assumption of the model is fundamental to the formation of a capillary barrier sandwiched between the zone of enhanced moisture content and the proposed repository horizon preventing liquid water from reaching the waste during the heating regime. Consequently, gravity driven flow such as dripping, which may be an important process for container life and source term evaluations, cannot be described within the confines of the ECM. Alternate conceptualizations, such as multiple interacting continua, may provide a better description of fracture flow. Validation of the

thermal-hydrologic-chemical coupling may be attempted through an analysis of field samples in the vicinity of YM originating from paleohydrothermal sources. Field samples have been collected and are being analyzed.

The effects of cementitious materials on the near-field environment have been estimated using available data mainly at near-ambient temperatures. However, considerable uncertainties exist regarding stability of the calcium silicate hydrate gel phase that may determine the pH of the fluid contacting the cement. If the gel phase recrystallizes at higher temperatures, the pH may not attain as high a value as calculated from room temperature data. It is also important to couple these essentially batch calculations with a transport model such as MULTIFLO to estimate the spatial extent of the change in pH due to cement water interactions.

The investigation of microbiological activity has shown that bacterial colonies native to the host rock at YM are viable even after exposure to 120 °C for a short period of time. However, activity and the effects on near-field environment through interaction with cementitious materials may be limited by the concentration of oxidizable sulfur species.

The primary focus of resolving this KTI will be on bounding the environment around WPs sufficiently well so that WP performance can be estimated. Time to wetting and the effects of aqueous chemistry on container life appear to be critical factors. Adequacy of ECM models for estimating these factors remains to be investigated.

Container Life and Source Term KTI

The DOE updated WCIS for the proposed repository at YM has the primary goals of near-complete containment of radionuclides within WPs for several thousand years and acceptably low annual doses to a member of the public living near the site. Among the system attributes recognized in the DOE strategy to be most important in accomplishing these goals are the WP lifetime (containment), rate of release of radionuclides from breached WPs, and radionuclide transport through engineered and natural barriers. The objective of the Container Life and Source Term (CLST) KTI is to evaluate these attributes independently and provide input to the performance assessment (PA) of the overall proposed repository.

Several subissues delineated within the CLST KTI directly address the DOE WCIS: (i) evaluating methodologies for extrapolating short-term laboratory data to long-term performance; (ii) evaluating factors affecting waste form alteration products and the release of radionuclides; (iii) determining effect of long-term thermal exposure and mechanical loads on the mechanical stability of the container materials; (iv) assessing the effect of microbiological organisms on the performance of container materials; and (v) performing sensitivity analyses on the effects of thermal loading, near-field environment, and galvanic coupling on container life using the Engineered Barrier System Performance Assessment Code (EBSPAC). The DOE performed a probabilistic analysis of container life in TSPA-95 (TRW Environmental Safety Systems, Inc., 1995) using the Waste Package Degradation (WAPDEG) code. Similar methodologies may be used in the DOE VA through TSPA-VA. The sensitivity analyses performed in this KTI will enable the NRC and the CNWRA staffs to evaluate methodologies used by the DOE in TSPA-95 (TRW Environmental Safety Systems, Inc., 1995) and compare the container life cumulative distribution curves predicted by EBSPAC and WAPDEG. These analyses will also facilitate evaluating the significance of these subissues to the overall system performance.

In the most common WP design proposed by the DOE, 21 pressurized water reactor or 40 boiling water reactor spent fuel (SF) assemblies are contained in a type 316L stainless steel multi-purpose canister (MPC) (3.5-cm thick wall). The MPC is surrounded by an inner overpack of corrosion-resistant alloy (2.5-cm thick wall), contained in an outer overpack of corrosion-allowance material (10-cm thick wall). The container life evaluations in this KTI focused on the inner and outer overpacks.

Calculations of container life using EBSPAC indicated that two parameters are of great importance to container life: (i) the areal mass loading (AML), as defined by the thermal loading strategy, which determines the near-field temperature as well as the chemistry of the environment contacting the WP; and (ii) the degree of galvanic coupling between the outer carbon steel overpack, once it is breached, and the inner nickel-base alloy overpack, which determines the failure time of the inner overpack. In the absence of galvanic coupling, the container life exhibits a minimum at an intermediate AML. At high AML, the container remains dry for long periods of time and the overall life of the container is long. At low AML, container wetting occurs shortly after emplacement but corrosion processes are not as severe and life is extended just beyond 10,000 yr. For example, the critical potential above which localized corrosion occurs increases with decreasing temperature so the likelihood of localized corrosion for a given chemical environment decreases with decreasing temperature. These two competing factors lead to a minimum container life at an intermediate AML. If efficient galvanic coupling occurs, calculated container life can exceed 10,000 yr, regardless of the AML value.

The effect of long-term thermal exposure on susceptibility to mechanical failure of the steel outer overpack (thermal embrittlement) was evaluated on the basis of a review of the literature. Thermal embrittlement may occur due to segregation of phosphorus (an incidental impurity in steel) to grain boundaries. It was concluded that the candidate steels considered for the outer overpack are susceptible to thermal embrittlement if the WP surface temperature exceeds 200 °C for significant periods (thousands of years). The investigation also revealed that low-alloy steels are more susceptible to thermal embrittlement than plain carbon steels.

Even if the container surface remains dry and aqueous corrosion is obviated, dry oxidation may be a determining factor in container performance. Literature on the kinetics of dry oxidation of plain carbon and low-alloy steels at temperatures anticipated in the proposed repository was evaluated critically. It appears that dry oxidation and intergranular penetration of these steels are not important factors at the predicted temperatures. Further but limited investigation may be necessary to resolve this issue.

The DOE strategy in extending the life of containers is to use two dissimilar metals so the outer overpack protects the inner overpack from corrosion through a galvanic coupling effect. Implicit in this strategy is the assumption that a critical potential exists for a given environment/material combination below which localized corrosion does not occur. This critical potential is identified as the repassivation potential, E_{rp}. Long-term corrosion tests, ongoing for over 2 yr, have shown that when the potential is maintained below E_{rp} for Alloy 825, localized corrosion has not occurred.

A factor that often affects corrosion of materials exposed to natural environments is microbiological activity. Microbiological organisms can adversely affect the susceptibility to localized corrosion of a material by either increasing the corrosion potential, E_{corr}, (called ennoblement) or decreasing the E_{rp}. Investigations conducted using a model organism, *Shewanella putrefaciens*, originally

isolated from a corroded oil supply line, show that the bacterium has no significant effect on E_{corr} of stainless steel but decreases E_{rp} in an anaerobic environment containing thiosulfate.

The literature on dry oxidation and fracturing of SF was evaluated because these phenomena could enhance radionuclide release rate by increasing the surface area and solid-state diffusion of relatively volatile radionuclides, followed by dissolution or colloid formation under aqueous conditions. It was concluded that higher oxides (i.e., greater than $UO_{2.4}$) may not form below 150 °C due to slow diffusion of oxygen. Although colloids are formed by oxidative dissolution of SF, there are uncertainties regarding the significance of colloids to the source term. Natural analog, experimental, and thermodynamic studies indicate that the properties of secondary uranyl minerals such as uranophane will control the source term. Experimental studies were initiated to determine fundamental thermodynamic properties of uranophane to reduce the uncertainties in solubility calculations. Pure uranophane was synthesized for this purpose.

The subissue of extrapolating short-term laboratory tests on corrosion can be resolved by using repassivation potential as a bounding value for onset of localized corrosion. Efficiency of galvanic corrosion remains to be investigated.

Thermal Effects on Flow KTI

Prediction of thermally driven redistribution of moisture through partially saturated, fractured porous media caused by the emplacement of heat-generating HLW with acceptable uncertainty is the focus of the Thermal Effects on Flow (TEF) KTI. It is necessary to understand the spatial and temporal effects of the thermal load on temperature as well as liquid and gas phase flux in the vicinity of the proposed repository to have confidence in predictions of containment and long-term waste isolation. The DOE is developing a strategy to demonstrate that waste can be contained and isolated at the proposed YM repository site. Evaluating this strategy necessitates a detailed understanding of thermally driven moisture flow through partially saturated, fractured porous media. This KTI was divided into three resolvable subissues in pursuit of this understanding: (i) is the DOE thermal testing program sufficient to assess the likelihood of gravity driven refluxing occurring in the near field, (ii) is the DOE thermal modeling approach adequate for assessing the nature and bounds of thermally induced flux in the near-field, and (iii) will the DOE thermal loading strategy result in thermally induced flux in the near-field and humidity at the WP surface to meet the performance objectives? Resolution of these subissues establishes the knowledge base necessary to predict with acceptable uncertainty thermally driven redistribution of moisture through partially saturated, fractured porous media.

The objective of this KTI is to resolve the subissues to a level of acceptable uncertainty. Activities designed to reduce uncertainties in these subissues in FY96 were both reactive and proactive: (i) reviewing and evaluating the DOE thermohydrology program, including the DOE peer review activity; (ii) benchmark testing of computer codes; (iii) providing sensitivity analyses; and (iv) evaluating conceptual models. Results from the DOE and the NRC activities (i), (ii), and (iii) are summarized here. Evaluations of alternative conceptual models are only preliminary and will be reported in future documents.

The review and evaluation concluded that the DOE Thermohydrologic Testing and Modeling Program adequately addresses most, but not all, critically relevant technical issues. It was noted in the DOE peer review team (PRT) report, and supported here, that the DOE has not demonstrated that it has plans to evaluate the conceptual models as rigorously as needed. The importance of near-field flow and

transport calculations will depend upon the degree to which WP performance is affected. The current DOE models may not adequately include all important transport mechanisms. Either the current models will need to be modified or different models used if these mechanisms are to be included. Additionally, in neither the PRT recommendations nor the DOE response to the PRT report was it demonstrated that the DOE bounding assumptions and analyses of the thermal-hydrological-chemical coupled effects are conservative. The review noted that the discontinuance of surface based hydrologic testing may result in unacceptably high uncertainty in infiltration estimates. The importance of acceptable predictions of infiltration rates is manifested in thermohydrologic flow models whose predictions are highly sensitive to prescribed infiltration rates at the upper boundary.

Benchmark testing (i.e., code-to-code comparisons) was conducted on four general thermohydrologic codes: TOUGH2, FEHM, CTOUGH, and MULTIFLO; the first two codes are currently being used by the DOE while the latter two are NRC codes. Primary differences among the codes were in computational efficiency—the MULTIFLO code was substantially faster than the other three codes. The FEHM code experienced computational difficulties in two test cases; one with high infiltration rates and the other with flow in fractured porous media. With respect to computational precision, simulation results from all codes were sufficiently similar that differences in future predictions from either of the codes can be attributed to differences in input and not computational inconsistencies.

Sensitivity and numerical scoping analyses helped identify the relative importance of specific types of information that contribute to the evaluation of thermally driven moisture flow through partially saturated fractured porous rock. This is of interest because the presence of liquid water or water vapor in the repository environment is important in corrosion analyses of the WP and transport of radionuclides once released from the WP. These sensitivity analyses indicate that (i) placement of backfill materials can lead to increased temperatures at the WP and decreased temperatures at the drift wall; (ii) varying the hydraulic properties of the PTn and CHnv within reasonable limits can produce a factor of 10^4 change in the unsaturated hydraulic conductivity of the CHnv located below the proposed repository horizon; (iii) vertically oriented fracture zones that intersect the emplacement drifts can decrease peak temperatures by 20 °C at the WP and 15 °C at the drift wall; (iv) ventilation can reduce drift wall temperatures by as much as 45 °C and induce dryout 5 m into the drift wall; and (v) geologic structures at YM are capable of forming perched water bodies; heating within these structures can lead to increased saturation in, above, and below the proposed repository horizon during early times after the onset of heating.

FY96 activities of the TEF KTI made significant progress toward resolution of subissues. Comments and recommendations made on the DOE Thermohydrologic Testing and Modeling Program provide input to the basis for the resolution in FY97 of the subissue on the sufficiency of the DOE thermal testing program to assess the likelihood of gravity driven refluxing occurring in the near-field. The identification, through sensitivity study of important parameters, features, and processes that may significantly affect the moisture flow and postclosure performance of the repository, will provide additional input for the resolution in FY97 of the subissue on the sufficiency of the DOE thermal testing program to assess the likelihood of gravity driven refluxing occurring in the near-field. There remain two areas that still contribute to the uncertainty in resolving the subissues in the TEF KTI. High levels of uncertainty exist regarding the effect of heterogeneities and geologic structure on thermally driven moisture movement, even though insight has been gained in this area. A second major contributor to the high level of uncertainty in this KTI is the absence of evidence to support a conceptual model adequately representative of the heat and mass transfer mechanisms present in partially saturated fractured rock. These are two target areas for future evaluation and resolution in FY98 of the subissue on the adequacy of the DOE thermal modeling approach for assessing the nature and bounds of thermally induced flux in the near-field.

Repository Design and Thermal-Mechanical Effects KTI

The main focus of the Repository Design and Thermal-Mechanical Effects (RDTME) KTI is the evaluation of time-dependent thermal-mechanical (TM) coupled effects on the heated rock mass near the repository horizon for repository design and preclosure and postclosure repository performance. There are three resolvable subissues associated with this KTI: (i) design of a proposed repository to meet preclosure and postclosure performance objectives, (ii) evaluation of thermal effects on design of the underground facility, and (iii) role of repository seals in meeting performance objectives. In addition, this KTI also supports examination of two of the DOE hypotheses regarding the ability of the proposed YM repository to isolate wastes: (i) flow of water into the repository will be low and (ii) engineered barriers, possibly including backfill, will limit migration of radionuclides into the host rock and any sources of groundwater. The objective of the RDTME KTI during FY96 was to address certain components of the first and second subissues. The associated activities included (i) review of the DOE repository design program with emphasis on technical reviews of DOE seismic design methodology, regulatory compliance review report, and Exploratory Studies Facility (ESF) design report; (ii) a TM parametric study of drift stability to identify important parameters that may affect repository design; and (iii) development of a prediction tool for TM analysis.

Review of the DOE Seismic Topical Report No. 2 (TR2) *Seismic Design Methodology for a Geologic Repository at Yucca Mountain* indicated that the proposed seismic performance categories are not consistent with the NRC categories 1 and 2 design basis events in the proposed rule changes to 10 CFR Part 60. This inconsistency could potentially pose a problem during license review of repository design. This topical report did not adequately link proposed preclosure seismic methodology and postclosure performance considerations. The proposed treatment of repeated seismic loadings as low-probability/low-consequence events is not justifiable given that limited information is available regarding seismic activity at YM. Furthermore, the proposed methodology did not provide sufficient details regarding fault-specific investigations needed to define set-back distance for fault avoidance. These concerns are currently being addressed by the DOE in its revised topical report. These concerns will be resolved if the revised topical report is found acceptable by the NRC.

As a part of the activity for resolving the NRC concerns on the DOE design control process—an integral part of the DOE repository design program—a DOE regulatory compliance review report was reviewed during early FY96. The focuses of the review were to verify that the DOE identified applicable 10 CFR Part 60 design requirements to be addressed in ESF design and assess if these design requirements were correct and if the flow-down to the design specifications was objective and traceable. Review of the document made it possible to conclude that the NRC concerns related to the DOE design control process can be considered resolved. The only outstanding item remaining is to assess the DOE implementation of the improved design control process. The NRC recommendations made on DOE design of the ESF Main Drift will provide guidelines to the DOE in its future repository design considerations.

An enhanced model has been developed to simulate the response of natural rock joints under cyclic loads taking into account the primary, secondary, and higher-order asperities present on the joint surfaces. This model will provide review tools to the NRC and the CNWRA staffs to assess stability of drifts in the context of preclosure safety and retrievability. Review of seismic TR2, ESF design package, and DOE regulatory compliance review report, and development of a rock joint model provided a basis for resolving the subissue on design of the proposed repository to meet preclosure and postclosure performance objectives.

The first phase TM parametric study of drift stability investigated the potential effects of inherent variation of thermal and mechanical properties of the rock mass and site characteristics on emplacement drift stability without backfill during the operation period. The range of properties used in the study are those currently considered to be representative of the site. Various combinations of nine rock mass parameters were included in the parametric study using numerical modeling with the Universal Distinct Element Code. Statistical analyses of the parametric study results based on certain performance measures were conducted. These performance measures include maximum and minimum principal stress, maximum joint shear displacement, maximum joint closure and separation, convergence of excavated openings, and extent of yield zone around the excavation. Results indicate that thermal load and thermal expansion coefficient are important parameters that affect most of the performance measures studied while other rock mass properties affect drift stability to various degrees of significance. Among them, intact rock cohesion and friction angle were found to have less significant effects on the performance measures related to joint behavior. However, they have a relatively significant effect on the extent of yield zone. These findings will bring necessary focus in development of review procedures and acceptance criteria for resolution of RDTME KTI and in review of the DOE ESF design packages.

The NRC and CNWRA staffs reviewed the DOE ESF thermal tests program through DOE/NRC technical interactions and a site visit to the ESF thermal testing alcove. Objectives related to the RDTME KTI in the first ESF Thermal Test are developing information on rock mass thermal and mechanical properties at elevated temperature through the single heater test, and investigating interactions between the rock mass and various ground support systems through the drift-scale heater test. The locations for both tests are in a relatively competent rock mass. The NRC and the CNWRA anticipate that the mechanical properties and responses obtained from these tests will be near the high end of the range encountered in the emplacem area. The TM parametric study and review of the DOE ESF heater tests led to identification of thermal load and site specific rock mechanical and thermal parameters that may significantly affect emplacement drift stability and waste retrievability. These will provide input to the basis for resolution of the subissue on consideration of thermal effects in underground facility design.

Total System Performance Assessment and Integration KTI

Licensing decisions regarding the proposed HLW repository at YM will be largely based on the quantitative determination of compliance over relatively long time periods (e.g., 10,000 yr). This determination of compliance will be made by the NRC through a predictive analysis referred to as a TSPA. Simply stated, TSPA is a broad based engineering analysis that (i) considers the features, events, and processes (FEPs) that significantly affect the proposed repository; (ii) examines the effects of these FEPs on the proposed repository system (composed of engineered and natural barriers); and (iii) estimates the probability and consequences in terms of dose (or risk). Results of the TSPA are expressed in a probabilistic context because of the broad uncertainties associated with the large spacial scale of the complex geologic setting and the long compliance period.

The primary objective of the Total System Performance Assessment and Integration (TSPAI) KTI is to assess compliance of the proposed repository with regulatory standards. Such assessments must identify and analyze the features, processes, and events relevant to the site, as well as account for uncertainties in conceptual models, abstracted mathematical models, future system states, and model parameters. The resolution of this issue will, in part, be accomplished by completing development of the TPA code. Full resolution will be achieved with application of the TPA code to evaluations of the DOE TSPA-VA and review of the TSPA for license application.

A number of subissues were identified that are essential to resolution of the primary issue: (i) do the hypotheses described in the DOE WCIS adequately represent the major performance characteristics of the YM repository, (ii) what is the relative importance of the individual NRC KTIs and is there is a need for change in emphasis, and (iii) are major components of the DOE TSPA methodology (e.g., model abstractions, probability and consequences of relevant FEPs, parameter and model uncertainties, and bounding assumptions) sufficiently comprehensive to provide a defensible safety case? In addition to these subissues, work performed under this KTI involved conducting independent assessments for prelicensing review, developing guidance on the use of expert judgment, promoting integration among KTIs, and assisting the NRC with maintenance of the advanced computer system and Consolidated DOCument System (CDOCS).

Significant progress was made this FY in addressing a number of the TSPAI KTI tasks. Through the conduct of an audit (i.e., prelicensing) review of the DOE TSPA-95 (TRW Environmental Safety Systems, Inc., 1995) report, the NRC and the CNWRA staffs made substantive progress on the subissue dealing with the DOE TSPA methodology. The KTI teams conducting the audit review identified a number of significant vulnerabilities in the DOE TSPA-95 (TRW Environmental Safety Systems, Inc., 1995) primarily associated with nonconservative assumptions, inadequate model abstractions, inconsistencies with field data, and inconsistencies with previous DOE TSPA analyses. Specific recommendations for improving analyses were made to the DOE and support contractors at a technical exchange meeting on TSPA-95. Regarding the use of expert judgment, a branch technical position was prepared and published for public review and comment. In addition, the CDOCS software was documented and successfully installed on the NRC advanced computer system.

Activities Related to Development of the U.S. Environmental Protection Agency Yucca Mountain Standard KTI

The primary objectives for this KTI are to (i) support the NRC in interactions with the EPA regarding development of an EPA Standard for the YM site and (ii) subsequent to promulgation of the EPA Standard, assist in developing the technical bases for future revisions to the NRC regulations to conform with the new EPA Standard. A number of subissues were defined that must be addressed to constrain exposure scenarios for TSPA: (i) defining a compliance period and method, (ii) selecting a critical group(s), (iii) evaluating results of potential human intrusion, and (iv) considering disruptive events. Results of the analyses conducted during FY96 on these subissues are summarized briefly in the following paragraphs.

The relative radiological hazard of a repository containing only SF is initially about four orders of magnitude greater than that of an equivalent hypothetical ore body. The hazard diminishes rapidly over the first few hundred to few thousand years—by 90 percent at 100 yr; 99 percent at 1,000 yr; and 99.9 percent at 10,000 yr. An apparent increase in hazard at 100,000 to 500,000 yr is due to the ingrowth of radionuclides such as ^{230}Th, ^{229}Th, ^{226}Ra, and ^{210}Pb. By 10,000 yr the relative radiological hazard will be within an order of magnitude of the hypothetical ore body. A time period of regulatory interest (TPI) for a repository of about 10,000 yr would, therefore, focuses attention on the period when the waste hazard has a significant man-made component that is readily discernable from an equivalent hypothetical ore body, even after considering uncertainties associated with solubilities and release rates. The findings of this study are consistent with those of earlier studies (U.S. Environmental Protection Agency, 1982, 1985).

Calculations were made of expected peak dose to a hypothetical member of a critical group residing in the Amargosa Valley region for an extrusive volcanism scenario, assuming a lifestyle as

described in NUREG-1538[7]. These calculations considered doses for different locations of this individual on the earth surface (i.e., 20, 25, and 30 km directly south of the proposed repository) immediately after the event. These analyses show that increasing the TPI has the effect of increasing the importance of low-probability, high-consequence events such as extrusive volcanism when compared with scenarios that are certain to occur regardless of the TPI (e.g., undisturbed repository). The magnitude of this increase was found to be about a factor of 4, although this estimate is somewhat uncertain due to large variances in the expected dose values.

A scoping analysis on dilution effects found that dilution at the YM site is not likely to produce large reductions in groundwater concentrations of radionuclides (or the associated radiologic doses). In the immediate vicinity of the proposed repository, dilution factors (DF) on order of 2 to 10 are expected based on model calculations. Relatively low DFs are likely if the plume is confined to fracture zones that are pervasive in the tuff aquifer (Geldon, 1993). Alternatively, if the plume spreads vertically, as a result of flow through vertical fractures or faults, the DFs will tend toward the higher end of the range. Passive mixing along the long flow path (from the proposed repository site to the Amargosa Valley region) will contribute to dilution but is unlikely to increase DFs by many orders of magnitude. This scoping analysis did not identify any methodology issues with regard to implementation of an individual dose-based requirement. Characterization of the local and regional groundwater system is more important for demonstrating compliance with a dose-based standard than for a derived standard based on integrated releases to the accessible environment (i.e., the containment requirements of 40 CFR Part 191). This increased emphasis on characterizing the groundwater system will hold for individual risk-based requirements as well. Additional tracer tests, such as those being conducted by the DOE in the C-Well complex (Geldon, 1995), may be needed to acquire data on transport parameters (e.g., mass dispersivities and effective porosities).

The NRC staff concluded from preliminary analyses of the consequences of a stylized human intrusion at YM that exploratory drilling appears to be an unlikely, low consequence event, if restricted to reasonable assumptions. The staff also found that such an analysis need not be directly incorporated into a total system performance demonstration. If the revised EPA Standard requires such stylized calculations, the NRC staff recommends that analysis be constrained to specific reasonable scenarios identified in the regulatory framework.

General conclusions from the peak dose analysis presented in this report are that (i) a relatively small number of long-lived, mobile radionuclides will be important to performance; (ii) there do not appear to be any major technical difficulties that might preclude estimating an annual individual dose; and (iii) assumptions concerning critical group location and lifestyle could be very important in determining an appropriate approach for establishing radionuclide concentrations at receptor locations.

Sections of this report also describe continuing efforts for this KTI to determine appropriate critical group(s), reference biosphere assumptions, and parameter values for a stylized human intrusion scenario.

Unsaturated and Saturated Flow Under Isothermal Conditions KTI

---

[7]Nuclear Regulatory Commission. 1996. *Preliminary Performance Assessment Analyses Relevant to Dose-Based Performance Measures.* In preparation. NUREG-1538. Washington, DC: Nuclear Regulatory Commission.

Yucca Mountain was selected as a potential HLW repository site in part due to the favorable hydrogeologic conditions provided by an unsaturated zone up to 700 m thick. Low moisture fluxes and water contents reduce the likelihood of waste canister corrosion, SF dissolution, and rapid transport to the water table. It has also been postulated that dissolved radionuclides that reach the water table will be rapidly diluted by relatively large saturated zone flow rates. The Unsaturated and Saturated Flow Under Isothermal Conditions (USFIC) KTI is responsible for assessing aspects of the ambient hydrogeologic regime of YM that have the potential to compromise performance of the proposed repository. The DOE developed a WCIS for YM that defines low seepage and saturated zone dilution as two of three key natural barriers for a geologic repository at YM. The primary goal of the USFIC KTI is to develop technical procedures and conduct technical investigations to assess the adequacy of the DOE strategy for characterizing and modeling hydrogeologic processes and features at YM. Three subissues related to shallow infiltration, unsaturated zone conditions above the repository, and ambient flow condition through the repository were identified in the KTI, whose resolution will aid in assessing the DOE low seepage hypothesis. One subissue addresses the saturated zone and the dilution hypothesis. During FY96, efforts were primarily focused on those FEPs that most strongly affect shallow infiltration, unsaturated zone conditions above the repository and flow conditions from the repository horizon to the water table.

Progress was made toward resolving differences with the DOE on methods for bounding the effects of climate changes on hydrogeologic conditions and on estimates of shallow infiltration. It appears likely that changes in climate at YM may be bounded using available paleoclimatic data to establish temporal patterns, likely limits on precipitation, and expected changes in water table elevation. Estimates for net infiltration have been made for an area including YM using a numerical simulator. Resulting distributions are similar to those made by the DOE using different codes and somewhat different modeling assumptions.

Technical investigations related to the formation of perched water zones, the spatial distribution of infiltration, and focused recharge were conducted. These investigations were designed to address subissues related to the shallow infiltration, unsaturated zone conditions above the repository, and flow conditions from the repository horizon to the water table and accordingly evaluate the low seepage WCIS hypotheses. Numerical models were developed to investigate the formation and persistence of perched water bodies at YM and whether simulated perched zones were consistent with measured ^{14}C residence times. An average deep recharge rate of 6.2 mm/yr was estimated to sustain a perched water body and application of hydrologic and geochemical constraints suggests that perched zones may contain a combination of older pluvial water and younger water from more recent infiltration. The spatial distribution of infiltration at YM was estimated by abstracting detailed one-dimensional simulations into a response surface for annual-average infiltration (AAI) as a function of hydraulic properties, annual average meteorologic input, and depth of surficial cover. Analyses indicate that after precipitation and temperature, AAI is most sensitive to colluvium depth. Development of a distributed watershed model was initiated to evaluate the possibility for focused recharge in the YM area. Calculations were made for a portion of the northern end of Solitario Canyon. Preliminary results indicate that channel recharge can be calculated for Solitario Canyon but better estimates for key hydraulic and infiltration parameters are required.

Based on paleoclimate data, an upper bound on future precipitation can be estimated to be 2–3 times the present rate. This bound will help resolve the subissue of estimating deep percolation through the repository horizon. The near agreement between the range of near-surface infiltration estimated through modeling by the CNWRA and measured in the field by the DOE will also contribute to resolution of this KTI.

Radionuclide Transport KTI

The Radionuclide Transport (RT) KTI was designed to conduct technical investigations of processes that affect radionuclide transport from the proposed YM repository to the accessible environment and thereby affect the overall system performance. Matrix diffusion, sorption, and dilution that may reduce radionuclide concentrations during transport are key attributes of the DOE WCIS. The primary goals of the RT KTI are to determine which processes are critical to meeting overall system performance objectives and develop criteria with respect to data sufficiency, process representation in system models, and parameter values to resolve this KTI.

Technical investigations were conducted to address a subset of radionuclide transport issues. Fast transport paths at YM have been indicated by the presence of bomb-pulse ^{36}Cl in data collected by the DOE in the ESF. Available data and associated interpretations were evaluated. The consensus interpretation is that groundwater moved from the surface to the proposed repository horizon, mainly along faults and fractures within the last 50 yr. Data from the Nopal I deposit within the Peña Blanca District, an analog site, were measured and interpreted to evaluate radionuclide transport at tens of meters scale in hydrologically unsaturated tuffs. These interpretations indicate that long-term (hundreds of thousands of years) radionuclide transport is affected by changes in hydrologic conditions and document the role of fracture transport in unsaturated tuffs. Furthermore, observations of the incorporation of uranium (U) within fracture minerals suggest that retardation is not a fully reversible process.

Retardation processes were evaluated by interpreting a combination of U and neptunium (Np) sorption data from the CNWRA experiments and from the literature to show that the magnitude of sorption of a given actinide is similar for different minerals if normalized to the number of available sorption sites. Additionally, these studies indicate that U and Np sorption coefficients can be constrained using approaches that account for changes in aqueous and surface speciation over wide ranges of geochemical conditions. To study regional-scale flow and mixing, hydrochemistry data for the YM region have been gathered and entered into a geographic information system database. This system will allow analysis of hydrochemical signatures for different aquifers to evaluate the possibility of dilution of radionuclide-contaminated groundwater upon mixing with the regional groundwater system as postulated by the DOE. A conceptual model of hydrologic flow has been outlined to test the DOE simulations of transport through fractures and matrix. This conceptual model may allow development of a numerical approach for fracture and matrix transport that can be compared with site data.

The path to resolution for this KTI includes estimating the effects of geochemical conditions on retardation through TSPA. This will help identify those radionuclides that require retardation, in addition to dilution, for the site and proposed repository to comply with applicable standards. The resolution will then focus on estimating lower bounds for retardation of these radionuclides.

1.5 CONCLUSIONS

The refocused program is expected to provide an efficient and effective way to streamline the NRC prelicensing program and enhance the emphasis on safety of the proposed repository program in an environment of constrained resources. This program provides the essential technical basis for fulfilling NRC responsibilities independent of the DOE, including establishing implementable regulations consistent with EnPA direction and evaluating the sufficiency of at-depth site characterization and the proposed waste forms during the prelicensing period in accordance with the NWPA. Focusing on KTIs that are potential

licensing vulnerabilities is a robust approach that is not highly dependent on DOE products and thus less likely to be impacted by potential future changes to the DOE program. Finally, the approach is flexible enough to allow necessary changes to issues or priority of activities based on new site information or insights about repository performance.

This report provides a summary of the progress made in FY96 on developing paths to resolution for various subissues in the ten KTIs. The NRC work is clearly keyed to those issues that most impact repository performance. Recognizing the uncertainties in description of the natural system and processes that lead to release from the engineered system, migration through the geosphere, and eventual dose to humans in the biosphere, the effort is directed toward estimating appropriate bounds for factors that are important to performance.

1.6 REFERENCES

Geldon, A.L. 1993. *Preliminary Hydrogeologic Assessment of Boreholes UE-25c #1, UE-25c #2, and UE-25c #3, Yucca Mountain, Nye County, Nevada.* Denver, CO: U.S. Geological Survey.

Geldon, A.L. 1995. *Results and Interpretation of Preliminary Aquifer Tests in Boreholes UE-25c #1, UE-25c #2, and UE-25c #3, Yucca Mountain, Nevada.* United States Geological Survey Water-Resources Investigations Report 94-4177. Washington, DC: U.S. Geological Survey.

McConnell, K.I., M.E. Blackford, and A.K. Ibrahim. 1992. *Staff Technical Position on Investigations to Identify Fault Displacement Hazards and Seismic Hazards at a Geologic Repository.* NUREG-1451. Washington, DC: Nuclear Regulatory Commission.

TRW Environmental Safety Systems, Inc. 1995. *Total System Performance Assessment—1995: An Evaluation of the Potential Yucca Mountain Repository.* B00000000-01717-2200-00136. Las Vegas, NV: TRW Environmental Safety Systems, Inc.

U.S. Environmental Protection Agency. 1982. *Population Risks from Disposal of High-Level Radioactive Wastes in Geologic Repositories.* EPA 520/3-80-006. Washington, DC: U.S. Environmental Protection Agency.

U.S. Environmental Protection Agency. 1985. *High-Level and Transuranic Radioactive Wastes—Background Information Document for Final Rule.* EPA 520/1-85-023. Washington, DC: U.S. Environmental Protection Agency.

Table 1-1. Overview of the Nuclear Regulatory Commission program activities in FY96

<u>**Key Funded NRC Activities**</u>

— Work cooperatively with the EPA to develop a YM-specific HLW standard consistent with NAS recommendations. Perform independent analyses to evaluate the implementability of these standards.

— Review the DOE data related to KTIs and conduct modeling and sensitivity analyses to independently evaluate whether the issues pose a risk to repository licensing.

— Continue interactions with DOE and other parties through use of video conferencing and enhanced role of on-site representatives.

— Use TSPA to provide the framework for both verifying and resolving the NRC KTIs, and for evaluating the DOE WCIS.

— Develop acceptance criteria and review procedures necessary to evaluate KTI resolution.

— Conduct independent investigations for specific KTIs most significant to repository performance and having a high likelihood of success before licensing.

<u>**Reduced NRC Program Activities**</u>

— NRC quality assurance observation audits and in field verifications significantly reduced.

— Oversight of DOE field work reduced.

— Review of DOE study plans and test procedures for collection of data eliminated.

— Review of DOE Site Characterization Plan progress reports not planned.

— Reviews of DOE designs limited.

— Peer reviews of CNWRA work conducted through peer-review journal publications and limited review by external experts.

— Use of CNWRA consultants reduced.

— License Application Review Plan development deferred.

— Research efforts eliminated (including field investigations, laboratory testing, and model development for KTIs on igneous activity, unsaturated flow, container life, and radionuclide transport).

2 IGNEOUS ACTIVITY

Primary Authors: ***B.E. Hill, C.B. Connor, and J.S. Trapp***

Technical Contributors: ***C.B. Connor, F.M. Conway, D.A. Ferrill, S.L. Greenan, D.B. Henderson, B.E. Hill, M.S. Jarzemba, P.L. LaFemina, S.B. Magsino, R.H. Martin, J.A. Stamatakos, and J.S. Trapp***

Key Technical Issue Co-Leads: ***H.L. McKague (CNWRA) and J.S. Trapp (NRC)***

2.1 INTRODUCTION

The Igneous Activity (IA) Key Technical Issue (KTI) has been defined by the Nuclear Regulatory Commission (NRC) as "Predicting the probability and consequences of IA affecting the repository in relationship to the overall system performance standard." The hypothesis to be evaluated by the U.S. Department of Energy (DOE) Waste Containment and Isolation Strategy (WCIS) is "Volcanic events within the controlled area will be rare and the consequences of volcanism will be acceptable";[1] subsurface IA is not thought by the DOE to demonstrably affect repository performance (e.g., Wilson et al., 1994). In addition to directly releasing waste material into the accessible environment, IA could alter groundwater flow paths and initiate mechanical, chemical, and thermal effects that could cause degradation of the waste package and other engineered barriers. A concern with the DOE IA program and WCIS is that a reasonable range of probability and consequences of future IA have not been bounded by the DOE. Data and models developed by the NRC, the Center for Nuclear Waste Regulatory Analyses (CNWRA), and others provide an independent technical basis for defining the concern and data to support resolution of this issue.

IA has been factored by the NRC into three subissues that contain numerous technical foci. The first subissue, probability, focuses on definition of igneous events, determination of recurrence rates, and examination of geologic factors that control timing and location of IA. A recent expert elicitation by the DOE concluded "the aggregate expected annual frequency of intersection of the repository footprint by a volcanic event is 1.5×10^{-8}, with a 90 percent confidence interval of 5.4×10^{-10} to 4.9×10^{-8}." (U.S. Department of Energy, 1996a). Based on additional qualitative arguments, DOE[2] suggests the probability of volcanism could be even less than currently estimated. Technical investigations presented in Connor and Hill (1995) and in this chapter will show that the geologic evidence supports most annual probability estimates between 1×10^{-7} and 1×10^{-8} per yr. In addition, a new probability model incorporating structural control of volcanic events is presented.

The second subissue consists of the range of expected consequences for IA within the proposed repository setting. Primary focus areas are definition of the physical characteristics of igneous events, determination of the eruption characteristics for modern and ancient basaltic igneous features in undisturbed geologic settings, models of the effects of the disturbed geologic setting of the proposed repository on igneous processes, evaluation of waste and repository characteristics with regard to behavior during igneous events, and determination of geologic system characteristics. Historically, small-volume

---

[1]U.S. Department of Energy. 1996. *Highlights of the U.S. Department of Energy's Updated Waste Containment and Isolation Strategy for the Yucca Mountain Site.* DOE Concurrence Draft, July 1996.

[2]*Ibid.*

basaltic volcanism has not been studied in the same detail as large-volume volcanic systems, primarily because of a relatively low level of hazards and lack natural resources associated with cinder cone systems. Of primary importance in performance models is determining the ability of cinder cone eruptions to fragment and transport subsurface material. Detailed sensitivity analyses have been performed on a model routinely used to simulate ash transport in volcanic eruptions (Suzuki, 1983).[3] Results of these analyses are presented in this chapter. These analyses provide an alternative interpretation to a critical assumption in the DOE performance models regarding limited tephra dispersion (Link et al., 1982) which is a primary basis for the conclusion that "the consequences of volcanism will be acceptable."[4]

The third subissue is the viability of data sets used to make probability and consequence analyses. In essence, this subissue is designed to evaluate the precision and accuracy of data used in the characterization program and licensing process. At times, multiple sources provide contradictory data regarding age, location, and characteristics of the Yucca Mountain region (YMR) volcanoes. Recent CNWRA field technical investigations in the YMR will be presented in this report to document there is an insufficient technical basis to conclude the probability of future silicic eruptions in the YMR is negligible. Ground magnetics surveys (Connor et al., 1996)[5] and ongoing technical investigations show that buried igneous features continue to be discovered and characterized within 25 km of the proposed repository site. Analysis of the DOE characterization program consisted of two Appendix 7 meetings; one on geophysics in December 1995 to review and better understand the status of the DOE geophysics program, and one on tectonic models in May 1996 to evaluate various tectonic models and determine which models can still be considered viable. Results of these meetings are presented in the respective trip reports. In addition, staff observed the DOE Quality Assurance (QA) audit of the Los Alamos program on September 16–20, 1996. Further details on this audit can be found in the DOE audit report.

2.2 OBJECTIVES AND SCOPE OF WORK

The main objective of work within this KTI is to evaluate the significance of IA to repository performance by reviewing and independently confirming the data, and evaluating and developing alternative conceptual models for the probability and consequence of IA at YM. The scope of work includes review of various DOE documents as well as applicable documents in the open literature, participation in meetings with the DOE to discuss issues related to the KTI, observation of QA audits of the DOE, and independent technical investigations. This technical investigation is designed to address key licensing issues regarding IA in the YMR. Although none have been published to date, issue resolution reports are intended to be an important programmatic aspect starting in FY97.

CNWRA technical investigation is designed to provide an independent assessment of the probability and consequences of future IA in the YMR using physical data from YMR and analog

[3]Jarzemba, M.S. 1996. Stochastic radionuclide distributions after a basaltic eruption for performance assessments of Yucca Mountain. *Nuclear Technology*. In press.

[4]U.S. Department of Energy. 1996. *Highlights of the U.S. Department of Energy's Updated Waste Containment and Isolation Strategy for the Yucca Mountain Site*. DOE Concurrence Draft, July 1996.

[5]Stamatakos, J.A., C.B. Connor, and R.H. Martin. 1996. Quaternary basin evolution and basaltic volcanism of Crater Flat, Nevada, from detailed ground magnetic surveys of the Little Cones. *Journal of Geology*. In press.

volcanoes applied to empirical, deterministic, and probabilistic models that link directly into iterative performance assessment. For example, physical volcanological data and samples were collected during the 1995 eruption of Cerro Negro volcano in Nicaragua. These data and subsequent laboratory analyses are used in this report to test the accuracy of tephra dispersion models currently used in Performance Assessment (PA). Theoretical studies regarding the sensitivity of ground magnetic measurements to detect buried igneous features (Connor and Sanders, 1994) prompted field studies to better define known buried igneous features in the YMR (Connor et al., 1996) and to investigate igneous features that are present but uncharacterized by previous site characterization work.

Issue resolution regarding probability will be achieved by gaining agreement on reasonable mechanisms and realistic ranges of the critical parameters necessary to evaluate the likelihood and character of future IA at or near the proposed repository. This will require an evaluation of existing data and models from the DOE, CNWRA, and others to arrive at a reasonably conservative range for the probability of future IA at the proposed repository site. Probability models will need to reflect the resolution capabilities of YMR characterization activities along with the uncertainties associated with understanding igneous processes. In accordance with regulatory requirements, there must be reasonable assurance that values used do not underestimate possible effects of IA on the proposed repository site. The activities described in the following sections provides the basis for resolving this issue.

Issue resolution for the consequences of IA will be more difficult to achieve, as the direct and indirect effects of igneous intrusion through a waste repository have no known geological analog. In addition, the physical, chemical and thermal effects of magma on engineered systems are poorly understood and often are well beyond the design limits of these systems. Thus, expert opinions are likely to vary widely on how the proposed repository might be affected by future IA. Resolution of consequences will be achieved through comparison of results from independently derived data and models with those from the DOE program and through agreement on reasonable mechanisms and realistic ranges of parameters necessary to evaluate IA on repository total system performance. Critical to this resolution is the ability of performance models to reasonably reproduce igneous processes measured directly at active and historically active basaltic volcanoes.

IA KTI subissues on probability and consequences require that available data are correctly presented and used as part of the characterization and licensing process. Inherent in this use is an evaluation of the precision and accuracy of the data. At times, multiple sources provide contradictory data regarding age, location, and characteristics of YMR volcanoes. These contradictions must be evaluated and incorrect data removed from consideration to achieve issue resolution in this area.

2.3 SIGNIFICANT TECHNICAL ACCOMPLISHMENTS

2.3.1 Stabilize Database

Probability models are critically dependent on accurately determining age, location, and characteristics of igneous features. In order to achieve issue resolution on the probability of future IA in the YMR, this KTI evaluates several aspects of IA that are factors in assessing the probability of future volcanism in the YMR.

Age and location of basalts younger than about 12 Ma and currently thought by CNWRA staff to be part of the YMR magma system through time are shown in figure 2-1.[6] Recent work has shown that the YMR magma system may extend south and west into the Death Valley area (Yogodzinski and Smith, 1995; Hill and Connor, 1996). Mid-Pliocene basalts of the Funeral Formation in the Greenwater Range, California, rest unconformably on volcanic and volcaniclastic rocks of the Miocene Greenwater Formation (figure 2-1). The timing of volcanism of the Funeral Formation is poorly constrained by several K-Ar ages and is considered to have erupted between 4 and 4.8 Ma (e.g., Wright et al., 1991). Geochemical data from Yogodzinski and Smith (1995) and Hill and Connor (1996) show that Funeral Formation basalts have the same, relatively unique isotopic signature as YMR basalts. The Funeral Formation is, however, in a different structural setting than most YMR basalts and immediately follows a period of distributed silicic volcanism (e.g., Wright et al., 1991).

Few vent structures in the Funeral Formation in the Greenwater Range are identified on regional and local geologic maps (e.g., McAllister, 1970). Satellite imagery (multispectral Landsat Thematic Mapper (TM) images and high-resolution panchromatic images) and high-altitude, side-looking airborne radar indicate that more than 20 vents crop out within the Funeral Formation. Vents are predominantly cinder cones, but at least one shield volcano consisting of more than 20 cooling units is present in the northern part of the Greenwater Range. Additionally, well-log data from more than 150 wells drilled by U.S. Borax Corporation show a number of vents buried beneath late-stage lava flows. Well-log data indicate an average thickness of 130 m for basaltic lava flows and interbedded conglomerates. Preliminary calculations suggest a minimal volume of about 11 km^3 for Funeral Formation basalt.

The immediate significance of the Funeral Formation to proposed repository performance is that inclusion of these vents would increase Pliocene recurrence rates to about seven volcanoes per m.y. (v/m.y.), which is equal to Quaternary recurrence rates. Weibull-process probability models used by, for example, Ho (1991) are extremely sensitive to the timing of past volcanic events. Maintaining a relatively constant Plio-Quaternary recurrence rate of seven v/m.y. would lower most probability estimates from Weibull-process models that assume volcanic recurrence rates have increased in the Quaternary (e.g., Ho, 1991; U.S. Department of Energy, 1996a). In addition, inclusion of the Funeral Formation basalts into the YMR igneous system gives a more northerly trend to many of the statistically defined zones used in the probability models in U.S. Department of Energy (1996a). Funeral Formation vents are too old and too distant from the proposed repository site to significantly affect the results of nonhomogeneous Poisson spatio-temporal probability models (e.g., Connor and Hill, 1995) that will form the basis for issue resolution. Other classes of probability models, however, that place more reliance on volcano timing (e.g., Ho, 1991) or source-zone definition (e.g., U..S. Department of Energy, 1996a) can be affected to varying degrees by inclusion of Funeral Formation vents in the YMR system. Because of uncertainty about the relationship of Funeral Formation basalts to basalts closer to YM, including Funeral Formation basalts into recurrence calculations appears prudent.

Silicic volcanoes can erupt much more explosively than basaltic volcanoes. In addition, the geologic processes that produce basaltic magmatism are significantly different from those that produce silicic magmatism. DOE investigations indicate that there has been no silicic activity in the YMR since 7.5 Ma at the Stonewall Mountain caldera (more than 100 km northwest of Crater Flat) or 9 Ma at the Black Mountain caldera (60 km northwest of Crater Flat) (U.S. Department of Energy, 1993; Crowe et al.,

---

[6]Fleck, R.J., U.S. Geological Survey, Menlo Park. Unpublished K-Ar dates for basalt lava in MSH-C drill core and Dome Mountain. Personal communication to B. Hill, 1996.

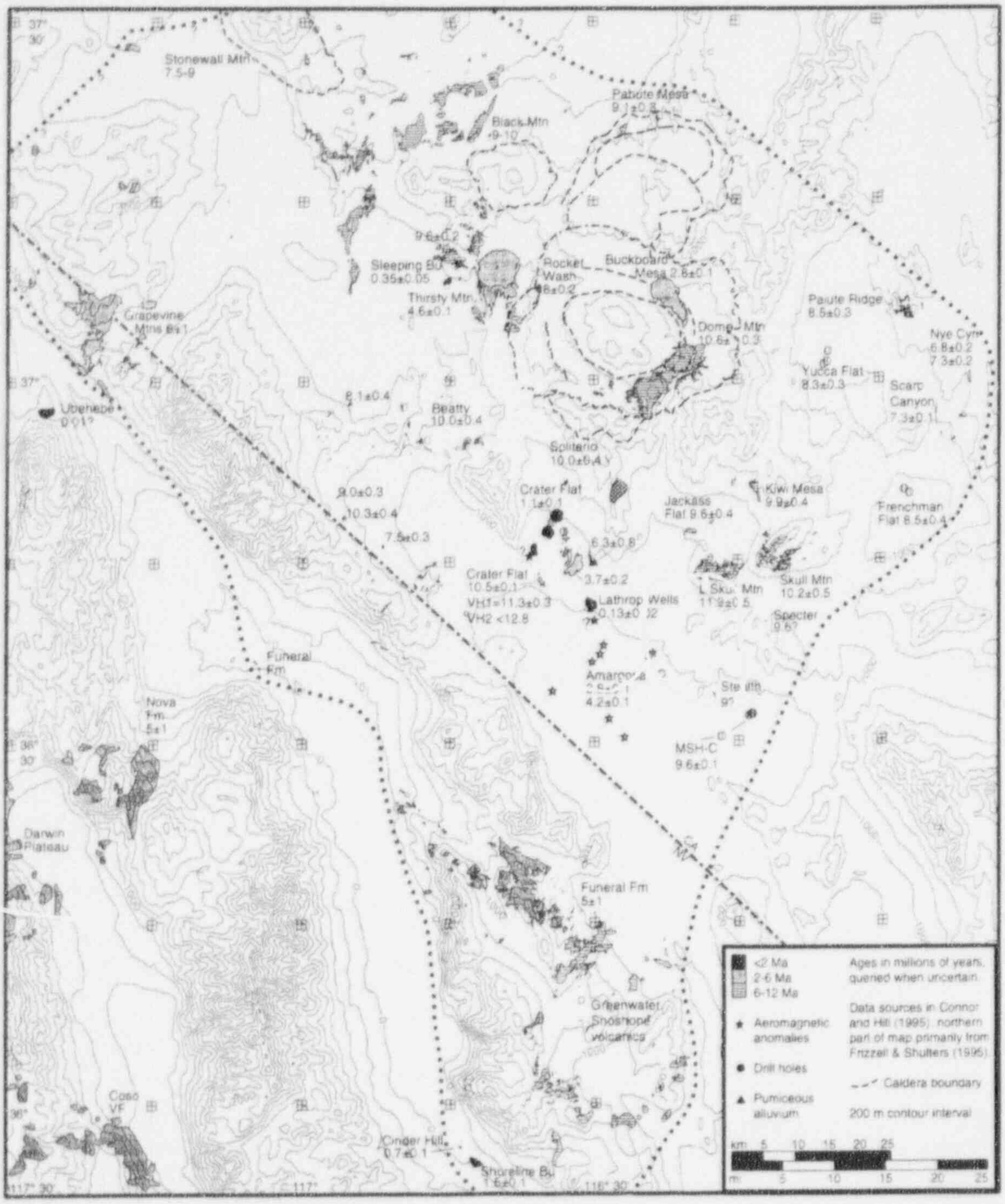

Figure 2-1. Distribution of post-12 Ma basalts of the YMR. Dotted line defines boundary of the YM-Death Valley isotopic province of Yogodzinski and Smith (1995) and Hill and Connor (1996). Unpublished dates for MSH-C and Dome Mountain from R. Fleck.[1] Other data sources in Connor and Hill (1995), Fleck et al. (1996), and this report.

1995; U.S. Department of Energy, 1996a,b). These analyses form the basis of the DOE conclusion that "the potential for future silicic volcanism . . . is considered to be negligible for the post-closure period of the repository." (U.S. Department of Energy, 1996b). The DOE investigations, however, have not considered all available data.

Carr (1982) described silicic pumice beneath the easternmost 3.7±0.2 Ma basalts of Crater Flat (figure 2-1). This pumice has a zircon fission-track date of 6.3±0.8 Ma and does not correlate petrographically or chronologically with known Miocene pyroclastic deposits in the Crater Flat area (Carr, 1982). Recent CNWRA work shows that the pumice is relatively pristine, subangular to subrounded lapilli ranging in size from 2-to-6 cm in diameter, with an average maximum diameter of 4.4 cm. The pumice is disseminated in massive, medium to coarse-grained sandy alluvium that is extensively bioturbated. Pumice abundances increase downwards from trace amounts at the basalt contact to roughly 30 percent at 2 m below the basalt. At least two 10–15 cm beds of generally matrix-free reworked pumice occur within 2 m of the base of the overlying 3.7±0.2 Ma basalt. The deposit is only weakly indurated and shows no evidence of thermal or chemical alteration that could reset a zircon fission-track date. The deposit most likely represents a pumice-fall tuff that has been locally reworked and buried by alluvium in Crater Flat. At present, silicic volcanism is not considered a concern at YM, based on a lack of nearby Pliocene or younger eruptions. The CNWRA will, however, continue to perform some confirmatory investigations of the uncertainties represented by this post-caldera silicic deposit. These investigations will examine the age and petrogenesis of the Crater Flat pumice deposit and should lead to either resolution of the issue or definition of a potential concern.

2.3.2 Probability Estimates of Volcanic Disruption

In an area of active volcanism such as the YMR, a probabilistic hazard analysis starts with the null hypothesis that the site will be affected by volcanic activity during the expected performance period and an alternate hypothesis that the site will not be affected by volcanic activity. The primary goal of the probabilistic hazard analysis is to estimate the confidence with which the null hypothesis can be accepted or rejected. The sensitivity of probability estimates to uncertainty about volcanological and volcano-tectonic processes, such as structural control on dike propagation and the distribution of volcanic events, must therefore be assessed as part of a probabilistic hazard assessment (e.g., Smith et al., 1990; Sheridan, 1992; Crowe et al., 1995). The following analyses explore the bounds of probability estimates of volcanic disruption using models based on spatial patterns of basaltic volcanism, regional recurrence rates of volcanic activity, and structural control on volcanism in the YMR.

In areas where magma is available, the crust is being extended and dike injection can accommodate crustal strain. In this sense, dikes and faults play the same role in responding to extension (Parsons and Thompson, 1991). Faults with a high dilation-tendency in the current stress state of the crust can act as conduits for magma transport through the crust. The abundance of these faults may indicate areas that, because they are extending, are likely areas of dike injection, given a magma supply. Thus, the frequency of faults may be an indicator of future volcanism. In this sense basin bounding faults such as the Bare Mountain fault (BMF) may provide low energy pathways for magma ascent to the surface (McDuffie et al., 1994). A comparison of the distribution of Miocene and younger basalts and faults in the YMR supports this hypothesis. For example, one way to view basaltic volcanism in Crater Flat is that this volcanism is localized in the hangingwall of the BMF. Other basalts in the YMR are associated with major mapped faults with significant vertical displacements: the Miocene Beatty basalts along the Fluorspar Canyon fault and the Little Skull Mountain and Kiwi Mesa basalts along the Rock Valley and Wahmonic faults (figure 2-2).

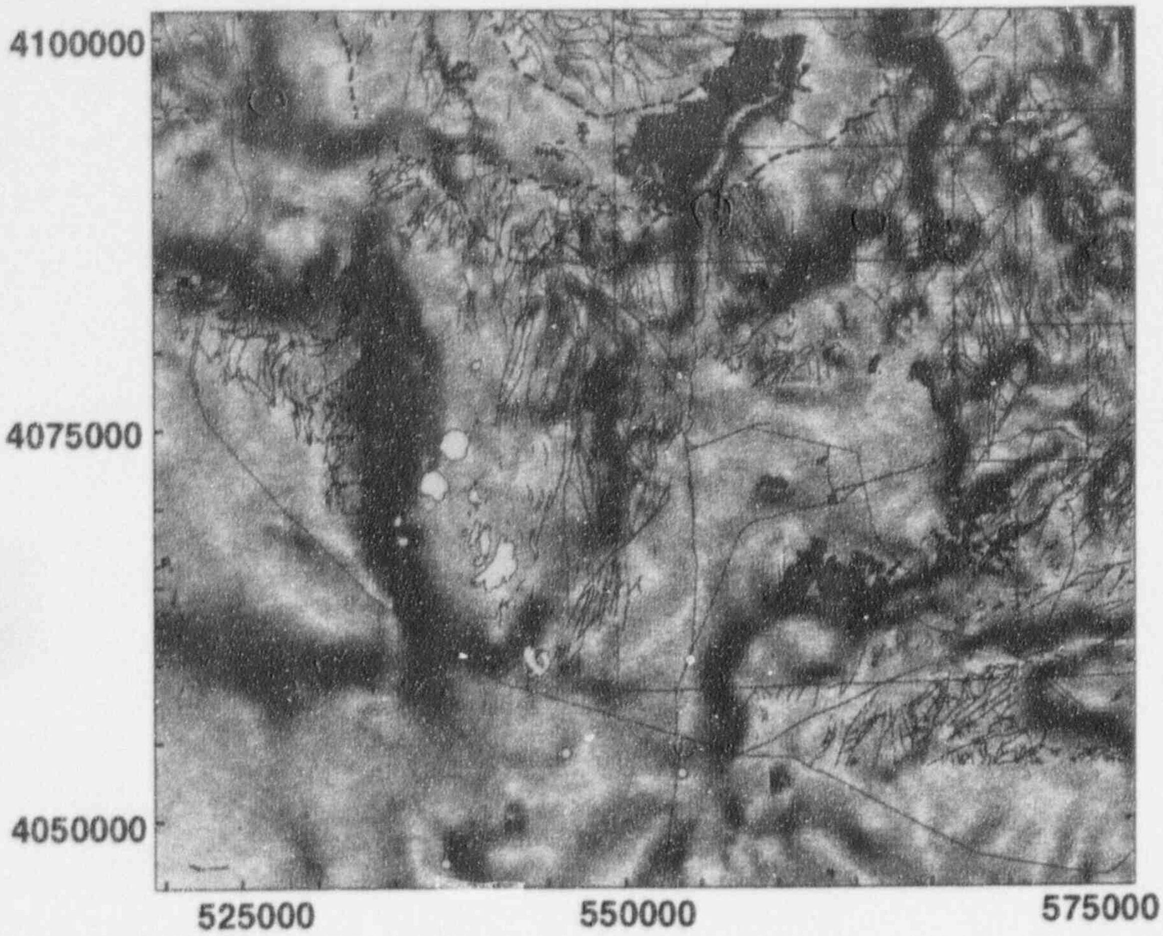

Figure 2-2. Map of horizontal gravity-gradient, faults, and volcanoes near the proposed repository site. Plio-Quaternary basalt in yellow, Miocene basalt in cyan, and mapped caldera boundaries outlined by dashed lines. Areas of high-amplitude horizontal gravity-gradient are shown in dark shading; low gradient is indicated by light shading. Faults from Frizzell and Shulters (1990) gravity data are summarized in Oliver et al. (1995).

This relationship between structure and volcanism has been used to suggest both higher and lower probabilities of volcanic disruption of the proposed repository than are predicted using spatio-temporal patterns alone. A wide variation in probability estimates is a direct result of the varying ways in which these source zones have been drawn. Smith et al. (1990) suggested that a narrow NE-trending structurally controlled zone of potential volcanism extends through Lathrop Wells and the proposed repository site, resulting in probabilities much greater than indicated by spatio-temporal patterns (e.g., Connor and Hill, 1995). Sheridan (1992) also incorporated NE-trending dikes into a probabilistic model but did not restrict these dikes to a narrow zone. Alternatively, some structure models exclude the repository from zones of potential volcanism. For example, Crowe and Perry (1989) proposed the Crater Flat Volcanic Zone (CFVZ), a NNW-trending zone through the Crater Flat and Sleeping Butte volcanoes with the eastern boundary located west of the proposed repository site. Similar source-zone models that exclude the proposed repository site have been used elsewhere (Crowe et al., 1995; U.S. Department of Energy, 1996a). Because these models exclude the repository from the potential source-zone of volcanism,

their application results in low estimates for the probability of volcanic disruption of the proposed repository compared with spatio-temporal models.

Analyses presented here avoid the source-zone concept altogether by casting structural information as a discretized density distribution, readily comparable to spatial and spatio-temporal probability distributions. Two data sets are used in this analysis: (i) gravity data, which reveal large-scale variations in crustal density and hence basin development and extension and (ii) distribution of high dilation-tendency faults, which indicates areas of past extension and areas where crustal strain may be accommodated by dike injection.

2.3.2.1 Gravity Data

Yucca Mountain and Crater Flat are part of a structural half-graben, bounded on the west by the BMF, an eastwardly dipping master fault, and on the east by a diffuse set of westward dipping normal faults. Variations in the intensity of the earth's gravitational field, reflecting major changes in the density of subsurface rocks, can be used to define the structural boundaries of the Crater Flat basin. A large volume of gravity data have been collected in the YMR during the last 40 yr. This data set, summarized in Oliver et al. (1995), consists of approximately 16,000 gravity stations. A subset of these complete Bouguer gravity data, consisting of approximately 8,000 gravity stations, was obtained from the Lawrence Berkeley Laboratory where these data are archived.

Langenheim and Ponce (1995) interpreted the depth to pre-Cenozoic basement in the YMR from gravity data by iterative calculation of expected gravity using density-depth estimates. Their preliminary results suggest that the depth to pre-Cenozoic basement in southern Crater Flat is approximately 2.5 km. The gravity data suggest that anomalously deep pre-Cenozoic basement (greater than 0.5 km) extends south into the Amargosa Desert from Crater Flat. The amplitude of the horizontal gravity-gradient indicates the position of the boundaries of this basement low (figure 2-2). For example, the BMF produces a steep gravity-gradient on the western edge of Crater Flat. The amplitude of the horizontal gravity-gradient increases and the width of the anomaly decreases from north to south along the BMF. This is consistent with an increasing dip of the BMF from north to south, a geometry supported by additional modeling of gravity data (e.g., Oliver et al., 1995) and structural models of the evolution of the Bare Mountain block (Ferrill et al., 1996). The eastern boundary of Crater Flat basin is less distinct, but it is clear from the gravity-gradient map (figure 2-2) that the steepest gravity-gradients lie east of the topographic edge of the basin beneath YM and the proposed repository site. The southern topographic margin of Crater Flat basin also correlates with a rapid change in depth to basement. Comparatively steep gravity-gradients, however, also continue south of Crater Flat along the projection of the BMF into Amargosa Desert. Steep N-trending gradients are found on the eastern margin of Amargosa Desert that likely indicate a major N-trending fault in the northern part of Amargosa Desert (Healey and Miller, 1971; Oliver et al., 1995).

These observations are important to volcanic hazard assessment because many of the known Plio-Quaternary volcanoes in the YMR lie within or at the margins of this basement low. Plio-Quaternary volcanoes in Crater Flat all lie within or near high gravity-gradient areas associated with the Crater Flat basin. Two episodes of volcanism, the eruption of the Little Cones[7] and the eruption of Miocene basalt

---

[7]Stamatakos, J.A., C.B. Connor, and R.H. Martin. 1996. Quaternary basin evolution and basaltic volcanism of Crater Flat, Nevada, from detailed ground magnetic surveys of the Little Cones. *Journal of Geology*. In press.

south of the Little Cones (figure 2-2), and a possible third episode suggested by the presence of a shallowly buried body of highly magnetized rock in southern Crater Flat, all occur very close to the steepest gravity-gradient in the region. The repetition of volcanic activity in this small area of the basin suggests that the BMF may provide a pathway for ascending magmas. Topographically, Lathrop Wells cinder cone lies outside Crater Flat but, based on the gravity data, is within the larger N-trending basin and at the margin of the prominent basement low in southernmost Crater Flat. Aeromagnetic anomalies A-E (Langenheim et al., 1993) in the Amargosa Desert also lie within or at the margins of the southern extension of this basin. The largest of these anomalies, (B), is the easternmost Plio-Quaternary volcano in the Crater Flat area and lies close to N-trending gravity anomaly demarcating the eastern edge of Amargosa Desert. Thus, the horizontal gravity-gradient appears to adequately represent crustal structures that have controlled past volcanism, especially the Plio-Pleistocene. It has been used here as a discrete density function to add structural data to the overall probability estimates.

2.3.2.2 Fault Dilation-Tendency

The ability of any fault or fracture to dilate is directly related to the normal stress acting across the fault or fracture surface. The relative tendency for a fault of a given orientation to dilate in a given stress state can be expressed by comparing the normal stress acting across the fault with the differential stress. Dilation tendency of the fault can be expressed as (Morris et al., 1996)

$$T_d = \frac{(\sigma_1 - \sigma_n)}{(\sigma_1 - \sigma_3)} \qquad (2\text{-}1)$$

where σ_1 and σ_3 are the maximum and minimum compressional stresses and σ_n is the normal stress acting across the fault or fracture surface. In the YMR, σ_1 is vertical, σ_2 is horizontal and oriented 28°, and σ_3 is horizontal and oriented 300°. The relative magnitudes of $\sigma_1 : \sigma_2 : \sigma_3$ are 10:9:1.8 (Stock et al., 1985; Morris et al., 1996). As a result of this stress pattern, NE-trending vertical or steeply dipping faults have a greater tendency to dilate than faults of other orientations and there is a good correlation between the density of high dilation-tendency faults and extended terrains. Areas with higher concentrations of high dilation-tendency faults also may be more likely sites for future volcanic activity. Thus, in addition to the gravity data, the effect of structure on potential volcanic hazards can be further assessed by casting the distribution of high dilation-tendency faults as a density distribution and comparing this distribution to patterns of past volcanic activity.

2.3.2.3 Method of Using Structural Data in the Hazard Analysis

Incorporation of structural data into the probability estimate proceeds in several steps. First, an estimate of the spatial recurrence rate is made based on distribution and timing of past volcanic events. Connor and Hill (1995) reviewed patterns in volcanic activity in basaltic volcanic fields and found that nonhomogeneous methods provide estimated spatial and spatio-temporal recurrence rates that capture the clustered nature of volcanism and shifts in the location of volcanism through time within these volcanic fields.

The following equation shows an $m = 8$ near-neighbor spatio-temporal estimate of recurrence rate

$$\lambda_n(x,y) = \frac{m}{\sum_{i=1}^{n} u_i t_i} \tag{2-2}$$

where t_i is the time elapsed since formation of volcano i, m the number of near-neighbor volcanoes, and u_i the area of a circle having a radius equal to the distance between the point x,y and the i^{th} volcano. The resulting map of recurrence rate is normalized using a constant, k_1, so that

$$\int_X \int_Y \frac{1}{k_1} \lambda_n(x,y) dy dx = 1 \tag{2-3}$$

where the limits X and Y correspond to the geographic extent of the map, well beyond the boundaries of the volcanic field and the area of the probability assessment. The resulting map of $\lambda_n(x,y)$ shows expected volcanic events/km^2 based on distribution and timing of past volcanic events.

Other methods of estimating $\lambda_n(x,y)$ are discussed in Connor and Hill (1995) and U.S. Department of Energy (1996a). These include use of the Epanechnikov kernel estimate of the density distribution (Connor and Hill, 1995). The near-neighbor and Epanechnikov kernel models produce a range of probability estimates and both approaches are used in the following bounding analysis.

In the second step, this map of $\lambda_n(x,y)$ based on either the near-neighbor or Epanechnikov kernel methods is multiplied with a map having the distribution of structural features represented by a surface, $s(x,y)$, calculated over the same geographic area, X,Y, and at the same grid spacing as the recurrence rate map. In the case of gravity data, a grid of complete Bouguer corrected gravity values was first constructed by minimum-tension bicubic spline interpolation. The amplitude of the horizontal gravity-gradient is then given by

$$s(x,y) = \sqrt{\left[\frac{\partial g}{\partial x}\right]^2 + \left[\frac{\partial g}{\partial y}\right]^2} \tag{2-4}$$

where g is the complete Bouguer gravity anomaly interpolated at location x,y.

Alternatively, $s(x,y)$ can be calculated based on distribution of faults with high dilation-tendency. To accomplish this, mapped faults in the YMR (Frizzell and Shulters, 1990) were discretized at 50 m intervals along their lengths. The number of fault segments within a circle of radius r about a grid node at point x,y is $n_f(x,y)$; the number of high dilation-tendency fault segments within the same area is $n_t(x,y)$. Here, r is chosen to be 4,850 m and the threshold for high dilation-tendency faults is chosen to be $T_d > 0.8$. Then

$$t(x,y) = \frac{n_t(x,y)}{\sum\limits_X \sum\limits_Y n_t} - \frac{n_f(x,y)}{\sum\limits_X \sum\limits_Y n_f} \tag{2-5}$$

Map areas where $t(x,y) < 0$ correspond to uplifted Paleozoic basement, resurgent areas within Timber Mountain caldera, and similar zones where bedrock that was not faulted predominantly in the current crustal stress-state is exposed. In contrast, terrains extended in the Neogene and Quaternary have predominantly high dilation-tendency faults and $t(x,y) > 0$. One of the central difficulties in using mapped fault distribution in hazard analysis is that in areas covered by Quaternary alluvium, both $n_f(x,y)$ and $n_t(x,y) = 0$. High dilation-tendency fault density is likely to be high, and is possibly greatest, in alluvial basins because these regions have experienced extension in the Neogene and Quaternary. Mapped fault density, however, is very low in these areas because of alluvial cover, resulting in low values of $t(x,y)$ that do not reflect true crustal-scale structure. For example, a detailed ground magnetic survey of Northern Cone[8] reveals a large number of high dilation-tendency faults associated with the cone, although mapped fault density in the alluvium is low. Unfortunately, such detailed geophysical data are not available for much of Crater Flat or for other alluvial basins in the region. One means of addressing a lack of understanding of the fault density in alluvial basins is to assign a minimum value of $t(x,y)$ to areas of alluvial cover. This minimum value, n_k, was chosen so that $0 \le n_k < \max[t(x,y)]$. Then

$$s(x,y) = \begin{cases} t(x,y), & t(x,y) > n_k \\ n_k, & 0 < t(x,y) < n_k \\ 0, & t(x,y) < 0 \end{cases} \tag{2-6}$$

Choosing a large value for n_k assumes that fault density is high in alluvial areas and heavily weights these areas in the probability analysis. Choosing a small value of n_k assumes that fault density is low in alluvial basins and letting $n_k \to 0$ results in $s(x,y)$ depending solely on mapped fault distribution.

To cast $s(x,y)$, calculated from either the horizontal gravity-gradient or the relative distribution of high dilation-tendency faults, as a probability density distribution, a constant, k_2, is determined so that

$$\int_X \int_Y \frac{1}{k_2} s(x,y)\,dy\,dx = 1 \tag{2-7}$$

The resulting probability density distribution is multiplied by the near-neighbor model or any other probability density distribution based on location and timing of past volcanic events. The resulting map can be renormalized so that probability of volcanism across the region is unity. The resulting

[8]Connor, C.B., LaFemina, P.L., Magsino, S.B., Hill, B.E. Unpublished ground magnetic survey on Northern Cone, August 1996.

expected recurrence rate of volcanism in a particular small area, $\Delta x \cdot \Delta y$, is $\lambda_s(x,y)$ given that volcanism will recur in the region X, Y.

It is important to note that s may be weighted in a variety of ways. For example, assigning a low weight to s by attenuating this matrix yields a solution that approaches the results of the near-neighbor analysis alone (i.e., λ_n). Conversely, assigning a large weight to s diminishes the role of the near-neighbor analysis, essentially suggesting that spatial distribution of volcanic events is well-represented and predicted by the distribution of crustal structure. Thus, both geologic interpretation and uncertainty are reflected in the relative weighing of λ_n and s in the calculation of λ_s. A simple weighing scheme commonly used in risk analysis (e.g., Griesmeyer and Okrent, 1981) is

$$\lambda_s(x,y) = \frac{1}{k_3}\left(\lambda_n(x,y) \cdot s(x,y)^w\right),\ 0 < w \tag{2-8}$$

where w is the weight assigned to $s(x,y)$ and k_3 is a proportionality constant so that the integral of $\lambda_s(x,y)$ across the region is unity.

In the fourth step of the spatial analysis, the likelihood that a volcanic event at a given location will result in disruption of the proposed repository is assessed. One way to do this is to use an effective repository area, such as the actual area of the proposed repository, currently estimated to be approximately 5.6 km^2, plus some buffer area (e.g., Connor and Hill, 1995). A second approach, adopted here, is to estimate the probability that an event at a given location will produce a dike that will intersect the repository (e.g., Sheridan, 1992; U.S. Department of Energy, 1996a). In this analysis it is assumed that dike length has a uniform random probability distribution $U[d_1, d_2]$, d_1 = 1,000 m and d_2 = 5,000 m, and that dikes will be oriented at an azimuth of 28°, perpendicular to the regional minimum horizontal compressional stress. Other distributions for dike length and dike orientation can be used (U.S. Department of Energy, 1996a) and yield similar probability distributions. The volcanic event is assumed to centered on the dike, thus

$$\begin{aligned} h_1 &= \frac{\min\{U[d_1,d_2]\}}{2} \\ h_2 &= \frac{\max\{U[d_1,d_2]\}}{2} \end{aligned} \tag{2-9}$$

then

$$d_L(x,y) = \frac{(h_2 - d(x,y))}{(h_2 - h_1)} \tag{2-10}$$

where $d(x,y)$ is the distance from a grid point at location x,y to the proposed repository boundary along a 28° azimuth. The frequency of dike intersection becomes

$$\lambda_d(x,y) = \begin{cases} 1, d(x,y) \le h_1 \\ d_L, h_1 < d(x,y) < h_2 \\ 0, h_2 \le d(x,y) \text{ } or \text{ } d(x,y) \text{ is undefined} \end{cases} \tag{2-11}$$

The probability of one or more volcanic events disrupting the repository is given by

$$P[N \ge 1] = 1 - \exp\left[-t\lambda_t \int_X \int_Y \lambda_s(x,y) \cdot \lambda_d(x,y) dy dx\right] \tag{2-12}$$

where X and Y are the limits of integration across the region of interest, λ_t is the regional recurrence rate of volcanic events, and t is the time interval of interest (e.g., 10,000 yr). The regional recurrence rate of volcanism is taken to be a constant in this analysis. U.S. Department of Energy (1996a) and Ho (1991) have explored the possibility of time-dependence of λ_t in detail.

2.3.2.4 Results

Two examples of spatial analysis and the resulting distribution of λ_s are shown in figures 2-3a–e. The calculation of λ_n using $m = 8$ near-neighbor volcanoes results in a high probability of volcanism in southern Crater Flat and a zone of lower probability that extends along a NNW-trend. Connor and Hill (1995) present a full range of probability estimates based on different nonparametric estimates of λ_n. Application of the Epanechnikov kernel method results is a similar overall map pattern, but probability is more uniform in high probability areas, where distances to nearby volcanoes are less than h and uniformly low outside these zones (Connor and Hill, 1995).

The gravity-gradient map is normalized so that the sum of $s(x,y)$ across the map is unity (figure 2-3). Multiplying the two maps (figures 2-3a,b) with $w = 1$ [Eq. (2-8)] produces a map of λ_s (figure 2-3c) that is considerably different from probability maps based on the near-neighbor model alone (e.g., figure 2-3a). High gravity-gradients along the BMF elongate and narrow the probability distribution in Crater Flat. The highest probabilities are located within 5 km of the surface expression of the BMF and are limited to the BMF hangingwall in Crater Flat. Conversely, probabilities based on λ_s are less than those based on λ_n across most of Bare Mountain because of the low gravity-gradients within this block. The pattern is slightly more complicated on the eastern margin of Crater Flat at YM. Gravity-gradients are relatively high at YM and south of YM along the Stagecoach fault delimiting the eastern boundary of the structural basin. This structure increases the probability of volcanism at YM. The calculated probability is, however, also more variable in this area than elsewhere in the basin.

An example of s calculated using high dilation-tendency fault density [Eq. (2-6)] is given in figure 2-3d with n_k equal to the average $t(x,y)$ across YM and $w = 1$ [Eq. (2-8)]. An important feature of this map is that $s(x,y)$ is zero where Paleozoic rocks crop out and in the Timber Mountain caldera

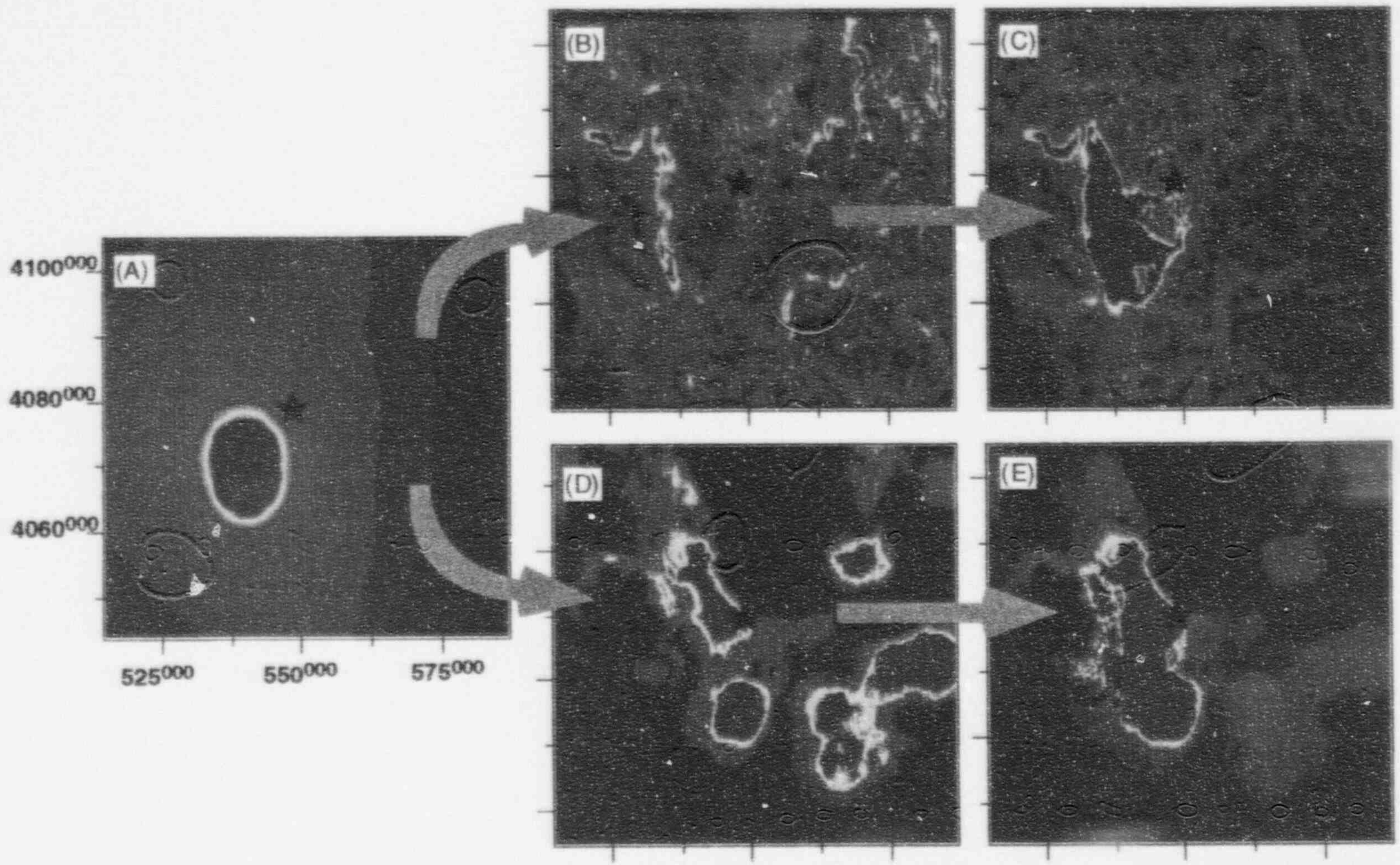

Figure 2-3. Maps illustrating the steps in calculation of the probability estimate. (a) Spatio-temporal model based on a near-neighbor model [Eq. (2-2)]; (b) Normalized horizontal gravity-gradient and (c) Resulting map with w = 1; (d) Normalized density of high dilation-tendency faults with n_k equal to the average of $t(x,y)$ across YM, and (e) Resulting probability map with w=1. Proposed repository location indicated by star (exact boundary used in analysis shown in figure 2-2).

complex—areas that have not extended significantly in the Quaternary. Multiplying the high dilation-tendency fault density map with λ_n results in an estimate of λ_s which is quite similar to that obtained from the horizontal gravity-gradient. Probabilities are highest in Crater Flat and this high probability zone extends in a NNW direction. The proposed repository site is located at the eastern edge of this relatively high probability zone.

Results of the spatial probability analysis depend on assumptions made about the relative weight given to s and λ_n and the type of spatio-temporal model used to estimate λ_n. Sensitivity of the probability estimates to these assumptions was explored using various weights, w, in Eq. (2-8) for both the near-neighbor and Epanechnikov models. Eight near-neighbor volcanoes were chosen for the near-neighbor model and a smoothing parameter of $h = 20$ was selected for the Epanechnikov model because the resulting maps provide lower and upper bounds on spatio-temporal recurrence rate in the site vicinity. With $w = 0$, the probability of dike intersection with the proposed repository is that obtained from the spatio-temporal recurrence rate model alone, and ranges from approximately $P[N \geq 1] = 0.005$ to 0.0075 with $\lambda_t = 1$. Letting w vary from 0 to 4.5 increases the probability of dike intersection with maximum probabilities between $w = 2$ and 2.5. Varying λ_t between 2 and 10 v/m.y. gives a probability of volcanic disruption between 1×10^{-8}/yr and 1.4×10^{-7}/yr (figure 2-4).

The effect of n_k and w on the probability calculated using the high dilation-tendency fault model is shown in figure 2-5. If the distribution of faults in alluvium is estimated to be the same as the average fault density at YM, the effect on probability is minimal. Although the probability of volcanism decreases in areas like Bare Mountain, probability is not significantly redistributed over large regions of the map. Probabilities are greatest for $n_k = 0$ when analysis is restricted to mapped faults. In this case, probability values are higher at YM because of the high density of high dilation-tendency faults mapped on and around YM. Assigning $w = 1 - 1.5$ gives the highest probability of dike intersection of the proposed repository, with probabilities ranging from 0.014 for the $m = 8$ near-neighbor model to 0.019 for the $h = 20$ km Epanechnikov kernel model, given that a volcanic event will occur in the area $(\lambda_t = 1)$. Using $\lambda_t = 2 - 10$ v/m.y., probability estimates of volcanic disruption of the proposed repository that incorporate fault dilation-tendency vary between 1×10^{-8}/yr and 1.9×10^{-7}/yr (figure 2-5), essentially the same range estimated from the horizontal gravity-gradient.

2.3.2.5 Discussion

Results of this analysis indicate that structural models increase probability of volcanic disruption of the proposed repository site compared to models that do not incorporate structure explicitly. This result primarily reflects that fact that YM is structurally part of the Crater Flat basin (Ferrill et al., 1996) with geophysical data suggesting a rapid change in the depth to Paleozoic basement beneath the eastern edge of YM and high dilation-tendency faults bounding and penetrating YM itself. Because of the presence of these structures, a lower limit on probability estimates is represented by the spatio-temporal recurrence rate models that do not incorporate structure (e.g., Connor and Hill, 1995). This result is contrary to numerous source-zone models that suggest the presence of structure decreases the probability of volcanism at YM (Crowe et al., 1995; U.S. Department of Energy, 1996a). For example, the CFVZ as proposed by Crowe and Perry (1989), is a distinctive feature on the maps of λ_s calculated using both gravity and fault dilation-tendency models. However, the same structural features that tend to enhance the probability of volcanism within this zone occur at YM, albeit possibly to a lesser degree.

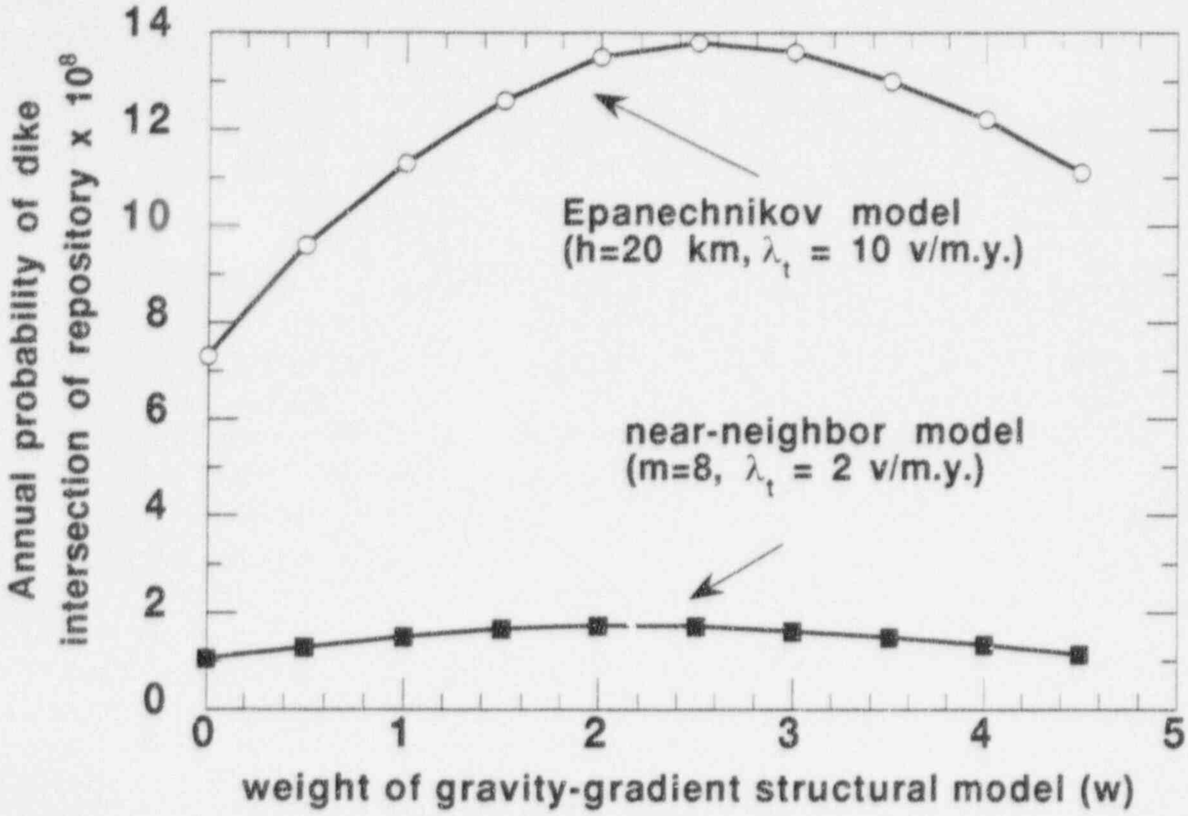

Figure 2-4. Range of probability estimates of dike intersection of the proposed repository, based on Epanechnikov and near-neighbor estimates, and amplitude of the horizontal gravity-gradient weighted by w (Eq. 2-8) for λ_t = 2 to 10 v/m.y.

Data sets other than the horizontal gravity-gradient and distribution of high dilation-tendency faults can be used to calculate s and λ_s. Estimators of s might include depth to Paleozoic basement based on integrated geological and geophysical models, improved models of fault distribution, or stress maps based on *in situ* stress measurements or microseismicity. Such estimates of s may provide further insight into the sensitivity of probability estimates to alternative conceptual models of the relationship between volcanism and structure. It is anticipated, however, that the range of probability estimates identified here (i.e., 1×10^{-8} – 2×10^{-7}) will not change substantially given uncertainties associated with the regional recurrence rate of volcanism, λ_t, and the area affected by dike injection represented by λ_d.

2.3.3 Dispersion of Tephra from Basaltic Eruptions

2.3.3.1 Introduction

One of the key parameters in calculating risks associated with basaltic volcanic activity is accurately modeling how far erupted material can be transported from the vent into the accessible environment. For basaltic volcanic eruptions, the primary mode of dispersal is through aerial transport commonly extending tens of kilometers from the vent. Additional material accumulates at the vent through ballistic transport with lava flows commonly extending for several kilometers from the source. This section

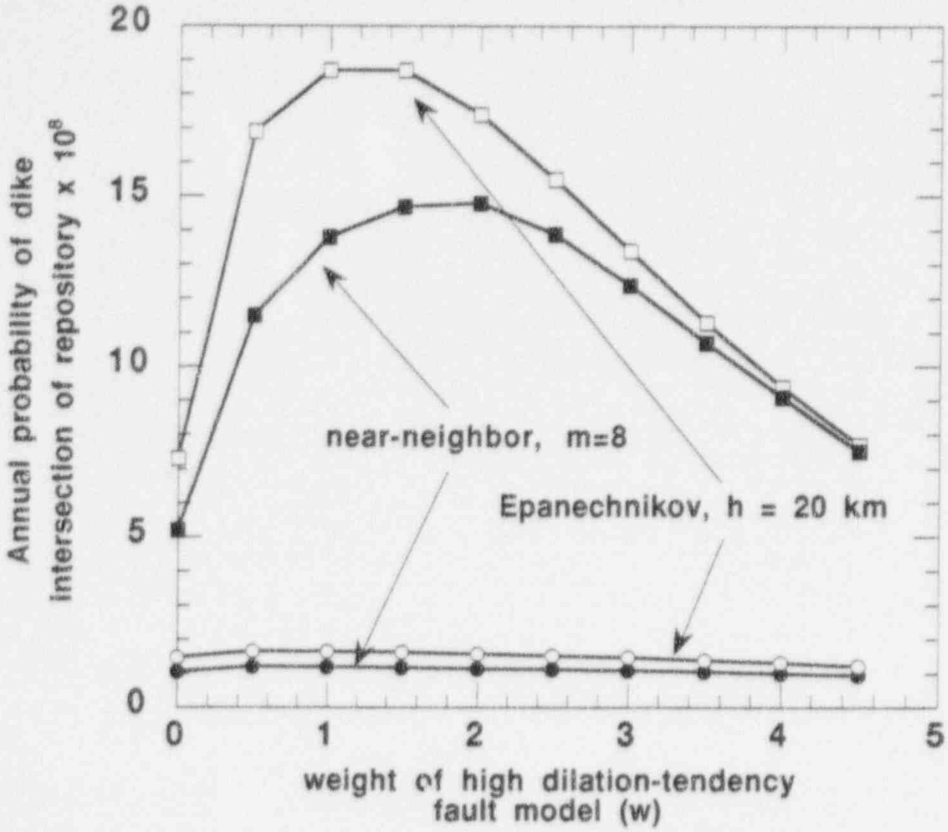

Figure 2-5. Range of probability estimates of dike intersection of the proposed repository based on Epanechnikov and near-neighbor estimates and density of high dilation-tendency faults weighted $0<w<4.5$ (Eq. 2-8) for $\lambda_t = 2$ (circles) to 10 v/m.y. (squares)

examines recent work on modeling the dispersion of basaltic tephra using the model of Suzuki (1983) as implemented in Jarzemba.[9] The primary emphasis of this section is to determine Suzuki (1983) model sensitivities to a range of input parameters that are derived from the literature and recent CNWRA field studies at active analog volcanoes. The results of the Suzuki (1983) model are then compared to tephra distribution patterns for the 1995 Cerro Negro eruption in Nicaragua, which has the detailed volcanological and granulometric data necessary for model evaluation.

The DOE efforts at modeling tephra distribution are described in Link et al. (1982). In summary, tephra with diameters greater than 0.06 mm are assumed to remain within 8 km of the vent with deposit thicknesses less than 1 cm beyond 8 km (Link et al., 1982). Work presented in this section will show that basaltic eruptions comparable or smaller in volume to Quaternary events in the YMR are capable of transporting tephra greater than 0.1 mm in diameter tens of kilometers from the vent and producing deposits centimeters thick. Link et al. (1982) modeled tephra with diameters less than 0.06 mm using a

[9] Jarzemba, M.S. 1996. Stochastic radionuclide distributions after a basaltic eruption for performance assessments of Yucca Mountain. *Nuclear Technology*. In press.

modified Gaussian plume equation. Jarzemba[10] notes that a Gaussian plume model may not be appropriate for volcanic eruptions because the eruption column is a distributed source rather than a point source of particulates release. This may overestimate the dispersal capability of a basaltic eruption and thus underestimate radiation exposure to persons in a critical group.[11]

2.3.3.2 Model Parameters

The Suzuki (1983) dispersal model is described in detail in Jarzemba.[12] In summary, Suzuki (1983) simulates the dispersal of tephra using a two-dimensional diffusion model in the atmosphere and relates the accumulation of tephra on the ground to the total mass of the tephra, grain size and density characteristics, height of the eruption column, and eruption and wind velocity. The Suzuki (1983) model successfully reproduced distribution patterns of tephra from the 1977 eruption of Usu volcano in Japan (Suzuki, 1985) and the 1986 eruption of Lascar volcano in Chile (Glaze and Self, 1991), both of which are short-duration plinian style eruptions from composite volcanoes.

Many of the input parameters for the Suzuki (1983) model can be sampled stochastically using a range of values for basaltic volcanic eruptions[13] or entered directly for eruptions with detailed data. Critical parameters are (i) height of the eruption column, (ii) eruption duration, (iii) total tephra mass, (iv) mean particle diameter for the entire deposit, (v) standard deviation of particle diameter, (vi) average particle density, (vii) particle shape, and (viii) wind velocity. In addition, Suzuki (1983) uses constants for eddy diffusivity (C) and diffusion within the eruption column (β). Sensitivity of the Suzuki (1983) model to each of these input parameters is discussed in section 2.3.4.4.

2.3.3.3 Analog Volcano Data

The tephra deposits from YMR volcanoes have been removed by erosion and thus their dispersal characteristics must be inferred. Comparison with historically active basaltic volcanoes of similar size and eruption style provides a means to evaluate the tephra dispersal characteristics of ancient YMR volcanoes and to construct accurate models for use in PA. Using computer-assisted cartography, Quaternary volcanoes of the YMR have density-corrected volumes of roughly 0.002 km^3 for Northern Cone and NE Little Cone, 0.02 km^2 for Hidden Cone, Little Black Peak and SW Little Cone,[14] and 0.08 km^3 for Lathrop Wells, Red and Black Cones. Historically active analog volcanoes (Connor, 1993; Hill, 1995) have density corrected volumes of 0.52 km^3 for 1975 Tolbachik (Budinkov et al., 1983), 0.92 km^3 for

---

[10]Jarzemba, M.S. 1996. Stochastic radionuclide distributions after a basaltic eruption for performance assessments of Yucca Mountain. *Nuclear Technology*. In press.

[11]*Ibid.*

[12]*Ibid.*

[13]*Ibid.*

[14]Stamatakos, J.A., C.B. Connor, and R.H. Martin. 1996. Quaternary basin evolution and basaltic volcanism of Crater Flat, Nevada, from detailed ground magnetic surveys of the Little Cones. *Journal of Geology*. In press.

1943 Parícutin (Luhr and Simkin, 1993), 0.18 km^3 for 1973 Heimaey (Self et al., 1974), 0.015 km^3 for 1968 Cerro Negro (Taylor and Stoiber, 1973), 0.025 km^3 for 1971 Cerro Negro (Rose et al., 1973), 0.012 km^3 for 1992 Cerro Negro (McKnight, 1995), and 0.008 km^3 for 1995 Cerro Negro (Global Volcanism Network, 1995).

The dispersal characteristics of these analog volcanoes are shown in figure 2-6. With the exception of Heimaey volcano, all of the analog volcanoes have deposit thicknesses greater than 1 cm at distances greater than 10 km from the vent. Heimaey volcano, which is a mantle hot-spot volcano located on a mid-oceanic ridge, represents the lower range of possible dispersion from a low-energy basaltic eruption. In addition to the dispersal characteristics, grain-size data are available for several of these eruptions. For the 1995 Cerro Negro eruption, 82.9 percent of the fall deposit is coarser than 0.1 mm at 20.1 km from the volcano. This percent increases to 86.1 at 6 km from Cerro Negro. The 1975 eruption of Cone 1 at Tolbachik volcano produced fall deposits with 70 percent of the material coarser than 0.1 mm (Budinkov et al., 1983). These data and figure 2-6 show that significant thicknesses and material coarser than 0.1 mm extends tens of kilometers from the vent and there is an insufficient technical basis to truncate volcanic dispersion models at 8 km (i.e., Link et al., 1982).

Data from the 1995 eruption of Cerro Negro was chosen as an initial test for the Suzuki (1983) model because the data were collected during and immediately after the eruption and all parameters necessary for detailed modeling were obtained. One fundamental problem in modeling basaltic volcanism is that eruption duration commonly is greater than the period of intense activity that produced the tephra fall deposits. Although these differences are well recognized in observed eruptions (e.g., Self et al., 1974; Budinkov et al., 1983; Luhr and Simkin, 1993), eruption durations reported in the literature rarely distinguish between total duration and duration of the main tephra producing phase. In addition, column heights vary significantly during the eruption and often are visually estimated from distant locations. These problems do not occur with the 1995 Cerro Negro eruption data. Errors introduced through erosion and diagenesis of the tephra deposits also were avoided.

2.3.3.4 Sensitivity Analysis

Before conducting the sensitivity analyses, the CNWRA computer code of the Suzuki (1983) model was tested by using the model parameters in Suzuki (1983) to reproduce the reported dispersal patterns. Small deviations (less than 10 percent) between output from the code and values reported in Suzuki (1983) were deemed acceptable and can be accounted for by the level of precision under which the code is routinely run. Slightly higher precision is possible, but involves an order of magnitude increase in computational time that was not judged effective for these analyses.

The Suzuki (1983) model calculates mass of basalt per unit area with distance from the vent. Calculating deposit thicknesses requires that the *in situ* bulk density of the deposit is known. Because of systematic changes in the size and sorting of the deposit with distance from the vent, deposit density will also vary systematically in pyroclastic falls (e.g., Cas and Wright, 1987). For the 1995 Cerro Negro eruption, proximal (i.e., less than 5 km) fall deposits have a measured bulk density of 1,100 kg m^{-3}. Distal deposits (i.e., greater than 5 km) have a measured bulk density of 600 kg m^{-3}. These values are used to calculate deposit thicknesses in the following analyses.

Deterministic parameters from the 1995 Cerro Negro eruption used in the sensitivity analyses are a column height of 2.0 km, eruption duration of 3.456×10^6 s, total ash mass of 1.667×10^9 kg, mean particle diameter for the entire deposit of 0.5 mm, standard deviation of particle diameter of 0.5 mm,

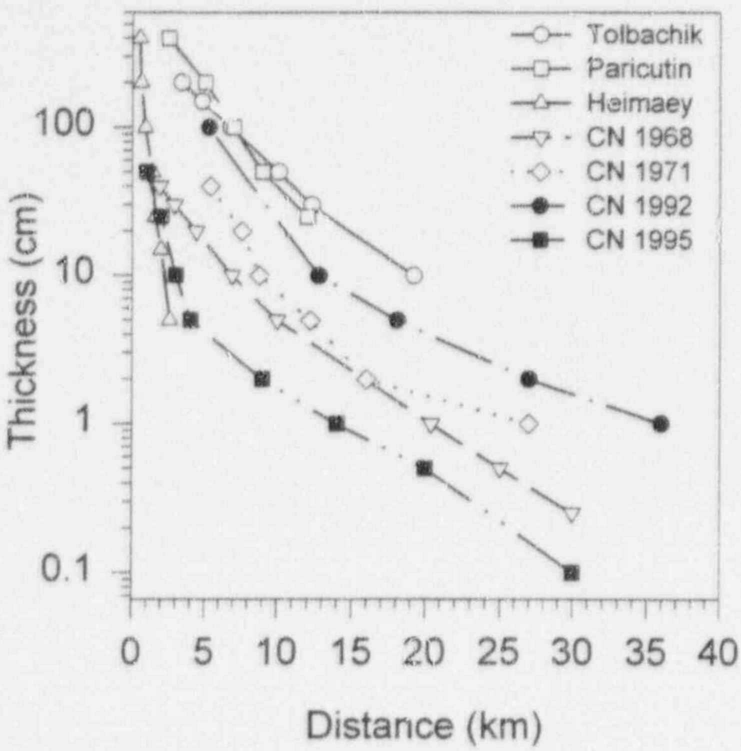

Figure 2-6. Dispersal characteristics for analog basaltic eruptions. Data sources in text. Thicknesses measured along main dispersal axis as reported in original isopach maps. Note significant thicknesses extend beyond 8 km from the vent, even for eruptions much smaller than those of the YMR.

particle shape factor of 0.5, β of 0.01, and *C* of 400. Average particle density ranged from 800 to 1,200 kg m^{-3} with a log-triangular distribution that was sampled stochastically (Jarzemba and LaPlante, 1996).

Wind speed is the most sensitive parameter in the Suzuki (1983) model, with a 100 percent increase in wind speed resulting in 200 percent increases in deposit thicknesses for lower wind velocities. During the 1995 eruption of Cerro Negro, wind speeds at ground level were estimated at 9 m s^{-1} (i.e., 20 mi hr^{-1}). Satellite imagery also shows wind speeds between 8 and 10 m s^{-1} during the eruption (Global Volcanism Network, 1995). Although the Suzuki (1983) model accurately calculates deposit thicknesses within 5 km of the vent using observed wind speeds and eruption characteristics, it underestimates distal thicknesses (i.e., greater than 5 km) by approximately 60 percent (figure 2-7a). A wind speed of 18 m s^{-1} (40 mi hr^{-1}) agrees well with observed distal thicknesses but overestimates proximal thicknesses by 100 percent (figure 2-7a). Analyses presented later in this section will show that this sensitivity to wind speed cannot be overcome by selecting reasonable values for other critical parameters. This discrepancy may be important as the distal component of a repository-penetrating eruption will transport most of the waste material into the accessible environment (e.g., Jarzemba and LaPlante, 1996). The remaining analyses will show a range of wind speeds, to present a sense of scale to model parameter sensitivities.

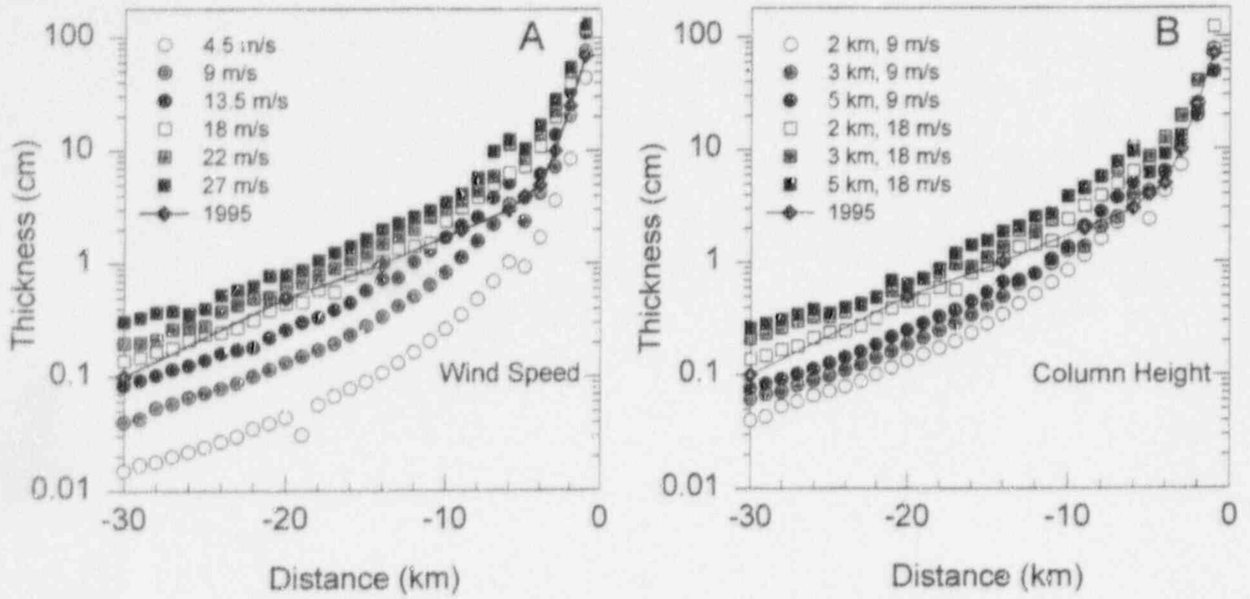

Figure 2-7. a) Variations in deposit thicknesses with distance from the vent as a function of wind speed using the tephra dispersal model of Suzuki (1983) and data from the 1995 Cerro Negro eruption. Observed wind speeds were 9 m s^{-1} during the eruption; 1995 deposits shown by symbol 1995. b) Variations in deposit thicknesses with distance from the vent as a function of column height. Observed column heights were 2 km during the eruption.

Variations in the eruption column height also have a demonstrable effect on modeled deposit thicknesses, although this effect is significantly less than the effect of wind speed. Increasing the column height from 2 to 5 km, while maintaining a constant eruption volume, increases distal deposit thicknesses by roughly 50 percent (figure 2-7b). To maintain mass balance, however, the eruption duration must decrease to 3 hr to sustain a 5 km high column. Similarly, a 3-km-high column could only be sustained for 1 d given the observed eruption mass. Direct observation and calculation of mass accumulation rates show the main tephra-producing phase of the eruption must have lasted 3.5–4 d. Thus, small variations in column height (i.e., ±0.5 km) cannot account for discrepancies between modeled and measured deposit thicknesses beyond 5 km from the vent.

Order of magnitude variations in the median particle diameter can produce less than 50 percent variations in deposit thicknesses using the Suzuki (1983) model. For the 1995 Cerro Negro eruption, 50 percent of the tephra volume is contained within the 5 cm isopach which extends to 5 km from the vent and has a bulk deposit median grain-size diameter of about 0.5 mm. For comparison, 50 cm thick deposits 1 km from the vent have median diameters of 2 mm, whereas deposits at 20 km from the vent are 0.5 cm thick with median diameters of only 0.2 mm. Varying particle diameter between 0.5 and 2 mm produces only minor variations in deposit thicknesses (figure 2-8a) and cannot account for the discrepancies between observed and calculated dispersal for the 1995 Cerro Negro eruption.

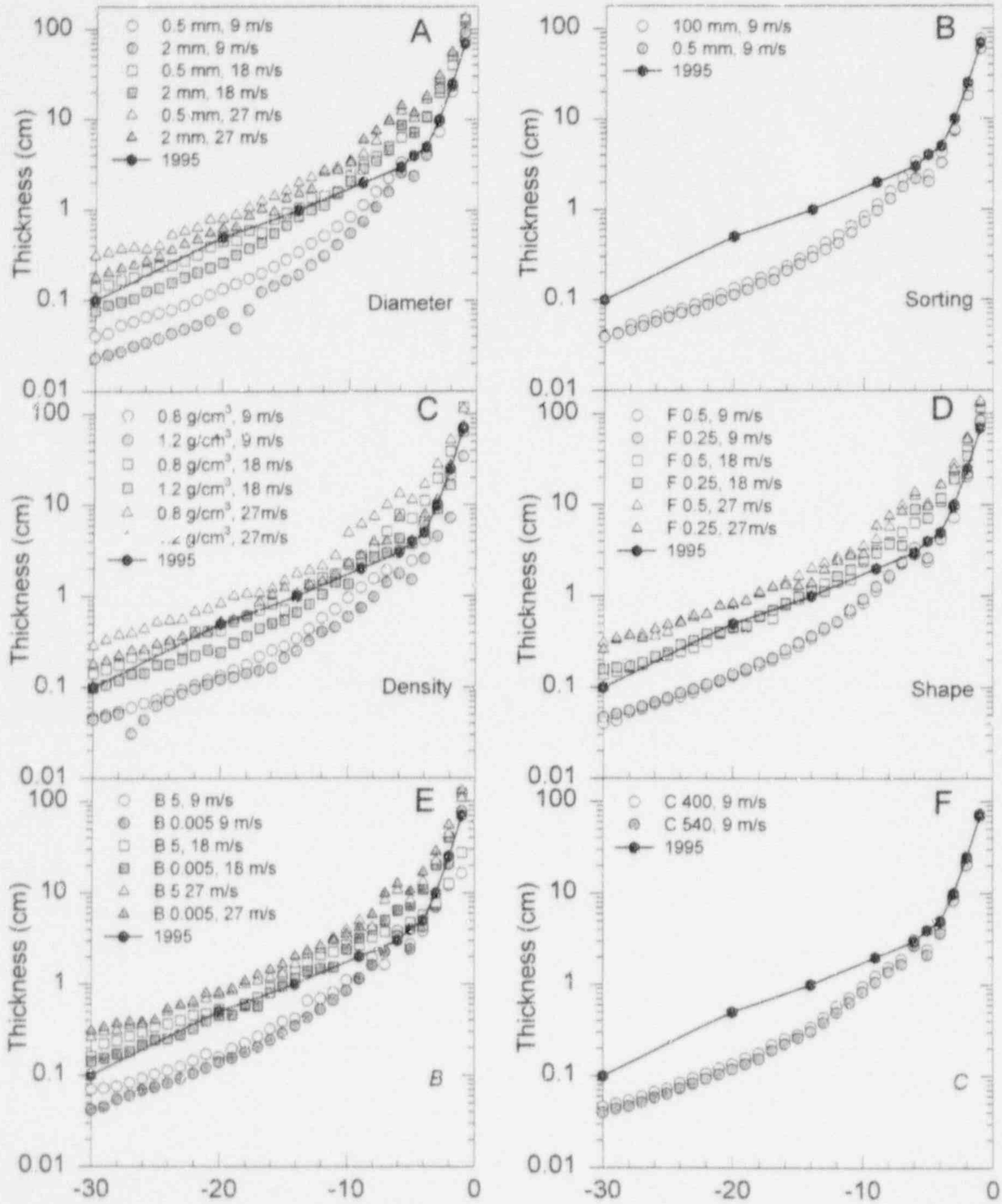

Figure 2-8. Sensitivity of the Suzuki (1983) model to variations in a) Average particle diameter; b) Particle sorting; c) Particle density; d) Particle shape; e) Constant β for vertical diffusion; and (f) Constant *C* for eddy diffusivity. Models are shown for a range of wind speeds and compared with data from the 1995 Cerro Negro eruption.

Other particle size and shape characteristics have even less effect on dispersal patterns using the Suzuki (1983) model. With clast density fixed at 800 kg m^{-3}, sorting (i.e., the distribution of different particle sizes within a deposit) has only a minor effect on deposit thicknesses (figure 2-8b). Deposits from the 1995 Cerro Negro eruption have a relatively narrow range of grain sizes and are thus considered well sorted (i.e., sorting = 0.5 mm). Increasing the range of grain sizes (i.e., sorting) within the deposit to 100 mm only results in a roughly 10 percent increase in deposit thicknesses. Changes in particle density have variable but small effects on deposit thicknesses (figure 2-8c), although these variations are less systematic than those associated with most other parameters. Decreasing particle density from 1,200 kg m^{-3} to 800 kg m^{-3} increases deposit thicknesses about 20 percent for 9 m s^{-1} wind speeds, with a roughly 40 percent increase for 27 m s^{-1} wind speeds (figure 2-8c). Changing the shape of the tephra has a negligible effect on thickness distributions (figure 2-8d). Decreasing the shape parameter F from 0.5 (roughly equant) to 0.25 (roughly tabular) increases the cross-sectional area of the particle and thus increases particle settling times. This increase in settling times, however, results in a less than 5 percent increase in deposit thicknesses.

Several important physical constants are used in the Suzuki (1983) model of tephra dispersion. Suzuki (1983) uses the constant β to control the mass diffusion pattern from the eruption column. Variations of β in Suzuki (1983) between 0.5 and 0.02 produce very different diffusion patterns, with broader and greater dispersion of material for larger values of β. It is important to note that the CNWRA computer code successfully reproduced the distribution patterns reported in Suzuki (1983) when using his eruption conditions. In contrast, similar variations in β produced barely discernable variations in deposit thicknesses for the 1995 Cerro Negro eruption conditions (figure 2-8e). Increasing β from 0.005 to 0.5 results only in a 10 percent average increase in deposit thicknesses for all wind speeds. Increasing β to 5 results in a 24 percent increase in distal deposit thicknesses, relative to β equal to 0.005. This value of β, however, results in an approximately 50 percent underestimation of thicknesses within several kilometers of the vent (figure 2-8e). Increasing β to 0.5 results in the maximum tephra mass per unit area occurring at a significant distance from the vent (Suzuki, 1983) rather than immediately at the vent as observed in basaltic eruptions. Thus, values of β above 0.5 do not appear justified.

The relative insensitivity of β likely results from the small column-height for basaltic cinder cone eruptions. Because these eruptions columns ascend to only around 5 km or less, there is limited opportunity for lateral diffusion or spreading within the rising column. Thus, particles are released from essentially a point-source at the top of the column rather than from a broad area as commonly observed for larger eruptions [cf. Suzuki, 1983 figures (2-3)–(2-4)]. Suzuki (1983) uses another constant, C, in equations governing eddy diffusivity (i.e., horizontal transport). Data presented in Suzuki (1983) for a range of eruption sizes result in a value for C of 400. Restricting these data to only relatively small eruptions results in a value of 540 for C. As shown in figure 2-8, using a value of 540 for C results in a less than 10 percent decrease in deposit thicknesses.

A final set of simulations were run for conditions that best represent the 1995 Cerro Negro eruption: column height of 2.0 km, eruption duration of 3.456×10^6 s, total ash mass of 1.667×10^9 kg, mean particle diameter for the entire deposit of 0.5 mm, standard deviation of particle diameter of 0.5 mm, particle shape factor of 0.25, average particle density of 800 kg m^{-3}, β of 0.5 and C of 400. These conditions were used with wind speeds of 9 m s^{-1} (i.e., observed) and 18 m s^{-1}. The latter results in the best apparent fit of the model to observed tephra distributions (figure 2-9a) although this wind velocity

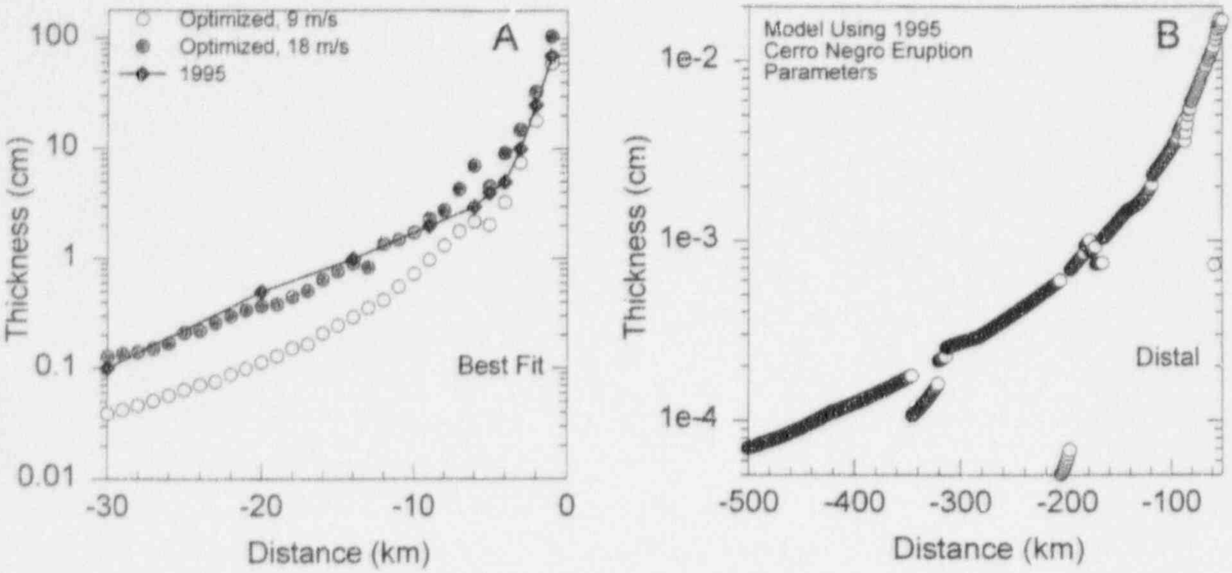

Figure 2-9. a) Distribution of tephra modeled using Suzuki (1983) optimized to conditions from the 1995 Cerro Negro eruption compared with measured deposit thicknesses. Wind speed during the eruption was 9 m s^{-1}, whereas speeds of approximately 18 m s^{-1} are required to generate measured deposit thicknesses at 5–30 km from the vent. b) Deposit thicknesses to 500 km from the vent, using same conditions as 1995 Cerro Negro eruption including wind speeds of 9 m s^{-1}.

is twice that observed during the eruption. Using measured wind velocities, the model underestimates deposit thicknesses by 50 percent at distances of 5 to 30 km from the vent.

2.3.3.5 Discussion

The Suzuki (1983) model successfully produces tephra-fall thicknesses observed for the 1995 Cerro Negro eruption at distances less than 5 km from the vent. Optimizing the Suzuki (1983) model for parameters measured during the 1995 Cerro Negro eruption, or at the reasonable upper bounds of these parameters, underestimates deposit thicknesses by 50 percent at distances 5–30 km from the vent. In addition, the volume of the 1995 Cerro Negro eruption is significantly smaller than most Quaternary YMR volcanoes and mass discharge rate also is relatively low (about 4 m^3 s^{-1}). This eruption thus should not overestimate the dispersal characteristics for YMR-type eruptions. The sensitivity of key parameters in the Suzuki (1983) model has been examined in detail. The model is highly sensitive to wind velocity, moderately sensitive to column height, particle diameter and density, and relatively insensitive to the degree of sorting, particle shape, and constants related to column diffusivity and eddy diffusivity. The sensitivity to wind speed is especially important to repository performance models, where average wind

speeds of 3–7 $m\ s^{-1}$ are used.[15] Current versions of the Suzuki (1983) model likely underestimate deposit thicknesses, and thus volume of waste material dispersed, by 50 percent in regions critical to determining radiation releases within the accessible environment (Jarzemba and LaPlante, 1996).[16]

The implementation of the Suzuki (1983) model on the CNWRA systems has been checked and found to accurately reproduce distribution patterns and parameter sensitivities shown in the original reference. Currently, the cause for underestimation of deposit thicknesses is speculative, but presumably relates to a conceptual problem with the Suzuki (1983) model as applied to small column height, low mass-flow basaltic eruptions. Apparently, mass distribution is not accurately accounted for in these small-volume eruptions and there is insufficient horizontal transport of material along the depositional axis. To test for mass conservation, tephra dispersal was modeled over a 50×50 km area. This area contains nearly all of the deposit down to thicknesses of 0.1 mm. The material modeled within this area underestimates the mass deposited from the 1995 Cerro Negro eruption by 36 percent (i.e., 1×10^{12} g), which is in relative agreement with the 50 percent underestimation of deposit thicknesses solely along the main fall axis. In addition, deposit thicknesses down to 0.001 mm were modeled to a distance of 500 km from the vent (figure 2-9b). Construction of reasonable isopachs from these data can only account for about 25 percent of the missing mass.

For comparison, calculations using the well-recognized exponential thinning of fall deposits with distance from the vent (e.g., Fierstein and Nathenson, 1992) show that only 25 percent of the 1995 Cerro Negro fall deposits should be present in deposits thinner than 1 mm. One of the characteristics of basaltic eruptions, however, is that magma fragmentation is relatively weak, resulting in a lack of ≤1 mm tephra (e.g., Walker, 1973; 1981). It is thus highly unlikely that 25 percent of the Cerro Negro deposits are contained in deposits thinner than 1 mm, whereas such volumes are possible for more highly fragmented silicic eruptions (e.g., Fierstein and Nathenson, 1992).

2.3.4 Conclusions

Calculations of the probability of future igneous activity at the proposed repository site are dependent on accurate identification and characterization of igneous features within the YMR. Pliocene volcanism in the Funeral Formation suggests that Plio-Quaternary recurrence rates may be relatively constant through time. This is an alternative interpretation to that used in many Weibull-process probability models which assume volcanism recurrence rates increase during the Quaternary (e.g., Ho, 1991; U.S. Department of Energy, 1996a). In addition, Funeral Formation volcanoes may affect probability models that use vent location to control definition of spatial trends to the YMR volcanic field, so that the probability of future igneous activity at the proposed repository site could be greater than calculated by some models in U.S. Department of Energy (1996a). Reworked, coarse-grained 6.3±0.8 Ma silicic pumice in Crater Flat alluvium cannot be correlated with any known silicic eruption in the YMR and likely indicates a previously unrecognized episode of silicic magmatism in the YMR. The risk of future silicic igneous activity was thought to be negligible based on the absence of post-caldera silicic eruptions in the YMR (U.S. Department of Energy, 1993). The post-caldera Crater Flat pumice shows that determining

[15]Jarzemba, M.S. 1996. Stochastic radionuclide distributions after a basaltic eruption for performance assessments of Yucca Mountain. *Nuclear Technology*. In press.

[16]*Ibid.*

the risks presented by future silicic eruptions requires an additional evaluation of the YMR geologic setting to see if the conditions that led to the production of this pumice are present or could be present during future periods of interest.

Integration of fault dilation-tendency with spatio-temporal Poisson probability models shows that many of the faults in and proximal to the proposed repository site are in high dilation orientations, which favors magma ascent. Other areas, such as Bare Mountain, lack such faults. The probability of future igneous activity should be lower in areas lacking high dilatancy faults than calculated strictly by spatio-temporal methods but proportionally higher in areas of high dilation-tendency. Integrated dilation-tendency probability models show that the probability of future volcanic disruption of the proposed repository site ranges between 1×10^{-8} and 2×10^{-7} per year. In contrast, U.S. Department of Energy (1996a) concluded, based in large part on the definition of preferred structural zones, that this probability is 1.5×10^{-8} with a 90 percent confidence interval of 5.4×10^{-10} to 4.9×10^{-8}.

Data from basaltic volcanoes analogous to those of the YMR and modeling shows that significant amounts of material can be transported tens of kilometers from a small-volume basaltic eruption. In contrast, the DOE models assume that only material with diameters less than 0.06 mm can be transported more than 8 km from the vent, forming deposits less than 1 cm thick. Current models being used in the CNWRA research underestimate tephra deposit thicknesses by about 50 percent at distances of 5–30 km. These distances are important to evaluating releases of radioactive material into the accessible environment. Tephra dispersion models are highly sensitive to wind speed and a lesser extent to eruption column height, particle diameter, and density. Whereas wind speed can be sampled stochastically, the other eruption parameters will need to be estimated accurately for the poorly preserved to absent deposits at YMR volcanoes. Data from historically active analog volcanoes will be critical to constraining these parameters.

The DOE WCIS concludes "Volcanic events within the controlled area will be rare and the consequences of volcanism will be acceptable." Based on information presented herein, the current understanding of the YMR volcanic and structural setting indicates the probability of future basaltic volcanic events at the proposed repository site ranges between 10^{-8} and 10^{-7} per year. The probability of future silicic volcanic events is unknown, but the available data shows that silicic pyroclastic eruptions likely occurred in the YMR at least several million years after cessation of caldera-forming activity. The consequences of volcanism on repository performance are incompletely bounded, but the current understanding of small-volume basaltic eruption processes is sufficient to show that significant amounts of material can be transported tens of kilometers from the vent into the accessible environment.

2.4 ASSESSMENT OF PROGRESS TOWARD MEETING OBJECTIVES

Work completed in FY96 continued to provide independent assessments of the probability of future igneous activity in the YMR and of processes important to consequence analyses. Detailed field investigations have shown that significant igneous features remained present but undetected or poorly characterized including post-caldera silicic eruptions. These activities will ensure that all relevant information is used in assessing risks associated with igneous activity including the quantification of uncertainty associated with these analyses. Important progress also was made through the integration of fault dilation-tendency into spatio-temporal probability models, which provides a significantly different interpretation of the effects of structure on igneous activity than presented in many DOE models (e.g., U.S. Department of Energy, 1996a). Work on probability issues not reported herein also has continued on

understanding the petrogenetic evolution of the YMR volcanic field and integrating field and geochronological data from other western U.S. volcanic fields to construct robust tests of probability model accuracies.

Understanding the consequences of igneous activity on proposed repository performance also has progressed well during FY96. Data from analog basaltic volcanoes, most importantly from the December 1995 Cerro Negro eruption, continue to provide an independent means to develop and test consequence models. The sensitivity analysis of the Suzuki (1983) dispersion model shows that accurately quantifying the column height and grain-size characteristics for YMR volcanoes is important to calculating risks of radiological releases into the accessible environment. Additional major work during FY96 related to consequences included integration of data from analog volcanoes on thermal and degassing effects associated with basaltic igneous activity, field and laboratory analyses to determine critical eruption characteristics from tephra deposits, and studies of wall-rock fragmentation and entrainment processes at historically active and YMR volcanoes.

In addition to the technical accomplishments, significant progress was made on closure of open items. Between the Site Characterization Analysis and study plan reviews, the NRC generated 57 open items of which six had been closed prior to FY96. During FY96, the NRC closed an additional 18 open items and a re-analysis of the open items based on information contained within the new DOE Program Plan suggests that review of U.S. Department of Energy (1996a), along with the proposed DOE Geophysical Synthesis report, should allow the closure of a significant number of other open items during FY97.

Work in FY97 will shift to greater emphasis on consequence analyses, primarily related to waste fragmentation, entrainment mechanisms, and dispersal modeling. Previous and ongoing PA analyses (e.g., Jarzemba and LaPlante, 1996) have shown these to be critical processes to determining risks associated with igneous activity. In FY97 resources will need to be devoted to review of the DOE reports and planned documents including U.S. Department of Energy (1996a) and a volcanism synthesis report.

Although the DOE mean probability value is within the range reported in section 2.3.3, significant differences in approach to consideration of processes that control location of igneous activity, including shallow and deep structural setting, topography, and definition of "source zones." One example is the detailed ground magnetic studies by CNWRA staff, which revealed north-trending faults in eastern Crater Flat that offset tuff beneath a thin carapace of alluvium. These faults apparently localized volcanism at Northern Cone at a stratigraphic level above the repository horizon. Many DOE source-zone models, which form the basis for the DOE WCIS, are inconsistent with these volcano-fault relationships. Understanding the processes that control volcanism is important because the probability of future igneous activity is low but may be large enough to influence repository performance. Regardless of these differences and because of the proposed revisions to the U.S. Environmental Protection Agency standard, from a regulatory perspective issue resolution is possible in FY97. Both DOE and NRC agree that while volcanic activity affecting the repository is a low probability event, probability is sufficiently high that the consequences of such activity must be considered in PA. Although technical differences apparently exist, an Issue Resolution Report is planned for FY97 to attempt to resolve the probability subissue. This report will evaluate existing data and models from the DOE, CNWRA, and others to arrive at a reasonably conservative range on the probability of future igneous activity at the proposed repository site.

2.5 INTEGRATION WITH OTHER KEY TECHNICAL ISSUES

IA has relied heavily on input from the Structural Deformation and Seismicity (SDS) KTI in developing fault dilation-tendency probability models and understanding the structural and geophysical setting of the YMR. Output from igneous activity to SDS include the integration of geophysical data that constrains the structural setting of the YMR and the timing and nature of post-caldera volcanism as tectonic indicators. IA also is strongly linked with the Total System Performance Assessment and Integration (TSPAI) KTI, providing input on volcanic processes and probabilities for performance models, review of DOE TSPA-95 (TRW Environmental Safety Systems, Inc., 1995), and development and testing of the tephra dispersal model. These links will strengthen in FY97, especially for model development and integration with TSPAI. In addition, some integrated study is expected with Container Life and Source Term KTI staff to better understand the effects of igneous activity on waste package integrity.

2.6 REFERENCES

Budinkov, V.A., Ye.K. Markhinin, and A.A. Ovsyannikov. 1983. The quantity, distribution and petrochemical features of pyroclastics of the great Tolbachik fissure eruption. S.A. Fedotov and Ye.K. Markhinin, eds. *The Great Tolbachik Fissure Eruption*. New York, NY: Cambridge University Press: 41–56.

Carr, W.J. 1982. *Volcano–Tectonic History of Crater Flat, Southwestern Nevada, as Suggested by New Evidence from Drill Hole USU–VH–1 and Vicinity*. U.S. Geological Survey Open-File Report 82-457. Reston, VA: U.S. Geological Survey.

Cas, R.A.F., and J.V. Wright. 1987. *Volcanic Successions*. Winchester, MA: Unwin Hyman Inc.

Connor, C.B. 1993. *Technical and Regulatory Basis for the Study of Recently Active Cinder Cones*. San Antonio, TX: Center for Nuclear Waste Regulatory Analyses.

Connor, C.B., and B.E. Hill. 1995. Three nonhomogeneous Poisson models for the probability of basaltic volcanism: Application to the Yucca Mountain region, Nevada, U.S.A. *Journal of Geophysical Research* 100(B6): 10,107–10,125.

Connor, C.B., and C.O. Sanders. 1994. *Geophysics Review Topical Report: Application of Seismic Tomographic and Magnetic Methods to Issues in Basaltic Volcanism*. CNWRA 94-013. San Antonio, TX: Center for Nuclear Waste Regulatory Analyses.

Connor, C.B., R.H. Martin, P.G. Hunka, J.A. Stamatakos, D.B. Henderson, and R.V. Klar. 1996. *Ground Magnetic Survey of the Little Cones, Crater Flat, Nevada*. CNWRA 96-002. San Antonio, TX: Center for Nuclear Waste Regulatory Analyses.

Crowe, B.M., and F.V. Perry. 1989. Volcanic probability calculations for the Yucca Mountain site: Estimation of volcanic rates. *Proceedings Nuclear Waste Isolation in the Unsaturated Zone, Focus '89*. La Grange Park, IL: American Nuclear Society: 326–334.

Crowe, B.M., F.V. Perry, J. Geissman, L. McFadden, S. Wells, M. Murrell, J. Poths, G.A. Valentine, L. Bowker, and K. Finnegan. 1995. *Status of Volcanic Hazard Studies for the Yucca Mountain Site Characterization Project.* Los Alamos National Laboratory Report LA-12908-MS. Los Alamos, NM: Los Alamos National Laboratory.

Ferrill, D.A., J.A. Stamatakos, S.M. Jones, B. Rahe, H.L. McKague, R.H. Martin, and A.P. Morris. 1996. Quaternary slip history of the Bare Mountain fault (Nevada) from the morphology and distribution of alluvial fan deposits. *Geology* 24(6): 559–562.

Fierstein, J., and M. Nathenson. 1992. Another look at the calculation of fallout tephra volumes. *Bulletin of Volcanology* 54: 156–167.

Fleck, R.J., B.D. Turrin, D.A. Sawyer, R.G. Warren, D.E. Champion, M.R. Hudson, and S.A. Minor. 1996. Age and character of basaltic rocks of the Yucca Mountain region, southern Nevada. *Journal of Geophysical Research* 100(B4): 8,205–8,227.

Frizzell, V.A. Jr., and J. Shulters. 1990. *Geologic Map of the Nevada Test Site, Southern Nevada.* U.S. Geological Survey Miscellaneous Investigations Map I-2046. Reston, VA: U.S. Geological Survey.

Glaze, L.S., and S. Self. 1991. Ashfall dispersal for the 16 September 1986 eruption of Lascar, Chile, calculated by a turbulent diffusion model. *Geophysical Research Letters* 18(7): 1,237–1,240.

Griesmeyer, J.M., and D. Okrent. 1981. Risk management and decision rules for light water reactors. *Risk Analysis* 1: 121–136.

Global Volcanism Network. 1995. Cerro Negro, Nicaragua. *Bulletin of the Global Volcanism Network* 20(11/12): 2–4.

Healey, D.L., and C.H. Miller. 1971. *Gravity Survey of the Amargosa Desert Area of Nevada and California.* U.S. Geological Survey Report USGS-474-308. U.S. Geological Survey Technical Letter NTS-99: 30 pp.

Hill, B.E. 1995. *Expert-Panel Review of CNWRA Volcanism Research Programs.* CNWRA 95-002. San Antonio, TX: Center for Nuclear Waste Regulatory Analyses.

Hill, B.E., and C.B. Connor. 1996. Volcanic Systems of the Basin and Range *NRC High-Level Radioactive Waste Research at CNWRA, July–December 1995.* B. Sagar, ed. CNWRA 95-02S. San Antonio, TX: Center for Nuclear Waste Regulatory Analyses. 5-1 to 5-21.

Ho, C.-H. 1991. Time trend analysis of basaltic volcanism at the Yucca Mountain site. *Journal of Volcanology and Geothermal Research* 46: 61–72.

Jarzemba, M.S., and P.A. LaPlante. 1996. *Preliminary Calculations of Expected Dose from Extrusive Volcanic Events at Yucca Mountain.* IM 5078-771-610. San Antonio, TX: Center for Nuclear Waste Regulatory Analyses.

Langenheim, V.E., K.S. Kirchoff-Stein, and H.W. Oliver. 1993. Geophysical investigations of buried volcanic centers near Yucca Mountain, southwest Nevada. *Proceedings of the Fourth Annual International Conference on High-Level Radioactive Waste Management*. La Grange Park, IL: American Nuclear Society: 1,840–1,846.

Langenheim, V.E., and D.A. Ponce. 1995. Depth to Pre-Cenozoic basement in southwest Nevada. *Proceedings of the Sixth Annual International Conference on High-Level Radioactive Waste Management*. La Grange Park, IL: American Nuclear Society: 129–131.

Link, R.L., S.E. Logan, H.S. Ng, F.A. Rokenbach, and K.-J. Hong. 1982. *Parametric Studies of Radiological Consequences of Basaltic Volcanism.* Sandia National Laboratory Report SAND 81-2375. Albuquerque, NM: Sandia National Laboratory.

Luhr, J.F., and T. Simkin. 1993. *Paricutin, the Volcano Born in a Mexican Cornfield*. Phoenix, AZ: Geoscience Press.

McAllister, J.F. 1970. *Geology of the Funeral Creek Borate Area, Death Valley, Inyo County, California*. California Division of Mines and Geology Map Sheet 14. Sacramento, CA: California Division of Mines and Geology.

McDuffie, S.M., C.B. Connor, and K.D. Mahrer. 1994. A simple 2-D stress model of dike-fracture interaction. *EOS, Transactions of the American Geophysical Union* 75(16): 345.

McKnight, S.B. 1995. *Geology and Petrology of Cerro Negro Volcano, Nicaragua*. M.S. Thesis. Tempe, AZ: Arizona State University.

Morris, A., D.A. Ferrill, and D.B. Henderson. 1996. Slip-tendency analysis and fault reactivation. *Geology* 24(3): 275–278.

Oliver, H.W., D.A. Ponce, and W.C. Hunter. 1995. *Major Results of Geophysical Investigations at Yucca Mountain and Vicinity, Southern Nevada*. U.S. Geological Survey Open-File Report 95-74. Reston, VA: U.S. Geological Survey.

Parsons, T., and G.A. Thompson. 1991. The role of magma overpressure in suppressing earthquakes and topography: Worldwide examples. *Science* 253: 1,399–1,402.

Rose, W.I., Jr., S. Bonis, R.E. Stoiber, M. Keller, and T. Bickford. 1973. Studies of volcanic ash from two recent Central American eruptions. *Bulletin Volcanologique* 37: 338–364.

Self, S., R.S.J. Sparks, B. Booth, and G.P.L. Walker. 1974. The 1973 Heimaey strombolian scoria deposit, Iceland. *Geological Magazine* 111: 539–548.

Sheridan, M.F. 1992. A Monte Carlo technique to estimate the probability of volcanic dikes. *Proceedings of the Third International Conference on High-Level Radioactive Waste Management*. La Grange Park, IL: American Nuclear Society: 2,033–2,038.

Smith, E.I., T.R. Feuerbach, and J.E. Faulds. 1990. The area of most recent volcanism near Yucca Mountain, Nevada: Implications for volcanic risk assessment. *Proceedings of the International Topical Meeting on High-Level Radioactive Waste Management*. La Grange Park, IL: American Nuclear Society: 81–90.

Stock, J.M., J.H. Healy, S.H. Hickman, and M.D. Zoback. 1985. Hydraulic fracturing stress measurements at Yucca Mountain, Nevada, and relationship to regional stress field. *Journal of Geophysical Research* 90 (B10): 8,691–8,706.

Suzuki, T. 1983. *A Theoretical Model for the Dispersion of Tephra*. D. Shimozuru and I. Yokiyama, eds. Arc Volcanism: Physics and Tectonics. Tokyo, Japan: Terra Scientific Publishing Company: 95–113.

Suzuki, T. 1985. Analysis of the 1977 tephra of Usu volcano by the turbulent diffusion model. *Bulletin of the Volcanological Society of Japan* 30: 231–251.

Taylor, P.S., and R.E. Stoiber. 1973. Soluble material on ash from active Central America volcanoes. *Geological Society of America Bulletin* 84: 1,031–1,042.

TRW Environmental Safety Systems, Inc. 1995. *Total System Performance Assessment—1995: An Evaluation of the Potential Yucca Mountain Repository*. (B00000000-01717-2200-00136). Las Vegas, NV: TRW Environmental Safety Systems, Inc.

U.S. Department of Energy. 1993. *Study Plan for Study 8.3.1.8.5.1., Characterization of Volcanic Features, Revision 1*. Washington, DC: U.S. Government Printing Office.

U.S. Department of Energy. 1996a. *Probabilistic Volcanic Hazards Analysis for Yucca Mountain, Nevada*. Civilian Radioactive Waste Management System Management and Operating Contractor BA0000000-1717-2200-00082, Rev. 0. Washington, DC: U.S. Government Printing Office.

U.S. Department of Energy. 1996b. *Study Plan for Study 8.3.1.8.1.1., Probability of Magmatic Disruption of the Repository, Revision 3*. Washington, DC: U.S. Government Printing Office.

Walker, G.P.L. 1973. Explosive volcanic eruptions—a new classification scheme. *Geologische Rundsche* 62: 431–446.

Walker, G.P.L. 1981. Generation and dispersal of fine ash and dust by volcanic eruptions. *Journal of Volcanology and Geothermal Research* 11: 81–92.

Wilson, M.L., and 24 others. 1994. *Total-System Performance Assessment for Yucca Mountain—SNL Second Iteration (TSPA-1993)*. Sandia National Laboratories Report SAND93-2675. Albuquerque, NM: Sandia National Laboratories.

Wright, L.A., R.A. Thompson, B.W. Troxel, T.L. Pavlis, E.H. DeWitt, J.K. Otton, M.A. Ellis, M.G. Miller, and L.F. Serpa. 1991. Cenozoic magmatic and tectonic evolution of the east-central Death Valley region, California. M.J. Walawender and B.B. Hanan, eds. *Geological Excursions in Southern California and Mexico, Guidebook for the 1991 Annual Meeting of the Geological Society of America.* San Diego, CA: San Diego State University: 93–127.

Yogodzinski, G.M., and E.I. Smith. 1995. Isotopic domains and the area of interest for volcanic hazard assessment in the Yucca Mountain area. *EOS, Transactions of the American Geophysical Union* 76(46): F669.

3 STRUCTURAL DEFORMATION AND SEISMICITY

Primary Authors: J.A. Stamatakos, P.S. Justus, D.A. Ferrill, R. Chen, and G.I. Ofoegbu

Technical Contributors: D.P. Cederquist, J.R. Firth, R.V. Klar, H.L. McKague, B.R. Rahe, K.J. Smart, G.L. Stirewalt, and G.W. Wittmeyer

Key Technical Issue Co-Leads: H.L. McKague (CNWRA) and P.S. Justus (NRC)

3.1 INTRODUCTION

Yucca Mountain (YM) lies within the central Basin and Range Province of the western North American Cordillera [see figure 1 of Wernicke (1992), p 554], a region characterized by complex interactions of strike-slip and extensional deformation active since the onset of the Cenozoic 65 m.y. ago. The region is still tectonically active as indicated by Quaternary (including Holocene) faulting, volcanism, and historic seismicity (including the 1992 Little Skull Mountain earthquake). Continuing structural deformation and seismicity at YM and in the Yucca Mountain region (YMR) pose a risk of noncompliance with radiological safety, health, and environmental protection standards because these tectonic processes might modify existing groundwater flow, damage waste packages (WPs), degrade stability of underground openings, and disrupt surface and other preclosure operations including retrievability.

The primary objective of the Structural Deformation and Seismicity (SDS) Key Technical Issue (KTI) is to evaluate structural deformation, seismicity, and related hazards on safe disposal of high-level nuclear waste (HLW) at the proposed YM, Nevada, repository. As part of that task, the SDS KTI evaluates hypotheses outlined in the U.S. Department of Energy (DOE) Waste Containment and Isolation Strategy (WCIS) regarding potential effects of seismicity and structural deformation (U.S. Department of Energy, 1996)[1]. Pertinent hypotheses are (i) the amount of movement on faults through the potential repository horizon will be too small to bring waste to the surface and too small and infrequent to significantly impact containment during the next few thousand years and (ii) the severity of ground motion expected in the repository horizon for tens of thousand of years will only slightly increase the amount of rockfall and drift collapse. In addition, the SDS KTI provides critical structural and seismicity information to other KTIs to evaluate the DOE WCIS hypotheses concerning seepage, containment, radionuclide mobilization, radionuclide transport, dilution, and volcanism.

In addition to evaluations of the DOE WCIS hypotheses, the SDS KTI evaluates conclusions regarding SDS in the DOE 1995 Total System Performance Assessment (TSPA-95) (TRW Environmental Safety Systems, Inc., 1995) in preparation for the upcoming TSPA Viability Assessment (TSPA-VA). Notwithstanding tectonic activity of the region, the DOE concluded on page 2-14 in TSPA-95 (TRW Environmental Safety Systems, Inc., 1995) that future consequences of faulting and seismicity will be negligible on release of radionuclides to the accessible environment. The DOE did not explicitly include external events in TSPA-95. Its conclusion about negligible affects of structural deformation and seismicity on total system performance was based primarily on the DOE Probabilistic Seismic Hazard Analysis (PSHA) (Wong et al., 1995) and auxiliary performance assessment (PA) calculations (e.g., Gauthier et al., 1995) in which only a subset of possible externally induced natural phenomena were considered (e.g., WP

[1]U.S. Department of Energy. 1996. Highlights of the U.S. Department of Energy's Updated Waste Containment and Isolation Strategy for the Yucca Mountain Site. DOE Concurrence Draft.

rupture or enhanced degradation from faulting and fracture or bulk rock seepage flow, and seismicity-induced water table fluxuations). Moreover, the DOE data used to constrain faulting characteristics were based solely on trenching studies of suspected Quaternary faults in alluvium (Pezzopane, 1995). These estimates are not considered conservative because they yield minimum fault-slip values (Ferrill et al., 1996a). Alternative methods for gauging fault-slip (e.g., apatite fission-tracks, geodetic surveys, alluvial fan studies, and ground magnetic surveys) indicate greater slip-rates than those proposed by the DOE [Ferrill et al. (1996b; 1996c); Stamatakos et al. (1996)[2]]. In addition, the DOE TSPA-95 did not consider potential effects of faulting and seismicity on disruption of groundwater flow, thermal perturbations, or structural control of magma injection along faults and fractures.

SDS KTI evaluations are also relevant to DOE PSHA, Probabilistic Fault Displacement Hazard Analysis (PFDHA), corresponding deterministic fault-displacement and seismic hazard analyses, and controlled design assumptions concerning faults and fractures. The DOE plans to complete its expert elicitation on PSHA and PFDHA in Fiscal Year 1997 (FY97) and present those findings in early FY98. The PSHA and PFDHA results will be used by DOE for both preclosure design and operation safety decisions as well as input to the TSPA-VA.

SDS has been subdivided by Nuclear Regulatory Commission (NRC) into five subissues that serve as focal points for SDS KTI technical tasks. The first subissue focuses on data, which provide the basis for evaluations of tectonic, structural, and seismological models, DOE hypothesis and assumptions, as well as PSHA and TSPA. The SDS KTI continues to assess and independently evaluate critical SDS data and complete resolution of this issue is not expected in FY97. However, an important component of this subissue was resolved in FY96. Type I faults have been identified based on a deterministic assessment of seismicity in the YMR. Those findings are presented in McKague et al. (1996) and are summarized in section 3.3.4.

The second subissue comprises model validation and verification that provide the basis for the three-dimensional (3D) geologic framework model of the site, methodologies and results of seismic and fault-displacement hazards assessments, and coupled mechanical-thermal-hydrologic-chemical process models. A significant component of SDS KTI work in FY96 related to possible structural control of volcanism Connor et al. (1996a), Conway et al. (1996),[3] Connor et al. (1996b), and Stamatakos et al. (1996).[4] Integration of structural models in volcanic probability models is presented in chapter 2 of this report. The SDS KTI developed hydrological applications in the Center for Nuclear Waste Regulatory Analyses (CNWRA) 3D geologic framework model (Stirewalt and Henderson, 1995a; 1995b; 1996). Technical investigations presented in section 3.3.3 summarize modeling result of faulting and

---

[2]Stamatakos, J.A., C.B. Connor, and R.H. Martin. 1996. Quaternary volcanism and basin evolution of Crater Flat, Nevada, from detailed ground magnetic surveys of the Little Cones. *Journal of Geology*. Accepted for publication.

[3]Conway, F.M., D.A. Ferrill, C.M. Hall, A.P. Morris, J.A. Stamatakos, C.B. Connor, A. Halliday, and C. Condit. 1996. Timing of volcanism along the Mesa Butte fault in the San Francisco Volcanic Field, Arizona, from $^{40}Ar/^{39}Ar$ ages: Implications for the longevity of cinder cone alignments. *Journal of Geophysical Research*. Submitted for publication.

[4]Stamatakos, J.A., C.B. Connor, and R.H. Martin. 1996. Quaternary volcanism and basin evolution of Crater Flat, Nevada, from detailed ground magnetic surveys of the Little Cones. *Journal of Geology*. Accepted for publication.

seismicity along the Bare Mountain fault (BMF) and possible co-seismic links to slip on antithetic YM faults is examined using ABAQUS (v.5.5).

The third subissue centers on alternative conceptual (tectonic) models (ACM). Identification and appropriate use of tectonic models is critical to the overall assessment of SDS effects on proposed repository performance. Tectonic models provide a common reference frame that exposes gaps in data acquisition, deficiencies in data analysis, and a focal point for future investigations. These models provide bounds for probability and consequence analyses and offer a vehicle to link structural and seismological features with other geological processes such as groundwater flow and volcanism. Finally, tectonic models provide a basis for representative abstractions of SDS in TSPA calculations. Results of SDS KTI investigations of the YMR tectonic setting, including analyses of contemporary strain and *in situ* stress, are given in Ferrill et al., 1996,[5] Rahe et al. (1996),[6] (Stamatakos and Ferrill, 1996b); and Stamatakos et al. (1996).[7] On the basis of an Appendix 7 meeting on viable tectonic models held in San Antonio in May 1996, tentative agreement was reached between the DOE, the CNWRA, the State of Nevada, and the United States Geological Survey (USGS) that only 5 of the more than 12 proposed tectonic models for the YMR are supported by existing data. Results of the Appendix 7 meeting are summarized in section 3.3.1. In addition, the potential for additional seismic sources from buried faults implied in two of the five viable models was investigated by analog deformation experiments using a sandbox deformation apparatus. Results of the analog experiments are presented in section 3.3.2.

The fourth subissue relates to potential for disruption of WPs, underground openings, and surface facilities/operations. The SDS KTI completed a detailed review of DOE Topical Report 1 (TR1), *Methodology to Assess Fault Displacement and Vibratory Ground Motion Hazard at Yucca Mountain*, (U.S. Department of Energy, 1994). In the review, the NRC concluded that sufficient information exists to close all comments and resolve the methodology to evaluate seismic hazards at YM. The SDS KTI is also investigating the effects of faulting on repository performance using the faulting module (Stirewalt et al., 1996), a PA code designed to assess WP disruption from faulting within the repository block.

The fifth subissue is concerned with the potential for disruption of flow due to structural deformation or seismicity. The SDS KTI investigated this subissue at two scales of observation. Technical investigations of the role of fractures, faults, and *in situ* stress on regional groundwater flow are summarized in 3.3.5. The evaluation is based in part on dilation-tendency analysis using 3DStress (v.1.2). Results suggest that regional groundwater flow may converge near the eastern boundary of the proposed repository. Local-scale variations in groundwater flow and infiltration resulting from possible dilation of joints and fractures (with concomitant increases in porosity and permeability) in the hangingwall blocks above a series of active normal fault was investigated using UDEC (v.2.01). These results are presented

---

[5]Ferrill, D.A., A.P. Morris, S.M. Jones, and J.A. Stamatakos. 1996. Geometric, thermal, and temporal constraints on the development of extensional faults at Bare Mountain (Nevada) and implications for seismicity in the Yucca Mountain region. *Geological Society of America Bulletin*. Submitted for publication.

[6]Rahe, B., D.A. Ferrill, and A.P. Morris. 1996. Physical analog modeling of pull-apart basin evolution. *Tectonophysics*. Submitted for publication.

[7]Stamatakos, J.A., C.B. Connor, and R.H. Martin. 1996. Quaternary volcanism and basin evolution of Crater Flat, Nevada, from detailed ground magnetic surveys of the Little Cones. *Journal of Geology*. Accepted for publication.

in section 3.3.6 and show significant dilation of fractures in the hangingwall block after each faulting event.

3.2 OBJECTIVES AND SCOPE OF WORK

The SDS KTI seeks to ensure that significant SDS conditions and hazards are identified, sufficiently understood, fully considered, and used appropriately to evaluate repository performance. This objective requires review and independent confirmation of data, numerical models and alternative conceptual tectonic, structural, and seismic models, and PA, PSHA, and PFDHA calculations. The scope of work includes review of the DOE documents, review of applicable peer-reviewed literature, meeting participation to discuss SDS related issues with the DOE, observation of quality assurance (QA) audits, and independent technical investigations. The independent technical investigations are designed to provide guidance to the NRC on critical SDS licensing issues and associated reviews of upcoming DOE reports, most notably the DOE PSHA and PFDHA, the DOE WCIS strategy, and SDS aspects of the DOE TSPA-VA. Forthcoming issue resolution reports are intended to be an integral programmatic component of the NRC effort.

Technical investigations by the CNWRA are based on geological and geophysical data; numerical, conceptual, and analog models; and deterministic and probabilistic fault and seismic analyses. These investigations provide important and independent results on SDS conditions that can ultimately be linked to iterative PA, PSHA and PFDHA. For example, recent geological and geophysical investigations of the BMF (Ferrill et al., 1996b) indicate fault slip-rates up to one order of magnitude greater than the DOE estimates (Pezzopane, 1995). These values provide independent assessments of faulting in the CNWRA PSHA and PFDHA. These fault slip estimates also provide alternative estimates of faulting in planned PA sensitivity studies of WP disruption using the FAULTING module, which will then feed into the iterative total performance assessment (TPA) calculations.

Issue resolution will be achieved when the following three conditions are met. First, the DOE has collected data of sufficient extent and quality to identify and characterize all significant Quaternary and contemporary SDS conditions and SDS hazards necessary to assess potential repository performance. Second, the DOE has evaluated relevant data and uncertainties and developed alternative conceptual models of the contemporary and projected seismo-tectonic systems and structural geologic features and conditions. Third, the DOE has appropriately integrated these data and concepts into its process models and assessments of future repository performance. SDS KTI work on resolution of the five subissues is so directed that, when resolved, they would provide a technical basis for reasonable assurance that public safety, health, and environmental protection standards will be met.

3.3 SIGNIFICANT TECHNICAL ACCOMPLISHMENTS

3.3.1 Tectonic Models

Staff members from the DOE, the NRC, the Advisory Committee on Nuclear Waste (ACNW), the Nuclear Waste Technical Review Board (NWTRB), the Electric Power Research Institute (EPRI), the CNWRA, the USGS, and the State of Nevada met in San Antonio on May 7–8, 1996 for an Appendix 7[8] meeting to discuss conceptual tectonic models of the Crater Flat-YM area. The meeting was initiated by

[8]Informal meetings between the staff of NRC and DOE for the purpose of information exchange.

the NRC and the CNWRA to facilitate resolution of this subissue. In this meeting, tectonic models proposed for the YMR were reviewed in the context of the most recent geological and geophysical data. Of the 11 tectonic models proposed, the DOE, the NRC, the CNWRA, USGS, and the State of Nevada informally agreed that only five were presently supported by existing data. Although this agreement on the remaining five models was not unanimous and the participants still disagree on the relative importance of each model, tentative agreement forms the basis for resolution of the subissue related to tectonic models. In addition, there was no general consensus on which models are truly independent and which may be subsets of others.

The SDS KTI refers to the five viable tectonic models as the

- deep detachment fault (12–15 km) model (Ferrill et al., 1996b, figures 2-3, 2-6)
- moderate detachment fault (6–8 km) model (Ferrill et al., 1996b, figures 2-3, 2-6)
- planar faults with internal block deformation model (Janssen, 1995)
- pull-apart basin model Fridrich (1996),[9] (McKague et al., 1996, figures 4-3, 4-7)
- Amargosa shear model (Caskey and Schweichert, 1992; McKague et al., 1996, figure 4-3)

In a broader sense, these five models can be considered in two general categories. The first three are dominantly related to extensional deformation and the latter two are dominantly related to strike-slip deformation. Moreover, the five models are not mutually exclusive. Locally extensional-dominated deformation (within Crater Flat, for example) can exist within a larger region of transtensional deformation related to a pull-apart basin. In addition, none of the viable tectonic models explicitly supports partitioning Crater Flat into separate magma-probability domains (in which the probability of magma is significantly lower at YM versus Crater Flat) as implied by recent DOE volcanic hazard assessments (e.g., Crowe et al., 1995).

3.3.2 Analog Modeling of Pull-Apart Basins

Of the five viable tectonic models, the pull-apart basin model proposed by the USGS Fridrich (1996)[10] and the Amargosa shear proposed by the State of Nevada (Schweickert, 1989) present the greatest seismogenic risks to overall repository safety and performance. These two models imply significant buried or blind seismic sources in Crater Flat adjacent to YM that are not currently accounted for in PSHA or in plans for repository design and operations. The nature of these risks has been the focus of the CNWRA analog model studies of pull-apart deformation. Specifically, scaled sandbox deformation experiments were conducted as analogs to the geologic evolution of pull-apart basins. From this modeled evolution, changes in seismic risks are inferred. By comparing the analog models to the geometry of faults in Crater Flat and the surrounding region, implicit seismic risks of the pull-apart and Amargosa Shear

[9]Fridrich, C.J. 1996. Tectonic evolution of the Crater Flat Basin, Yucca Mountain region, Nevada. Cenozoic Basins of the Death Valley Region. L. Wright, ed. *Geological Society of America Special Paper*. In press.

[10]*Ibid.*

models can be better constrained. Results presented here are a followup to preliminary results of Stamatakos and Ferrill (1996a). A more detailed description of the analog sandbox models and analyses of the evolution of pull-apart basins is given in Rahe et al. (1996).[11] Results from this work bear directly on subissues of the SDS KTI associated with (i) data, (ii) model verification, (iii) alternate conceptual models, and (iv) potential for disruption of WPs.

3.3.2.1 Sequential Development of Pull-Apart Basins

Pull-apart basins are structural depressions formed by localized extension along strike-slip fault zones (Burchfiel and Stewart, 1966). In the classic conceptual model of pull-apart basin formation (Burchfiel and Stewart, 1966), pull-apart basins form within the brittle crust above a horizontal detachment in the lower crust. Although active pull-apart basins can exist for millions of years, they are geologically transient features that evolve and eventually become inactive (Zhang et al., 1989). Pull-apart basin evolution can be divided into four steps: incipient, early, early mature, and late mature (figure 3-1).

Incipient pull-apart basins are characterized by initiation of closely spaced normal faults parallel to oblique steps between main strike-slip displacement zones that define the boundaries of a graben or half graben. Motion along faults is partitioned between normal and strike-slip faults in relatively small and unconnected individual fault segments (e.g., Stamatakos and Ferrill, 1996). Strike-slip faults are not recognizable within the pull-apart basin at the surface (figure 3-1a). Earthquake hazards are mitigated by fault segmentation in which rupture is limited to the isolated fault segments (Sibson, 1986). Normal and strike-slip faults are segmented from each other in the incipient and early stages of basin development.

During the early stage (figure 3-1b) basin-bounding normal fault systems are characterized by lateral variations of fault throw that produce localized relay ramps. Pull-apart basins exhibit additional normal faults toward the basin interior inward from the original bounding faults, as well as cross-basin strike-slip faults that cut diagonally across the basin interior (figure 3-1b). Relay ramps are described as accommodating displacement transfer from one fault segment to another, while maintaining continuity between the footwall and hangingwall (Peacock and Sanderson, 1991; Trudgill and Cartwright, 1994). Relay ramps form early in fault system development as individual normal faults increase rupture area and begin to interact, but prior to coalescence of the deformation onto a single through-going strike slip fault. Relay ramps also form along developing sections of normal faults that bound the growing pull-apart basin.

At the early and late mature stages (figures 3-1c and 3-1d), strike-slip and normal faults join to completely bound the pull-apart basin at the surface. Displacement associated with cross-basin faults causes development of a through-going strike-slip fault that defines these stages. This fault cuts through the center of the pull-apart basin, linking the two main strike-slip displacement zones and typically represents continued activity on segments of the original cross-basin faults and formation of new connecting strike-slip fault segments. This linking of main strike-slip displacement zones dramatically enlarges the overall fault area capable of rupture and thus increases potential for large-magnitude earthquakes. Late in this stage, normal faults bounding the outer margins of the basin commonly show a decrease in fault activity. This decrease consistently occurs on normal faults bounding the side of the pull-apart basins experiencing less strike-slip displacement relative to the fixed basement.

---

[11]Rahe, B., D.A. Ferrill, and A.P. Morris. 1996. Physical analog modeling of pull-apart basin evolution. *Tectonophysics*. Submitted for publication.

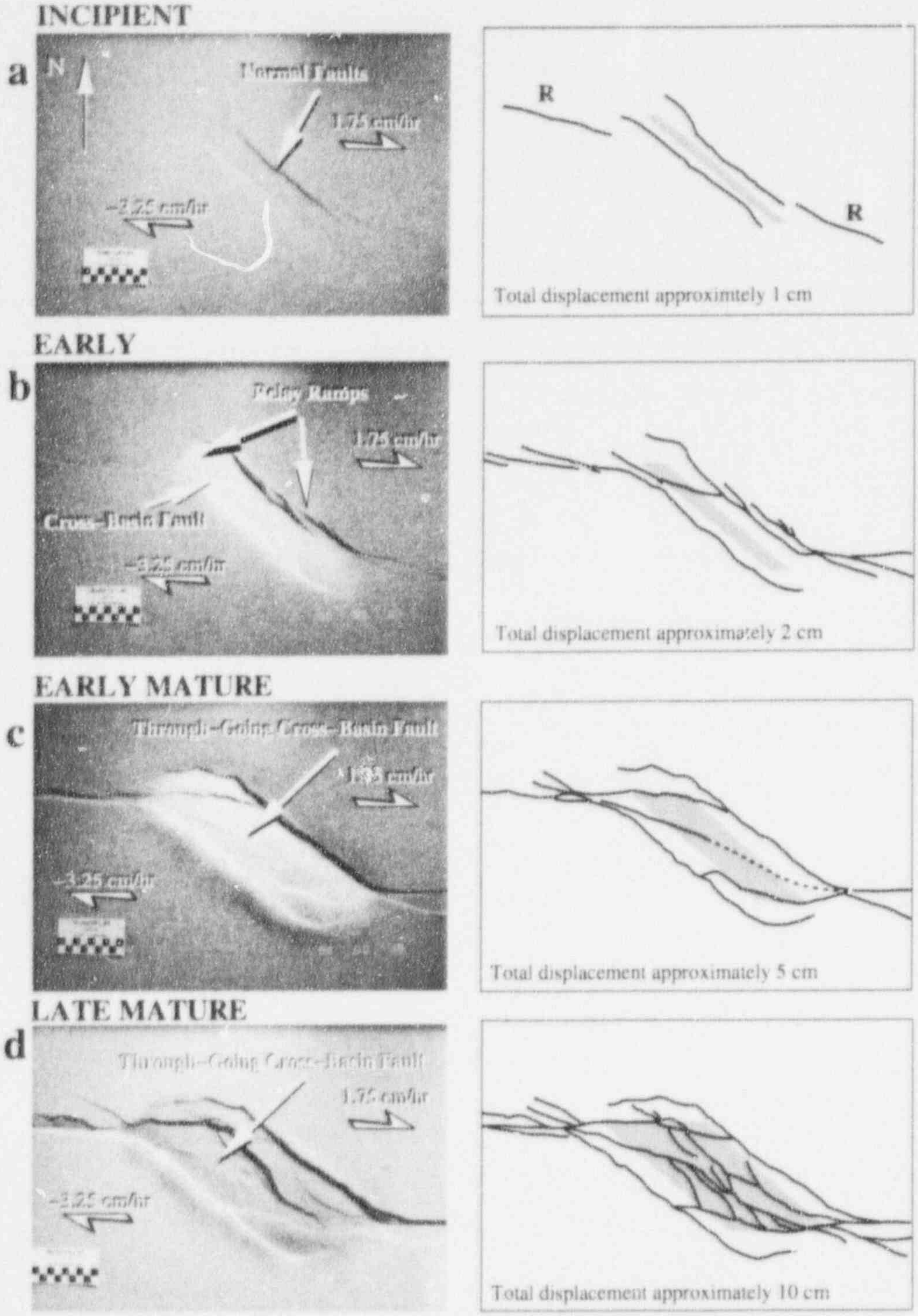

Figure 3-1. Photographs and corresponding line drawings showing evolution of a pull-apart basin from analog modeling experiments. Stages of development are (a) incipient, (b) early, (c) early mature, and (d) late mature. Shaded area in line drawings represents displacement at the base of the basin. R in line drawings are the expected Riedel shear orientation.

The observed evolution of pull-apart basins (e.g., Zhang et al., 1989) is favorably represented by sequential deformation of the CNWRA analog models. In these analog models, cross-basin faults formed as one or two separate small faults with orientations along the Riedel (R) shear orientation, 15° to the main shear direction. In the incipient stage, these cross-basin faults connected the tips (corners) of the basin with the center of the basin-bounding normal faults on the opposite margin of the basin (figure 3-1b). As further strike-slip displacement separated the active tips of the pull-apart basin (corresponds to bends in the controlling fault at deptn), the basin widened relative to its length. When the basin reached optimal configuration (with a length-width ratio of about 2.4:1.0), new cross-basin faults (which still formed in a R shear orientation) connected the active tips of the basin (figures 3-1c and 3-1d). These cross-basin faults effectively linked slip on the formerly segmented master strike-slip faults. The result is a single, through-going strike-slip fault system (with a large potential rupture plane and correspondingly large earthquake magnitude) and inactive basin bounding normal faults.

3.3.2.2 Implications to Seismic Hazard Analyses

Results from the analog models reinforce concerns about potential seismic hazards of strike-slip dominated tectonics (Stamatakos and Ferrill 1996; McKague et al., 1996). The primary concern for repository performance is the potential for significant blind seismic sources. Current DOE PSHA analyses do not include the potential for seismicity generated from blind faults (e.g., Wong et al., 1995). In addition, these models predict substantial strike-slip or oblique-slip deformation on most faults related to the pull-apart basin. Yet, in recent paleoseismic investigations that rely on trenching studies in alluvium (e.g., Klinger and Anderson, 1994) only fault throw (the vertical component of slip) is factored into estimates of recurrence and slip rate. The viability of the pull-apart or Amargosa shear models suggests paleoseismic investigations may underestimate fault activity.

The pull-apart model of Fridrich (1996)[12] proposes a highly elongated pull-apart rhombochasm or sphenochasm that extends from northern Crater Flat to the Death Valley-Furnace Creek fault system. This geometry corresponds to the incipient or young stage of pull-apart evolution (figure 3-1) where a significant fraction of deformation is accommodated by bounding normal faults. The master strike-slip faults and cross-basin faults are segmented, and considerable widening of the basin is required (roughly an additional 8 km of right slip on the Death Valley-Furnace Creek fault system) before the cross-basin faults could link the active tips at the corners of the basin. The most significant implication of this model to seismic hazard analyses is the potential of an earthquake on one of the cross-basin faults. These faults would have moderate rupture areas that would yield earthquakes with maximum moment magnitudes (M_m) of 6.6 to 6.8 (McKague et al., 1996). Because of their proximity to YM, however, such earthquakes have the potential to generate relatively large peak accelerations (0.76 g or larger) at the potential repository site (McKague et al., 1996).

In the Amargosa shear model, Schweickert (1989) envisions Crater Flat as a shear zone accommodating right-lateral shear on a proposed buried strike-slip system that trends northwest from southeast of Pahrump to northwest of the Miocene Caldera complex. Although Schweickert (1989) does not explicitly depict the shear zone as a pull-apart, it shares many structural features with a mature stage pull-apart basin. The Amargosa shear zone is interpreted to result from a releasing bend along a strike-slip fault system, and deformation is accommodated by a combination of strike-slip and extensional faulting.

---

[12]Fridrich, C.J. 1996. Tectonic evolution of the Crater Flat Basin, Yucca Mountain region, Nevada. Cenozoic Basins of the Death Valley Region. L. Wright, ed. *Geological Society of America Special Paper*. In press.

The most significant implication of this model is the potential for a large earthquake near YM. The size of the proposed Amargosa system is comparable to the Death Valley-Furnace Creek fault or to segments of the San Andreas. Thus the Amargosa shear has the potential for earthquakes with $M_m \geq 7.8$. Depending on how close the boundary of the proposed shear zone is located to the repository site, such a large earthquake could produce peak accelerations at the site well in excess of 1.0 g (McKague et al., 1996).

3.3.3 Mechanical (Numerical) Analyses of Faulting at Bare Mountain and Yucca Mountain

Most conventional PSHA estimate peak accelerations by assuming fault length and surface distance to source parameters. Based on these assumptions, paleoseismicity is reconstructed from the mapped trace-length of faults and recurrence estimates from fault-trenching studies. Recent earthquakes in the western United States, however, challenge these assumptions. The 1992 Landers earthquake ruptured along several previously distinct fault segments (with a surface magnitude Ms=7.6) that by themselves would not seem capable (based on their mapped trace-length) of generating such a large magnitude earthquake (e.g., Hart et al., 1993; Sieh et al., 1993; Sowers et al., 1994). In addition, the Landers earthquake was part of a coseismic sequence of earthquakes (see Ferrill et al., 1994 for summary) that apparently initiated with the Joshua Tree (Ms=6.3) earthquake on April 22, 1992 and terminated with the Little Skull Mountain (Ms=5.4) earthquake on June 29, 1992 (Harmsen, 1994). The 1994 Northridge (Ms=6.9) earthquake (Hauksson et al., 1995) occurred along a previously unmapped blind fault that did not produce any surface rupture and resulted in anomalously large near-field peak accelerations. The implication of these earthquakes to the potential HLW repository is that the DOE data used in YM PSHA may not accurately reflect future seismicity and thus has relevance to SDS KTI data subissue. Therefore, seismicity data used by the DOE in future PA and in evaluation of the WCIS hypotheses that the severity of ground motions expected in the repository horizon for tens of thousands of years will only slightly increase the amount of rockfall, and drift collapse may not be reasonably conservative. To investigate the significance of this potential data deficiency, mechanical analyses were conducted to simulate fault-slip on BMF. Specifically the following were examined:

- Distribution of fault displacement along the BMF; in particular, the relationship between magnitude of fault displacement at the ground surface (surface fault displacement), average fault displacement, and maximum fault displacement. In developing historical earthquake data based on observations of geologic structures, fault-rupture parameters such as surface fault displacement and rupture length are used in empirical relationships (e.g., Wells and Coppersmith, 1994) to estimate maximum earthquake magnitudes associated with existing faults. In these empirical relationships, however, it is not clear if there are significant differences among the earthquake magnitudes calculated using different fault-rupture parameters, such as fault rupture at depth.

- Distribution of ground-motion amplitudes to determine if the magnitudes of acceleration at the ground surface and at depths of 200–500 m are consistent with assumptions commonly made in developing ground-motion attenuation curves.

- Possibility that slip on the BMF could trigger slip on YM faults and how the potential for triggered slip may vary with the proposed geometry of the YM faults given in the moderate and deep detachment models.

Analyses were based on a model of the Bare Mountain-Yucca Mountain fault system; BMF is interpreted as a listric fault with a detachment at about 12 km depth and the YM faults are steeply dipping faults in the hangingwall (see figure 2-3, p. 2-6, Ferrill et al., 1996b). Two YM faults were modeled in the analyses, representing faults that terminate at either the steeply dipping (YM1) or detachment (YM2) segments of the BMF (figure 3-2). Analyses were conducted using the finite element code ABAQUS (v.5.5). Each fault was modeled as a 100 m thick zone of isotropic and elastic-plastic material with a yield strength defined using the Drucker-Prager failure criterion (e.g., Ofoegbu and Ferrill, 1995) and the surrounding rock mass isotropic and linear-elastic.

Each analysis was conducted in two steps. First, initial static equilibrium was established under a specified initial stress state (based on vertical stress gradient of 25 MPa/km and vertical-to-horizontal stress ratio of 1:0.25), gravitational body force, and boundary restraints. Second, a shear-stress pulse was applied over a selected (~ 2-km) segment of the BMF through dynamic analysis, thereby simulating the release of seismic energy over the selected fault segment (an earthquake) and the response of the model was monitored for about 10 s. The focus of the simulated earthquake (i.e., the fault segment over which the shear-stress pulse was applied) was varied to simulate a shallow-focus earthquake (Case sc01 at 1.5 km depth), an intermediate-focus earthquake (Case sc02 at 6 km depth), a deep-focus earthquake on steep fault segment (Case sc03 at 10 km depth), and another deep-focus earthquake on the detachment segment (Case sc04 at 12 km depth).

Results calculated from the model suggest values of earthquake magnitude based on empirical relationships with surface fault displacement (Wells and Coppersmith, 1994) give satisfactory estimates of potential earthquake magnitudes for moderate to deep sources on steeply dipping faults, but overestimate magnitudes for shallow sources and underestimate magnitudes for low-angle faults (table 3-1). The first two sets of values in table 3-1 are based on Wells and Coppersmith (1994) empirical relationships, whereas the third is based on Hanks and Kanamori (1979). The latter requires evaluation of seismic moment, based in part on the rupture area, A_r. Because A_r cannot be calculated directly from a two-dimensional (2D) model, its value is estimated from data on subsurface fault lengths and down-dip rupture lengths from Wells and Coppersmith (1994). As a result, a range of magnitudes (instead of a single magnitude) is presented for each case. The three methods of earthquake-magnitude calculation give similar values for Cases sc02 and sc03 (intermediate and deep earthquakes on steep-fault), while the magnitude based on surface displacement is too small for Case sc04 (low-angle fault) and too large for sc01 (shallow focus).

The model results also indicate that an earthquake originating on the BMF at a depth of 5 km or more produces larger ground motions at a distance away from the fault (in the YM area in this simulation) than near the surface rupture (in the BM region in this simulation). Figure 3-2 shows seismic energy from a planar source (such as a fault surface) travels away from the source along a path perpendicular to the fault. Because the source is not a point, as assumed in ground-motion attenuation functions, the wave paths are not attenuated spherically. The largest ground-motion amplitudes do not occur at the epicenter (directly above the focus) but at a point near the intersection of the fault normal plane (or line) that passes through the focus of the earthquake and the surface. Thus, maximum ground motions will not necessarily be at the epicenter but could occur a short distance away. For example, the magnitudes of ground acceleration illustrated in figure 3-2 are about 0.2–0.4 g (horizontal) and 0.2–0.5 g (vertical) in the YM area, but smaller than 0.1 g in the immediate vicinity of the surface trace of the BMF. Such a distribution of ground accelerations could not have been predicted using a ground-motion attenuation relationship that estimates maximum ground motions solely on site-to-source distance.

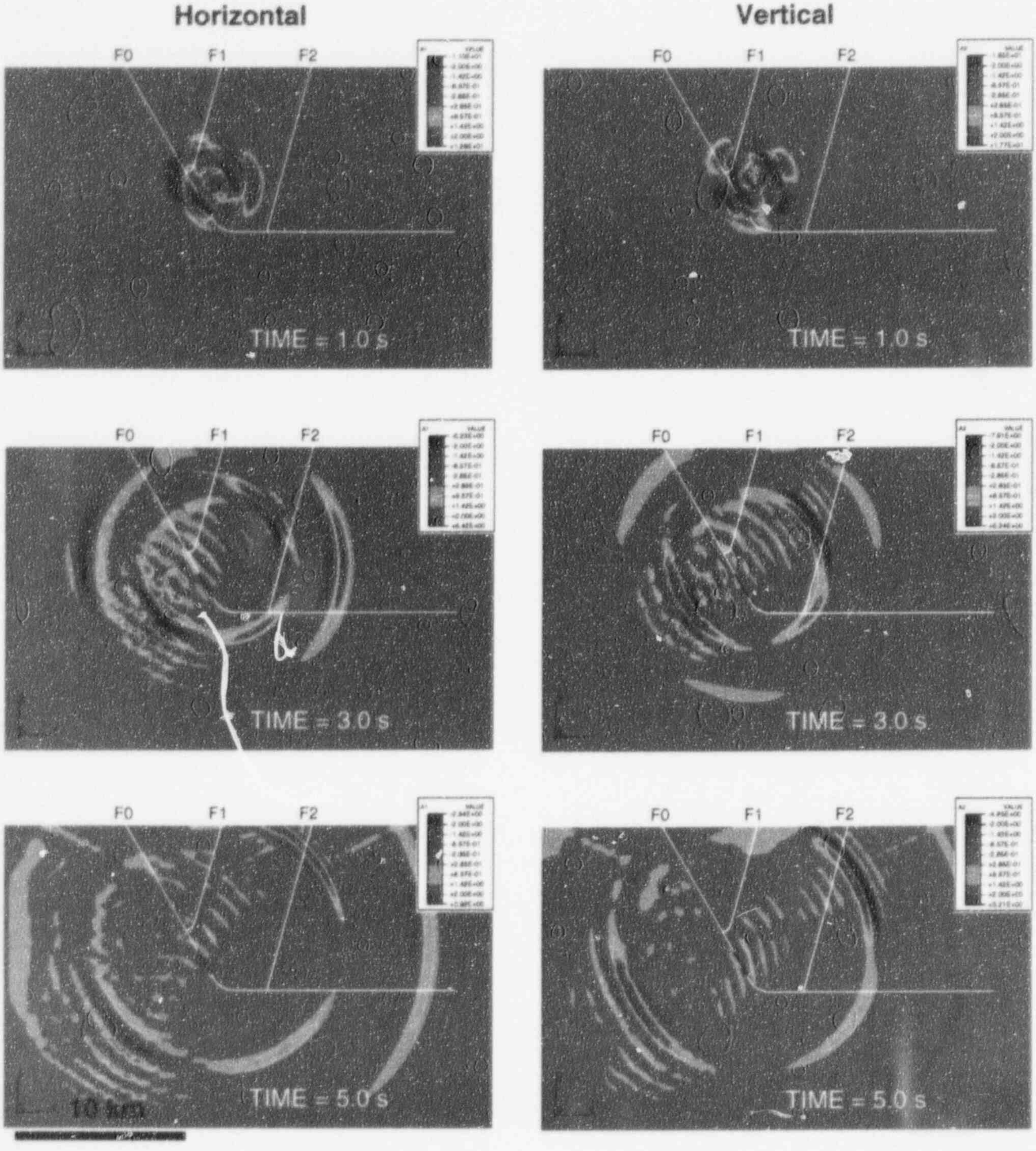

Figure 3-2. Contour of horizontal (left column) and vertical (right column) components of ground accelerations in m/s^2 for model case sc03. Plots are shown for times of one, three, and five seconds after the simulated seismic event. BMF is simulated along with the two subsidiary YM faults (YM1 and YM2). The source zone is shown by the dark line segment on the BMF. For horizontal accelerations, positive is toward the right and negative is toward the left; for vertical accelerations, positive is up and negative is down.

Table 3-1. BMF displacement, down-dip rupture length, and earthquake magnitudes

	Fault Displacement (m)				Magnitude Based On		
Model Case	Surface	Average	Maximum	DRL[1] (km)	Surface Displ.[2]	DRL[2]	Seismic Moment[3]
sc01	2.92	1.07	4.00	18.50	6.9	6.7	6.3 to 6.7
sc02	4.12	3.03	11.60	27.68	7.0	7.1	6.9 to 7.2
sc03	2.39	3.08	13.90	26.44	6.9	7.0	6.9 to 7.2
sc04	0.05	0.65	4.43	23.71	5.7	6.9	6.3 to 6.7

[1]Down-dip rupture length
[2]Moment magnitudes calculated from empirical formulas of Wells and Coppersmith (1994)
[3]Rupture area range calculated from ratio of subsurface rupture length and down-dip rupture width for normal fault data compiled by Wells and Coppersmith (1994). Moment magnitude is calculated from formulas of Kanamori and Anderson (1975) and Hanks and Kanamori (1979)

The model results also suggest that a BMF earthquake may trigger slip on YM faults, but for the modeled geometry of faults the magnitude of triggered slip is small compared to BMF slip. This may be a function of the sharp curvature of the listric portion of the BMF. Previous results from Ofoegbu and Ferrill (1995) suggest the likelihood of triggered slip is greater when the listric geometry of the BMF is more gently curved. For the four simulated earthquake cases (table 3-2), the largest triggered slip of 0.26 m occurs on YM2 (in response to a deep-focus earthquake originating from the steep segment of BMF). The shallow-focus case, sc01, does not induce measurable slip on the YM faults, whereas all other cases trigger slip. This suggests that an earthquake originating on the BMF at a depth of 5 km or more may produce measurable displacement on faults in the YM vicinity.

Collectively, these analyses suggest uncertainty in ground-motion attenuation functions, especially when used for sources in the near-field (i.e., for faults close enough to the site so they no longer can be considered point sources). Although earthquake magnitude estimation based on surface-rupture parameters may be satisfactory, ground accelerations calculated from these magnitudes in conventional ground-motion attenuation curves may underestimate peak ground accelerations at the proposed repository site because they fail to account for asymmetric radiation of seismic energy caused by the geometry of the seismic source. Future effort in the SDS KTI will be directed toward investigating the relationship between ground accelerations calculated in the numerical model and those calculated using empirical ground-motion attenuation relationships.

Table 3-2. Fault displacements on YM faults triggered by slip on BMF

	Fault F1 (Figure 3-2)		Fault F2 (Figure 3-2)	
Model Case	Surface Displacement (m)	Maximum Displacement (m)	Surface Displacement (m)	Surface Displacement (m)
sc01	No Slip	No Slip	No Slip	No Slip
sc02	0.09	0.13	0.04	0.05
sc03	0.02	0.13	0.26	0.26
sc04	0.06	0.10	0.02	0.07

3.3.4 Type I Faults

Adequate PSHA and related faulting and seismic hazard analyses require consideration of only those faults in the YMR posing significant potential risk to long-term waste isolation and short-term safety and retrievability objectives specified in the Title 10 Code of Federal Regulations (CFR) 60.111, 60.112, and 60.113. Identification of these faults is also important to design criteria for the Geologic Repository Operations Area (GROA) that require design of structures, systems, and components so anticipated natural phenomena (e.g., vibratory ground motion or direct repository rupture from slip on active faults) will not interfere with necessary safety functions [10 CFR part 60.131(b) (1)].

The criteria for selecting Type I faults (i.e., those that could affect repository design or performance) are from McConnell et al. (1992). Application of those criteria to the more than 400 faults within a 100 km radius of YM indicates that 52 faults may be considered Type I faults (McKague et al., 1996). McKague et al. (1996) serves as the focus for issue resolution with the DOE regarding Type I faults and provides a technical basis for the NRC evaluation of the DOE submittals. Issue resolution, however, only addresses the effects of seismicity that may be important. It does not include resolution on rates or recurrence of faulting or on faults that may serve as pathways or barriers to groundwater or magma flow, heat, or refluxation.

McKague et al. (1996) reports three main findings. First, the report develops a database of 52 Type I faults. Significant faults not considered Type I faults are the Pagany Wash, Sever Wash, and Yucca Wash faults. Despite having surface areas capable of producing peak accelerations greater than 0.1 g at YM, these faults lack evidence of significant Quaternary slip and have unfavorable orientations for slip in the current stress field. Beatty Wash Scarp is the only remaining Type II fault (i.e., there was insufficient data available to determine whether it is Type I or not) because differing opinions of its origin exist (it may not be a fault). Of the 52 Type I faults, the 24 capable of generating peak accelerations greater than 0.3 at the site all lie within a 10 km radius of YM. Important faults more distant from the potential repository include the BMF, Stagecoach Road, and Rock Valley faults, all capable of generating peak accelerations at YM greater than 0.25 g.

Second, the likelihood for slip within the present *in situ* stress state was estimated. Review of slip tendency for the YMR shows that nearly all faults at YM have relatively high slip tendency values in the current *in situ* stress field, except northwest trending faults. In the current stress state, maximum and intermediate principal stresses have nearly equal magnitudes. Thus, N trending right-lateral strike-slip, NNE trending left-lateral strike-slip faults and NE trending normal faults could slip without significant changes in the regional stress as observed in the aftershock sequence following the 1992 Little Skull Mountain earthquake. In addition, slip tendency analysis performed on several alternative cross sections (drawn across Crater Flat from BM to Jackass Flat) indicate active faults penetrating the entire thickness of the brittle crust pose the most significant potential seismic hazard. In contrast, faults that intersect a detachment at shallower crustal levels (e.g., at ~7 km depth) or where deformation is greatest at the surface and diminishes with depth, have limited potential as seismic hazards.

Third, additional constraints on fault and seismic hazard assessment were evaluated in light of alternative tectonic models and fault scaling relationships. For example, scaling relationship of fault-trace length versus cumulative vertical displacement (throw) indicates that most faults in the YMR fall within the expected range established from fault data sets worldwide. Mapped trace-lengths of the BMF, Windy Wash (WW), and Ghost Dance (GD) faults are anomalous. The mapped trace-length of the BMF is anomalously short for its cumulative offset and thus a longer BMF needs to be considered in future seismic hazard analyses. In contrast, the mapped trace-length of the WW and GD faults are too long for their accumulated throws, suggesting that either the offset estimates are too small or these faults are actually composed of a series of smaller distinct fault segments. If the latter is correct, then maximum moment magnitude and peak accelerations estimated from these faults may presently be overestimated because lengths used in the attenuation functions are too long.

3.3.5 Dilation-Tendency of Faults and Fractures and Implications for Groundwater Flow in the Yucca Mountain Region

Technical questions about the influence of faulting and fractures on groundwater flow relate to SDS KTI subissues involving tectonic models and disruption of flow. In addition, these analyses are critical to the evaluation of the DOE WCIS hypotheses on containment, radionuclide mobilization, radionuclide transport, and dilution.

Groundwater in the volcanic tuffs of YM and in the regional aquifer system consisting of Paleozoic strata is dominantly transmitted through networks of fractures. The fractures in tuff are the products of thermal contraction (cooling), tectonic deformation, and unloading. Fractures in the Paleozoic strata of the regional aquifer system are dominantly from tectonic deformation. Field observations from tuffs at YM suggest that dilation of fractures may change with time and is dependent on the stress field. In general, a propagating extension fracture will terminate against an older extension fracture that is open. An open fracture dissipates the high crack-tip stresses associated with propagating fractures, causing a younger extension fracture (joint) to abut pre-existing fractures. In the case where an earlier fracture is tightly closed due to high normal stress across perfectly matched surfaces or the fracture is healed by a mineral filling (vein), the propagating fracture may continue across the earlier fracture producing a mutually cross-cutting relationship. Faults (shear fractures), however, are typically capable of cutting earlier unfilled joints.

Studies of rock pavements at YM revealed three sets of cooling joints and at least three sets of tectonic joints (Barton and Hsieh, 1989; Barton et al., 1993; Throckmorton and Verbeek, 1995; Sweetkind

and Williams-Stroud, 1995), Sweetkind et al. (1996).[13] Because cooling joints were the first to form, the fractures of the first set of cooling joints (C1) tend to be relatively long and continuous compared with other fractures. Fractures of the first set of tectonic joints (T1) generally trend N-S, tend to be relatively long and commonly cross cooling joints (e.g., C1). The number of T1 joints appears to be inversely proportional to the number of cooling joints (Throckmorton and Verbeek, 1995). This observation suggests that extensional strain (dilation) may have been locally accommodated by dilatant reactivation of cooling joints rather than formation of new tectonic joints. The most prominent sets of later tectonic joints are the NW-trending T2 set and NE-trending T3 set. T2 and T3 joints typically abut cooling joints and pre-existing (T1) tectonic joint sets.

Dilation-tendency (tendency for dilation in the direction normal to a fracture plane) is by definition high at the time of extension fracture formation. It appears that cooling joints were relatively tightly closed at the time of formation of crossing T1 joints but may have later reopened. Dilatant reactivation of cooling joints would explain the complex abutting relationships with later tectonic joints (e.g., crossing of T1 joints versus abutting of T2 and T3 joints). Furthermore, some cooling joints and early tectonic joints were apparently reactivated as small displacement faults that may have caused formation of ancillary fractures (e.g., T, R, and R′ shears) which may explain localized development of additional tectonic fracture sets Sweetkind et al.(1996).[14] Early formed fractures (e.g., cooling joints), or fractures that encounter no barriers to propagation (e.g., T1 joints that cross cooling joints) will typically be the most continuous and may, if open, present preferential pathways for groundwater flow. These may, if open, represent fast pathways for radionuclides, but could also favorably prevent pooling of groundwater around WPs by draining groundwater from the proposed repository horizon.

3.3.5.1 Dilation-Tendency

Fracture aperture depends on fracture dilation, mismatched irregularities on the fracture walls, presence of mineral fillings and coatings or wall-rock material within the fracture, and the resolved normal stress (the stress acting perpendicular to the fracture surface to close the fracture). Fractures within a 3D stress field experience a normal stress determined by the magnitudes and directions of the principal stresses in relation to the plane of the fractures. The ability of a fracture to open (dilate) and transmit fluid is directly related to the normal stress acting across the fracture as well as the fluid pressure. Once formed or opened a change in the stress field can cause the effective normal stress to close the fractures, unless the fractures are propped open (i.e., by fragments of wall rock within the open fracture, precipitated mineral coating on fracture walls, or offset of irregular fracture walls) so that opposing fracture surfaces do not match across the fracture. The magnitude of the normal stress can be computed for surfaces of all possible orientations within a known or hypothesized stress field that can be normalized by comparison with differential stress. Dilation-tendency (T_d) for a surface is defined (Ferrill et al., 1995) as

---

[13]Sweetkind, D.S., S. Williams-Stroud, and J. Coe. 1996. Characterizing the fracture network in the unsaturated zone at Yucca Mountain, Part 1. Collection and interpretation of geologic data: Case studies. T.E. Hoak and P.K. Blomquist, eds. Fractured Reservoirs: Descriptions, Predictions, and Applications: Rocky Mountain Association of Geologists 1996 Guidebook. In press.

[14]*Ibid.*

$$T_d = (\sigma_1 - \sigma_n)/(\sigma_1 - \sigma_3) \qquad (3\text{-}1)$$

Analysis of dilation-tendency can be used to evaluate populations of existing faults and fractures that may act as pathways for fluid flow. Additionally, dilation-tendency analysis can be used to assess relative risks of magma injection along existing faults. This application is described in chapter 2.

Two factors, with respect to *in situ* stress and fractures, may contribute significantly to anisotropy of transmissivity in fractured rock. First, existing fractures that are at a high angle to the maximum horizontal stress may be preferentially closed by the maximum horizontal stress, thereby reducing transmissivity parallel to the minimum *in situ* stress (Ferrill et al., 1995; Wittmeyer et al., 1994; Wittmeyer and Ferrill, 1994). New fractures will form in orientations parallel (model 1 tensile fractures) or at a relatively low oblique angle (<45°; model 2 shear fractures) to the minimum principal stress. In either case, the *in situ* stress directly affects fracture orientation, fracture aperture, and resulting bulk transmissivity of the rock. Transmissivity will tend to be relatively higher in the plane normal to the minimum principal stress direction. Analysis of dilation tendency of natural fractures in granite at the Juktan underground hydroelectric power plant in northern Sweden (Carlsson and Olsson, 1979) showed close agreement with both measured transmissivity anisotropy and observed groundwater flow into tunnels along fractures (Ferrill et al., 1995).

3.3.5.2 Dilation-Tendency Analysis of Yucca Mountain Area Faults and Fractures

Dilation-tendency analysis of faults and fractures at YM was performed to evaluate the relative likelihood for fractures or faults to dilate in the contemporary stress field. Estimates of contemporary stress in the YM area consistently indicate that the regional minimum principal stress (σ_3) is horizontal and trends W-NW and the maximum horizontal stress (τ_1) is horizontal and trends N-NE (Zoback et al., 1981; Zoback, 1992; Zoback et al., 1992; Stock et al., 1985; Harmsen 1994; Morris et al., 1996). Stress estimates indicate the YM stress regime may be intermediate between a normal faulting regime, typified by vertical σ_1 and a strike-slip faulting regime characterized by vertical σ_2. Dilation-tendency analysis was performed assuming the maximum principal stress is vertical, the minimum principal stress is horizontal trending 120°, and the intermediate principal stress (maximum horizontal stress) is horizontal and trending 030°. The resulting analyses illustrate that subvertical fractures and faults that trend 030° have the highest dilation-tendency and there is a range of strikes of ±35° and dips of between 65° and 90° where fractures have >80 percent of the maximum possible dilation-tendency within the stress field. Dilation-tendency is independent of scale and may apply to small joints or major faults. Dilation-tendency analysis of faults in and around YM illustrates an abundance of N-NE trending faults that have high dilation-tendency (figure 3-3).

3.3.5.3 Sensitivity Analysis of Transmissivity Anisotropy on Groundwater Flow

In developing maps depicting the regional groundwater flow regime for a laterally extensive area, it is usually assumed that flow is perpendicular to potentiometric contours. The direction of flow and driving force (negative gradient of the potentiometric surface), however, are only parallel if the transmissive properties of the aquifer are isotropic or if the driving force is everywhere parallel to either the major or minor semi-axes of the transmissivity tensor. Geologic evidence indicates flow in the aquifers in the YM area is primarily through fractures and faults, some of which have been widened by dissolution

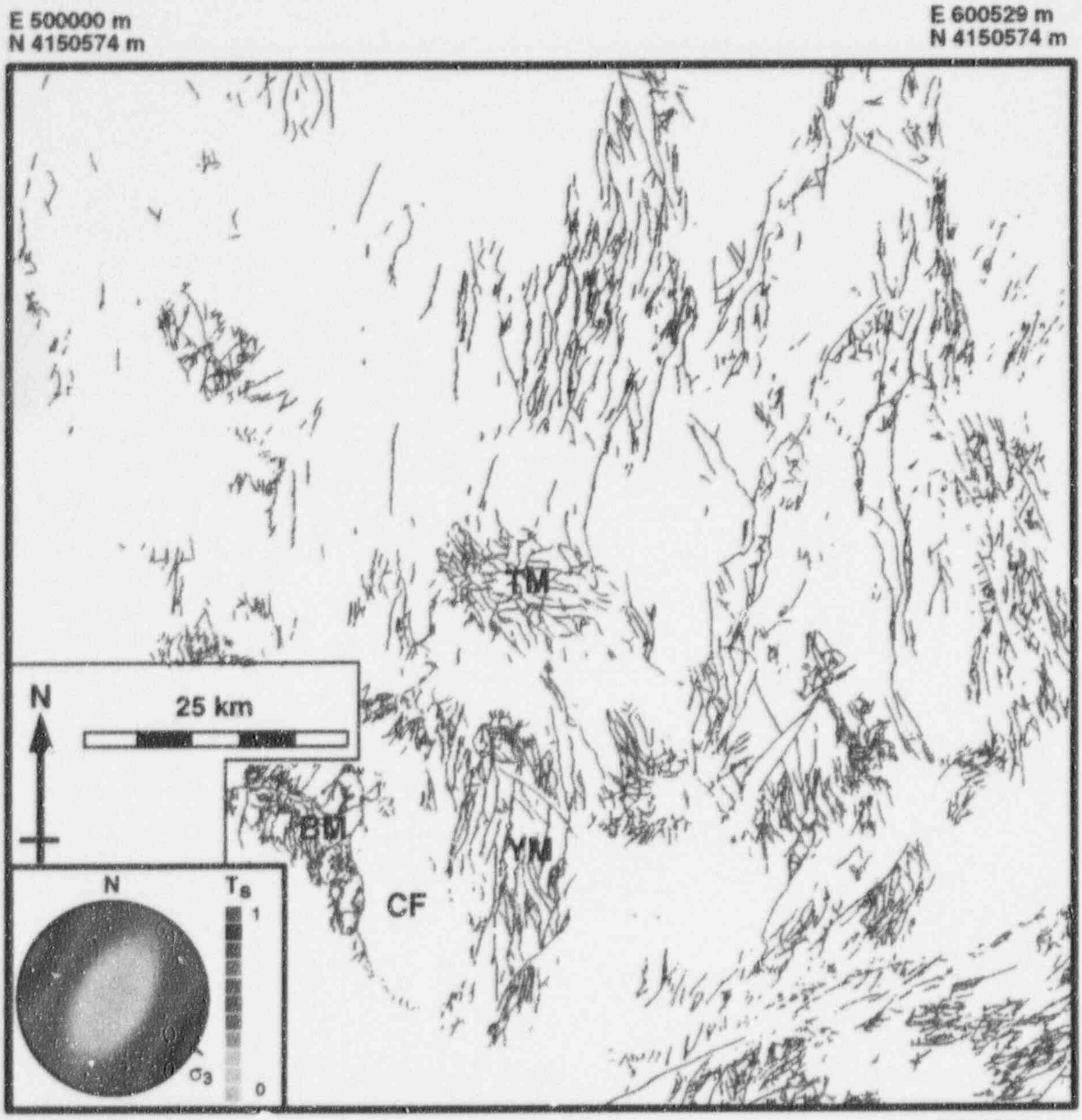

Figure 3-3. Dilation-tendency analysis of faults in and around YM based on fault maps (Frizzell and Schulters, 1990; Monsen et al., 1992; and Sawyer et al., 1995)

in carbonate rocks. Fractured aquifers most commonly have anisotropic transmissivity. The orientation of the horizontal stress ellipse is herein used to analyze the sensitivity of transmissivity anisotropy, assuming that fracture frequency or aperture and therefore transmissivity is affected by the contemporary stress field. Analyses of subregional flow directions were conducted following the approach of Wittmeyer et al. (1994) and Wittmeyer and Ferrill (1994). The subregional potentiometric surface was constructed from the interpreted steady-state water levels measured in and around YM (after Wittmeyer et al., 1995). Contouring the potentiometric surface illustrates the steep hydraulic gradient north and northeast of YM and an area of very low gradient beneath Fortymile Wash and Jackass Flat. In the study area, the saturated zone is within fractured Tertiary tuff and Paleozoic strata, however, the water table is in alluvium at the southern end of Jackass Flat.

A contaminant plume released into the saturated zone beneath the proposed repository site would be expected to move SE away from the potential repository to Jackass Flat and turn south beneath Jackass Flat and migrate to Amargosa Valley. Assuming anisotropic transmissivity in the fractured aquifer (maximum transmissivity parallel to τ_1) flow directions will rotate toward τ_1. Because of curvature of potentiometric contours at YM, modified flow directions produce local variations in flow direction that may serve to focus or channelize flow. The results illustrate (figure 3-4) that flow pathways in the vicinity of the proposed repository site show a marked convergence near the eastern edge of the proposed repository site. The result has two important implications for performance. First, converging flow near the proposed repository would reduce the area where lateral spreading of released radionuclides would occur, and thus may reduce dilution. Second, a contaminant plume localized along fractures could be exceedingly difficult to recognize and monitor unless a monitoring well was favorably placed directly along a flow pathway. This channelization mechanism is of course highly dependent on existing sets of open fractures, orientation of the stress tensor, and magnitude of the resulting transmissivity anisotropy.

Recent multiwell pumping tests at the C-Well complex (conducted by USGS for the DOE) indicate that the local maximum transmissivity lies along the NW trending axis between wells C-2 and C-3, a distance of 30 m. This is contrary to the results presented here but is not all that surprising because the C-Well test is only indicative of local variations in fracture intensity and orientation. Interpreting hydraulic properties of a fractured aquifer via continuum theory requires fracture density within the test area large enough for the fractured aquifer to be considered a porous medium. At the 30-to-70 m scale of the C-Well complex, there may be too few fractures to validate the results presented previously, which are based on a view of fractures as a continuum. The phenomena described in this section need to be tested at a scale larger than that at the C-Well complex.

3.3.6 Hangingwall Deformation from Normal Faulting—UDEC (v.2.01) Modeling Calculations

Fault related deformation in fault blocks and fault zones can cause significant changes in fracture aperture, thereby altering porosity, permeability, and hydraulic conductivity. Zhang and Sanderson (1996) studied fluid flow and deformation in regions of jointed rock around extensional faults and observed that during faulting, significant dilation and fluid flow occurred in vertical-subvertical joints in the hangingwall and within the fault zone itself. Because the near surface tectonic setting at YM is characterized by a system of extensional faults (e.g., Scott, 1990), increases in permeability and fluid flow in the hangingwall from normal faulting could facilitate flow of groundwater at YM, especially drainage of perched water. The purpose of SDS KTI work was to investigate this possibility and to evaluate its significance to waste isolation at YM.

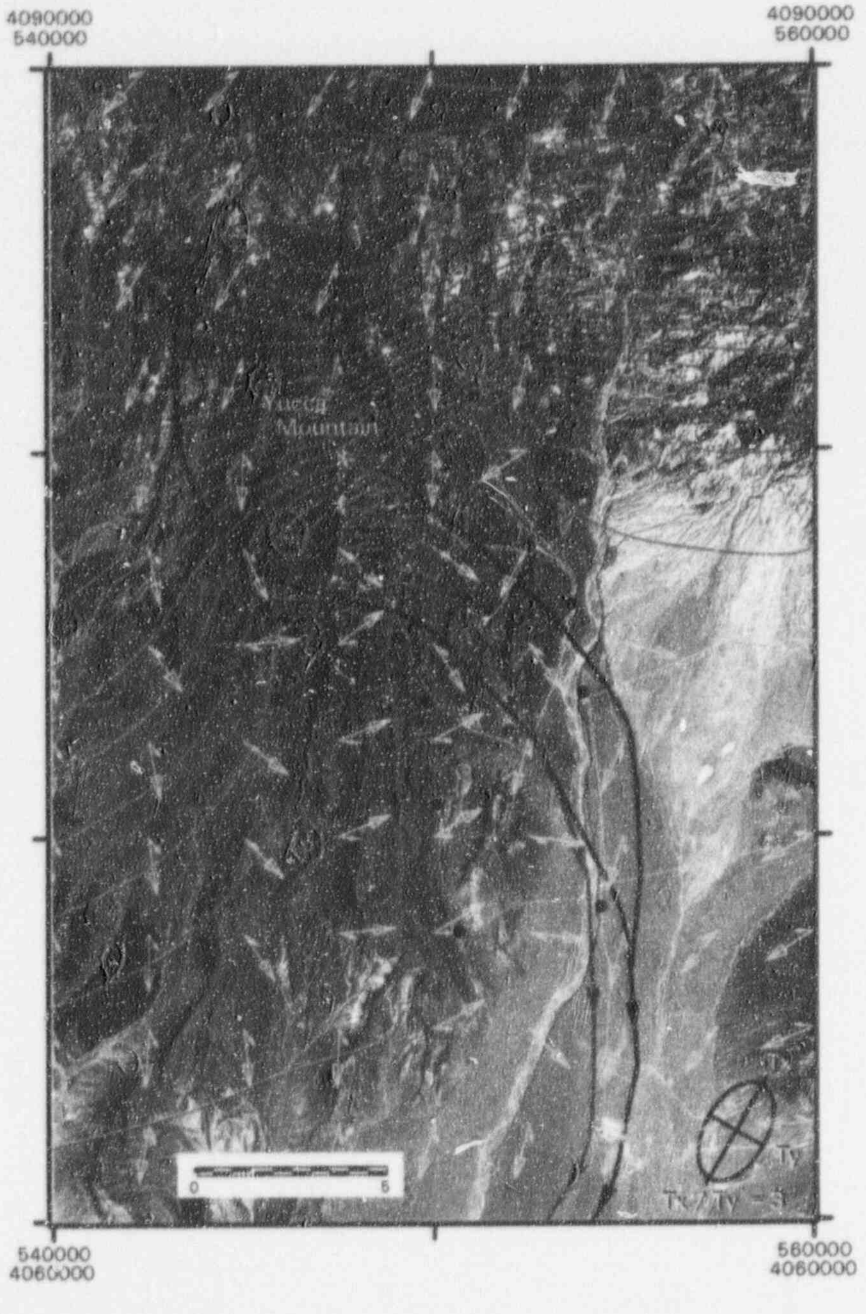

Figure 3-4. Contours representing potentiometric surface based on interpreted steady-state water levels (after Wittmeyer et al., 1995) overlaid on Landsat Thematic Mapper image. Short arrows indicate flow directions (driving force) assuming isotropic transmissivity; long arrows illustrate flow directions assuming a horizontal transmissivity ratio of three ($\tau x/\tau y = 3$) with maximum principal transmissivity parallel to the maximum horizontal stress direction. Black dots show well locations.

The 2D models were analyzed using the distinct element code UDEC (v.2.01) (Itasca Consulting Group, Inc., 1993) in which a fracture porosity and fully coupled mechanical-hydraulic analysis is performed assuming impermeable blocks (i.e., water flows through fractures only). The first model was a modification of the 50×40 m rectangular model used by Zhang and Sanderson (1996). The second model was a simple fault model based on an east-west cross section through the proposed repository taken from the CNWRA 3D geological framework model for YM (Stirewalt and Henderson, 1995b). The model configuration consisted of three fault zones and two joint sets (vertical and horizontal at spacings of 100 and 200 m above an unjointed basement (figure 3-5a). The fault zones modeled were analogous to the Solitario Canyon (SC), GD, and Bow Ridge (BR) faults. Each fault is represented as a 75 m wide zone and modeled as a highly fractured zone with two joint sets parallel and perpendicular to the fault zone. Mechanical and hydrologic properties are assumed to be similar to the Topopah Spring welded tuff (Ahola et al., 1996). The *in situ* stresses include vertical stress caused by gravitational loading and horizontal stress related to vertical stress by an assumed Poisson's ratio. Fluid pressure in the model is assumed to be hydrostatic.

The first model was simulated following the sequence described by Zhang and Sanderson (1996). Simulation of the YM fault model started with an initial stage to achieve steady-state mechanical and hydraulic conditions followed by 1 m displacement of three fault zones in a predefined sequence. Displacement of each fault zone was simulated by allowing vertical movement of the basement beneath the hangingwall region to produce 1 m of slip parallel to the fault zone. Changes in porosity associated with each fault slip were then estimated. Such changes do not reflect porosity changes that may occur in geologic time between successive fault slip events.

Simulation of the first model basically reproduced the results obtained by Zhang and Sanderson (1996). Similar results were also observed in the YM fault model simulation. Figures 3-5b through 3-5d show the distribution of joint apertures after each fault slip in the sequence of BR, GD, and SC, where the thickness of solid lines is proportional to the magnitude of joint aperture. Joint dilation from slip of BR mainly occurred between the GD and SC faults in the hangingwall close to each fault zone and within each fault zone (figure 3-5b). About 100 percent increase in overall porosity was observed in regions between and within the fault zones. Although joint dilation occurred mainly on the vertical joints, some degree of increased dilation was also observed on the horizontal joints. Slip of GD resulted in greater dilation of fractures and joints in the areas between fault zones and within GD and SC faults (figure 3-5c). The combined effect of slip on the BR and GD faults resulted in a more than 150 percent increase in porosity. Slip of SC fault mainly increased joint apertures in its hangingwall with little change in its footwall (figure 3-5d). The calculations only address the potential for change immediately following a normal earthquake. Other processes that could reduce porosity, such as fracture filling or the compressive effects of *in situ* stresses, are not considered.

Two additional simulations were conducted with 1 m slips of each fault in the sequences, GD-SC-BR and SC-GD-BR, to study the effects of slip sequence on dilation. Both these scenarios resulted in more aperture dilation in the area between GD and SC faults and less aperture dilation in the area between GD and BR faults and along horizontal joints. In summary, fault-slip appears to increase joint apertures, especially along vertical joints and existing fault zones in the hangingwall of the fault zone that slipped. The amount and location of fracture dilation also appear to be sensitive to different slip sequences. The resulting magnitude and distribution of joint apertures change depending on relative locations of the fault zones. Further analyses need to be performed to better understand faulting-induced aperture changes. These include investigations of the (i) effect of fault zone structure and irregularities in fault geometry; (ii) inclusion of stratigraphic information specific to YM, especially existing joint patterns in each thermal-

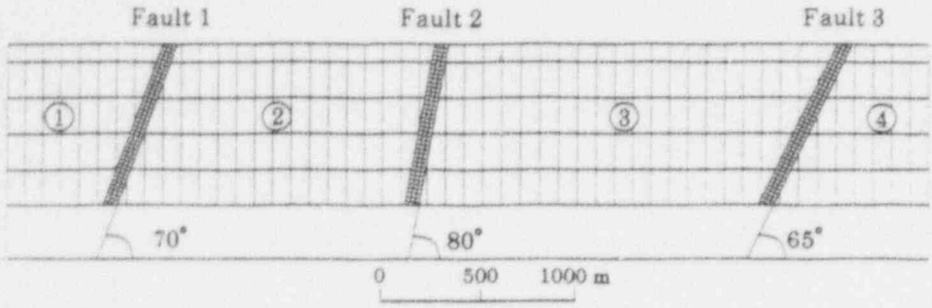

(a) Model Geometry and Mesh

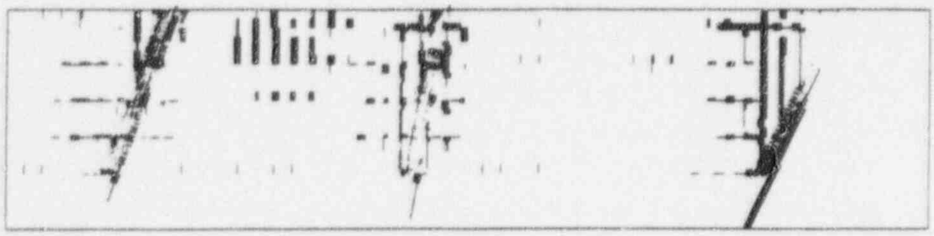

(b) After slip on Fault 3 only

(c) Slip on Fault 2 after slip on Fault 3

(d) Slip on Fault 1 after slip on Faults 2 and 3

Figure 3-5. Geometry of YM fault used in UDEC (v.2.01) modeling. (a) Model consists of three fault zones, SC, GD, and BR faults and two regional joint sets (vertical and horizontal) above an unjointed basement. Cross section shows location and thickness of joints (solid lines) after 1 m slip of the BR fault, (b) after 1 m slip of the GD fault, and (c) after 1 m slip of the SC fault (d).

mechanical unit; (iii) modeling of unsaturated flow to simulate drainage of perched water; and (iv) effects of a significantly large population of fractures and joints in the model. In addition, the methods in which fault slip and the associated boundary conditior- were applied needs to be explored further to more closely simulate fault slip that occur *in situ*.

3.3.7 Summary

Technical investigations by the SDS KTI addressed components of all five subissues deemed essential to resolution of the SDS KTI primary objective—evaluation of the effects of SDS and related hazards on safe disposal of HLW at the proposed YM repository. Technical work presented in this report represents significant progress toward resolution of these five subissues. Activities summarized in this chapter include overviews of the identification of Type I faults (McKague et al., 1996) and identification of viable conceptual tectonic models of the YMR. In addition, technical investigations on (i) analog models of pull-apart basins, (ii) numerical modeling of faulting at BM and YM, (iii) dilation-tendency analysis of faults and fractures and implications for groundwater flow in the YMR, and (iv) hangingwall deformation from normal faulting are presented.

To facilitate resolution of the ACM subissue, the NRC and the CNWRA convened an Appendix 7 meeting on May 7-8, 1996 with technical representatives from the DOE, USGS, ACNW, NWTRB, EPRI, and the State of Nevada. A dozen tectonic models proposed for the YMR were reviewed in terms of the most recent geological and geophysical data. Informal agreement among meeting participants was reached that five models are presently supported by the existing data, although agreement on the five models is not unanimous and the participants still differ on the relative importance of each model. Of these five models, the two proposed by representatives of the State of Nevada and the USGS [Crater Flat (CF) is interpreted as a pull-apart basin] pose the greatest seismic risk because of the potential for blind or buried faults not currently accounted for in the DOE PSHA.

The CNWRA investigations examined development of pull-apart basins through a series of analog sandbox experiments constructed to simulate strike-slip deformations like those proposed for Death Valley and CF. Results of the experiments show that evolution of pull-apart basins can be characterized in four stages (incipient, early, early mature, and late mature). The relative level of seismic hazard potential appears to vary significantly during this evolutionary sequence. Greatest risk is during the mature stage. The cross-basin faults can be linked directly with the master strike-slip fault forming a single, thoroughgoing structure with the potential for large-magnitude earthquakes. Comparisons of the analog models to the tectonic models show that the so-called Amargosa Shear model (Schweickert, 1989) presents the greatest potential seismic risk. In that model, CF is envisioned as a right-lateral (clockwise) shear zone very similar to a mature pull-apart basin. Proposed concealed faults beneath CF would be capable of earthquakes with maximum magnitudes in excess of M_m=7.8 (McKague et al., 1996). In contrast, the sphenochasm model Fridrich (1996)[15] would best correspond to an incipient or early mature pull-apart and thus would present a less hazardous alternative to the Amargosa Shear model. However, even in this tectonic model, the potential for seismicity on concealed cross-basin faults near the repository remains an important consideration in PSHA.

---

[15]Fridrich, C.J. 1996. Tectonic evolution of the Crater Flat Basin, Yucca Mountain region, Nevada. Cenozoic Basins of the Death Valley Region. L. Wright, ed. *Geological Society of America Special Paper*. In press.

Identification of only those faults in the YMR that pose significant potential risk to repository performance (i.e., Type I faults) is an integral component of an adequate PSHA. The SDS KTI has identified 52 Type I faults from the more than 400 faults within a 100 km radius of YM (McKague et al., 1996). This analysis provides guidance to the NRC for resolution of this aspect of the data subissue and for upcoming review and comment on the DOE PSHA. In addition to the criteria in NUREG-1451 (McConnell et al., 1992), McKague et al. (1996) used an analysis of fault slip from 3DStress (v.1.2) to assess the seismic potential of faults within the current, *in situ* stress state.

Finite element modeling using ABAQUS (v.5.5) was performed to investigate seismicity and faulting along the BMF. Results indicate that earthquake magnitudes estimated from surface offsets are reasonably representative for moderately deep earthquakes on steeply dipping portions of the fault plane but appear to overestimate magnitudes of shallow earthquakes and underestimate magnitudes of deep earthquakes on low-angle segments of the fault. The models also suggest that for the assumed deep detachment geometry with narrowly confined listric curvature, slip on the BMF does not produce appreciable compensatory slip on YM faults. The most significant result of the modeling is that radiation patterns of seismic energy may be anisotropic so that the largest ground-motion amplitudes do not occur at the epicenter but at a point between the epicenter and the intersection of a line or plane normal to the fault-plane originating at the earthquake focus and extending to the surface. Given the geometry of an east-dipping BMF, peak accelerations may be highest near YM for an earthquake at BM because seismic energy from slip on the BMF at depth radiates to the surface towards YM. The implication of this result is that predicted ground accelerations derived from traditional attenuation functions may significantly underestimate expected peak accelerations from sources in the near-field (near the fault).

Dilation-tendency analysis was used to evaluate the potential effect of horizontal stress on groundwater flow. Modeling indicates that flow pathways converge near the eastern boundary of the proposed repository site. Implications of this result are (i) convergence would limit lateral spreading of any contaminated plume near the site, thereby reducing dilution, and (ii) a plume localized along fractures, like the one predicated in the models, would be difficult to recognize and assess in PA calculations. The models show that localization along fractures is highly sensitive to the orientation of existing fracture sets relative to the orientation of horizontal stress. These results suggest that dilution may be reduced, limiting dilution as a favorable condition as indicated in the DOE WCIS (U.S. Department of Energy, 1996).[16]

Models of YM faulting were also analyzed using the distinct element code UDEC (v.2.01) to investigate the possibility that normal faulting could alter groundwater flow patterns in the hangingwall blocks above active normal faults. Impermeable blocks that restricted flow to fractures and joints were modeled. To simulate conditions at YM, the models contained three faults (GD, SC, and BR) with a geometry derived from the CNWRA 3D geologic framework model and two sets of orthogonal fractures (horizontal and vertical). Deformation was modeled as a series of faulting events on the three faults. Results from the analysis showed significant changes in porosity in selected regions between the fault zones and within the fault zones themselves. Dilation mainly occurred in vertical joints and fractures, although some dilation of horizontal joints was also observed. Changes in porosity were sensitive to the order in which faults slipped. The greatest porosity changes occurred with combined slip on the GD and BR faults. Slip on the SC fault increased fracture dilation in its hangingwall with little change in its footwall (i.e., the hangingwall blocks of the GD and BR faults).

---

[16]U.S. Department of Energy. 1996. Highlights of the U.S. Department of Energy's Updated Waste Containment and Isolation Strategy for the Yucca Mountain Site. DOE Concurrence Draft.

3.4 ASSESSMENT OF PROGRESS TOWARD MEETING OBJECTIVES

3.4.1 Resolution of Main Key Technical Issue

Significant progress was made by the NRC and the CNWRA staffs toward meeting the main SDS KTI objective. These investigations included field geological and geophysical studies that help to constrain the viable tectonic models and tectonic processes in the YMR, laboratory studies that constrained ages and rates of deformation, analyses of fault coverages that identified potential performance affecting faults, as well as laboratory studies and numerical analysis that provide insight into possible styles of deformation in the YMR. These investigations, independently and in combination, reduced uncertainties and provided the basis for issue resolution with the DOE.

Progress within the SDS KTI treated several needs: (i) communication with the DOE on site characterization during prelicensing, (ii) evaluation of the DOE progress toward resolving issues critical to supporting license application, and (iii) preparation for review of a license application for YM. It has been necessary for the SDS KTI to act proactively to ensure these needs are treated, given the constraints arising from the DOE schedule and prioritization. The Appendix 7 meeting on alternative conceptual tectonic models demonstrates that this proactive approach is mutually beneficial to the DOE and the NRC. The meeting resulted in a common recognition that more than half the proposed conceptual tectonic models for the YM geologic setting are not presently supported by geologic evidence. The five remaining models significantly reduce and simplify conceptualization of YMR tectonics.

Alternatively, there is greater difficulty in proactively treating numerical modeling of tectonic processes, especially as they relate to performance. The consequences of structural deformation and seismicity on performance are often indirect. As a result, they received limited treatment in early PAs which, unfortunately, were used to argue that consequences of structural deformation and seismicity are negligible. Focused technical investigations of structural and seismic processes reported here provide compelling evidence that such processes need to be considered within the limited expenditure of resources.

Progress toward resolution of the following five subissues is a prerequisite to resolution of the main issue.

1. Data. The preliminary identification of Type I faults using the NUREG-1451 (McConnell et al., 1992) methodology resolved a component of this subissue. The DOE has also compiled preliminary identification of Type I faults (Whitney, 1996). The SDS KTI staff is prepared to discuss with the DOE its seismic source term database and resolve this component of this subissue. Conceptual models also provided insight into adequacy of data sets. For example, several viable tectonic models suggest unidentified (blind) faults that are not in fault data sets. Tectonic models discussed with the DOE at the Appendix 7 meeting and evaluation of pull-apart scale model experiments at the CNWRA generated important information on potential blind seismic sources of large-magnitude earthquakes and blind faults.

2. Model (numerical) validation and verification. The SDS KTI independently evaluated sensitivity of ground motion to seismic attenuation models and is prepared to move toward issue resolution as appropriate. The SDS KTI modeled groundwater flow anisotropy using fracture aperture changes in changing *in situ* stress fields as a surrogate for bulk transmissivity. The methodology of using dilation-tendency analysis in groundwater studies is a pioneering effort by the CNWRA,

and the SDS KTI is prepared to assimilate the results of PA calculations. In light of the Type I fault report (McKague et al., 1996), analysis of BM-YM fault connectivity, considerations of strike-slip dominant tectonic models, and upgrading SEISM 1.1 code, the SDS KTI staff is prepared to present input on PSHA and PFDHA to the DOE at its FY97 workshops on PSHA.

3. ACMs. The Appendix 7 meeting on Alternative Tectonic Models (ATMs) was an important step toward resolution of this subissue on identification of viable tectonic models for the YMR. The DOE and the NRC appear to agree that five ACMs are presently supported by existing data. Much of that data was generated from the CNWRA field, laboratory, and numerical studies of the YMR tectonic setting and associated tectonic processes.

4. Potential for disruption of WP, underground openings and surface facilities/operations. The DOE postponed its consideration of disruptive processes and events scenarios from TSPA-95 (TRW Environmental Safety Systems, Inc., 1995) to TSPA-VA. The NRC and the CNWRA staffs are presently using the FAULTING module to evaluate potential breaching of WPs by faulting, including sensitivity studies of faulting on alterative estimates of faulting activity (Ferrill et al., 1996b; Pezzopane, 1995).

5. Potential for disruption of flow. Sensitivity of transmissivity to the *in situ* stress field YM area was investigated by the SDS KTI with input from the Unsaturated and Saturated Flow Under Isothermal Conditions (USFIC) KTI. In addition, effects of fault displacement on joint aperture in the hangingwall and footwall of a normal fault were investigated. Preliminary results indicate measurable changes in fracture and joint aperture in the hangingwall. Analysis of anisotropic flow as a result of the interaction of the *in situ* stress and fractures provided insight into the potential for convergence of flow near the eastern edge of the potential repository which could lead to useful quantifications of dilution. Future work will focus on developing more complex and detailed models with the intent of assessing the sensitivity of porosity changes to both variations in faulting parameters (ship and recurrence) and fracture intensity, orientation, and distribution.

3.4.2 Evaluation of the U.S. Department of Energy Testable Hypotheses

The DOE based the organization, management, and explanations of its rationale for testing and analyses of total system performance on 15 testable hypotheses (U.S. Department of Energy, 1996).[17] Two hypotheses that fall within the purview of this KTI are potential disruptive processes and events (faulting and seismicity) that the DOE intends to analyze for effects on the predicted doses to the public (described in section 3.1). These hypotheses are: "The amount of movement of faults through the repository horizon will be too small to bring waste to the surface, and too small and infrequent to significantly impact containment during the next few thousand years," and "The severity of ground motion expected in the repository horizon for tens of thousands of years will only slightly increase the amount of rockfall and drift collapse."

The first hypothesis is being directly tested by the NRC and the CNWRA using the FAULTING module. Preliminary calculations of cumulative fault displacements based on even the most conservative

---

[17]U.S. Department of Energy. 1996. Highlights of the U.S. Department of Energy's Updated Waste Containment and Isolation Strategy for the Yucca Mountain Site. DOE Concurrence Draft.

slip rate estimates indicate that faults acting alone will produce insufficient displacement to transport waste to the surface in the next ten thousand years. The significance of faulting on containment, however, has not yet been evaluated. Results will be described in the NRC detailed review of TSPA-95 (TRW Environmental Safety Systems, Inc., 1995) in FY97.

The second hypothesis is being evaluated in part by this KTI. Preliminary analyses described in sections 3.3.2, 3.3.3, and 3.3.4 indicate that the potential severity of ground motion could be higher than currently considered by the DOE. Results will be presented to the DOE in FY97 in issue resolution status reports on identification of tectonic models and Type I faults, and in the DOE workshops on PSHA, where CNWRA staff have been invited to participate.

3.4.3 Evaluation of Selected U.S. Department of Energy Assumptions

The DOE controlled design assumption #23 concerning subsurface fault standoff is being evaluated in part by this KTI (i.e., location of Type I faults, main trace of faults, characteristics of GD fault). The DOE notes that to the extent practical, repository openings will be located to avoid Type I faults. For unavoidable Type I faults that intersect emplacement drifts, the DOE plans to allow 15 m standoff from the edge of the fault zone to the nearest WP. Avoidance is assumed to be adequate by using a 60 m offset from the main trace of a fault at the proposed repository level. They further note that a 120 m standoff should be used on the west side of the GD fault because the Exploratory Studies Facility (ESF) Topopah Spring main drift will be excavated before the GD fault characteristics are fully investigated (Controlled Design Assumption Document Rev. 2, 12/19/95, B00000000-01717-4600-0032, p 6–24).

Selection of particular standoff distances is an issue to be resolved jointly with the SDS, Container Life and Source Term, USFIC, Evolution of the Near-Field Environment, and Repository Design and Thermal-Mechanical Effects (RDTME) KTIs. Faults that are not Type I and fractures that may be fast pathways in some scenarios may need to be considered by the DOE for avoidance or setback. This KTI considers the subissue of identification of Type I faults will be resolved in FY97.

The DOE assumption concerning future seismic effects on flow was not explicitly evaluated in FY96. The DOE states that increases in water table elevation due to seismic effects can be bounded at 20–30 m, which should have no adverse impact on performance (U.S. Department of Energy, 1996)[18]. Field measurements from past worldwide occurrences of water table fluctuation in response to seismic events are well known (Ofoegbu et al., 1995). Work in progress at the CNWRA relating slip and dilation-tendency to flow bears on this assumption and will be reported in FY97.

The DOE hypotheses concerning future faulting and fracturing effects on flow is in the early stage of evaluation by computer modeling at the CNWRA (section 3.3.7 and 3.3.8). The DOE states that hydrologic characteristics of faults and fractures at YM represent cumulative effect of numerous tectonic events and thus, they consider that future events are unlikely to significantly change those hydrologic

---

[18]U.S. Department of Energy. 1996. Highlights of the U.S. Department of Energy's Updated Waste Containment and Isolation Strategy for the Yucca Mountain Site. DOE Concurrence Draft.

characteristics (U.S. Department of Energy, 1996)[19]. Quantitative analyses of the potential change of fracture characteristics, such as numerical analysis of fracture aperture changes resulting from faulting (section 3.3.5), do not necessarily support this DOE hypothesis. Significant changes in the hydrologic characteristics may result from a single tectonic event. Thus, the DOE hypothesis is valid only for those characteristics that can be shown to result from cumulative events and not simply result from the latest tectonic event(s). Additionally, the hypothesis does not consider the potential effects on flow driven through fractures by an internal thermal source. The characteristics of faults/fractures to heat transport and consequent refluxation remain to be evaluated.

3.5 INTEGRATION WITH OTHER KEY TECHNICAL ISSUES

Preliminary review of geophysical data and discussions with USGS, the State of Nevada, and others at the Appendix 7 meeting on alternative tectonic models for YM indicate that CF and Yucca Flat lie in the same structural domain with no obvious indication of different magma probability zones beneath CF and YMR. Numerical modeling of the intersection of a rising magma with a weak fault zone suggest that any future magmatism would be controlled by moderate to steeply dipping faults. These activities support Igneous Activity KTI contentions of structural controls and probability of volcanism. Refinement of tectonic models based on resolution of crustal geophysical survey data may help constrain uncertainties about the deeper crustal structural controls on magma generation, flow, and transport in the Crater Flat–YM area. Improved understanding of deep seated faults and crustal zones of accommodation of uplift and subsidence have implications for probability, location, and consequences of future volcanism. In addition, the identification of Type I faults and development of the FAULTING module for the TSPA analysis provided input into the role of structural deformation and seismicity on the potential for waste package failure.

Collection, review, and analysis of the DOE data on fracture origin, length, aperture characteristics, and orientation were started in FY96. Such data will contribute to the sensitivity and bounding calculations of hydrologic flow in the saturated and unsaturated zones in both the near- and far-field regions surrounding the proposed repository. Analysis of fracture patterns with 3DStress suggest concentration of flow along the east side of YM and thus provides an important constraint for the USFIC KTI. The SDS KTI will also continue to provide structural analyses of DOE ESF-wall and surface-outcrop fracture and fault mapping.

Finally, a number of SDS KTI activities are near completion for integration of the PA KTI, including development of the FAULTING module software, review and redefinition of the lithostratigraphic columns of the subregions of the TSPA repository model, and additional development and modifications to the 3D geologic framework model. This work was accomplished with input from the USFIC, RDTME, and Total System Performance Assessment and Integration (TSPAI) KTIs.

3.6 REFERENCES

Ahola, M.P., R. Chen, H. Karimi, S.M. Hsiung, and A.H. Chowdhury. 1996. *Parametric Study of Drift Stability in Jointed Rock Mass, Phase I: Discrete Element Thermal-Mechanical Analysis of Unbackfilled Drifts*. CNWRA 96-009. San Antonio, TX: Center for Nuclear Waste Regulatory Analyses.

---

[19]U.S. Department of Energy. 1996. Highlights of the U.S. Department of Energy's Updated Waste Containment and Isolation Strategy for the Yucca Mountain Site. DOE Concurrence Draft.

Barton, C.C., and P.A. Hsieh. 1989. Physical and hydrologic flow properties of fractures: Field Trip Guidebook T385: 28th International Geologic Congress. Washington, DC: *American Geophysical Union* 36

Barton, C.C., E. Larsen, W.R. Page, and T.M. Howard. 1993. *Characterizing Fractured Rock for Fluid-Flow, Geomechanical, and Paleostress Modeling: Methods and Preliminary Results from Yucca Mountain, Nevada*. U.S. Geological Survey Open-File Report 93-269. Reston, VA: U.S. Geological Survey.

Burchfiel, B., and J. Stewart. 1966. "Pull-apart" origin of the central segment of Death Valley, California. *Geological Society of America Bulletin* 77: 439–442.

Carlsson, A., and T. Olsson. 1979. Hydraulic conductivity and its stress dependence. *Proceedings, Organization for Economic Cooperation and Development and International Atomic Energy Agency, 1979*. Paris, France: 249–259.

Caskey, S.J., and R.A. Schweickert. 1992. Mesozoic deformation in the Nevada Test Site and vicinity: Implications for the structural framework in the Cordilleran and thrust belt and tertiary extension north of the Las Vegas Valley. *Tectonics* 11: 1,314–1,331.

Connor C.B., R.H. Martin, P.G. Hunka, D.B. Henderson, and R.V. Klar. 1996a. *Ground Magnetic Survey of the Little Cones, Crater Flat, Nevada*. CNWRA 96-002. San Antonio, TX: Center for Nuclear Waste Regulatory Analyses.

Connor, C.B., J.A. Stamatakos, D.A. Ferrill, and B.E. Hill. 1996b. Integrating structural models into probabilistic volcanic hazard analyses: An example from Yucca Mountain, Nevada. *Geological Society of America Abstracts with Program 1996 Annual Meeting*. Boulder, CO: Geological Society of America: 28: 192.

Crowe, B.M., F.V. Perry, J. Geissman, L. McFadden, S. Wells, M. Murrell, J. Poths, G.A. Valentine, L. Bowker, and K. Finnegan. 1995. *Status of Volcanic Hazard Studies for the Yucca Mountain Site Characterization Project*. Los Alamos National Laboratory Report LA-12908-MS. Los Alamos, NM: Los Alamos National Laboratory.

Ferrill, D.A., S.R. Young, G.L. Stirewalt, A.P. Morris, and D.B. Henderson. 1994. Tectonic processes in the central Basin and Range region. *NRC High-Level Radioactive Waste Research at CNWRA January–June 1994*. B. Sagar, ed. CNWRA 94-01S. San Antonio, TX: Center for Nuclear Waste Regulatory Analyses: 139–160.

Ferrill, D.A., A.P. Morris, D.B. Henderson, and R.H. Martin. 1995. Tectonic processes in the central Basin and Range region. *NRC High-Level Radioactive Waste Research at CNWRA July–December 1994*. B. Sagar, ed. CNWRA 95-01S. San Antonio, TX: Center for Nuclear Waste Regulatory Analyses: 121–139.

Ferrill, D.A., J.A. Stamatakos, and A.P. Morris. 1996a. Structural controls of progressive deformation of the Yucca Mountain (Nevada) region. *Geological Society of America Abstracts with Program 1996 Annual Meeting*. Boulder, CO: Geological Society of America: 28: 192.

Ferrill, D.A., G.L. Stirewalt, D.B. Henderson, J.A. Stamatakos, A.P. Morris, K.H. Spivey, and B.P. Wernicke. 1996b. *Faulting in the Yucca Mountain Region: Critical Review and Analyses of Tectonic Data from the Central Basin and Range*. NUREG/CR-6401. Washington, DC: Nuclear Regulatory Commission.

Ferrill, D.A., J.A. Stamatakos, S.M. Jones, B. Rahe, H.L. McKague, R.H. Martin, and A.P. Morris. 1996c. Quaternary slip history of the Bare Mountain fault (Nevada) from the morphology and distribution of alluvial fan deposits. *Geology* 24: 559–562.

Frizzell, V.A., and J. Shulters. 1990. *Geologic Map of the Nevada Test Site, Southern Nevada*. U.S. Geological Survey Miscellaneous Investigations Series, Map I-2046, Scale 1:100,000. Denver, CO: U.S. Geological Survey.

Gauthier, J.H., M.L. Wilson, D.J. Borns, and B.W. Arnold. 1995. Impacts of seismic activity on long-term repository performance at Yucca Mountain. *Methods of Seismic Hazard Evaluation, Focus '95*. Las Vegas, NV: American Nuclear Society: 159–168.

Hanks, T.C., and H. Kanamori. 1979. A moment-magnitude scale. *Journal of Geophysical Research* 84: 2,348–2,350.

Harmsen, S.C. 1994. The Little Skull Mountain earthquake of 29 June 1992: Aftershock focal mechanisms and tectonic stress field implications. *Bulletin of the Seismological Society of America* 84: 1,484–1,505.

Hart, E.W., W.A. Bryant, and J.A. Treiman. 1993. Surface faulting associated with the June 1992 Landers earthquake, California. *California Geology* 46(1): 10–16.

Hauksson, E., L.M. Jones, and K. Hutton. 1995. The 1994 Northridge earthquake sequence in California: Seismological and tectonic aspects. *Journal of Geophysical Research* 100: 12,335–12,355.

Itasca Consulting Group, Inc. 1993. *UDEC Version 2.0 User's Manual*. Minneapolis, MN: Itasca Consulting Group.

Janssen, B. 1995. *Numerical Modelling of Extension of the Earth's Crust with Example from the Basin and Range, United States*. Ph.D. Dissertation. Shasburg, France: l'Universite' Louis-Pasteur de Strasburg.

Kanamori, H., and D.L. Anderson. 1975. Theoretical basis of some empirical relations in seismology. *Bulletin of the Seismological Society of America* 65: 1,073–1,096.

Klinger, R.E., and L.W. Anderson. 1994. Topographic profiles and their implications for late Quaternary activity of the Bare Mountain Fault, Nye County, Nevada. *Geological Society of America Abstracts with Program 1994 Annual Meeting*. Seattle, WA: Geological Society of America 26(2): A-63.

McConnell, K.I., M.E. Blackford, and A.K. Ibrahim. 1992. *Staff Technical Position on Investigations to Identify Fault Displacement Hazards and Seismic Hazards at a Geologic Repository*. NUREG-1451. Washington, DC: Nuclear Regulatory Commission.

McKague, H.L., J.A. Stamatakos, and D.A. Ferrill. 1996. *Type I Faults in the Yucca Mountain Region*. CNWRA 96-007. San Antonio, TX: Center for Nuclear Waste Regulatory Analyses.

Monsen, S.A., M.D. Carr, M.C. Reheis, and P.A. Orkild. 1992. *Geologic Map of Bare Mountain, Nye County, Nevada*. U.S. Geological Survey Miscellaneous Investigations Series, Map I-2201, Scale 1:24,000. Denver, CO: U.S. Geological Survey.

Morris, A.P., D.A. Ferrill, and D.B. Henderson. 1996. Slip-tendency analysis and fault reactivation. *Geology* 24: 275–278.

Nuclear Regulatory Commission. 1996. *Disposal of High-Level Radioactive Waste in Geologic Repository. Title 10. Energy, Part 60 (10 CFR Part 60)*. NUREG-1451. Washington, DC: U.S. Government Printing Office.

Ofoegbu, G.I., and D.A. Ferrill. 1995. *Finite Element Modeling of Listric Normal Faulting*. CNWRA 95-008. San Antonio, TX: Center for Nuclear Waste Regulatory Analyses.

Ofoegbu, G.I., S. Hsuing, A.H. Chowdhury, and J. Philip. 1995. *Field Site Investigations: Effects of Mine Seismicity on Groundwater Hydrology*. NUREG/CR-6283. Washington, DC: Nuclear Regulatory Commission.

Peacock, D., and D. Sanderson. 1991. Displacements, segment linkage and relay ramps in normal fault zones. *Journal of Structural Geology* 13: 721–733.

Pezzopane, S.K. 1995. *Preliminary Table of Characteristics of Known and Suspected Quaternary Faults in the Yucca Mountain Region*. U.S. Geological Survey Administrative Report. Reston, VA: U.S. Geological Survey.

Sawyer, D.A., R.R. Wahl, J.C. Cole, S.A. Minor, R.J. Laczniak, R.G. Warren, C.M. Engle, and R.G. Vega. 1995. *Preliminary Digital Geological Map Database of the Nevada Test Site Area, Nevada*. U.S. Geological Survey Open-File Report 95-0567. Scale 1:100,000. Denver, CO: U.S. Geological Survey.

Schweickert, R.A. 1989. Evidence for a concealed strike-slip fault beneath Crater Flat, Nevada. *Geological Society of America Abstracts with Program 1989 Annual Meeting*. Denver, CO: Geological Society of America 28: 21.

Scott, R.B. 1990. Tectonic setting of Yucca Mountain, southwest Nevada. Basin and Range extensional tectonics near the latitude of Las Vegas, Nevada. B.P. Wernicke, ed. *Geological Society of America Memoir* 176: 251–282.

Sibson, R. 1986. Rupture interaction with fault jogs. S. Das, J. Boatwright, and C. Scholz eds., *Earthquake Source Mechanics*. Washington, DC. American Geophysical Union Geophysical Monograph 37(6): 157–167.

Sieh, K., L. Jones, E. Hauksson, K. Hudnut, D. Eberhart-Phillips, T. Heaton, S. Hough, K. Hutton, H. Kanamori, A. Lilje, S. Lindvall, S.F. McGill, J. Mori, C. Rubin, J.A. Spotila, J. Stock, H.K. Thio, J. Treiman, B. Wernicke, and J. Zachariasen. 1993. Near-field investigations of the Landers earthquake sequence, April to July, 1992. *Science* 260: 171–176.

Sowers, J.M., J.R. Unruh, W.R. Lettis, and T.D. Rubin. 1994. Relationship of the Kickapoo fault to the Johnson Valley and Homestead faults, San Bernadino County, California. *Bulletin of the Seismological Society of America* 84(3): 532–536.

Stamatakos, J.A., and D.A. Ferrill. 1996a. Tectonic processes in the Central Basin and Range region. *NRC High-Level Radioactive Waste Research at CNWRA July–December 1995*. B. Sagar, ed. CNWRA 95-02S. San Antonio, TX: Center for Nuclear Waste Regulatory Analyses: 6–1 to 6–25.

Stamatakos, J.A., and D.A. Ferrill. 1996b. Kinematic constraints of central Basin and Range tectonism from paleomagnetic and fission track studies at Bare Mountain, Nevada. *Geological Society of America Abstracts with Program 1996 Annual Meeting*. Denver CO: Geological Society of America: 28: 125.

Stirewalt, G.L., and D.B. Henderson. 1995a. A preliminary three-dimensional geological framework model for Yucca Mountain. *Proceedings of the Sixth Annual International Conference on High-Level Radioactive Waste Management*. La Grange Park, IL: American Nuclear Society: 16–118.

Stirewalt, G.L., and D.B. Henderson. 1995b. *A Three-Dimensional Geological Framework Model for Yucca Mountain, Nevada, with Hydrologic Application: Report to Accompany 1995 Model Transfer to the Nuclear Regulatory Commission*. CNWRA 94-023. San Antonio, TX: Center for Nuclear Waste Regulatory Analyses.

Stirewalt, G.L., and D.B. Henderson. 1996. Development of three-dimensional hydrostratigraphic models for the potential high-level radioactive waste repository site at Yucca Mountain, Nevada. *Association of Engineering Geologists 39th Annual Meeting Program and Abstracts*. Bryan, TX Association of Engineering Geologists: 67–68.

Stirewalt, G.L., S.M. McDuffie, and R.D. Manteufel. 1996. A consequence analysis module to simulate fault displacement in the repository block at Yucca Mountain. *Proceedings of the Topical Meeting on Methods of Seismic Hazard Evaluation: Focus '95*. Las Vegas, NV: American Nuclear Society. 169–177.

Stock, J.M., J.H. Healy, S.H. Hickman, and M.D. Zoback. 1985. Hydraulic fracturing stress measurements at Yucca Mountain, Nevada, and relationship to regional stress field. *Journal of Geophysical Research* 90: 8,691–8,706.

Sweetkind, D.S., and S. Williams-Stroud. 1995. Controls on the genesis of fracture networks, Paintbrush Group, Yucca Mountain, Nevada. *EOS, Transactions, American Geophysical Union* 76: F597.

Throckmorton, C.K., and E.R. Verbeek. 1995. *Joint Networks in the Tiva Canyon and Topopah Spring Tuffs of the Paintbrush Group, Southwestern, Nevada.* U.S. Geological Survey Open-File Report 95-2. Denver, CO: U.S. Geological Survey.

Trudgill, B., and J. Cartwright. 1994. Relay-ramp forms and normal-fault linkages, Canyonlands National Park, Utah. *Geological Society of America Bulletin* 106: 1,143–1,157.

TRW Environmental Safety Systems, Inc. 1995. *Total System Performance Assessment—1995: An Evaluation of the Potential Yucca Mountain Repository.* (B00000000-01717-2200-00136). Las Vegas, NV: TRW Environmental Safety Systems, Inc.

U.S. Department of Energy. 1994. *Methodology to Assess Fault Displacement and Vibratory Ground Motion at Yucca Mountain.* DOE Topical Report 1, YMP/TR-002-NP. Washington, DC: U.S. Department of Energy.

Wells, D., and K. Coppersmith. 1994. New empirical relationships among magnitude, rupture length, rupture width, rupture area, and surface displacement. *Bulletin of the Seismological Society of America* 84: 974–1,002.

Wernicke, B. 1992. Cenozoic extensional tectonics of the U.S. Cordillera. The Cordilleran Orogen: Conterminous U.S. B.C. Burchfiel, P.W., Lipman, and M.L. Zoback, eds. The Geology of North America G-3. Boulder, CO: *Geological Society of America*: 553–581.

Whitney, J.W. 1996. *Seismo Tectonic Framework and Characterization of Faulting at Yucca Mountain, Nevada.* Denver, CO: U.S. Geological Survey.

Wittmeyer, G.W., and D.A. Ferrill. 1994. Effect of contemporary regional stress on the anisotropy of transmissivity in fractured rock aquifers. *EOS, Transactions, American Geophysical Union* 75:(44): 258.

Wittmeyer, G.W., W.M. Murphy, and D.A. Ferrill. 1994. Regional hydrologic processes of the Death Valley Region. *NRC High-Level Radioactive Waste Research at CNWRA, January–June 1994.* San Antonio, TX: B. Sagar, ed. CNWRA 94-01S. Center for Nuclear Waste Regulatory Analyses: 189–212.

Wittmeyer, G., R. Klar, G. Rice, and W. Murphy. 1995. *The CNWRA Regional Hydrogeology Geographic Information System Database.* CNWRA 95-009. San Antonio, TX: Center for Nuclear Waste Regulatory Analyses.

Wong, I.G., S.K. Pezzopane, M. Mengas, R.K. Green, and R.C. Quittmeyer. 1995. Probabilistic seismic hazard analyses of the exploratory studies facility at Yucca Mountain, Nevada. *Methods of Seismic Hazard Evaluation, Focus '95.* Las Vegas, NV: American Nuclear Society. 51–63.

Zhang, P., B. Burchfiel, S. Chen, and Q. Deng. 1989. Extinction of pull-apart basins. *Geology* 17: 814–817.

Zhang, Z., and D.J. Sanderson. 1996. Numerical modeling of the effects of fault slip on fluid flow around extensional faults. *Journal of Structural Geology* 18: 109–119.

Zoback, M.L. 1992. First- and second-order patterns of stress in the lithosphere: The World Stress Map Project. *Journal of Geophysical Research* 97(B8): 11,703–11,728.

Zoback, M.L., R.E. Anderson, and G.A. Thompson. 1981. Cenozoic evolution of the state of stress and style of tectonism of the Basin and Range Province of the western United States. *Philosophical Transactions of the Royal Society of London* A300: 407–434.

Zoback, M.L., and 36 Project participants. 1992. World Stress Map—maximum horizontal stress orientations. *Journal of Geophysical Research* 87(B8).

4 EVOLUTION OF THE NEAR-FIELD ENVIRONMENT

Primary Authors: *P.C. Lichtner, R.T. Pabalan, N. Sridhar, W.M. Murphy, B.W. Leslie, and P.J. Angell*

Technical Contributors: *P.J. Angell, B.W. Leslie, P.C. Lichtner, W.M. Murphy, R.T. Pabalan, and N. Sridhar*

Key Technical Issue Co-Leads: *N. Sridhar (CNWRA) and B.W. Leslie (NRC)*

4.1 INTRODUCTION

The U.S. Department of Energy (DOE) updated Waste Containment and Isolation Strategy (WCIS) for the proposed repository at Yucca Mountain (YM)[1] has the primary goals of near-complete containment of radionuclides within waste packages (WPs) for several thousand years and acceptably low annual doses to a member of the public living near the site. Among the system attributes recognized in this strategy to be most important in accomplishing these goals are the rate of seepage of water into the proposed repository, WP life time (containment), release rate of radionuclides from breached WPs, and radionuclide transport through engineered and natural barriers. The objective of the Evolution of the Near-Field Environment (ENFE) Key Technical Issue (KTI) is to evaluate these attributes as they relate to the transient near-field environment and provide bounding calculations of near-field environmental conditions for use in total system performance assessment (TSPA) calculations.

The near field is that portion of the proposed repository where physical and chemical properties have been altered by the proposed repository construction operations and radioactive waste emplacement affecting performance of the proposed repository (Wilder, 1993a). The spatial extent of the near-field environment varies depending on the specific process considered. For example, the near-field environment can extend to a considerable distance from the waste emplacement horizon if transport of radionuclides is considered, whereas the processes of importance to spent fuel dissolution occur in a much smaller region.

Expected near-field environmental processes for the proposed YM repository were reviewed previously (Glassley, 1986; Murphy, 1991; Wilder, 1993a,b). However, these evaluations were focused on the older Site Characterization Plan (SCP) design of the engineered barrier system (EBS) involving borehole emplacement of a thin (12.5 mm), single-walled container (U.S. Department of Energy, 1988). Recently, a new WP design called the Advanced Conceptual Design (ACD) has evolved involving thick (120 mm), multiple-wall containers (TRW Environmental Safety Systems, Inc., 1996b). The emplacement geometry has also changed from a vertical borehole concept to a horizontal drift concept. The DOE thermal loading strategy also has evolved, with the aim of higher thermal loading to create a longer dryout period. Processes affecting the near-field environment and WP performance must be considered in light of changes in the EBS design. For example, the effect of gamma radiolysis on corrosion of container materials is unimportant because of shielding provided by the thick overpacks. On the other hand, effects of corrosion of outer overpack on the corrosion of inner overpack must be considered in

---

[1] U.S. Department of Energy. 1996. *Highlights of the U.S. Department of Energy's Updated Waste Containment and Isolation Strategy for the Yucca Mountain Site.* DOE Concurrence Draft. July 1996. Washington, DC: U.S. Department of Energy.

the new design. Similarly, the large volume of iron containing material is expected to affect the radionuclide transport processes through generation of colloids and secondary iron-containing minerals. Also, the higher thermal load expected in the new design may extend the spatial scale of the near-field environment. The present report focuses on the ACD concept in evaluating the processes affecting the near-field environment. Baseline conditions prior to proposed repository construction and waste emplacement have been described extensively in previous reports (Wilder, 1993a,b; U.S. Department of Energy, 1988).

This chapter describes sensitivity analyses of the near-field environment conditions conducted through use of the computer code MULTIFLO, auxiliary analyses of pH changes due to cement-water interactions, and assessment of the viability of microbial organisms and effects in the near-field environment. The focus of these technical accomplishments, and this chapter, is the subissues concerning containment, radionuclide mobilization, and radionuclide transport.

The ENFE KTI has been divided into four subissues directly linked to four system attributes (seepage, containment, radionuclide mobilization, and radionuclide transport) of the DOE WCIS.[2] One subissue within the ENFE KTI addresses three of the DOE hypotheses within the seepage attribute: (i) limited fracture flow at the proposed repository depth (Hypothesis #2); (ii) capillary retention reduces seepage into the drifts (Hypothesis #3); and (iii) bounds can be placed on thermally-induced changes in seepage rates (Hypothesis #4). However, in FY96 the ENFE KTI did not address the subissue related to seepage. The second ENFE subissue will evaluate the DOE hypothesis of slow corrosion at low humidity within the DOE containment attribute (Hypothesis #7). Evaluating the DOE hypothesis that radionuclide release from waste forms due to surface area exposed, dissolution, colloid formation, and microbial activity will be low (Hypothesis #9) is the focus of the third ENFE subissue. The final ENFE subissue focuses on the DOE hypothesis that transport properties of both engineered and natural barriers will significantly reduce radionuclide concentration (Hypothesis #10).

Each of the ENFE subissues has been addressed during FY96 activities in a multidisciplinary evaluation conducted of near-field processes and the evolution of the near-field environment at YM (Angell et al., 1996). An objective of this review was to judge the sensitivity of proposed repository performance to near-field environmental effects, and a set of subjective prioritized recommendations was provided as an overview and justification for the technical work described in this chapter. Two primary system characteristics significant to performance were identified in the near-field evaluation report (Angell et al., 1996). Coupled thermal-hydrological-geochemical processes were concluded to have the greatest priority. These processes will have big effects on the near-field environment; they will affect proposed repository performance by having dominant effects on containment, release, and radionuclide transport; and predicting these effects will be difficult. The chemistry of the near field will evolve as a result of thermal-hydrologic-geochemical processes associated with heat output of radioactive waste. Chemical composition of water in the near field that could come in contact with the WP, including its oxidation state, pH, chloride concentration, and other compositional variables, is important to the WP life time and radionuclide release from the EBS. Chemistry of the near field could also be important for transport of radionuclides through its impact on speciation, sorption, and coprecipitation of radionuclides. In addition, chemical changes in the near field could affect fracture permeability and the rate of seepage into drifts.

---

[2]U.S. Department of Energy. 1996. *Highlights of the U.S. Department of Energy's Updated Waste Containment and Isolation Strategy for the Yucca Mountain Site.* DOE Concurrence Draft. July 1996. Washington, DC: U.S. Department of Energy.

Another important system characteristic is the effect of engineered materials on the near-field environment. Large amounts of container materials, cementitious materials, waste form materials, and their alteration products will have strong effects on the near-field environment. Uncertainties in the properties and behavior of these materials under proposed repository conditions make predictions of performance difficult. Nevertheless, expected processes such as the influence of cementitious materials on water chemistry, the effects of container alteration products on radionuclide transport, and the role of secondary products of waste form materials on radionuclide releases indicate that engineered materials will be significant to performance.

Three other issues were identified in the near-field evaluation report to be of lower priority (Angell et al., 1996). Microbiology is of concern because of uncertainty with regard to its potential effects. Radiolysis can affect radionuclide speciation and release. Also, near-field rock stability under long-term conditions of elevated temperature is uncertain.

4.2 OBJECTIVES AND SCOPE OF WORK

The objective for the ENFE KTI is to conduct activities that will lead to resolution of subissues within the KTI using both proactive and reactive approaches. Resolving the ENFE KTI and its subissues will require evaluating the range of near-field environment (temperature, saturation, and chemical composition) that may result from the interactions of emplaced waste and other materials introduced during proposed repository operations with the host rock and fluids at YM. The breadth of reactive work during FY96 included evaluation of the DOE preliminary near-field environment report (Wilder, 1993a,b), an audit review of the DOE assumptions of the near-field environment used in TSPA-95 (Baca and Brient, 1996; TRW Environmental Safety Systems, Inc., 1995), and evaluating the extent to which the DOE heater tests could be used to constrain the range of expected near-field geochemical conditions. These reactive activities evaluated the information and its relationship to the DOE WCIS hypotheses.[3] In addition, the reactive tasks provided constraints that focused technical work accomplished in the ENFE KTI during FY96 on aspects of the subissues that lead to issue resolution.

Proactive work during FY96 focused on development of computer modeling capabilities that allow sensitivity analyses to be conducted on the near-field environment conditions, auxiliary analyses of pH changes due to cement-water interaction, and evaluation of the viability and effects of microbial organisms in the near field. Field work under this KTI focused on collection and analysis of altered rock samples in the vicinity of YM. These samples are being examined in the laboratory to determine the patterns and characteristics of mineral alteration. Observations will be used to support predictive modeling of chemical alteration of the near-field environment. Laboratory efforts during FY96 for the ENFE KTI focused on study of the viability of microbial organisms under expected near-field conditions. These experiments form the basis for resolving the subissue on the importance of microbial organisms on radionuclide mobilization.

The development of the MULTIFLO code (Seth and Lichtner, 1996; Lichtner and Seth, 1996), and the cement-water and microbial organism studies, provide the NRC the capability and information necessary to evaluate the DOE assumptions on processes and parameters used in TSPA. These technical

[3]U.S. Department of Energy. 1996. *Highlights of the U.S. Department of Energy's Updated Waste Containment and Isolation Strategy for the Yucca Mountain Site*. DOE Concurrence Draft. July 1996. Washington, DC: U.S. Department of Energy.

activities also allow evaluation of the assumptions used by DOE to support the hypotheses in WCIS. Thus, each of these proactive activities has or will contribute (when completed in FY97) to subissue resolution within the ENFE KTI and in other KTIs.

4.3 SIGNIFICANT TECHNICAL ACCOMPLISHMENTS

4.3.1 Sensitivity Analyses Using MULTIFLO

4.3.1.1 Introduction

Model calculations of the redistribution of moisture resulting from emplacement of nuclear waste at the proposed YM high-level waste (HLW) site in Nevada indicate that heat produced from the decay of fission products contained in the waste creates a dryout zone surrounding the proposed repository with enhanced zones of saturation above and below the proposed repository horizon caused by condensation of water (Buscheck and Nitao, 1993; Pruess and Tsang, 1993). The degree of dryness and time to rewet the proposed repository depends on the heat load of radioactive waste and hydraulic properties of the host rock.

As a result of evaporation, condensation, and flow during heating of the proposed repository, salinity and pH may increase in the near-field region. The amount of water that can be evaporated depends on initial saturation and porosity of the rock and water flow toward the WPs. Salts could form on the WP and in the near field as a result of evaporation (Walton, 1993). High pH fluids could react with the silicate host rock producing calcium silicate hydrates (CSHs) and could affect sorption characteristics, porosity, and permeability of the host rock. Precipitation of minerals on fracture surfaces could limit the effect of retardation of radionuclides by matrix diffusion. At high thermal loads, concentrations in dissolved species such as chloride and elevation in the pH are expected to occur near the boiling front surrounding the proposed repository. In regions of condensation, a reduction in concentration is expected due to dilution. In addition, an inverted fluid density gradient will occur below the proposed repository leading to unstable conditions. A further complication is that the boiling front is predicted to change continuously in position in response to the changing thermal load as waste decays with time. Prediction of such effects can only be achieved with models that couple thermal, hydrologic, and chemical (THC) processes.

Few models have been presented that account for THC coupled processes (White, 1995). Robinson[4] carried out a two-dimensional calculation using a repository scale model with a single component, SiO_2. Robinson[5] concluded that the dryout zone could be extended due to changes in permeability and porosity caused by precipitation and dissolution of quartz. However, the permeability-porosity relation used by Robinson[6] seems questionable. He associated a six order of magnitude change in permeability with a variation in porosity from 0.09 to 0.13. No attempt was made to estimate changes in pH and salinity due to evaporation and condensation processes.

---

[4]Robinson, B. 1994. *Status of Coupled Thermohydrologic/Geochemical Modeling*. Presented at the DOE/NRC Technical Exchange Meeting. Las Vegas, NV: November 9, 1994.

[5]*Ibid.*

[6]*Ibid.*

Current codes that describe coupled thermal-hydrologic processes, such as TOUGH, TOUGH2, VTOUGH, FEHM, and NUFT (Pruess, 1987; Nitao, 1989, 1996; Zyvoloski et al., 1992), do not include multicomponent chemistry suitable for describing rock-water interaction or the effects on solution chemistry due to evaporation and condensation processes. Reaction path codes, such as EQ3/6 (Wolery, 1992), that provide sophisticated descriptions of chemical interaction, do not include explicitly spatial-dependent processes. The code MULTIFLO, developed under the ENFE KTI, provides the capability to model THC processes for multicomponent-multiphase systems in one, two, or three spatial dimensions (Lichtner and Seth, 1996; Seth and Lichtner, 1996).

4.3.1.2 Description of the Code MULTIFLO

MULTIFLO sequentially couples two-phase fluid flow and reactive transport of aqueous and gaseous species. It is composed of two modules: Mass and Energy TRAnsport (METRA), a two-phase fluid flow code; and General Electrochemical Migration (GEM), a reactive transport code that takes into account multicomponent chemical reactions involving aqueous, gaseous, and mineral species. METRA and GEM may each be run in stand-alone mode or in coupled mode. In coupled mode, METRA is called first to compute the pressure, temperature, saturation state, and liquid and gas velocities for a single time step. These quantities are then fed to GEM to solve the reactive transport equations in a partially saturated medium. The equivalent continuum model (ECM) is used by METRA to represent the interaction between fractures and matrix. GEM accounts for reactions within the aqueous and gas phases assuming local chemical equilibrium and ion-exchange and kinetic reaction with minerals. Thermodynamic data are provided by an equivalent form of the EQ3/6 database data0.com.r16 applicable for temperatures to 300 °C (Wolery, 1992).

4.3.1.3 Application to the Proposed Nuclear Waste Repository at Yucca Mountain, Nevada

Using the code MULTIFLO, predictions of solution composition, temperature, saturation, and mineral reaction for the proposed YM HLW are based on a moderate heat loading of 80 MTU/acre. With this heat load, a liquid phase is always present. The YM host rock is modeled as pure quartz with an initial volume fraction of 90 percent and a porosity of 10 percent. The ECM is used to represent interaction between fractures and matrix. The chemical model for the aqueous solution used in the calculations consists of 7 primary species and 14 secondary species as listed in table 4-1. The initial fluid composition is presented in table 4-2, abstracted from J-13 groundwater sampled from the saturated zone at YM (Harrar et al., 1990). The unsaturated zone water has even higher concentrations of dissolved solids than the saturated zone water and, therefore, even higher concentrations than predicted here would occur due to evaporation. Calcite and tobermorite precipitate as secondary alteration products. Effective rate constants for quartz, calcite, and tobermorite were chosen to approximate local equilibrium. Material properties of the host rock used in the calculation were taken from Pruess and Tsang (1993).

4.3.1.4 Results

Results are presented for a one-dimensional calculation using MULTIFLO along a vertical line through the center of the proposed repository. The proposed repository horizon is located 375 m below the ground surface and 225 m above the water table. An initial heat load of 80 MTU/acre assuming 26-yr-old spent fuel was used in the calculation with a decaying heat load corresponding to the average WP used in TSPA-95 (TRW Environmental Safety Systems, Inc., 1995). The temperature profile plotted as a function of distance above the water table is shown in figure 4-1 for times ranging from 10 to 10,000 yr. The maximum temperature obtained for this heat load is approximately 130 °C. The deflection

Table 4-1. Chemical species used in MULTIFLO calculations

Primary Species	Other Aqueous Species	Minerals	Gases
Ca^{2+}	OH^-	Quartz (SiO_2)	CO_2(g)
Na^+	CO_2(aq)	Calcite ($CaCO_3$)	
K^+	CO_3^{2-}	Tobermorite ($Ca_5Si_6H_{21}O_{27.5}$)	
H^+	$CaCO_3$(aq)		
SiO_2(aq)	$CaHCO_3^+$		
HCO_3^-	$CaOH^+$		
Cl^-	$CaCl_2$(aq)		
	$NaHCO_3$(aq)		
	NaCl(aq)		
	NaOH(aq)		
	KCl(aq)		
	$H_3SiO_4^-$		
	$H_2SiO_4^{2-}$		

in the temperature profile at approximately 100 °C indicates the presence of a heat pipe.

The corresponding liquid saturation profile is shown in figures 4-2(a) and (b). Above and below the proposed repository horizon regions of enhanced saturation form and expand with time. In these regions, the pore spaces become almost fully saturated during the period of relative dryness at the proposed repository horizon. The saturation state is a dynamic condition caused by continuous evaporation of liquid drawn toward the proposed repository by capillary forces and gravity above the repository horizon and by condensation farther away in cooler regions. Within the heat pipe region the velocity of water vapor is approximately 1,600 times faster than the liquid velocity.

The pH profile is shown in figures 4-2(c) and (d) and the chloride concentration in figures 4-3(a) and (b). The pH increases to values above 10 as CO_2 degasses from the liquid phase at evaporation fronts above and below the proposed repository horizon. The increase in pH is a consequence of degassing of $CO_{2(g)}$ according to the reaction

$$CO_3^{2-} + 2H^+ \rightleftharpoons CO_{2(g)} + H_2O \tag{4-1}$$

The pH decreases at the condensation fronts above and below the proposed repository horizon. The chloride concentration increases by over a factor of 10 from its ambient value at the evaporation front. At the condensation fronts the chloride concentration decreases from its ambient value because the condensing liquid is devoid of salts. Quartz and calcite dissolve in the condensate zones and precipitate in the regions of evaporation. Tobermorite ($Ca_5Si_6H_{21}O_{27.5}$) precipitates in the high pH region.

Concentrations of total and free $SiO_{2(aq)}$ are shown in figure 4-3(c) and (d). At high pH, $H_3SiO_4^-$ becomes the dominant silica species. The reaction rate for quartz is shown in figures 4-4(a) and (b) at two different times: 25 and 250 yr. A positive value indicates precipitation and a negative value dissolution. Regions of dissolution and precipitation move with the evaporation and condensation zones. This minimizes change in porosity and variations in permeability at any point. Minimal change in porosity are predicted over the height of the rock column during simulation time.

Table 4-2. Initial fluid composition corresponding to that of J-13 well water

Species	Concentration, Molality
Ca^{2+}	2.9×10^{-4}
Na^{+}	2×10^{-3}
K^{+}	1.4×10^{-4}
HCO_3^{-}	2.7×10^{-3}
$SiO_2(aq)$	1.1×10^{-3}
Cl^{-}	1.8×10^{-4}
pH = 6.9	

The pH and chloride concentration corresponding to different thermal heat loads are indicated in figures 4-4(c) and (d). A time of 25 yr was chosen because complete dryout occurs at longer times for the 100 MTU/acre heat load. The increase in chloride concentration due to evaporation could have important consequences on corrosion rates of the steel overpack and the stainless steel inner liner. Carbon steel becomes passivated at $pH > 8$. However, pitting becomes important for chloride concentrations $\geq 3 \times 10^{-3}$ M at $pH \sim 8.4$ if the corrosion potential is greater than the repassivation potential. The repassivation potential is a function of temperature and chloride concentration, and the corrosion potential is a function of temperature, pH, and dissolved oxygen concentration. For Alloy 825, there is no effect on repassivation potential due to pH in the range $2 \leq pH \leq 12$. Pitting becomes important for a chloride concentration $\geq 10^{-2}$ M. Future work will consider more realistic host rock compositions and extend the calculation to two spatial dimensions. Including feldspars can be expected to affect the pH and provide a supply of silica and other cations which could lead to precipitation of salts such as halite. The results of calculations of the kind presented here can be used to provide bounding estimates of chloride concentration, pH, and other variables in total system performance models and to provide constraints for sensitivity analyses for container life, source term, and radionuclide transport.

4.3.2 Effects of Manmade Materials: Cement-Water Interactions

An important aspect of the evolution of the near-field environment is the interaction of groundwater with cementitious materials that could affect WP corrosion and waste form alteration, radioelement speciation, dissolution/precipitation, sorption/desorption reactions, and radionuclide transport. Cementitious materials will be introduced during the construction of the nuclear waste proposed repository primarily in roadways and as ground support for the estimated 228,000 m of proposed repository excavation (TRW Environmental Safety Systems, Inc., 1996a). Roadways for construction and emplacement, particularly for ramps and service mains, will include concrete inverts, stabilized and strengthened by grouting and overlain by reinforced cast-in-place concrete caps. Cementitious materials for ground support may exist as (i) shotcrete or fibercrete (as full or partial circle structural lining); (ii) grout (typically to encapsulate and secure rock bolts, but also to consolidate and strengthen the rock mass); and (iii) concrete lining (pre-cast or cast-in-place, with or without reinforcement). Concrete may also be used for WP pedestals (TRW Environmental Safety Systems, Inc., 1996a).

Cements are fine-grained, high surface area materials containing soluble phases [e.g., CSH gels], metastable with respect to crystalline CSHs. These properties make the materials potentially reactive in the near-field environment and could significantly alter near-field geochemistry. Pore fluids in contact with hydrated cementitious materials are characterized by alkaline pH (> 10) conducive to precipitation of radionuclides, including transuranics (Glasser et al., 1985; Atkins et al., 1990). Cement hydration products can also provide sorption sites that could aid in retarding radionuclide migration (Atkins et al., 1990; 1991) from the EBS to the host rock. In addition, alkaline conditions can provide an environment resulting in formation of a tightly adhering passive film on carbon steel overpack which protects it from uniform corrosion.

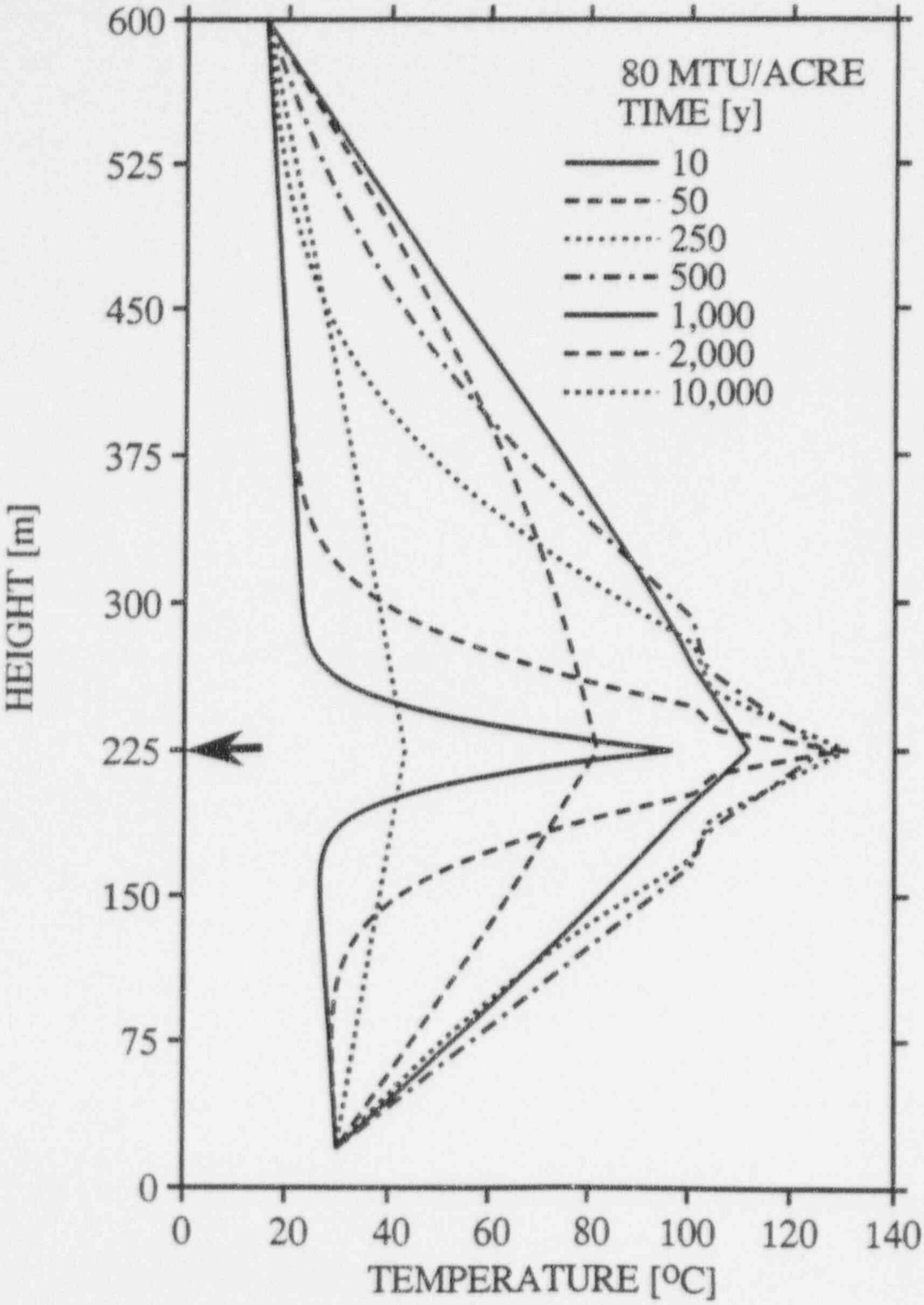

Figure 4-1. Temperature plotted as a function of distance above the water table at times ranging from 10 to 10,000 yr. The arrow depicts the horizon of the proposed repository.

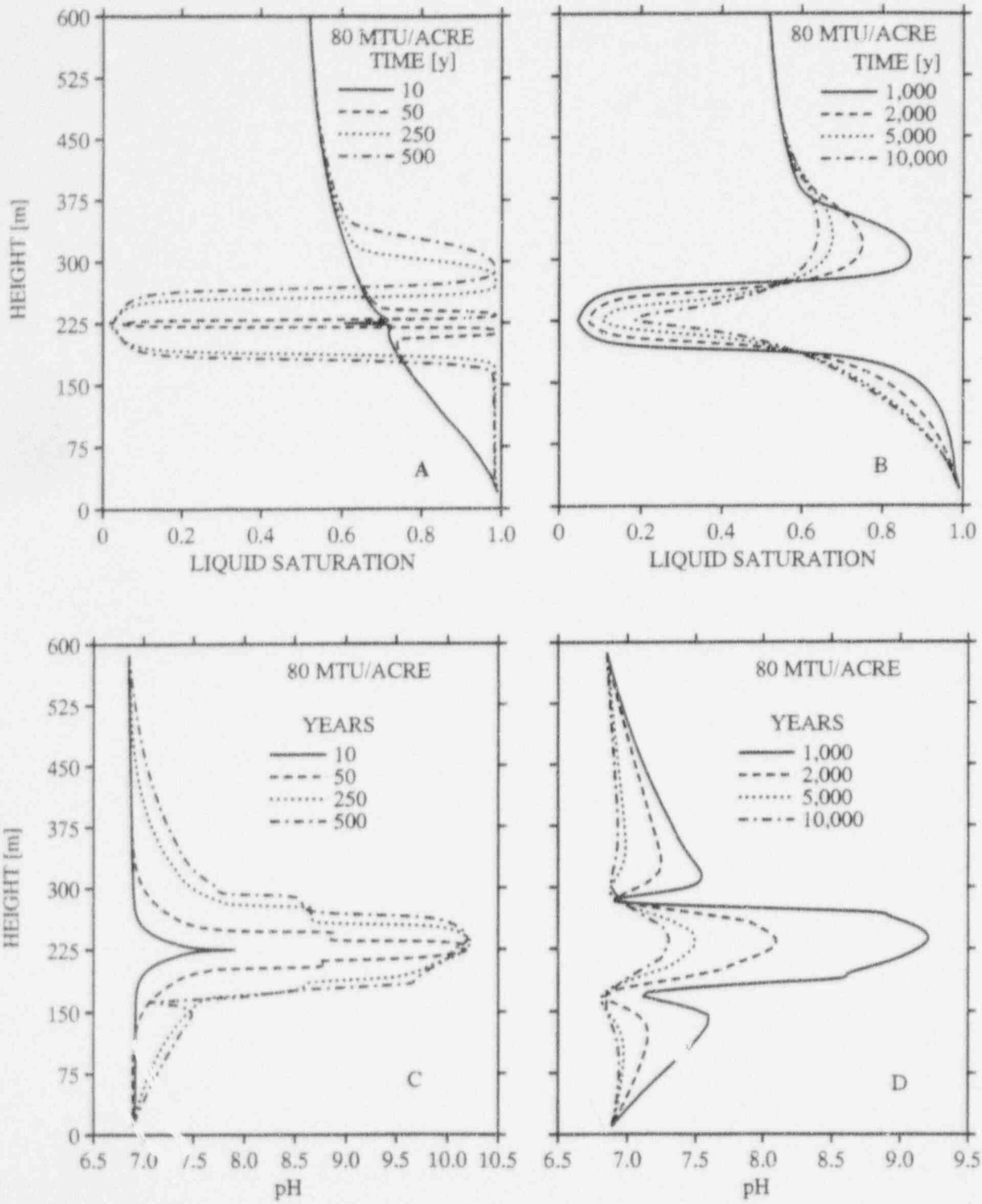

Figure 4-2. Liquid saturation [(a) and (b)] and pH [(c) and (d)] plotted as a function of distance above the water table at times ranging from 10 to 10,000 yr

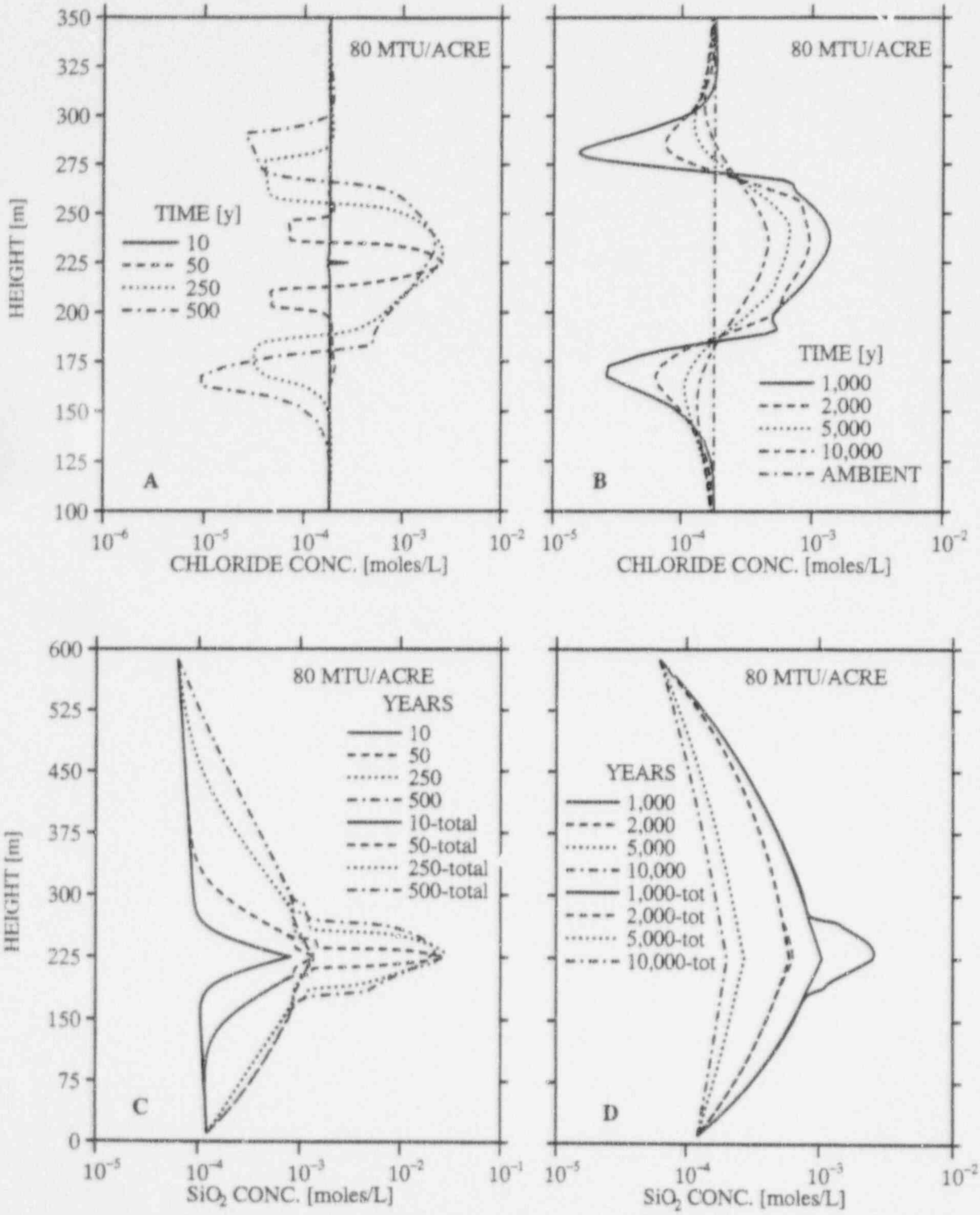

Figure 4-3. Chloride [(a) and (b)] and silica concentration [(c) and (d)] plotted as a function of distance above the water table at times ranging from 10 to 10,000 yr

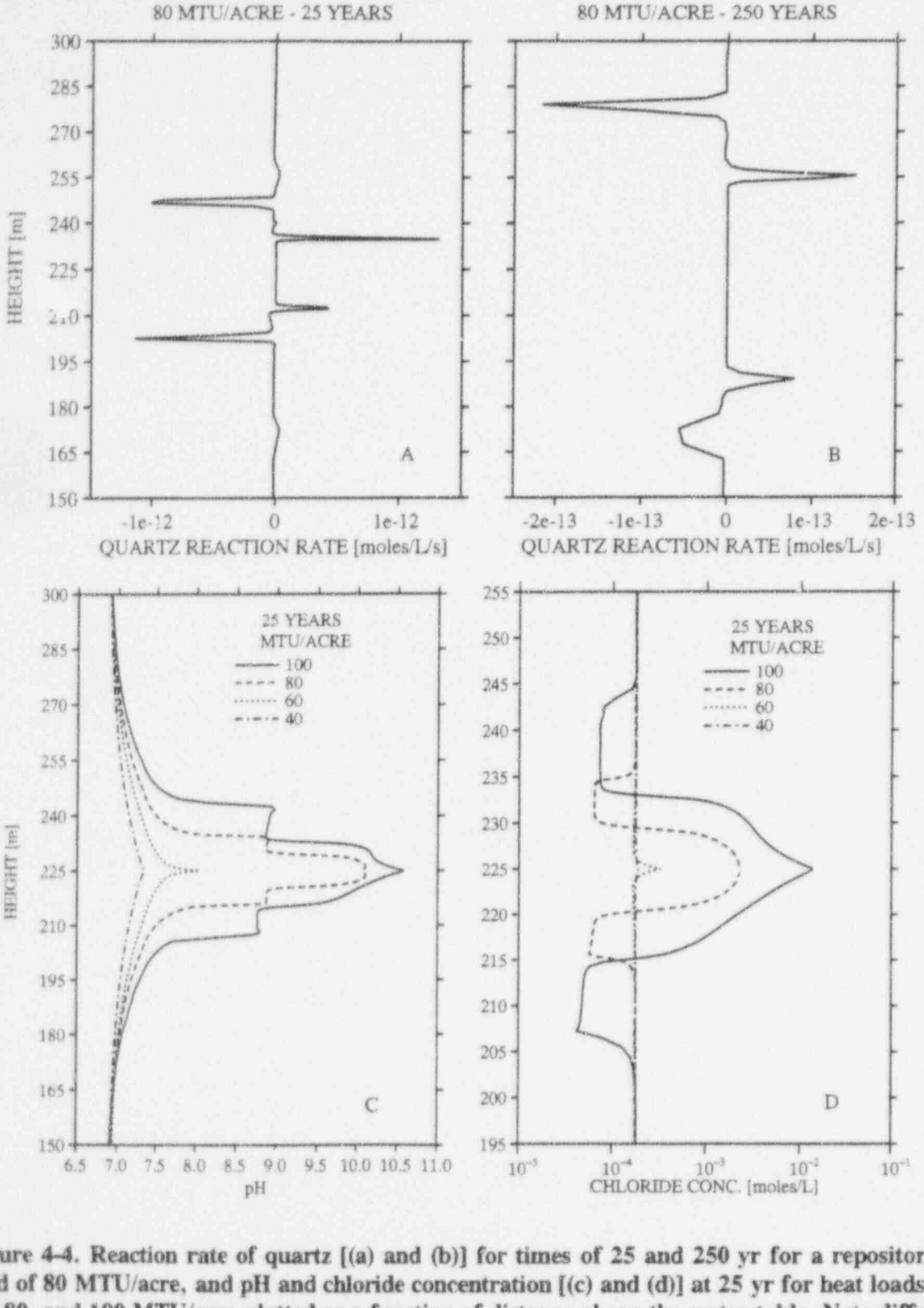

Figure 4-4. Reaction rate of quartz [(a) and (b)] for times of 25 and 250 yr for a repository heat load of 80 MTU/acre, and pH and chloride concentration [(c) and (d)] at 25 yr for heat loads of 40, 60, 80, and 100 MTU/acre plotted as a function of distance above the water table. Note differences in the vertical scale.

Alkaline conditions can be detrimental to the stability of nuclear waste glass and mineral components of the geologic barrier. Experiments by Heimann (1988) indicated that cement/glass interaction leads to accelerated dissolution/alteration of nuclear waste glass compared to a system without cement. Minerals common at YM such as clinoptilolite, mordenite, and montmorillonite, which is also an important component of bentonite backfill material, become unstable at high pH (Komarneni and Roy, 1983; Angus et al., 1983). Mineral alteration due to alkaline solutions and precipitation of secondary phases could affect the sorptive and retardation ability of the geologic barrier and its hydraulic properties (porosity and permeability). Results from U and Np sorption experiments discussed in chapter 5 illustrate the strong dependence of actinide sorption on pH. For example, at atmospheric pCO_2 conditions, U(6+) sorption decreases by four orders of magnitude from pH ~ 6 to pH ~ 9 and Np(5+) sorption decreases by more than two orders of magnitude from pH ~ 8 to pH ~ 10. The release of radionuclides from the container and from the EBS could be affected by cement/water interactions. Lichtner and Eikenberg (1995) analyses indicated that interaction between a hyperalkaline plume released from a cement-based radioactive waste repository and a marl host rock could result in a rapid decrease in porosity of the host rock several meters from the repository due to precipitation of secondary phases. This study also indicated that porosity could increase at the interface of the marl host rock and the cement due to mineral dissolution. Precipitation of calcite would also occur as the low CO_2-high Ca cement pore waters mixed with the ambient fluids containing high CO_2 concentrations (Steefel and Lichtner, 1994). Another important consideration is the durability of rock bolts encapsulated with cementitious grout and of shotcrete planned to be used in emplacement drifts for ground support. The durability of these ground supports may be weakened by cement/tuff reactions and increase the likelihood of rock falls that could damage the waste containers. In addition, carbon steel can undergo localized corrosion or cracking if the external environment is alkaline. As indicated in chapter 5, localized corrosion of carbon steel overpack may occur in the form of pitting or crevice corrosion when the external environment is moderately alkaline (pH ~ 8 to 10), and stress corrosion cracking can occur in a HCO_3^-/CO_3^{2-} environment at a pH of about 10 and when the corrosion potential reaches a critical value.

To address the consequences of cementitious materials in the near field, one must be able to predict changes in near-field chemistry as caused by cementitious materials, particularly with respect to solution pH, a key parameter controlling radionuclide sorption/transport, mineral dissolution/precipitation, waste form degradation, and container corrosion. These predictions are possible for near ambient temperature conditions using available hydration models, geochemical equilibrium codes, and thermodynamic data for cement phases (e.g., Berner, 1992; Atkins and Glasser, 1992; Reardon, 1992).

Simulations of cement/water interactions were conducted as part of this KTI using the equilibrium code SIMUL developed by Reardon (1992). Compositions of porewaters in equilibrium with hydrated Type II Portland cement were calculated. This type of cement is used in the production of concrete inverts for the ESF[7] and is likely to be the predominant type of cement material used for proposed repository construction. The calculations were based on composition data for anhydrous Type II Portland cement [table 4-3, Clifton et al. (1991)] assuming a water/cement ratio of 0.38 and a setting time of 90 d. The setting time is used in the Reardon (1992) model to estimate the degree of hydration of each cement component and the bound water content as a function of time, whereas the water/cement ratio determines the amount of water available in the system and influences the calculated concentration of aqueous species. A water/cement ratio of 0.38 is the value used in production of concrete inverts for the

---

[7]N. O'Connor. 1996. Personal Communication.

ESF. A setting time (90 d) greater than the value used in constructing the concrete inverts (28 d)[8] was assumed for the simulation to partially account for further hydration reactions which occur over time.

Porewater chemical composition predicted to be in equilibrium with CSH gel, portlandite, brucite, ettringite, and hydrogarnet, the principal phases present at later stages of cement hydration (Reardon, 1992), is shown in table 4-4. CSH has a variable Ca/Si ratio and is the principal binding phase in Portland cements. The predicted hyperalkaline pH (13.9) of the pore fluid arises from the preferential partitioning of Na and K into the aqueous phase due to the absence of solid phase controls on these elements in a mature cement. Although Na and K concentrations in the cement material are low (table 4-3), these are dominant cations in the pore fluid. Due to charge balance constraints, Na^+ and K^+ concentrations must be balanced by an equivalent concentration of anions, predominantly OH^-. Alkali content of the cement paste determines the pH of porewater and influences the solubility of other phases in cementitious material.

Table 4-3. Composition of Type II Portland cement (taken from Clifton et al., 1991)

Oxide Component	Weight Percent
SiO_2	21.0
Al_2O_3	4.4
Fe_2O_3	3.1
CaO	63.5
MgO	3.4
SO_3	2.94
Na_2O	0.26
K_2O	0.50
Loss on Ignition	1.00

The major influence of alkalies on porewater chemistry and mineral solubilities could be short-lived if advection and diffusion processes dilute the concentration of alkalies. Where alkali concentration is small, porewater pH is buffered by dissolution of portlandite (Atkins and Glasser, 1992; Reardon, 1992; Berner, 1992). The predicted composition of porewater in equilibrium with alkali-free Type II Portland cement is given in table 4-5, indicating a pH of 12.5. Eventual depletion of portlandite causes the pore fluid pH to decrease from 12.5 to approximately 11, controlled by the incongruent dissolution of the CSH gel, particularly the Ca/Si ratio of the gel (Berner, 1992). When dissolution of CSH is complete, the pH of the cement pore fluid continues to decrease to a value approaching that of the groundwater.

The pH of water from tuffaceous aquifers at YM and vicinity falls in the range 7 to 9.2, with most samples in the 7 to 8 range (Kerrisk, 1987). The large difference in chemical potential between groundwater and pore fluid in cementitious materials provides a driving force for reactions between the two systems. These reactions will lead to a range of water chemistries that need to be considered in evaluating the performance of waste containers and the transport of radionuclides.

Several models have been developed to predict the evolution of pH in cementitious low- and intermediate-level waste repositories (e.g., Berner, 1987). A study by Atkinson et al. (1989) indicated that interaction of groundwater typical of a clay environment with cement could maintain a pH above about 10.5 for a time period on the order of a few hundred thousand years under the low flow rates assumed in that study. At those pH conditions, passive film formation would protect carbon steel, a material proposed as an overpack for HLW containers, unless high concentrations of chloride, sulfate,

[8]N. O'Connor. 1996. Personal Communication.

Table 4-4. Predicted solid and porewater composition for hydrated Type II Portland cement with initial composition given in table 4-3: water/cement ratio of 0.38 and setting time of 90 d. Solute concentrations are millimolal. Solid quantities are in millimoles per kilogram of water in the cement paste [total of bound and unbound water].

Species	Concentration mmol/kg H_2O	Activity Coefficient	Solid Phase	Log Saturation Index
OH^-	1.06×10^{-3}	0.682	Brucite	0
Ca^{2+}	0.67	0.018	Portlandite	0
Mg^{2+}	6.61×10^{-7}	0.038	Ettringite	0
$MgOH^+$	6.47×10^{-6}	0.436	CSH Gel	0
Na^+	584	0.636	Hydrogarnet	0
K^+	763	0.719	Amorphous Silica (SiO_2)	−5.32
$Al(OH)_4^-$	0.23	0.524	Sepiolite [$Mg_4Si_6O_{15}(OH)_2 \cdot 6\ H_2O$]	−11.01
$H_3SiO_4^-$	0.223	0.504	Gibbsite [$Al(OH)_3$]	−2.88
$H_2SiO_4^{2-}$	6.61	0.060	Calcite ($CaCO_3$)	−9.2
SO_4^{2-}	136	0.048	Gypsum ($CaSO_4 \cdot 2\ H_2O$)	
Brucite [$Mg(OH)_2$]	$1.33\times10^{+3}$	1.000	Syngenite [$K_2Ca(SO_4)_2 \cdot H_2O$]	−2.38
Portlandite [$Ca(OH)_2$]	$1.19\times10^{+4}$	1.000	Monosulfate ($Ca_4Al_2O_6SO_4 \cdot 12\ H_2O$)	−1.09
Ettringite [$Ca_6Al_2O_6(SO_4)_3 \cdot 32\ H_2O$]	299	1.000	Arcanite (K_2SO_4)	−0.93
CSH Gel ($x\ CaO \cdot SiO_2 \cdot x\ H_2O$, $x = Ca/Si$)	$7.25\times10^{+3}$	1.000	Glaserite [$K_3Na(SO_4)_2$]	−1.79
Hydrogarnet [$Ca_3Al_2(OH)_{12}$]	$1.1\times10^{+3}$	1.000		
pH	13.88			
Ionic Strength (mole/Kg H_2O)	1.49			
Bound H_2O	66.60%			
Ca/Si_{CSH}	1.03			

Table 4-5. Predicted solid and porewater composition for hydrated alkali-free Type II Portland cement. Solute concentrations are millimolal. Solid quantities are in millimoles per kilogram of water in the cement paste [total of bound and unbound water].

Species	Concentration mmol/kg H_2O	Activity Coefficient	Solid Phase	Log Saturation Index
OH^-	42.2	0.682	Brucite	0
Ca^{2+}	21.1	0.018	Portlandite	0
Mg^{2+}	3.54×10^{-5}	0.038	Ettringite	0
$MgOH^+$	8.61×10^{-5}	0.436	CSH Gel	0
$Al(OH)_4^-$	5.82×10^{-3}	0.524	Hydrogarnet	0
$H_3SiO_4^-$	1×10^{-3}	0.504	Amorphous silica	−6.03
$H_2SiO_4^{2-}$	4.29×10^{-4}	0.060	Sepiolite	−15.47
SO_4^{2-}	2.75×10^{-2}	0.048	Gibbsite	−2.88
Brucite	$1.33 \times 10^{+3}$	1.000	Gypsum	−2.68
Portlandite	$6.54 \times 10^{+3}$	1.000	Monosulfate	−1.14
Ettringite	314	1.000	Calcite	−6.35
CSH Gel	$7.25 \times 10^{+3}$	1.000		
Hydrogarnet	$1.08 \times 10^{+3}$	1.000		
pH	12.48			
Ionic Strength (mole/kg H_2O)	0.0634			
Bound H_2O	66.90%			
Ca/Si_{CSH}	1.76			

and/or carbonate are present which could lead to localized corrosion. However, results of current models of cement/water interactions are highly dependent on the assumptions used, particularly the reliance of pH evolution on solubility and persistence of a CSH gel known to be thermodynamically metastable. The same study by Atkinson et al. (1989) indicated that if recrystallization of the CSH gel occurred in the long term, lower pH could result due to the lower solubility of the crystalline CSH phases. If groundwater pH is buffered in the range 8 to 10 by crystalline CSH phases, localized corrosion or stress corrosion cracking of carbon steel overpack may be enhanced and adversely affect performance of the

waste canister. The possibility of CSH recrystallization is high in an HLW repository due to the long timeframe involved and the elevated temperatures imposed by radioactive decay heat from emplaced nuclear wastes. Even modest temperature excursion to 55 °C for 6 to 12 mo can result in partial transformation of CSH gel to more stable, though poorly crystallized, phases such as jennite and tobermorite (Atkins and Glasser, 1992). Thus, modeling of cement/near-field interactions in an HLW repository must consider the likelihood that cement chemistry is dominated by phases other than those present in the initial material.

The effects of cementitious materials on the evolution of the near-field environment at YM are difficult to quantify because of uncertainties in the amount that will be used in the estimated 228,000 m of excavation. Although an estimate of 560,000 m^3 of shotcrete for ground support was reported (Bruton et al., 1993) based on the SCP (U.S. Department of Energy, 1988), mostly competent ground has been encountered during construction of the Exploratory Studies Facility (ESF). Although qualitative information regarding effects of cementitious materials on the near-field environment can be derived using chemical models for cement/water interactions, a detailed analysis specific to the proposed YM repository environment will require specific information regarding inventory and location of these materials.

4.3.3 Effect of Microorganisms in the Near Field

Horn and Meike (1995) concluded that microorganisms are potentially important in three areas relative to proposed repository performance at YM: (i) alteration of groundwater and host rock chemistry, (ii) corrosion of the EBS, and (iii) mobility of radionuclides. Another important factor of microbial action on the evolution of the near field is its potential to affect flow of water both in the matrix and in fractures. It is known that growth of bacteria and the resultant production of exopolymeric substances can lead to a decrease in the porosity of tuff and other rocks. This effect on porosity can affect transport of radionuclides away from the proposed repository and water flow to containers and waste forms. Microbial plugging of pores and fractures could prevent resaturation of the proposed repository following dryout and could also increase the time necessary to achieve dryout. The DOE has partially characterized the microbiology of the proposed YM repository site. This survey showed that a number of microorganisms that could have an impact on the proposed repository are present at the site. However, this limited survey looked for a partial list of microorganisms, focusing particularly on those implicated in microbial corrosion processes. The current or anticipated level of activity of those organisms has not been addressed.

The Center for Nuclear Waste Regulatory Analyses (CNWRA) studies concentrated on the viability of a natural population following exposure to various temperatures to determine whether the proposed repository will be self sterilizing due to heating by the waste. A sample of tuff obtained from the proposed repository horizon at YM was cored providing an undisturbed sample which was crushed and a 2–4-mm-size fraction collected. Samples of crushed tuff were heated to various temperatures for 200 hr and bacterial viability assessed. A Gram-positive spore former maintained viability at temperatures to 120 °C for the extended time exposures and showed variable viability for shorter 150 °C exposures. Only aerobic heterotrophic bacteria were screened in this study. With a heat load of 83 MTU, the maximum predicted temperature is 130 °C. Therefore, these results indicate that microorganisms can survive over short periods in the near-field environment, although probably not on the containers themselves. Later, when suitable conditions prevail, they can become active. Although these bacteria have not been fully characterized, it is possible that as Gram-positive spore formers producing acid from glucose and capable of anaerobic growth, they are members of the genus *Clostridium*. This group of

bacteria is often associated with MIC due to the ability to produce organic acids. They are also a common isolate from corroded pipes. These isolates produce extracellular polymeric substances potentially affecting hydraulic properties of the host rock and other near-field components.

Two factors have been suggested to limit the effects of microbiological organisms on the performance of the EBS and proposed repository (TRW Environmental Safety Systems, Inc., 1996b):

(i) Diffusion of oxygen destabilizes anaerobic conditions needed by obligate anaerobes. This argument neglects anaerobic niches known to form in the environment in oxidizing conditions. For example, Lee et al. (1993) demonstrated that formation of a biofilm on a surface can lead to conditions necessary for anaerobic sulfate reducing bacteria to grow.

(ii) The level of oxidizable sulfur species found at the proposed repository horizon is insufficient to maintain bacteria such as Thiobacilli. A potentially important area is the microbial degradation of concrete. Milde et al. (1993) first reported microbially induced degradation (MID) of concrete in a Hamburg sewer system. They were able to link the degradation to the action of Thiobacilli, a group of bacteria capable of oxidizing sulfur compounds to sulfuric acid. Recently, Hamilton et al. (1996) surveyed a number of large concrete structures above ground which showed evidence of severe degradation. They identified many sites with severe degradation that also had high numbers of Thiobacilli; in each case, they identified a source of reducible sulfur. The DOE site characterization has shown that Thiobacilli are present but not a suitable supply of sulfur. However, potentially large amounts of sulfate are available from Portland cement.

Although the action of the Thiobacilli on MID of concrete is potentially limited by lack of oxidizable sulfur, potential corrosive action on steel may be important. *Thiobacillus ferrooxidans* is a unique member of the Thiobacilli that can obtain energy axotrophically from the oxidation of iron without an organic carbon source, using carbon dioxide instead. Again, its action on the canisters is limited at elevated temperatures. Literature on this bacteria reports its growth in pure planktonic cultures. Under these conditions, it is known to be acidophilic requiring low pH. However, biofilm cells are distinct from the physiology of planktonic cultures. Therefore, the CNWRA experiments are determining whether *T. ferrooxidans* can grow and oxidize iron at the pH anticipated in the proposed repository.

4.4 SUMMARY OF TECHNICAL ACCOMPLISHMENTS

THC coupled processes were examined using the MULTIFLO code. The code was used to assess the range of near-field environmental conditions as a function of areal mass loading. Calculations show that significant changes in pH and salinity could occur with moderate thermal loading of the proposed repository. With increasing heat load, higher concentrations of dissolved solutes are expected. At the extreme case of complete dryout, salts are expected to precipitate during the heating regime and dissolve during the cooling phase as the proposed repository rewets. It is expected that for the higher heat loads, when complete dryout occurs, an evaporite deposit will form in the near field with the deposition of salts occurring throughout the dryout zone in the near-field region. The effect of this evaporite deposition on fluid composition during the rewetting stage is being investigated.

One of the main limitations of the present calculation is the use of the ECM. In this model, the fractured porous medium is represented as a single average continuum. Capillary equilibrium is assumed

to be maintained between the fracture and matrix. As a consequence of this assumption, it is not possible for flow to take place in the fracture network without the matrix becoming fully saturated at the same time. This assumption of the model is fundamental to the formation of a capillary barrier sandwiched between zones of enhanced moisture content and the proposed repository horizon preventing liquid water from reaching the waste during the heating regime. Consequently, gravity driven flow such as dripping, which may be an important process for container life and source term, can not be described within the confines of the ECM. Alternate conceptualizations, such as multiple interacting continuua, may provide a better description of fracture flow. Verification or validation of the THC coupling may be attempted through an analysis of field samples at YM originating from paleohydrothermal sources. Field samples have been collected and are being analyzed. Alternatively, idealized laboratory experiments may be performed if suitable methods of accelerating the processes can be found and the results compared to model predictions for validating models. However, these have not been attempted in FY96.

The effects of cementitious materials on near-field environment has been estimated using available data mainly at near-ambient temperatures. However, considerable uncertainties exist regarding the stability of the CSH gel phase that may determine the pH of the fluid contacting the cement. If the gel phase recrystallizes at higher temperatures, the pH may not attain as high a value as calculated from room temperature data. It is also important to couple these essentially static calculations with a transport model such as MULTIFLO to estimate the spatial extent of the change in pH due to cement-water interactions.

The investigation of microbiological activity has shown that bacterial colonies native to the host rock at YM are viable even after exposure to 120 °C. However, their activity and the effects on near-field environment through interaction with cementitious materials may be limited by the absence of oxidizable sulfur species.

4.5 ASSESSMENT OF PROGRESS TOWARD MEETING OBJECTIVES

The completion of the ENFE evaluation report (Angell et al., 1996) enabled a prioritization of those aspects of the evolution of the near-field environment that are likely to affect the attributes of the DOE WCIS. Completion of the ENFE evaluation report (Angell et al., 1996) also prepared the ENFE KTI team to review the two near-field DOE synthesis reports (mineralogy/petrology and near-field environment), which are anticipated to be released in FY97, and the DOE TSPA-95 effort (TRW Environmental Safety Systems, Inc., 1995). Development of computer modeling capabilities allowed sensitivity analyses of the near-field environment to be determined and projection of expected THC effects for the DOE heater tests. These sensitivity analyses will be used to address DOE hypotheses related to low corrosion, mobilization of radionuclides, and slow transport. In addition, sensitivity analyses results will be directly incorporated in the NRC detailed TSPA-95 review effort. Both the cement-water interaction study and the laboratory microbial investigations focused on aspects of the near-field environment important to performance (Angell et al., 1996), that support resolution of subissues, and that address DOE hypotheses related to low corrosion and slow transport. Cement-water calculations provide an upper limit on the pH of fluids significantly higher than that used by the DOE in TSPA-95 (TRW Environmental Safety Systems, Inc., 1995) and provides for a basis to resolve the appropriate range of environmental conditions to use in performance calculations. The microbial studies provide a scientific basis for determining the importance of microbial interactions on radionuclide transport and a footing to resolve this aspect of the limited radionuclide transport subissue. In general, studies of these issues

address overall performance because near-field conditions affect the rate of container corrosion, alteration of waste forms and radionuclide release, and transport of radionuclides through the near field.

No new subissues for this KTI were discovered during FY96 as a result of the ENFE team effort. However, two aspects of existing subissues were brought to light as being currently under-emphasized in the ENFE effort. The importance of fractures on the transport of fluids needs to be evaluated for staff to resolve the ENFE subissue of low infiltration into emplacement drifts. In addition, the importance of man-introduced materials, such as cementitious materials, has been demonstrated to be an important control of fluid chemistry. However, the impacts of degradation of the WP including the waste have not been incorporated into determining importance to the evolution of the chemistry of the near-field environment. The ENFE subissue addressing the DOE hypothesis of low seepage into the emplacement drift requires answering the question of what are the changes in fracture permeability due to interactions of fluids with the rock matrix and fractures. Two lines of evidence suggest the importance of resolving this question.

(i) The MULTIFLO modeling effort and modeling completed by the Thermal Effects on Flow (TEF) KTI indicate the formation of a heat pipe. Geologic evidence of fossil heat pipes has been recently interpreted to indicate downward flow of liquid condensate within vapor-filled fractures.[9]

(ii) High pH fluids derived from interaction with cementitious material have been suggested to affect the porosity and permeability of the interacting host rock (Steefel and Lichtner, 1994).

For the case of the proposed repository, both evaporative processes and fluid interaction with cementitious material will drive fluids to a high pH. The net result of the high pH will be to strengthen the importance of water rock interaction and its consequences on hydrologic characteristics of the fractures. To help resolve this subissue, hydrologic models for near-field interactions, other than ECMs, will be required. The ENFE subissue addressing the DOE hypothesis of limited radionuclide transport from the EBS to the host rock requires definition of the bounding environmental factors affecting radionuclide transport from the EBS. At present, the importance of the degradation of the WP and release from the source have not been incorporated into evaluation of bounding conditions. Completion of the EBSPAC module in the Container Life and Source Term (CLST) KTI should allow for some estimates of possible bounding geochemical conditions to be determined.

4.6 INTEGRATION WITH OTHER KEY TECHNICAL ISSUES

Development and beta testing of the MULTIFLO code required input and assistance from the TEF and Total System Performance Assessment and Integration (TSPAI) KTI teams. The assistance provided by other teams include specifying information that the model would need to provide to the other KTIs and providing boundary conditions for beta testing the model.

Output from the ENFE KTI for FY96 are predominately related to development of the MULTIFLO computer code. The MULTIFLO code is the basis for many of the thermal analyses currently being conducted under the TEF KTI. Calculations performed using MULTIFLO are also being

[9]S. Ingebritsen. 1996. Personal Communication.

used as input in the EBSPAC calculation of CLST by the CLST KTI team. Currently, these codes are not directly linked. Additionally, the METRA part of the MULTIFLO code is being used by the Repository Design and Thermal-Mechanical Effects (RDTME) KTI to benchmark temperature calculations performed using an effective conductivity model. The temperature calculations from the effective conductivity model are then being used in the EBSPAC.

Two subissues, low infiltration into emplacement drifts and radionuclide transport, will need additional effort to approach resolution. Currently under the ENFE KTI implementation plan, ENFE does not obtain input from the Structural Deformation and Seismicity (SDS) KTI. To complete an analysis of the importance of fractures on the evolution of the near field will require input from the SDS of a simplified or abstracted model of faults and their geometry. Discussions with the SDS team to refine the informational needs of the ENFE KTI have been initiated. Bounding the chemical composition of near-field pore fluids will require increased interactions with the CLST team. Currently, the degradation products of the engineered barrier and waste form and importance to pore fluid chemistry have not been factored into efforts to bound near-field fluid chemistry. Finally, the linkage and pathway between information generated in the ENFE sensitivity analyses and the actual input needs of the TSPA team should be refined.

In support of the TSPAI KTI, sections of TSPA-95 (TRW Environmental Safety Systems, Inc., 1995) related to near-field environment were reviewed with particular attention to an evaluation of the dependence of the results of performance calculations on geochemical characteristics of the near field. In general, this review concluded that important near-field characteristics are fairly well recognized in qualitative descriptions of model development. However, minimal recognition of these characteristics was employed in the performance calculations.

4.7 REFERENCES

Angell, P., J.A. Apps, G.A. Cragnolino, S.-M. Hsiung, P.C. Lichtner, W.M. Murphy, R.T. Pabalan, D.A. Pickett, N. Sridhar, S.A. Stothoff, and D.R. Turner. 1996. *Evolution of the Near-Field Environment in the Proposed High-Level Waste Repository at Yucca Mountain, Nevada*. W.M. Murphy, ed. CNWRA Letter Report. San Antonio, TX: Center for Nuclear Waste Regulatory Analyses.

Angus, M.J., C.E. McCulloch, R.W. Crawford, F.P. Glasser, and A.A. Rahman. 1983. Kinetics and mechanism of the reaction between Portland cement and clinoptilolite. *Advances in Ceramics 8*. G.G. Wicks and W.A. Ross, eds. Columbus, OH: Nuclear Waste Management: American Ceramic Society: 429–440.

Atkins, M., and F.P. Glasser. 1992. Application of Portland cement-based materials to radioactive waste immobilization. *Waste Management* 12: 105–131.

Atkins, M., J. Cowie, F.P. Glasser, T. Jappy, A. Kindness, and C. Pointer. 1990. Assessment of the performance of cement-based composite material for radioactive waste immobilization. *Scientific Basis for Nuclear Waste Management XIII Symposium Proceedings*. M. Oversby and P.W. Brown, eds. Pittsburgh, PA: Materials Research Society: 176: 117–127.

Atkins, M., F.P. Glasser, and A. Kindness. 1991. Phase relations and solubility modelling in the $CaO-SiO_2-Al_2O_3-MgO-SO_3-H_2O$ system: For application to blended cements. *Scientific Basis for Nuclear Waste Management XIV Symposium Proceedings*. T. Abrajano, Jr. and L.H. Johnson, eds. Pittsburgh, PA: Materials Research Society: 212: 387–394.

Atkinson, A., N.M. Everitt, and R.M. Guppy. 1989. Time dependence of pH in a cementitious repository. *Scientific Basis for Nuclear Waste Management XII Symposium Proceedings*. W. Lutze and R.C. Ewing, eds. Pittsburgh, PA: Materials Research Society: 127: 439–446.

Baca, R.G., and R.D. Brient. 1996. *Total System Performance Assessment 1995 Audit Review*. CNWRA Letter Report. San Antonio, TX: Center for Nuclear Waste Regulatory Analyses.

Berner, U.R. 1987. Modelling porewater chemistry in hydrated Portland cement. *Scientific Basis for Nuclear Waste Management X Symposium Proceedings*. J.K. Bates and W.B. Seefeldt, eds. Pittsburgh, PA: Materials Research Society: 44: 319–330.

Berner, U.R. 1992. Evolution of pore water chemistry during degradation of cement in a radioactive waste repository environment. *Waste Management* 12: 201–219.

Bruton, C.J., A. Meike, B.E. Viani, S. Martin, and B.L. Phillips. 1993. Thermodynamic and structural characteristics of cement minerals at elevated temperature. *Proceedings of the Topical Meeting on Site Characterization and Model Validation (Focus '93)*. La Grange Park, IL: American Nuclear Society: 150–156.

Buscheck, T.A., and J.J. Nitao. 1993. The analysis of repository-heat-driven hydrothermal flow at Yucca Mountain. *Proceedings of the Fourth Annual International Conference on High-Level Radioactive Waste Management*. La Grange Park, IL: American Nuclear Society: 1: 847–867.

Clifton, J.R., L.I. Knab, E.J. Garboczi, and L.X. Xiong. 1991. *Chloride Ion Diffusion in Low Water-to-Solid Cement Phases*. NUREG/CR-5727. Washington, DC: Nuclear Regulatory Commission.

Glasser, F.P., M.J. Angus, C.E. McCulloch, D. Macphee, and A.A. Rahman. 1985. The chemical environment in cements. *Scientific Basis for Nuclear Waste Management VIII Symposium Proceedings*. C.M. Jantzen, J.A. Stone, and R.C. Ewing, eds. Pittsburgh, PA: Materials Research Society: 44: 849–858.

Glassley, W.E. 1986. *Reference Waste Package Environment Report*. UCRL-53726. Livermore, CA: Lawrence Livermore National Laboratory.

Hamilton, M.A., R.D. Rogers, R. Veeh, and M. Zolynski. 1996. Evaluation of microbially-influenced degradation of massive concrete structures. *Scientific Basis for Nuclear Waste Management XIX Symposium Proceedings*. W.M. Murphey and D.A. Knecht, eds. Pittsburgh, PA: Materials Research Society: 412: 469–474.

Harrar, J.E., J.F. Carley, W.F. Isherwood, and E. Raber. 1990. *Report of the Committee to Review the Use of J-13 Well Water in Nevada Nuclear Waste Storage Investigations*. UCID-21867. Livermore, CA: Lawrence Livermore National Laboratory.

Heimann, R.B. 1988. Interaction of cement and radioactive waste forms in multicomponent systems tests at 200 °C, Part 2: Mineralogical changes of cement. *Cement Concrete Research* 18: 554–560.

Horn, J.M., and A. Meike. 1995. *Microbial Activity at Yucca Mountain*. UCRL-ID-122256. Livermore, CA: Lawrence Livermore National Laboratory.

Kerrisk, J.F. 1987. *Groundwater Chemistry at Yucca Mountain, Nevada, and Vicinity*. LA-10-29-MS. Los Alamos, NM: Los Alamos National Laboratory.

Komarneni, S., and D.M. Roy. 1983. Hydrothermal interactions of cement or mortar with zeolites or montmorillonites. *Scientific Basis for Nuclear Waste Management VI Symposium Proceedings*. D.G. Brookins, ed. Pittsburgh, PA: Materials Research Society: 15: 55–62.

Lee, W., Z. Lewandowski, M. Morrison, W.G. Characklis, R. Avci, and P.H. Nielsen. 1993. Corrosion of mild steel underneath aerobic biofilms containing sulfate-reducing bacteria, Part II: At high dissolved oxygen concentration. *Biofouling* 7: 217–239.

Lichtner, P.C., and J. Eikenberg. 1995. *Propagation of a Hyperalkaline Plume into the Geological Barrier Surrounding a Radioactive Waste Repository*. PSI 95-01. Wurenlingen, Switzerland: Paul Scherrer Institute.

Lichtner, P.C., and M.S. Seth. 1996. *User's Manual for MULTIFLO: Part II—MULTIFLO 1.0 and GEM 1.0. Multicomponent-Multiphase Reactive Transport Model*. CNWRA 96-010. San Antonio, TX: Center for Nuclear Waste Regulatory Analyses.

Milde, K., W. Sand, W. Wolff, and E. Bock. 1993 Thiobacilli of the corroded concrete walls of the Hamberg sewer system. *Journal of General Microbiology* 129: 1,327–1,333.

Murphy, W.M. 1991. Performance assessment perspectives with reference to the proposed repository at Yucca Mountain, Nevada. *Proceedings from the Technical Workshop on Near-Field Performance Assessment for High-Level Waste*. Madrid, Spain: Swedish Nuclear Fuel and Waste Management Co.: 11–12.

Nitao, J.J. 1989. *V-TOUGH—An Enhanced Version of the TOUGH Code for the Thermal and Hydrologic Simulation of Large-Scale Problems*. UCID-21954. Livermore, CA: Lawrence Livermore National Laboratory.

Nitao, J.J. 1996. *Reference Manual for the NUFT Flow and Transport Code, Version 1.0*. UCRL-ID-113J20. Livermore, CA: Lawrence Livermore National Laboratory.

Pruess, K. 1987. *TOUGH User's Guide*. LBL-20700. Berkeley, CA: Lawrence Berkeley Laboratory.

Pruess, K., and Y. Tsang. 1993. Modeling of strongly heat-driven flow processes at a potential high-level nuclear waste repository at Yucca Mountain, Nevada. *Proceedings of the Fourth Annual International Conference on High-Level Radioactive Waste Management*. La Grange Park, IL: American Nuclear Society: 1: 568–575.

Reardon, E.J. 1992. Problems and approaches to the prediction of the chemical composition in cement/water systems. *Waste Management* 12: 221–239.

Seth, M.S., and P.C. Lichtner. 1996. *User's Manual for MULTIFLO: Part I—METRA 1.0β, Two-Phase Nonisothermal Flow Simulator*. CNWRA 96-005. San Antonio, TX: Center for Nuclear Waste Regulatory Analyses.

Steefel, C., and P.C. Lichtner. 1994. Diffusion and reaction in rock matrix bordering a hyperalkaline fluid-filled fracture. *Geochimica et Cosmochimica Acta* 58: 3,595–3,612.

TRW Environmental Safety Systems, Inc. 1995. *Total System Performance Assessment—1995: An Evaluation of the Potential Yucca Mountain Repository*. B00000000-01717-2200-00136. Las Vegas, NV: TRW Environmental Safety Systems, Inc.

TRW Environmental Safety Systems, Inc. 1996a. *Mined Geologic Disposal System Advanced Conceptual Design Report. Volume II of IV, Repository*. B00000000-01717-5705-00027. Rev. 00. Las Vegas, NV: TRW Environmental Safety Systems, Inc.

TRW Environmental Safety Systems, Inc. 1996b. *Mined Geologic Disposal System Advanced Conceptual Design Report. Volume III of IV, Engineered Barrier Segment/Waste Package*. B00000000-01717-5705-00027. Rev. 00. Las Vegas, NV: TRW Environmental Safety Systems, Inc.

U.S. Department of Energy. 1988. *Site Characterization Plan, Yucca Mountain Site, Nevada Research and Development Area, NV*. DOE/RW-0199. Washington, DC: Office of Civilian Radioactive Waste Management: U.S. Department of Energy.

Walton, J.C. 1993. Effects of evaporation and solute concentration on presence and composition of water in and around the waste package at Yucca Mountain. *Waste Management* 13: 293–301.

White, S.P. 1995. Multiphase nonisothermal transport of systems of reacting chemicals. *Water Resources Research* 31: 1,761–1,772.

Wilder, D.G. 1993a. *Preliminary Near-Field Environment Report. Vol. I: Technical Bases for EBS Design*. UCRL-LR-107476. Livermore, CA: Lawrence Livermore National Laboratory.

Wilder, D.G. 1993b. *Preliminary Near-Field Environment Report. Vol. II: Scientific Overview of Near-Field Environment and Phenomena*. UCRL-LR-107476. Livermore, CA: Lawrence Livermore National Laboratory.

Wolery, T.J. 1992. *EQ3/6, A Software Package for Geochemical Modeling of Aqueous Systems: Package Overview and Installation Guide. Version 7.0.* UCRL-MA-110662. Part 1. Livermore, CA: Lawrence Livermore National Laboratory.

Zyvoloski, G., Z. Dash, and S. Kelkar. 1992. *GEHMN 1.0: Finite Element Heat and Mass Transfer Code.* LA-12062-MS. Rev. 1. Los Alamos, NM: Los Alamos National Laboratory.

5 CONTAINER LIFE AND SOURCE TERM

Primary Authors: ***G.A. Cragnolino, S. Mohanty, T.M. Ahn, H.K. Manaktala, D.S. Dunn, P.J. Angell, W.M. Murphy, and N. Sridhar***

Technical Contributors: ***B.J. Davis, S. Larose, Y.-M. Pan, and R.A. Rapp***

Key Technical Issue Co-Leads: ***N. Sridhar (CNWRA) and K.C. Chang (NRC)***

5.1 INTRODUCTION

The U.S. Department of Energy (DOE) updated Waste Containment and Isolation Strategy (WCIS) for the proposed repository at Yucca Mountain (YM)[1] has the primary goals of near-complete containment of radionuclides within waste packages (WPs) for several thousand years and acceptably low annual doses to a member of the public living near the site. Among the system attributes recognized in this strategy to be most important in accomplishing these goals are the WP life time (containment), rate of release of radionuclides from breached WPs, and radionuclide transport through engineered and natural barriers. The objective of the Container Life and Source Term (CLST) Key Technical Issue (KTI) is to evaluate these attributes independently and provide input to the performance assessment (PA) of the overall proposed repository.

Several subissues have been delineated within the CLST KTI that directly address the DOE WCIS. These include (i) evaluation of methodologies for extrapolating short-term laboratory data to long-term performance, (ii) evaluation of factors affecting waste form alteration products and the release of radionuclides, (iii) determining the effect of long-term thermal exposure and mechanical loads on the mechanical stability of the container materials, (iv) assessing the effect of microbiological organisms on the performance of container materials, and (v) performing sensitivity analyses on the effects of thermal loading, near-field environment, and galvanic coupling on container life using the Engineered Barrier System Performance Assessment Code (EBSPAC). The DOE performed a probabilistic analysis of container life in TSPA-95 using the Waste Package Degradation (WAPDEG) code. Similar methodologies may be used in the DOE viability assessment (VA) through TSPA-VA. The sensitivity analyses performed in this KTI will enable the Nuclear Regulatory Commission (NRC) and the Center for Nuclear Waste Regulatory Analyses (CNWRA) staffs to evaluate methodologies used by DOE in TSPA-95 and compare the container life cumulative distribution curves predicted by EBSPAC and WAPDEG. These analyses will also facilitate the evaluation of the significance of these subissues to the overall system performance.

The major component of the Engineered Barrier System (EBS) is the WP, which includes the waste form [spent fuel (SF) and vitrified waste], fuel cladding, filler, canisters [multi-purpose canister (MPC) and pour canister], and disposal overpacks. In addition to the WP, the EBS consists of backfill, concrete inverts, emplacement pedestals, drip shields, and other components used in the proposed repository construction. Some components affect the waste containment indirectly through their effects on near-field environment (e.g., concrete inverts, rock bolts), while other components affect containment

[1]U.S. Department of Energy. 1996. *Highlights of the U.S. Department of Energy's Updated Waste Containment and Isolation Strategy for the Yucca Mountain Site*. DOE Concurrence Draft. July 1996. Washington, DC: U.S. Department of Energy.

directly (e.g., overpacks, cladding). Evaluation of the components of EBS that affect containment and radionuclide release directly is considered in this KTI.

Several WP designs have been proposed by the DOE over the history of the proposed YM repository program. Of these designs, the canistered fuel design is considered the primary choice (TRW Environmental Safety Systems, Inc., 1996). In this design, either 21 pressurized water reactor (PWR) or 40 boiling water reactor (BWR) SF assemblies are contained in a type 316L stainless steel MPC (3.5-cm wall thickness) in which a fuel basket, probably made of borated stainless steel, provides criticality control and enhances heat transfer. The MPC is surrounded by an inner overpack made of a corrosion-resistant alloy (2.5-cm wall thickness), in turn contained in an outer overpack made of a corrosion-allowance material (10-cm wall thickness). The proposed outer length of such a WP is 5.682 m and the outer diameter is 1.802 m. The total surface area is about 37 m^2 and the loaded weight is about 65,000 Kg. Alternate designs include WP for uncanistered fuel (no MPC), small canistered fuel (12 PWR or 24 BWR SF assemblies), and vitrified reprocessed waste. A list of candidate materials for the overpacks is shown in table 5-1 with the materials that are the primary choices in the present design indicated. In addition to providing an independent evaluation of containment for specific materials in the present WP and radionuclide release from the EBS, the CLST KTI addresses the appropriateness of predictive methodologies which are generally applicable to a wide variety of materials.

5.2 OBJECTIVES AND SCOPE OF WORK

This KTI has three objectives:

(i) Evaluate the scope and quality of the DOE WP program and WP design

(ii) Conduct sensitivity analyses on performance of the EBS in relation to uncertainties in conceptual models and data

(iii) Provide input to the PA of the overall repository

To accomplish the first objective, the DOE planning documents on the WP program and Total System Performance Assessment (TSPA)-95 (TRW Environmental Safety Systems, Inc., 1995) calculations were reviewed. The second objective is being accomplished through detailed evaluations of specific failure processes and incorporation of abstracted models in the EBSPAC. The third objective will be accomplished through the incorporation of EBSPAC as a source term module into the NRC/CNWRA Total Performance Assessment (TPA) code.

This section of the annual report describes some of the sensitivity analyses of WP performance through the use of EBSPAC, a detailed evaluation of dry oxidation and thermal embrittlement of the outer steel overpack, the applicability of the repassivation potential concept for long-term prediction of inner overpack performance, and some of the factors affecting radionuclide release from SF. Some of these detailed analyses have already been abstracted in EBSPAC. The integration between this KTI and some of the other KTIs is briefly described.

Table 5-1. Candidate materials in the advanced conceptual design (modified from TRW Environmental Safety Systems, Inc., 1996)

Component	Materials	
	Primary	**Alternate**
Inner Overpack	Alloy 825 (UNS N08825)	Ni-Base Alloys Alloy C-22 (UNS N06022) Alloy G-30 (UNS N06030) Alloy C-4 (UNS N06455) Alloy G-3 (UNS N06985) Alloy N08221 (Not in commercial production) Ti-Base Alloys Grade 12 (UNS R53400) Grade 16 (UNS R52402)
Outer Overpack	ASTM A516, Grade 55 Carbon Steel (UNS K01800)	Fe-Base Alloys ASTM A27 Grade 70-40 (UNS J02501) cast steel ASTM A387 Grade 22 (UNS K21590) alloy steel Cu-Base Alloys 90-10 CuNi (UNS C70600) 70-30 CuNi (UNS C71500) Ni-Base Alloy Alloy 400 (UNS N04400)
Outer Overpack, HLW Glass	70-30 CuNi (UNS C71500)	

5.3 SIGNIFICANT TECHNICAL ACCOMPLISHMENTS

5.3.1 Sensitivity Analyses Using the Engineered Barrier System Performance Assessment Code

The overall strategy for EBSPAC development consists of concurrent development of detailed analyses or models of physical and physicochemical processes affecting WP performance and abstraction of these models for incorporation into EBSPAC. Models and computational approaches used previously in SOTEC (Sagar et al., 1992) and SCCEX (Cragnolino et al., 1994) codes have been incorporated with appropriate modifications in the current version of EBSPAC (Mohanty et al., 1996).

Sensitivity analyses provide an adequate methodology to evaluate the relative importance of certain processes and the associated variables or parameters on the performance of WPs. Although detailed conceptual and numerical models exist for many corrosion and mechanical failure processes, material specific parameters for these models, that should be adapted to the conditions prevailing in a repository under partially saturated conditions, are scarce. These parameters are obtained through reviews

of published literature and information reported by the DOE, combined with data obtained in the experimental investigations program conducted within this KTI. In some cases, lack of reliable data for a given parameter justifies the use of sensitivity analyses as a tool to evaluate the need for acquiring new data.

In EBSPAC, Version 1.0β (Mohanty et al., 1996), only the largest canistered fuel WP design for 21 PWR or 40 BWR SF assemblies in a horizontal drift emplacement, as currently envisioned by the DOE (TRW Environmental Safety Systems, Inc., 1996), was considered. As a set of external calculations to EBSPAC, the thermal model provides the temperature distribution as a function of time and position within the EBS as well as in the surrounding geosphere. The temperature and relative humidity (RH) at the WP surface as functions of time are used to predict the conditions that affect the occurrence and rate of corrosion of the WP and the subsequent release of radionuclides. The chemical composition, pH, and oxygen concentration of the fluid able to come in contact with the WP is determined by the environment model, where the evaporative effects produced by heat released by radioactive decay are considered.

Below a critical value of RH, air oxidation of steel is modeled as the dominant process for the steel overpack. Mechanical failure as a result of thermal embrittlement of the steel promoted by long-term exposure to temperatures above 150 °C is evaluated at each time step. If the RH is higher than the critical value, the occurrence of aqueous corrosion of the steel overpack is evaluated. No distinction is made in EBSPAC between humid air corrosion and aqueous corrosion because both processes are governed by the same fundamental principles. The corrosion models calculate the rates of uniform and localized corrosion. The corrosion process at any given time depends on the corrosion potential and the critical potential required to initiate a particular localized corrosion process. Following penetration of the outer container, electrical contact of the inner and outer container through the presence of an electrolyte path such as that provided by modified groundwater promotes galvanic coupling assuming that metallic contact always exists between both containers. The galvanic coupling model evaluates whether penetration of the inner container by localized corrosion is possible; otherwise, uniform corrosion or mechanical fracture becomes the predominant failure mechanism because the inner container becomes protected against localized corrosion.

Once penetration of the inner container occurs, the RH criterion is applied to determine whether air oxidation or aqueous dissolution of SF is the subsequent process to be evaluated. Air oxidation of SF leads to gaseous release of C-14 predominantly from the fuel cladding, whereas I-129, Cl-36, and C-14 are released as gases from the fuel pellets and the pellet/cladding gap. In Version 1.0β of EBSPAC, aqueous release of radionuclides from SF only includes congruent releases with solubility constraints of the radionuclides contained in the irradiated UO_2 matrix. Only the bathtub model is used in Version 1.0β of EBSPAC, although dripping of modified groundwater on the SF will be implemented in future versions. Aqueous releases are treated only as dissolution rate limited release or solubility limited release.

EBSPAC performs deterministic calculations for a single cell, not for the overall repository, through two separate, distinctive parts. One part deals with WP failure calculations and the other, essentially a separate code, with release calculations; no feedback exists from the release part into the failure part. The release code includes the incorporation of radionuclide decay, generation of daughter products in the chains, temporal variation of inventory in the WP, and spatial variations in the properties of the surrounding material. However, the degree of complexities incorporated varies from model to model to accomplish necessary simplifications while ensuring conservatism in calculations of radionuclide release.

As an example of the capabilities of the EBSPAC, a set of calculations was performed to demonstrate the effect of galvanic coupling on the failure time of the WP. In Version 1.0β of EBSPAC a simplified approach is used to account for galvanic coupling effects between the inner and the outer overpacks. The corrosion potential of the galvanic couple formed when the wall of the outer container is penetrated by a pit, E_{corr}^{wp}, is estimated by using experimentally measured values of the potential of the bimetallic couple, E_{couple}, for a well-defined area ratio between both components. Then E_{corr}^{wp} is determined through a linear combination of E_{corr} of the outer overpack, as calculated by the code at the time of its through-wall penetration, and E_{couple}, according to the following expression

$$E_{corr}^{wp} = (1 - \eta)E_{corr} + \eta E_{couple} \tag{5-1}$$

where η is the efficiency of the galvanic coupling with the condition $0 \leq \eta \leq 1$. A value of E_{couple} equal to $-0.46\ V_{SHE}$ was adopted on the basis of results reported by Scully and Hack (1984) for a galvanic couple made of steel and alloy 625 (a nickel-base alloy similar in electrochemical behavior to alloy 825) with an area ratio 1:1 and exposed to sea water. The values adopted for the different parameters needed to calculate E_{corr} and those establishing the dependence of the critical potentials with chloride concentration and temperature are reported elsewhere (Mohanty et al., 1996). A chloride concentration of 0.3 mol/L has been used in this set of calculations, instead of 3×10^{-3} mol/L as provided by MULTIFLO calculations (Mohanty et al., 1996), to attain failure within the 10,000-yr simulation period for $\eta = 0$.

Figure 5-1 shows the WP failure time as a function of the galvanic coupling efficiency for two values of the areal mass loading (AML), currently a repository design variable. The calculations correspond to the thermal model cases (Mohanty et al., 1996) in which neither ventilation is assumed during the initial 100 yr operations period nor backfill after permanent closure. It is seen that at 80 MTU/acre, which is close to the value adopted by the DOE in TSPA-95 for the high thermal loading case, η has an important effect on the WP failure time, which increases abruptly from 2,736 yr to more than 10,000 yr (the simulation time) for η values close to 0.2. A similar effect is observed at 40 MTU/acre where failure time increases from 472 yr to more than 10,000 yr for η values just above 0.08. On the contrary, no effect of η is found at 20 MTU/acre, a case where failure time is greater than 10,000 yr regardless of the value of η. If galvanic coupling is completely ineffective ($\eta = 0$), the shortest failure time occurs at the intermediate AML (40 MTU/acre). The wetting time is also the shortest at the intermediate AML, but the differences in failure times are only explainable by the effect of temperature on the initiation of localized corrosion. The wetting times, corresponding to a critical value of RH equal to 65 percent, are 153, 50, and 2,336 yr for 20, 40, and 80 MTU/acre, respectively.

Although penetration by localized corrosion of the outer container occurs in a few hundred years, as illustrated in figure 5-2, for 20 MTU/acre, only slow passive dissolution of the inner alloy 825 container takes place subsequently because E_{corr} is lower than the critical potential for localized corrosion at the relatively low temperatures encountered at this low AML. In this case, the inner container is undermined just after 10,000 yr. In summary, the critical potential above which localized corrosion occurs increases with a decrease in temperature so the likelihood of localized corrosion for a given chemical environment decreases with a decrease in AML. At high AML, WP remains dry for a long period, and the container life is long. These two competing factors lead to a minimum container life at

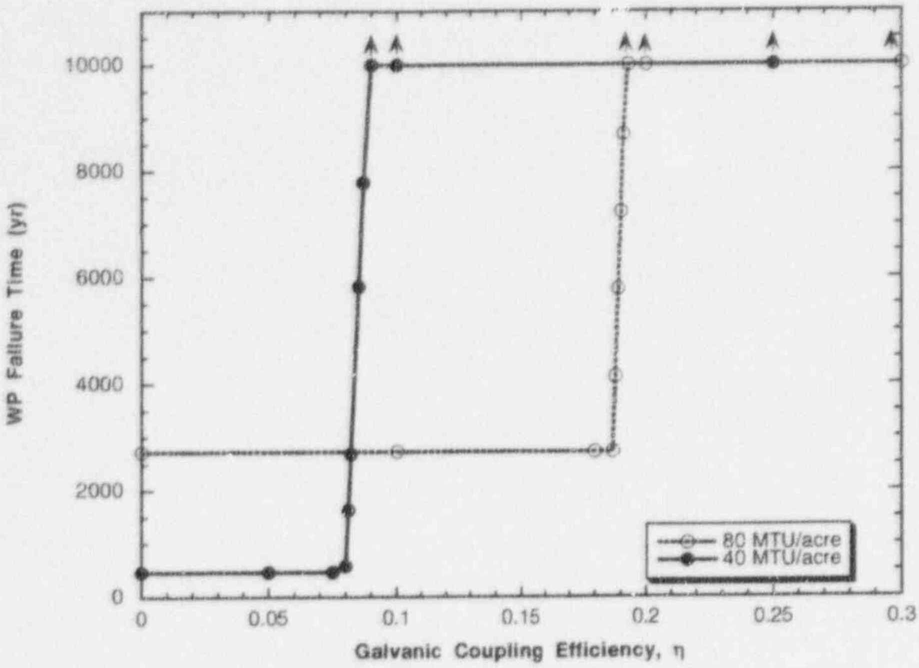

Figure 5-1. Effect of galvanic coupling on the waste package failure time for two values of areal mass loading in the absence of ventilation and backfilling. Arrows indicate no failure within the simulation time (10,000 yr).

an intermediate AML. If efficient galvanic coupling occurs, container life can be greater than 10,000 yr, independent of the AML value. Additional sensitivity analyses currently being accomplished with Version 1.0β of EBSPAC include the effect on the failure time of varying several parameters of interest such as chloride concentration and critical RH, among others.

5.3.2 Thermal Embrittlement of Carbon Steel

Depending upon the thermal loading strategy, WP materials can be exposed to temperatures well above 100 °C for thousands of years. In addition, backfilling can induce a sharp increase in temperature of the WP surface above 100 °C, followed by a gradual decrease with time.[2] In the DOE TSPA-95 (TRW Environmental Safety Systems, Inc., 1995), no consideration was given to the effect of prolonged exposures at these temperatures on material stability and specific mechanical properties. Thermal embrittlement is related to the well-known phenomenon of temper embrittlement that affects tempered low-alloy steels as a result of isothermal heating or slow cooling within the temperature range of 325 to 575 °C. Temper embrittlement is a major concern to the integrity of engineering components that operate within that critical temperature range and also to heavy section components that are slowly cooled through the critical temperature range after heat treatment or welding operations. Examples of such components

[2]Manteufel, R.D. 1996. Effects of ventilation and backfill on an underground nuclear waste repository. *International Journal of Heat and Mass Transfer*. Accepted for publication.

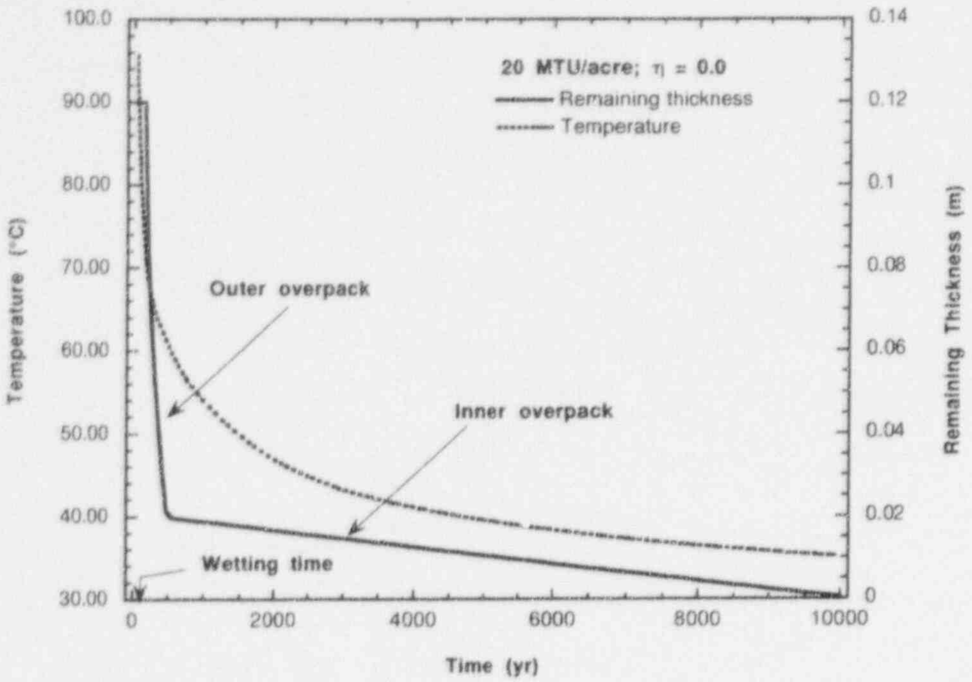

Figure 5-2. Temperature of the waste package and remaining wall thickness as a function of time for the lowest areal mass loading in the absence of galvanic coupling

are pressure vessels and turbine rotors. This phenomenon leads to a shift in the ductile-brittle transition temperature (DBTT), as shown schematically in figure 5-3, where the variation of the impact fracture energy for notched specimens is represented as a function of test temperature. However, the potential for embrittlement of carbon and low-alloy steels at temperatures lower than 300 °C as a result of extended exposures (hundreds to thousands of years) expected under repository conditions has never been experimentally investigated (Cragnolino et al., 1996). Lack of information is undoubtedly related to the extended times that could be required to induce the occurrence of this phenomenon, if it occurs, at these relatively low temperatures.

Temper embrittlement occurs when impurities originally present in the steel, such as Sb, Sn, P, Si, and As, segregate along prior austenite grain boundaries during exposure to temperatures ranging from 300–600 °C. Of these elements, P is the most common embrittling element found in commercial low-alloy steels. According to Briant and Banerji (1983), this detrimental role of P is a consequence of the following facts: (i) it segregates during austenitization and tempering, as well as during aging; (ii) it segregates rapidly even at low temperatures; and (iii) its concentration in commercial steels is usually greater than that of other embrittling elements. In importance, P is followed by Sn and Si, since Sb and As are not generally present in sufficiently large quantities in commercial steels. The segregation of P promotes fracture of notched specimens upon impact and leads to a change in the low-temperature fracture mode from transgranular cleavage to intergranular fracture.

By reviewing the available literature on temper embrittlement of low-alloy steels (Cragnolino et al., 1996), useful thermodynamics and kinetics expressions based on the segregation model originally developed by McLean (1957) were found for predicting long-term behavior at lower temperatures. These expressions have been successfully applied to the diffusion and segregation of P following long-term aging

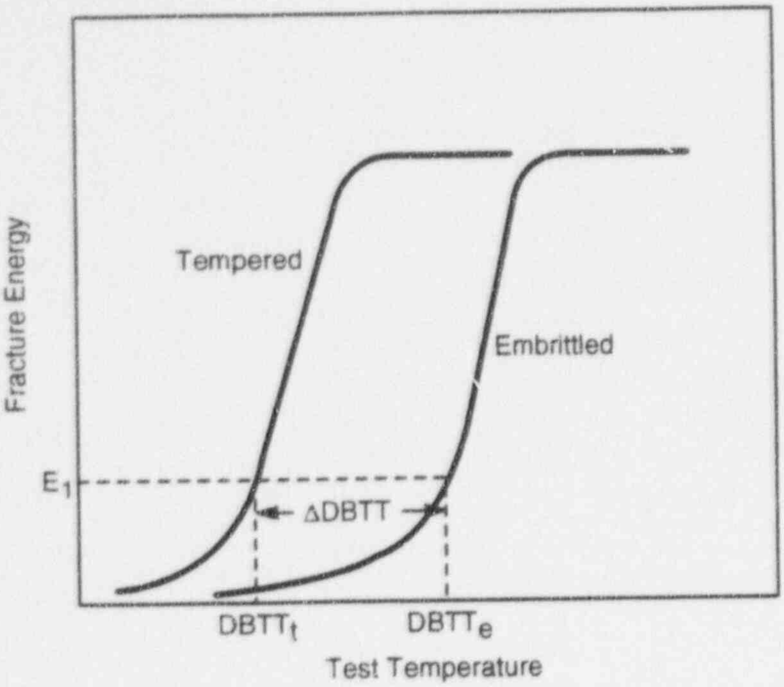

Figure 5-3. Schematic diagram of the effect of embrittlement on the ductile-brittle transition temperature as a function of test temperature

(20,000 hr) at temperatures above 300 °C in steels such as A508 and A533B which are used as pressure vessel materials in nuclear power plants (Druce et al., 1986; Hudson et al., 1988). The grain boundary P segregation and the embrittlement data for alloy A533B are clearly correlated via a linear relationship shown in figure 5-4 (Druce et al., 1986). On the basis of Druce's work, it is estimated that P concentrations above 0.06 weight percent may lead to noticeable embrittlement.

Although McLean's model can be used for predicting the segregation kinetics of P as applied by Druce et al. (1986) to pressure vessel steels, the prediction is primarily dependent on the validity of certain critical modeling parameters, such as the diffusion coefficient for P in steels. The diffusion coefficient of P was evaluated through a compilation of high temperature diffusion data for iron and various steels from the literature, from which the following Arrhenius expression was derived

$$D(cm^2/s) = 0.017 \exp\left[\frac{-179.22(kJ/mol)}{RT}\right] \tag{5-2}$$

Thus, kinetics of phosphorous segregation to grain boundaries at temperatures prevailing at the WP overpack can be predicted. A sensitivity analysis was performed by varying the diffusion coefficient, as depicted in figure 5-5. A significant P enrichment can be attained at lower temperatures (200 °C) but longer times.

It was also found that an important metallurgical factor controlling the degree of embrittlement is grain size (Wada and Hagel, 1976; Lonsdale and Flewitt, 1978; Ucisik et al., 1978). The degree of embrittlement has been evaluated in various studies by comparing base materials and welds, as well as the associated heat affected zones (HAZs) using weldments or simulated microstructures. It appears that

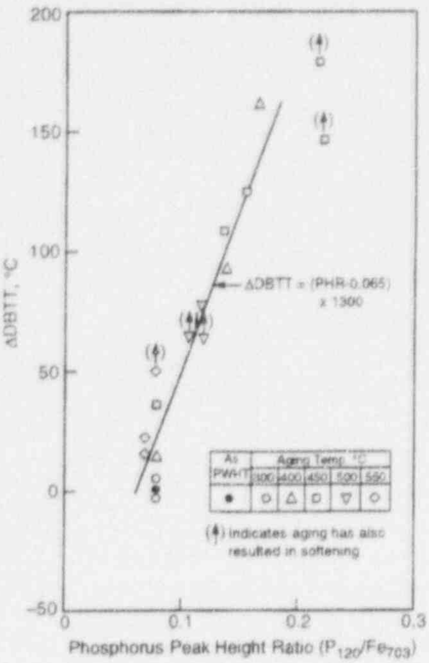

Figure 5-4. Embrittlement as a function of phosphorus segregation in A 533B-Class 1 simulated coarse-grained heat affected zone (Druce et al., 1986, reprinted with permission from Elsevier Science Ltd)

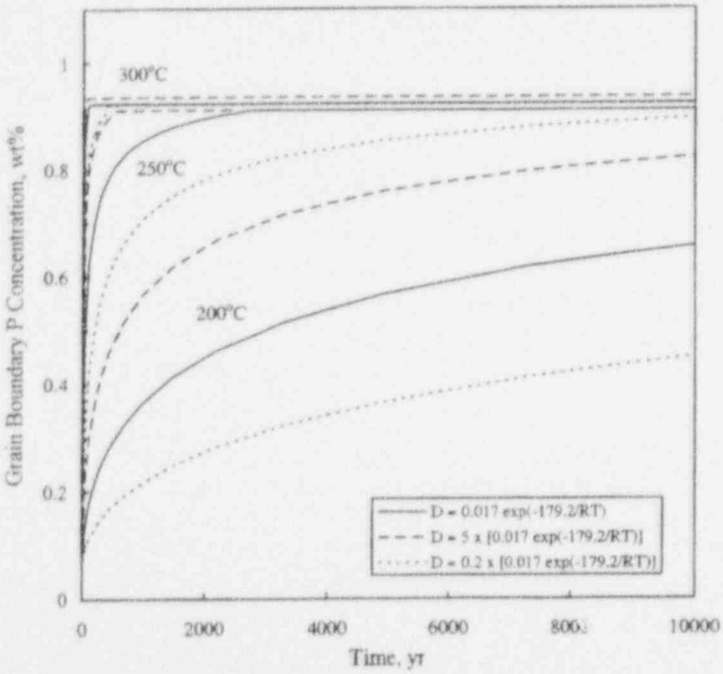

Figure 5-5. Grain boundary concentration of phosphorus at various temperatures calculated on the basis of the values of the diffusion coefficient given by Eq. (5-2) and upper and lower bounds obtained at each temperature by multiplying such values by 5 and 0.2, respectively

welds are less susceptible than the base metal, but coarse grain microstructures developed in the HAZ could be significantly more embrittled than the base metal (Tavassoli et al., 1984). Empirical equations relating embrittlement with chemical composition of steels have been developed, in which the effect of alloying elements and detrimental impurities is included (i.e., Watanabe et al., 1974; Bruscato, 1970; Newhouse, 1972; Viswanathan and Bruemmer, 1985). It should be noted that significant variability has been reported for components made from the same nominal grade of pressure vessel steel. Correlations used to estimate fracture toughness, K_{IC}, by using values of impact energy obtained with Charpy V-notched specimens (i.e., Iwadate et al., 1985; Rolfe and Novak, 1970) have also been compiled (Cragnolino et al., 1996).

The concern about susceptibility to thermal embrittlement of some candidate materials for the WP outer disposal overpack can be reduced through appropriate selection of the chemical composition of steel or processing techniques. There are two potentially promising processing methods: (i) reducing the amount of P in the steel through a two-step process combining the basic oxygen furnace (BOF) and the ladle refining furnace (LRF) process (Kusuhara et al., 1980), and (ii) adding small but controlled amounts of Al and B accompanied by reductions in Si content (Nakanishi et al., 1984).

Based on review of the literature, it is concluded that low-alloy steels, such as A387 Grade 22, and eventually C-Mn steels, such as A516 Grade 55, may be susceptible to a substantial degradation in toughness as a consequence of long-term thermal aging at repository temperatures anticipated for the high heat-loading concept (i.e., >200 °C). The investigation also revealed that low-alloy steels are more susceptible to thermal embrittlement than plain carbon steels. Therefore, it is preferable to use plain carbon steels if thermal embrittlement is the only consideration. However, it is preferable to use low-alloy steels to resist humid-air and aqueous corrosion, which may become more significant under low thermal loading strategy. Hence, selection of outer overpack must involve a balance between these considerations and the thermal loading strategy.

5.3.3 Dry Oxidation of Carbon Steel Overpack

Under dry conditions of an RH of less than 65 percent, one degradation mode of the outer steel container is dry oxidation caused by the interaction with gaseous oxygen in air. The proposed YM repository site is considered buffered with air. Currently, the DOE postulates that dry oxidation of the outer container would be negligible for the Mined Geological Disposal System planned at the YM repository site leading to penetrations of 0.40, 0.86, and 1.84 μm, after 100, 1,000, and 10,000 yr at 200 °C (Stahl, 1993). In FY96, a preliminary report was prepared to evaluate this dry oxidation (Ahn, 1996). A detailed review of the state of knowledge regarding dry oxidation of carbon and low-alloy steel was performed independently by Professor R.A. Rapp, Ohio State University (Larose and Rapp, 1996) under a CNWRA contract. This section summarizes the conclusions from these reports.

A preliminary analysis of localized oxidation was conducted at the NRC, focusing predominantly on iron-base alloys with significant alloy content (Ahn, 1996). At temperatures above 600 °C, iron-base alloys often show localized dry oxidation (Shida and Moroishi, 1992; Otsuka and Fujikawa, 1991; Newcomb and Stobbs, 1991; Tasovac et al., 1989; Mayer and Smeltzer, 1973). This localized oxidation is normally much deeper than uniform oxidation. The extrapolated values suggest thin (at most 100 μm at 200 °C) penetration by localized dry oxidation. However, simple extrapolations may underestimate the real penetration. Dry oxidation can be more localized than that observed above 600 °C for noncandidate alloys. Lower concentration of alloying elements and lower performance temperature can be the main

cause for this further localization in candidate alloys. Additionally, if all metal ions, mobile at high temperatures, are essentially frozen under repository conditions, oxygen will be the main mobile species. Consequently, oxidation can be deeper as promoted by oxygen diffusion compared with the oxidation by metal diffusion. On the other hand, if iron oxides formed at lower temperatures are protective to a certain extent, there would be less localized oxidation. Extreme diffusion calculations show that oxygen can penetrate through the 10-cm container wall in less than 10,000 yr at both 150 and 200 °C. The consequences of this penetration may include (i) container breach, and (ii) easy mechanical failure of container by localized oxidation or by (atomic or gaseous) oxygen embrittlement. The reasonableness of the extreme diffusion calculations need to be assessed through further literature evaluation or focused experiments.

Larose and Rapp (1996) undertook a more detailed examination of the potential for dry oxidation at repository temperatures, with a specific focus on candidate overpack steels (C-Mn and low-alloy steels). As a baseline, the thermodynamics and kinetics of pure iron oxidation were considered. Thermodynamics of the Fe-O system from room temperature to 1,600 °C was used to understand the oxide phases important within the small temperature range of interest to the repository. The literature on oxidation of iron or steel at temperatures beyond 567 °C is not considered relevant because the stable oxide phase at low oxygen fugacities beyond this temperature is wüstite, corresponding to $Fe_{1-y}O$, which is slightly deficient in Fe (Muan and Osborne, 1965). At lower temperatures, the oxide scale on iron has two phases, an inner magnetite (Fe_3O_4) and an outer hematite (Fe_2O_3) phase. The kinetics of oxide growth at temperatures below 567 °C are dictated by cation diffusion outwards not by oxygen transport inwards. Grain boundaries in the oxide scale are known to influence the diffusivities in oxides, but the values are not known at the temperatures of interest. Oxidation of pure iron between 400 and 550 °C is especially affected by delamination of the scale due to condensation of cation vacancies at the metal-oxide interface. The oxidation rate of steel at low temperatures increases with the carbon content in steel. At 250 °C, carbon steels containing 0.2 weight percent carbon are expected to lose about 4 μm in thickness, while steels containing 2.25 weight percent chromium and 1 weight percent molybdenum (another candidate container material) are expected to undergo a thickness loss of about 3 μm in 1,000 yr at the same temperature. They concluded that because low-temperature oxidation in carbon and low-alloy steels following a parabolic rate law is controlled by outward diffusion of iron rather than inward diffusion of oxygen, intergranular penetration of oxide would not be significant. The discrepancies between these two analyses of dry oxidation need to be resolved through further investigation.

5.3.4 Long-Term Corrosion Prediction

As reported in chapter 4, modeling of the evolution of the near-field environment has shown that the saturation increases above and below the repository horizon and the chemistry of this saturated zone water is alkaline. Such conditions can promote the passivation of carbon steel (Pourbaix, 1974). In addition, the presence of small amounts of chloride in the groundwater is well known for promoting localized attack (pitting or crevice corrosion) on carbon steel, typically considered a corrosion-allowance-type material (Szklarska-Smialowska, 1986; Marsh et al., 1985). Finally, the presence of microbiological organisms can alter the local environment adjacent to the WP and accelerate the corrosion rate.

Activities in the CLST KTI focused on developing a methodology to predict localized corrosion initiation and propagation. Localized corrosion is assumed to occur when E_{corr} of the overpack is greater then the repassivation potential E_{rp}. In the last year, efforts at the CNWRA emphasized measuring the E_{rp} of ASTM A516 grade 60 carbon steel, which is similar to the candidate outer overpack material, and

alloy 825, a candidate inner overpack material, in a wide range of test solutions. The data generated from these tests are used in EBSPAC to predict container life time. Long-term testing of alloy 825 is conducted to determine if E_{rp} is a conservative parameter for predicting localized corrosion.

5.3.4.1 Effect of Solution Composition on Repassivation Potential for A516 Grade 60 and Alloy 825

Measurement of the E_{rp} for A516 grade 60 was performed using cyclic potentiodynamic polarization (CPP) tests in solutions containing 3×10^{-4} to 5 M chloride and a total carbonate concentration of 0.012 M as sodium carbonate (Na_2CO_3) and sodium bicarbonate ($NaHCO_3$). The carbonate/bicarbonate ratio was adjusted for each test solution to obtain a solution pH of 9.0. These solutions were deaerated with 99.999 percent N_2. Tests were conducted at both 65 and 95 °C. The test procedure used was similar to that given by ASTM G-61 (American Society for Testing and Materials, 1995) and details provided in a previous report (Sridhar et al., 1995).

The CPP scans exhibited significant hysteresis characteristic of pitting or localized attack. Observation of the specimens using a 70× stereoscope revealed that all specimens exhibited some shallow pitting along with uniform corrosion. The E_{rp} for ASTM A516 Grade 60 was found to be

$$E_{rp} = -620.3 + 0.47T + (-95.2 + 0.88T)\log\left[Cl^-\right] \tag{5-3}$$

where T is the temperature in °C and the chloride concentration is expressed in molar units.

Previously, acquired CPP test data for alloy 825 specimens along with crevice repassivation potential data reported by Tsujikawa and Okayama (1990) were similarly analyzed. However, for this material, pitting corrosion was not observed at chloride concentrations lower than 3×10^{-3} M. In addition, E_p was not found to be a function of temperature. The regression equation for E_{rp} at temperatures above 50 °C is

$$E_{rp} = 422.8 - 4.1T + (-64 - 0.8T)\log\left[Cl^-\right] \tag{5-4}$$

The previous expressions were incorporated in EBSPAC, Version 1.0β (Mohanty et al., 1996) as the electrochemical basis for evaluating WP failure time in conjunction with calculations of E_{corr}.

5.3.4.2 Long-Term Testing of Alloy 825

Potentiostatic tests with alloy 825 specimens were conducted over 2 yr to gain further confidence in the use of E_{rp} for long-term prediction of container life. The test apparatus and procedures have been previously described (Sridhar et al., 1995; Dunn et al., 1996). Tests were conducted in 1,000 ppm (0.028 M) chloride solutions at 95 °C. The electrochemical parameters, such as potential, current density, E_{corr}, etc., were continuously monitored and the specimens were periodically inspected for signs of localized corrosion.

Results of the long-term tests are shown in figure 5-6 where specimens that exhibited localized corrosion are indicated by solid symbols. It is apparent from this figure that the initiation of crevice

corrosion occurs much more readily than that of pitting corrosion. Also, the time necessary to initiate localized corrosion decreases as the potential of the specimen increases. No localized attack was observed in potentiostatic tests conducted at potentials lower than E_{rp}, as depicted by the open symbols in figure 5-6.

To further verify that the initiation of localized corrosion requires as a condition that E_{corr} becomes greater than E_{rp}, a test under naturally exposed conditions (open-circuit potential) is being conducted in an aerated 1,000 ppm Cl^- solution. The results of this test, shown in figure 5-7, indicate that E_{corr} is highly variable but in general tends to become more noble with time. On two occasions, as indicated in the figure, E_{corr} was found to be greater than E_{rp} for brief periods. At the conclusion of these test intervals, localized corrosion in the form of crevice corrosion on the mill-finished surface was observed. However, since E_{corr} did not remain above E_{rp} for an extended period, the depth of the localized attack was shallow.

5.3.5 Effects of Microbial Growth on High-Level Nuclear Waste Containers

Microbially influenced corrosion (MIC) is currently acknowledged as a phenomenon that may affect the performance of high-level waste (HLW) containers. It was shown in chapter 4 that microbial populations can survive exposures to temperatures on the order of 120 °C for short periods. However, they become active only when the temperature decreases, upon reintroduction of water and nutrients. Although there is no consensus on the detailed mechanisms involved, MIC is recognized as a modification of abiotic localized corrosion (Thierry and Sand, 1995). It was shown in section 5.3.4 that localized corrosion in abiotic media occurs when E_{corr} exceeds E_{rp}. Microbiological organisms can adversely affect the susceptibility to localized corrosion of a material by either increasing E_{corr} (called ennoblement) or decreasing the E_{rp}. In the present program, two materials were used to examine these two processes: (i) type 316L stainless steel representing a typical corrosion-resistant alloy, and (ii) A 516 carbon steel representing a corrosion-allowance material. Classically, bacteria involved in MIC have been divided into three broad phenotypic groups: (i) acid producers (APB), (ii) sulfate reducers (SRB), and (iii) iron oxidizers (IOB) (Little et al., 1991). The DOE research has concentrated on and identified bacteria representative of each of these phenotypic groups as part of the natural flora at the proposed HLW repository site at YM (Pitonzo et al., 1996).

Microbial biofilms are known to grow in environments where growth nutrients are present only at growth limiting levels (Costerton et al., 1995). Bacteria are able to grow due to the efficiency with which biofilms are capable of scavenging available nutrients. Many of the accepted mechanisms of MIC involve the oxidation or reduction of nutrients releasing corrosive metabolic products, such as reduced sulfur species and acids, as well as products of the oxidation or reduction of various other species, including metal cations that can potentially alter E_{rp} or E_{corr}. These metabolic products can then be concentrated in the surface area covered by the bacteria leading to localized concentration cells. It is therefore necessary to determine what reactions are important to the container life and which are possible at the repository site under anticipated near-field environmental conditions.

The MIC research at the CNWRA has used the model bacterium *Shewanella putrefaciens*, a thiosulfate reducing bacteria (TRB), that was originally isolated from a corroded oil supply line. *S. putrefaciens* is capable of using a number of terminal electron acceptors (TEA) including oxygen, iron

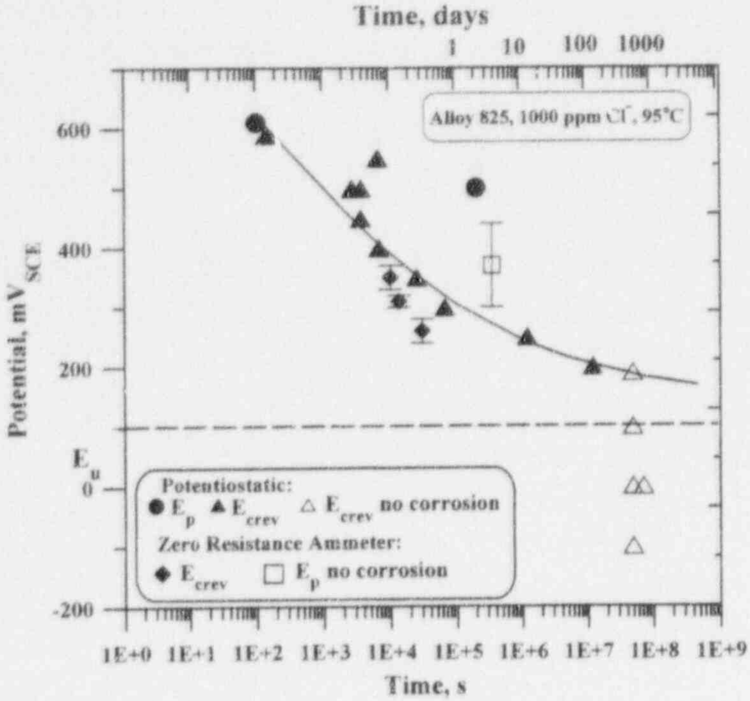

Figure 5-6. Effect of potential on initiation and repassivation of localized (pitting and crevice) corrosion of alloy 825 in 1,000 ppm Cl^- solution at 95 °C using potentiostatic and zero resistance ammeter measurements

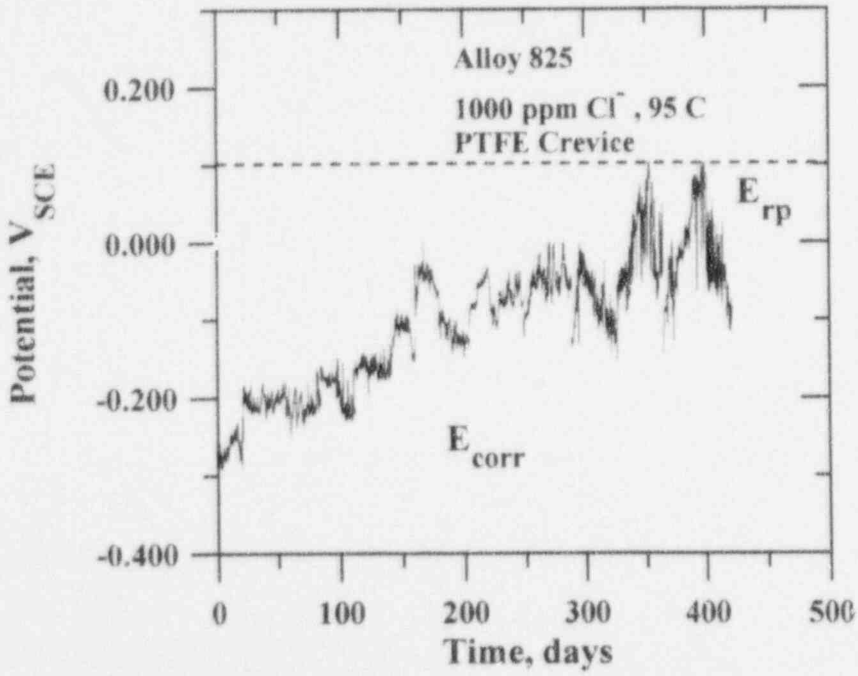

Figure 5-7. Corrosion potential of alloy 825 (creviced specimen) as a function of time in an air saturated 1,000 ppm Cl^- solution at 95 °C

(III), nitrate, manganese dioxide, and thiosulfate. Various MIC processes are linked to the microbial reduction of many of these compounds. By modifying the metabolic pathways of this bacterium and, hence, the metabolic products, their effects on E_{corr} and E_{rp} can be examined independently. Multiple electrode probes were exposed to *S. putrefaciens* grown in batch reactors where the medium composition was altered to promote the use of various TEAs. The experimental procedures have been reported elsewhere (Angell et al., 1996).

S. putrefaciens produced no ennoblement under the conditions so far examined on 316L stainless steel. *S. putrefaciens* grown under aerobic conditions, with oxygen as the TEA, caused a small increase in E_{corr} with no evidence of localized corrosion. The addition of either nitrate or thiosulfate (2 mM) to the medium caused essentially no change to E_{corr} under aerobic conditions because oxygen is the preferential TEA. When oxygen is removed and the bacteria is cultured in anaerobic conditions *S. putrefaciens* will continue to grow by reducing whatever other TEA has been selected. Nitrate used as the anaerobic control again showed there was little variation on E_{corr} and no evidence of localized corrosion, with the metal exhibiting only passive behavior.

The reduction of thiosulfate resulting in the production of sulfide had little effect on E_{corr} that remained well below E_{rp} as measured by cyclic polarization in abiotic conditions in the same medium with thiosulfate, but no metabolic sulfide. However, visual inspection revealed pitting on a number of specimens. EIS confirmed these results with the appearance of two time constants on the Bode and Nyquist plots. It is suggested that this is due to localized breakdown of the passive film on the 316L specimen. This may appear to contradict the findings in abiotic environments that E_{corr} had to exceed E_{rp} to initiate localized corrosion. However, it is possible that E_{rp} in the biotic solution was lower than that in the abiotic solution. While relatively low levels of thiosulfate (2 mM), added to simulate the metabolic product of this bacterium, had little effect on E_{rp} in abiotic solutions, there was evidence of localized attack in biotic solutions. It is postulated that bacteria are able to concentrate their metabolic products at specific sites leading to localized areas where the chemistry could be significantly different from the bulk solution leading to localized changes in E_{rp}. This hypothesis is currently being evaluated experimentally. This finding, if verified, is of significance for the prediction of the effects of MIC on container life. Whereas groundwater in the vicinity of the proposed repository site at YM has 25 ppm sulfate, microbial action could lead to a micro-environment with a possible sulfide concentration in the range of the reported values of 10^{-2} M necessary to induce pitting (Newman et al., 1982). It should also be noted that the ratio of sulfide to chloride is an important factor in localized pitting.

5.3.6 Factors Affecting Radionuclide Release from Spent Fuel

Studies of the behavior of SF in the proposed repository at YM have advanced on several fronts. An analysis of literature on dry oxidation and fracturing of SF (Ahn, 1995a) concluded that volume changes due to oxidation causes fracturing. Dry oxidation and fracturing enhance the potential for radionuclide releases because of increases in surface area, solid state diffusion of relatively volatile radionuclides, and subsequent dissolution or colloid formation under aqueous conditions. The rate of dry oxidation may depend on diffusion of oxygen in the SF matrix or reaction kinetics. Diffusion limited oxidation is slow on a 10,000-yr time scale, and oxidation reaction kinetics decrease strongly with decreasing temperature so that higher oxides (i.e., greater than $UO_{2.4}$) may not form below 150 °C under dry conditions.

Dissolution of SF releases highly soluble and gaseous species and may generate colloids of low solubility radioelements (Ahn, 1995b). Secondary solid phases form in SF dissolution tests, but they may not be protective with regard to oxidative dissolution of SF. Colloids form during oxidative dissolution of SF and can form by nucleation in supersaturated solutions, dispersion (physical breakup), or sorption of radioelements on existing colloids. Many uncertainties persist regarding the stability and mobility of colloids, resulting in uncertainties on the significance of colloids to the source term.

Natural analog, experimental, and thermodynamic studies indicate that the properties of secondary uranyl minerals will control the source term for uranium and minor, low solubility radioelements incorporated in these phases in the proposed repository at YM. Uranophane, a common hydrated calcium uranyl silicate, is a preponderant uranyl mineral at the Nopal I natural analog site (and elsewhere) (Pearcy et al., 1994). Similarities between this site and YM and the common enrichment in Ca of secondary minerals at YM suggest that uranophane will significantly affect the performance of the repository. Nevertheless, uncertainties in the properties of uranophane preclude accurate predictions of its role. Experimental studies were initiated to determine fundamental thermodynamic properties of uranophane. Obtaining appropriate materials has been a significant challenge. Attempts to separate adequately pure uranophane from geologic samples failed because of its fine grain size and intimate intergrowths with other minerals. Efforts succeeded to synthesize a phase from chemical reagents that has the structure (based on x-ray diffraction data) and stoichiometric chemical composition of uranophane. This phase is being used in solubility experiments and was intended for use in future studies of actinide (Np and/or Pu) coprecipitation studies.

5.3.7 Future Developments

EBSPAC was developed to conduct PAs of the EBS taking into consideration the need to evaluate the failure of the WP and subsequent release of radionuclides. EBSPAC will be incorporated into the TPA code as the source term module.

With minor modifications, EBSPAC is applicable to various designs of the EBS that involve different thermal and environmental conditions, distinct types of SF combinations, and dissimilar overpack materials and WP designs. Alterations in the radionuclide composition, including chains, can be accommodated by modifying the radionuclide input data file. However, the current version of the code needs additional modifications to be used for the vitrified HLW.

To keep the source term calculation simple, EBSPAC focuses on a single cell. However, post- and pre-processors can be written to integrate EBSPAC as a source term module into the TPA code for overall PA studies. It should be noted that this version of EBSPAC has been developed mainly as framework for future improvements. Depending upon available resources and in order of priority, these developments include

- Implementation of the results of MULTIFLO calculations to obtain a better description of the evolution of the chemical composition and variables of the near-field environment, such as pH and f_{O_2}, as a function of temperature and time. Future MULTIFLO calculations will address the definition of the near-field environment at the drift scale, including the effects of various heat loads, host rock compositions, and initial fluid compositions.

- Incorporation of more developed corrosion models for the description of wet/dry periods, including the effect of through-wall penetrations of various sizes on the outer container and their related influence on galvanic coupling effects, as well as the consideration of stress corrosion cracking models.

- Improvement of the mechanical failure model through appropriate implementation of the methodology described for analysis of thermal embrittlement of the steel outer overpack.

- Incorporation of a SF dissolution rate-limited model to address the release of relatively soluble radionuclides such as Tc-99, I-129, Np-237, and Cs-135 and implementation of simplified models to account for colloidal transport of the actinides.

- Evaulation of the effect of partially failed containers on radionuclide release, including the influence of partially failed MPC and cladding.

- Determination of the effects of uranyl silicates as potential secondary alteration products of SF in the presence of high-silica concentration groundwater anticipated to be encountered by the WP because these alteration products could play an important role in enhancing the dissolution of SF and the release of radionuclides.

- Consideration of variable water infiltration into the EBS that will require modification of modules where liquid release calculations are performed to have a full implementation of the effect of time varying flow rate on radionuclide release from SF.

- Incorporation of cladding failure models, including creep, localized corrosion, and delayed hydride cracking.

- Consideration of criticality as a result of the degradation of the WP, water intrusion, and geometry changes due to instability of basket materials.

- Evaluation of radionuclide release from vitrified HLW.

The principal steps for development of a complete assessment of the potential for thermal embrittlement of the outer steel overpack are (i) predicting the level of grain boundary P segregation using acceptable models; (ii) estimating the toughness degradation of the steel using the relationship between P segregation and the degree of embrittlement as measured by DBTT parameter; (iii) combining the previous steps for estimating the variation of toughness, ΔDBTT, with time; (iv) calculating the evolution of fracture toughness, K_{IC}, with time using an appropriate K_{IC}-CVN correlation; and (v) calculating the change in the critical crack size, a_{cr}, as K_{IC} changes with time using fracture mechanics. A successful thermal stability assessment would require sufficient information for the specific material conditions to fully define both the segregation model parameters and the embrittlement potencies.

The results of these activities would provide the NRC with a better understanding of the potential for thermal embrittlement of overpack materials due to long-term aging. These studies are needed to support sensitivity analyses and to address uncertainties in models [i.e., applicability of Guttmann and McLean theory to C-Mn steels (Guttmann and McLean, 1979)], parameters (i.e., coefficient diffusion of P in steels), and data (i.e., correlations between ΔDBTT and K_{IC}). A more

complete evaluation of the embrittlement of steel overpacks under repository conditions will provide staff with the knowledge base needed to assess adequacy of the DOE treatment of this potential failure mode.

Some additional work may be needed to attain a complete assessment of the potential for intergranular oxidation of steel in dry air because discrepancies in mechanistic interpretations may lead to different estimates of intergranular penetration of oxide. However, this phenomenon may not affect the performance of the steel overpack as inferred by extrapolating data obtained in the temperature range of 400 to 576 °C to predict the behavior at repository temperatures. Long-term testing of alloy 825, extended for about 30 mo seems to indicate that E_{rp} is a robust parameter to assess the performance of the inner overpack. It is expected that the continuation of these tests during FY97 and FY98 would be valuable to confirm the validity of the current observations. In this regard, it is important to emphasize that the DOE should conduct a critical assessment of the relevance of using initiation potentials for localized corrosion, instead of repassivation potentials, as valid parameters to predict WP performance.

To date, the DOE has paid little attention to MIC; in TSPA-95 reference was made to MIC but it was not accounted for in the current models. The only work seen is a preliminary report in the form of an extended abstract (Pitonzo et al., 1996). These authors looked at the effect of axenic and mixed cultures of bacteria isolated from YM on the corrosion rate of 1020 carbon steel. A mixed culture of IOB, APB, and SRB was the only one to show significant corrosion rates (1.3 mm yr^{-1}). This rate was three to four times that of the abiotic control. Due to the limited nature of this abstract, it is difficult to fully relate the results to the waste repository.

5.4 ASSESSMENT OF PROGRESS TOWARD MEETING OBJECTIVES AND PATHS TO RESOLUTION

One of the objectives in the CLST KTI is being achieved through the development of EBSPAC to evaluate the failure of WPs and ultimately the release of radionuclides from the EBS. The technical description and user's manual for Version 1.0β of EBSPAC was recently issued (Mohanty et al., 1996). Preliminary calculations conducted using EBSPAC Version 1.0β clearly indicate there are two parameters of greatest importance to container life: (i) the AML, which determines the WP temperature and the RH as well as the chemical composition of the near-field environment; and (ii) the degree of galvanic coupling between the outer carbon steel overpack once it is breached and the inner nickel-base alloy overpack, which determines the failure time of the WP inner overpack. Additional sensitivity analyses will be needed to complete the goal of assessing the influence of other dominant environmental and materials factors on WP life and hence, the potential for radionuclide release within the initial thousands of years after repository closure.

With the incorporation of a probabilistic driver, Version 1.0β of EBSPAC can be used to conduct an independent review of the container life cumulative distribution functions (CDFs) presented by the DOE in TSPA-95. As noted previously, models and computational approaches used in SOTEC (Sagar et al., 1992) and SCCEX (Cragnolino et al., 1994) codes were incorporated with appropriate modifications in the current version of EBSPAC. In addition, the development of EBSPAC benefited from the data obtained in the experimental investigation program conducted within this KTI. The critical potentials used in EBSPAC for assessing the susceptibility to localized corrosion of ASTM A516 steel and alloy 825 have been generated in this program in conjunction with data extracted from the open literature. Experimental confirmation is now available indicating that E_{rp}, as measured in relatively short tests, is a reliable parameter for evaluating the long-term susceptibility to localized corrosion.

In TPSA-95, the DOE did not address the potential for mechanical failure of the carbon steel overpack due to thermal embrittlement. The propensity to thermal embrittlement of the outer steel overpack was evaluated through a review of the literature (Cragnolino et al., 1996). Calculations indicate that thermal embrittlement susceptibility could be significant only at WP temperatures exceeding 200 °C over extended periods (thousands of years). Sources of uncertainties in the degree of embrittlement related to uncertainties in models, parameters, or data have been identified, but additional work could be necessary following appropriate sensitivity analyses. Based on the current assessment, there is a need to determine the DOE design parameters prior to resolving this issue.

Different interpretations have been developed regarding the mechanisms of dry oxidation of steels (Ahn, 1996; Larose and Rapp, 1996) which lead to different values of oxide penetration by extrapolating high-temperature data. Nevertheless, it can be concluded, at least for C-Mn steels, that this phenomenon is not a matter of primary concern. Limited investigation can lead to a complete resolution of this issue.

Experimental work at the CNWRA on MIC demonstrated that localized corrosion of corrosion-resistant materials such as type 316L stainless steel can occur in the presence of *S. Putrefaciens*. The effect cannot be attributed to an increase in E_{corr} but to a decrease in E_{rp} that can be due to the concentration of metabolic products such as sulfide in localized areas of the metal surface. These results combined with observations reported by Pitonzo et al. (1996) of the existence of several species of bacteria responsible for MIC failures as part of the natural flora in the proposed site at YM confirm the need for a complete assessment of the effects of MIC on WP failure. The possibility of microorganism influence on radionuclide release from the EBS should be addressed.

5.5 INTEGRATION WITH OTHER KEY TECHNICAL ISSUES

The evaluation of thermal embrittlement of the outer overpack steel required knowledge of the container temperature as a function of time. This was provided by the temperature calculations performed in the Repository Design and Thermal-Mechanical Effects (RDTME) KTI using an effective conductivity approach.

Calculation of the time required to form an aqueous condensate film on the WP (time to wetting) is necessary to evaluate container life. Time to wetting is a function of the RH, calculated in the RDTME KTI. Results were provided to EBSPAC as a table.

Initiation of localized corrosion is dependent on the chloride concentration and pH of the aqueous solution contacting the WP. MULTIFLO calculations have been performed in the Evolution of the Near-Field Environment KTI on a repository scale to determine the spatial and temporal distribution of these variables. Results of MULTIFLO calculations have not been directly incorporated in the current version of EBSPAC. However, these calculations formed the basis for assumptions regarding the chemistry of the environment contacting the containers in EBSPAC.

Preliminary calculations were performed regarding failure of overpack materials and dispersion of radionuclides due to magmatic activity. For this purpose, the high temperature creep and stress rupture properties of the overpack materials were considered. The grain-size distribution of SF pellets, as affected by prior oxidation, was considered for determining the dispersion of radionuclides. These results were provided to the Igneous Activity KTI for consequence analyses.

EBSPAC is envisioned as a source term module to be incorporated in the NRC/CNWRA TPA code and reflects a significant activity integrated with the TSPA and Integration (TSPAI) KTI. Since EBSPAC is designed in a modular fashion to calculate container life and radionuclide release separately, evaluation of the CDFs of container life in TSPA-95 can be made using EBSPAC. Additionally, EBSPAC can assess the importance of factors such as thermal loading strategy on container life and source term, which will assist in the sensitivity analyses performed in the TSPAI KTI.

5.6 REFERENCES

Ahn, T.M. 1995a. *Dry Oxidation and Fracture of LWR Spent Fuels*. NUDOC Accession Number: 9512220279. Washington, DC: Nuclear Regulatory Commission.

Ahn, T.M. 1995b. *Long-Term Kinetic Effects and Colloid Formations in Dissolution of LWR Spent Fuels*. NUDOC Accession Number: 9508030112. Washington, DC: Nuclear Regulatory Commission.

Ahn, T.M. 1996. *Dry Oxidation of Waste Package Materials*. NUDOC Accession Number: 9607290014. Washington, DC: Nuclear Regulatory Commission.

Angell, P., D.S. Dunn, and G.A. Cragnolino. 1996. Effect of microbial action on the corrosion potential of austenitic alloy containers for high-level waste. *Scientific Basis for Nuclear Waste Management XIX Symposium Proceedings*. W.M. Murphy and D.A. Knecht, eds. Pittsburgh, PA: Materials Research Society: 412: 539–546.

American Society for Testing and Materials. 1995. *G-61-86, Standard Test Method for Conducting Cyclic Potentiodynamic Polarization Measurements for Localized Corrosion Susceptibility of Iron-, Nickel-, or Cobalt-Based Alloys*. Vol. 3.02. Philadelphia, PA: American Society for Testing and Materials.

Briant, C.L., and S.K. Banerji. 1983. Intergranular fracture in ferrous alloys in nonaggressive environments. *Treatise on Materials Science and Technology. Volume 25: Embrittlement of Engineering Alloys*. C.L. Briant and S.K. Banerji, eds. New York, NY: Academic Press: 21–58.

Bruscato, R. 1970. Temper embrittlement and creep embrittlement of 2 1/4Cr-1Mo shielded metal-arc weld deposits. *Welding Research Supplement* 49: 148s–156s.

Costerton, J.W., Z. Lewandowski, D.E. Caldwell, D.R. Korber, and H.M. Lappin-Scott. 1995. Microbial biofilms. *Annual Review of Microbiology* 49: 711–746.

Cragnolino, G.A., N. Sridhar, J. Walton, R. Janetzke, T. Torng, J. Wu, and P. Nair. 1994. *"Substantially Complete Containment"—Example Analysis of a Reference Container*. CNWRA 94-003. San Antonio, TX: Center for Nuclear Waste Regulatory Analyses.

Cragnolino, G.A., H.K. Manaktala, and Y-M. Pan. 1996. *Thermal Stability and Mechanical Properties of High-Level Radioactive Waste Container Materials: Assessment of Carbon and Low-Alloy Steels*. CNWRA 96-004. San Antonio, TX: Center for Nuclear Waste Regulatory Analyses.

Druce, S.G., G. Gage, and G. Jordan. 1986. Effect of ageing on properties of pressure vessel steels. *Acta Metallurgica* 34: 641–652.

Dunn, D.S., G.A. Cragnolino, and N. Sridhar. 1996. Localized corrosion initiation, propagation, and repassivation of corrosion resistant high-level nuclear waste container materials. *CORROSION/96*. Paper No. 97. Houston, TX: NACE International.

Guttmann, M., and D. McLean. 1979. Grain boundary segregation in multicomponent systems. *Interfacial Segregation*. W.C. Johnson and J.M. Blakely, eds. Metals Park, OH: American Society for Metals: 261-350.

Hudson, J.A., S.G. Druce, G. Gage, and M. Wall. 1988. Thermal ageing effects in structural steels. *Theoretical and Applied Fracture Mechanics* 10: 123–133.

Iwadate, T., J. Watanabe, and Y. Tanaka. 1985. Prediction of fracture toughness K_{IC} of 2 1/4Cr-1Mo pressure vessel steel from Charpy V-notch test results. *Flaw Growth and Fracture*. ASTM-STP 631. Philadelphia, PA: American Society for Testing and Materials: 493–506.

Kusuhara, Y., T. Sekine, T. Enami, and H. Ooi. 1980. BOF-LRF refined ultralow phosphorous 2.25Cr-1Mo steel plate of low temper embrittlement susceptibility. *Proceedings of the Fourth International Conference on Pressure Vessel Technology*. London, U.K.: Institute of Mechanical Engineers.

Larose, S., and R.A. Rapp. 1996. *Review of Low-Temperature Oxidation of Carbon Steels and Low-Alloy Steels for Use as High-Level Radioactive Waste Package Materials*. San Antonio, TX: Center for Nuclear Waste Regulatory Analyses.

Little, B., P. Wagner, and F. Mansfeld. 1991. Microbiologically influenced corrosion of metals and alloys. *International Materials Review* 36: 253–272.

Lonsdale, D., and P.E.J. Flewitt. 1978. The role of grain size on the ductile brittle transition of a 2.25 pct Cr-1 pct Mo steel. *Metallurgical Transactions* 9A: 1,619–1,623.

Marsh, G.P., K.J. Taylor, I.D. Bland, C. Wescott, P.W. Tasker, and S.M. Sharland. 1985. Evaluation of localized corrosion of carbon steel overpacks for nuclear waste disposal in granite environments. *Scientific Basis for Nuclear Waste Management IX Symposium Proceedings*. L.W. Werme, ed. Pittsburgh, PA: Materials Research Society: 59: 421–428.

Mayer, P., and W. Smeltzer. 1973. Internal oxidation and decarburization properties of an Fe-1w/oMn and Fe-1w/oC alloy in carbon dioxide-carbon monoxide atmosphere at 1000 °C. *Canadian Metallurgical Quarterly* 12: 23–34.

McLean, D. 1957. *Grain Boundaries in Metals*. London, U.K.: Oxford Press.

Mohanty, S., G.A. Cragnolino, T. Ahn, D.S. Dunn, P.C. Lichtner, R.D. Manteufel, and N. Sridhar. 1996. *Engineered Barrier System Performance Assessment Code: EBSPAC Version 1.0 β, Technical Description and User's Manual*. CNWRA 96-011. San Antonio, TX: Center for Nuclear Waste Regulatory Analyses.

Muan, A., and E.F. Osborn. 1965. *Phase Equilibria Among Oxides in Steelmaking*. Reading, MA: Addison-Wesley Publishing Company, Inc.

Nakanishi, M., S. Watanabe, and J. Furusawa. 1984. On the improvement of ductility and toughness in welded joints of Al-B treated thick plates for pressure vessels. Paper No. 42. *International Conference on the Effects of Residual, Impurity, and Microalloying Elements on Weldability and Weld Properties*. Cambridge, U.K.: The Welding Institute.

Newcomb, S., and W. Stobbs. 1991. The effects of a grain boundary on the compositional fluctuations inherent in the oxidation of Fe-10Cr-34Ni. *Oxidation of Metals* 35: 69–88.

Newhouse, D.L. 1972. Temper embrittlement study of nickel-chromium-molybdenum-vanadium rotor steels, I: Effects of residual elements. *Temper Embrittlement of Alloy Steels*. STP 499. Philadelphia, PA: American Society for Testing and Materials: 3–36.

Newman, R.C., H.S. Isaacs, and B. Alman. 1982. Effects of sulfur compounds on the pitting behavior of type 304 stainless steel in near-neutral chloride solutions. *Corrosion* 38: 216–265.

Otsuka, R., and H. Fujikawa. 1991. Scaling of austenitic stainless steels and nickel-base alloys in high-temperature steam at 973 K. *Corrosion* 47: 240–248.

Pearcy, E.C., J.D. Prikryl, W.M. Murphy, and B.W. Leslie. 1994. Alteration of uraninite from the Nopal I deposit, Peña Blanca District, Chihuahua, Mexico, compared to degradation of spent nuclear fuel in the proposed U.S. high-level nuclear waste repository at Yucca Mountain, Nevada. *Applied Geochemistry* 9: 713–732.

Pitonzo, B., P. Castro, P. Amy, D. Bergman, and D. Jones. 1996. Microbially-influenced corrosion capability of Yucca Mountain bacterial isolates. *Proceedings of the Seventh Annual International Conference on High-Level Radioactive Waste Management*. La Grange Park, IL: American Nuclear Society and New York, NY: American Society of Civil Engineers: 12–18.

Pourbaix, M. 1974. *Atlas of Electrochemical Equilibria in Aqueous Solutions*. Houston, TX: National Association of Corrosion Engineers: 307–321.

Rolfe, S.T., and S.R. Novak. 1970. Slow-bend K_{IC} testing of medium-strength high-toughness steels. *Review of Developments in Plain-Strain Fracture Toughness Testing*. ASTM-STP 463. Philadelphia, PA: American Society for Testing and Materials: 124–159.

Sagar, B., R.B. Codell, J. Walton, and R.W. Janetzke. 1992. *SOTEC: A Source Term Code for High-Level Nuclear Waste Geologic Repositories User's Manual: Version 1.0*. CNWRA 92-009. San Antonio, TX: Center for Nuclear Waste Regulatory Analyses.

Scully, J.R., and H.P. Hack. 1984. Galvanic corrosion prediction using long- and short-term polarization curves. *CORROSION/84*. Paper No. 34. Houston, TX: National Association of Corrosion Engineers.

Shida, Y., and T. Moroishi. 1992. Effect of aluminum and titanium additions to Fe-21%Cr-32%Ni on the oxidation behavior in an impure helium atmosphere at high temperatures. *Oxidation of Metals* 37: 327–348.

Sridhar, N., G.A. Cragnolino, and D.S. Dunn. 1995. *Experimental Investigations of Failure Processes of High-Level Nuclear Waste Container Materials*. CNWRA 95-010. San Antonio, TX: Center for Nuclear Waste Regulatory Analyses.

Stahl, D. 1993. *Waste Package Corrosion Inputs*. CRWMS M&O Interoffice Correspondence. Las Vegas, NV: TRW Environmental Safety Systems, Inc.

Szklarska-Smialowska, Z. 1986. *Pitting Corrosion of Metals*. Houston, TX: National Association of Corrosion Engineers: 224–231.

Tasovac, A., R. Marković, and Ž. Štrbački. 1989. Comparative investigation of some austenitic chromium-nickel steels in hot air. *Materials Science and Engineering* A120: 229–234.

Tavassoli, A.A., A. Bougault, and A. Bisson. 1984. The effect of residual elements on the temper embrittlement susceptibility of large A508, Class 3, vessel forgings. Paper No. 43. *International Conference on the Effects of Residual, Impurity, and Microalloying Elements on Weldability and Weld Properties*. Cambridge, U.K.: The Welding Institute.

Thierry, D., and W. Sand. 1995. Microbially influenced corrosion. *Corrosion Mechanisms in Theory and Practice*. P. Marcus and J. Oudar, eds. New York, NY: Marcel Dekker, Inc.: 457–499.

TRW Environmental Safety Systems, Inc. 1995. *Total System Performance Assessment—1995: An Evaluation of the Potential Yucca Mountain Repository*. B00000000-01717-2200-00136. Las Vegas, NV: TRW Environmental Safety Systems, Inc.

TRW Environmental Safety Systems, Inc. 1996. *Mined Geologic Disposal System Advanced Conceptual Design Report. Vol. III of IV. Engineered Barrier Segment/Waste Package*. B00000000-01717-5705-00027. Rev. 00. Las Vegas, NV: TRW Environmental Safety Systems, Inc.

Tsujikawa, S., and S. Okayama. 1990. Repassivation method to determine critical conditions in terms of electrode potential, temperature and NaCl concentration to predict crevice corrosion resistance of stainless steels. *Corrosion Science* 31: 441–446.

Ucisik, A.H., C.J. McMahon, Jr., and H.C. Feng. 1978. The influence of intercritical heat treatment on the temper embrittlement susceptibility of P-doped Ni-Cr steel. *Metallurgical Transactions* 9A: 321–329.

Viswanathan, R., and S.M. Bruemmer. 1985. In-service degradation of toughness of steam turbine rotors. *Transactions of the ASME. Journal of Engineering Materials and Technology* 107: 316-324.

Wada, T., and W.C. Hagel. 1976. Effect of trace elements, molybdenum, and intercritical heat treatment on temper embrittlement of 2 1/4Cr-1Mo steel. *Metallurgical Transactions* 7A: 1,419-1,426.

Watanabe, J., Y. Shindo, Y. Murakami, T. Adachi, S. Ajiki, and K. Miyano. 1974. Temper embrittlement of 2 1/4Cr-1Mo pressure vessel steel. *29th Petroleum Mechanical Engineering Conference.* New York, NY: American Society of Mechanical Engineers.

6 THERMAL EFFECTS ON FLOW

Primary Authors: R.T. Green, A.C. Bagtzoglou, R.D. Manteufel, P.C. Lichtner, and G.I. Ofoegbu

Technical Contributors: R. Chen, M.E. Hill, S.M. Hsiung, K.M. James, M.A. Muller, G.I. Ofoegbu, and G. Rice

Key Technical Issue Co-Leads: A.H. Chowdhury (CNWRA) and J.A. Pohle (NRC)

6.1 INTRODUCTION

Prediction of thermally driven redistribution of moisture through partially saturated, fractured porous media caused by the emplacement of heat-generating high-level radioactive waste (HLW), with acceptable uncertainty, is the focus of the Thermal Effects on Flow (TEF) Key Technical Issue (KTI). Redistribution of moisture driven by heat may result in extended periods of dryness in the proposed repository during either the period of high heat or during cooling. Also, redistribution of moisture driven by heat could result in channeling moisture toward waste packages (WP). Thus, it is necessary to understand the spatial and temporal effects of the thermal load on temperature as well as liquid and gas phase flux in the vicinity of the proposed repository to have confidence in predictions of containment and long-term waste isolation. The U.S. Department of Energy (DOE) is developing a waste containment and isolation strategy to demonstrate that waste can be contained and isolated at the proposed Yucca Mountain (YM) site. The DOE strategy defines attributes of the disposal system deemed important to containment and isolation. DOE has identified hypotheses that address attributes to be evaluated within this KTI. Three of these hypotheses are: (i) there will be low humidity at the WP surface; (ii) there will be low percolation flux and limited fracture flow at repository depth; and (iii) thermally induced flux can be bounded. Evaluating these hypotheses necessitates understanding thermally driven flow of moisture through partially saturated and fractured porous media. This KTI was divided into three resolvable subissues in pursuit of this understanding: (i) is the DOE thermal testing program sufficient to assess the likelihood of gravity driven refluxing occurring in the near field, (ii) is the DOE thermal modeling approach adequate for assessing the nature and bounds of thermally induced flux in the near field, and (iii) will the DOE thermal loading strategy result in thermally induced flux in the near field and humidity at the WP surface to meet the performance objectives? Resolution of these subissues will establish the knowledge base necessary to predict, with acceptable uncertainty, thermally driven redistribution of moisture through partially saturated fractured porous media. The DOE hypotheses can then be evaluated using these predictive capabilities.

The FY96 activities of TEF KTI reported herein address all three subissues. In section 6.2, these activities and results are discussed to assess the extent the subissues have been resolved through FY96.

6.2 OBJECTIVES AND SCOPE OF WORK

The objective of this KTI is to understand heat and mass transfer through geologic materials to predict thermally driven redistribution of moisture through partially saturated fractured porous media at the proposed repository with acceptable uncertainty. Specific laboratory-scale experiments, analysis of existing field-scale test results, and predictive numerical modeling are being conducted to achieve this objective. Planned work has been prioritized to identify tasks whose resolution is both achievable within available resources and that will lead to significant reduction in uncertainty. Tasks designed to reduce uncertainties in these subissues in FY96 are both reactive and proactive: (i) review and evaluate the DOE

thermohydrology program, including the DOE peer review activity; (ii) benchmark test computer codes; (iii) provide sensitivity analyses; and (iv) evaluate conceptual models. Pursuit of these four activities were relevant to the first two subissues in the TEF KTI. The third subissue, will DOE thermal loading strategy result in thermally induced flux in the near field and humidity at the WP surface to meet the performance objectives, will be resolved using information gained during the resolution of the first two subissues.

Review and evaluation of the DOE thermohydrology program included (i) review of a DOE peer review team (PRT) report, (ii) the DOE response to PRT recommendations, (iii) PRT comments to the DOE response to PRT recommendations, (iv) attendance at an Appendix 7 meeting on Exploratory Studies Facility (ESF) thermal testing including site visit, and (v) participation in a DOE/Nuclear Regulatory Commission (NRC) ESF video conference. This activity also included a presentation to the Advisory Committee on Nuclear Waste on thermal-hydrological coupled processes.

Benchmark testing (i.e., code-to-code comparisons) was conducted of DOE and NRC thermohydrologic codes. The DOE codes, TOUGH2 and FEHM were tested against the NRC codes CTOUGH and MULTIFLO. The TOUGH2 and FEHM codes are currently being used to support Total System Performance Assessments (TSPAs) while CTOUGH and MULTIFLO are being used by the Center for Nuclear Waste Regulatory Analyses (CNWRA) in reviewing the DOE TSPAs. Various test problems were used to (i) compare and contrast code capabilities, (ii) identify and understand any significant differences that may arise, and (iii) assess robustness and computational efficiencies of the codes.

Work performed in regard to sensitivity analysis included the effects of (i) backfill on temperature and saturation; (ii) media properties on prediction of moisture redistribution at proposed repository scale; (iii) ventilation on rock dryout and drift relative humidity; (iv) geologic structure and features on the evolution of perched water body; and (v) geologic structure and media hydrologic properties on temperature and saturation. Temperature and saturation at the WP will influence the integrity of the canister. Once released from the WP, transport of radionuclides will be influenced by thermally driven moisture at and below the repository horizon.

6.3 SIGNIFICANT TECHNICAL ACCOMPLISHMENTS

6.3.1 Review and Evaluation of the Department of Energy Thermohydrology Program

The purpose of the review of the DOE thermohydrology program was to provide an independent evaluation of the DOE Yucca Mountain Site Characterization Office (YMSCO) Thermohydrologic Testing and Modeling Program. This review was conducted to evaluate whether the DOE thermohydrologic program would enable the DOE to conservatively predict thermally driven flow at the proposed repository with acceptable uncertainty. In particular, the central question is: will the DOE program provide the information necessary to resolve the subissues identified in the TEF KTI? For this review, it was assumed that information regarding the YMSCO Thermohydrologic Testing and Modeling Program contained in previous DOE reports was superseded by data in three recent documents and supported by information provided during an Appendix 7 meeting and a DOE/NRC ESF video conference meeting. The three documents are: (i) PRT Record Memorandum Report and Recommendations submitted to the DOE in January, 1996, (ii) the DOE response to PRT recommendations distributed in July 1996, and (iii) the PRT comments to the DOE response to PRT recommendations dated July 30, 1996. No additional documents regarding this review process have been released by DOE as of September 1996.

Further insight into the YMSCO Thermohydrologic Testing and Modeling Program was gained during the DOE/NRC Appendix 7 meeting on July 24, 1996 and during the quarterly DOE/NRC ESF video conference meeting September 12, 1996. The Appendix 7 meeting on thermal testing was held at YM and included a visit to the ESF and thermal alcove experiments. Results of this review were submitted to the NRC as a letter report in September 1996 and are summarized here.

The review concluded that the DOE YMSCO Thermohydrologic Testing and Modeling Program, as represented in the information available for this review, adequately addresses most, but not all critical relevant technical issues. It was noted in the PRT report, and supported here, that the discontinuance of surface based hydrologic testing may result in unacceptably high uncertainty in infiltration estimates. The importance of acceptable predictions of infiltration rates is manifested in thermohydrologic flow models whose predictions are highly sensitive to prescribed infiltration rates at the upper boundary. It was also noted in both reports that the DOE does not have plans to evaluate the conceptual models as rigorously as needed to ensure that their analyses provide conservative and acceptably accurate predictions of proposed repository performance. It is possible that heater tests designed for conditions different from those expected at the proposed repository may provide misleading results. Results from a field-scale heater test with an excessively high thermal load may support an equivalent continuum model (ECM) conceptual model, however, the ECM might not accurately incorporate important moisture redistribution mechanisms, such as refluxing and dripping, that would be experienced under repository conditions. For example, a drift-scale heater conducted with drift wall temperatures > 200 °C could conceivably minimize the potential for reflux dripping from the drift ceiling. The heater test would thereby concur with ECM conceptual models which do not predict dripping, a mechanism not yet predicted in any analyses, but which has been observed in previous heater tests (i.e., Climax, G-tunnel, and the road tunnel near Superior, AZ). Analyses of WP integrity and radionuclide transport from the WP may not be conservative if thermally driven moisture flow near the WP is not conservatively modeled (Pruess and Tsang, 1993, 1994). In future prelicensing interactions with DOE, the potential benefits of a spatially variable thermal load for the drift-scale heater test will be suggested as a way to test for the potential of this mechanism.

In neither the PRT report nor the DOE response to the PRT report was it demonstrated that DOE bounding assumptions and analyses of the thermo-hydrological-chemical (THC) processes are conservative. At high thermal loads, significant concentrations in dissolved species such as chloride and elevation in pH can be expected to occur near the boiling front surrounding the repository (Walton, 1993). As a consequence corrosion rates and sorption properties of the host rock will be affected. Prediction of such effects can only be achieved with models which adequately couple THC processes (Lichtner and Seth, 1996). The current codes mentioned by the PRT and DOE (TOUGH, TOUGH2, VTOUGH, FEHM, and NUFT) do not include chemistry suitable for describing rock-water interaction and the effects on solution chemistry due to evaporation and condensation processes. An additional code mentioned in the DOE response, GIMRT/OS3D, is a fully saturated code that does not include two-phase fluid flow. The code EQ3/6, a geochemical reaction path model, does not appear adequate for the analysis either, although use of this code was recommended by the PRT. This is because the problem to be solved is fundamentally a moving boundary problem. Reaction fronts will not remain stationary with time and therefore, it is difficult to see the utility of using EQ3/6 which does not incorporate fluid transport to model such processes. Analyses which omit critical THC processes may not be conservative. It is important that the DOE YMSCO Thermohydrological Testing and Modeling Program be designed to address these and the above mentioned issues.

6.3.2 Benchmark Testing of Computer Codes

Thermohydrologic codes used by the DOE and NRC/CNWRA were assessed through benchmark testing (i.e., code-to-code comparisons) and the results were used to (i) compare and contrast code analysis capabilities, (ii) identify and understand any significant differences that may arise, and (iii) assess robustness and computational efficiencies of the codes. Benchmark testing (Baca and Seth, 1996) included four general thermohydrologic codes: TOUGH2, FEHM, CTOUGH, and MULTIFLO. The TOUGH2 and FEHM codes are actively being used by DOE contractors, while the CTOUGH and MULTIFLO codes are being used by the NRC/CNWRA. The benchmark testing of these four thermohydrologic codes was conducted using two sets of computational test cases. Each set of cases consisted of one- and two-dimensional (2D) simulations of isothermal and nonisothermal flow involving both porous and fractured-porous media systems. In general, the benchmark testing showed that three of the four codes tested (TOUGH2, CTOUGH, and MULTIFLO) appear to possess sufficient capability to simulate some of the hydrologic and thermohydrologic conditions expected to be important at the proposed HLW repository at YM. In all the test cases considered, it was found that the numerical results produced by these three thermohydrologic codes agreed. The primary differences were in computational efficiency and it was found the MULTIFLO code was substantially faster than the other codes. FEHM solved most of the test cases and the numerical results agreed adequately well with results of the other three codes. However, the FEHM code that was tested experienced computational difficulties in two test cases due to prohibitively large execution times that occurred as a result of repetitive reductions of the time step; one with high infiltration rates and the other with flow in fracture-porous media. The overall results of the benchmarking study suggest that the use of distinct thermohydologic codes by DOE and NRC will not lead to contentious methodology issues.

6.3.3 Sensitivity Analysis

A robust, accurate two-phase numerical simulator was needed to perform a sensitivity analysis of thermally driven flow through partially saturated fractured porous rock. Therefore, the first task of this analysis was to evaluate and select a two-phase numerical simulator to be used in predictive modeling. Results from previously conducted scoping analyses using C-TOUGH (Lichtner, 1994) were compared with similar analyses predicated on an ECM performed using MULTIFLO, a multicomponent, multiphase, nonisothermal reactive transport code developed at the CNWRA (Seth and Lichtner, 1996). MULTIFLO proved to be more efficient and capable in these and other comparative analyses (Baca and Seth, 1996) and was selected as the two-phase simulator in the sensitivity analyses. In addition, TOUGH2 (Pruess, 1991), a two-phase simulator used by the DOE contractors, is used to provide an independent comparison of MULTIFLO results and to assess a dual continuum conceptual model. Limited use of DCM-3D (Updegraff et al., 1991) has been initiated to test an alternative conceptual model of matrix/fracture interactions. Other than this limited testing, however, all simulation of thermally driven moisture through partially saturated fractured rock that was performed as part of this KTI was accomplished using an ECM conceptual model and computed with MULTIFLO. Although limitations in the ECM have been recognized, future analysis will also use the ECM with MULTIFLO until an acceptable model or code is identified.

Sensitivity analyses were conducted to assess the importance of variations in thermal loading schemes, drift engineering design, backfill material, hydraulic properties, and geologic structures and features. Effects are presented in terms of predicted temperature and saturation. Results from these analyses were used to address the subissue to identify the nature and bounds of thermally induced flux in the near field. Moisture conditions at the WP will affect canister integrity and thermally driven moisture flow at and below the proposed repository horizon will affect radionuclide transport.

6.3.3.1 Effects of Backfill on Temperature and Saturation

Engineered barriers such as backfill may play a role in containing waste and inhibiting radionuclide transport by providing structural control of near field rock movements, deterring human entry, and creating a diversionary path for episodic water intrusions. In addition, the selective use of backfill material with a low thermal conductivity has been considered as a proactive procedure to engineer the hydrothermal conditions near the WP (Buscheck et al., 1995).

A series of simulations was performed with the MULTIFLO code to evaluate the effects of backfill on temperature and saturation at the WP and the drift wall. The evaluation included assessments of: (i) backfill versus no backfill materials, (ii) effect of saturation of the backfill materials, and (iii) effect of the thermal conductivity of backfill materials. A vertically oriented, 2D numerical model spanning from ground surface to the water table was used for these analyses. The model was configured with six hydrostratigraphic layers similar to that used in the 1995 DOE Total System Performance Assessment (TSPA-95) (TRW Environmental Safety Systems, Inc., 1995). Each layer was represented as a uniform equivalent continuum combining the effects of matrix and fractures (Klavetter and Peters, 1986). The vertical boundaries were no heat or fluid flow. The surface and water table were established as constant temperature and pressure boundaries. The upper boundary was assigned a uniform, steady infiltration rate of 0.3 mm/yr as was used in TSPA-95 (TRW Environmental Safety Systems, Inc., 1995). The WPs are assumed to be initially stored in open drifts. After 100 yr, the drift voids are filled with backfill material. The assigned package spacing equates to an areal power density of 83 MTU/Ac. The model geometry, property values, and heat load are consistent with TSPA-95 (TRW Environmental Safety Systems, Inc., 1995).

The temperature effect of emplacing backfill materials into a drift 100 yr after emplacement of 30 yr old spent fuel is illustrated in figure 6-1. Before the backfill is emplaced, temperature in the drift at the surface of the WP increases steadily for approximately 50 yr then declines as the waste decays. Immediately after emplacement of the backfill materials, the temperature in the drift decreases by 15 °C from evaporation of pore water in the backfill (in this case, the initial saturation of the backfill was assumed to be 0.5). After the pore water of the backfill materials is evaporated, the backfill acts as an insulator and the temperature at the WP increases by about 10 °C above its pre-emplacement level. Temperatures elevated due to the insulating effect of the backfill persist for about 1,500 yr.

The effects of variable saturation of the backfill were examined for initial backfill saturations of 0.01, 0.5, and 0.99 compared to measured *in situ* Topopah Spring Welded (TSw) saturations that vary from about 0.5 to 0.99. The saturation of backfill material will be affected by drying mechanisms associated with the manner in which the backfill materials are mined, transported, stored, and possibly processed. Analysis for initial saturations of 0.01, 0.5, and 0.99 provide the range of possibilities that could be encountered. Increased saturation in the backfill causes temporary lower temperatures after emplacement, however, after 10–20 yr there is negligible difference in the predicted temperatures or saturations (figure 6-2).

It has been asserted by the DOE (Buscheck et al., 1995) that emplaced backfill material with low thermal conductivity will elevate the WP temperature, decrease the drift wall temperature, and decrease the extent of the boiling isotherm with the advantageous effect that water condensed above the drifts will be more easily shed away and downward from the WP. Analyses were conducted within the TEF KTI to evaluate this assertion. Initially, a literature search was conducted to collate existing measurements and estimates for thermal conductivity values of geologic units at YM. Most of the measurements were made on intact rock whereas backfill materials will most certainly be crushed or

Effect of Backfill on Temperature (83 kW/Ac)

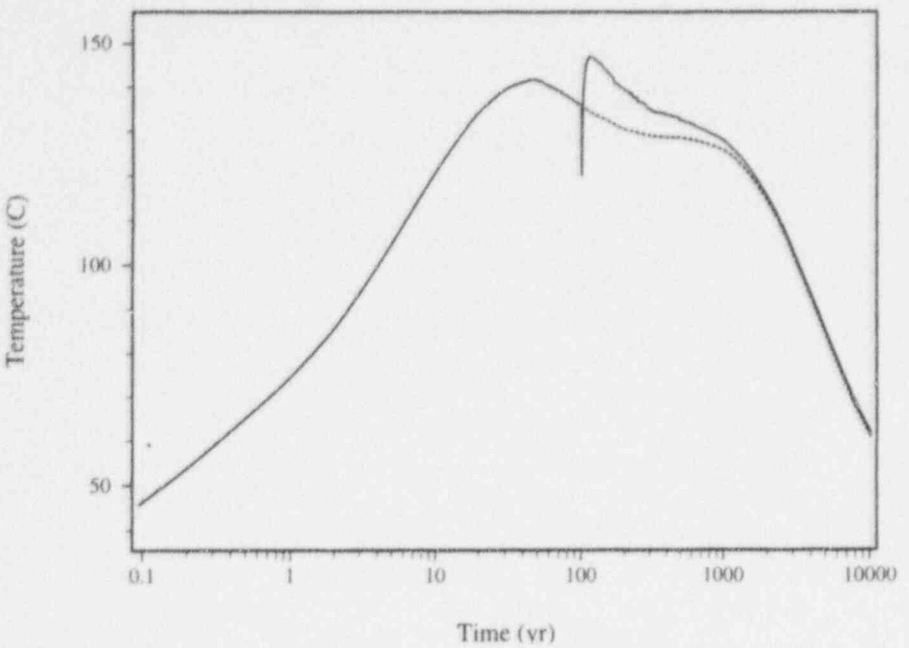

Figure 6-1. Effects of backfill on temperature at the waste package; dotted line denotes no backfill

Effects of Initial Saturation of Backfill (83 kW/Ac)

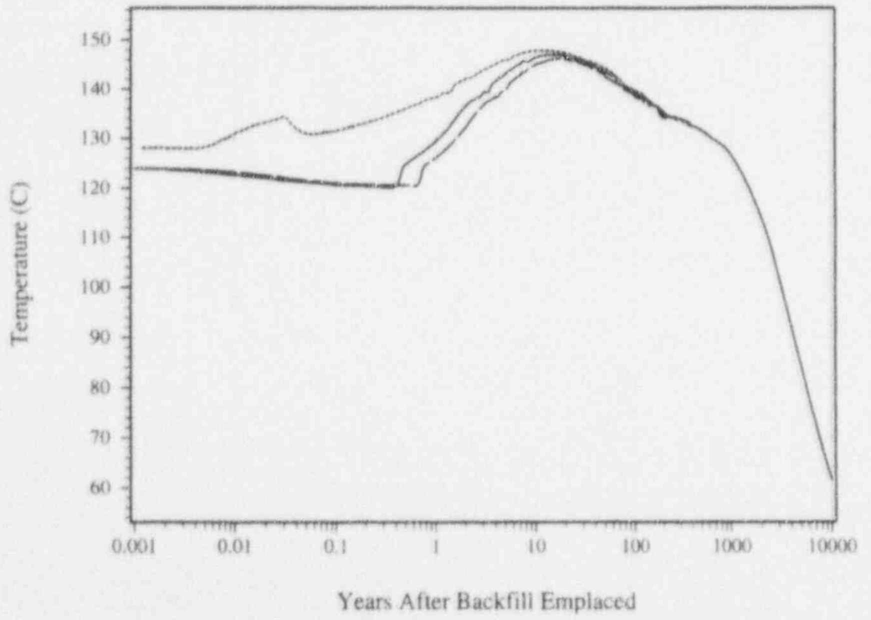

Figure 6-2. Waste package temperature as a function of initial saturation of backfill for initial saturations of 0.01 (dotted line), 0.5 (solid line), and 0.99 (dashed line)

granulated. For this reason, a steady-state laboratory apparatus was assembled to measure the bulk thermal conductivity of crushed rock over a range of temperatures and saturations. Using reasonable estimates of thermal conductivity identified in the literature search and laboratory testing, numerical analyses were then conducted to assess the relative effect of backfill materials exhibiting different values for thermal conductivity, K_t. Following is a discussion of this assessment.

Previous studies that measured and/or estimated the thermal conductivities of the thermal-mechanical units at YM have been conducted by Lappin (1980), Lappin et al. (1982), Sass and Lauchenbruch (1982), Lappin and Nimick (1985), Nimick and Lappin (1985), and Sass et al. (1988). Nimick (1990a,b) rejects most of the thermal conductivity values obtained in the aforementioned investigations because of uncertainties and errors cited by authors or their peers. The DOE Reference Information Base (RIB) (U.S. Department of Energy, 1993) cites Nimick (1990a,b) measured and estimated values of thermal conductivity for the thermal-mechanical units at YM. The DOE RIB values for thermal conductivity by Nimick are, therefore, assumed to be most representative of the thermal-mechanical units at YM. The classification of the thermal-mechanical units at YM used by Nimick is compared to that used in TSPA-95 (TRW Environmental Safety Systems, Inc., 1995) in table 6-1. The measured and estimated values of thermal conductivity values obtained by Nimick (1990a,b) and referenced in the RIB are presented in table 6-2.

To date, measurements of thermal conductivities at steady-state conditions are not available for bulk crushed samples collected from YM (Wilson et al., 1994). To gain a better understanding of the parameters that may affect these estimates, laboratory measurements of the thermal conductivity were made of crushed tuff materials, such as those being considered for use as backfill at the proposed repository. A steady-state thermal conductivity apparatus was constructed to measure the thermal conductivity of bulk rock samples. A schematic diagram of the apparatus is shown in figure 6-3. The cell accepts 1.35 m^3 of sample material and will accommodate dry to fully saturated samples over a temperature range of 10 to 230 °C, although only dry samples were measured for temperatures in excess of 100 °C.

Preliminary thermal measurements were performed on welded tuff collected from the Apache Leap Test Site (ALTS). Core samples from ALTS were broken, crushed, and sieved into a fraction consisting of very angular to subangular rock pieces between 1.6 and 4 cm in diameter. The crushed tuff was dried for two days at 90 °C then loaded into the thermal conductivity cell. A total of six measurements was conducted on the same sample, although the sample was more tightly packed in tests 2 through 6 than in test 1 (the cell contained about 0.1 m^3 more rock in tests 2–6). As expected, thermal conductivity of the more tightly packed sample increased from 0.246 to 0.266 W/m-K, with all other variables remaining constant.

Measurements were also performed to determine if thermal conductivity is sensitive to variations in the temperature of the boundaries of the sample. Heat flux was controlled by varying the temperature difference between the top and bottom aluminum plates (e.g., increasing or decreasing the temperature of the heater or heat sink or both). The heat flux was varied from 20.74 to 115.80 W/m^2 and the average temperature varied from 26.41 to 66.93 K. Thermal conductivity is illustrated in figure 6-4 as a function of temperature. Although subtle, there is a linear relationship between temperature and thermal conductivity. Test 1, which was loosely packed, departs slightly from this linear relationship. In all of the test runs, the sample attained thermal equilibrium within a few days. Results of these preliminary measurements are presented in table 6-3.

Table 6-1. Classification of thermal-mechanical units at Yucca Mountain

Nimick (1990a,b)		TSPA-95 (TRW Environmental Safety Systems, Inc., 1995)	
Unit	Depth[1] (m)	Unit	Depth (m)
TCw	0-60	TCw	0-95
PTn	60-125	PTn	95-148
TSw1	125-300	TSw	148-482
TSw2	300-400		
TSw3	400-420	TSv	474-482
CHn1	420-570	CHnv	482-563
CHn2	570-590	CHnz	563-684
CHn3	590-600		

[1]approximations

Table 6-2. Measured and estimated values of thermal conductivity, κ_t

Formation	κ_t at *In Situ* Saturation (W/m-K)	κ_t Ambient Saturation Not Indicated (W/m-K)	κ_t Saturated (W/m-K)	κ_t Dry (W/m-K)
TCw	1.59-1.73[1]			1.51-1.64[1]
PTn	1.55-1.67[1]	1.68-1.94[2]		
TSw	1.59-2.18[1]		1.6-2.1[2]	1.58-2.36[2]
TSv	1.26-1.28[1]	1.20-2.09[2]		
CHnv	0.84-1.21[1]	1.17-1.44[2]		
CHnz	1.26-1.57[1]		1.16-1.83[2]	0.54-.076[2]

[1]Estimated values
[2]Measured values

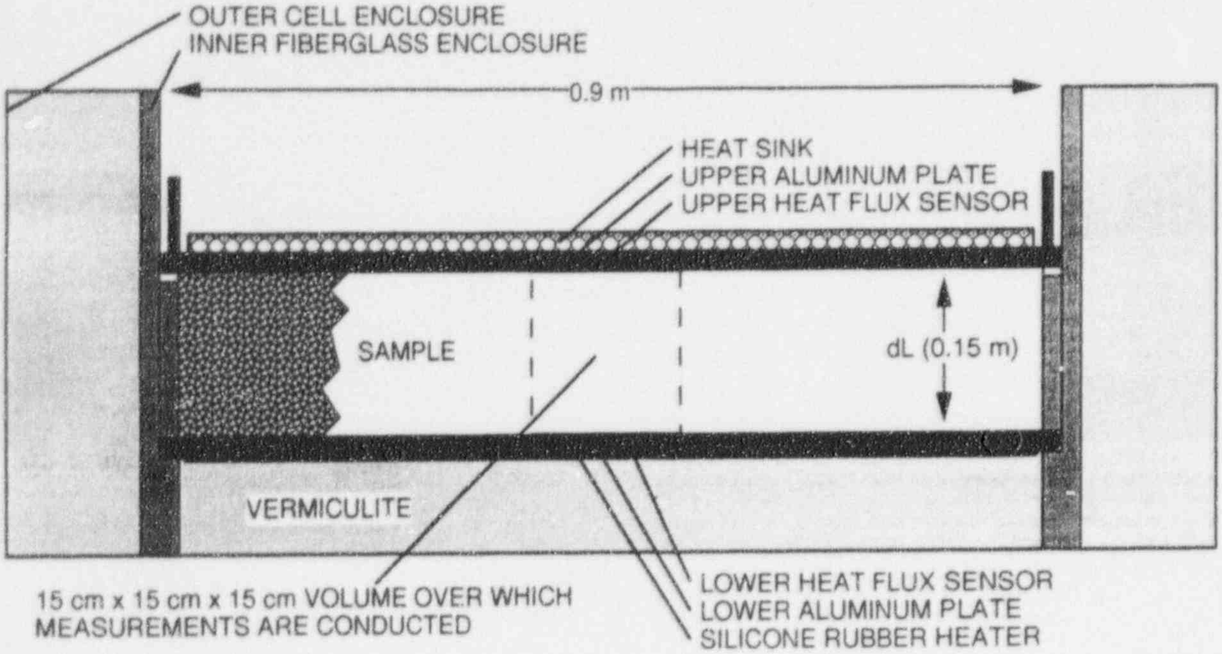

Figure 6-3. Schematic of bulk thermal conductivity measurement apparatus

The numerical model used in analyses to assess the effect of the thermal conductivity of backfill materials was similar to that used in the previous backfill analyses. The time history of WP temperature with backfill thermal conductivities of 0.2, 0.6, 2.0, and 10.0 W/m-K is illustrated in figure 6-5. The first three thermal conductivities are similar to those of tuff backfill materials and intact tuff. The high value of 10 W/m-K exceeds the thermal conductivities of common geologic materials but approaches a value equivalent to radiative heat transfer through air over short distances. This figure indicates that backfill with a lower thermal conductivity acts as an insulator and results in higher WP temperatures; higher conductivity backfill acts as a conductor and can lower WP temperatures. This effect is most pronounced immediately emplacement of the backfill and gradually becomes insignificant with time as temperatures and heat after flux diminish. It is interesting to note that although backfill thermal conductivity affects temperature at the WP, it has little effect on temperature at the drift wall. Temperature at the WP, roof, sidewall, and within the pillar are illustrated in figure 6-6 for a backfill thermal conductivity of 0.2 W/m-K. This figure shows that the temperature at locations other than the WP do not differ significantly with change in thermal conductivity of the backfill. Similarly, backfill thermal conductivity has no appreciable effect on saturation near the drift wall.

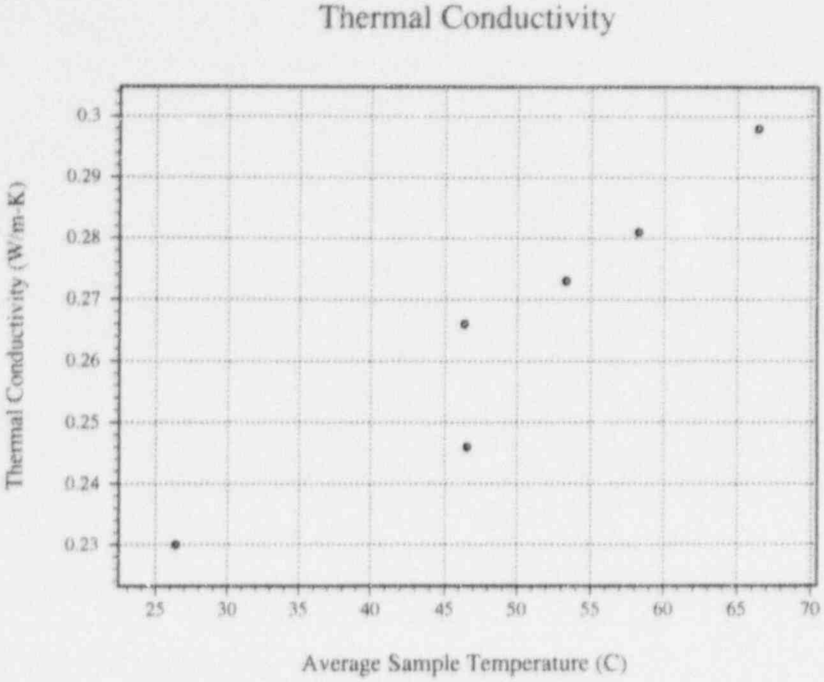

Figure 6-4. Thermal conductivity of dry bulk tuff from the Apache Leap Test site as a function of temperature

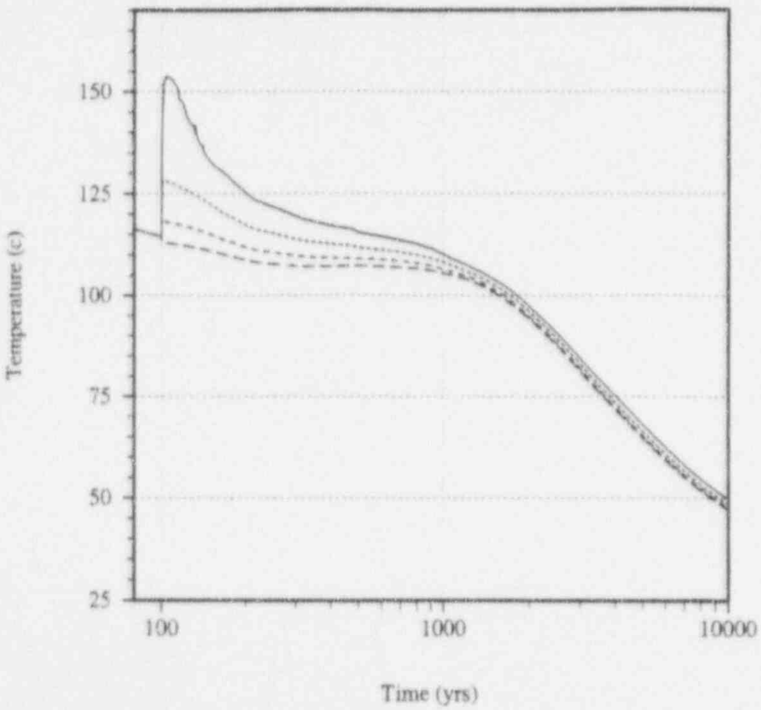

Figure 6-5.Waste package temperature as a function of backfill thermal conductivity of 0.2 (solid line), 0.6 (dotted line), 2.0 (short dash), and 10.0 W/m-K (long dash)

Table 6-3. Unsaturated thermal conductivity measurements of ALTS tuff. Uncertainties in the thermal conductivity values were calculated based on errors in sample thickness, temperature measurement, and accuracy of the heat flux sensors.

Test Number	Temperature of Top Plate (°C)	Temperature of Bottom Plate (°C)	Average Sample Temperature (°C)	Heat Flux (Q) (W/m^2)	Thermal Conductivity (κ_T) (W/m-K)
1	23.14	70.00	46.57	75.52	0.246±0.026
2	23.35	69.40	46.38	80.36	0.266±0.028
3	39.94	76.60	58.27	67.59	0.281±0.029
4	40.42	92.44	66.43	101.75	0.298±0.031
5	20.98	85.66	53.22	115.80	0.273±0.029
6	19.53	33.28	26.41	20.74	0.230±0.024

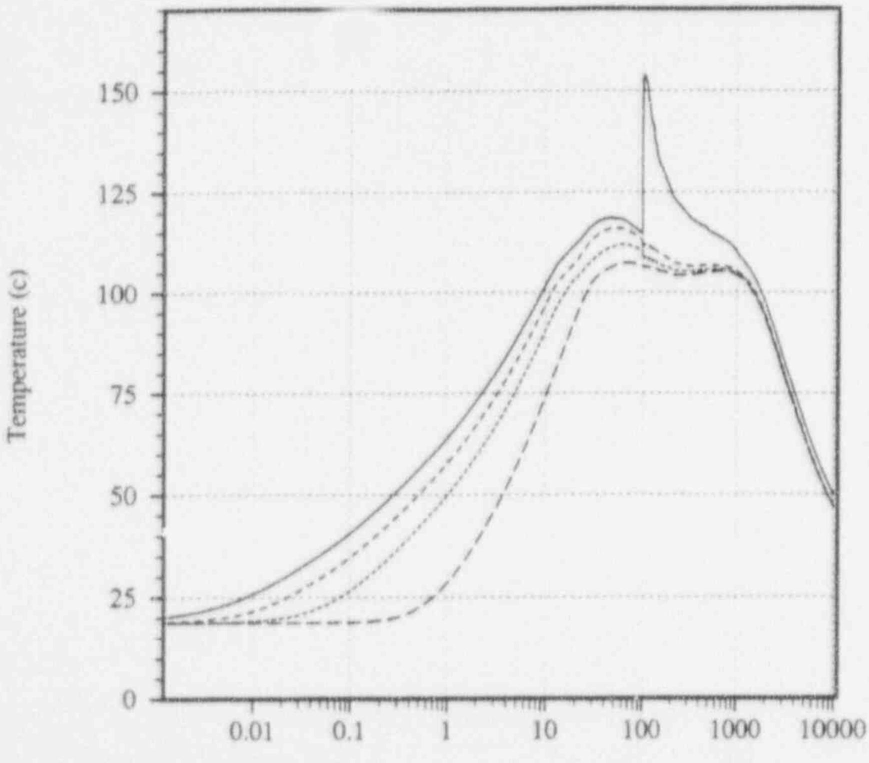

Figure 6-6. Temperature at waste package (solid line), drift roof (dotted line), drift sidewall (short dash), and pillar center (long dash) for backfill with a thermal conductivity of 0.2 W/m-K

6.3.3.2 Effect of Media Properties on Prediction of Moisture Redistribution at Yucca Mountain

Variations in the hydraulic properties of partially saturated porous media can have significant effects on the redistribution of moisture driven by heat generated from HLW emplaced at the proposed geologic repository at YM. The objective of this part of the sensitivity analysis was to evaluate the hydraulic conditions at YM for different, yet reasonable, homogeneous hydraulic property values assigned to the Paintbrush Tuff (PTn) and Calico Hills (CHnv) units located above and below the proposed repository horizon, respectively, in the presence of heat-generating HLW. The six-layer model is similar to that described in the backfill simulations. Model description and basecase properties were taken from TSPA-95 (TRW Environmental Safety Systems, Inc., 1995). Details of the analyses can be found in Green (1996).

In this analysis, the importance of media property values was assessed by how saturation and hydraulic conductivity, K(θ), are affected in the presence of heat-generating waste at the proposed HLW repository. The hydraulic properties of the PTn and CHnv units were varied to determine their effect on saturation. Saturation of the units alone is of limited use, however, knowledge of saturation and the saturation/pressure relationship of a medium allows calculation of K(θ), a direct indication of flow rates or groundwater travel times, because the flow of groundwater and any radionuclides released from WP would probably be downward, hydraulic conditions in the unsaturated units below the repository, particularly the CHnv, are of greatest interest.

It was found that saturation of the PTn and CHnv units could be increased from 0.2–0.3 to near full saturation by decreasing either the van Genuchten α or n parameters or by decreasing permeability (van Genuchten, 1980). In general, emplacement of the heat source resulted in negligible moisture change in the PTn, some moisture increase in the CHnv, and significant redistribution of moisture in the tuff units between the PTn and CHnv units in all cases studied. However, there is considerable variability in unsaturated hydraulic conductivity, K(θ), of CHnv depending on the properties assigned to PTn and CHnv (table 6-4). In particular, K(θ) for the CHnv directly below the proposed repository decreased by a factor of 10^2 at 100 and 1,000 yr and by 10^4 at 10,000 yr after the onset of heating when the hydraulic properties of the PTn and the CHnv were varied from values given in TSPA-95 (TRW Environmental Safety Systems, Inc., 1995) to values selected from the 1993 DOE Total System Performance Assessment (TSPA-93) report (Wilson et al., 1994). Consequently groundwater flow through the CHnv below the proposed repository would be significantly less if hydraulic properties taken from the TSPA-93 (Wilson et al., 1994) are found to be more appropriate than TSPA-95 (TRW Environmental Safety Systems, Inc., 1995) values. The wide range of values predicted for K(θ) indicate the large uncertainty (i.e., a factor of 10^2 to 10^4) associated with these calculations.

6.3.3.3 Effects of Ventilation on Rock Dryout and Drift Humidity

The most recent proposed repository designs call for an extended time period up to 150 yr before permanent closure of the proposed repository (TRW Environmental Safety Systems, Inc. 1993, 1994). During this preclosure period, it will be necessary to ventilate the subsurface facility to permit inspection and observation. If ventilation is employed over such a long time, some heat and groundwater will be removed from the facility. The removal of heat will reduce the peak WP temperature and the removal of groundwater will create a drier, less-corrosive environment. Even after permanent closure, ventilation may have some long lasting effects. In most earlier analyses, the proposed repository was assumed to be sealed and both heat and groundwater were conserved within the mountain for thermohydrologic calculations. Motivated by the changing designs, this analysis addresses the effects of ventilation on temperature reduction and groundwater removal. If ventilation is found to have a significant

Table 6-4. Saturation and unsaturated hydraulic conductivity (m/s) in CHnv at 100, 1,000, and 10,000 y for TSPA-95 (TRW Environmental Safety Systems, Inc., 1995) basecase and TSPA-93 (Wilson et al., 1994)

Case	100 yr		1,000 yr		10,000 yr	
	θ	K(θ)	θ	K(θ)	θ	K(θ)
TSPA-95	0.25	1.03e-9	0.28	1.89e-9	0.18	3.51e-10
TSPA-93	0.21	1.46e-11	0.24	2.55e-11	0.07	5.46e-14

impact on the WP environment, then it may be incorporated in future designs and TSPAs (Nuclear Regulatory Commission, 1995; TRW Environmental Safety Systems, Inc., 1995).

During the construction and operation of the proposed repository, ventilation will be used to provide oxygen to workers. Current designs call for a minimum ventilation capacity of 125 m^3/s of air for normal operations and a maximum of nearly 600 m^3/s for cooling if needed (TRW Environmental Safety Systems, Inc., 1994). The potential for groundwater removal is great because of increased underground temperatures (i.e., more moisture can be contained in a cubic meter of air when temperatures are increased). But because the permeability of the subsurface rock is low for liquid flow, the groundwater will not readily flow into the drifts. A reasonably conservative approach is to assume that the groundwater is immobile and does not flow to the drift walls. The groundwater in the host rock will vaporize *in situ* as if a vaporization front penetrates into the medium. After being vaporized, the water can flow due to gas pressure differences or by molecular diffusion. The gaseous permeability of a fractured rock mass is generally orders of magnitude greater than the liquid permeability so that small pressure gradients can motivate significant amounts of gas flow. At this time, the gradient in gas pressure was neglected because ventilation can strongly affect gas pressures in the drift. Ventilation could be used to maintain low gas pressures in the drift, hence drawing vapor into the drift and increasing groundwater mechanism. Hence, this work underestimates the removal of groundwater due to ventilation.

In this work, a drift-scale model was used to predict the three-dimensional (3D) transient temperature field in the vicinity of an emplacement drift. The model extends from the ground surface to the proposed repository horizon (~350 m below the ground surface and ~250 m above the water table) to 750 m below the water table. The model consisted of seven homogenous but distinct layers of rock whose thermal properties were based on Wilson et al. (1994) that are primarily from DOE (1993). The spacing between WP along a drift and the spacing between parallel drifts affect the areal mass loading (AML). To study the effects of ventilation, an intermediate AML of 40 MTU/acre was used. In the model, heat flux applied to the drift wall was reduced to compensate for heat removed by sensible heating of the ventilated air and latent heating of the vaporized groundwater. Figure 6-7 shows three thermal sources histories considered. The reference case (first scheme) has no ventilation. The other two cases are considered to evaluate the potential effects from increased heat removal by ventilation and are discussed in Manteufel (1996). In all three cases the drift has been filled with backfill materials 150 yr after the onset of heating and there is no additional ventilation.

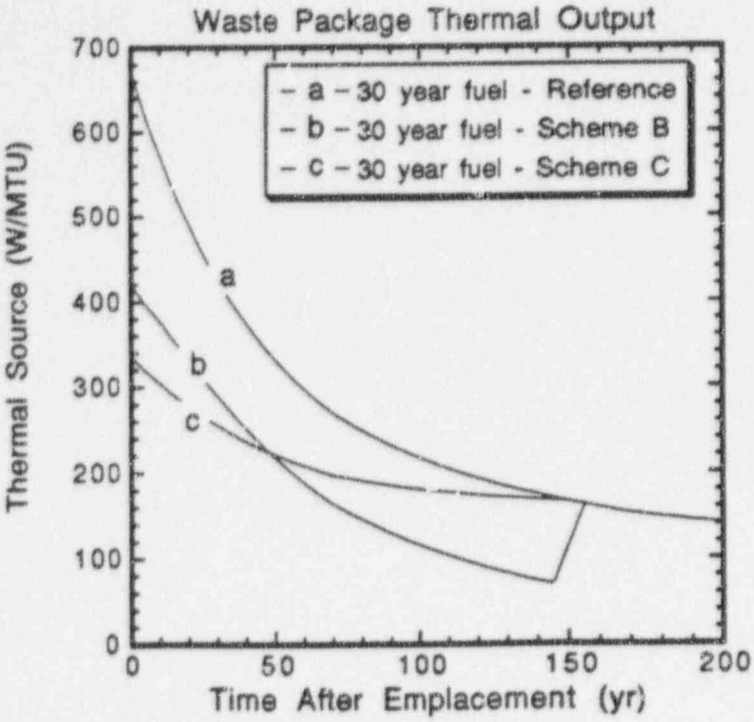

Figure 6-7. Thermal output of waste package for no ventilation (reference scheme, 30 yr old fuel) and two ventilation schemes

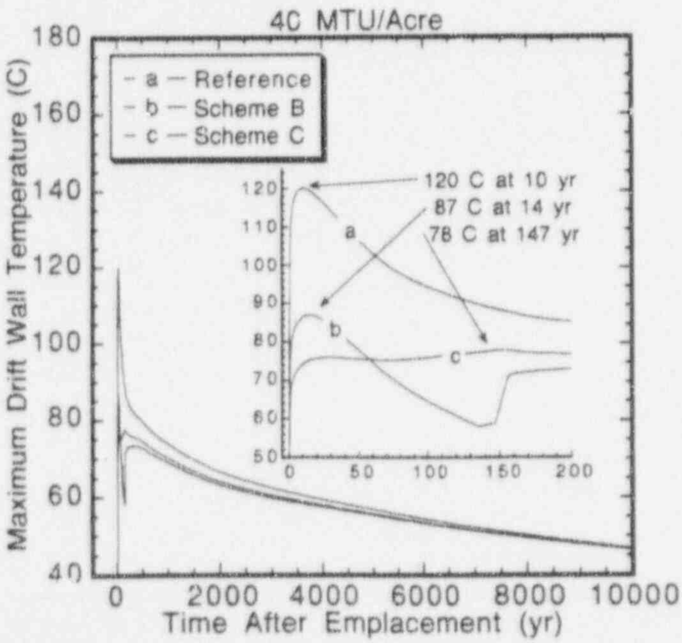

Figure 6-8. Maximum drift wall temperature for three schemes

Figure 6-8 illustrates maximum drift wall temperatures to 10,000 yr. Both ventilation cases have a strong effect on the wall temperature to 150 yr. Without ventilation, the maximum temperature is 120 °C at 10 yr. With ventilation, the temperature is either 33 °C lower (87 °C at 14 yr) or 42 °C lower (78 °C at 147 yr). Both ventilation schemes moderate the wall temperature over time. Scheme C gives the most steady temperature profile with the maximum wall temperature maintained about 75 °C for at least the first 200 yr. The long-term effects are less significant between schemes. After 1,000 yr the wall temperatures are within 10 °C for all schemes and the differences continue to diminish with time.

A model was also developed to predict the rate and extent of dryout. The model is based on immobile groundwater that is locally vaporized. This model is reasonably conservative and is expected to predict the minimum rate of dryout. Other mechanisms and features that would enhance dryout are not included such as lower gas pressures in the drift and the existence of fractures through which vapor can more readily flow into the drift. Both schemes produced nearly the same wall temperatures and about the same dryout. The dryout is diffusion limited hence, the position of the vaporization front scales with the square root of time. This implies the vapor mass flux into the drift scales as the inverse of the square root of time. Over 150 yr, the extent of dryout is predicted be about 4 to 5 m for either ventilation scheme.

In summary, these results suggest that ventilation during the first 150 yr can moderate underground temperatures. For two hypothetical yet plausible ventilation schemes, the maximum drift wall temperature was 87 °C at 14 yr and 78 °C at 147 yr as compared with 120 °C at 10 yr without ventilation. In addition to extracting heat, ventilation provides a removal mechanism for water vapor. The extent of dryout was about 4 to 5 m over 150 yr for both cases. This suggests that ventilation can be an effective thermal management tool in addition to AML (drift and WP spacing) and age of waste. In future prelicensing interactions with the DOE, it will be suggested that the possible benefits of long-term ventilation be explored.

6.3.3.4 Effects of Geologic Structure and Features on the Evolution of Perched Water Bodies

The formation of perched water bodies either above, within, and below the proposed repository horizon can potentially cause, at some point in time, liquid water to contact or elevated humidity to exist near waste canisters. The exposure of WP to water could in turn increase the rate of waste canister failure resulting in greater releases of radionuclides. In general, perched water bodies tend to be transient features formed where there is a contrast in hydrologic properties (Freeze and Cherry, 1979). Contrasts may result from differences at boundaries between various ash flows and also by low hydraulic conductivity strata being adjacent to more permeable and conductive strata along structural features such as faults or other persistent discontinuities. YM is dissected by numerous faults (Frizzell and Shulters, 1990), thus substantially increasing the probability of locally saturated conditions occurring.

It has been hypothesized that in the vicinity of the proposed repository rock drying by repository heat may cause perched water zones to form. This process involves vaporization of water around the proposed repository. It is expected that water vaporized by radiogenic heat will move away from the waste canisters until it reaches a location where the rock temperature is low enough to permit condensation. If the condensed water encounters low permeability material, rock water saturations may increase and form a perched zone. These multiphase flow conditions and their effects on the formation and dissipation of perched water bodies could significantly affect the performance of waste canisters in a repository. Sensitivity analyses have been performed using MULTIFLO to simulate the evolution of perched water bodies in the presence of heat-generating HLW at YM. As an initial component to these analyses, the presence of pre-existing perched water bodies at YM was first assessed. Second, the further evolution of perched water induced by multiphase conditions was numerically simulated.

The geographical area considered for this analysis is the vicinity of the intersection of Ghost Dance fault (GDF) and Sundance fault in the proposed repository area of the YM site. The modeled area is a north-facing, 2D vertical section along the Sundance Fault, 1,100 m wide by 650 m deep, taken from the CNWRA Geological Framework Model (GFM). Note that the effects of the Sundance Fault are not considered in these analyses. The area of interest is above the water table and primarily updip of GDF. GFM includes lithostratigraphy, hydrostratigraphy, and geologic structure (Stirewalt et al., 1994; Stirewalt and Henderson, 1995) of the YM region. Lithostratigraphy and geologic structure are based on surface geologic maps of the site (Scott and Bonk, 1984). Subsurface geology is constrained by borehole data from the DOE site characterization activities (e.g., Flint and Flint, 1990) and through construction of balanced cross sections. Thermal and hydrologic property values assigned to the matrix of each of the different lithostratigraphic units were assumed homogeneous and isotropic. Data used in this study were adopted from TSPA-95 (TRW Environmental Safety Systems, Inc., 1995). The GDF was modeled only as a geological boundary, without any specific properties assigned. If the GDF acted as a conduit to flow, the formation of a perched water zone updip of the fault may be suppressed. Future work will address the behavior of the flow system taking into consideration fault properties. The lithostratigraphic units represented in the model are (from top to bottom): (i) Tiva Canyon Welded (TCw), (ii) PTn, (iii) TSw 1,2,3, (iv) CHn, and (v) Prow Pass Welded (PPw).

The spatial mesh of this model is rectangular with a Δx=20-m and Δz=10-m (x and z are horizontal and vertical directions respectively). The left and right boundaries are no-flow, the top boundary is constant flux, and the bottom boundary is a water table condition. A uniform initial saturation value of 0.25, corresponding to the bubbling pressure for most YM units, was assigned to the entire modeled region. Initial conditions were based on a constant flux rate of 0.3 mm/yr, similar to TSPA-95 (TRW Environmental Safety, Systems, Inc., 1995). Solution of the transient flow equation under isothermal conditions produced pressure head results, transformed to saturation values. These saturations indicated the presence of existing perched water zones. At various points in time, the volume of moisture within zones with saturation equal to or in excess of an *a priori* selected saturation value (typically 0.998, 0.9998, and 1.00) was then calculated, thus providing the time variation of the perched water volume.

Under the influence of a constant surface flux of 0.3 mm/yr and isothermal conditions, the flow system exhibits the following behavior. The PTn unit, having a high permeability, allows water to flow freely down through it. When the water encounters the TSw unit with low permeability, downward flow is inhibited. This causes the water to be channelled downdip in the PTn until it reaches the GDF. The footwall of the fault has been uplifted so that the PTn in the hangingwall is juxtaposed against the relatively impermeable TSw unit in the footwall of the fault. This produces a trap where water begins to accumulate producing a perched water zone. As it continues to accumulate, some water percolates slowly downward through the TSw unit, extending the perched water body well into the TSw unit. The perched body continues to grow as long as inflowing water exceeds the rate at which water percolates through the TSw. The simulated perched zone attains a steady-state condition characterized by high saturation values (i.e., 0.99 and higher) immediately updip of the GDF (figure 6-9a).

The isothermal results were used as the initial condition for the nonisothermal analysis. A uniform thermal load of 83 MTU/acre was applied over the entire simulated repository (1,100 m long by 10 m thick) at a depth of 340 m below the top boundary. The time history of the heat load was taken from TSPA-95 (TRW Environmental Safety Systems, Inc., 1995). In less than one yr after the onset of heating, the thermal effects of the proposed repository are manifested by increased saturation and liquid and gas phase velocities within the proposed repository horizon (figure 6-9a,b,c). These effects are amplified beneath the area of highest saturation values predicted for prerepository conditions. As time progresses, a high saturation zone develops at the proposed repository horizon, immediately updip of the GDF. The

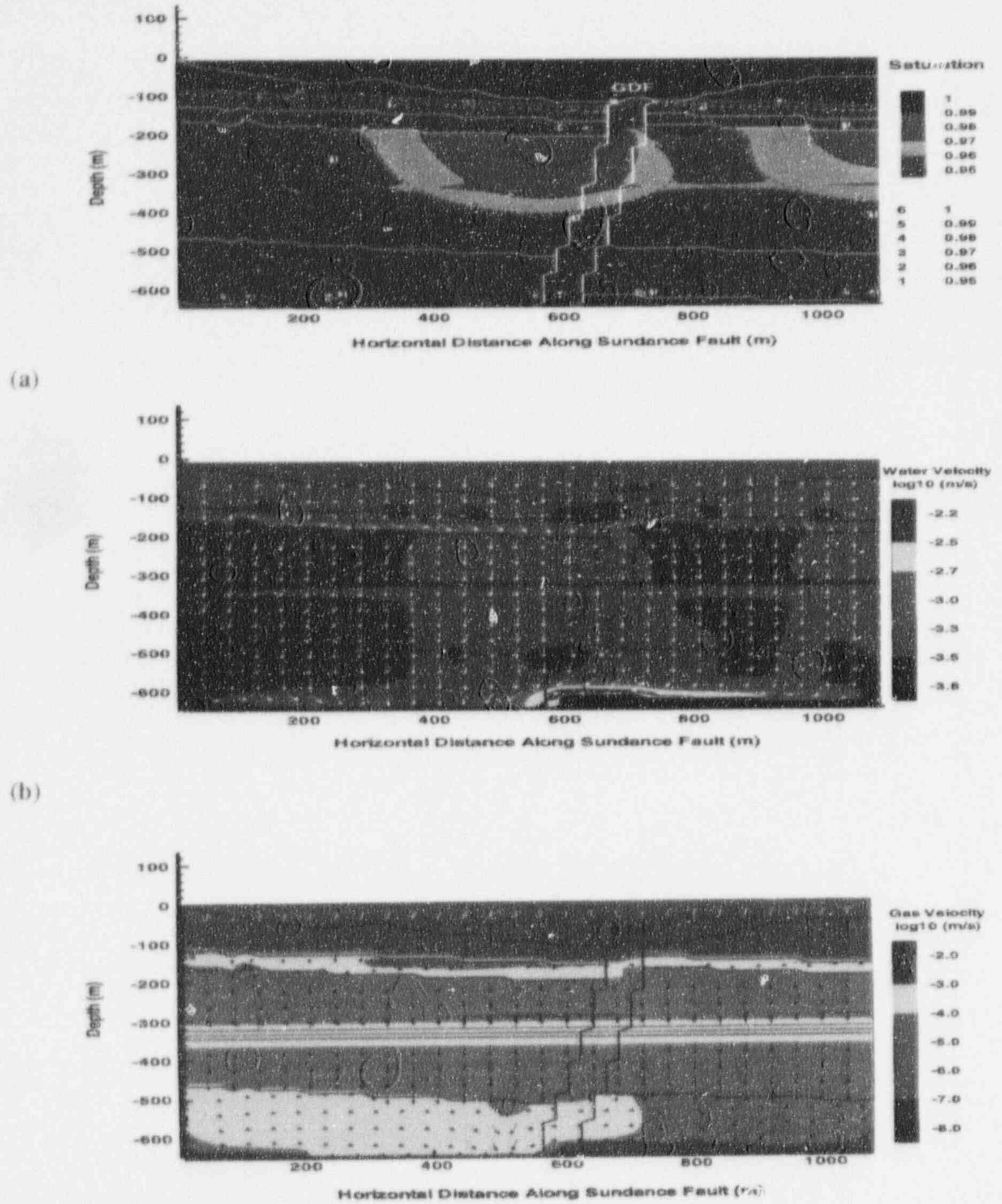

Figure 6-9. Results of nonisothermal flow analyses after 1 yr of repository heating with isothermal analyses steady-state results as initial conditions. Solid white lines represent the geologic structure and topographic relief, (a) Saturation, dashed black lines correspond to steady-state saturation values obtained from isothermal analyses; (b) liquid-phase velocity; and (c) gas-phase velocity.

size of the perched water volume increases with time, reaches a maximum value at about 100 yr (figure 6-10), starts decreasing under the influence of elevated temperatures, and is no longer evident by 250 yr (figure 6-11). The proposed repository eventually dries out completely by 1,000 yr.

The time varying volume of perched water for three saturation thresholds (0.998, 0.9998, and 1.00) is shown in figure 6-12. Several observations can be made from this figure. First, though the isothermal analyses produced high saturations giving water volumes (per unit section thickness) of 7,500 and 4,800 m^3 within zones with saturations higher than 0.998 and 0.9998, respectively, there was no zone with saturation values equal to 1.0. Under the influence of proposed repository heating, however, a perched water body based on a 1.0 saturation threshold is formed, reaches a maximum volume of 4,000 m^3 after 100 yr, and dissipates totally after 1,000 yr. Similar behavior is exhibited by the other two threshold saturations with the exception that the maximum volume occurs around 45 yr followed by an abrupt decrease in the volume. The abrupt decrease in volume for both the 0.998 and 0.9998 saturation values is attributed to condensation effects caused by the thermal pulse having been reached and moved beyond the area of high saturation under isothermal conditions.

It is also worth noting that even though the multiphase effects of proposed repository heating are rapidly propagated throughout the model domain, a long time is required for the thermohydrologic system to return to its preheating state. As illustrated in figure 6-13, this difference is easily seen in the comparison of the liquid phase velocity magnitude contours and direction vectors after a period of 10,000 yr with those simulated for preexisting isothermal conditions (figure 6-9b).

Model results were examined to understand the physical phenomena associated with formation of perched water bodies in the vicinity of the proposed repository under nonisothermal conditions. The introduction of heating causes general movement of gas (water vapor) away from the proposed repository area, whereas water movement directional patterns remain essentially the same as were established prior to proposed repository heating. The combined effect of water accumulation and gas expulsion leads to the development of full saturation, first in the preheating zone of highest saturation. The volume of the full saturation zone initially increases with time and later migrates downwards to a depth of about 360–400 m that is below the proposed repository level. Thereafter, the saturation zone begins to break up and eventually disappears.

Results calculated in this sensitivity analysis indicate that the initial effect of proposed repository heating (under the condition of steady averaged infiltration) can lead to increased water saturation within the proposed repository area. Such increased saturation may result in sustained perched water volumes that grow in size within the first 100 yr of proposed repository heating and begin to dissipate thereafter. The specific effects of such perched water zones on the total system performance have not yet been assessed, however, elevated saturated levels at the proposed repository horizon could affect WP corrosion rates and subsequent radionuclide transport.

6.3.3.5 Effects of High Permeability Features on Temperature and Saturation

Numerical analyses were conducted to assess what effect a zone of higher permeability intersecting the drift would have on the thermohydrology of the drift. This effect was assessed for temperature, saturation, and relative humidity within the drift and at the drift wall. The model extended vertically from the ground surface to the water table and horizontally from the center line of the drift to the mid-distance separating drifts. Rock mass was represented as an ECM. Material properties were taken from TSPA-95 (TRW Environmental Safety Systems, Inc., 1995). Initial conditions were determined for

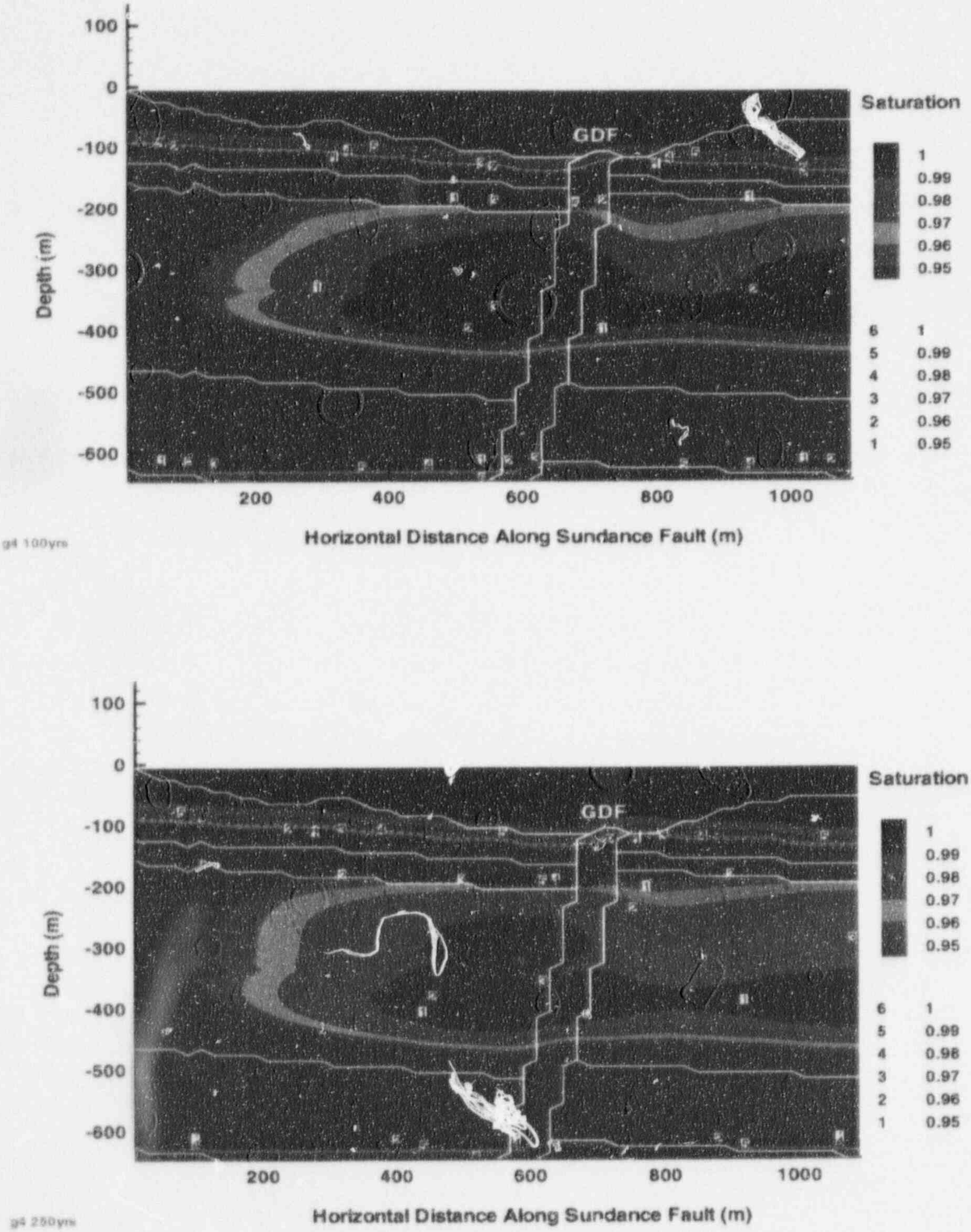

Figure 6-11. Saturation after 250 yr of heating. Dashed black lines correspond to steady-state saturation values obtained from isothermal analyses.

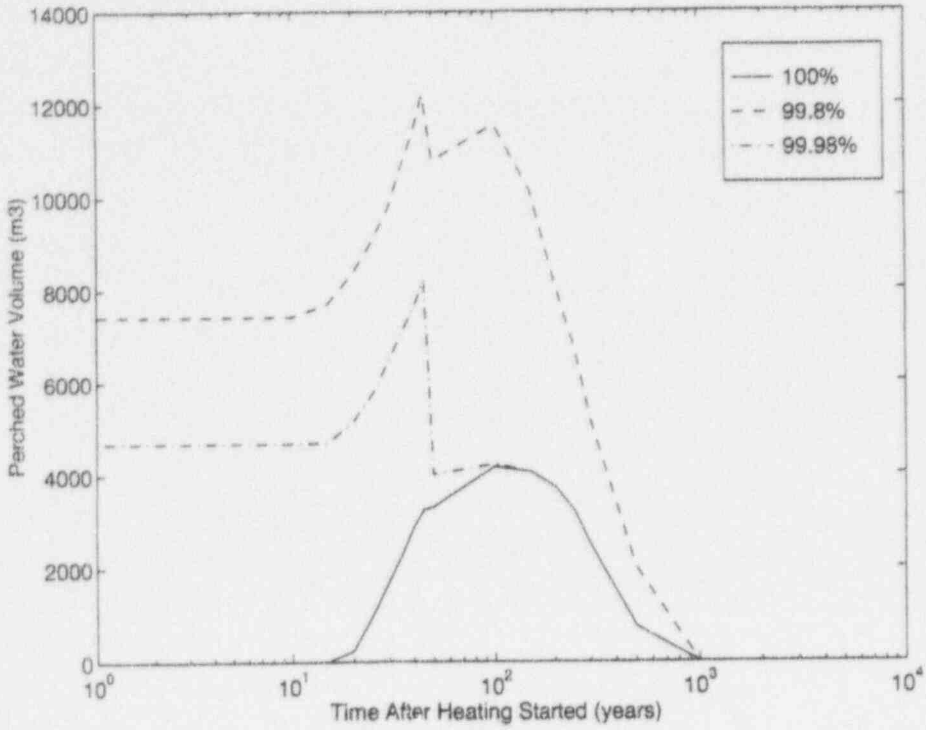

Figure 6-12. Time history of water volume for parts of the domain with saturations higher or equal to 0.998, 0.9998, and 1.00

a uniform infiltration rate of 0.3 mm/yr applied at the upper boundary. Fracture zones that extended from ground surface to the water table and intersected the drifts were simulated. Fracture zone widths varied from 1 to 140 cm. The fracture zones were assigned permeabilities a factor of five greater than that assigned to the matrix of the TSw and a factor of ten less than the permeability assigned to fractures in the TSw. An exponentially decaying heat load with an AML of 83 MTU/acre was assigned to the WP. The void of the drift was initially left empty then filled with backfill material 100 yr after the onset of heating. The MULTIFLO code (Seth and Lichtner, 1996) was used in all analyses.

Simulations conducted with ECM properties assigned to the rock mass were compared to similar simulations but with vertically oriented fracture zones of variable widths intersecting the drift. In general, simulations with fracture zones allowed gas and heat to escape from the drift more easily than was experienced for simulations with no fracture zone. This resulted in reduced temperatures at the WP (a decrease in the maximum from 147 to 120 °C) and to a lesser extent at the drift wall (a decrease in the maximum of 131 to 117 °C) (figure 6-14). Temperature reductions caused by fracture zones persisted at the WP for approximately 3,000 yr (figure 6-15). Varying the width of the fracture zone to about 20 cm indicated that the reduction in temperature is dependent on width of the fracture zone. Increases in the fracture zone width greater than 20 cm however, did not result in any additional decrease in temperature. For example, the 25 °C decrease in temperature at the WP and the 15 °C temperature decrease at the drift wall for a 20 cm wide fracture zone were approximately the same as predicted for fracture zones that vary in width from 20 to 140 cm (figure 6-14). The cause of the slight increase in temperature predicted for fracture zones greater than 80 cm was not identified but may have resulted from excessively coarse numerical discretization.

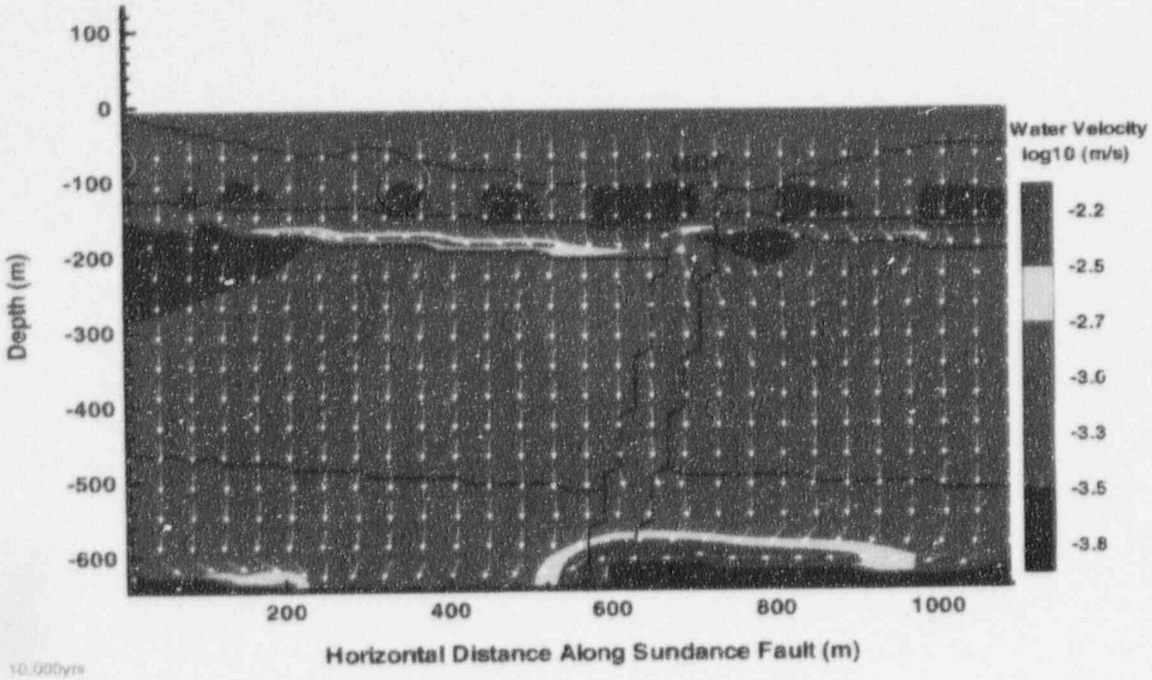

Figure 6-13. Liquid-phase velocity magnitude contours and direction vectors at 10,000 yr

The results of this analysis are consistent with analyses by Buscheck and Nitao (1995), both indicating that the high permeable features that intersect the drift result in lower temperatures at both the WP and at the drift wall. Although a 15 to 25 °C drop in drift wall temperature may not seem consequential, particularly relative to the high level of uncertainty associated with the predictions, temperature decreases from 131 to 117 °C at the drift wall can have added significance. Lower drift wall temperatures permit refluxing waters to approach more closely to the drift wall before vaporizing. There is also the added possibility of liquid water being present near the drift wall at temperatures greater than 100 °C as a result of elevated salt content and capillary pressure. These effects combine to increase the potential for flow down fractures near the drift wall and dripping into the drift, possibly onto WP. Water dripping onto canisters heated to above 100 °C has been experienced during field-scale heater tests in heater tests at G-tunnel, Climax, and at the Apache Leap Test site. Based on these observations, the effect of high permeability features such as these should be considered when evaluating the validity of conceptual models and performing assessments of various thermal loading strategies.

6.3.3.6 Summary of Sensitivity Analyses

Results from the previous sensitivity analyses provide some insight to the importance of thermal and hydraulic properties, geologic features, and their attendant impact on heat and mass transfer mechanisms. Use of backfill materials is found to affect the temperature and saturation within the drift and within the first few meters of rock near the drift. The transient magnitude of these effects has been quantitatively determined, thus contributing to the subissues of the TEF KTI, namely assessing the bounds of thermally induced flux in the near field and humidity at the WP surface. In addition, the knowledge gained will be useful to future reviews of the DOE thermohydrology program.

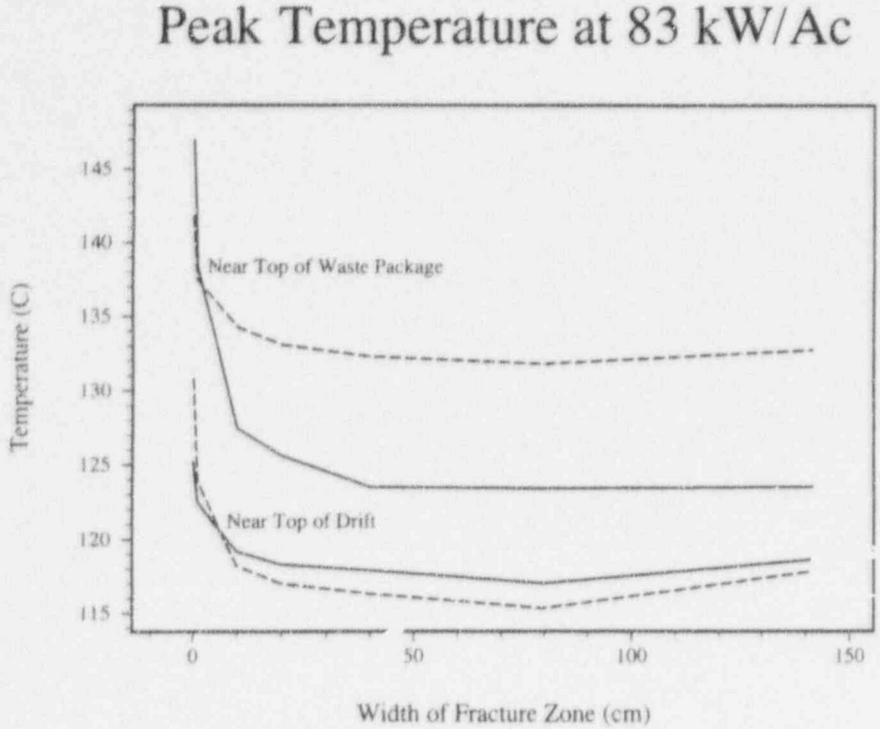

Figure 6-14. Maximum temperature before backfill (dashed line) and after backfill (solid line) at waste package and drift roof as a function of width of a vertically oriented fracture zone intersecting drift

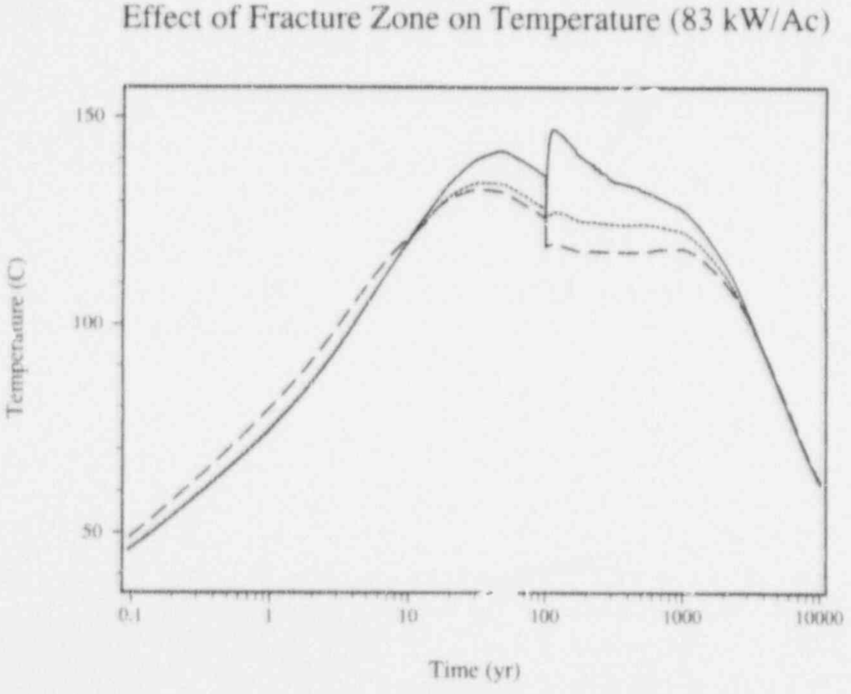

Figure 6-15. Maximum waste package temperature with no fracture (solid line), a 10-cm wide fracture zone (dotted line), and a 140-cm wide fracture zone (dashed line)

The hydraulic properties of two stratigraphic units, the PTn and CHnv, have proved to have a significant effect on flow of water below the repository horizon, in particular, flow through the CHnv. Similarly, ventilation through the drift and geologic features and structures with hydraulic properties different from the rock matrix could have a significant effect on temperature, saturation, and relative humidity within the drift and within the first few meters of rock near the drift. This information contributes directly to the subissue that addresses the bounds of thermally induced flux in the near field.

6.4 ASSESSMENT OF PROGRESS TOWARD MEETING OBJECTIVES

The results of activities conducted in the TEF KTI during FY96 contributed to the reduction of uncertainties associated with the subissues listed in section 6.1. Work was prioritized to identify tasks whose resolution is both achievable within available resources and able to provide significant reduction in uncertainty relative to committed resources. Tasks designed to reduce uncertainties in these subissues in FY96 are both reactive and proactive: (i) review and evaluate the DOE thermohydrology program, including the DOE peer review activity; (ii) benchmark testing of computer codes, (iii) provide sensitivity analyses; and (iv) evaluate conceptual models.

Review and evaluation of the DOE thermohydrology program included review of a DOE PRT, the DOE response to peer review recommendations, the peer review response to the DOE response to PRT recommendations, attendance at an Appendix 7 meeting on ESF thermal testing including site visit, and participation at a DOE/NRC ESF video conference. The review concluded that the DOE Thermohydrologic Testing and Modeling Program, as represented in the information available for this review, does not adequately address several technical issues. It was noted in this review and in PRT recommendations that the DOE has not demonstrated that it has plans to evaluate the alternative conceptual models as rigorously as needed. It is possible that heater tests designed for conditions different from those expected at the proposed repository may provide misleading results. For example, results from a heater test with an excessively high heat load (e.g., one that results in drift wall temperature > 200 °C) may support an ECM conceptual model since high drift wall temperatures (i.e. > 200 °C) could limit the occurrence of reflux dripping into the drift. However, potential difficulties could arise because the ECM might not accurately incorporate important moisture redistribution mechanisms, such as refluxing and dripping, that would be experienced under proposed repository conditions. Additionally, neither the PRT report nor the DOE response to PRT recommendations recognize the potential significance of thermal-hydrological-chemical coupled effects. It was noted that the discontinuance of surface based hydrologic testing may result in unacceptably high uncertainty in infiltration estimates at YM. It is important the DOE Thermohydrological Testing and Modeling Program be designed to address these issues. The comments and recommendations made on the DOE thermohydrology testing and modeling program will provide input to the basis for the resolution in FY97 of the subissue on the sufficiency of the DOE thermal testing program to assess the likelihood of gravity driven refluxing occurring in the near field.

Sensitivity and numerical scoping analyses helped identify the relative importance of specific types of information that contribute to the evaluation of thermally driven moisture through partially saturated fractured rock. It was observed that the emplacement, initial saturation, and thermal conductivity of backfill may be important during those times of the heating period when WP temperatures are high. Conceptual uncertainty regarding the effect of backfill materials has been reduced in the sense of delineating cause and effect relationships, however, the full effect of drift ventilation is not fully resolved. Analyses indicated that selective use of geologic materials that exhibit particularly low thermal conductivities can elevate WP temperatures and decrease drift wall temperatures. The hydraulic

characteristics of particular key geologic units, namely the nonwelded PTn and CHnv whose properties are inherently different from the welded tuffs most common at YM, can have a significant effect on flow through the nonwelded units below the proposed repository horizon (i.e. reasonable variations in hydraulic properties assigned to the PTn and CHnv can result in a factor of 10^4 change in the unsaturated hydraulic conductivity of the CHnv). In summary, these sensitivity analyses identified the relative importance of specific features of the proposed repository site and design. These will provide additional input to the basis for the resolution in FY97 of the subissue on the sufficiency of the DOE thermal testing program to assess the likelihood of gravity driven refluxing occurring in the near field.

Results from a repository-scale model that assumes a constant infiltration rate of 0.3 mm/yr and geologic structure but assumes that each of the hydrostratigraphic units is homogeneous and represented by a uniform matrix continuum indicated that the initial effect of repository heating can lead to increased water saturation within the proposed repository area. Such increased saturation may result in sustained perched water volumes that grow in size within the first 100 yr of proposed repository heating and begin to dissipate thereafter.

The DOE thermohydrologic codes TOUGH2 and FEHM were benchmark tested against the NRC/CNWRA codes CTOUGH and MULTIFLO. In general, the benchmark testing showed that three of the four codes tested (TOUGH2, CTOUGH, and MULTIFLO) appear to possess sufficient capability to simulate the wide range of hydrologic and thermohydrologic conditions expected to be important at the proposed HLW repository at YM. The primary differences noted were in computational efficiency and it was found that the MULTIFLO code was substantially faster than the other codes. The fourth code, FEHM, experienced computational difficulties in two test cases; one with high infiltration rates and the other with flow in fracture-porous media. This testing has provided confidence that the use of distinct thermohydrologic codes will not produce contentious methodology issues.

There remain two areas that still contribute to the uncertainty in resolving the subissues in the TEF KTI. There remain high levels of uncertainty regarding the effects of heterogeneities and geologic structure on thermally driven moisture movement, even though some insight has been gained in this area. A second major contributor to the high level of uncertainty in this KTI is the absence of evidence to support a particular conceptual model that is adequately representative of the heat and mass transfer mechanisms present in partially saturated fractured porous rock. These two areas are target areas of future studies and evaluations for resolution in FY98 of the subissue on the adequacy of the DOE thermal modeling approach for assessing the nature and bounds of thermally induced flux in the near field.

6.5 INTEGRATION WITH OTHER KEY TECHNICAL ISSUES

Information gained in the conduct of the TEF KTI is provided to other KTIs. Similarly information from other KTIs contribute to the information base from which the TEF KTI is resolved. Included here is a summary of the integration of the TEF KTI with other KTIs.

The Unsaturated and Saturated Flow Under Isothermal Conditions (USFIC) KTI provided initial saturation conditions and infiltration boundary conditions to the TEF KTI. Techniques for modeling fault hydraulic properties and flow in fractured medium that are being developed in the TEF KTI will be provided to the USFIC KTI for modeling of isothermal flow. The Structural Deformation and Seismicity KTI provided updated hydrostratigraphy and structural features information to the TEF KTI.

The TEF KTI provided to the Container Life and Source Term KTI updated values of waste package temperature, saturation distributions, and relative humidity for use in EBSPAC analysis. Similarly, the TEF KTI provided to the Evolution of the Near-Field Environment KTI updated values of temperature, saturation distribution, and relative humidity in the near field. Fracture aperture changes calculated by the Repository Design and Thermal-Mechanical Effects KTI were provided to the TEF KTI for use in these sensitivity analyses.

The TEF KTI provided thermohydrologic analyses to the Total System Performance Assessment and Technical Integration KTI for the audit review of TSPA-95 (TRW Environmental Safety Systems, Inc., 1995) and will provide additional information for the detailed review and input to the TSPA code. Specifically, the TEF KTI provided time-dependent waste package temperature and relative humidity at the waste package for proposed repository AMLs.

6.6 REFERENCES

Baca, R.G., and M.S. Seth. 1996. *Benchmark Testing of Thermohydrologic Computer Codes*. CNWRA 96-003. San Antonio, TX: Center for Nuclear Waste Regulatory Analyses.

Buscheck, T.A., and J.J. Nitao. 1995. *Thermal-Hydrological Analysis of Large-Scale Thermal Tests in the Exploratory Studies Facility at Yucca Mountain*. UCRL-ID-121791. Livermore, CA: Lawrence Livermore National Laboratory.

Buscheck, T.A., J.J. Nitao, and L.D. Ramspott. 1995. Localized dryout: An approach for managing the thermal-hydrological effects of decay heat at Yucca Mountain. *Proceedings of the XIX International Symposium on the Scientific Basis for Nuclear Waste Management*. Pittsburgh, PA: Materials Research Society.

Flint, L.E., and A.L. Flint. 1990. *Preliminary Permeability and Water-Retention Data for Nonwelded and Bedded Tuff Samples, Yucca Mountain Area, Nye County, Nevada*. U.S. Geological Survey Open-File Report 90-569. Denver, CO: U.S. Geological Survey.

Freeze, A.R., and J.A. Cherry, 1979. *Groundwater*. Englewood Cliffs, NJ: Prentice-Hall.

Frizzell, V.A., Jr., and J. Shulters. 1990. *Geologic Map of the Nevada Test Site, Southern Nevada*. U.S. Geological Survey Miscellaneous Investigations Series Map I-2046, Scale 1:100,000. Denver, CO: U.S. Geological Survey.

Green R.T. 1996. The effect of media properties on prediction of moisture redistribution at a high-level nuclear waste repository. *Proceedings of the Seventh Annual International Conference on High-Level Radioactive Waste Management*. La Grange, Park, IL: American Nuclear Society.

Green, R.T., G. Rice, and K.A. Meyer. 1995. *Hydraulic Characterization of Hydrothermally Altered Nopal Tuff*. NUREG/CR-6356. Washington, DC: Nuclear Regulatory Commission.

Klavetter, E.A., and R.R. Peters. 1986. *Estimation of Hydrologic Properties of an Unsaturated, Fractured Rock Mass*. SAND84-2642. Albuquerque, NM: Sandia National Laboratory.

Lappin, A.R. 1980. *Thermal Conductivity of Silicic Tuffs: Predictive Formalism and Comparison with Preliminary Experimental Results*. SAND80-0769. Albuquerque, NM: Sandia National Laboratories.

Lappin, A.R., and F.B. Nimick. 1985. *Bulk and Thermal properties of the Functional Tuffaceous Beds in Boreholes USW G-1, UE-25a#1, and USW G-2, Yucca Mountain, Nevada*. SAND82-1434. Albuquerque, NM: Sandia National Laboratories.

Lappin, A.R., R.G. van Buskirk, D.O. Enniss, S.W. Butters, F.M. Prater, C.S. Muller, and J.L. Bergosh. 1982. *Thermal Conductivity, Bulk Properties, and Thermal Stratigraphy of Silicic Tuffs from the Upper Portion of Hole USW-G1, Yucca Mountain, Nye County, Nevada*. SAND81-1873. Albuquerque, NM: Sandia National Laboratories.

Lichtner, P.C. 1994. *Multi-Phase Reactive Transport Theory*. CNWRA 94-018. San Antonio, TX: Center for Nuclear Waste Regulatory Analyses.

Lichtner, P.C., and M. Seth. 1996. Multiphase-multicomponent nonisothermal reactive transport in partially saturated porous media: Application to the Proposed Yucca Mountain HLW Repository. *Proceedings of the International Conference on Deep Geologic Disposal of Radioactive Waste. Canadian Nuclear Society, September 16–19*. Winnipeg, Manitoba, Canada: 3-133–3-142.

Manteufel, R.D. 1996. Groundwater removal near heat dissipating waste packages. *International Conference and Engineering Exhibition*. New York, NY: American Society of Mechanical Engineers.

Nimick, F.B. 1990a. *The Thermal Conductivity of the Topopah Spring Member at Yucca Mountain, Nevada*. SAND86-0090. Albuquerque, NM: Sandia National Laboratories.

Nimick, F.B. 1990b. *The Thermal Conductivity of Seven Thermal/Mechanical Units at Yucca Mountain, Nevada*. SAND88-1387. Albuquerque, NM: Sandia National Laboratories.

Nimick, F.B., and A.R. Lappin. 1985. *Thermal Conductivity of Silicic Tuffs from Yucca Mountain and Ranier Mesa, Nye County, Nevada*. SAND83-1711J. Albuquerque, NM: Sandia National Laboratories.

Nuclear Regulatory Commission. 1995. *Phase 2 Demonstration of the NRC's Capability to Conduct a Performance Assessment for a High-Level Waste Repository*. NUREG-1464. Washington, DC: Nuclear Regulatory Commission.

Pruess, K. 1991. *TOUGH2. A General Purpose Numerical Simulator for Multiphase Fluid and Heat Flow*. LBL-29400. Berkeley, CA: Lawrence Berkeley Laboratory.

Pruess, K., and Y. Tsang. 1993. Modeling of strongly heatdriven flow processes a potential high-level nuclear waste repository at Yucca Mountain, Nevada. *Fourth International High-Level Radioactive Waste Management Conference*. La Grange Park, IL: American Nuclear Society.

Pruess, K., and Y. Tsang. 1994. Thermal modeling for a potential high-level nuclear repository at Yucca Mountain, Nevada. LBL35381. Berkeley, CA: Lawrence Berkeley Laboratory.

Sass, J.H., and A.H. Lachenburch. 1982. *Preliminary Interpretation of Thermal Data from the Nevada Test Site*. U.S. Geological Survey Open-File Report 82-9730. Washington, DC: United States Geologic Survey.

Sass, J.H., A.H. Lachenburch, W.W. Dudley, Jr., S.S. Priest, and R.J. Monroe. 1988. *Temperature, Thermal Conductivity, and Heat Flow near Yucca Mountain, Nevada*. U.S. Geological Survey Open-File Report 87-649. Washington, DC: United States Geologic Survey.

Scott, R.B., and J. Bonk. 1984. *Preliminary Geologic Map (1:12,000 scale) of Yucca Mountain, Nye County, Nevada, with Geologic Cross Sections*. U.S. Geological Survey Open-File Report 84-494. Denver, CO: U.S. Geological Survey.

Seth, M.S. and P.C. Lichtner. 1996. *User's Manual for MULTIFLO: Part 1 Metra 1.0 Beta*. CNWRA 96-005. San Antonio, TX: Center for Nuclear Waste Regulatory Analyses.

Stirewalt, G.L., and D.B. Henderson. 1995. A preliminary three-dimensional geological framework model for Yucca Mountain. *Proceedings of the Sixth Annual International Conference on High-Level Radioactive Waste Management*. La Grange Park, IL: American Nuclear Society: 116–118.

Stirewalt, G., B. Henderson, and S. Young. 1994. *A Preliminary Three-Dimensional Geological Framework Model for Yucca Mountain, Nevada: Report to Accompany Model Transfer to the Nuclear Regulatory Commission*. CNWRA 94-023. San Antonio, TX: Center for Nuclear Regulatory Analyses.

TRW Environmental Safety Systems, Inc. 1993. *FY93 Thermal Loading Systems Study Final Report*. B00000000-01717-57-5-00013 Rev. 01. Las Vegas, NV: TRW Environmental Safety Systems, Inc.

TRW Environmental Safety Systems, Inc. 1994. *Initial Summary Report for Repository/Waste Package Advanced Conceptual Design*. B00000000-0-5705-00015 Rev. 00. Las Vegas, NV: TRW Environmental Safety Systems, Inc.

TRW Environmental Safety Systems, Inc. 1995. *Total System Performance Assessment—1995: An Evaluation of the Potential Yucca Mountain Repository*. B00000000-01717-2200-00136. Las Vegas, NV: TRW Environmental Safety Systems Inc.

Updegraff, C.D., C.E. Lee, and D.P. Gallegos. 1991. DCM-3D: *A Dual-Continuum, Three-Dimensional, Groundwater Flow Code for Unsaturated, Fractured, Porous Media*. NUREG/CR-5536. Washington, DC: Nuclear Regulatory Commission.

U.S. Department of Energy. 1993. *Yucca Mountain Site Characterization Project Reference Information Base*. YMP/93-02. Las Vegas, NV: U.S. Department of Energy.

U.S. Geological Survey. 1981. *Subsurface-Water Flow and Solute Transport—Federal Glossary of Selected Terms.* Subsurface-Water Glossary Working Group, Ground-Water Subcommittee, Interagency Advisory Committee on Water Data. Washington, DC: U.S. Geological Survey.

van Genuchten, M.Th. 1980. A closed-form equation for predicting the hydraulic conductivity of unsaturated soils. *Soil Science Society of America Journal* 44: 892–898.

Wang, J.S.Y., and T.N. Narasimhan. 1986. *Hydrologic Mechanisms Governing Partially Saturated Fluid Flow in Fractured Welded Units and Porous Nonwelded Units at Yucca Mountain.* LBL-21022. Berkeley, CA: Lawrence Berkeley Laboratory.

Walton, J.C. 1993. Effects of evaporation and solute concentration on presence and composition of water in and around the waste package at Yucca Mountain. *Waste Management*: 13: 293–301.

Wilson, M.L., J.H. Gauthier, R.W. Barnard, G.E. Barr, H.A. Dockery, E. Dunn, R.R. Eaton, D.C. Guerin, N. Lu, M.J. Martinez, R. Nilson, C.A. Rautman, T.H. Robey, B. Ross, E.E. Ryder, A.R. Schenker, S.A. Shannon, L.H. Skinner, W.G. Halsey, J.D. Gansemer, L.C. Lewis, A.D. Lamont, I.R. Triay, A. Meijer, and D.E. Morris. 1994. *Total-System Performance Assessment for Yucca Mountain—SNL Second Iteration (TSPA—1993)* Volume 2. SAND93-2675. Albuquerque, NM: Sandia National Laboratories.

7 REPOSITORY DESIGN AND THERMAL-MECHANICAL EFFECTS

Primary Authors: ***S.M. Hsiung, R. Chen, A.H. Chowdhury, A. Ghosh, M.S. Nataraja, and B.N. Jagannath***

Technical Contributors: ***M.P. Ahola, H. Karimi, G.I. Ofoegbu, R. Chen, A.H. Chowdhury, A. Ghosh, S.M. Hsiung, B.N. Jagannath, and M.S. Nataraja***

Key Technical Issue Co-Leads: ***A.H. Chowdhury (CNWRA) and B.N. Jagannath (NRC)***

7.1 INTRODUCTION

Evaluation of time-dependent thermal-mechanical (TM) coupled response of jointed rock mass is the primary focus of the Repository Design and Thermal-Mechanical Effects (RDTME) Key Technical Issue (KTI). Postclosure performance assessment (PA) requires an understanding of the TM response of the jointed rock mass over the compliance period (thousands of years) as it influences near-field environment and waste package (WP) degradation, performance of seals, and flow; and radionuclide transport mechanisms. Design for the preclosure operation period (≈100 y) requires an understanding of the TM response of the jointed rock mass as it influences drift stability and waste retrievability. Study of TM effects in the near-field environment of the proposed high-level waste (HLW) repository has two components: (i) stability of underground excavations for both opening design and input for PA and (ii) change of hydrological properties of rock fractures due to TM perturbation of the rock mass for input to design and PA.

The U.S. Department of Energy (DOE) has formulated several hypotheses that, if confirmed, would demonstrate that waste can be isolated at the proposed Yucca Mountain (YM) site for long periods of time. These hypotheses include: (i) flow of water into the repository will be low and (ii) the engineered barriers, possibly including backfill, will limit migration of radionuclides into the host rock and any sources of groundwater. Testing these hypotheses will necessitate an understanding of time-dependent TM coupled effects of jointed rock mass on design of the proposed repository and WPs, and repository seals program. Study of stability of underground excavations is needed to test the DOE hypothesis that the engineered barriers will limit migration of radionuclides into the host rock and any sources of groundwater. Investigation on changes of hydrological properties of rock fractures due to TM perturbation is needed to test the other DOE hypothesis that the flow of water into the repository will be low. The main issue of the RDTME KTI has been divided into resolvable subissues. Resolution of the subissues will lead to resolution of the main issue.

There are three subissues associated with this KTI: (i) design of the proposed repository to meet preclosure and postclosure performance objectives, (ii) evaluation of thermal effects on design of the underground facility, and (iii) the role of repository seals in meeting performance objectives. The FY96 activities reported herein address two RDTME KTI subissues. Comments on seismic topical report no. 2 (TR2); development of a rock joint model; and reviews of Exploratory Studies Facility (ESF) design and the DOE regulatory compliance review report address several components of the KTI subissue on design of the proposed repository to meet preclosure and postclosure performance objectives. A parametric study of drift stability in a jointed rock mass and a review of the DOE *in situ* heater test address some components of the subissue on evaluation of the thermal effect on design of the underground facility. These activities and results will be discussed to assess the extent to which these subissues have been resolved through FY96.

7.2 OBJECTIVES AND SCOPE OF WORK

During FY96, the primary objective of the RDTME KTI was to address some components of subissues (i) and (ii) discussed in the previous section. The main activities in accomplishing the objective include review of the DOE repository design program with emphasis on technical reviews of the DOE seismic design methodology topical report, ESF design reports, and design control process reports. Other activities included identification of thermal load and site specific rock mechanical and thermal parameters that may significantly affect the emplacement drift stability and waste retrievability through a TM parametric study and review of DOE ESF heater tests. An additional activity was to selectively develop prediction tools for the TM analysis of jointed rock mass under cyclic pseudostatic and seismic loads.

The scope of work for review of the DOE design of the proposed repository included review of the DOE seismic TR2 including participation in two DOE/Nuclear Regulatory Commission (NRC) Appendix 7 meetings, review of ESF design and supporting documents, and review of the DOE regulatory compliance review report. The review of ESF heater tests included an DOE/NRC Appendix 7 meeting and a site visit.

Work performed in regard to independent evaluation of thermal effects on stability of the underground excavations included a parametric study of unbackfilled drifts involving nine thermal, mechanical, and site characteristic parameters, each at two levels, using the Universal Distinct Element Code (UDEC). A 1/8 fractional factorial experimental design approach was used in this parametric study.

The review tools preparation activity included enhancement of the basic rock joint model developed in FY95 and development of methodologies for determination of the parameters associated with the enhanced model.

Significant accomplishments associated with these activities are reported in section 7.3. An assessment of the extent to which the above-mentioned subissues have been resolved through FY96 activities is provided in section 7.4.

7.3 SIGNIFICANT TECHNICAL ACCOMPLISHMENTS

7.3.1 Repository Seismic Design

Due to the long-term performance requirements for the proposed repository, the potential influence of repeated seismic events will need to be addressed by the DOE. Currently available seismic design methodologies may not provide an adequate demonstration that a particular design has appropriately considered seismic effects in the context of repository performance. Consequently, the DOE is attempting to develop a coherent seismic design methodology that is suitable for use in the repository design.

The DOE topical report "Seismic Design Methodology for a Geologic Repository at Yucca Mountain" reviewed by the NRC is the second in a series of three seismic topical reports. Altogether, the reports describe the seismic design process that the DOE plans to implement for the YM Geologic Repository Operations Area (GROA). Seismic topical report no. 1 (TR1) describing the DOE methodology to assess vibratory ground motion and fault displacement hazards has already been reviewed and accepted by the NRC (Nuclear Regulatory Commission, 1996). Seismic TR2 presents the DOE seismic design methodology and criteria for the YM GROA to meet the NRC preclosure safety requirements. The seismic

topical report no. 3 (TR3), scheduled for preparation after completion of TR2, will describe the DOE assessment of seismic hazards for the YM GROA and determination of ground motion and fault displacement values appropriate for design of GROA structures, systems, and components and inputs for postclosure PA objectives. After review and acceptance of TR2 and TR3, it is anticipated the NRC will develop and issue a prelicensing evaluation report to address the seismic design process the DOE plans to implement for YM GROA (Nuclear Regulatory Commission, 1996).

A review of TR2 and associated DOE/NRC technical interactions generated eight comments: (i) inadequacy of linkages between the proposed preclosure seismic design methodology and the postclosure performance considerations, (ii) lack of relationship between the DOE proposed four seismic performance categories and the NRC category 1 and category 2 design basis events in the proposed rule change to 10 CFR Part 60, (iii) lack of rationale for choosing mean probabilistic seismic hazards to determine ground motion and fault offset design basis events, (iv) inappropriateness of treatment of repeated seismic loadings as low-probability/low-consequence events, (v) lack of verified or generally accepted methods for the design of underground openings under the loads and time frame of interest for repository performance, (vi) nonconservative safety factors for combining seismic load with *in situ* stress and thermal loads, (vii) lack of details regarding fault-specific investigations needed to define values of set-back distance for fault-avoidance, and (viii) lack of details regarding investigations that the DOE intends to conduct to define the set-back distance for type 1 faults.

Specific recommendations to each of the eight comments were made and transmitted to the DOE. The DOE is currently revising its TR2 addressing these comments. Review of the revised TR2 by the NRC in early FY97 is expected to resolve the concerns related to seismic design methodology.

7.3.2 Design Control Process

7.3.2.1 Background

As a result of past DOE/NRC interactions in the area of ESF/GROA design and associated quality assurance issues, the NRC identified deficiencies in the DOE design control process. It has long been recognized by the NRC that it is impossible for the NRC and Center for Nuclear Waste Regulatory Analyses (CNWRA) staffs to conduct a thorough review of all the DOE design documents given the limited resources at NRC disposal. Consequently, the NRC has used a vertical slice approach in which the NRC and CNWRA staffs would selectively review some important aspects of the DOE ESF/GROA design packages and observe the DOE internal reviews looking for trends that can be used as examples to provide feedback and guidance to the DOE. The NRC has paid particular attention to design of the ESF because it will eventually become a part of the GROA if the YM site is found to be suitable and, therefore, many regulatory requirements applicable to the GROA would also be applicable to the ESF. The DOE found it difficult to demonstrate to the NRC the traceability of regulatory requirements and provide necessary documentary evidence to clearly show that all applicable requirements were indeed being applied to various design components. To thoroughly examine this issue, the NRC conducted a phased in-field verification to evaluate the DOE design control process (Nuclear Regulatory Commission, 1996). There are a number of open items (OI) that resulted from this in-field verification, past DOE/NRC interactions, and the NRC review of the DOE ESF/GROA design documents related to this issue. All of these OI are being monitored by the RDTME KTI and a number of them have been closed during FY96 as a result of staff reviews and interactions with the DOE. Some of the main FY96 activities conducted to help resolve the remaining OI and subissues are reported in this section.

7.3.2.2 Regulatory Compliance

To address the NRC concerns on the design control process, the DOE submitted a regulatory compliance review report (U.S. Department of Energy, 1995a; 1995b) to the NRC. The report attempts to provide the NRC staff a description of steps taken by the DOE and criteria used by the Civilian Radioactive Waste Management System Management and Operating Contractor to identify, evaluate, and minimize potential impacts to the proposed site as a result of the ongoing site characterization program. Also included in the report is the description of how 10 CFR Part 60 requirements applicable to the ESF Design Package 2C have been incorporated into the current design. The regulatory compliance review report presents an evaluation of 42 selected requirements for their allocation and traceability into the design solutions of the 11 configuration items included in ESF Design Package 2C. On October 22, 1995, the DOE submitted a letter to the NRC further elaborating the steps taken to improve this design control process (U.S. Department of Energy, 1995c).

The regulatory compliance review report was evaluated as a part of the NRC staff Phase 3 In-Field Verification activities using NUREG-1439 (Gupta et al., 1991) as the basis for compliance determination. The review indicated that, in general, the DOE identified 10 CFR Part 60 design requirements applicable to the ESF Design Package 2C. The assessment of 10 CFR Part 60 design requirements included in the report is acceptable.

As a result of this review, the open items in the checklist of the Phase 3 In-Field Verification related to verifying that appropriate regulatory requirements are being applied to ESF Design Package 2C were closed. To complete the Phase 3 In-Field Verification, assertions made by the DOE in its October 25, 1995, letter (U.S. Department of Energy, 1995c) regarding improvement of the design control process will be verified and implementation of the improved design control process in the ESF design packages will be evaluated in FY97.

7.3.2.3 Exploratory Studies Facility Design

The DOE Title II design package of ESF Main Drift (Design Package 8A) consists of a series of design analysis documents. These design analysis documents are released by the DOE in installments. The design analysis reports reviewed by the NRC include ESF Alcove Ground Support Analysis (BABEE0000-01717-0200-00001 REV 01C) and ESF Ground Support—Structural Steel Analysis (BABEE0000-01717-1200-00003 REV 00B). In addition to these two design analysis reports, three supporting reports were also reviewed by the NRC: Fracture Analysis and Rock Quality Designation Estimation for the Yucca Mountain Site Characterization Project (Lin et al., 1993), Geotechnical Characterization of the North Ramp of the Exploratory Studies Facility, Volume I of II: Data Summary (Brechtel et al., 1995), and Drift Design Methodology and Preliminary Application for the Yucca Mountain Site Characterization Project (Hardy and Bauer, 1991).

ESF Alcove Ground Support Analysis is a part of the DOE Title II design package of the ESF Main Drift (Design Package 8A). This report deals with analysis of the stability of the Bow Ridge test alcove (Alcove 2) and two radial borehole tests alcoves (Alcoves 3 and 4) using empirical and analytical methods. Both FLAC3D and 3DEC codes were used in the analysis; no support system was considered in the models analyzed. It was concluded that the effect of 80 and 100 kw/acre of thermal loads would not be significant due to the location of the alcoves relative to the repository horizon. Analysis carried out with *in situ* and seismic loads did not include discrete joints in the rock mass. The modeling results given in this report indicated a significant amount of damage (both tensile and shear failures) in the roof, floor,

and sidewalls of the excavations, and in the pillar between the alcoves and the North Ramp. The report on ESF Ground Support—Structural Steel Analysis deals with the analysis, design, and selection of structural steel ground support members and components. The computer program STAAD-III was used for the analysis and American Institute of Steel Construction Specifications (American Institute of Steel Construction, 1989) were used for the design of steel members and components.

Review of the three supporting reports did not raise any major concerns, however, the two design analysis documents resulted in two observations. These observations are helpful to the DOE in its future repository design exercises. The first observation is that the numerical analysis to determine the stability of ESF drifts and Alcoves 2, 3, and 4 is based on continuum modeling and does not consider the effect of existing joint sets in the rock mass. The extensive rock mass damage predicted by this analysis under *in situ* and seismic load is expected to increase significantly if discontinuum analysis is performed. The second observation indicates that the duration of input shear wave used in the dynamic analysis of the stability of ESF drifts and alcoves is unrealistically low.

7.3.3 *In Situ* Heater Test

The First ESF Thermal Test is planned by the DOE to study the effects of thermal load on hydrology, chemistry, and rock mass-ground support interaction, with an ultimate goal of providing information needed for viability assessment of the proposed YM site for permanent disposal of HLW. This test consists of two phases. The first phase—a single heater test—was started on August 26, 1996 and the second phase—a drift-scale heater test—will be initiated next year. The First ESF Thermal Test will be conducted in Alcove 5 (Thermal Testing Facility) located in the Topopah Spring welded unit (TSw2), lithophysae-poor, south of the North Ramp and east of the ESF Main Drift at Station 28+27 m from the portal. An Appendix 7 meeting was held at the site on July 24, 1996, to discuss the First ESF Thermal Test. As a result of the meeting, concerns related to TM coupling were generated and are summarized in the following paragraphs.

One of the objectives of the single heater test is to develop information on rock mass thermal and mechanical properties at elevated temperatures. The rock mass at the instrumentation location for the single heater test appears to be competent with a relatively smaller number of fractures/joints compared to the rock mass conditions at several other locations within the ESF. Therefore, the rock mass thermal and mechanical properties obtained at this location at elevated temperatures may not be transferrable to other repository locations with extensive fractures/joints. Some effort will need to be made to either obtain rock mass thermal and mechanical properties at elevated temperatures at locations with extensive fractures/joints or develop a reasonable approach for data extrapolation. Otherwise, the usefulness of the rock mass thermal and mechanical properties obtained from this single heater test will be somewhat limited. It is not clear how this issue will be addressed by the DOE. There are additional concerns expressed by other KTIs on the single heater test (see sections 4 and 6).

The planned drift-scale heater test includes activities for investigating interactions between the rock mass and ground support systems. Various ground support systems including those used in the North Ramp and ESF Main Drift are planned to be evaluated in a drift about 66 m long. The main focus of the planned test is to identify potential interaction processes that may affect ground support design. It is likely the planned instrumentation drift will be in a competent rock mass, given its proximity to the single heater test. Thus, interaction processes in the relatively less competent rock mass may not be identified. These processes may affect the stability of emplacement drifts during waste emplacement operations and potential

waste retrieval, and therefore deserve attention during site characterization testing. During interaction with the NRC, the DOE expressed confidence that the 66 m long drift will cover the range of rock conditions expected to be encountered in the TSw2 thermo-mechanical unit. This will be verified during FY97.

7.3.4 Parametric Study of Drift Stability—Phase I: Discrete Element Thermal-Mechanical Analysis of Unbackfilled Drifts

Construction of a geological repository in a jointed rock mass at YM will change the state of stress and cause deformation of surrounding rock and joints. Emplacement of radioactive waste in the proposed repository provides a heat source that will be active over an extended period of time and thus complicate the understanding and prediction of rock mass responses. There are two issues that involve TM effects in the near-field environment: stability of underground openings for both design and input for PA and change of hydrological properties of rock fractures due to TM perturbation of the rock mass for input to design and PA. The objectives of the TM parametric study are to understand rock mass response to drift excavation and waste emplacement as a function of time and to identify mechanical, thermal, and site characteristic parameters that would affect the preclosure and postclosure performance of the proposed repository under heated and seismic conditions. The focus of the phase I TM study is to conduct a parametric investigation of emplacement drifts with no backfill, rock support, or seismic load for 100 yr of heating.

7.3.4.1 Study Method and Model Setup

The study comprised a series of numerical modeling exercises using UDEC (Itasca Consulting Group, Inc., 1993). A total of 74 UDEC calculations were performed, including 10 scoping runs and 64 final runs. The scoping runs were aimed at identifying the effect of joint patterns. The final runs were selected based on a 2^k fractional factorial experiment design methodology to systematically probe the effects of joint patterns and thermal and mechanical parameters [see Ahola et al. (1996) for details of 2^k fractional factorial design and parameter combinations for all UDEC run cases]. The scoping calculations considered five distinct joint patterns, each containing at least two joint sets (subhorizontal and subvertical, except for several cases that contained an additional subvertical or ubiquitous joint set), while thermal and mechanical properties of rock matrix and joints remained fixed at their representative mean values.

Scoping calculations showed that joint patterns did not appear to have a large impact on rock mass response at a distance of more than five diameters away from the drift. Based on the results of scoping analyses, it was decided that for the final UDEC runs only two joint sets would be simulated: one subvertical with varying spacing and orientation and one subhorizontal with fixed spacing and varying orientation. Also, based mostly on engineering judgment and past modeling experience, it was decided the additional parameters considered in the final set of UDEC runs would include joint friction angle, intact rock cohesion, intact rock friction angle, intact rock Young's modulus, and thermal expansion coefficient. The upper and lower values of these parameters are given in table 7-1. Thermal loads considered in both the scoping and final UDEC calculations were selected to encompass the DOE hot and cold repository concepts which included a high (100 MTU/acre) and a low (20 MTU/acre) thermal loading strategy. The heat generation of the spent fuel within the WP was modeled as a simple exponentially decaying thermal flux applied directly to the wall of the circular emplacement drift. The decay constant used was 3.2197×10^{-10}/s and the waste was assumed to be 20 yr old at the time of emplacement. Therefore, a total of nine parameters were considered in the final runs including thermal load, three joint geometric parameters, and five rock and joint thermal and mechanical properties.

Table 7-1. Upper and lower values for UDEC final analyses

Parameter	Value		Unit
	Upper	Lower	
Subvertical Joint Inclination	85	70	degree
Subhorizontal Joint Inclination	20	10	degree
Subvertical Joint Spacing	0.5	0.2	m
Joint Friction Angle	38	28	degree
Thermal Load	100	20	MTU/acre
Intact Rock Friction Angle	43	18	MPa
Intact Rock Cohesion	50	20	degree
Intact Rock Young's Modulus	32	16	MPa
Thermal Expansion Coefficient	12×10^{-6}	6×10^{-6}	K^{-1}

The final calculations were evaluated in terms of the effect of each parameter on certain performance measures chosen based on the scoping calculations. These performance measures included maximum and minimum principal stresses around the excavation, maximum joint shear displacement, maximum joint closure and separation, roof-to-floor convergence, and extent of yield zone around the excavation.

The UDEC model included a single drift 5 m in diameter and one unit cell width governed by drift to drift spacing, depending on the areal thermal loading selected. The vertical extent of the UDEC models was determined so that the ambient temperatures applied along the upper and lower boundaries did not artificially impact the results for the total selected simulation time of 100 yr. The vertical boundaries represented lines of symmetry based on the assumption of multiple parallel emplacement drifts, and therefore, were assigned with zero horizontal velocity and zero heat flux boundary conditions. To maintain a reasonable number of blocks and finite difference zones, only a region approximately one drift diameter into the rock mass was modeled as having the specified joint spacings assigned for each case. Beyond this region, the size of the blocks was scaled up accordingly as depicted in figure 7-1.

The modeling procedures consisted of obtaining model equilibrium under the *in situ* stress. The drift was then excavated and a new equilibrium stage was reached. From this stage on, thermal load was applied and coupled TM simulations conducted for 100 yr.

7.3.4.2 Discussion of Modeling Results

The scoping analyses considering five joint patterns and two thermal loadings show that, in general, joint pattern does not appear to affect the response of the rock mass at a distance of more than five diameters away from the drift. However, joint pattern affects the magnitude and distribution of stresses in the immediate vicinity of the drift (up to about five diameters into the wall) and, therefore, controls the stability of drifts.

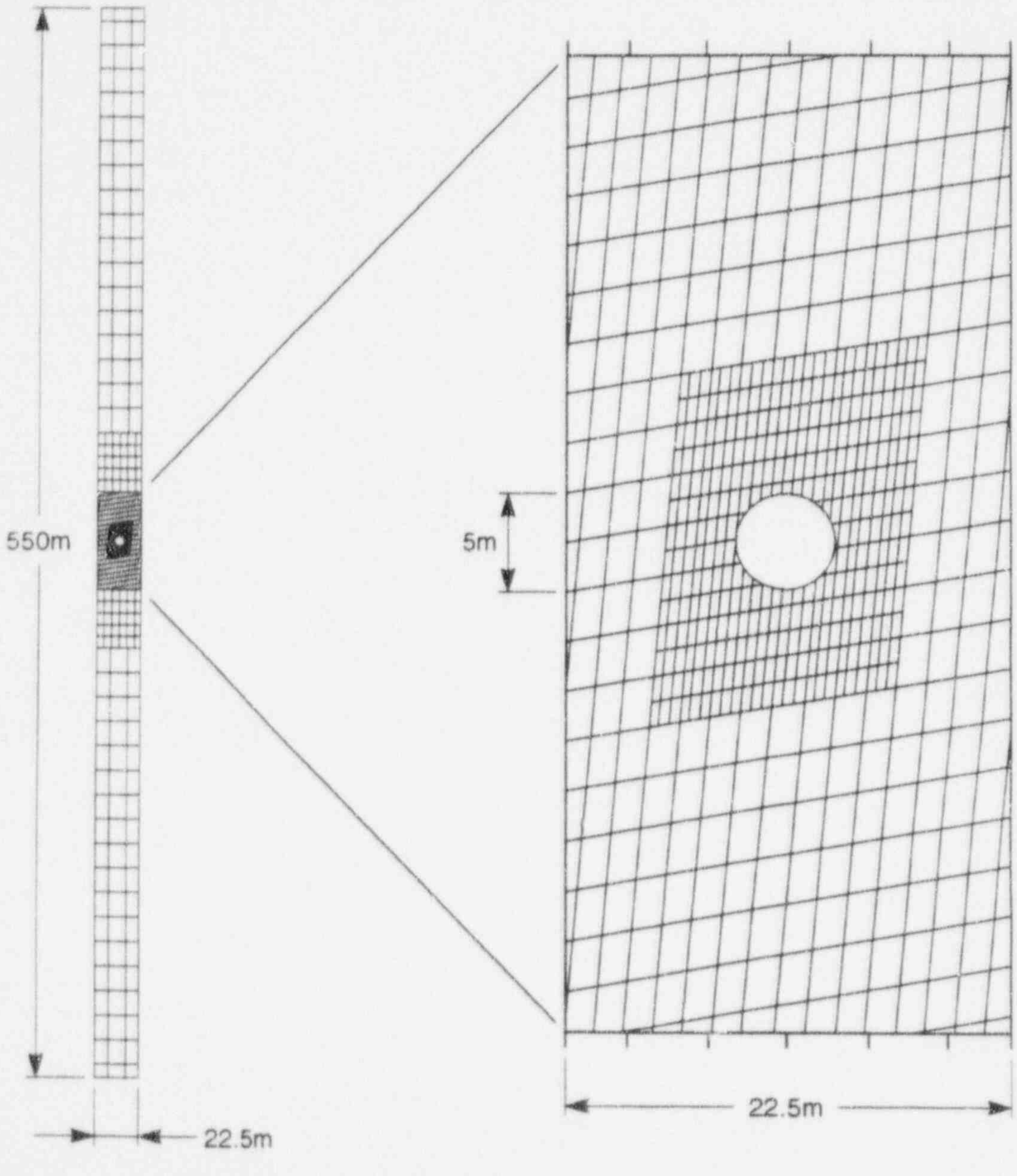

Figure 7-1. UDEC model showing block geometry for one particular joint set pattern and thermal loading

Results of UDEC final runs indicate that thermal loading is an important parameter affecting most performance measures: magnitudes of maximum principal stress, maximum joint shear displacement, maximum joint closure and separation, and extent of yield zone increase as thermal load increases. An increase in thermal load reduces opening convergence. The effects of important parameters on affected performance measures are given in table 7-2.

Table 7-2. Effects of parameters studied on selected performance measures

Parameter Increased	Performance Affected					
	Maximum Principal Stress	Maximum Joint Shear Displacement	Maximum Joint Closure	Maximum Joint Separation	Maximum Roof-to-Floor Convergence	Extent of Yield Zone
Subvertical Joint Inclination	I	N (50 yr) I (100 yr)	N	D	D (50 yr) N (100 yr)	N
Subhorizontal Joint Inclination	N	N	N	I	N	N
Subvertical Joint Spacing	I	N (50 yr) D (100 yr)	N	N	N (50 yr) D (100 yr)	D
Joint Friction Angle	N	N	N	D	D	D
Thermal Load	I	I	I	I	D	I
Intact Rock Friction Angle	N	N	N	N	N	D
Intact Rock Young's Modulus	I	N (50 yr) I (100 yr)	N (50 yr) I (100 yr)	I	D (50 yr) N (100 yr)	I
Intact rock Cohesion	N	N	N	N	N	N (50 yr) D (100 yr)
Thermal Expansion Coefficient	I	N	I	I	D (50 yr) N (100 yr)	I

Note: I = increase; D = decrease; N = no effect

General results show that shear displacement usually occurs along joints near the drift following excavation and increases after heating, particularly along the horizontal-subhorizontal joint set. Although in most cases the extensiveness and magnitude of joint shear displacement are limited, there are cases in which thermally enhanced joint shear displacement becomes so extensive that it could greatly increase shear-induced permeability (Barton et al., 1985) and, therefore, increase the possibility of groundwater flowing into the drift. Figure 7-2 depicts the distribution of joint shear displacements after heating for Case 12 [case numbers and associated input parameters are described in Ahola et al. (1996)].

Yielding occurs in some of the cases after heating, mostly by tensile failure. Although yield zones in most cases are localized to the immediate areas around the drift, they cover the entire pillar in the worst cases. Figure 7-3 shows yielding zones after 100 yr heating for Case 26. Most studies show that yielding of intact rock causes the rock mass to dilate which, in turn, could increase rock permeability (Wawersik and Brace, 1971; Wawersik and Fairhurst, 1970; Bieniawski, 1969; Ofoegbu and Curran, 1992). It is important in emplacement drift design to make sure the extent of yielding is limited to avoid direct hydraulic connections between drifts and overlying strata that could facilitate groundwater inflow from potential perched water zones.

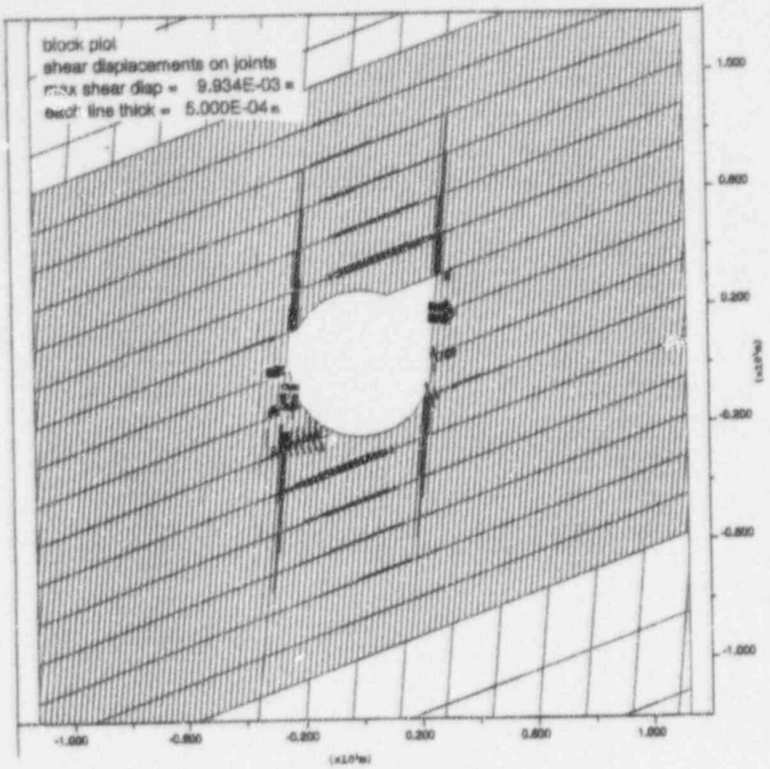

Figure 7-2. Distribution and magnitude of joint shear displacements after 100 yr of heating for Case 12

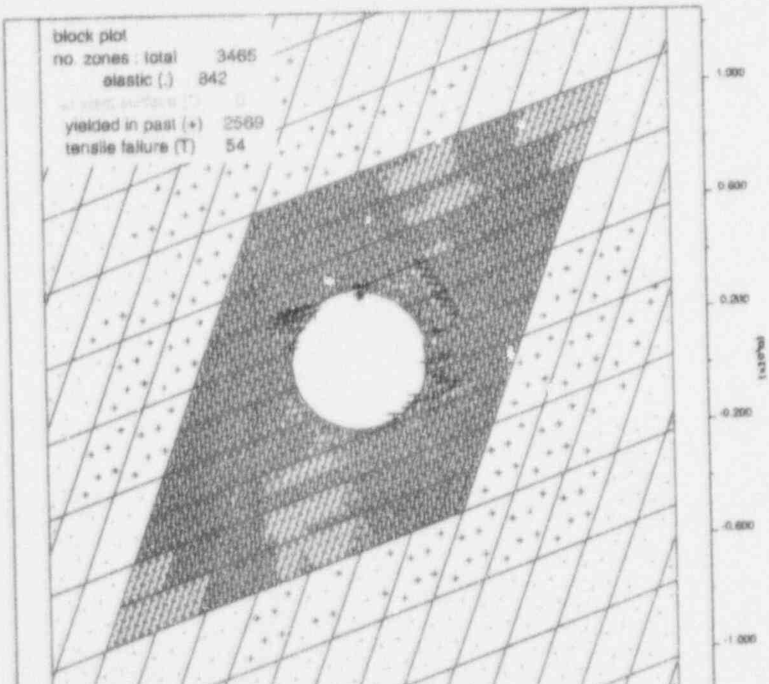

Figure 7-3. Failure distribution after 100 yr of heating for Case 26

In most cases, subvertical joints near the sidewalls of the drift tend to dilate due to stress relaxation immediately after drift excavation. This dilation tends to increase during heating. However, the extent of the zone where joints dilate does not appear to increase significantly during heating. Heating increases closure along subvertical joints above and below the drift. In general, the extent of these zones of joint dilation is less than one drift diameter. Figure 7-4 shows the distribution of joint opening and closure for a typical case.

The maximum compressive stress usually occurs in drift sidewalls following excavation. Its magnitude increases and its location shifts to the immediate roof and floor areas as heating progresses. Although tensile stresses are predicted following drift excavation as well as after heating, heating appears to change the location of the maximum tensile stress from roof and floor areas to the sidewalls of the drift. Circumferential stress generally increases in the roof with heating, while it decreases in the ribs of the drift due to thermal expansion. This phenomenon occurs because thermal expansion creates a stress state that tends to counteract with the mining-induced stresses in the rib of the drift while enhance the mining-induced stresses on the roof and floor areas.

Increasing the coefficient of thermal expansion increases the magnitude of maximum principal stress, maximum joint separation, maximum joint closure, and extent of yield zone, and reduces the short-term convergence. Increasing the intact rock Young's modulus results in higher maximum principal stress, greater maximum joint separation, more extensive yield zone, and increased maximum joint shear displacement and closure after 100 yr of heating while it reduces short-term drift convergence. Higher subvertical joint inclination seems to be associated with higher maximum principal stress when either subhorizontal joint inclination or the coefficient of thermal expansion is at its higher value. Increasing the subhorizontal joint inclination increases maximum joint separation, whereas increasing the subvertical joint spacing reduces joint shear displacement, drift convergence, and extent of yield zone, and increases maximum principal stress. These effects are observed only after 100 yr heating. Joint friction angle has a significant effect on maximum joint separation, convergence, and extent of yield zone. Intact rock friction angle affects only the extent of the yield zone (i.e., a larger intact rock friction angle results in less extensive yielding). Variation of intact rock cohesion does not appear to have an effect on any performance measures other than the extent of the yield zone after 100 yr of heating; that is, an increase in intact rock cohesion reduces the extent of the yield zone.

7.3.4.3 Summary

The most interesting aspects of the results are the increase in joint shear displacement and in the extent of yielding zones around the drift due to heating. As discussed earlier, heating causes significant increases in joint shear displacements over a large area and induced yielding of almost the entire pillar in some extreme cases. Both joint shear displacement and yielding of intact rock could induce dilation that would increase permeability of the rock mass and therefore, affect groundwater flow and radionuclide transport. Phase I TM parametric study shows that thermal load is an important parameter affecting most of the performance measures studied herein. Other parameters also influence drift stability by affecting certain performance measures to various degrees of significance.

7.3.5 Development of Rock Joint Model

Seismic events at YM will take place in an environment of *in situ*, excavation-induced, and thermal stresses. Seismic load will affect both drift stability and hydrological properties of the rock mass in the near-field environment of the proposed HLW repository at YM. Thus, it is necessary to study the effect of seismic load, including the effect of repeated seismic load (Nuclear Waste Technical Review

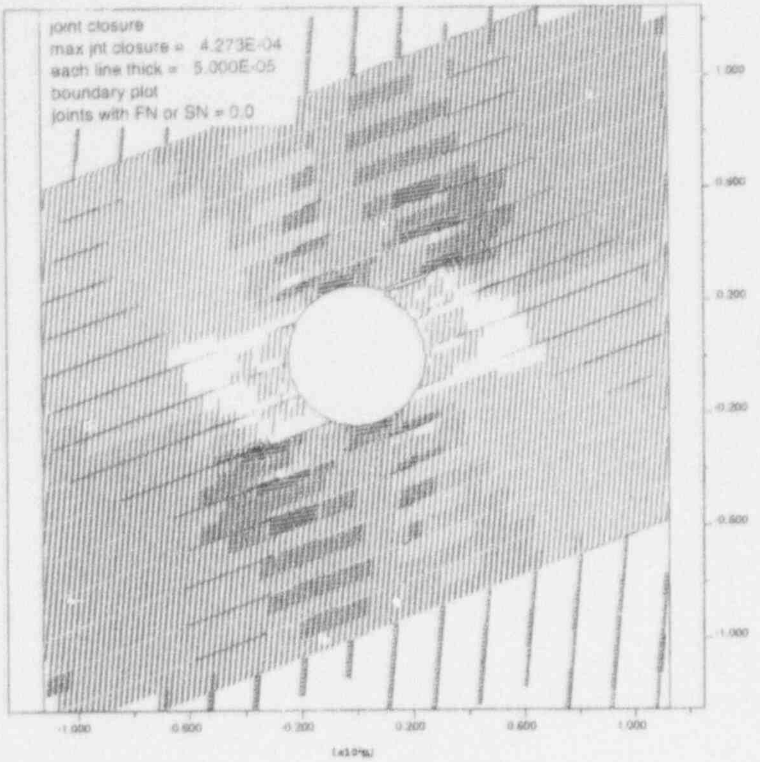

Figure 7-4. Distribution of joint opening and closure after 100 yr of heating for typical UDEC run case

Board, 1992) on proposed repository performance. Experimental results of direct shear tests on joints subjected to cyclic pseudostatic and dynamic loads (Celestino and Goodman, 1979; Gillette et al., 1983; Zubelewicz et al., 1987; Fishman, 1988; Jing et al., 1992; Huang et al., 1993; Wibowo et al., 1993; Hsiung et al., 1994a) have shown that rock joint responses, in terms of both shear strength and dilation, appear to be different in forward and reverse directions of shearing. In reverse shearing, the shear strength is smaller than that in the forward direction. Moreover, dilation realized in forward shearing is almost completely recovered in the reverse direction. Hsiung et al. (1994b) showed that three commonly used rock joint models were unable to simulate joint behavior in reverse shear. Using these models could result in an overestimation of excavation stability, as well as prediction of an unreasonable pattern of fast water flow paths. The objective of developing a new rock joint model, using results of the rock mechanics research project (Hsiung et al., 1994a), is to provide an improved prediction tool to assess seismic effects on the pre- and post-closure performance of the proposed repository and to assist in testing the two DOE hypotheses relevant to the RDTME KTI.

From observation of fractal characteristics of natural rock joint surfaces (Hsiung et al., 1994b), a conceptual model was proposed to represent the joint surfaces in direct shear tests [figure 7-5(a)]. The joint surfaces in this model contain three components: primary, secondary, and tertiary and higher-order asperities. The first component is the basic V-shape of the surface (primary asperity) with an inclination angle ϕ_1 that acts as an additional friction angle [figure 7-5(b)]. Friction realized by secondary asperities has an equivalent friction angle ϕ_2, whereas the friction realized by tertiary and higher-order asperities has an equivalent friction angle of ϕ_3 [figure 7-5(c)]. Both secondary and tertiary and higher-order

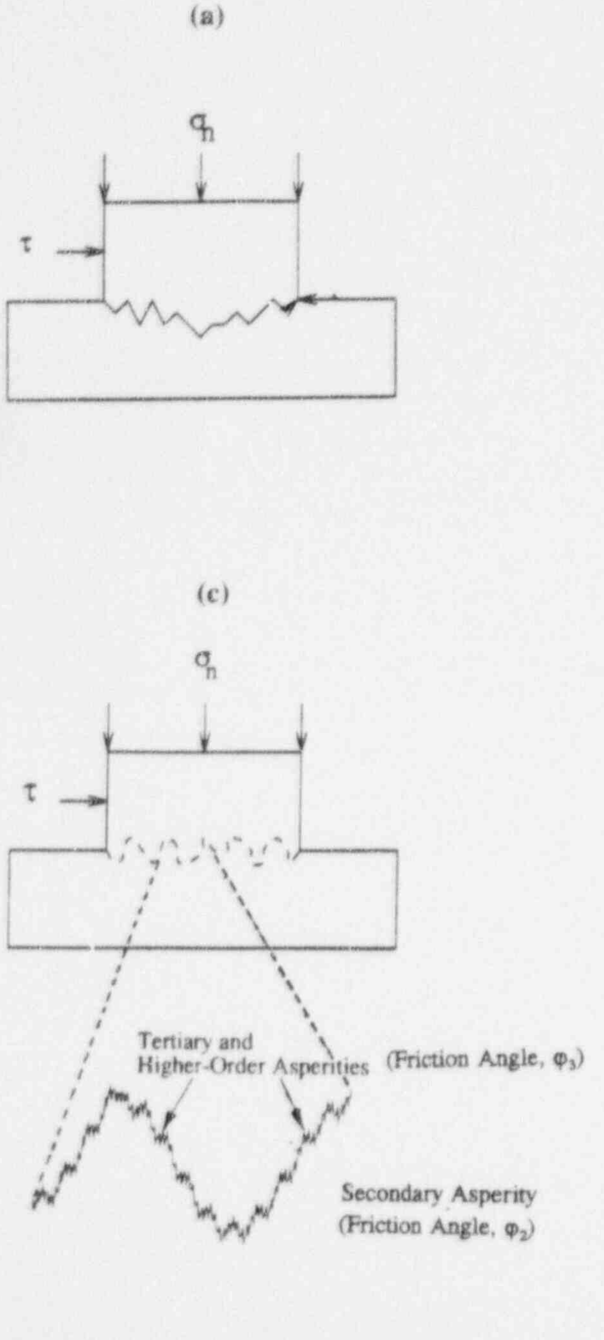

Figure 7-5. Schematic diagrams of rock surface conceptual model

asperities wear off quickly with shear displacement; tertiary and higher-order asperities (ϕ_3) wear off at a much faster rate than secondary asperities (ϕ_2). If shear displacement is continued for a long time, the joint surface will tend toward a perfectly smooth and plane surface [figure 7-5(d)] (ϕ_1, ϕ_2, and ϕ_3 approaching zero) having the basic friction angle ϕ_b.

Based on the previous discussion on the rock joint model, shear response of the natural rock joint subjected to cyclic pseudostatic load in the forward direction is

$$\tau = \sigma_n \tan\left[Sign(v)\left(\phi_b + \phi_3 e^{-C_3 W^p} + \phi_2 e^{-C_2 W^p}\right) + \phi_1 \tanh(\eta u_s) e^{-C_1 W^p}\right] \qquad (7\text{-}1)$$

In this equation, τ is the shear stress of the joint subjected to a normal stress σ_n and u_s is the shear displacement. C_3 is the rate of wearing of ϕ_3. Similarly, C_2 and C_1 are the rates of wearing of ϕ_2 and ϕ_1. W^p is the plastic work and the product of normal stress and cumulative shear displacement. $Sign(v)$ is the sign of the shear velocity v (either positive or negative). Shear velocity is a vector quantity and is negative in the reverse direction. Therefore, the resultant shear stress takes the negative sign when the top block is shearing in the reverse direction. η is an empirical constant. $\tanh(\eta u_s)$ basically controls the smooth transition of the shear stress versus shear displacement curve in the reverse direction. In the reverse direction, the effect of the downslope (angle ϕ_1) is to help movement of the sheared block, whereas the available friction from surface roughness will oppose the motion.

There is one more aspect of cyclic shearing that warrants discussion. When the top block passes the initial point during reverse shearing from one side of the initial starting point to the other (i.e., from side marked A in figure 7-6 to side marked B), it experiences the fresh surface of the bottom block. Consequently, the frictional resistance offered by these blocks will be higher than when the top block was at the other side of the initial point. Although the rate of wear may remain the same on both sides, the amount of wear needs to be accounted for separately on both sides of the initial point for appropriate modeling. Therefore, one version of the Eq. (7-1) must be provided for each side of the blocks, namely, A and B. Cumulative shear displacement for calculation of plastic work can then be determined separately for each side. Figure 7-7 shows a plot of shear stress versus shear displacement curves for test no. 20 of Hsiung et al. (1994a) and predicted results using the proposed model. The characteristics of the curve are similar to those of the experimental results.

When one rough surface slides past another rough surface, the volume change of the interface or change in aperture is generally described by the normal displacement (dilation) of the interface. In this model, joint dilation at a given shear displacement is proportional to the mobilized friction angle at that shear displacement. The mobilized friction angle is ($\phi_2 + \phi_3 + \phi_1$) in the forward direction and ($\phi_2 + \phi_3$) in the reverse direction. Friction angle for tertiary and higher-order asperities ϕ_3 will wear off relatively quickly during the first cycle and make a small contribution to the dilation. Methods for generating the equation constants (including ϕ_1, ϕ_2, ϕ_3, C_1, C_2, C_3, and η) are currently under development.

7.4 ASSESSMENT OF PROGRESS TOWARD MEETING OBJECTIVES

Activities conducted during FY96 as reported in section 7.3 were aimed at addressing certain components of two of the three KTI subissues: (i) design of the repository to meet preclosure and

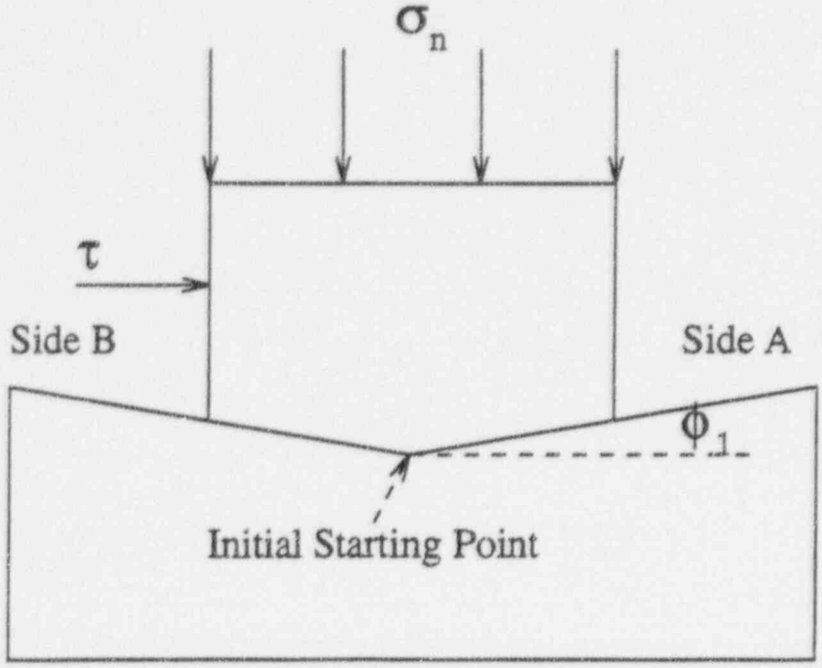

Figure 7-6. Schematic diagram of the rock joint model

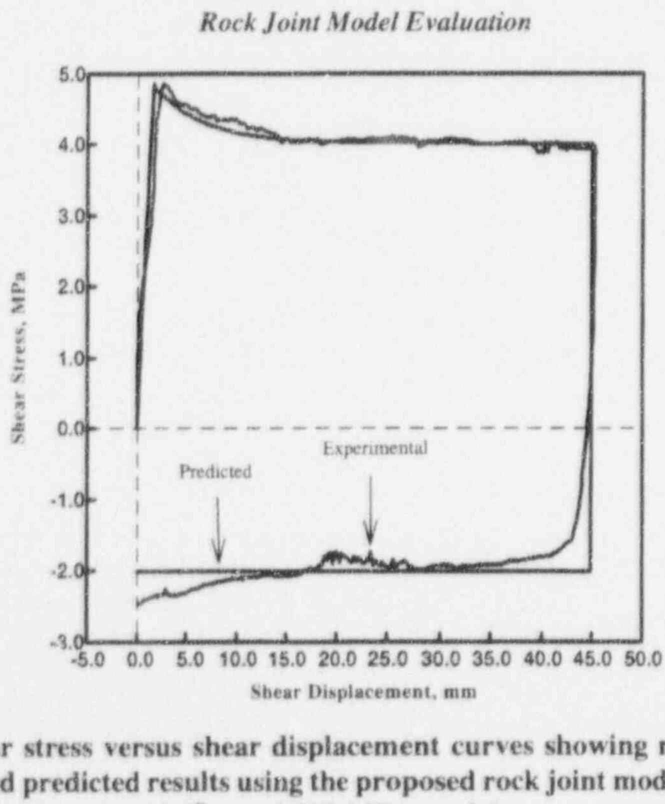

Figure 7-7. Plot of shear stress versus shear displacement curves showing results from test no. 20 (Hsiung et al., 1994a) and predicted results using the proposed rock joint model (ϕ_1=18.46°, ϕ_2=2.03°, ϕ_3=5.53°, C_1=0.05, C_2=0, C_3=0, ϕ_b=24.7°, σ_n=3.988 MPa, η=3.0)

postclosure performance objectives and (ii) evaluation of thermal effects on design of the underground facility. Specifically, activities related to review of seismic TR2, rock joint model development, ESF design package review, and review of the DOE regulatory compliance review report attempted to address concerns related to the DOE design program for subissue (i). The concern related to identification of TM parameters and effects for subissue (ii) is addressed through activities on parametric study of drift stability in jointed rock mass and the DOE *in situ* heater tests.

Review of the DOE seismic TR2, ESF Main Drift design report, and regulatory compliance review report contributed to resolution of NRC concerns related to the DOE repository design program. The NRC and CNWRA recommendations made to modify the DOE proposed seismic design methodology, if accepted by DOE, will resolve the NRC concerns in early FY97. The NRC recommendations made on DOE design of the ESF Main Drift will provide guidelines to the DOE in its future repository design considerations. These will also be factored into the NRC development of review procedures and acceptance criteria for repository design. Review of DOE design control process report made it possible to resolve all related NRC concerns. The only item left is to assess DOE implementation of the NRC-approved design control process.

A TM parametric study and review of DOE ESF heater tests identified thermal load and site specific rock mechanical and thermal parameters that may significantly affect emplacement drift stability and waste retrievability. These will provide input to the basis for resolution of the RDTME subissue on consideration of thermal effects in underground facility design.

The enhanced rock joint model, when completed and incorporated in the TM compliance determination codes UDEC and 3DEC, will be used as a prediction tool to resolve the RDTME KTI subissue on design of the proposed repository to meet preclosure and postclosure performance objectives.

7.5 INTEGRATION WITH OTHER KEY TECHNICAL ISSUES

The Structural Deformation and Seismicity (SDS) KTI provided updated YM seismic ground vibration and fault displacement data to RDTME KTI for the review of seismic TR2. RDTME KTI provided to SDS KTI fault and fracture modeling tools and techniques that have been used for fault slip study, hangingwall deformation investigation, and FAULTING module development. Integration between RDTME and SDS KTIs will continue in areas involving site geologic and geomechanics parameters, seismic and faulting hazard assessments, prediction tools and techniques for these assessments, and underground and surface facilities design against seismic and faulting hazards.

The RDTME KTI provided comments to the audit review of the 1995 DOE Total System Performance Assessment (TSPA-95) (TRW Environmental Safety Systems, Inc., 1995), which was coordinated by the Total System Performance Assessment and Integration (TSPAI) KTI, using the updated TM parametric study data. The effects of thermal and seismic loads on repository postclosure performance will be provided by the RDTME KTI to the TSPAI KTI through the EBSPAC and SEISMO codes, which will be incorporated as models in the TPA code. Updated data on the importance of thermal and seismic loads and seals on repository performance will be provided to the RDTME KTI by the TSPAI KTI based on its TPA sensitivity analysis results.

The RDTME KTI provided to the Evolution of the Near-Field Environment (ENFE) KTI the mechanical and hydrological field investigation data from the Lucky Friday Mine, shaking table rock mass

test data, and TM parametric study data for review of the hypotheses on evolution of the near-field environment.

Integration between the RDTME and Container Life and Source Term (CLST) KTIs is through input to the EBSPAC code (Mohanty et al., 1996). Because the DOE is considering the option of not backfilling the emplacement drifts, TM effects related to drift stability are expected to become important for postclosure system performance. The EBSPAC code has the option to incorporate mechanical and hydrological effects on WP caused by instability of emplacement drifts. The RDTME KTI will provide the CLST KTI with predictions of drift stability and rock fall under thermal and seismic loads. Likewise, the CLST KTI will identify important parameters and data needed from RDTME KTI for the EBSPAC module.

The temperature distribution and fracture opening data predicted by TM parametric study have been provided by the RDTME KTI to the Thermal Effects on Flow (TEF) KTI. These data were used by the TEF KTI for review of the DOE thermal testing program.

7.6 REFERENCES

Ahola, M.P., R. Chen, H. Karimi, S.M. Hsiung, and A.H. Chowdhury. 1996. *A Parametric Study of Drift Stability in Jointed Rock Mass, Phase I: Discrete Element Thermal-Mechanical Analysis of Unbackfilled Drifts*. CNWRA 96-009. San Antonio, TX: Center for Nuclear Waste Regulatory Analyses.

American Institute of Steel Construction. 1989. *Manual of Steel Construction, Allowable Stress Design, Ninth Edition*. Chicago, IL: American Institute of Steel Construction.

Barton, N., S. Bandis, and K. Bakhtar. 1985. Strength, deformation and conductivity coupling of rock joints. *International Journal of Rock Mechanics of Mining Sciences & Geomechanics Abstracts* 22: 121–140.

Bieniawski, Z.T. 1969. Behavior of fractured rock under multiaxial compression. *Structure, Solid Mechanics and Engineering Design*. M. Te'eni, ed. Toronto, Canada: Wiley Interscience: 1:589–598.

Brechtel, C.E., M. Lin, E. Martin, and D.S. Kessel. 1995. *Geotechnical Characterization of the North Ramp of the Exploratory Studies Facility*. SAND95-0488/1. Albuquerque, NM: Sandia National Laboratories.

Celestino, T.B., and R.E. Goodman. 1979. Path dependency of rough joints in bi-directional shearing. *Fourth International Congress on Rock Mechanics Proceedings*. Lisbon, Portugal: Society for Rock Mechanics: 91–98.

Fishman, K.L. 1988. *Constitutive Modeling of Idealized Rock Joints Under Quasi-Static and Cyclic Loading*. Ph.D. Dissertation. Tucson, AZ: University of Arizona.

Gillette, D.R., S. Sture, H.-Y. Ko, M.C. Gould, and G.A. Scott. 1983. Dynamic behavior of rock joints. *24th U.S. Symposium on Rock Mechanics Proceedings*. College Station, TX: Texas A&M University: 163–179.

Gupta, D., J. Peshel, and J. Bunting. 1991. *Staff Technical Position on Regulatory Considerations in the Design and the Construction of the Exploratory Shaft Facility*. NUREG-1439. Washington, DC: Nuclear Regulatory Commission.

Hardy, M.P., and S.J. Bauer. 1991. *Drift Design Methodology and Preliminary Application for the Yucca Mountain Site Characterization Project*. SAND89-0837. Albuquerque, NM: Sandia National Laboratories.

Hsiung, S.M., M.P. Ahola, A.H. Chowdhury, and A. Ghosh. 1994a. *Laboratory Characterization of Rock Joints*. NUREG/CR-6178. Washington, DC: Nuclear Regulatory Commission.

Hsiung, S.M., A. Ghosh, A.H. Chowdhury, and M.P. Ahola. 1994b. *Evaluation of Rock Joint Model and Computer Code UDEC Against Experimental Results*. NUREG/CR-6216. Washington, DC: Nuclear Regulatory Commission.

Huang, X., B.C. Haimson, M.E. Plesha, and X. Qiu. 1993. An investigation of the mechanics of rock joints Part I—Laboratory investigation. *International Journal of Rock Mechanics and Mining Sciences & Geomechanics Abstracts* 30: 3.

Jing, L., E. Nordlund, and O. Stephansson. 1992. An experimental study on the anisotropy and stress-dependency of the strength and deformability of rock joints. *International Journal of Rock Mechanics and Mining Sciences & Geomechanics Abstracts* 39: 6.

Itasca Consulting Group, Inc. 1993. *UDEC: Universal Distinct Element Code. Volume I: User's Manual, Version 2.0*. Minneapolis, MN: Itasca Consulting Group, Inc.

Lin, M., M.P. Hardy, and S.J. Bauer. 1993. *Fracture Analysis and Rock Quality Designation Estimation for the Yucca Mountain Site Characterization Project*. SAND92-0449. Albuquerque, NM: Sandia National Laboratories.

Mohanty, S., G.A. Cragnolino, T. Ahn, D.S. Dunn, P.C. Lichtner, R.D. Manteufel, and N. Sridhar. 1996. *Engineering Barrier System Performance Assessment Code: EBSPAC Version 1.0β—Technical Description and User's Manual*. CNWRA 96-011. San Antonio, TX: Center for Nuclear Waste Regulatory Analyses.

Nuclear Waste Technical Review Board. 1992. *Fifth Report to the U.S. Congress and the U.S. Secretary of Energy*. Washington, DC: U.S. Government Printing Office.

Nuclear Regulatory Commission. 1996. *Letter of July 25, 1996 from Michael J. Bell to Stephan Brocoum*. Washington, DC: Nuclear Regulatory Commission.

Ofoegbu, G.I., and J.H. Curran. 1992. Deformability of intact rock. *International Journal of Rock Mechanics and Mining Sciences & Geomechanics Abstracts* 29(1): 35–48.

TRW Environmental Safety Systems, Inc. 1995. *Total System Performance Assessment—1995: An Evaluation of the Potential Yucca Mountain Repository*. B00000000-01717-2200-00136. Las Vegas, NV: TRW Environmental Safety Systems Inc.

U.S. Department of Energy. 1995a. *Regulatory Compliance Review Report. Yucca Mountain Site Characterization Project, March 1995*. Washington, DC: U.S. Department of Energy, Office of Civilian Radioactive Waste Management.

U.S. Department of Energy. 1995b. *Regulatory Compliance Review Report. Yucca Mountain Site Characterization Project, July 1995*. Washington, DC: U.S. Department of Energy, Office of Civilian Radioactive Waste Management.

U.S. Department of Energy. 1995c. *Letter of October 25 from Stephan J. Brocoum to Joseph J. Holonich*. Washington, DC: Nuclear Regulatory Commission.

Wawersik, W.R., and W.F. Brace. 1971. Post-failure behavior of a granite and diabase. *Rock Mechanics* 3: 61–85.

Wawersik, W.R., and C.A. Fairhurst. 1970. A study of brittle rock fracture in laboratory compression experiments. *International Journal of Rock Mechanics and Mining Sciences & Geomechanics Abstracts* 7: 561–575.

Wibowo, J.T., B. Amadei, S. Sture, R.H. Price, and A.B. Robertson. 1993. *Effect of Boundary Conditions on the Strength and Deformability of Replicas of Natural Fractures in Welded Tuff: Data Report*. SAND92-853. Albuquerque, NM: Sandia National Laboratories.

Zubelewicz, A., K. O'Connor, C.H. Dowding, T. Belytschko, and M. Plesha. 1987. A constitutive model for the cyclic behavior of dilatant rock joints. *Second International Conference on Constitutive Laws for Engineering Materials: Theory Applications Proceedings. Volume II*. C.S. Desai, E. Krempl, P.D. Kiousis, and T. Kundu, eds. New York, NY: Elsevier: 1,137–1,144.

8 TOTAL SYSTEM PERFORMANCE ASSESSMENT AND INTEGRATION

Primary Authors: R.G. Baca, R.B. Codell, A.R. DeWispelare, R.D. Manteufel, S.A. Stothoff, T.J. McCartin, and R.G. Wescott

Technical Contributors: R.G. Baca, R.B. Codell, A.R. DeWispelare, R.W. Janetzke, M.S. Jarzemba, M.P. Lee, R.D. Manteufel, T.J. McCartin, S. Mohanty, N. Sridhar, S.A. Stothoff, and R.G. Wescott

Key Technical Issue Co-Leads: R.G. Baca (CNWRA) and R.G. Wescott (NRC)

8.1 INTRODUCTION

The standard currently being developed by the U.S. Environmental Protection Agency (EPA) for the Yucca Mountain (YM) site is expected to require the proposed repository to meet both dose and risk limits. To determine compliance with such a standard, the Nuclear Regulatory Commission (NRC) will conduct a total system performance assessment (TSPA) to evaluate the isolation performance of the engineered and natural barriers. In this evaluation, the TSPA will address, in a probabilistic manner, the propagation of uncertainties associated with inherently complex natural phenomena such as unsaturated flow in fractured-porous media and repository processes such as waste package (WP) corrosion. Where appropriate, the TSPA will use bounding assumptions to compensate for uncertainties in both data and technical knowledge. In addition, TSPA takes into account uncertainties in model parameters and conceptual models as well as the relevant features, events, and processes (FEPs) (for both anticipated and unanticipated conditions) into an analysis that estimates the radiologic risks to a hypothetical member of a critical group. The integration aspect of TSPA ensures that the key technical issues (KTIs) develop technical bases for use in issue resolution and that the transfer of information among program areas will result in assessments of compliance that are transparent, defensible, and sufficiently comprehensive.

A long compliance period (e.g., 10,000 yr) may require consideration of combinations of disruptive events, coupling of processes, and possible changes to the flow and transport in the geologic system. To ensure the proposed repository does not pose an unacceptable risk to public health and safety or the environment, such complex phenomena cannot be considered only within the subsystem process models but must be reflected in the modeling from an overall system perspective. Examples of such complex phenomena include the distribution of water over WPs in the proposed repository and how this distribution can change with time; quantification of thermal, hydrologic, and chemical processes in the near-field of the WP and determination of how these processes may interact with each other; and radionuclide dilution and transport in the groundwater system, including interaction with the biosphere. Analyzing total system performance requires a broad knowledge and modeling expertise from a variety of technical disciplines. The need for strong coordination among KTI teams is recognized as an essential aspect to the success of a TSPA and must be pursued in a deliberate manner.

The three principal subissues associated with the Total System Performance Assessment and Integration (TSPAI) KTI consist of

- Do the hypotheses described in the U.S. Department of Energy (DOE) Waste Containment and Isolation Strategy[1] (WCIS) adequately represent and rigorously test the major performance characteristics of the proposed YM repository?

- What is the relative importance of the individual NRC KTIs and is there is a need for change in emphasis?

- Are the major components of the DOE TSPA methodology (e.g., model abstractions, probability and consequences of relevant FEPs, parameter and model uncertainties, and bounding assumptions) sufficiently comprehensive that it will provide a defensible safety case?

In addition to addressing these subissues, the TSPAI KTI was tasked with developing and maintaining an independent technical assessment capability, reviewing the DOE Total System Performance Assessment (TSPA-95) (TRW Environmental Safety System, Inc., 1995)[2], and supporting documents, promoting technical integration among KTIs, and developing the Consolidated DOCument System (CDOCS) software. The fiscal year (FY) 96 accomplishments in this KTI discussed in greater detail are (i) audit review of the DOE TSPA-95, (ii) expert elicitation, (iii) CDOCS, and (iv) Licensing Support System Pilot Program (LSSPP). Progress on other activities include (i) initiation of a detailed review of TSPA-95, (ii) work on an acceptable scenario analysis methodology, and (iii) development of an independent technical assessment capability.

8.2 OBJECTIVES AND SCOPE OF WORK

The major objectives of the TSPAI KTI are two-fold: enhance the NRC capability to conduct independent reviews of the DOE TSPAs [such as the forthcoming TSPA-Viability Assessment (VA)] and use the TSPA capability to evaluate the relative importance of the NRC KTIs. Specific programmatic objectives pursued this fiscal year included providing technical comments to the DOE on TSPA-95, issuing generic guidance on an acceptable procedure for use in formal elicitations of expert judgment, and completing the CDOCS software and transferring it to the NRC for use in a variety of prelicensing activities within the NRC high-level waste (HLW) program.

An audit review of the DOE TSPA-95 report was conducted for the purposes of identifying vulnerabilities of the assessment and recommending approaches for enhancing the defensibility of future DOE TSPAs. The audit review consisted of independent analyses of selected components of the TSPA, direct comparisons of calculational results with those produced by the DOE, and then identification of primary factors causing the differences. In general, the major calculational differences were explained by distinct conceptual models, mathematical modeling approaches, bounding assumptions, and/or interpretations of available data. The independent analyses performed for the audit review provided the basis for developing constructive technical comments transmitted to the DOE in presentations at the

[1]U.S. Department of Energy. 1996. *Highlights of the U.S. Department of Energy's Updated Waste Containment and Isolation Strategy for the Yucca Mountain Site*. DOE Concurrence Draft. July 1996. Washington, DC: U.S. Department of Energy.

[2]The DOE TSPA-95 document is extensively referenced in this chapter. For ease of reading, the reference to TRW Environmental Safety Systems, Inc., is omitted from all subsequent citations.

DOE/NRC Technical Exchange on the Audit Review of TSPA-95, and transmitted in a technical report (Baca and Brient, 1996). The success of the audit review is reflected in the TSPA-VA Plan (TRW Environmental Safety Systems, Inc., 1996) which makes note of the NRC comments/recommendations and outlines actions to be taken by the DOE in the conduct of the TSPA-VA.

Because of the pervasive nature of expert judgment in the repository program, the NRC recognized the need for guidance on an acceptable expert elicitation procedure. To meet this need, a general elicitation procedure was developed and demonstrated for the case of future climate scenarios for the YM site. This work established the framework for guidance documented in a draft branch technical position (BTP). The BTP was then distributed for public comments, revised in accordance with resolutions and issued as NUREG-1563 (Kotra et al., 1996).

The CDOCS software was developed to provide the Division of Waste Management (DWM) technical staff with an enhanced computer capability for management, retrieval, and visualization of technical and regulatory information (DeWispelare et al., 1993). CDOCS-related work included development of the CDOCS software, preparation of the user's manual, and conduct of a technology transfer seminar. Assistance was also provided to the NRC with the installation and testing of the document management system on the NRC advanced computer system.

8.3 SIGNIFICANT TECHNICAL ACCOMPLISHMENTS

8.3.1 Audit Review of the U.S. Department of Energy Total System Performance Assessment-95

The DOE recently issued the third in a series of TSPAs for the proposed repository at YM. The latest TSPA report referred to as TSPA-95 presents the DOE performance assessment approach, assumptions, data, and principal findings of the evaluation. Overall system performance is quantified in the TSPA-95 report using both cumulative release at 5 km (over 10,000 y) and peak dose (i.e., drinking water dose assuming 2 L/d).

In accordance with the NRC Overall Review Strategy (Johnson, 1993), the NRC conducted an audit review of TSPA-95 (Baca and Brient, 1996). The review consisted of technical comments developed by the NRC and the Center for Nuclear Waste Regulatory Analyses (CNWRA) staffs. These comments formed the basis for presentations and discussions at the DOE/NRC Technical Exchange on the Audit Review of TSPA-95 on May 22–23, 1996. This audit review identified some areas of agreement and a number of areas of technical difference (i.e., methodology issues). Most of these technical differences were clarified during the technical exchange and in some cases resolved.

The audit review consisted of a two-level review process that involved probing component model abstractions of the TSPA-95 and a broad review of TSPA methodology. In the first level, independent analyses were conducted to evaluate such aspects as the appropriateness of technical approach, adequacy of treatment of parameter uncertainties, appropriateness of conservatism through the use of bounding assumptions, sufficiency of site data. Calculational results from these independent analyses were used to develop specific technical comments regarding the DOE performance evaluation. The more general comments addressed aspects that the TSPA-95 asserted were not significant but did not specifically address in the TSPA-95 report. For example, the TSPA-95 states that disruption scenarios associated with igneous activity and seismicity are not considered significant to overall performance. To clearly present the NRC

position on this statement, general comments were prepared to indicate that the DOE had not provided sufficient basis (in a TSPA context) to support such a statement.

The audit review focused on five primary review topics:

- Infiltration and Deep Percolation
- Groundwater Dilution
- Temperature and Humidity
- WP Failure Modes
- Subsystem Abstractions

These five review topics were selected because of their relevance to WCIS (U.S. Department of Energy, 1996). The fact that the NRC/CNWRA staffs had performed detailed technical studies on these topics was also a consideration. Each of the focus topics was probed through the conjunctive use of abstracted and detailed process models, as well as through the application of the NRC Iterative Performance Assessment (IPA) Phase 2 (Nuclear Regulatory Commission, 1995) version of the total performance assessment code. These areas are discussed in the following sections.

8.3.1.1 Infiltration and Deep Percolation

Distribution of percolation flux is identified in TSPA-95 as the primary site characterization issue because of impacts on WP degradation and radionuclide transport rates through the unsaturated zone. The infiltration rate at the soil surface and percolation flux at depth are highly correlated. Both quantities are water fluxes. If no significant lateral diversion of flow can be demonstrated, then the assumption that percolation flux is synonymous with infiltration rate is bounding.

Water fluxes and velocities in the matrix and fractures are not directly calculated in the total system simulations reported in TSPA-95. Rather, an abstracted representation for these quantities is used. Using a single representative vertical column with constant thickness, random matrix properties obtained from Schenker et al. (1995) [essentially identical to the properties used in the TSPA-93 report (Wilson et al., 1994)], and a single set of constant fracture properties for all stratigraphic layers, the velocities and fluxes obtained from simulations using TOUGH2 (Pruess, 1987; 1991) for a small number of material-property realizations are abstracted into probability distribution functions (PDFs) for matrix velocity, fracture velocity, and a flux-partitioning factor distributing flux between matrix and fractures.

To independently assess the impact of the assumptions used for the unsaturated flow abstraction, the method presented in the TSPA-95 was evaluated for several flux rates The particle travel times were calculated for each pathway in the one-dimensional (1D) column where a pathway consists of a combination of matrix flow for some layers and fracture flow for the remaining layers. The fastest pathway typically consists of fracture flow for each of the layers and the slowest pathway consists of matrix flow. The fastest and shortest pathways have the shortest and longest overall travel times. The largest flux pathway represents the most likely pathway for a particle, since the largest fraction of the flux goes through the pathway. For conservatism, particles were assumed not to move between matrix and fracture within a layer but may transition at layer interfaces.

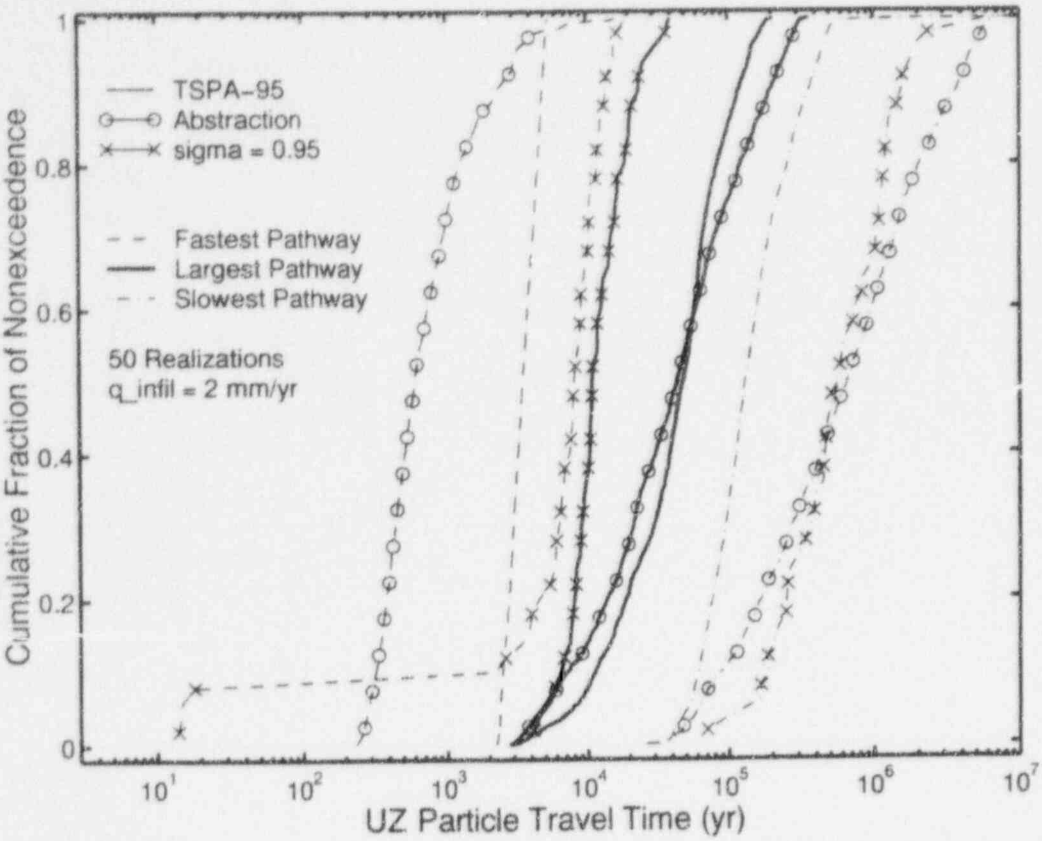

Figure 8-1. Comparison of process-level simulations with abstractions for an infiltration flux of 2 mm/yr

The highest infiltration rate considered in the TSPA-95 report was 2 mm/yr. This value was used to compute the fastest, slowest, and largest flux pathways shown in figure 8-1. The line style for a curve represents the type of pathway and the symbol type denotes whether the curve represents process-level simulations (sigma = 0.95), the abstraction based on the simulations (abstraction), or the TSPA-95 abstraction (TSPA-95). Each curve was constructed using results from 50 process-level realizations. The cumulative fraction of realizations with the particle travel time for a specified pathway not exceeding a given particle travel time is presented for each pathway. The process-level simulations were performed by integrating Darcy's law from the water table to the proposed repository, using the steady-state calculational methodology described by Baca et al. (1994) and adapted to incorporate the equivalent continuum model. As a comparison, the corresponding pathway analysis was performed for the TSPA-95 abstraction.

For the 2 mm/yr case shown in figure 8-1, the statistical character of the particle travel times for the process-level pathways is distinct from the behavior of the corresponding abstraction pathways. In particular, the process-level simulations exhibit a relatively low but non-negligible probability of extremely fast pathways, on the order of decades, while the largest-flux pathways and most of the fastest

pathways are on the order of thousands of years. Incorporating a total of 320 simulations (not shown here due to space limitations) suggests there is a small probability that the largest flux pathways may also be on the order of decades. On the other hand, the abstraction from these process-level simulations indicates a minimum of 200 yr for the fastest pathways but more typically on the order of 1,000 yr. The largest flux pathways generally tend to be several times slower than the corresponding process-level simulations. By comparing the 50 process-level realizations with the TSPA-95 abstraction, it can also be seen that considering 50 rather than 10 realizations has the effect of making the fastest pathways faster and the slowest pathways slower.

Specific recommendations (Baca and Brient, 1996) made at the NRC/DOE Technical Exchange on TSPA-95 as a result of this independent analysis included (i) modifying the equation to calculate pore velocity to account for saturation level, (ii) increasing the number of realizations in their process-level models, and (iii) reviewing the abstractions incorporated in Markovian particle model that result in relatively long particle travel times (i.e., solute residence times) in the unsaturated zone. The recently issued TSPA-VA Plan (TRW Environmental Safety System, Inc., 1996) notes and discusses these recommendations. From the technical activities identified in the TSPA-VA Plan (TRW Environmental Safety System, Inc., 1996), it appears the DOE will be implementing the recommendations.

8.3.1.2 Groundwater Dilution

Groundwater dilution at the YM site is a component of the DOE WCIS and may be of key importance to a dose- or risk-based standard. Consequently, the estimation of dilution merits a combination of (i) groundwater modeling, detailed site scale (e.g., 5 km) and regional scale (e.g., 30 km); (ii) evaluation of geochemical parameters indicating the degree of mixing; and (iii) estimation of macro-scale dispersivities based on field tracer test data. Such a combination of investigations would better support the DOE development of a more defensible basis for the TSPA-VA (TRW Environmental Safety System, Inc., 1996). In the DOE TSPA-95, groundwater dilution was quantified by a dilution factor defined as the ratio of steady-state radionuclide concentration in the unsaturated zone to the concentration in the saturated zone. Defined in this manner, the dilution factor accounts for groundwater mixing immediately below the repository and along the saturated zone flow path.

In TSPA-95, two models were used to estimate dilution factors: a stirred-tank mixing model and a line source advection-dispersion model. The stirred tank model implicitly assumes that radionuclides leaving the proposed repository are uniformly distributed throughout the entire repository footprint and, upon reaching the water table, are instantaneously and completely mixed over a 50-m-thick zone (i.e., screen-interval depth). In contrast, the advection-dispersion model makes no assumption of mixing depth but rather assumes that radionuclides enter the saturated zone along a line equal to the width (e.g., 4 km) of the proposed repository and that macro-scale dispersion reduces concentrations along the flow path from the proposed repository to Amargosa Desert.

Based on the stirred tank model, TSPA-95 calculates dilution factors ranging from 8×10^2 to 3.3×10^4 for a 5 km path length. With the advection-dispersion model, TSPA-95 estimates centerline dilution factors of 4.5×10^3 to 1.9×10^5 for a 5 km path length and 3.1×10^4 to 1.3×10^6 for 30 km. Embedded in the calculations with the advection-dispersion model is the assumption that dispersion coefficients are linearly dependent on path length.

Using an advection-dispersion model, independent estimates of dilution factors were calculated and presented in table 8-1. These calculations differ from TSPA-95 calculations only by having more

Table 8-1. Dilution factors computed using conservative values for transverse dispersivity and unsaturated zone flux

Unsaturated Zone Flux (m/yr)	Dilution Factor (DF)	
	5 km	30 km
1.25×10^{-3}	9.5×10^{2}	8.0×10^{3}
3.0×10^{-5}	4.0×10^{4}	3.4×10^{5}

conservative values of transverse dispersivity and saturated zone flux, which can be supported by information in the technical literature (Gelhar et al., 1985; Gelhar, 1993; Whitfield et al., 1985; Wittwer et al., 1995).

These calculated dilution factors are about 1/3 to 1/5 of those estimated in TSPA-95. In addition to these estimates, the maximum dilution factors calculated using assumptions from the NRC IPA Phase 2 (Nuclear Regulatory Commission, 1995) are about two to three orders of magnitude smaller than those calculated in TSPA-95. The much smaller dilution factors arise primarily because the infiltration rates from IPA Phase 2 are much larger than those assumed in TSPA-95 and the estimated saturated zone fluxes are much smaller than those assumed in TSPA-95. Similarly, TSPA-93 (Wilson et al., 1994) presents results for a detailed three-dimensional (3D) transport model indicate dilution factors at 5 km in the range of $5 \leq DF \leq 20$. These estimates are again smaller than those in TSPA-95. It is important to acknowledge, however, that dilution factor estimates derived from the TSPA-93 (Wilson et al., 1994) transport calculations are likely to be more conservative than those of TSPA-95 because they neglect the initial mixing and dilution immediately below the repository.

In summary, the conclusion was that the DOE assessment of dilution may be overly optimistic. Moreover, the large dilution factors postulated in TSPA-95 appear to be inconsistent with the heterogeneous hydrochemistry evident from available field data. It was recommended (Baca and Brient, 1996) at the NRC/DOE Technical Exchange on TSPA-95 that the defensibility of dilution factor estimates could be enhanced through the use of improved modeling techniques as well as available field tracer and geochemical data. Alternatively, more conservative bounds for dilution effects could be developed. The recently issued TSPA-VA Plan (TRW Environmental Safety System, Inc., 1996) paraphrases these recommendations. It is evident from technical activities identified in the TSPA-VA Plan (TRW Environmental Safety System, Inc., 1996) that the DOE will be implementing the recommendations.

8.3.1.3 Temperature and Humidity

One conclusion of TSPA-95 is that the thermohydrologic environment of WPs strongly affects the initiation and rate of aqueous corrosion. Because the thermohydrologic environment of the WP affects many near-field processes important to TSPA, independent calculations were initiated to reproduce TSPA-95 results using the same data and dimensions and evaluate the differences introduced by using a 3D instead of a two-dimensional (2D) model.

In TSPA-95, the FEHM thermohydrologic code (Zyvoloski et al., 1995) is used to predict the evolving hydrothermal conditions near WPs. TSPA-95 results appeared to have anomalies in the predictions prior to backfilling, hence independent calculations were performed by the CNWRA to reproduce the results using the ABAQUS (1995) and MULTIFLO (Seth and Lichtner, 1996) codes. METRA, a submodule of MULTIFLO, simulates coupled heat and mass transfer in a porous medium—the same processes included in the DOE FEHM code. ABAQUS simulates transient conduction heat transfer, considered the dominant mode of heat transfer for low and intermediate areal mass loadings (AMLs). ABAQUS uses the finite element method and accurately represents the geometry of the system. MULTIFLO uses rectangular grids.

A portion of the computational mesh near the WP is provided in figure 8-2 for a 2D model similar to that used in TSPA-95 and a 3D model. For clarity, the backfill elements are not shown in the figure but do exist in the mesh. The 2D model averages the heat source along the drift (in the third dimension). This tends to produce lower WP temperatures. The 3D model has a more accurate representation of the geometry and should yield more accurate predictions of WP conditions. Both conceptual models were considered in the CNWRA investigations.

Calculations were performed for the 25 MTU/acre and 83 MTU/acre AMLs. Thermohydrologic parameters were taken from figure 4.2-1 and table 4.2-3 of TSPA-95. Because a few thermal properties were not fully described in TSPA-95 some judgment and interpretation was necessary. Key assumptions were made that the package supports and concrete inverts have a conductivity of 1.0 W/(m-C) and that the effective conductivity of the drift prior to backfilling was 10 W/(m-C).

Relative humidity (RH) was calculated using the same approach as Eq. 4.2-1 on page 4-6 of TSPA-95. RH is a measure of the tendency for liquid films to develop on the WP surface. Within the emplacement drift, the absolute humidity was assumed to be uniform because the relative ease with which vapor flows within the drift. The vapor pressure at the WP surface was then dictated by the vapor pressure at the drift wall.

In figure 8-3, TSPA-95 and the CNWRA results are compared for the 25 MTU/acre case. The temperatures and RH are in good agreement at long times for the 2D models. For the first hundred years, the TSPA-95 results show a higher WP temperature and lower RH. After reviewing TSPA-95, it is believed that this trend is due to underestimating the rate of heat transfer from the WP to the drift wall prior to 100 yr. This could not be confirmed because of sparse documentation of details in TSPA-95. The report states that a radiative transfer model was employed but does not discuss how view factors were calculated or provide emissivity values for the package and drift wall.

The differences arising from using a 2D instead of a 3D model were also compared. It was found that the 3D model calculated WP temperatures that were about 55 °C higher than the 2D results for times after backfill was assumed to be emplaced (140 °C compared to 85 °C) for the 25 MTU/acre case. The RH was also affected so that the 3D model predicted lower values. The overall effect of higher WP temperatures and lower RH on system performance was unclear and depends on the sensitivities of the WP corrosion and source term models. Unless the 2D models are shown to be more conservative (predict earlier WP failure times and higher radionuclide release rates), then the DOE should consider use of 3D models because they can more accurately predict WP conditions.

In summary, the independent calculations reproduced many of the thermohydrologic results found in TSPA-95. Some differences were noted where TSPA-95 has higher WP temperatures before backfilling.

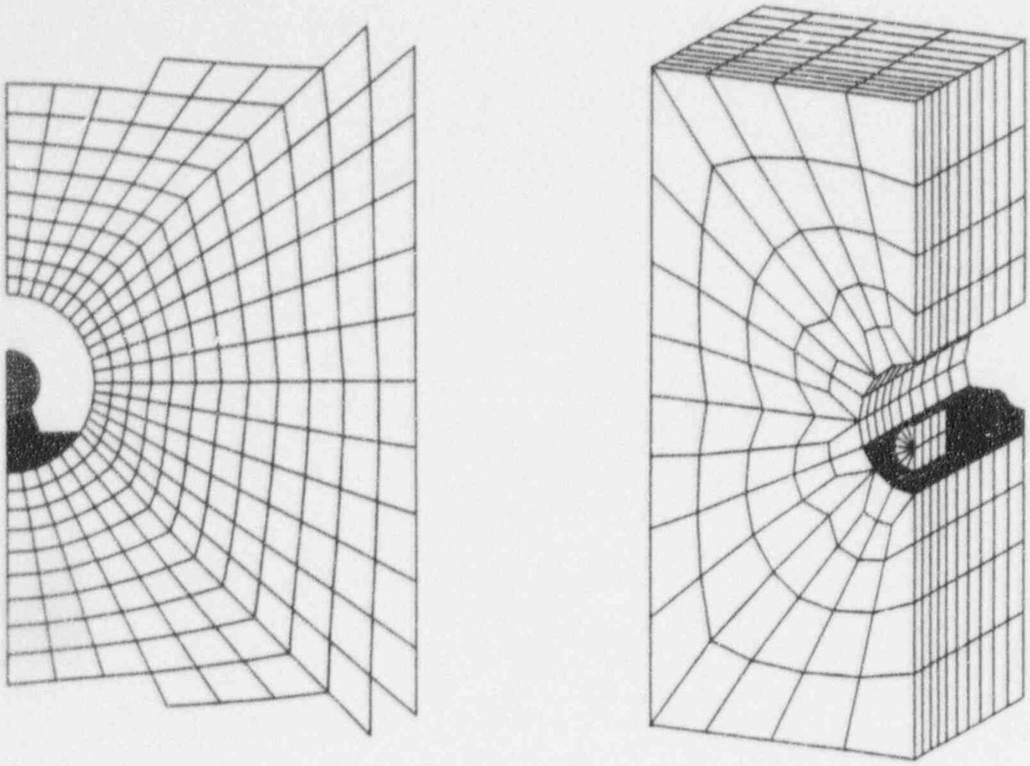

Figure 8-2. Two and three-dimensional computational models near the waste package

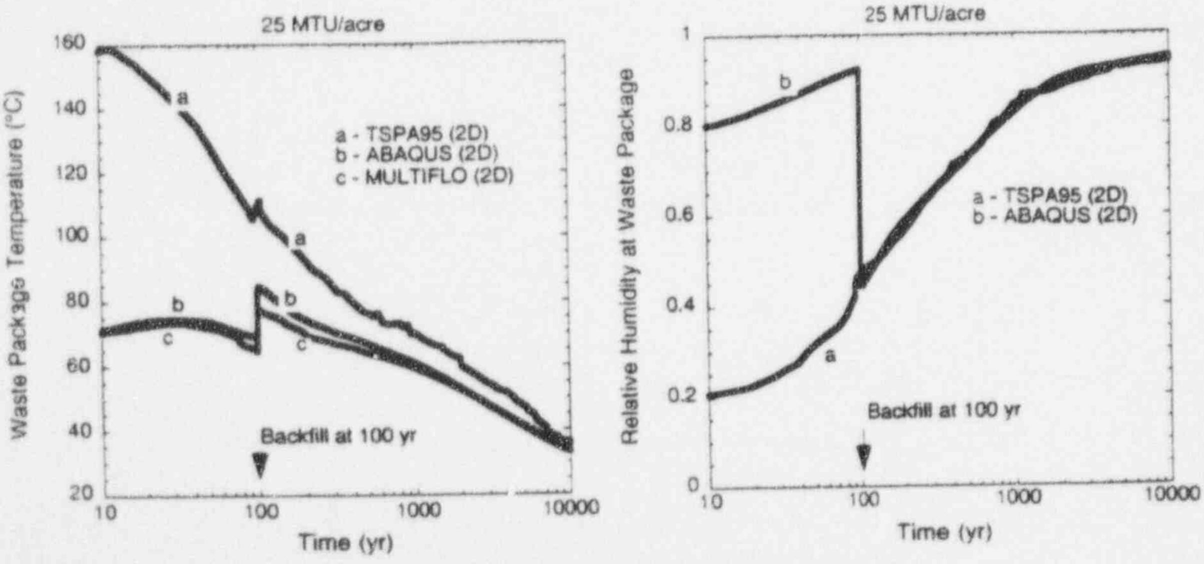

Figure 8-3. Comparison for 25 MTU/acre areal mass loading

As a result of this work, it was recommended (Baca and Brient, 1996) that the DOE review the heat transfer models used in the unbackfilled drift case and consider using a 3D model to more accurately predict WP conditions. The TSPA-VA (TRW Environmental Safety System, Inc., 1996) notes this (and other recommendations) and indicates that the DOE is implementing this recommendation for the 3D analyses. It also indicates that the DOE is considering other NRC recommendations made at the DOE/NRC Technical Exchange on the Audit Review of TSPA-1995 (Baca and Brient, 1996).

8.3.1.4 Waste Package Failure Modes

The performance characteristics of the current conceptual design of the WP for spent fuel (U.S. Department of Energy, 1994) were evaluated in TSPA-95 using a stochastic WP performance model. The design of the WP used in TSPA-95 is a significant departure from the single-wall container concept evaluated in TSPA-93 (Wilson et al., 1994). The design consists of an outer disposal overpack of a corrosion-allowance material (carbon steel) and an inner container of a corrosion-resistant alloy (Alloy 825). An additional containment barrier of a moderately corrosion-resistant material such as Alloy 400 is included in the low thermal-load repository design (U.S. Department of Energy, 1994). This additional containment barrier was not considered in TSPA-95 because models for predicting the performance of this type of material are not currently available. Also, the multi-purpose canister made of type 316L stainless steel and the pour canister for vitrified defense HLW are not included in TSPA-95 since no credit is assigned by the DOE to these canisters as containment barriers.

Although several corrosion modes, including crevice corrosion, stress corrosion cracking, microbially influenced corrosion, and galvanic corrosion, are briefly mentioned in TSPA-95 as potential failure modes for the WP, the performance calculations in TSPA-95 include only general corrosion and pitting corrosion as relevant models. Calculations in TSPA-95 are considered to be nonconservative because relevant failure modes, such as crevice corrosion, stress corrosion cracking, microbially influenced corrosion, and thermal embrittlement of steel, are not included in the analysis and the chemistry of the environment contacting the WP does not correspond to bounding environments described in the DOE long-term testing program (Lawrence Livermore National Laboratory, 1995). Furthermore, no technical basis was provided for consideration of various atmospheric and river water corrosion test results as representative of corrosion in the expected repository environment.

In summary, a number of potential failure mechanisms associated with container failure were not quantitatively addressed in TSPA-95. As a result of this review, it was recommended (Baca and Brient, 1996) that the DOE consider additional WP degradation modes, possible wet/dry near-field environments, and alternative waste dissolution models. The TSPA-VA (TRW Environmental Safety System, Inc., 1996) acknowledges these and other recommendations. In addition, it indicates the DOE will be improving the WP degradation model to take into account such phenomena as recommended.

8.3.1.5 Subsystem Abstractions

Currently, the DOE quantifies overall repository performance using a complementary cumulative distribution function (CCDF) plot of total radionuclide releases (at 5 km) to the accessible environment (over 10^4 yr) and CCDF of drinking water dose (for 2 L/d). Both the DOE and the NRC use computer codes to assess repository performance. Previous CCDFs calculated by the DOE TSPA codes such as Total System Analyzer (Wilson et al., 1994) and Repository Integration Program (RIP) (Golder Associates, Inc., 1993) differed significantly from those computed by the NRC/CNWRA TPA code, (Sagar and Janetzke, 1993). These differences in computational results are believed to be primarily because of distinct

- Model abstractions for repository subsystems

- Parameter ranges and distributions

- Underlying and/or bounding assumptions

In TSPA-95, a series of CCDFs computed with the RIP code are presented for various combinations of heat load, backfill, infiltration ranges, and alternative thermohydrologic models. None of these CCDF results are explained using causal factors or basic performance indicators [e.g., residence time in the engineered barrier system (EBS), timing of condensate refluxing, particle travel times through the unsaturated and saturated zones]. Thus, determining the correctness and reasonableness of CCDF results requires independent calculation.

The RIP code used in TSPA-95 is a generalized driver that can execute component models that describe (i) WP behavior and radionuclide release from the EBS, (ii) radionuclide transport pathways, (iii) disruptive events, and (iv) biosphere dose/risk. The components describing disruptive events and biosphere dose/risk, however, were not used in TSPA-95. The NRC/CNWRA developed the TPA computer code that was used in the NRC IPA Phase 2 (Nuclear Regulatory Commission, 1995). The approach in the audit review was to use the TPA code with WP lifetime and hydrostratigraphic representations to match those in TSPA-95. Independent CCDFs could then be generated and compared with those in TSPA-95. In this exercise, the WP lifetime was not calculated using the TPA code but a range of lifetimes was assumed based on digitizing figure 5.7-10a of TSPA-95.

In figure 8-4, two independently calculated CCDFs for cumulative release are compared with the corresponding CCDF from TSPA-95. The CCDFs generated by the TPA code used (i) the original IPA Phase 2 data and the digitized TSPA-95 WP lifetime curve together with (ii) the approximate representation of TSPA-95 input data and the digitized WP lifetime curve.

In the first case, the CCDF calculated with TPA code is within one order of magnitude of the EPA limit, whereas the CCDF taken from TSPA-95 (i.e., calculated with RIP) is about two orders of magnitude below the EPA limit. The TPA code calculations produced fewer lower releases and more high releases than indicated by the TSPA-95 result. This suggests that the IPA Phase 2 assumptions and site subsystem abstraction may be more conservative than those used in RIP. For example, in the TPA code calculations it was assumed that once a WP failed in a given zone of the repository, all WPs within that zone also failed—a more conservative assumption than that used in TSPA-95. Also, TSPA-95 computes radionuclide releases through a given number of pits/perforations. In contrast, the TPA code does not limit the releases by the number of perforations with the exception that the releases will not take place until the water in the WP reaches a certain level. The combined effect of these differences is relatively complex so that differences in the CCDF are not easily explained.

In addition to the CCDFs, TSPA-95 also presented results of calculations based on single values of parameters. One such calculation in TSPA-95 was the calculation of drinking water dose from ^{237}Np as a function of time based on expected values of infiltration and solubility limits. ^{237}Np was selected for this calculation because it is very long lived and an important contributor to dose. Thus the peak ^{237}Np dose occurring at long times will be insensitive to assumptions regarding the thermal period, waste container, and release rates for spent fuel. Two calculations were performed—one for the high infiltration rate (1.25 mm/yr), and one for the low infiltration rate (.03 mm/yr). For the staff calculation, the infiltration rate remained constant (in the TSPA-95 calculation, the infiltration rate increased). Results of

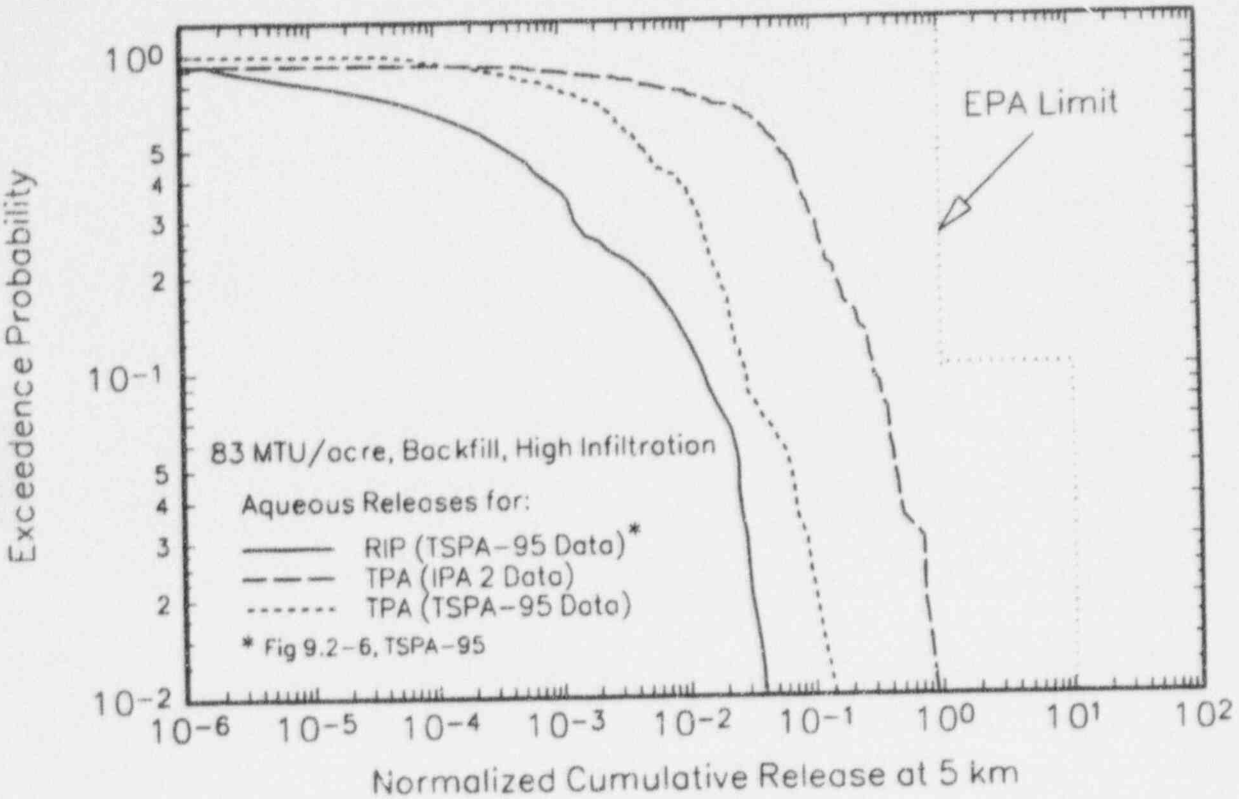

Figure 8-4. Comparison of complementary cumulative distribution functions for cumulative release

the calculation were approximately two orders of magnitude greater than doses presented in TSPA-95. The apparent extra dilution is believed to come from the model abstractions for interunit connectivity (Markovian particle approach) used in the DOE RIP code.

The model for radionuclide transport used in DOE TSPA-95 was compared to the model used in the NRC IPA Phase 2. In both models, particles moved along 1D flow paths representing either the fractures or the matrix in the Markovian particle approach (i.e., a particle starting in a given pathway-fracture or matrix—moves a distance Δx before transitioning to the other pathway). The time Δt for a particle to move Δx is sampled from an exponential distribution. Upon leaving a layer and entering the next, the process repeats itself until the particle translates all layers. The Phase 2 approach is similar, but particles move entirely through the layer in either the fracture or matrix flow paths, and only transition between layers.

The two models were compared for a four-layered unsaturated flow system using parameters typical of TSPA-95. Results for an instantaneous release of 5,000 particles showed obvious differences. The particle arrival times are much more spread out using the Markovian particle approach. The NRC

model would lead to a higher peak concentration at an earlier time. Conclusions from this analysis are that the Markovian particle approach may be taking unwarranted credit for diffusion between the fracture and matrix flow paths.

As a result of this work, it is recommended (Baca and Brient, 1996) that the DOE provide sufficient explanations of subsystem abstractions using basic physical factors and assess the potential optimism or conservatism of the abstracted models. Many abstractions appear prudent and defensible, but intermediate calculations and sensitivity studies would enhance reviewer understanding and confidence in the abstractions. One questionable abstraction is radionuclide transport along fractures. The Markovian particle approach used in TSPA-95 appears to neglect potential fast paths and, hence, it was recommended that alternative abstractions be pursued. The TSPA-VA (TRW Environmental Safety System, Inc., 1996) notes this recommendation and indicates that the DOE will be examining alternative modeling approaches.

8.3.2 Expert Elicitation

During this fiscal year, the staff issued a BTP on the formal use of expert elicitation in the HLW program. In the review of license applications, traditionally the NRC has accepted expert judgment in the evaluation and interpretation of the factual bases. Thus, it is expected that the NRC will give appropriate consideration to the judgments of the DOE experts regarding the geologic repository. In the BTP, designated NUREG-1563 (Kotra et al., 1996), the NRC staff proposed set forth technical positions that (i) provide general guidelines on those circumstances that may warrant the use of a formal process for obtaining the judgments of more than one expert (i.e., expert elicitation) and (ii) describe acceptable procedures for conducting expert elicitation when formally elicited judgments are used to support a demonstration of compliance with the NRC geologic disposal regulation.

In February 1996, the availability of a draft BTP for public comment was announced in the *Federal Register* (Nuclear Regulatory Commission, 1996). In its comments on the draft BTP, the DOE indicated it was in substantial agreement with the NRC staff technical positions (Brocoum, 1996). Moreover, the State of Nevada commented that the draft BTP was favorably responsive to earlier concerns regarding the DOE programmatic guidelines in this area (Loux, 1995). Thus, with issuance and acceptance of this guidance, the NRC staff was inclined to recommend a path to resolution of site characterization analysis comment no. 3 (Nuclear Regulatory Commission, 1989). Moreover, the staff also plans to review and possibly close open items related to expert elicitation.

The NRC and the DOE achieved a high level of agreement on an appropriate process for formal elicitations of expert judgment. For example, the DOE recently indicated to the Nuclear Waste Technical Review Board (NWTRB) that they plan to follow the NRC nine-step process (outlined in the BTP) in elicitations for the TSPA-VA (TRW Environmental Safety System, Inc., 1996). The recently issued DOE TSPA-VA (TRW Environmental Safety System, Inc., 1996) indicates that expert judgments will be used in a number of areas to supplement other sources of scientific and technical information.

8.3.3 Consolidated Document Management System

The CDOCS software was developed to provide the DWM technical staff with an enhanced computer capability for management, retrieval, and visualization of technical and regulatory information (DeWispelare et al., 1993). CDOCS Version 1.0 was documented and delivered to the NRC this fiscal

year. The NRC has a requirement for increased capability in making independent technical analysis to conduct prelicensing and licensing review activities.

CDOCS is intended to complement the technical computing capabilities of the NRC and the CNWRA technical staffs currently being provided by the Advanced Computer Review System. CDOCS provides the staffs with the capability to create, modify, and maintain documents containing both text and images in a full-text search and retrieval environment. This capability facilitates the capture of a broad spectrum of technical and regulatory materials making these available to the staffs to support work in the KTIs to resolve associated subissues, prepare for technical exchanges, review progress by the DOE, document concerns as open items, and track these open items.

As illustrated in figure 8-5, CDOCS uses a suite of commercial off-the-shelf (COTS) software combined by custom interface codes in a modern client-server network implementation supporting computers used by the NRC and the CNWRA staffs. The modular design of CDOCS allows for managed evolution of software products as their capabilities change over time. In figure 8-5, the database is continually updated by a custodian, to be then used by technical staff.

Currently, holdings in CDOCS include technical documents, technical document bibliographic headers, regulations, NUREGs, technical positions, regulatory records (compliance determination strategy and compliance determination method), and open items. CDOCS is implemented and available to staffs at the NRC and the CNWRA. Documents entered at either the NRC or the CNWRA are passed to servers at both locations for processing and inclusion into the local database. A synchronization process will be used to ensure that the NRC and the CNWRA databases are fully consistent.

8.3.4 Licensing Support System Pilot Program

The NRC License Support System (LSS) computer server test bed (LSSTB) was developed under a pilot program to evaluate the feasibility of a LSS concept using COTS technology. The LSSTB, accessible through the public Internet (outside the NRC network security firewall), will (i) provide a basic document search and retrieval capability from among a sample of HLW documents, (ii) allow downloading documents selected by the user, and (iii) obtain feedback from users by allowing on-line comments.

The CNWRA established a public Internet computer server site that can be accessed by commonly available World Wide Web (WWW) browsers (e.g., Netscape) as illustrated in figure 8-6. Authorization was obtained from the NRC before the server was placed on the Internet for public availability (URL: http://www.nrc.lsstb.gov). This server has an NRC LSSTB Home Page that was produced after design consultation with the NRC. The WWW server Home Page provides the user interface for searching the loaded-document repository. The WWW server application also provides for logging user comments and conducting four types of user searches (i.e., title, author, date, and document text). The server hardware uses a SUN workstation. The search and retrieval software used by the server is a COTS product that was quickly acquired.

The LSSTB was loaded with a sampling of documents from the HLW program including correspondence and SECY papers from the NRC Commission Data Tracking System, select CNWRA technical reports, and regulations. The goal of the LSSTB in FY97 is to provide downloading both text of documents and associated linked images, as well as provide a mechanism for users to submit/load pertinent documents. The full LSS will eventually document material of the DOE, the NRC, and others

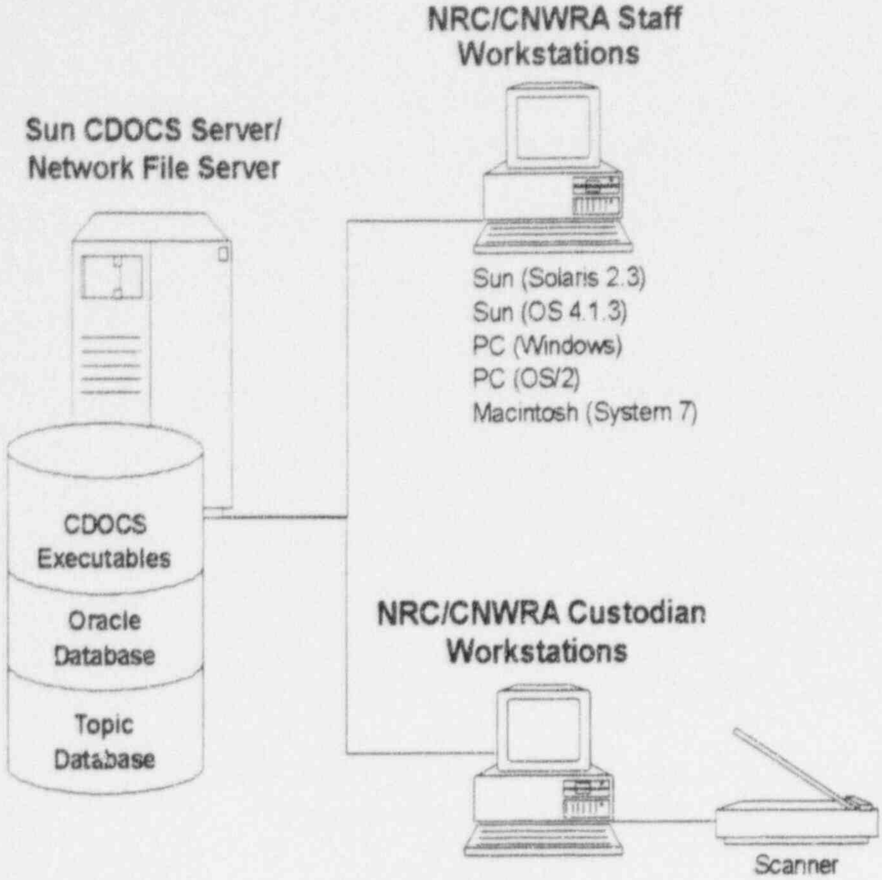

Figure 8-5. CDOCS architecture

to the HLW licensing proceeding that may be relevant to the license application review process. It is intended to facilitate the license review by supporting (i) electronic access to discoverable documents before the DOE license application is filled, (ii) early technical review of materials by all potential parties, and (iii) electronic transmission of all filings during the hearing.

8.4 ASSESSMENT OF PROGRESS TOWARD MEETING OBJECTIVES

The technical work conducted in the TSPA-95 audit review was completed in April 1996. Although all KTI teams participated, focus areas were chosen in four KTIs: Total System Performance Assessment and Integration, Unsaturated and Saturated Flow Under Isothermal Conditions, Thermal Effects on Flow, and Container Life and Source Term. Other KTI teams also provided technical comments that will be used in the detailed review of TSPA-95. Analyses performed for the audit review were discussed with the DOE in a technical exchange held on May 22–23, 1996. A letter summarizing the results of the audit review was sent to the DOE in July 1996 and a more detailed report of the analyses was transmitted to the DOE in September 1996. In addition, data collection and analyses on select topics were initiated as planned for the detailed review.

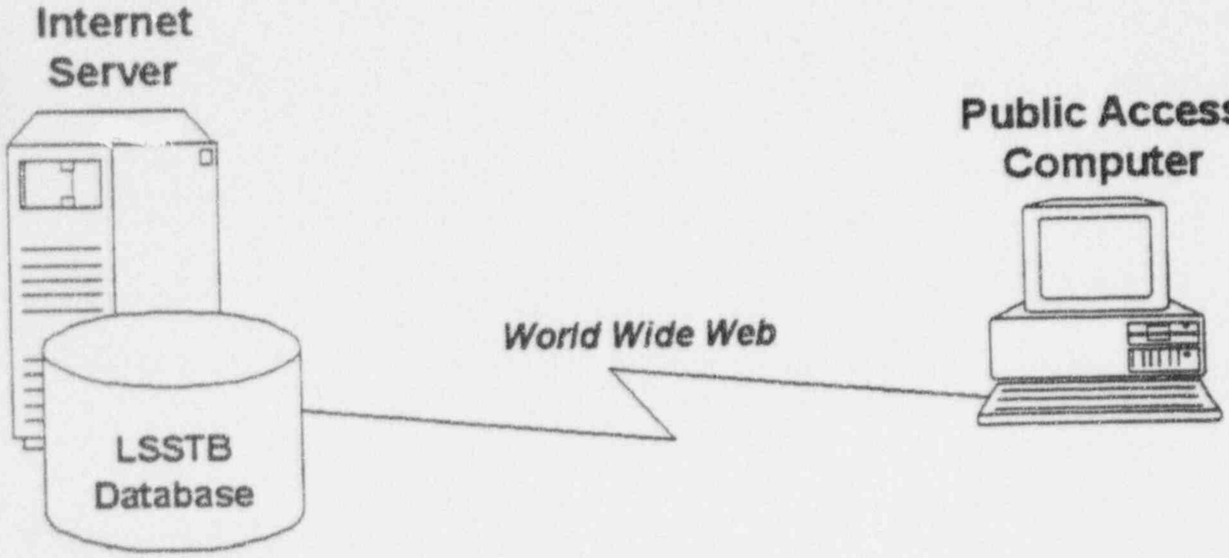

Figure 8-6. Licensing Support System Test Bed

A draft BTP on the Formal Use of Expert Elicitation in the High-Level Waste Program was issued for public comment in February 1996. Public comments were incorporated into a final version of the BTP that will be issued as NUREG-1563. The DOE provided favorable comments on the BTP and is expected to use this guidance in formal elicitations planned in FY97. The NRC staff believes that agreement has been achieved on an acceptable methodology for the formal use of expert elicitation. This acceptance is reflected in the recent DOE presentations to the NWTRB which states that the DOE will follow the elicitation procedure outlined in the NRC BTP. Additional work will be needed to develop guidance on acceptable techniques for aggregation of expert judgments.

Progress in scenario analysis methodology consisted of resolving three site characterization plan (SCP) comments: 101 (partial performance measures), 103 (Ross sequence numbers), and 115 (independence of scenario classes). Other comments about scenario analysis methodology were left open

and reasons explained: 95 (scenario development and screening) and 105 (justification for elimination of scenarios). Actions are based on a review of the DOE Mined Geologic Disposal License Application Annotated Outline distributed in March 1995. Results of this review were documented and sent to the DOE on March 28, 1996. This review helped provide some basic guidance to the DOE on an acceptable scenario analysis methodology. Specific disruptive scenarios needing to be considered in TSPAs, however, remain as a KTI subissue. Although the TSPA-95 contends that the volcanism and seismic disruption scenarios have been previously analyzed and found not to be of sufficient consequence, the DOE plan for the TSPA-VA (TRW Environmental Safety System, Inc., 1996) indicates these scenarios will be addressed.

Progress in developing an independent TSPA technical assessment capability was primarily concerned with modifying the IPA Phase 2 TPA code so it could be used in detailed reviews of the TSPA-95 and TSPA-VA (TRW Environmental Safety System, Inc., 1996). The TPA code is being updated to evaluate the latest repository designs and site characterization data. Assistance is also being provided to other KTI teams to develop updated modules to be added to the TPA code. Presently, the TPA code can run on a SUN workstation as well as on a Cray supercomputer. To make the code more user friendly, the TPA code is being modified to facilitate its general use in the evaluations of the remaining NRC KTIs and the corresponding DOE WCIS attributes.

8.5 INTEGRATION WITH OTHER KEY TECHNICAL ISSUES

Activities Related to Development of the EPA YM Standard KTI: The major input to the this KTI from TSPAI KTI was a scoping study for a human intrusion scenario. This and other scoping studies are expected to be included in a NUREG report. The information contained in the NUREG is planned to provide the basis for revising the NRC technical criteria for consistency with the EPA YM Standard. Information from the EPA Standard KTI includes tentative definitions of the reference biosphere used to guide near future TSPA calculations and likely criteria to be considered for dose and performance assessment (PA).

Unsaturated and Saturated Flow under Isothermal Conditions KTI: This KTI provided analyses for two focus topics to the audit review of TSPA-95 infiltration and dilution. Integration will continue with this KTI through the detailed review and the independent TSPA technical assessment capability effort. Using available geochemical data, the TSPAI KTI is working with this KTI to develop updated percolation flux distributions for the base case and pluvial climate case, groundwater dilution, and mixing parameters.

Container Life and Source Term (CLST) KTI: This KTI developed the Engineered Barrier System Performance Assessment Code (EBSPAC) (Mohanty et al., 1996) that will be used in the detailed review of TSPA-95 and as an integrated module within the TPA code. The CLST KTI also provided the results of technical evaluations as part of the audit review of TSPA-95. Because of FY97 budget reductions, no further development of EBSPAC code will be performed; maintenance and application of the code will be conducted under the TSPAI KTI. Discontinuance of EBSPAC code development is expected to limit the ability to independently review aspects of the DOE WP performance in the forthcoming TSPA-VA (TRW Environmental Safety System, Inc., 1996) report.

Evolution of the Near-Field Environment KTI: This KTI provided models and data to EBSPAC to be used within the TPA code. Insight gained from exercising the TPA code will be transmitted to the KTI regarding the relative importance of parameters and phenomena associated with the near-field

environment. This KTI will also prepare input to radionuclide transport models that will be incorporated in the TPA code.

Repository Design and Thermal-Mechanical Effects KTI: This KTI primarily focused on postclosure thermal-mechanical effects but also considered preclosure aspects such as drift stability and retrievability of the waste. As a result of FY97 budget reductions, the preliminary study of drift stability under thermal and seismic loads will be completed under the TSPAI KTI and, no further work on preclosure PA will be conducted. This will impact TPA code development in regards to repository system changes that occur during the 100–150 yr operational phase.

Igneous Activity KTI: This KTI prepared probability estimates for various types of igneous occurrences and is developing the modeling theory for eruption style and radionuclide transport. This model will be used to determine the contribution to risk from igneous activity through the airborne pathway. If this contribution is significant, the model will become part of the VOLCANO module in the TPA code.

Structural Deformation and Seismicity KTI: This KTI prepared an updated hydrostratigraphy for use in the detailed review of TSPA-95 and as input to the TPA code. The KTI developed the FAULTING module for evaluating the impact of fault displacement on WP lifetime. If fault displacement is found to contribute significantly to risk, the module will be added to the TPA code.

Thermal Effects on Flow KTI: This KTI furnished input to the audit review of TSPA-95 and will give additional information for the detailed review, as well as for the TPA code. Specifically, the KTI provided time-dependent WP temperature and RH for typical repository conditions under different AMLs.

Radionuclide Transport KTI: This KTI contributed to the audit review by using geochemical data to support estimates of mixing in the saturated zone. The KTI developed a geographic information system specific to hydrologic flow and transport. This was then combined with existing geographic information system coverages of geology and structure to support the detailed review. Because of budget reductions in FY97, no further work will be performed on determination of radionuclide transport properties (e.g., sorption and solubility) and dependence on such factors as pore fluid chemistry, mineralogy, and flow regime. Termination of this work will limit the NRC capability to review the DOE data and the appropriateness of certain input assumptions that may be used in the TSPA-VA (TRW Environmental Safety System, Inc., 1996).

8.6 REFERENCES

ABAQUS. 1995. *Theory and User Manuals*. Pawtucket, RI: Kibbitt, Karsson & Sorensen.

Baca, R.G., R.D. Manteufel, S. Mohanty, S.A. Stothoff, and G.W. Wittmeyer. 1994. Performance assessment research. *NRC High-Level Radioactive Waste Research at CNWRA, July–December 1993*. B. Sagar, ed. CNWRA 93-02S. San Antonio, TX: Center for Nuclear Waste Regulatory Analyses: 7-1 to 7-29.

Baca, R.G., and R.B. Brient, eds. 1996. *Total System Performance Assessment—1995 Audit Review*. Letter Report. San Antonio, TX: Center for Nuclear Waste Regulatory Analyses.

Brocoum, S.J. 1996. U.S. Department of Energy/Office of Civilian Radioactive Waste Management, Letter to U.S. Nuclear Regulatory Commission. *U.S. Department of Energy Comments on the U.S. Nuclear Regulatory Commission Draft Branch Technical Position on the Formal Use of Expert Elicitation in the High-Level Waste Program*. Las Vegas, NV: Yucca Mountain Site Characterization Office.

DeWispelare, A.R., R.D. Johnson, R.L. Marshall, and J.H. Cooper. 1993. *Development Plan for PASS/PADB System Design Version 3.0*. CNWRA 93-011. San Antonio, TX: Center for Nuclear Waste Regulatory Analyses.

Gelhar, L.W. 1993. *Stochastic Subsurface Hydrology*. Englewood Cliffs, NJ: Prentice Hall, Inc.

Gelhar, L.W., A. Mantoglou, C. Welty, and K.R. Rehfeldt. 1985. *A Review of Field-Scale Physical Solute Transport Processes in Saturated and Unsaturated Porous Media*. EPRI EA-4190. Palo Alto, CA: Electric Power Research Institute.

Golder Associates, Inc. 1993. *Application of the RIP (Repository Integration Program) to the Proposed Repository at Yucca Mountain: Conceptual Model and Input Data Set*. Redmond, WA: Golder Associates, Inc.

Johnson, R.L. 1993. *Overall Review Strategy for the Nuclear Regulatory Commission's High-Level Waste Repository Program*. NUREG-1323, Rev. 0. Washington, DC: Nuclear Regulatory Commission.

Kotra, J.P., M.P. Lee, N.A. Eisenberg, and A.R. DeWispelare. 1996. *Branch Technical Position on the Use of Expert Elicitation in the High-Level Waste Program*. NUREG-1563. Washington, DC: Nuclear Regulatory Commission.

Lawrence Livermore National Laboratory. 1995. *Scientific Investigation Plan for Yucca Mountain Project (YMP) WBS ELEMENT 1.2.2.5.1. Metal Barrier Selection and Testing*. SIP-CM-01, Rev. 2. Livermore, CA: Lawrence Livermore National Laboratory.

Loux, R.R. 1995. State of Nevada/Agency for Nuclear Projects, Letter to U.S. Nuclear Regulatory Commission. *Principles and Guidelines for Formal Use of Expert Judgement by the Yucca Mountain Site Characterization Project Office and Resolution of Site Characterization Analysis Comment 3*. Carson City, NV: Nuclear Waste Project Office.

Mohanty, S., G.A. Cragnolino, T. Ahn, D.S. Dunn, P.C. Lichtner, R.D. Manteufel, and N. Sridhar. 1996. *Engineered Barrier System Performance Assessment Code: EBSPAC Version 1.0 β, Technical Description and User's Manual*. CNWRA 96-011. San Antonio, TX: Center for Nuclear Waste Regulatory Analyses.

Nuclear Regulatory Commission. 1989. *NRC Staff Site Characterization Analysis of the Department of Energy's Site Characterization Plan, Yucca Mountain, Nevada*. NUREG-1347. Washington, DC: Nuclear Regulatory Commission.

Nuclear Regulatory Commission. 1995. *NRC Iterative Performance Assessment Phase 2: Development of Capabilities for Review of a Performance Assessment for a High-Level Waste Repository.* NUREG-1464. Washington, DC: Nuclear Regulatory Commission.

Nuclear Regulatory Commission. 1996. Availability of draft branch technical position on the use of expert elicitation in the high-level waste program. *Federal Register* 61(40): 7,568–7,569.

Pruess, K. 1987. *TOUGH User's Guide*. LBL-20700. Berkeley, CA: Lawrence Berkeley Laboratory.

Pruess, K. 1991. *TOUGH2—A General-Purpose Numerical Simulator for Multiple Fluid and Heat Flow.* LBL-29400. Berkeley, CA: Lawrence Berkeley Laboratory.

Sagar, B., and R.W. Janetzke. 1993. *Total System Performance Assessment Computer Code: Description of Executive Module (Version 2.0).* CNWRA 93-017. San Antonio, TX: Center for Nuclear Waste Regulatory Analyses.

Schenker, A.R., D.C. Guerin, T.H. Robey, C.A. Rautman, and R.W. Barnard. 1995. *Stochastic Hydrogeologic Units and Hydrogeologic Properties Development for Total-System Performance Assessments.* SAND94-0244. Albuquerque, NM: Sandia National Laboratories.

Seth, M.S., and P.C. Lichtner. 1996. *User's Manual for MULTIFLO.* CNWRA 96-005. San Antonio, TX: Center for Nuclear Waste Regulatory Analyses.

TRW Environmental Safety Systems, Inc. 1995. *Total System Performance Assessment—1995: An Evaluation of the Potential Yucca Mountain Repository.* B00000000-01717-2200-00136, Las Vegas, NV: TRW Environmental Safety Systems, Inc.

TRW Environmental Safety Systems, Inc 1996. *Total System Performance Assessment—Viability Assessment (TSPA-VA) Plan.* B00000000-01717-2200-00179, Las Vegas, NV: TRW Environmental Safety Systems, Inc.

U.S. Department of Energy. 1994. *Initial Summary Report for Repository/Waste Package Advanced Conceptual Design.* CRWMS M&O Document DOC No. B00000000-01717-5705-00015. Rev. 00. Las Vegas, NV: TRW Environmental Safety Systems, Inc.

Whitfield, M.S., E.P. Eshom, W. Thordarson, and D.H. Schaefer. 1985. *Geohydrology of Rocks Penetrated by Test Well USW H-4, Yucca Mountain, Nye County, Nevada.* Water-Resources Investigations Report WRI-85-4030. Denver, CO: U.S. Geological Survey.

Wilson, M.L., J.H. Gauthier, R.W. Barnard, G.E. Barr, H.A. Dockery, E. Dunn, R.R. Eaton, D.C. Guerin, N. Lu, M.J. Martinez, R. Nilson, C.A. Rautman, T.H. Robey, B. Ross, E.E. Ryder, A.R. Schenker, S.A. Shannon, L.H. Skinner, W.G. Haley, J.D. Gansemer, L.C. Lewis, A.D. Lamont, I.R. Triay, A. Meijer, and D.E. Morris. 1994. *Total-System Performance Assessment for Yucca Mountain—SNL Second Iteration (TSPA-93).* SAND93-2675. Albuquerque, NM: Sandia National Laboratory.

Wittwer, C., G. Chen, G.S. Bodvarsson, M. Chornack, A. Flint, L. Flint, E. Klicklis, and R. Spengler. 1995. *Preliminary Development of the LBL/USGS Three-Dimensional Site Scale Model of Yucca Mountain, Nevada.* LBL-37356, UC-814. Berkeley, CA: Lawrence Berkeley Laboratory.

Zyvoloski, G., Z. Dash, and S. Kelkar. 1995. *FEHM 1.0, Finite Element Heat and Mass Transfer Code.* LA-12062-MS, Rev.1. Los Alamos, NM: Los Alamos National Laboratory.

9 ACTIVITIES RELATED TO DEVELOPMENT OF THE U.S. ENVIRONMENTAL PROTECTION AGENCY YUCCA MOUNTAIN STANDARD[1]

Primary Authors: *P.C. Mackin, M.P. Lee, M.S. Jarzemba, R.G Baca, T.J. McCartin, and R.B. Codell*

Technical Contributors: *R.G. Baca, M.S. Jarzemba, P.A. LaPlante, P.C. Mackin, R.D. Manteufel, G.W. Wittmeyer, J.W. Bradbury, R.E. Cady, R.B. Codell, N.M. Coleman, B.J. Davis, J.R. Firth, J. Kotra, M.P. Lee, T.J. McCartin, S.M. McDuffie, R.B. Neel, R. Abu-Eid, C.W. Reamer, J.S. Trapp, and R.G. Wescott*

Key Technical Issue Co-Leads: *R.G. Baca (CNWRA) and T.J. McCartin (NRC)*

9.1 INTRODUCTION

Through the Energy Policy Act of 1992 (EnPA — Public Law 102-486), Congress directed the U.S. Environmental Protection Agency (EPA) to promulgate new environmental standards applicable to a potential geologic repository for high-level radioactive waste (HLW) at Yucca Mountain (YM). The EnPA stipulates that new EPA Standards be based on and consistent with the recent findings and recommendations of the National Academy of Sciences (NAS) (National Research Council, 1995). Once final standards are promulgated, the EnPA directs the NRC to modify its requirements in 10 CFR Part 60 to conform to the new EPA Standards. Under the EnPA, the Nuclear Regulatory Commission (NRC) has one year to make the necessary modifications.[2]

To support technical bases for revised disposal standards for YM, section 801(a)(2) of the EnPA directed NAS to provide EPA with recommendations on the following issues

- Whether health-based standards based on doses to individual members of the public from releases to the accessible environment . . . will provide a reasonable standard for protection of the health and safety of the general public.

- Whether it is reasonable to assume that a system of postclosure oversight of the proposed repository can be developed, based on active institutional controls, that will prevent an unreasonable risk of breaching the repository engineered or geologic barriers or increasing the exposure of individual members of the public to radiation beyond allowable limits.

---

[1]Revision to EPA HLW standard is currently under consideration. The NRC will need to consider revision to its geologic disposal regulation after a new EPA Standard for YM is promulgated. The information presented in the following chapter is not intended to convey a preference or position of the NRC or the CNWRA staffs regarding how either of these two regulations might be revised.

[2]In addition to recent NAS recommendations, Congress is contemplating other legislative proposals that would affect regulation of HLW at YM. See summary pp 46–48 in Nuclear Waste Technical Review Board (1995).

- Whether it is possible to make scientifically supportable predictions of the probability that the repository engineered or geologic barriers will be breached as a result of human intrusion over a period of 10,000 yr.

In August 1995, NAS issued its findings and recommendations on a revised environmental standard for HLW disposal. The NRC staff is coordinating with EPA to ensure development of reasonable and implementable HLW standards, considering the recommendations of NAS. Once EPA issues its final standards, the NRC must conform its regulations accordingly.

Important differences exist among NAS findings and recommendations, prior EPA Standards for HLW, and existing geologic disposal regulations in 10 CFR Part 60. Through the Activities Related to Development of the EPA Yucca Mountain Standard Key Technical Issue (KTI), the NRC staff is conducting requisite technical analyses to review and comment on EPA revised environmental standards, especially in those areas not addressed by previous HLW regulations. Some of the key subissues for evaluating a revised EPA Standard are (i) definition of the compliance period and the associated approach used in compliance calculation; (ii) specification of the exposure scenarios; (iii) treatment of disruptive events; and (iv) evaluation of the effects of human intrusion. Using its Iterative Performance Assessment (IPA) capability, the NRC staff and its technical assistance contractor—the Center for Nuclear Waste Regulatory Analyses (CNWRA)—undertook a series of focused technical analyses in FY96 to assess these subissues. Results of these analyses were documented by the respective staffs and are summarized in this report.

The primary objectives for this KTI are to (i) support the NRC in their interactions with the EPA regarding the development of an EPA Standard for the YM site and (ii) subsequent to promulgation of the EPA standard to assist in developing the technical bases for future revisions to NRC regulations required to conform with the new EPA Standard. As noted previously, a number of subissues have been defined that must be addressed to resolve the primary objective by providing specific staff assessment capabilities. These subissues are discussed in the following paragraphs.

- Defining a Compliance Period and Method: The current compliance period in the remanded HLW standards is 10,000 yr. NAS recommendations noted that long-term stability of the geologic setting at YM is on the order of one million years and recommended that compliance be evaluated for the time of peak risk. Selection of the appropriate compliance period must consider the recommendations of NAS as well as regulatory precedent and available assessment techniques. The specific assessment criterion (e.g., mean or median of dose to a specified group or individual) must also be specified.

- Selecting a Critical Group(s): Adoption of the NAS recommended critical group approach requires consideration of reference biosphere(s) and exposure pathways. There are numerous options for critical group parameter specifications, each presenting particular technical and regulatory uncertainties.

- Evaluating Results of Potential Human Intrusion: NAS determined there was no scientific basis for predicting the occurrence of human intrusion subsequent to repository closure and recommended that a stylized calculation be made to provide an indication of the resiliency of repository performance to such intrusions. The current regulations include requirements for considering human intrusion within the context of unanticipated processes and events which apply only to the containment limits for sites other than YM, Nevada. NAS

recommendations would require a consequence analysis for human intrusion to measure the resilience of the repository as measured by individual risk. The NRC must be able to evaluate the adequacy of any such stylized scenario calculation.

- Considering Disruptive Events: While NAS noted that the geologic setting in the YM area should be stable for approximately one million years, certain processes could occur in the region which might affect repository performance. These processes may include seismicity, volcanism, and climate change. Criteria for screening these processes and incorporating their effects into assessments of proposed repository performance must be evaluated.

To varying degrees, all of these issues were addressed in FY96. The following sections of this report detail the extent of these activities and their results.

9.2 OBJECTIVES AND SCOPE OF WORK

The previously applicable EPA environmental standards and the current NRC implementing regulations are somewhat different from the proposals for a health-based standard (e.g., limiting individual dose or risk) suggested by the EnPA. 40 CFR Part 191 establishes containment requirements that limit the releases of radioactive material to the accessible environment, weighted by a factor approximately proportional to radiotoxicity, and integrated over a period of time (e.g., a span of 10,000 yr is the current regulatory requirement) after permanent closure of the geologic repository. 10 CFR Part 60 incorporates 40 CFR Part 191 as the overall performance requirement for a geologic repository. The requirements in 10 CFR 60.112 establish an overall system performance objective that supports EPA containment requirements, whereas certain other sections (10 CFR 60.113) set forth subsystem performance objectives.[3]

The forthcoming revisions to both the EPA Standards and the NRC conforming regulations notwithstanding, it is expected that the NRC regulations will continue to require compliance with applicable EPA environmental standards as the overall system performance objective for the proposed repository, and that demonstration of compliance with this objective will necessitate a quantitative performance assessment (PA) to estimate postclosure performance of the repository system.

Among the NAS findings and recommendations is a key recommendation that the revised standard limit individual risk to a member of the public and abandon the existing quantitative release limit with its implied population protection basis. Specifically, NAS recommended that the level of protection provided by the new environmental standard be comparable to that level of risk considered acceptable to society at large, given that society currently tolerates certain *involuntary* risks (e.g., in the range of 10^{-5} to 10^{-6} fatalities per year). To demonstrate that the proposed geologic repository can be designed to provide comparable protection to society, NAS therefore recommended that assessments of individual risks be conducted for certain target populations in the YM vicinity, using the approach specified in 1985 by

[3]The use of subsystem performance objectives is consistent with the Commission multiple barrier, defense-in-depth concept. At their time of inclusion in 10 CFR Part 60, these criteria were viewed as important contributors to the NRC ability to find, with reasonable assurance, that the EPA Standards would be met.

the International Commission on Radiological Protection (ICRP) (e.g., "critical groups").[4] As EPA considers this particular recommendation, the NRC staff is evaluating how a PA methodology, used to demonstrate compliance with its implementing regulation, might be revised to accommodate such a standard. Anticipating that some type of dose-based standard will be adopted, the NRC has begun to evaluate methodologies for implementing such a standard to provide some insights into the subissues cited previously. For these reasons, the efforts of NRC staff in FY96 focused on the objectives presented in the following paragraphs.

Defining a Compliance Period and Method

> The objective for work on this subissue in FY96, was to provide some initial analyses of techniques for evaluating an appropriate compliance period. There is regulatory precedent related to this issue and selecting a compliance period that represents a departure from that precedent would require a supporting rationale. Accordingly, a comparative analysis of the hazards presented by a HLW repository and an equivalent uranium ore body was conducted. This comparative analysis provides insights on radiological hazard as a function of time and therefore supports decisions concerning an appropriate compliance period. A peak dose calculation was also completed, providing additional information on appropriate compliance determination periods and methods to be used in reviewing a proposed revised EPA Standard for YM.

Selecting a Critical Group(s)

> In FY96, efforts by the NRC focused on determining whether sufficient information exists to support identifying a critical group (or groups) for the Yucca Mountain region (YMR). Specific items addressed included (i) evaluation of the applicability of the critical group concept to the YMR, (ii) discussions with EPA staff to determine whether early drafts of the revised environmental standard would be compatible with the critical group concept, (iii) analysis of wells and water usage in the YMR to provide information related to lifestyles and exposure pathways, (iv) evaluation of approaches to defining exposure scenarios and reference biospheres, (v) reviews of previously compiled data on exposure pathways at YM, and (vi) considerations of the appropriate level of specificity to be used for including critical group parameters in a revised EPA Standard for YM.

Evaluating Results of Potential Human Intrusion

> The FY96 effort on this subissue was limited to examining whether using a stylized human intrusion scenario for the purpose of evaluating the resiliency of a repository to such intrusion was implementable through a revised EPA Standard for YM. Scoping calculations and evaluations were conducted for this purpose.

---

[4]The term dose generically refers to the quantity of radiation energy absorbed by body organs or tissue. The NRC defines dose for its regulatory purposes in 10 CFR Part 20. In its recommendations, the NAS adapts the ICRP terminology to its proposed risk-based framework.

In FY96, techniques for assessing the effects of volcanic disruption on the proposed repository were evaluated through refined modeling of the dispersion of radionuclides as a result of such disruption. The calculations included doses to persons who might reside at various distances from a proposed YM repository. These calculations could also assist in identifying the critical group. This assessment of volcanic disruption provides an example of methods that can be used to evaluate the incorporation of other disruptive events in a revised EPA Standard for YM.

These four particular topics were selected for study because they (i) provided some preliminary insights into NAS recommendations; (ii) focused on the major implementation issues that the Commission would need to address as it reviews and comments on a revised EPA Standard, and (iii) could be completed within the time constraints.

9.3 SIGNIFICANT TECHNICAL ACCOMPLISHMENTS

This section describes the technical accomplishments for the EPA Standard KTI during FY96. The significant technical accomplishments described herein are (i) scoping calculations that were performed to support the NRC review and comment on technical issues associated with a dose-based standard, (ii) documentation of investigations related to critical group(s) and reference biosphere, and (iii) documentation of background information to support the assessment of a stylized human intrusion calculation that may be required by a revised EPA Standard for YM.

9.3.1 Scoping Calculations for Interactions with the Environmental Protection Agency

The following sections provide short summaries of the analyses that are being published as NUREG-1538.[5]

9.3.1.1 Relative Hazards of High-Level Waste Over Long Time Periods

The time period of regulatory concern for geologic disposal of HLW is an issue that has been discussed and debated for well over 20 yr. The NAS recently recommended (National Research Council 1995)

> . . . [the] calculation of the maximum risks of radiation releases whenever they occur as long as the geologic characteristics of the repository environment do not change significantly. The time scale for long-term geologic processes at YM is on the order of approximately one million years.

NAS also stated that probably the most significant difference between their findings and recommendations and the existing HLW standard is the time period of regulatory interest (TPI) (National Research Council, 1995). Based on recent total system performance assessment (TSPA) studies, the time of maximum risk

---

[5]Nuclear Regulatory Commission. 1996. *Preliminary Performance Assessment Analyses Relevant to Dose-Based Performance Measures*. In preparation. NUREG-1538. Washington, DC: Nuclear Regulatory Commission.

may well be hundreds of thousands of years into the future (e.g., TRW Environmental Safety Systems, Inc., 1995). This NRC/CNWRA study examines one basis for limiting the time period of concern—the natural decrease in gross radioactivity and radiological hazard from a geologic repository hazard with time that results from radioactive decay.

A number of studies have examined the technical bases for limiting the TPI (Environmental Protection Agency, 1985; 1982a,b). Natural decay of the waste, in conjunction with other considerations, was used to support the limited time period for regulatory concern in the since-remanded standard 40 CFR Part 191. The 1985 version of the EPA Standard contained both a 1,000 yr time period for individual protection requirements and a 10,000 yr time period for the cumulative release requirement. A court remanded this regulation requesting (among other things) a more thorough explanation of the reasons underlying the choice of a 1,000 yr regulatory period. In 1993, EPA extended the time period for individual protection to 10,000 yr on the basis that it would encourage the selection of a good disposal site and robust barriers, but not because it was deemed necessary to ensure adequate protection for the environment or the public (Environmental Protection Agency, 1993a; 1993b).

A scoping study compared the variation in total radioactivity and radiological hazard for a geologic repository containing 70,000 MTU of spent nuclear fuel (SNF[6]) and a hypothetical equivalent uranium ore body, over a one hundred million year time period. The hypothetical ore body is defined to have the same amount of uranium and occupy the same volume as the proposed geologic repository at YM. The primary difference between the potential geologic repository and the hypothetical ore body is that repository waste has a significant man-made radioactive hazard (through neutron irradiation and fissioning) compared to the hazard from the ore body that is from naturally occurring nuclides.

In calculating the relative radiological hazard, the staff assumed the primary hazard would be from drinking contaminated groundwater, where the contamination was predicted using modeling assumptions and data specific to YM. The model consisted of steadily percolating groundwater flowing through the repository and into the saturated zone. Some of the percolating groundwater contacted some of the waste packages (WP). The water that contacted the waste became contaminated with radionuclides. For the analyses, 43 different radionuclides were considered from ten to one hundred million years after irradiation (Lozano et al., 1994). The drinking water pathway dose conversion factors (DCF_{dw}) were based on previously published results (Environmental Protection Agency, 1988; Department of Energy, 1988) and an assumed drinking rate of two L/d. The solubilities of the radionuclides were modeled with probability distributions based largely on earlier TSPA work (Wilson et al., 1994; Nuclear Regulatory Commission, 1995). The release of radionuclides was modeled as either solubility limited or rate limited. The limiting radionuclide release rate was based on subsystem requirements in 10 CFR 60.113 (Nuclear Regulatory Commission, 1995). The relative radiological hazard was defined as a ratio of doses

[6]The principal waste forms to be disposed at YM will be SNF and vitrified waste. Other waste forms that may possibly be disposed include low-level, greater than class C, or transuranic wastes. Only SNF was considered for this analysis.

$$\frac{D_{dw,rep}}{D_{dw,ob}} = \frac{\sum_i DCF_i \ \min(sol_{i,rep} \cdot F_g \cdot A_i \ , \ R_{i,rep} \cdot F_w \cdot I_{i,rep}/Q)}{\sum_i DCF_i \ \min(sol_{i,ob} \cdot F_g \cdot A_i \ , \ R_{i,ob} \cdot F_w \cdot I_{i,ob}/Q)} \tag{9-1}$$

where

$D_{dw,rep}$ = dose from drinking groundwater contaminated by the repository (rem/yr)
$D_{dw,ob}$ = dose from drinking groundwater contaminated by the ore body (rem/yr)
DCF_i = dose conversion factor from drinking groundwater contaminated by the i^{th} radionuclide [(rem/yr)/(Ci/L)]
$sol_{i,rep}$ = solubility of the i^{th} radionuclide in 70,000 MTU of waste (mol/L)
$sol_{i,ob}$ = solubility of the i^{th} radionuclide in hypothetical ore body (mol/L)
F_g = fraction of seeping groundwater that becomes contaminated (2 percent)
F_w = fraction of waste inventory that is contacted by groundwater (1 percent)
A_i = activity of the i^{th} radionuclide (Ci/mol)
$R_{i,rep}$ = maximum release rate for the i^{th} radionuclide in 70,000 MTU of waste (1/yr)
$R_{i,ob}$ = maximum release rate for the i^{th} radionuclide in hypothetical ore body (1/yr)
$I_{i,rep}$ = total inventory of i^{th} radionuclide in 70,000 MTU of waste (Ci)
$I_{i,ob}$ = total inventory of i^{th} radionuclide in hypothetical ore body (Ci)
Q = volumetric flow rate of groundwater through the repository/ore body (L/yr)

The minimum operator is used in Eq. (9-1) to select either solubility or rate limited release.

Figure 9-1 shows the range of relative radiological hazard due to uncertainties in radionuclide solubilities and release rates. For both the spent fuel repository and the hypothetical ore body, 100 distinct estimates were generated by sampling the radionuclide solubilities and release rates [the common logarithm of the release rate was assumed to be −5 with a standard error of 0.5 based on previous staff work (Nuclear Regulatory Commission, 1995)].

The relative radiological hazard of the spent fuel repository is initially about four orders of magnitude greater than that of the hypothetical ore body. The radiological hazard diminishes rapidly over the first few hundred to few thousand years. The relative hazard diminishes by 90 percent at 100 yr, 99 percent at about 1,000 yr, and 99.9 percent at 10,000 yr. By 10,000 yr, the relative radiological hazard will be within an order of magnitude of the hypothetical ore body. The apparent increase in hazard at 100,000 to 500,000 yr is due to the ingrowth of radionuclides such as ^{230}Th, ^{229}Th, ^{226}Ra, and ^{210}Pb. A TPI for a proposed repository of about 10,000 yr would therefore focus attention on the time period when the waste has a significant man-made hazard component that is readily discernable from a hypothetical ore body, even after considering uncertainties associated with solubilities and release rates. The findings of this study are consistent with those of earlier studies (Environmental Protection Agency, 1982a, 1985).

9.3.1.2 Preliminary Calculations of Expected Dose from Extrusive Volcanic Events at Yucca Mountain

The purpose of this analysis was to demonstrate a calculational technique and provide a preliminary estimate of radiation doses for an extrusive volcanic scenario at YM. Calculations are based in part on a probabalistic volcanic ash (tephra) distribution model developed by Suzuki (1983) and

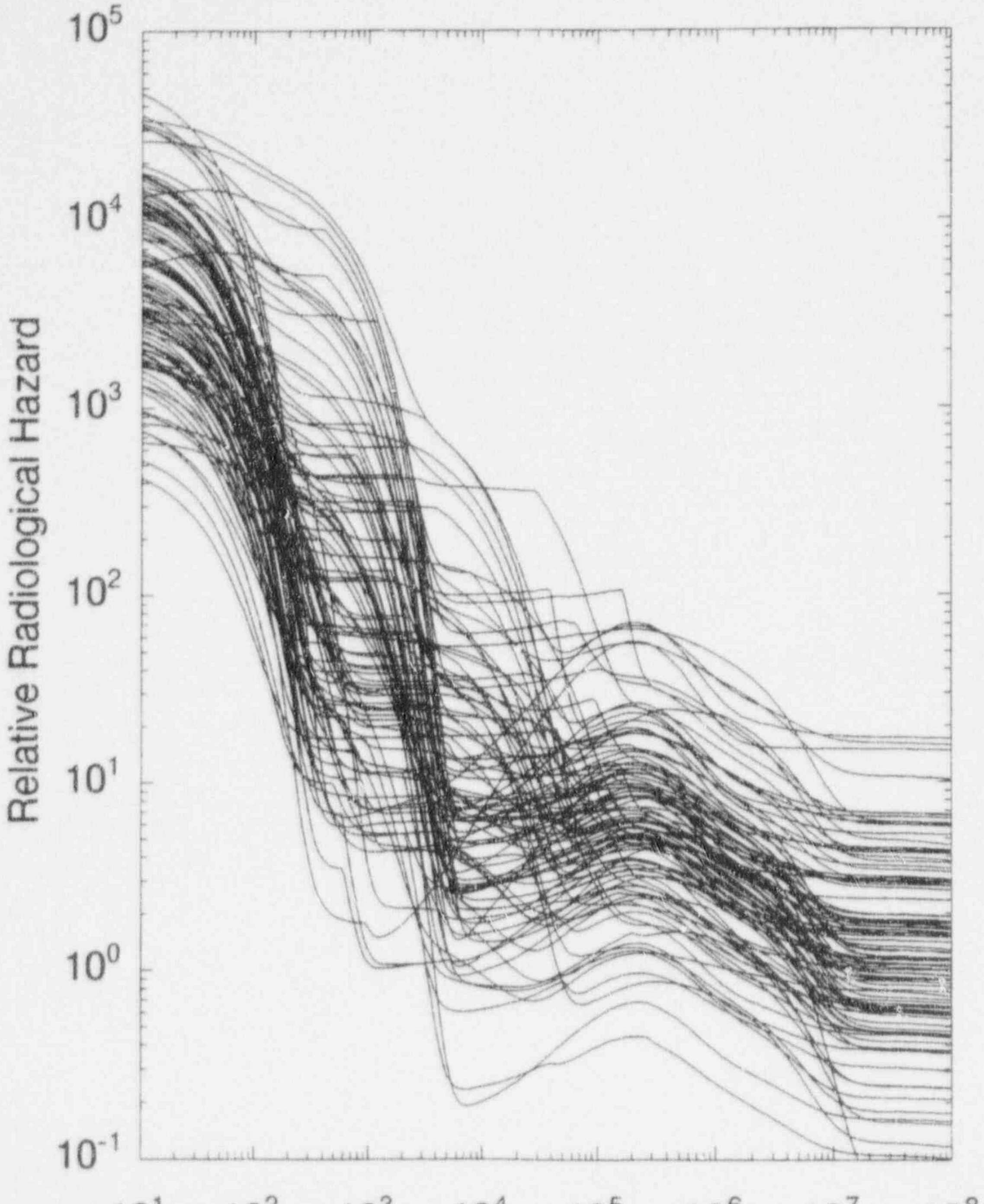

Figure 9-1. Comparison of spent nuclear fuel repository and hypothetical uranium ore body hazards accounting for uncertainties in radionuclide solubilities and release rates

extended by Jarzemba (1995). In addition, a new model for distributing only SNF within the ash particles has been developed to more realistically (than previous methods) model radionuclide distributions on the earth surface after a volcanic event. Dose modeling of radiation exposures from the contaminated ash blanket has also been performed. The dose pathways considered in these analyses were (i) ingestion from contaminated animal products and crops, (ii) inhalation from resuspension, and (iii) external radiation. Dose Conversion Factors (DCFs) as a function of these most important pathways, and as a total of all the pathways, were derived for contaminated soil for a hypothetical critical group resident at selected dose points on the earth surface [i.e., 20, 25, and 30 km directly south from the proposed repository (down gradient)] immediately after the volcanic event occurs. The extrusive volcanism analysis was performed for two different TPIs: 10,000 yr (current HLW regulations) and one million years (NAS proposed time frame).

The progression of events in the exposure scenario is as follows:

- Magma enters the repository and becomes contaminated with SNF particles.

- Contaminated magma forms into contaminated ash. The level of contamination of these particles is a function of the particle size (described in NUREG-1538).

- Eruption parameters are sampled according to the procedure given in Jarzemba (1995).

- The eruption column and contaminant plume form and produce volcanic ash fallout at distances and directions as determined in Jarzemba (1995).

- Doses are received by a member of the hypothetical critical group at specified dose points.

It is assumed the critical group member is exposed immediately after the particle plume deposits the contaminated ash blanket. The critical group in these investigations is composed of a single Amargosa Desert-type farmer/rancher at points 20, 25, and 30 km directly south of the proposed repository. For these preliminary analyses no other critical groups were investigated. NUREG-1538 contains a description of the lifestyle of this critical group. In addition, the following four assumptions were used:

- Volcanic ash dispersal model and parameter ranges described in Jarzemba (1995) are valid for modeling volcanic ash dispersals at YM.

- Doses are calculated for an Amargosa Desert farmer/rancher as described in LaPlante et al. (1995) with all of the associated assumptions and limitations.

- Selected dose points describe reasonable possible locations of the critical group.

- Assumptions used in modeling the SNF transport and subsequent dose calculations detailed in NUREG-1538 are valid.

Expected doses and standard deviations were calculated for the three dose points and the two TPIs. These results show a generally decreasing dose with distance from the location of the volcanic event (table 9-1). Increasing the TPI from 10,000 yr to one million years generally appears to increase the expected value of the peak effective dose equivalent by a factor of 2 to 4, although the magnitude of this change is somewhat uncertain because of the large standard deviation of the estimates. These results affirm

that by increasing the TPI, the importance of low-probability, high-consequence events such as volcanism is significantly enhanced when compared with scenarios that are certain to occur, such as an undisturbed repository leaching small amounts of radionuclides to the water table with subsequent drinking water pathway doses.

9.3.1.3 Dilution Analyses

Groundwater dilution is expected to be an issue of key importance in assessing the YM site because it directly determines the degree of dose reduction. For example, if mixing a contaminant stream with groundwater flow in the tuff aquifer produces a dilution factor of 100, then the dose (and associated radiologic risk) would be reduced by this same factor. Dilution of radionuclides released into the groundwater will be a result of mixing along the flow path between the source point(s) and the location where the contaminated groundwater is withdrawn. Mixing of a dissolved contaminant is, in general, the result of variations in both the magnitude of the fluid velocity and its direction (i.e., hydrodynamic dispersion). These variations are principally caused by small- and large-scale heterogeneities in the geologic media (Fetter, 1993). Large-scale features such as faults may in some instances induce flow variations and thereby enhance natural mixing, while in other cases they may produce highly channelized flow with limited mixing.

Only generic analyses of mixing and dilution have been performed by the DOE to date for the YM site (TRW Environmental Safety Systems Inc., 1995). These analyses suggest that natural or passive groundwater mixing will produce dilution factors (DF) on the order of 10^3 to 10^5 at 5 km from the edge of the proposed repository and 10^4 to 10^6 at 30 km. NRC and CNWRA staff believe these estimates are optimistic because (i) the technical bases were neither conservative nor bounding, (ii) such large DFs imply a homogeneous hydrochemistry—inconsistent with available data, and (iii) the DFs were much higher than those suggested by previous transport calculations in the DOE TSPA-93 (Wilson et al., 1994). The DOE estimates inferred from TSPA-93 calculations suggest DFs ranging from 5 to 20 at 5 km. In comparing the two independent dilution factor estimates, however, it is important to recognize that the TSPA-95 DFs take into account mixing below the repository whereas the DFs inferred from the TSPA-93 (Wilson et al., 1994) calculations neglect dilution immediately below the repository.

The scoping analysis was performed to study groundwater dilution characteristics associated with the proposed repository at YM. The objectives of the analysis were two-fold:

- Gain insight to the site specific factors that may affect groundwater mixing and attendant dilution of dissolved radionuclides at the YM site, and
- Determine if there are any methodology issues that may impact implementation of a dose- or risk-based standard as proposed by the NAS report.

Meeting these objectives provides a basis for staff review and comment on a revised EPA Standard for YM. As used in this analysis, the dilution factor was defined as the ratio of the peak groundwater concentration below the repository to the concentration at any other point in the saturated zone. This definition assumes that the initial mixing below the repository is small, which introduces conservatism.

Although available field data for the YM site were used, the scoping analysis did not consider parameter uncertainties associated with the spatial variability of hydraulic properties. In addition, the

Table 9-1. Expected values and standard deviations as a function of position and the time period of interest

Dose Point Number	Time Period of Interest (yr)	Dose Point Location		Expected Peak Annual Effective Dose Equivalent in the TPI (rem/yr)	Standard Deviation (rem/yr)
		x (km)	y (km)		
1	10,000	0	−20	2.7×10^{-6}	2.2×10^{-3}
2	10,000	0	−25	7.5×10^{-7}	7.6×10^{-4}
3	10,000	0	−30	2.5×10^{-7}	3.4×10^{-4}
1	1,000,000	0	−20	7.7×10^{-6}	6.1×10^{-4}
2	1,000,000	0	−25	1.8×10^{-6}	1.4×10^{-4}
3	1,000,000	0	−30	4.4×10^{-7}	4.1×10^{-5}

hydrogeologic system was treated as an equivalent porous continuum and no attempt was made to account for flow and transport through discrete fractures or include matrix diffusion effects. Mixing induced by water well pumping was also not considered.

To assess groundwater dilution and its dependence on the heterogeneous characteristics of the YM setting, a series of two-dimensional (2D) computer simulations of groundwater flow and radionuclide transport were performed. Computer models were applied to calculate four quantities: hydraulic head distributions, flow paths, particle travel times, and radionuclide plume distributions. Dilution of ^{99}Tc was modeled because it is a radionuclide of importance to dose and reflects the dilution behavior of radionuclides with relatively large inventories, long half-lives, and nonsorbing characteristics. Numerical calculations and graphical display of these four quantities were used to gain insight to the nature of the hydrogeologic processes that may control the degree of dilution at the YM site.

Two computer codes were used in performing the scoping analysis: (i) MAGNUM-2D, a saturated flow model (England, et al., 1985) and (ii) CHAINT, a multicomponent radionuclide transport model (Kline and Baca, 1985). Hydraulic head distributions simulated with the MAGNUM-2D code were used to calculate flow paths (i.e., streamlines) from various locations and associated particle travel times along the streamlines. Radionuclide concentrations computed with the CHAINT code were contoured to depict plume spreading and dilution patterns.

A model of lateral groundwater flow from the proposed repository site to the Amargosa Desert region was developed to assess the flow patterns through the relatively long and heterogeneous flow path. Groundwater flow paths and particle travel times for a particular parametric case are shown in figure 9-2a; circled numbers refer to the distinct hydrogeologic subregions of the flow domain. From this visualization it is evident that, depending on location of the release, mobile radionuclides could travel along paths with

very large particle travel times (i.e., on the order of ≈ 10,000 yr) or along more direct paths with smaller travel times (i.e., ≈ 5,000 yr). It can also be noted from figure 9-2a that structural features such as the Bow Ridge fault can play a role in determining flow directions. The range of Darcy fluxes, which are relevant to mixing, were calculated for each of the nine subregions. The magnitude of the flux in the tuff aquifer beneath the proposed repository foot print ranged from about 0.5 to 1.9 m/yr while immediately down gradient of the repository the flux was estimated to range from 0.01 to 3.7 m/yr. In the alluvium, where the Amargosa Valley region is located, the magnitudes of the Darcy fluxes ranged from about 0.4 to 0.7 m/yr.

Hypothetical releases of ^{99}Tc from discrete locations in the proposed repository site were also modeled to estimate possible spread and dilution of radionuclides. DFs were computed and contoured for various time frames. Depictions of the ^{99}Tc plumes at 10,000 yr (after the contaminant reaches the groundwater) are shown in figure 9-2b. From this radionuclide transport simulation, it appears that degree of dilution in the vicinity of the proposed repository would be relatively small. Even at long times, after the plume has reached the Amargosa Desert region, the DFs appear to be relatively low. Although these estimates may be relatively conservative, particularly at larger distances from the proposed repository, actual DFs would not be expected to be orders of magnitude larger.

Flow and transport along a cross section through the site was also modeled. The purpose of this part of the scoping analysis was to examine smaller scale mixing processes that occur immediately beneath the site. In this case, plume dilution is controlled by channelized flow through the complex geometry of the dipping hydrostratigraphic units, large permeability contrasts of adjacent units, and discontinuities associated with fault zones. The flow paths were calculated for the cross section defined by boreholes USW H-5 and USW H-4, shown in figure 9-3a. This figure depicts the streamlines originating from points along the Ghost Dance fault. The arrow heads placed along each streamline mark a 100 yr interval of particle travel time. From this visualization it is evident that flow paths are predominantly along hydrostratigraphic units except near fault zones where there are large discontinuities in the hydrostratigraphy. Transport calculations are for ^{99}Tc, assumed to be introduced at the Ghost Dance fault. The radionuclide distribution at 1,000 yr, shown in figure 9-3b, illustrates that (i) the plume remains near the surface of the water table, (ii) the DFs at the water surface are relatively small, and (iii) large fault zones can induce significant vertical mixing.

The overall finding of this preliminary scoping analysis was that dilution at the YM site is not likely to produce large reductions in groundwater concentrations of radionuclides (or the associated radiation doses). In the immediate vicinity of the proposed repository, DFs on the order of 2 to 5 are expected based on model calculations. Relatively low DFs are likely if the plume is confined to fracture zones that are pervasive in the tuff aquifer (Geldon, 1993). Alternatively, if the plume spreads vertically as a result of flow through vertical fractures or faults, then the DFs will tend toward the higher end of the range. Passive mixing along the long flow path (from the proposed repository site to the Amargosa Desert region) are conservatively estimated to produce DFs on the order of 5 to 50. Other factors, such as interbasin transfers and water well pumping, may contribute to enhanced dilution, but a much stronger technical basis and relevant field data are needed to support DFs of the magnitudes presented in the DOE (TRW Environmental Safety Systems, Inc., 1995).

While this scoping analysis did not directly identify any methodology issues related to implementing a dose- or risk-based standard, an important consequence of such a standard is that it will require the DOE to place greater emphasis on characterization of the local and regional groundwater system. Additional tracer tests such as those conducted in the C-well complex (Geldon, 1995) may be

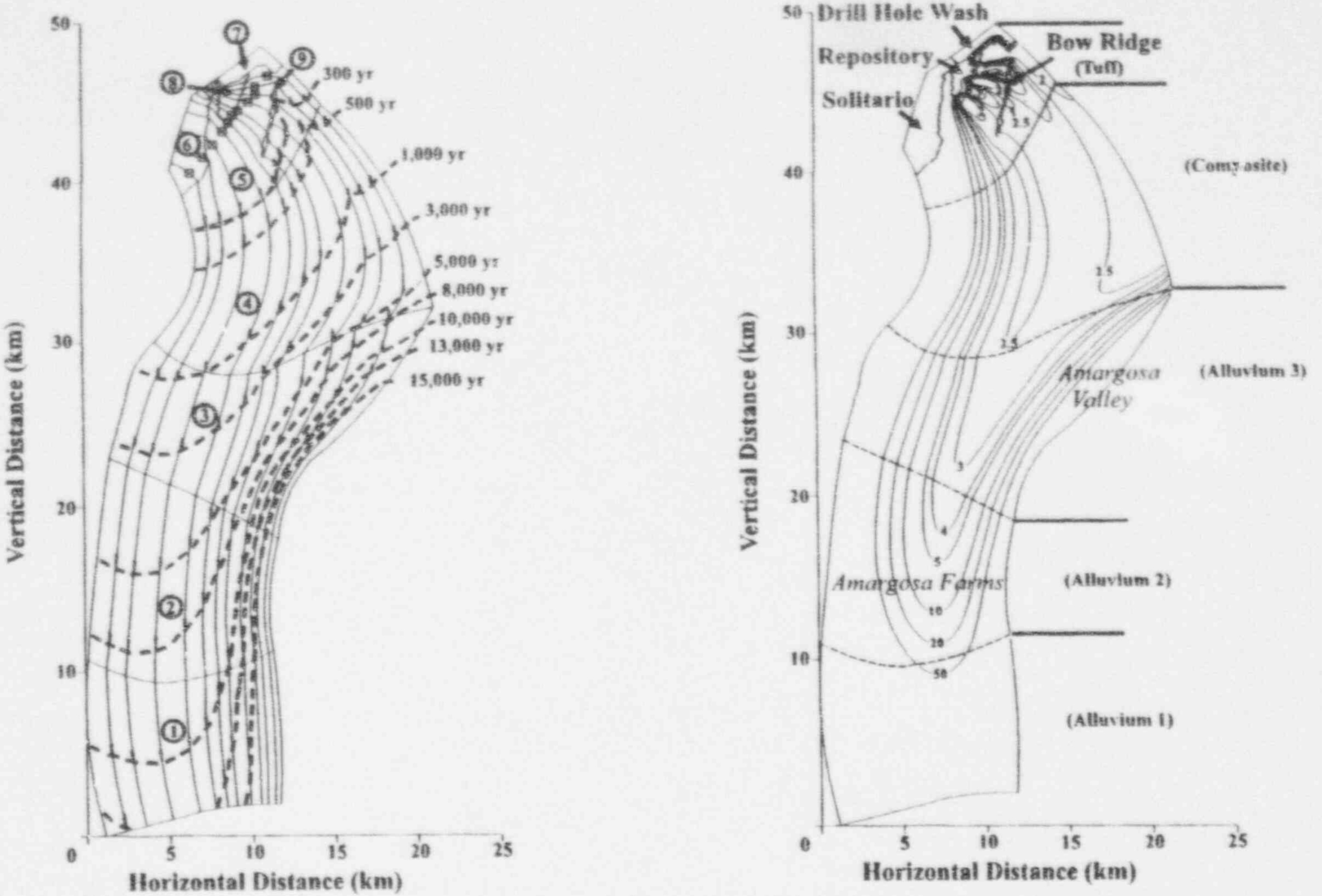

(a) Streamlines and travel times

(b) Dilution factor contours

Figure 9-2. Streamlines (solid lines), particle travel times (dashed lines), and plume for lateral flow model (solid lines with arrows)

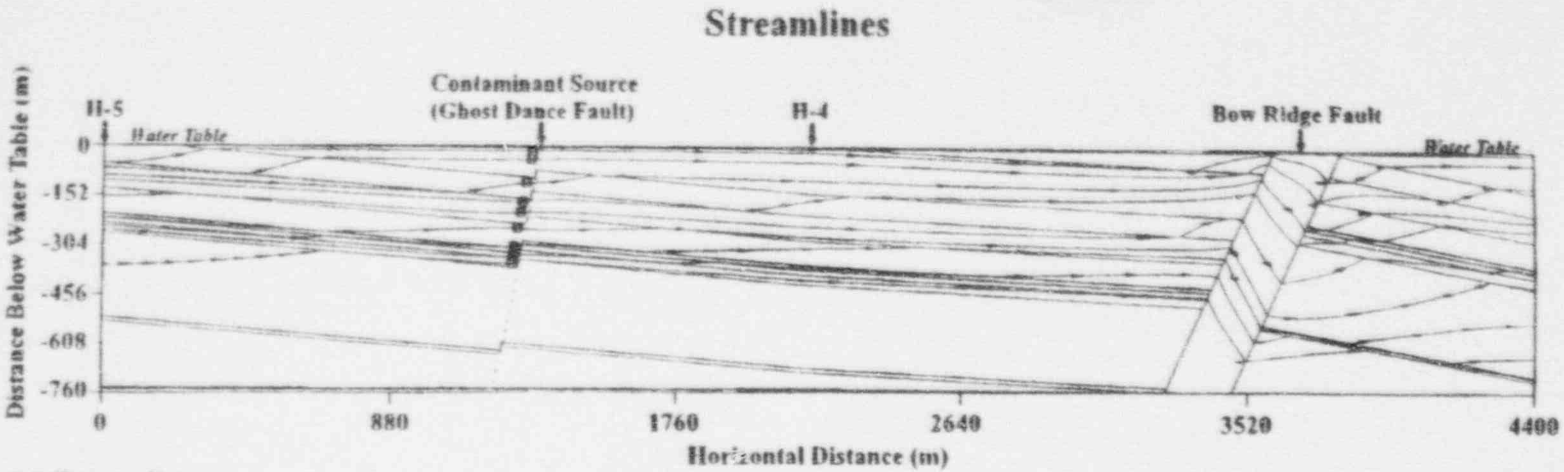

(a) Streamlines

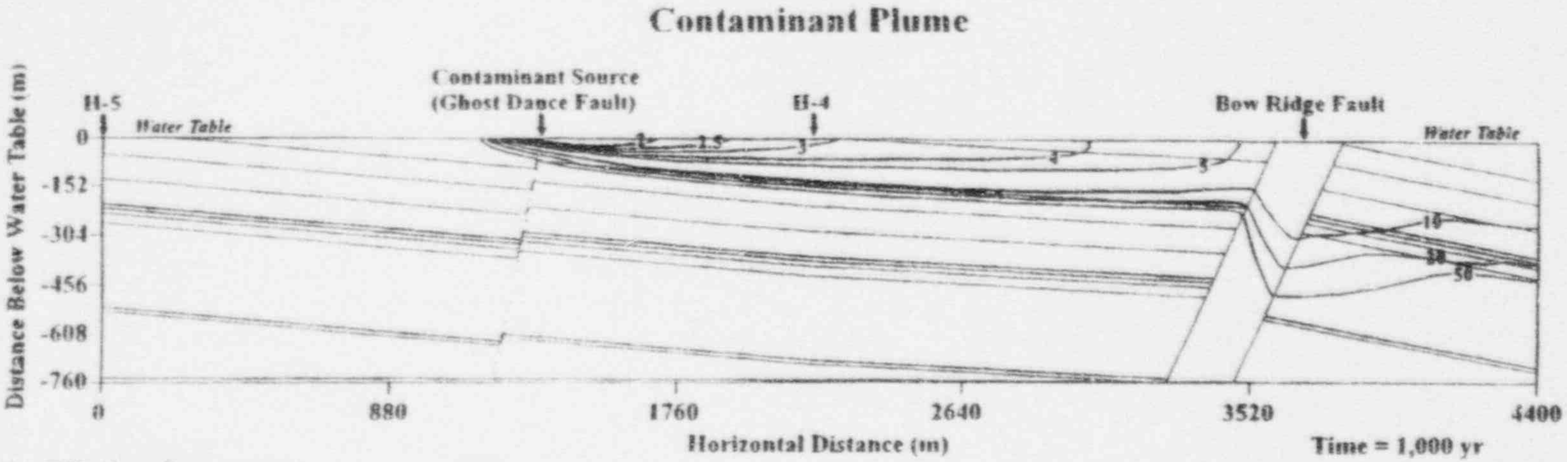

(b) Dilution factor contours

Figure 9-3. Streamlines (solid lines with arrows) and contaminant plume for vertical cross section model

needed to acquire data on transport parameters (e.g., mass dispersivities and effective porosities) but representative of larger length scales. The hydraulic properties of the various faults will also be important.

9.3.1.4 Human Intrusion

Human intrusion has been analyzed as a disruptive scenario in prior TSPAs [e.g., Codell, et al. (1992), Barnard, et al. (1995), Wilson, et al. (1984), and Nuclear Regulatory Commission, (1995)] performed to examine compliance with the requirements of 10 CFR Part 60. Each of these analyses required basic assumptions regarding human behavior and future technology. As stated in section 9.1 of this report, the NAS (National Research Council, 1995) determined that there was no scientific basis for predicting the occurrence of human intrusion. Consequently, the NRC staff performed scoping analyses to consider the requirements for a stylized calculation (consequences only) of human intrusion.

The scoping analysis for human intrusion consisted of calculating drinking water dose resulting from a single WP damaged by exploratory drilling from the ground surface. Neither direct exhumation nor other sources of human intrusion were considered in the analysis. The source term and transport of radionuclides were modeled using the methodology of section 9.3.1.5 as developed in the NRC IPA program (Nuclear Regulatory Commission, 1995). Dissolution of spent fuel and leaching of radionuclides from within a single WP were determined taking individual radionuclide solubilities into account, and radionuclide concentrations at a 5 km distant well were calculated, assuming a representative transport pathway. The first set of calculations assumed the WP to be damaged at times of 0, 500, 1,000, 10,000, and 100,000 yr after closure. For each of these times of failure, surface runoff was assumed to enter the borehole from a catchment of either 10 m^2, 1 m^2, or the inside area of the 150 mm diameter casing. Geochemical retardation was ignored so that the condition of either a fast fracture pathway or a nearby borehole path to the saturated zone could be approximated. Another purpose of this initial calculation was to determine the relative importance of time of failure and water inflow to consequence (drinking water dose). It was readily apparent that surface water inflow had a strong effect on dose and that time of failure had a relatively minor effect. It was also determined that water inflow affected the relative contributions of various radionuclides to dose.

The next set of analyses included geochemical retardation during transport. This was considered a more credible scenario than a direct short circuit to the saturated zone next to a damaged WP, given that the drilling event occurs. The inclusion of geochemical retardation reduced the calculated drinking water dose at the receiving well to about 1 millirem or less, depending on water inflow to the WP.

Considering such factors as (i) the depth to groundwater from the top of YM, (ii) the scarcity of water users and arable land on the mountain, and (iii) the absence of known resources below the proposed repository, it is reasonable to argue that disruption of the repository by exploratory drilling or drilling for water resources is relatively unlikely. Because of the expected low likelihood and low consequence, the NRC staff concludes that human intrusion from surface based drilling need not be directly incorporated into a TSPA.

9.3.1.5 Annual Individual Dose Estimates

Prior TSPAs for YM analyzed system performance primarily with respect to the integrated release requirement of the remanded EPA Standard. As discussed previously, NAS recommendations called for a performance objective based on an annual individual dose using a critical group approach. Preliminary dose calculations were conducted to gain insight on implementation issues associated with a

dose-based standard and the relative importance of site-specific assumptions and parameters at YM. These insights will be used to support the NRC analysis of a proposed EPA Standard for YM.

Evaluation of annual individual dose requires specification of an exposure scenario that defines the geosphere and biosphere pathways that can transport radionuclides released from a repository to a human receptor in the biosphere. Simulation of radionuclide release and transport in the geosphere was based on models already developed in the NRC IPA program (Nuclear Regulatory Commission, 1995). Some modifications were necessary to allow investigation of sensitivities of the dose calculation, improve calculational efficiencies, and allow the calculation to go beyond a 10,000 yr performance period to the time of peak dose. Two exposure pathways were developed for release of radionuclides to groundwater. One exposure pathway, consistent with the distance used for integrated release calculations performed in previous IPA efforts (Nuclear Regulatory Commission, 1995), assumes a critical group exists at a distance of 5 km. Radioactive exposure results from drinking water from a well that intercepts the potential release plume. The other exposure pathway, consistent with current populations in Amargosa Valley region, assumes a critical group is located approximately 30 km down gradient from YM. Radioactive exposure results from drinking contaminated water and consumption of locally grown crops irrigated using contaminated water.

The NRC staff performed probabilistic analyses to quantify the variation in dose estimates due to uncertainties in the geosphere models (i.e., source term release, hydrologic flow, and radionuclide transport) for the two critical group locations. Important attributes and assumptions of the analyses are as follows.

- Simplifications of the flow and transport models include a steady-state flow system; no thermal effects; fracture retardation assumed to be a fraction of the matrix retardation (a range of 0-10 percent was used for the uncertainty analyses); assumed WP container lifetime of 1,000 yr; disruptive scenarios not considered; and a source term based on leach rate, solubility, and amount of water contacting the waste.

- A continuous transport path is assumed to exist from the saturated zone below YM to the receptor locations at 5 and 30 km.

- All releases from the proposed repository eventually pass the receptor locations and are uniformly mixed in the annual volume of water pumped by the critical group (1 million gallons per day for the 5 km location and 8 million gallons per day for the 30 km location). Water usage was based on broad assumptions regarding minimum pumping rates required to intercept the entire contaminant plume (applied to the 5 km location) and water usage consistent with a farming critical group (applied to the 30 km location).

- The critical group at 5 km uses untreated groundwater for drinking water and household chores only.

- The critical group at 30 km uses untreated groundwater for home and irrigation. The average member of this critical group is assumed to supply half of the food needs and all the water and milk consumption from the farm/ranch.

The maximum annual individual dose [Total Effective Dose Equivalent, (TEDE)] for the pathways considered in the uncertainty analysis is presented in figures 9-4 and 9-5 for the 5 km location

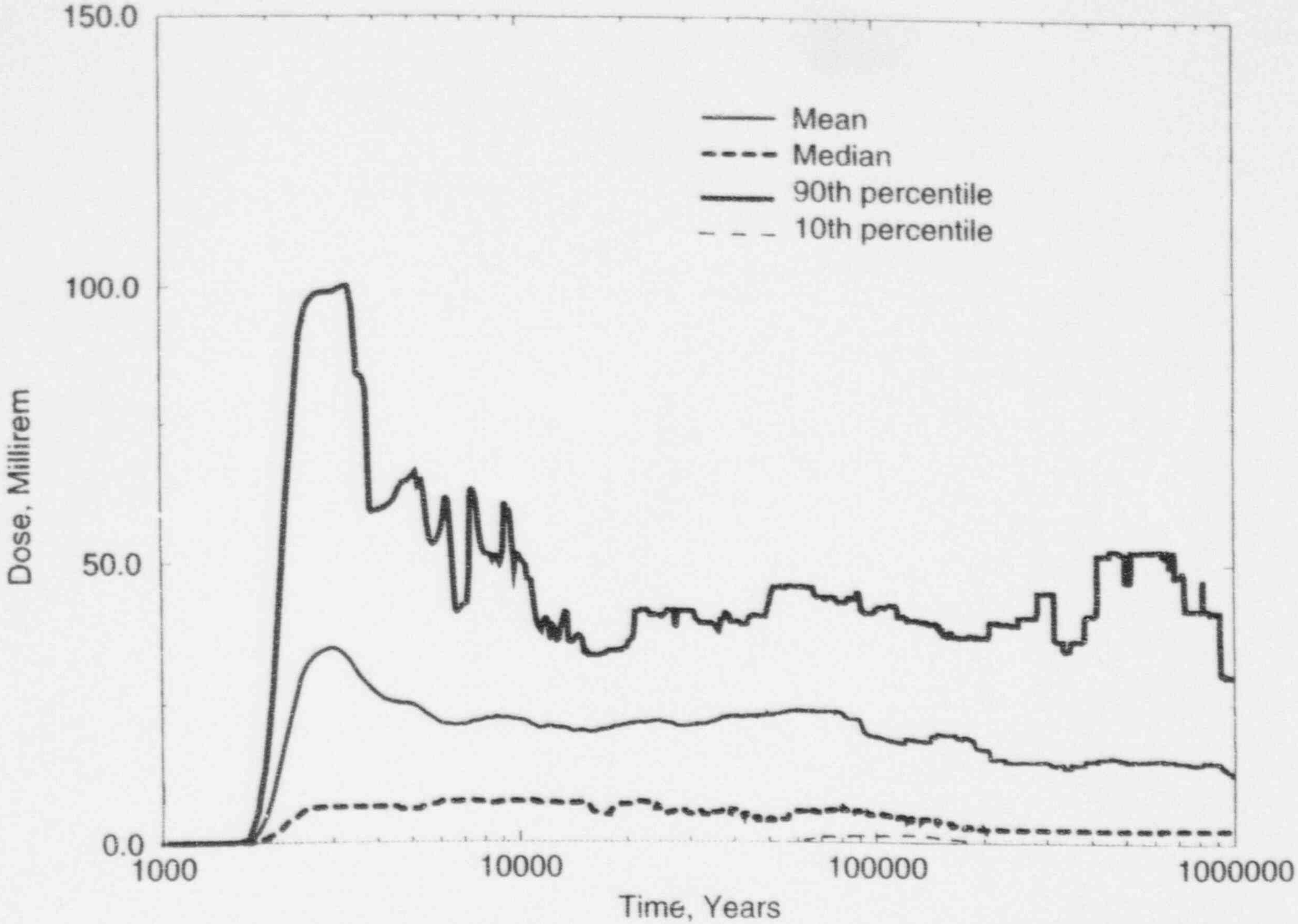

Figure 9-4. Uncertainty analysis of dose for one hundred vectors at a point 5 km down gradient from the proposed repository

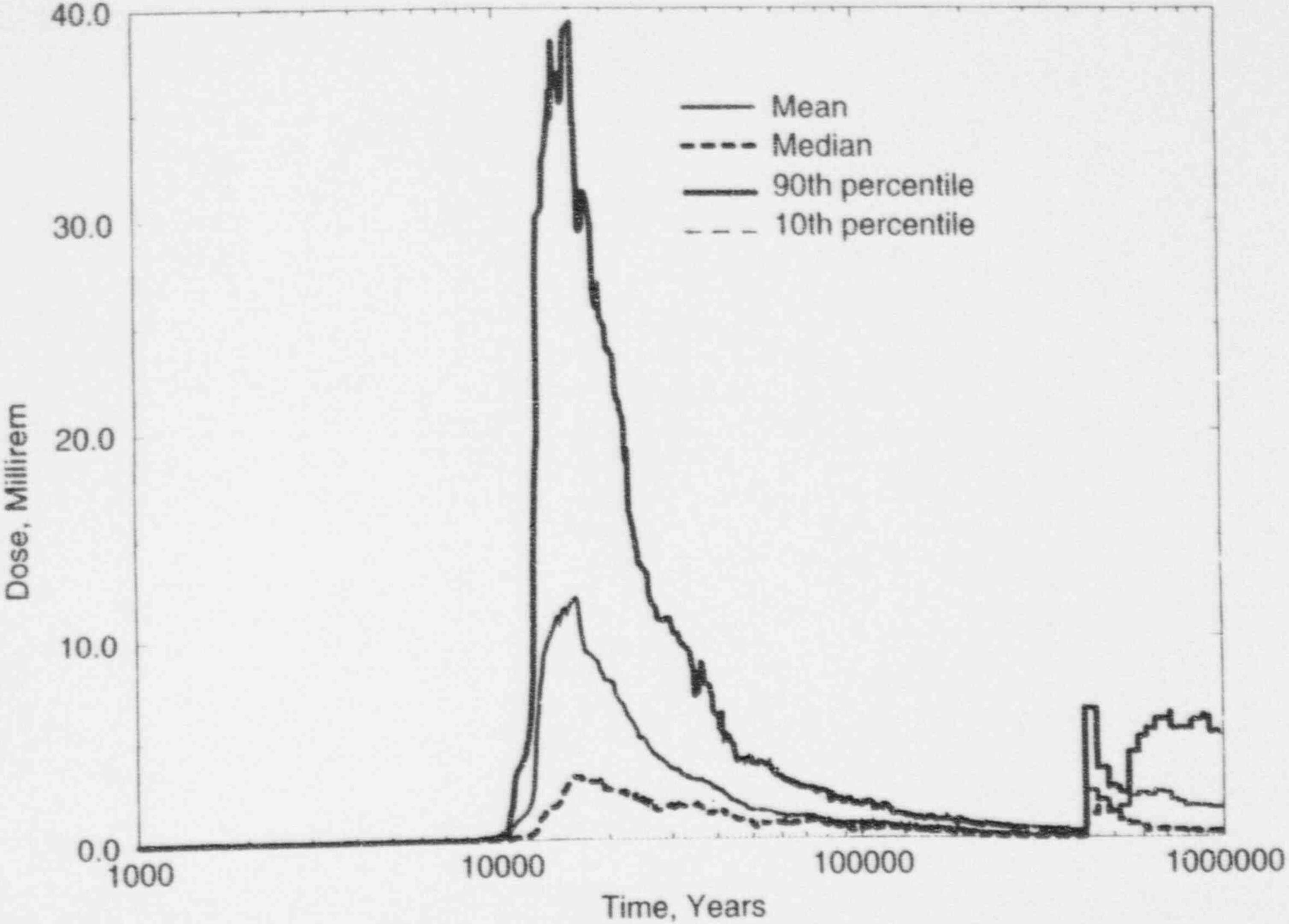

Figure 9-5. Uncertainty analysis of dose for one hundred vectors (all dose pathways) in the Amargosa Desert region 30 km down gradient from the proposed repository

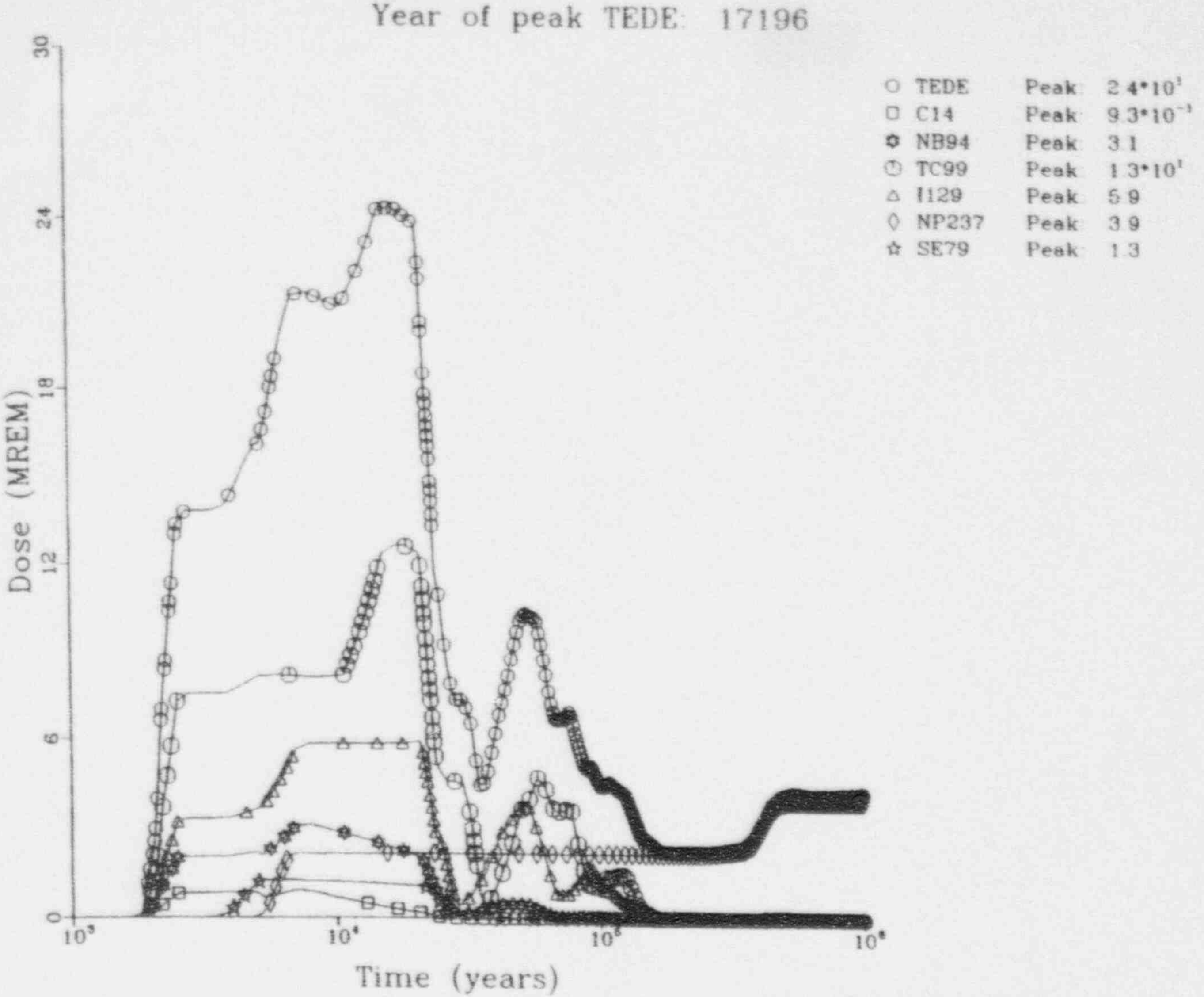

Figure 9-6. Annual individual dose from all radionuclides total effective dose equivalent and for selected radionuclides for the drinking water pathway at a distance of 5 km (mean parameter values were used including fracture retardation)

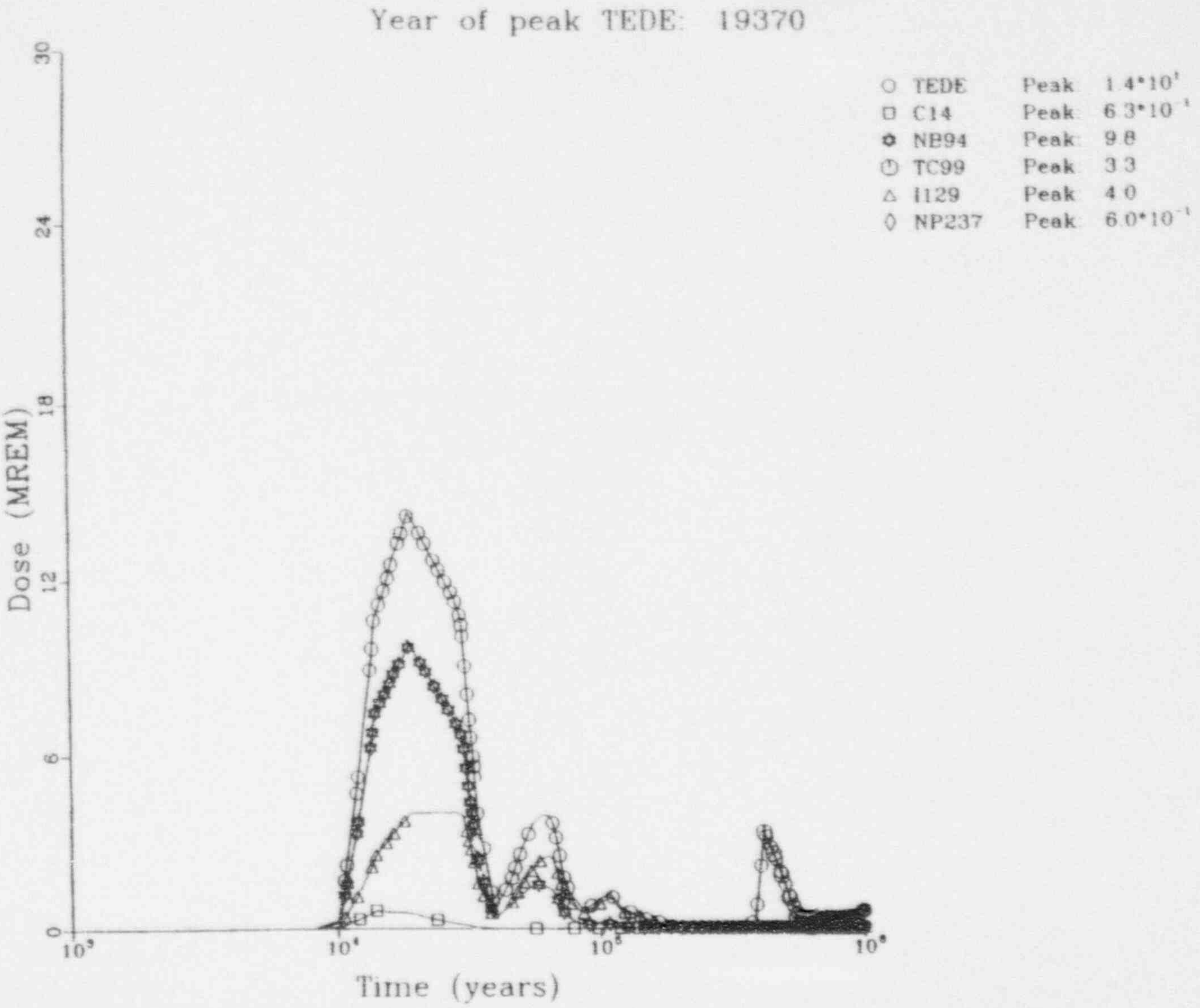

Figure 9-7. Annual individual dose from all radionuclides total effective dose equivalent and for selected radionuclides for the drinking water pathway at a distance of 30 km (mean parameter values were used including fracture retardation)

and the 30 km location, respectively. These figures represent the calculated annual individual dose at each point in time. Doses for 100 sampled vectors were calculated versus time, and the results were grouped into 100 yr bins. The values in each bin were then ranked, and the 10th, 50th, and 90th values in the rank (100 being the largest) were plotted to provide the curves denoted as 10th percentile, median, and 90th percentile, respectively. The curve marked mean is the arithmetic average of all the values in each bin. Note that over a large range of times for both curves, the 10th percentile value was essentially zero, and is coincident with the time axis. The maximum annual individual dose estimates for both locations occur shortly after the initial arrival time of radionuclides at the two locations. This result is believed to be due to high percolation values (deep percolation in the 2 to 5 mm/yr range) which result in large releases of a small set of long-lived, mobile radionuclides which arrive at the well location at generally overlapping times. After the initial peak, the dose versus time curve is complicated by both short duration spikes (e.g., spikes that appear between 3,000 and 8,000 yr in figure 9-4) and secondary peaks which are significantly less than the initial peak (e.g., secondary peaks at 50,000 and 700,000 yr in figure 9-4 and 700,000 yr. in figure 9-5). The short duration spikes are believed to be due to variation in arrival times of individual radionuclides due to varying flow velocities and retardation. The secondary peaks are due to the distinct arrival times from specific sub-areas of the repository (the repository was divided into seven sub-areas) or from the same sub-area but along differing flow paths (i.e., an initial peak could be due to releases which are transported in the fracture flow path with a later peak occurring from releases which are transported in the slower matrix flow path).

A set of mean value simulations that used mean values from the parameter ranges used in the uncertainty analysis was performed to determine the radionuclides most important to dose. While the mean simulation results are considered appropriate for identifying particular radionuclides, the probabilistic results (presented in figures 9-4 and 9-5) are more representative of total system behavior. The figures are in reasonable qualitative agreement, but there are differences between the probabilistic results and the deterministic results. Generally, attempts to draw inferences based on comparison of the probabilistic and deterministic results were not meaningful.

Figures 9-6 and 9-7 present the doses for specific radionuclides for two locations as well as the total dose for all radionuclides from the pathways considered, which is denoted in the legend as TEDE (for Total Effective Dose Equivalent). The parameter values for these simulations used mean values of the parameter ranges from the uncertainty analysis. A cursory examination of figures 9-6 and 9-7 reveals that: (i) the magnitudes for the peak dose for the two locations are quite similar (14 mrem versus 24 mrem), and (ii) the times of occurrence of the peaks are similar (both around 20,000 yr) although estimated releases initially arrive at the 5 km location at a much earlier time than for the 30 km location (2,000 yr versus 10,000 yr). This apparent similarity in results is due to several significant differences in key assumptions (see previous bullets) that have counterbalancing effects on the results. For example, the dose at the 5 km location should be larger than the dose at the 30 km location due to differences in the assumed dilution volumes [1 million gallons per day (MGD) versus 8 MGD] which reduce concentrations at the further location. If drinking water dose was the only ingestion pathway, then the dose at the 30 km location might have been an order of magnitude or more lower than the dose at the 5 km location. However, the increased dilution volume at the farther location is due to the greater water needs of an agricultural community which requires consideration of additional ingestion pathways from animal products and crops that are not included in the ingestion pathway for the 5 km location. Thus, doses at the 30 km location are increased due to inclusion of additional pathways, counterbalancing the decreased dose due to lower concentrations. The similarity in the two times for occurrence of the peak is a result of the different contributions from specific radionuclides responsible for time of the peak. At the 5 km location, the peak dose is significantly influenced by arrival of ^{99}Tc and ^{129}I from more than one sub-area as evidenced by the multiple peaks for ^{99}Tc (note: in the IPA flow and transport model, the repository is

represented by 7 sub-areas). At the 30 km location, the peak dose is influenced more by arrival of ^{94}Np. However, at both locations, it is long-lived, mobile radionuclides that are the key contributors to dose.

Three general conclusions may be drawn from the present analysis: (i) preliminary indications are that a relatively small number of long-lived, mobile radionuclides will be important to performance; (ii) there do not appear to be any technical difficulties that might preclude estimating an annual individual dose; and (iii) assumptions concerning critical group location and lifestyle could be important in determining an appropriate approach for establishing radionuclide concentrations at receptor locations.

9.3.2 Reference Biosphere/Critical Group

NAS recommended that the concepts of reference biosphere and critical group (RB/CG) be adopted for the revised EPA Standard for YM. These concepts were not included in prior EPA Standards (e.g., 40 CFR Part 191), and a number of new implementation issues must be considered by the NRC to prepare for review and comment on a new EPA Standard for YM. In addition, a joint NRC/CNWRA working group within the EPA KTI was formed to consider acceptable options that EPA might select for adopting the RB/CG concepts. This working group focused on understanding and summarizing relevant NAS recommendations and identifying important implementation issues regarding RB/CG at YM. The absence of a completed standard during FY96 required staff to limit consideration of issues to general concepts. When a standard is completed, the NRC implementing role will be clarified and details of the implementation approach will be addressed.

Initial efforts relating to RB/CG were directed at understanding relevant NAS recommendations. This effort was important for developing a common understanding of the recommendations, and to support discussions between the NRC and EPA on options for revised standards. The approach provided in appendix C of the NAS report (i.e., the probabilistic critical group) was found to be unnecessarily complex and confusing. Consistent with NAS recommendations, the KTI team concluded that an alternative approach, which also satisfies the NAS recommendations, would be preferable. Special attention was placed on examining how NAS recommendations helped to define and limit speculative assumptions about lifestyle characteristics and potential locations of the critical group(s).

NAS recommendations were considered by the KTI team to provide the staff with the flexibility needed to select alternative methods for implementation. The team agreed that RB/CG characteristics should be based on reasonable assumptions supported (to the extent possible) by site specific information. The team also agreed with NAS that the critical group concept is only a framework for performance assessment and is not intended to predict future human behaviors. Nonetheless, available information on present human populations provides a reasonable basis for defining critical group characteristics. It may be necessary for EPA or NRC to provide additional definition of critical group characteristics through rulemaking or issuance of supporting guidance; however, NAS recommendations relating to use of the critical group approach were found to be implementable.

Scoping calculations focused on providing EPA early input on current techniques, capabilities, and implementation issues to consider prior to drafting a dose-based standard. For the exposure assessment portion of the calculations in NUREG-1538, a site-specific farming/ranching exposure scenario representative of potential exposure conditions currently existing in the Amargosa Desert area was developed. Exposure scenario parameter information was adopted from previous staff efforts including NUREG-1464 (Nuclear Regulatory Commission, 1995) and LaPlante et al. (1995). Local information on

current farming practices, water use, climate, and soil characteristics was obtained and used. Additional information sources were investigated for population demographics and well water use.[7] Results of the scoping calculations were presented to EPA, and site specific data was provided to allow their staff to conduct exposure assessments and tests. Preliminary results of exposure scenario parameter sensitivity analyses were also provided to EPA for consideration. Discussion of issues within the KTI team helped formulate a general approach which was presented at a BIOMOVS conference and at the 84th Advisory Committee on Nuclear Waste meeting on Exposure Scenarios for YM (June 25, 1996). An examination was conducted to evaluate the EPA claim that a reasonably maximally exposed individual (RMEI) is essentially equivalent to the average member of the critical group recommended by NAS. While EPA did not demonstrate this quantitatively, upon consideration the NRC staff recognized that RMEI appeared to be an adequate concept to consider for the standard. The NRC currently awaits publication of the draft standard before more detailed review and comment can take place.

9.3.3 Background Information and Recommendations for a Stylized Human Intrusion Calculation at Yucca Mountain

The NAS report concluded: ". . . it is not possible to make scientifically supportable predictions of the probability that a repository's engineered or geologic barriers will be breached as a result of human intrusion over a period of 10,000 years." Based on this conclusion, the NAS recommended that the new standard(s) for YM not require that human intrusion be included directly in PAs of the proposed repository, but might instead require: ". . . [examination of] the site- and design-related aspects of repository performance under an assumed intrusion scenario to inform a qualitative judgement. In this approach, the objective would be to perform a consequences-only analysis without attempting to determine an associated probability for the analyzed scenario." NAS considered one exploratory borehole of a specified diameter drilled from the surface through the WP canister to the underlying aquifer. NAS suggested that: ". . . the simplest scenario that provides a measure of the ability of the repository to isolate waste and thereby protect the public health is the most appropriate scenario to use for this purpose."

The purpose of this work was to provide background information and recommendations for identification of characteristics of a representative (e.g., most likely) borehole at YM and identification of the important processes associated with boreholes that penetrate the proposed repository horizon. By studying related documents about exploratory drilling techniques typically used in mineral exploration and water well construction, and considering NAS recommendations for this scenario, the NRC staff developed concepts that will be used to review and comment on a proposed EPA Standard for YM. Building upon the findings of the scoping calculations for the human intrusion scenario described briefly in section 9.3.1.4, a rudimentary study of the size of the catchment area as a function of borehole position was also conducted. Other potentially important considerations associated with drilling that could affect repository performance were identified including borehole size, drilling fluid additives, the use of casing, and borehole sealing techniques.

9.4 ASSESSMENT OF PROGRESS TOWARD MEETING OBJECTIVES

This section evaluates the activities conducted in FY96 with respect to meeting the objectives discussed in section 2.0. The primary issue and each subissue will be discussed.

---

[7]Eisenberg, N.A. 1996. Staff Visit to Amargosa Valley: Trip Report. Memorandum to M. Federline, Acting Director, Division of Waste Management. May 14, 1996. Washington DC: Nuclear Regulatory Commission.

Significant progress was made in identifying and conducting the activities necessary to support review and comment on an EPA Standard for YM. Throughout the year, the NRC staff interacted frequently with EPA staff to provide the NRC perspectives on implementation issues regarding the NAS recommendations for a dose-based standard.

Defining a Compliance Period and Method

A number of proposals have been made to define the compliance period and method. These include (i) using the current 10,000 yr compliance period, (ii) evaluating compliance at the time of peak dose, and (iii) using deterministic calculations for shorter time periods with probabilistic methods for longer periods. Calculations of relative hazards and peak dose completed this year, combined with results of the previous NRC TSPAs, provided confidence that the NRC can evaluate any of the compliance periods or methods identified previously that might be proposed by the EPA Standard for YM.

Selecting a Critical Group(s)

Evaluations completed during FY96 show that there is information on conditions and lifestyles in the YM area which supports the identification of critical group characteristics that can be included in a revised EPA Standard. Exposure scenarios and pathways and reference biospheres can be adequately constrained. Issues remain concerning the level of detail for critical group parameters to be specified in the regulatory framework.

Evaluating Results of Potential Human Intrusion

Scoping calculations performed by the NRC staff in FY96 indicate that specifying a stylized human intrusion scenario and calculation is technically feasible. Details of the scenario and associated calculations require further definition in the regulatory framework.

Considering Disruptive Events

Scoping calculations completed for volcanic hazards in FY96 combined with increasing sophistication of the NRC TSPAs provide confidence that potential repository disruptive events can be examined in a technically defensible way. These calculations not only support PAs but also contribute directly to selection of a critical group.

9.5 INTEGRATION WITH OTHER KEY TECHNICAL ISSUES

Throughout FY96, the EPA Standard KTI coordinated its activities with other KTIs to ensure consistency of technical bases and assumptions and to provide results and information to other KTIs. The principal technical integration activities accomplished in FY96 were

- Information was provided to the TSPAI KTI consisting of tentative definitions of the reference biosphere and a critical group. Site specific characteristics (e.g., land use and water well practices) relevant to pathway modeling and dose calculations were compiled that will be used in future TSPAs for YM. In addition, scoping calculations for the human intrusion scenario were coordinated with those conducted in TSPAI KTI.

- Technical knowledge base and data regarding the hydrogeology of the site assembled as part of the USFIC (and previous CNWRA research projects) were used to conduct scoping calculations of the dilution characteristics of the proposed YM site.

- The RT KTI provided information regarding geochemical data for the regional groundwater system at YM that was useful in qualitative checks of the scoping calculations of dilution factors.

- The technical information necessary for modeling the volcanism scenario for YM was provided by the IA KTI. In close collaboration with the IA KTI team, this information was used to model hypothetical eruptions and to simulate the associated entrainment and airborne releases of radionuclides.

9.6 REFERENCES

Barnard, R.W., et al. 1992. *"TSPA 1991: An Initial Total System Performance Assessment for Yucca Mountain."* Albuquerque, NM. Sandia National Laboratories. SAND91-2795.

Codell, R.R. et al. 1992. *"Initial Demonstration of the NRC's Capability to Conduct a Performance Assessment for a High Level Waste Repository"*. NUREG—1327. Washington, DC: U.S. Nuclear Regulatory Commission.

England, R.L., K.J. Ekblad, and R.G. Baca. 1985. *MAGNUM-2D Computer Code: User's Guide.* RHO-BW-CR-143. Richland, WA: Rockwell International.

Fetter, C.W. 1993. *Contaminant Hydrogeology.* New York, NY: MacMillan Publishing Company.

Geldon, A.L. 1993. *Preliminary Hydrogeologic Assessment of Boreholes UE-25c #1, UE-25c #2, and UE-25c #3, Yucca Mountain, Nye County, Nevada.* Denver, CO: U.S. Geological Survey.

Geldon, A.L. 1995. *Results and Interpretation of Preliminary Aquifer Tests in Boreholes UE-25c #1, UE-25c #2, and UE-25c #3, Yucca Mountain, Nevada.* United States Geological Survey Water-Resources Investigations Report 94-4177. Washington, DC: U.S. Geological Survey.

Jarzemba, M.S. 1995. *Stochastic Radionuclide Distributions After a Basaltic Eruption for Performance Assessments of Yucca Mountain.* San Antonio, TX: Center for Nuclear Waste Regulatory Analyses.

Kline, N.W. and R.G. Baca. 1985. *CHAINT Computer Code: Users Guide. RHO-BW-CR-144.* Richland, WA: Rockwell International.

LaPlante, P.A., S.J. Maheras, and M.S. Jarzemba. 1995. *Initial Analyses of Site-Specific Dose Assessment Parameters and Exposure Pathways Applicable to a Groundwater Release Scenario at Yucca Mountain.* CNWRA 95-018. San Antonio, TX: Center for Nuclear Waste Regulatory Analyses.

Leigh, C.D., B.M. Thompson, J.E. Campbell, D.E. Longsine, R.A. Kennedy, et al. 1993. *User's Guide for GENII-S: A Code for Statistical and Deterministic Simulation of Radiation Doses to Humans from Radionuclides in the Environment.* SAND91-0561. Albuquerque, NM: Sandia National Laboratories.

Lozano, A.S., H. Karimi, J.P. Cornelius, R.D. Manteufel, and R.W. Janetzke. 1994. *INVENT: A Module for the Calculation of Radionuclide Inventories, Software Description, and User's Guide.* CNWRA 94-016. San Antonio, TX: Center for Nuclear Waste Regulatory Analyses.

National Research Council. 1995. Technical Bases for Yucca Mountain Standards. Washington, DC: National Academy Press.

Nuclear Regulatory Commission. 1995. *NRC Iterative Performance Assessment Phase 2: Development of Capabilities for Review of a Performance Assessment for a High-Level Waste Repository.* Wescott , R.G., M.P. Lee, T.J. McCartin, N.A. Eisenberg, and R.G. Baca, eds. NUREG-1464. Washington, DC: Nuclear Regulatory Commission.

Suzuki, T. 1983. A theoretical model for dispersion of tephra. *Arc Volcanism: Physics and Tectonics.* Tokyo: Terra Scientific Publishing: 95–113.

TRW Environmental Safety Systems Inc. 1995. *Total System Performance Assessment–1995: An Evaluation of the Potential Yucca Mountain Repository.* B00000000-01717-2200-00136. Las Vegas, NV: TRW Environmental Safety Systems, Inc.

U.S. Department of Energy. 1988. *Internal Dose Conversion Factors for Calculation of Dose to the Public.* DOE/EH-0071. Washington, DC: U.S. Department of Energy.

U.S. Environmental Protection Agency. 1982a. *Population Risks from Disposal of High-Level Radioactive Wastes in Geologic Repositories.* EPA 520/3-80-006. Washington, DC: Environmental Protection Agency.

U.S. Environmental Protection Agency. 1982b. *Draft Regulatory Impact Analysis for 40 CFR Part 191: Environmental Radiation Protection Standards for Management and Disposal of Spent Nuclear Fuel, High-Level and Transuranic Radioactive Wastes.* EPA 520/3-82-024. Washington, DC: Environmental Protection Agency.

U.S. Environmental Protection Agency. 1985. *High-Level and Transuranic Radioactive Wastes—Background Information Document for Final Rule.* EPA 520/1-85-023. Washington, DC: U.S. Environmental Protection Agency.

U.S. Environmental Protection Agency. 1988. *Limiting Values of Radionuclide Intake and Air Concentration and Dose Conversion Factors for Inhalation, Submersion, and Ingestion.* EPA 520/1-88-020, Washington, DC: Environmental Protection Agency.

U.S. Environmental Protection Agency. 1989. Title 40, Code of Federal Regulations, Part 191. *Environmental Radiation Protection Standards for Management and Disposal of Spent Nuclear Fuel, High-Level and Transuranic Radioactive Wastes.* Washington, DC: Office of the Federal Register.

U.S. Environmental Protection Agency. 1993a. *High-Level and Transuranic Radioactive Wastes—Background Information Document for Proposed Amendments.* EPA 402-R-93-007. Washington, DC: U.S. Environmental Protection Agency.

U.S. Environmental Protection Agency. 1993b. 40 CFR Part 191: Environmental Radiation Protection Standards for the Management and Disposal of Spent Nuclear Fuel, High-Level and Transuranic Radioactive Wastes, Final Rule. *Federal Register.* Vol 58, no. 242, 66,398-66,416. Washington, DC: U.S. Environmental Protection Agency.

Wilson, M.L., J.H. Gauthier, R.W. Barnard, G.E. Barr, H.A. Dockery et al. 1994. *Total-System Performance Assessment for Yucca Mountain—SNL Second Iteration (TSPA-1993).* SAND93-2675. Albuquerque, NM: Sandia National Laboratories.

10 UNSATURATED AND SATURATED FLOW UNDER ISOTHERMAL CONDITIONS

Primary Authors: A.C. Bagtzoglou, E.C. Pearcy, S.A. Stothoff, G.W. Wittmeyer, and N.M. Coleman

Technical Contributors: A.C. Bagtzoglou, E.C. Pearcy, S.A. Stothoff, T.L. Tolley, G.W. Wittmeyer, and D.A. Woolhiser

Key Technical Issue Co-Leads: E.C. Pearcy (CNWRA) and N.M. Coleman (NRC)

10.1 INTRODUCTION

Yucca Mountain (YM), Nevada has been proposed as a site for a geologic repository for high-level radioactive waste (HLW) in part because of the favorable hydrogeologic conditions provided by its 700 m thick unsaturated zone. YM is located in the southernmost portion of the Great Basin Desert where the sparse precipitation—a reflection of the Sierra Nevada rain shadow—is greatly exceeded by annual potential evapotranspiration and infiltration rates in the lower elevation valleys and mountain ranges are generally small. Because mean infiltration and deep percolation rates within YM are assumed to be small, it is postulated that waste canisters are unlikely to be contacted by significant amounts of water under ambient thermal conditions and are thus less likely to corrode and expose the waste form. Low flux rates also reduce the likelihood that waste form that is exposed to water will be dissolved and transported rapidly to the water table. When YM was originally proposed, the saturated zone was assumed to play little or no role in demonstrating repository performance inasmuch as applicable regulations were based on a maximum cumulative radionuclide release to the accessible environment and saturated zone transport times to the accessible environment were estimated to be small (less than 170 yr, U.S. Department of Energy, 1988). With the publication of the National Academy of Sciences (NAS) recommendation that the YM standard be risk- or dose-based rather than release-based, the study of mechanisms that may retard the transport of radionuclides in the saturated zone and thus reduce peak doses has received increased emphasis.

The U.S. Department of Energy (DOE) Waste Containment and Isolation Strategy (WCIS)[1] for YM defines seepage and saturated zone dilution as two of the three key attributes of the natural barrier system; radionuclide transport is the third key attribute. The WCIS (Department of Energy, 1996) states that "[p]erformance assessments have shown that seepage into the emplacement drifts is the most important determinant of the ability of the site to contain and isolate waste." Moreover, the DOE has developed a set of five specific hypotheses, which must be addressed in order to support the DOE assertion that seepage into the drifts will be low: (i) flux that percolates through the repository horizon is substantially less than net infiltration, (ii) rapid fracture flow occurs only within a limited volume of the repository block at any specific time, (iii) capillary effects will reduce seepage into the emplacement drifts to be a small percentage of deep percolation, (iv) effects of heat generated from the waste on the hydrogeologic regime can be bounded, and (v) the effect of climate change on seepage can be bounded. The DOE strategy for saturated zone dilution is to demonstrate that the flow of water that may contact the waste packages and transport dissolved waste to the water table is much smaller than the flow below

[1]U.S. Department of Energy. 1996. *Highlights of the U.S. Department of Energy's Updated Waste Containment and Isolation Strategy for the Yucca Mountain Site.* DOE Concurrence Draft. July 1996. Washington, DC: U.S. Department of Energy.

the water table. Moreover, the DOE strategy recognizes that further dilution may occur when water from a radionuclide plume is mixed with uncontaminated water in a producing water well. To address issues related to dilution strategy, the DOE proposed the following two hypotheses: (i) flow through the saturated zone beneath YM is much greater than the flow that may come in contact with waste packages and (ii) water that percolates through the repository horizon mixes with flow in the underlying welded tuff aquifer.

Specific technical subissues determined to be important to the resolution of this KTI have been identified. These technical subissues were framed as questions: (i) what is the key information needed to describe the hydrogeologic framework of YM, (ii) what is the amount and extent of present day shallow infiltration at YM, (iii) what are the hydraulic conditions in the unsaturated zone above the repository, (iv) what are the ambient flow conditions through the repository horizon to the water table, (v) what are the ambient flow conditions in the saturated zone, and (vi) which conceptual models provide conservative assessments of groundwater flow? By addressing each of these subissues in detail, it is hoped that technical bases can be developed that will assist in the timely review of the Site Suitability Report as well as the License Application. Moreover, by addressing these subissues the NRC hopes to resolve technical issues such as shallow infiltration and future climate prior to the issuance of the Site Suitability Report. Moreover, resolution of subissues (ii), (iii), and (iv) will directly address the reasonableness of the WCIS low seepage hypotheses, while resolution of (v) will address the reasonableness of the WCIS saturated zone dilution hypotheses.

10.2 OBJECTIVES AND SCOPE OF WORK

The primary objective of the Key Technical Issue (KTI) on Unsaturated and Saturated Flow under Isothermal Conditions (USFIC) is to assess all aspects of the ambient hydrogeologic regime of YM that have the potential to compromise the performance of the proposed repository. The secondary objective of this KTI is to develop technical procedures and to conduct technical investigations for assessing the adequacy of the DOE strategy for characterizing key site- and regional-scale hydrogeologic processes and features that may adversely affect the performance of the repository. These processes and features include (i) those likely to decrease radionuclide transport time from the repository to the accessible environment, (ii) those that affect corrosion of waste packages and dissolution of waste form, and (iii) those affecting saturated zone dilution of radionuclides. During FY96 it was determined that effort would primarily be focused on those processes and features that affect shallow infiltration and deep percolation.

For each subissue described previously, a number of specific technical criteria have been defined that describe in more detail the scope of each subissue. Because efforts during FY96 were focused primarily on shallow infiltration and deep percolation, only the specific technical criteria for subissues (ii) and (iii) will be defined. Specific technical criteria, which must be addressed to resolve subissue (ii) include determination of the average annual infiltration rate, the spatial distribution of infiltration, the maximum instantaneous infiltration rate, and the expected increase in infiltration during a pluvial period. Specific technical criteria for subissue (iii) include determining the potential for existing perched water bodies to flood portions of the repository, the likelihood that additional perched water bodies will form under a pluvial climate, whether perched water bodies are indicators of fast flow paths that extend to the surface, whether the Paintbrush nonwelded tuff (PTn) is laterally contiguous within a fault block and thus acts as a barrier to vertical flow, estimates of fast flow rates where the PTn is breached by faults or fracture zones, and whether radioactive tracers found at depth (e.g. ^{36}Cl) are indicators of fast pathways.

10.3 SIGNIFICANT TECHNICAL ACCOMPLISHMENTS

During FY96 significant progress was made in refining estimates of shallow infiltration and deep percolation, and improving understanding of mechanisms that lead to the development of perched water bodies and what the presence of perched water bodies at YM indicates about present and past hydrogeologic and climatic conditions. Three papers were prepared on these subjects and submitted to scientific journals for publication. In addition, significant progress has been made on development of a technical review procedure for assessing whether the DOE has adequately addressed the likelihood that existing or future perched water bodies may saturate the underground facility. Other efforts focused on resolving differences with the DOE on estimates of shallow infiltration and determining appropriate methods for bounding the effects of climatic changes on future hydrogeologic conditions.

10.3.1 Progress Toward Resolving Technical Issues at Yucca Mountain

Assessments of the performance of the proposed repository are unanimous in finding that moisture conditions in the drifts and moisture flux rates in the unsaturated zone below the repository critically impact performance of the repository (Nuclear Regulatory Commission, 1992, 1995b; Sandia National Laboratories, 1992; Wilson et al., 1994; TRW Environmental Safety System, Inc., 1995). Significant progress was made on determining appropriate methods for bounding the effects of climatic changes on future hydrogeologic conditions and resolving differences with the DOE on estimates of shallow infiltration. Both issues are concerned with linking current and possible future climatic conditions to current and possible future hydrologic conditions occurring at and below the proposed repository level.

10.3.1.1 Climate Change, Future Precipitation, and Water Table Rise

Current regulations of the U.S. Nuclear Regulatory Commission (NRC) require that any performance assessment supporting the license application for a HLW repository must consider potential changes in hydrologic conditions caused by reasonably foreseeable climatic conditions (Nuclear Regulatory Commission, 1995a). The requirement is important because climate will almost certainly change significantly during the many tens of thousands of years that disposed nuclear wastes will remain hazardous. More importantly, climate controls the range of precipitation, which in turn controls the rates of infiltration, deep percolation, and groundwater flux through a geologic repository located in an unsaturated environment. Changes in groundwater recharge will induce other changes such as fluctuations in elevation of the water table. Water table rise would reduce the thickness of the unsaturated zone barrier. Therefore, future changes in climate could significantly influence waste isolation in a repository at YM.

The importance of groundwater flux as the key parameter for waste isolation in an unsaturated zone is well known, and has been further emphasized by the DOE's most recent report (TRW Environmental Safety System, Inc., 1995) on total system performance assessment (TSPA). On page ES-30 of that report it is stated that "... in the overall TSPA analyses, an over-arching theme comes back again and again as being the driving factor impacting the predicted results. Simply stated, it is the amount of water present in the natural and engineered systems and the magnitude of aqueous flux through these systems that controls the overall predicted performance... Therefore, information on... [this issue]... remains the key need to enhance the representativeness of future iterations of TSPA." The DOE WCIS

(U.S. Department of Energy, 1996, p 5)[2] likewise states that "[p]erformance assessments have shown that seepage into the emplacement drifts is the most important determinant of the ability of the site to contain and isolate waste." The importance of infiltration as a hydrologic parameter was recognized by the NRC staff in Iterative Performance Assessment Phase 2. The NRC (1995b, p 10-4) states that "[a]lthough the flux of liquid water through the repository depends on the parameters infiltration, hydraulic conductivity, and porosity, performance correlates most strongly to infiltration."

The present environment of the HLW program is one of legislative and regulatory changes. The U.S. Environmental Protection Agency (EPA) is promulgating a new HLW standard. EPA current standard, 40 CFR Part 191, specifies a repository compliance period of 10,000 yr. A new standard may stipulate a similar period or a much longer time period on the order of hundreds of thousands of years. Under an extended compliance period climate change would be expected to play an even greater role in performance assessments. Even if the compliance period remains at 10,000 yr, the DOE may be required to provide longer-term estimates of peak doses dependent on likely climate scenarios to help support the NRC regulatory decisions.

As part of a pilot project in issue resolution, the NRC staff is preparing an issue resolution report that addresses three subissues under the KTI of Isothermal Hydrology. These subissues are future climate change and the related topics of future precipitation and water table rise. There appears to be a clear path to reach a scientific consensus on methods for evaluating past climates and estimating future climatic changes. It is suggested in the report that paleoclimatic and paleohydrologic data provide an excellent foundation to estimate the range of future climate states at YM. The NRC staff report emphasizes paleoclimatic methods to develop a reference scenario for future climate rather than placing reliance on extensive use of climate modeling. This approach is not expected to be significantly affected by any changes to EPA or the NRC HLW regulations that may result from the National Research Council (1995) recent review or by changes in the licensing of HLW repositories being considered in the Congress.

The NRC staff reviewed all available information, not just that provided by the DOE in previous submittals. Based on this prelicensing review, the issue resolution report suggests that sufficient paleoclimatic information exists in various forms to make the following observations:

- Methods based on paleoclimatic data can be used to adequately estimate the range of past climates in the YM region. In particular, the temperature proxy data from Devil's Hole provide one of the longest and best paleoclimatic records covering a continuous 500,000-yr period (Winograd et al., 1992).

- Variability of future climate over hundreds of thousands of years could be presumed to follow general patterns of the last 500,000 yr as inferred from paleoclimatic data. Glacial/interglacial cycles have typically lasted about 100,000 yr and interglacials have lasted about 20,000 yr (Winograd et al., 1992).

- Recent studies have shown that the water table in the YM region may at times have risen as much as 115 m during the Wisconsin glacial stage. The data also suggest that the water table

---

[2]U.S. Department of Energy. 1996. *Highlights of the U.S. Department of Energy's Updated Waste Containment and Isolation Strategy for the Yucca Mountain Site*. DOE Concurrence Draft. July 1996. Washington, DC: U.S. Department of Energy.

may never have been higher than that in the last 10+ million years, providing confidence that waste packages in a proposed repository at YM would never be inundated by the regional water table.

- Based on recent studies, mean annual precipitation at YM during past pluvial climates may have been two to three times greater than today. This range of precipitation can be used to estimate what might be expected during future pluvial climates and can help establish an upper bound to derive estimated ranges of future infiltration and deep percolation.

The NRC staff approach to issue resolution considers all available information, not just the information provided by the DOE in previous submittals. For this pilot topic the NRC staff is not responding to a specific topical report from the DOE, but instead performed an independent, prelicensing review of the broad scientific literature related to future climate. In general, there is sufficient information available today to reach resolution on the range of future climate variability and methods to determine upper thresholds for future precipitation and water table rise. When complete, the NRC staff issue resolution status report will be transmitted to the DOE, oversight committees, the State of Nevada, and other interested parties for review and comment.

10.3.1.2 Infiltration

To estimate deep percolation fluxes using numerical simulation, an estimate of net infiltration (percolation flux escaping the zone of evapotranspiration) is required over the surface of the subregional area. The DOE strategy evolved from potential infiltration maps based solely on matrix properties (Flint and Flint, 1994) as additional data [e.g., neutron-probe borehole measurements (Flint and Flint, 1995)] became available and as numerical simulators appropriate to the site have been developed.[3] The planned DOE strategy for estimating net infiltration over the performance period links climatic forcings to net infiltration using numerical simulators.[1] Current DOE efforts are tied to calibrating the numerical simulators to the neutron-probe data and estimating the spatial distribution of net infiltration.[1]

Independent attempts to use numerical simulators to predict the behavior and distribution of net infiltration are being conducted at the Center for Nuclear Waste Regulatory Analyses (CNWRA) (section 10.3.3). Based on experience gained from comparing modeling exercises to field measurements, it can be concluded that

- Numerical simulations can provide plausible estimates of the relative spatial and temporal distributions of net infiltration,

- Numerical simulations can provide reasonable estimates of hydraulic controls on infiltration,

- Numerical simulations can provide insights into how infiltration might change over time due to climatic changes, and

[3]Flint, A.L. 1996. Open-meeting presentation to the Nuclear Waste Technical Review Board on July 9–10, 1996 in Denver, CO.

* Numerical simulations only bound estimates of net infiltration to within ranges of perhaps 10 to 20 percent of precipitation.

Spatial distribution patterns for net infiltration predicted by the CNWRA are quite similar in character to patterns reported by Flint[1] (e.g., infiltration increases with increasing elevation and decreasing surface cover). The modeling approaches are similar, insofar as 1D simulations are used on a pixel-by-pixel basis, but the processes involved wit shallow infiltration are handled using somewhat different assumptions (e.g., bare-soil evaporation by the CNWRA versus evapotranspiration by the DOE). In addition, the estimated area-average net infiltration values are within a factor of 2 to 4, comparable in magnitude to the variation that the CNWRA model predicts over reasonable ranges of parameter values. Inasmuch as numerical modeling can only bound shallow infiltration estimates, it is appropriate to further constrain infiltration estimates using other sources of data. Various lines of evidence, including (i) age-dated fracture fillings, (ii) comparing 36_{Cl} measurements in the Exploratory Studies Facility (ESF) with transport simulations, and (iii) inverse modeling based on borehole measurements of moisture contents, tension, and temperature are cited[4] as suggesting that infiltration lies in the range of slightly under 1 mm/yr to perhaps greater than 10 mm/yr. As comparison, using the base-case CNWRA map, the average net infiltration is approximately 10 mm/yr, estimated over the length of the north ramp of the ESF through the turn to the main drift. As multiple lines of evidence are pointing to a range of values broadly within an order to magnitude for net infiltration, it can be concluded that considerable progress has been made on resolving the issue of estimating shallow infiltration.

10.3.2 Perched Water Bodies at the Yucca Mountain Site and Inferences for Recharge Rates

Specific technical subissues addressed in this section are the hydraulic conditions in the unsaturated zone above the repository, and the ambient flow conditions through the repository horizon to the water table. Resolution of both technical subissues involve evaluating the potential for formation of perched water bodies at YM. Perched water is defined as an unconfined saturated zone separated from an underlying saturated zone (water table) by an unsaturated zone and is deemed significant with respect to infiltration and groundwater flux (U.S. Geological Survey, 1981). Relative to the proposed repository, perched water bodies could occur above, within, and below the repository horizon. Of these three zones, perched water within the repository itself would be of most concern because it is believed that waste canisters will last longer in unsaturated rock than under saturated conditions. The formation of perched water bodies around waste canisters would likely increase the rate of waste canister failure resulting in greater releases of radionuclides. The potential for formation of perched water bodies is identified in federal regulations, for example, 10 CFR 60.122(c)(23), as a potentially adverse condition for the storage of HLW in a geologic repository. Perched water is common in arid environments. For example, perched water flows from seeps into the U12n tunnel through the zeolitized Indian Trail Tuff at Rainier Mesa, 50 km northwest of YM (Thordarson, 1965; Russell et al., 1987; Wang et al., 1993). Perched water bodies tend to be transient features that are formed where there is a contrast in hydrologic properties (Freeze and Cherry, 1979). Contrasts may result from differences between stratigraphic units. Contrasts may also occur by juxtaposition of low conductivity strata with more conductive strata along a structural feature such as a fault or other persistent discontinuity. YM is crisscrossed by numerous faults, thus substantially increasing the probability of locally saturated conditions occurring.

---

[4]Bodvarsson, G.S. Open-meeting presentation to the Advisory Committee on Nuclear Waste on September 26, 1996 in Las Vegas, NV.

Perched water bodies would be more likely to form or expand under future, wetter, climatic conditions that cause increased infiltration. It is possible that perched water bodies in the YM area are relict features formed by higher infiltration rates during former pluvial climates. If perched water bodies formed above the repository, this local saturation could induce localized fracture flow along vertical pathways downward into the repository. Past (and contemporary) occurrence of fracture flow that bypassed part of the unsaturated zone where matrix flow would normally predominate, thus transporting released contaminants at greater flow rates, has been recently inferred from ^{36}Cl measurements at the ESF within the repository host rock at YM (Fabryka-Martin et al., 1996). Elevated levels of ^{36}Cl, interpreted as being bomb-pulse in origin, was identified at a few distinct, highly fractured zones generally in the vicinity of faults, indicating that a small amount of water at these locations is less than 50 yr old and that it was, most probably, transported through extremely localized pathways.

10.3.2.1 Perched Water Body Occurrences at Yucca Mountain

A number of perched zones were found at several boreholes (USW UZ-1, UZ-14, NRG-7a, SD-7, and SD-9) at YM (Burger and Scofield, 1994; Yang et al., 1996). A vacuum-reverse-air-circulation drilling method was used for these boreholes to prevent contamination from drilling fluids and all perched water samples were collected using plastic or stainless steel bailers. As of June 1996, all perched water found occurs in the upper Calico Hills unit with the exception of UZ-14 and USW SD-9, where the perched water body is found on the basal vitrophyre in the Topopah Spring unit. Boreholes UZ-1 and UZ-14, which are on the same drilling pad, encountered a perched zone at a depth of 190 m above the water table. The zone was extensive enough to be pump tested at a rate of 0.204 m^3/hr for 67 hrs, and a total of 22.71 m^3 produced. It has been estimated, however, that this perched water zone is much more extensive than originally thought, with an approximate volume of 114,000 m^3 (Yang et al., 1996). In USW SD-9, perched water appeared to be just above the basal vitrophyre of the Topopah Spring unit, 120 m above the water table. Boreholes that encountered perched water within the Calico Hills Tuffs include USW SD-7 and USW NRG 7/7a. The perched zone encountered by SD-7 was extensive enough to be pump tested at a rate of 0.75 m^3/hr for 30 hrs and a total of 45.42 m^3 produced. This perched water zone is a relatively small body and its total volume estimated at approximately 300 to 500 m^3. It is quite possible that other perched zones may be discovered at YM during further site characterization.

Within 6 to 8 m sampling intervals in the five boreholes, large ^{14}C variations are detected ranging from 27.2 to 66.9 percent modern carbon (PMC) with an average of about 37 PMC, indicating a multitude of water sources that contribute to these perched water reservoirs. The apparent (uncorrected) ^{14}C ages of perched water range from 3,500 to 10,800 yr. If age corrections are made to account for caliche dissolution, perched water residence times of less than 7,000 yr are estimated. The uncertainty in ^{14}C measurements is $\pm$ 0.7 PMC (Yang et al., 1996).

10.3.2.2 Perched Water Body Modeling

This work addresses a specific mechanism that is known to promote development of perched water, the entrapment of water due to faults or fault zones. Faults can affect groundwater by enhancing flow rates, inhibiting flow, or acting in a neutral manner. In this work faults are considered to be neutral due to the lack of data supporting other hypotheses and thus only the effects of the relative positions of the layers of different and perhaps sharply contrasted hydrologic properties would affect the flow. Thus, the first question that needs to be answered is whether a perched water body can form and be sustained under the contrast conditions present at YM.

The effect of differing hydrologic properties of the stratigraphic layers may cause water that is percolating down to be channeled downdip when it encounters a relatively impermeable layer. Faults in YM are common and this faulting has produced offset of the stratigraphic units. If the offset of the fault is such that a relatively permeable unit within the downthrown fault-block is juxtaposed against a relatively impermeable unit downdip of the fault, then the channeled water will be inhibited from continuing downdip and eventually will become trapped at this location. The source of this water may be a combination of both infiltration of precipitation and relict water that accumulated during a cooler, wetter climatic period in the past. Spaulding (1985) conducted research with plant microfossils and dated remains found in packrat middens in the vicinity of the Nevada Test Site (NTS). Based on this work, Spaulding (1985) reported that the climatic conditions at the NTS about 45,000 yr before present (YBP) were similar to the present day conditions in northern Nevada. Even though it is fair to speculate that most of this recharge occurred in the areas of higher elevation north of YM, it is hypothesized that water was also able to find its way down in the area of the proposed repository, at higher rates than present. Moreover, evidence exists suggesting that the water table was approximately 115 m higher in the YM region than it is today (Quade et al., 1995).

Czarnecki (1985), following a numerical modeling approach, investigated the effects a wetter future climate would have on the water table and concluded that a 100 percent increase in precipitation could cause the water table at YM to rise by as much as 130 m. Such a rise in the water table would not be adequate to inundate the repository, but saturation levels above the higher water table would see an increase from present day values.

Some interesting questions pertaining to the YM system are (i) whether the flow system at YM could yield relict perched water bodies starting from a much wetter initial condition in the distant past, (ii) whether these perched water bodies could be sustained at present day levels (i.e., estimated reservoir volumes) under present day recharge conditions, and (iii) whether such sustained perched water bodies agree with ^{14}C residence times inferred from measurements at YM boreholes.

The first step toward enhancing modeling efforts is to construct a three-dimensional (3D) Geologic Framework Model (GFM) that embodies the current understanding of YM. Efforts at the CNWRA have developed a computerized GFM that includes lithostratigraphy, hydrostratigraphy, and geologic structure (Stirewalt et al., 1994; Stirewalt and Henderson, 1995) of the YM region. Lithostratigraphy and geologic structure are based on surface geologic maps of the site (Scott and Bonk, 1984). Subsurface geology is constrained by both borehole control and through the construction of balanced cross sections. Hydrologic properties include porosity, saturated hydraulic conductivity, and water content. For the hydrostratigraphic model, mean values for hydrologic properties are assigned as constant values for each of seven different lithostratigraphic units. Original data are from the DOE site characterization activities (e.g., Craig and Reed, 1991; Flint and Flint, 1990; Loscot and Hammermeister, 1992; Whitfield et al., 1993).

The area considered for current work is the vicinity of the intersection of the Ghost Dance and Sundance faults in the repository area of the YM site. The modeled area is 1,100 m wide by 650 m deep and is extracted electronically from the CNWRA GFM. The plane of view is the Sundance fault facing northward. The area of interest is above the water table and primarily updip of the Ghost Dance fault. The right border of this model represents an artificial no-flow boundary that causes water to accumulate, whereas in reality the water would continue flowing downdip past this boundary. Given the abundance of normal faults in the YM area, this condition may be a representative depiction since it corresponds to a periodic boundary condition (a fault every so many length units). Any perching to the right of the fault

is eliminated from subsequent calculations. The beds included in this analysis are (from top to bottom): (i) Tiva Canyon welded (TCw); (ii) PTn; (iii) Topopah Spring welded 1,2,3 (TSw); (iv) Calico Hills nonwelded (CHn); and (v) Prow Pass welded (PPw).

Initially, a uniform suction head value of 10 m (approximately equal to the bubbling pressure for most YM units) was assigned to the entire modeled region, which was then allowed to drain under gravity with no flux added in the system. Solution of the flow equation in a transient mode produced pressure head, which were transformed to saturation values. The volume of moisture within zones that exceeded an *a priori* selected percent saturation value (typically 99.95 percent) was then calculated, thus providing perched water volume as a function of time, $V(t)$. In this work, all flow simulations have been conducted with the BIGFLOW numerical code (Ababou and Bagtzoglou, 1993) that solves the local mass conservation equation in a slightly compressible and variably saturated porous medium without source/sink terms. The BIGFLOW code is based on a low order, seven point centered finite difference scheme in space and a fully implicit one step (Euler backwards) finite difference scheme in time. The spatial mesh used in this work is rectangular with a Δx=20 m and Δz=10 m and an automatic time stepping algorithm is invoked. The left and right boundaries are no-flow, the top boundary is constant flux, and the bottom boundary is a water table condition.

Once the $V(t)$ relationship has been obtained for the base-case state of the flow system (i.e., no flux added) the point of maximum perched water volume was used as an initial condition for a simulation with a uniformly distributed, prescribed flux added at the top of the domain. Depending on the value of this flux, any of the following situations is possible for the perched water volume: (i) it could eventually go to zero (system drained), (ii) it could eventually increase without bound (system flooded), and (iii) it could be sustained at a steady-state level. Figure 10-1 depicts two cases in schematic form: complete drainage and attainment of a steady-state volume consistent with the observed present day volume. Once such a match between predicted and observed volumes is attained, through repeated flow simulations with different input fluxes, the obtained flux is considered optimal and recorded. As indicated in figure 10-1, there exists two hydrological constraints that need to be satisfied. These are (i) $dV/dt(t=T_{tot})=0$, and (ii) $V(t=T_{tot})=V_{pres}$, where V_{pres} is the observed (present day) volume of the perched water reservoir. Finally, there exists the additional constraint that the steady-state condition has been attained within a time period less than 18,000 to 20,000 yr, the current climate period. Thus, $T_{tot} \leq 20{,}000$ yr is the third hydrological constraint that must be satisfied.

A means of refining computer models of flow at YM is to use available water and mineral chemistry to identify where perched water might have occurred in the geologic past. Hydrochemical facies and environmental tracers such as stable isotopes have long been used to distinguish water bodies and identify potential flow paths (National Academy of Sciences, 1992). Radiometric age dates can be determined for both mineral deposits and groundwater and used to estimate rates of fluid flow and timing of changes in paleohydrological conditions. Chemical data are being gathered at YM as part of the DOE site characterization efforts. These include groundwater chemistry of the unsaturated zone (Yang et al., 1988, 1996; Yang, 1992) and chemical and isotopic analyses of minerals deposited from past and present groundwater (e.g., Bish and Chipera, 1989; Whelan and Stuckless, 1992). Trends in these data have been used to interpret paleohydrology, fluctuations in the static water table (National Academy of Sciences, 1992), and climatic variations (Tyler et al., 1995).

An obvious second step in the work, presented herein, is to investigate whether ^{14}C data from the YM site could corroborate or refute hydrologically conditioned simulation results. Consider the mass balance of ^{14}C within a well-mixed reservoir (Pearson and Truesdell, 1978) expressed in PMC

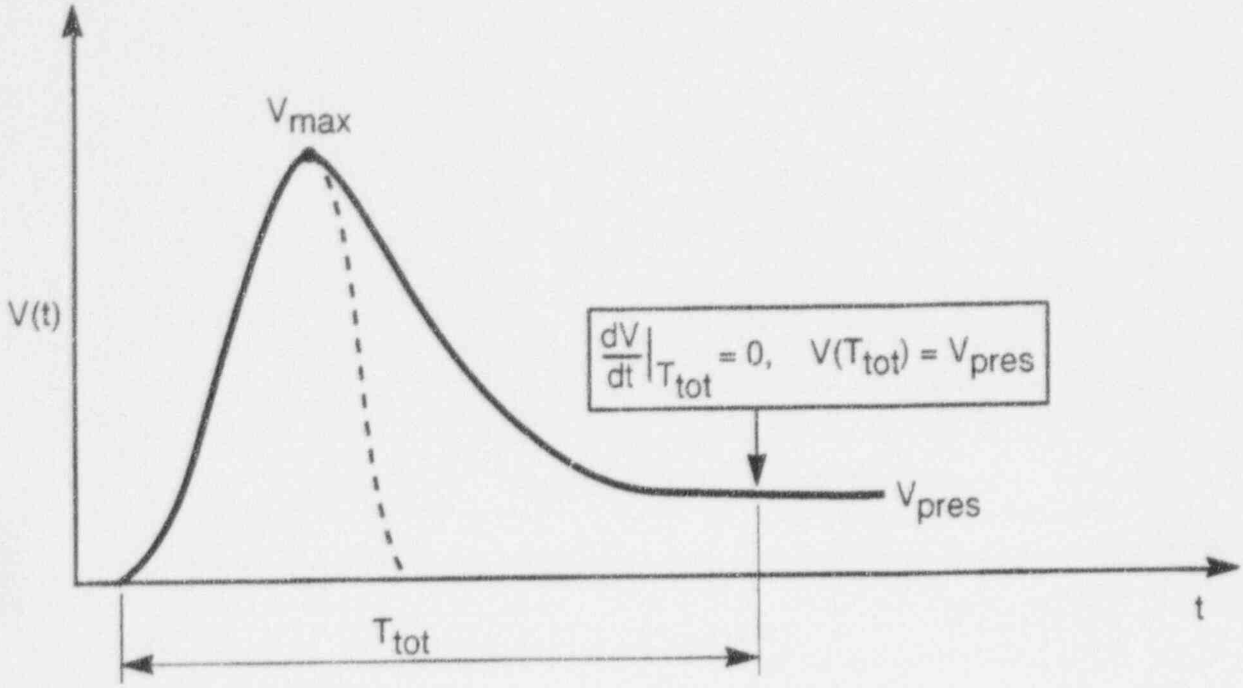

Figure 10-1. Schematic of perched water volume as a function of time for complete drainage and steady-state attainment simulations

$$\frac{d(CV)}{dt} = A\ q_i\ C_i - A\ q\ C - \lambda CV \qquad (10\text{-}1)$$

where C_i and C are the PMC of young (present day) and mixed-age water; $\lambda = 1.2097\times10^{-4}$ yr^{-1} is the radioactive decay constant for ^{14}C; A and V are the horizontal cross sectional area and volume of the perched water body, respectively; and q_i and q are the inflow and outflow rates, respectively. The well-mixed model assumes that all sources of water input to the reservoir are completely mixed with the water already in the reservoir. Solution of this equation is obtained by setting $A_1 = V_o$; $B_1 = A(q_i - q) = \frac{\Delta V}{\Delta t}$; $A_2 = A\ q_i + \lambda V_o = \frac{\Delta V}{\Delta t} + A\ q + \lambda V_o$, and $B_2 = \lambda\frac{\Delta V}{\Delta t}$ resulting in:

$$\frac{dC}{dt} = -\frac{A_2 + B_2 t}{A_1 + B_1 t}\,C + \frac{A\ C_i\ q_i}{A_1 + B_1 t} \qquad (10\text{-}2)$$

This is an ordinary differential equation that, unfortunately, has no closed form solution. In the process of arriving at this equation for ^{14}C, the following assumptions were made: (i) influx (q_i) is not changing with time; (ii) optimal flux estimates represent the areal average of a matrix-fracture continuum; (iii) no daughter product contribution ($C_{tot} = {}^{12}C + {}^{13}C + {}^{14}C$); (iv) transport system is lumped, exhibiting no spatial characteristics; and (v) no ^{14}C is partitioned in liquid and gas phases. Integration of (Eq. 10-2) was performed numerically using a fourth and fifth order Runge-Kutta-Fehlberg algorithm with a self-adapting

time step. The geochemical constraint that must be satisfied is that after a period of time equal to T_{tot}, the ^{14}C in the perched water body cannot be substantially different than a target value PMC_{pres} observed at YM boreholes.

To determine the likelihood of the repository site developing localized perched water zones, the potential for trapping and the areal extent of that perched water zone must be exhaustively evaluated. To do this, the hydraulic conductivity must be determined for all the rock units involved at all possible saturation levels. The hydrologic effects of the difference in hydraulic conductivities of various units must also be evaluated to determine the trapping potential of all the rock units at all saturation levels. Ideally, to make the best final probability estimate for the perching potential, an infinite number of combinations of hydraulic conductivity to saturation level and different saturation levels of different beds should be considered. For each of these combinations the areal extent of the region likely to become perched should be calculated. This task, however, would involve a vast number of calculations. The data used in this study were adopted from the 1993 Total System Performance Assessment (TSPA-93) for YM (Wilson et al., 1994). TSPA-93 uses 10 hydrogeologic units. Because the current CNWRA model of the YM site uses slightly different stratum classifications, some modifications were necessary. Some units are directly equivalent and others were combined by a weighted average based on their relative thicknesses. From the TSPA-93 data (mean, minimum, maximum, and coefficient of variation), a random sampling of possible values from a beta distribution curve were produced using the Latin Hypercube Sampling (LHS) approach (Iman and Shortencarier, 1984) to obtain sufficiently accurate results without using all possible combinations. However, results from only one realization are presented here for the sake of brevity.

10.3.2.3 Results and Discussion

The first realization used the mean values from the TSPA-93. As the system began to drain, with no flux added and an initial uniform head value of −10 m, water began to drain from some areas and to accumulate in others. The PTn unit, having a high matrix permeability, allowed water to flow freely down through it. When it encountered the low matrix permeability TSw unit its downward flow was inhibited. This caused the water to be channelled downdip in the PTn until it reached the Ghost Dance fault. The footwall of the fault has been uplifted such that the PTn in the hanging wall is juxtaposed against the relatively impermeable TSw unit in the footwall of the fault. This produces a trap where water that is channelled downdip through the PTn encounters the relatively impermeable TSw at the fault and begins to accumulate, producing a perched water body. As it continues to accumulate, it percolates slowly down through the TSw unit, thus extending the perched water body well in the TSw unit. The perched body continues to grow as long as there is enough water above it to supply water faster than can be dissipated. It reaches a maximum perched volume of 15,949 m^3 at 455 yr after which the perched water begins to dissipate until it is completely drained by about 1,600 yr.

Starting from the point in time with maximum perched water volume, a flux was added at the surface to approximate a mean infiltration rate. This was allowed to continue until the system reached an equilibrium condition, specifically until the perched water body disappeared or remained at a constant volume. Different flux rates were added until one was found that produced and sustained a perched water body of roughly the same volume of water as actual perched water bodies found in the area (e.g., SD-7), approximately 400 to 500 m^3. In this case, a constant flux of 6.2 mm/yr applied uniformly to the top of the system produced a sustained perched water volume of 528 m^3 right below the PTn/TSw interface. Figure 10-2 depicts the temporal evolution of the perched water volume for the draining simulation and the simulations with a recharge of 6.2 and 8.0 mm/yr. Note how the 8.0 mm/yr simulation diverges and floods the system, whereas the 6.2 mm/yr simulation reaches asymptotically the desired volume. This is

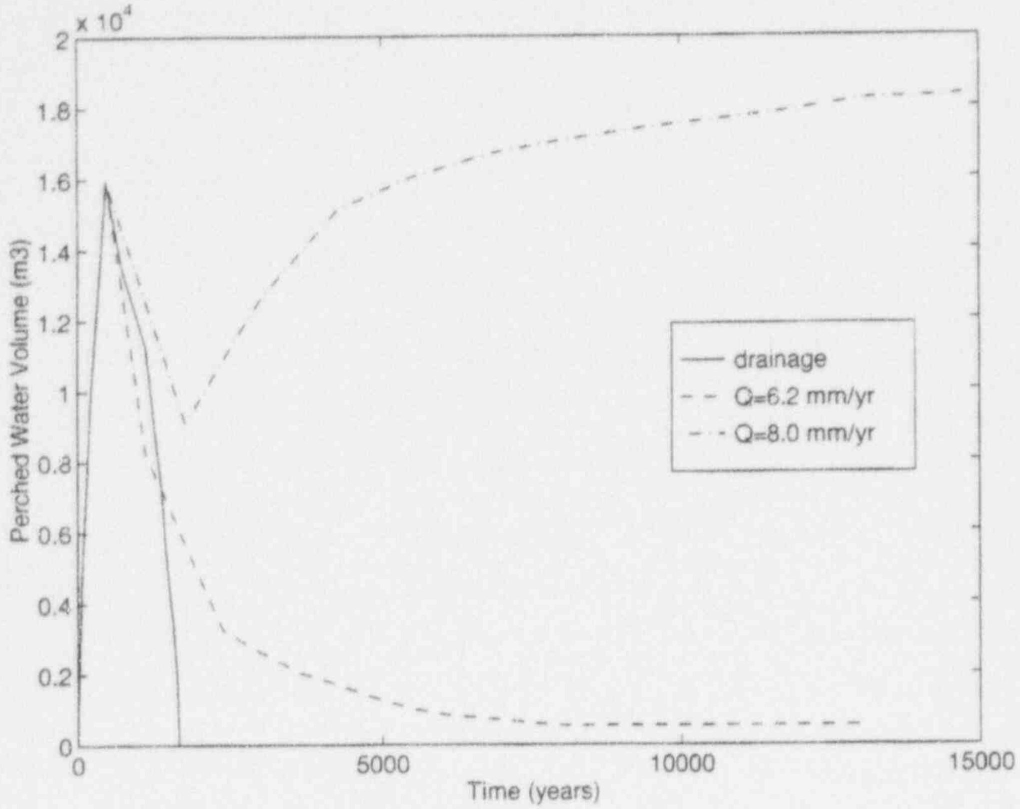

Figure 10-2. Temporal evolution of perched water volume for draining and for q=6.2 and 8.0 mm/yr simulations. Mean TSPA-93 hydrologic properties are used.

an indication that the perched water body exhibits a meta-stable behavior near the optimal value of 6.2 mm/yr. Any recharge higher than this optimal value exceeds its storage capacity and eventually floods the system. It is worth mentioning that even though this particular realization predicted perched water forming at a depth quite different from that observed at YM, other realizations predicted perched water forming at the base of the TSw unit.

Equation (10-2) was solved numerically with input the $V(t)$ behavior as inferred from the detailed flow simulations. Since the actual areal extent A of the perched water body is unknown, a set of simulations have been conducted by varying this parameter. Figure 10-3 depicts the ^{14}C depletion as a function of time for each material property realization and also for a set of three values for the areal extent parameter. Shown in figure 10-3 also is the reference simulation that corresponds to pure radioactive decay and the target value of PMC_{pres}=0.28. Several observations can be made from this figure. First, the q=6.2 mm/yr simulation, using mean TSPA-93 values, could reach the target PMC_{pres} after a residence time between 10,000 and 20,000 yr for realistic areal extent values. This timeframe is consistent with the time required for the volume to reach a dV/dt=0 and also with the change of the climate around 18,000 to 20,000 YBP. Therefore, this realization could be classified as plausible on the basis of the hydrological and geochemical constraints described earlier.

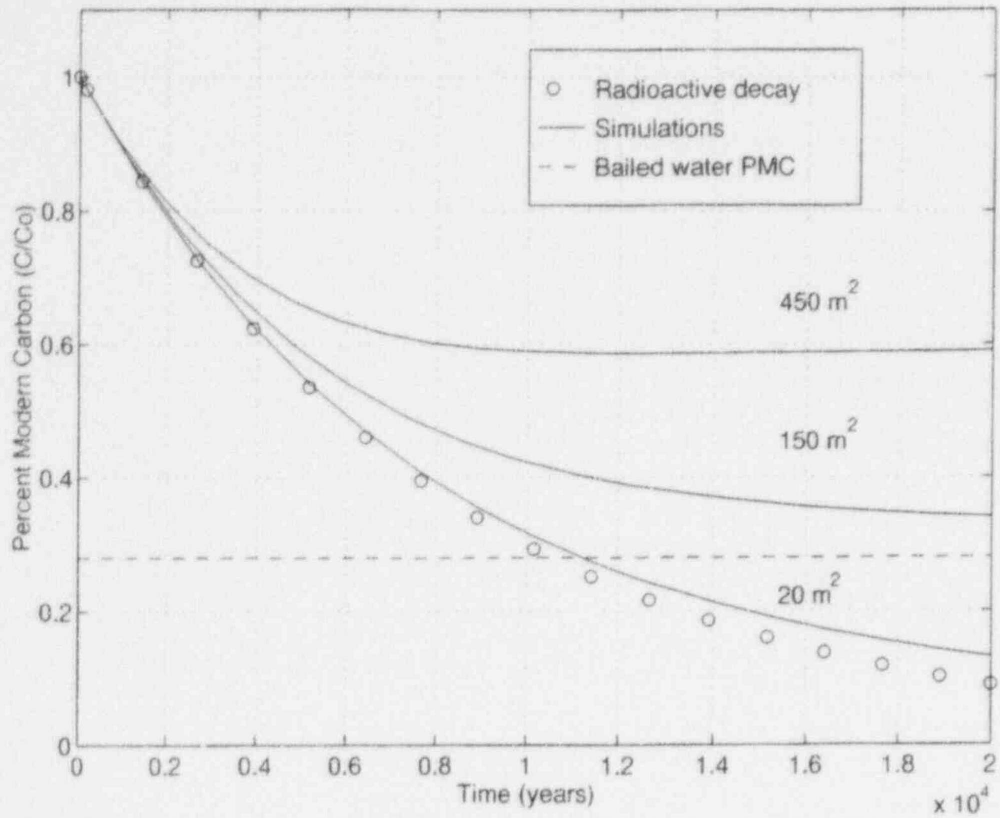

Figure 10-3. Depletion of perched water ^{14}C as a function of time for q=6.2 mm/yr and three areal extent values. Mean TSPA-93 hydrologic properties are used.

10.3.2.4 Conclusions

It must be stressed that the method presented in this section does not account for the hydraulic properties of fractures, which should be considered when modeling YM. Therefore, conclusions are only valid for the simplified system used to test the approach and may not be valid for YM. There are three major conclusions of this study: (i) a sustainable perched water body can be attained in the simplified system with an average deep recharge rate of 6.2 mm/yr; (ii) an approach that assists in the determination of plausible recharge rates, based on hydrological and geochemical constraints, was proposed and applied to an idealized YM site; and (iii) it appears that for the realization that satisfies both hydrological and geochemical constraints, a present day perched water body that consists of a combination of some minimal relict (past pluvial) water and young water from infiltration is an appropriate hypothesis.

10.3.3 Estimates of Infiltration at Yucca Mountain

The study presented in this section is part of an ongoing effort to examine the spatial distribution of shallow infiltration at YM using numerical simulations. A motivation for the study is to provide insight into the spatial distribution of boundary conditions appropriate for simulations of deep subsurface moisture redistribution and examine how these might be affected by hydraulic properties and climatic variation. The first efforts toward the study occurred under the Iterative Performance Assessment Project and a large part

of the work occurred under the Subregional Hydrogeologic Flow and Transport Processes Research Project.

The study abstracts detailed one-dimensional (1D) simulations into a response surface for average annual infiltration (AAI) as a function of hydraulic properties, average annual meteorologic inputs, and depth of surficial cover. Each input parameter to the response surface function is estimated for each pixel of a Digital Elevation Model (DEM) of the study area. Assuming that the response surface is appropriate over the scale of a DEM pixel, the set of input parameters at each pixel is used to predict AAI for the pixel. Using the average of AAI over the study area as a measure, the relative importance of each input parameter is assessed by examining the sensitivity of the measure to the input.

The basic methodology for the study was presented in the CNWRA semi-annual research reports (e.g., Stothoff et al., 1995; Stothoff and Bagtzoglou, 1996).[5] The primary efforts in FY96 have been to extend the breadth of cases considered, refine models, analyze the information already obtained, and document the work in refereed journal articles (Stothoff, 1996)[6]. In particular, efforts were made to (i) simulate the response of AAI to a more exhaustive set of input parameters, (ii) abstract the relationships between simulated AAI and input parameters, (iii) refine the predictive model for colluvial/alluvial depths, and (iv) examine the sensitivity of areal-average AAI to various input parameters.

10.3.3.1 One-Dimensional Simulator Description

The BREATH simulator used for the 1D simulations considers the coupled flow of moisture and energy in a porous medium and is described in detail by Stothoff (1995). All simulations presented herein use similar boundary conditions. At the bottom of the column, the gradients of saturation and temperature are assumed to be zero, allowing gravity drainage of water and advective losses of energy. At the top boundary of the column, the simulator is presented with 10 yr of meteorological input, based on hourly readings from the Desert Rock, Nevada, National Weather Service meteorologic station located approximately 30 miles east of YM (National Climatic Data Center, 1994); procedures for converting the National Weather Service readings into BREATH meteorological inputs are discussed by Stothoff et al. (1995). The meteorological record runs from March 1, 1983 through February 28, 1993. The decade of weather is repeated until the initial conditions are eliminated; all reported results are for the last simulated decade. One decade may be too short a time period to capture the full range of precipitation events in a statistically robust way, however, considerable insight can be gained on the behavior that might be expected from the columns over longer periods of time.

10.3.3.2 Deep-Alluvium Response Function Abstractions

A large number of 1D simulations were performed to systematically examine the impact of representative deep-alluvium hydraulic properties (Stothoff, 1996)[7] and representative meteorological input values[3] on AAI. To make direct comparisons between simulations, surface boundary conditions were

---

[5]Stothoff, S.A., H.M. Castellaw, and A.C. Bagztoglou. 1996. Simulating the spatial distribution of infiltration at Yucca Mountain, NV. *Water Resources Research*. In preparation.

[6]Stothoff, S.A. 1996. Sensitivity of long-term bare-soil infiltration simulations to hydraulic properties in an arid environment. *Water Resources Research*. Submitted for publication.

[7]*Ibid.*

based on the same 10 yr meteorological sequence. To investigate the impact of meteorological input values, one input value (e.g., precipitation, air temperature, etc.) was changed systematically for the entire sequence either by multiplying each hourly value by a constant or adding a constant to each hourly value.

All deep-alluvium simulations with intrinsic permeability k less than about 10^{-9} cm^2 [equivalent to silty sands (Freeze and Cherry, 1979)] yielded essentially zero AAI. For these simulations, evaporation from the ground surface was sufficient to reclaim any water not running off during precipitation. For simulations with k having a value of 10^{-8} cm^2 or greater, a scaling parameter $Y = \ln[(\text{AAI/AAP})k^{1/2}]$, where AAP is average annual precipitation, was found to be useful in describing the response of AAI to the hydraulic and meteorologic input properties. The scaling parameter accounts for the decrease in AAI with increasing intrinsic permeability observed in the simulations with maximum AAI occurring for k around 10^{-8} cm^2. The Y values obtained from the simulations can be expressed as a first order expansion about the Y value obtained for a base-case simulation. Over the range of parameters considered, Y appears to increase as the square of van Genuchten m, as the square root of air entry pressure, and as the inverse of porosity. As both m and air entry pressure increase as k increases for most porous media, AAI should also increase as k increases for most porous media when parameter correlations are considered.

Considerable additional work is required to verify the precise nature of the relationships between hydraulic properties, meteorologic inputs, and AAI in deep alluvium. It is expected, however, that vegetation may have a strong impact on AAI in deep alluvium, perhaps masking such relationships. To investigate the impacts of vegetation on AAI, future simulations are being planned that will incorporate the effects of representative YM vegetation on infiltration processes.

10.3.3.3 Colluvium/Fracture Response Function Abstractions

To estimate spatial distribution of AAI using estimates of hydraulic input, meteorologic input, and colluvium depths, a functional relationship between these variables is extremely useful. A set of empirical relationships was derived for these variables. One relationship characterizes the decay of AAI with increasing colluvium depth and a second relationship uses corrections to the AAI/depth relationship to characterize the impact of AAP and average annual temperature (AAT) on AAI. The relationships incorporate the impact of hydraulic properties through scaling parameters. Ongoing studies are examining the impacts of other meteorologic input.

The development of the shallow-colluvium functional relationships is discussed in detail by Stothoff et al.[8] The functional relationships reduce to

$$\log_{10}\left[\frac{\text{AAI/AAP}}{I_{D0}}\right] = -C_I\left(\frac{\varepsilon b}{b_r}\right)^{1/2}\left[1 + J_0\,(T,M)\right] \tag{10-3}$$

where ε is colluvium porosity, b is colluvium depth; b_r is a scaling depth; I_{D0} and C_I are material dependent coefficients; T is the relative change in AAT [$T = (\text{AAT}-\text{AAT}_0)/\text{AAT}_0$]; M is the change in the base-10 log of the AAP multiplier [$M = \log_{10}(\text{AAP}/\text{AAP}_0)$]; AAT_0 and AAP_0 are base-case values of AAT and AAP; and J_0 is a bicubic function of T and M. Arbitrarily choosing b_r to be 2 cm, regressed values for I_{D0} range from 0.641 through 1.21 and values for C_I range from 0.562 through 1.02. I_{D0} and C_I have a correlation coefficient of 0.93.

---

[8]Stothoff, S.A., H.M. Castellaw, and A.C. Bagztoglou. 1996. Simulating the spatial distribution of infiltration at Yucca Mountain, NV. *Water Resources Research*. In preparation.

Several points are significant about the scaling relationships:

- Porosity and colluvium depth act inversely (e.g., small depths and large porosity are similar to large depths and small porosity),
- The coefficients I_{D0} and C_I are highly correlated,
- Sensitivity to climate decreases with increasing AAI.

10.3.3.4 Refined Surface-Cover Model

Since infiltration is sensitively dependent on the distribution of the surface cover above bedrock (i.e., alluvium and colluvium) and a detailed map of surface cover depth is not available and may be difficult to measure, an alternative approach for estimating cover depth is followed here. Stothoff et al. (1995) presented a simple mechanistic model combining creep and weathering using a DEM for the underlying elevation controls. Based on cursory field observations, the model performed relatively well on ridgetops and sideslopes but predicted erroneously large alluvium depths in the upland channels. Accordingly, the model was enhanced to take into account erosion and sediment transport by water movement as well as soil creep and passive degradation. As a first step, the model only accounts for one generic particle size rather than considering a distribution of particle sizes. The model does not explicitly calculate erosion by rain splash or long-range transport by gravity (i.e., boulders rolling downhill). It is assumed that spatial variability in alluvium depths arises solely from the variability in surface elevation; all erosion-balance parameters are assumed constant in space. The original cover-balance mathematical model is based on work presented by Beaumont et al. (1992); the enhanced model, incorporating balance equations for overland flow and sediment transport, is based upon work presented by Woolhiser et al. (1990).

Each of the balance equations is solved using the same general finite-volume flow-routing approach. The DEM grid is discretized into square boxes, or nodes, with 1D connections to the nearest eight nodes. Taking advantage of the hyperbolic nature of the equations by assuming that upstream variables uniquely determine fluxes to downstream nodes, the nodes in the grid can be processed in order from highest to lowest elevation in one pass. The resultant predictions are reasonably consistent with field observations of bedrock cover ranging from zero in patches along crestlines, to tens of centimeters on sideslopes, to (in places) more than a meter at the base of some sideslopes above terraces. These trends in cover are also consistent with observations at neutron-probe boreholes (Flint and Flint, 1995). However, the model performs poorly in wash bottoms in large part due to insufficient spatial resolution. Accordingly, within regions having slopes less than 10 degrees and designated Quaternary alluvium by Scott and Bonk (1984) (i.e., terraces and channels), a regressed relationship between alluvium depth and slope is used to estimate the alluvium depth (Stothoff and Bagtzoglou, 1996). The resultant alluvium distribution is the base case spatial distribution of alluvium considered for sensitivity analysis.

10.3.3.5 Sensitivities of Spatial Distributions of Infiltration

Two issues are of particular interest when examining the spatial distribution of AAI. General trends in the spatial distribution of AAI are of interest (i.e., localized zones of high AAI), as is the sensitivity of the areal average AAI to the various input parameters. The first issue is examined by using reasonable values for hydraulic properties, colluvium and alluvium depths, and meteorologic input, in conjunction with the regression formulae developed in section 10.3.3.3, to predict the resultant distribution

of AAI. The second issue is investigated by using first order perturbations to the input parameters and examining the responses in the predicted areal average AAI.

To estimate the spatial distribution of infiltration, the subregional area was subdivided into three classes: deep alluvium, fractured welded bedrock overlain by colluvium, and nonwelded bedrock. Deep alluvium is classified as the area within the Scott and Bonk (1984) alluvium outline with g und slope less than 10 degrees, while the CNWRA 3D GFM (Stirewalt and Henderson, 1995) was used to determine the exposure of bedded nonwelded tuffs (PTn). The remaining area was presumed to consist of welded-tuff bedrock overlain by colluvium. The areas classified as deep alluvium and PTn are about 21 percent and 4 percent of the total subregional area.

Modeling AAI in PTn outcrop areas is problematic for several reasons:

- The layer is thin enough to make the semi-infinite assumption questionable.
- Bedding thicknesses are on the order of meters, making the assumption of homogeneous properties questionable.
- Roughly half of the measured permeabilities are less than 10^{-10} cm^2 (Schenker et al., 1995), thus should yield zero AAI, but some measured permeabilities are in the range of 10^{-8} to 10^{-9} cm^2 and would be expected to yield significant and even quite large AAI.
- Other PTn hydraulic properties are highly variable.

Because of the large uncertainty in PTn response, but relatively small exposure area, the simple approach of assigning a fraction of the AAP as AAI was adopted for PTn outcrops. The base case used 10 percent of AAP for AAI in the PTn outcrops regardless of colluvial cover; the sensitivity of areal average AAI to the PTn was assessed using 0 and 20 percent of AAP.

An estimated spatial distribution for AAI is shown in figure 10-4, based on using base-case surface-cover distribution, base-case reference properties shown in table 10-1, and present day meteorologic conditions. The average AAI over the subregional area for this example is 15.0 mm/yr; within the 3 km E-W×4 km N-S box surrounding the proposed repository footprint, the average AAI is 14.6 mm/yr. Within pixels classified as deep alluvium, PTn, and colluvium/fracture, average AAI is 2.4 mm/yr, 15.4 mm/yr, and 18.6 mm/yr. The largest AAI tends to be on ridgetops and sideslopes. Part of this trend is from enhancement of AAI through systematic meteorological variation; a larger part is from progressive thinning of colluvial thickness with elevation.

Using normalized sensitivity coefficients (Sykes et al., 1985), the sensitivity of areal average AAI to the generic parameter α_k is

$$S_k = \frac{\alpha_k}{AAI}\frac{dAAI}{d\alpha_k} \qquad (10\text{-}4)$$

The sensitivity coefficients are calculated by using first order derivatives between a high and low perturbation, normalized by a reference value. In general, sensitivity coefficients will change as the set of base input values change. Accordingly, sensitivity coefficients are calculated for a base-case AAI distribution and a set of alternate AAI distributions where the alternate AAI distributions result from

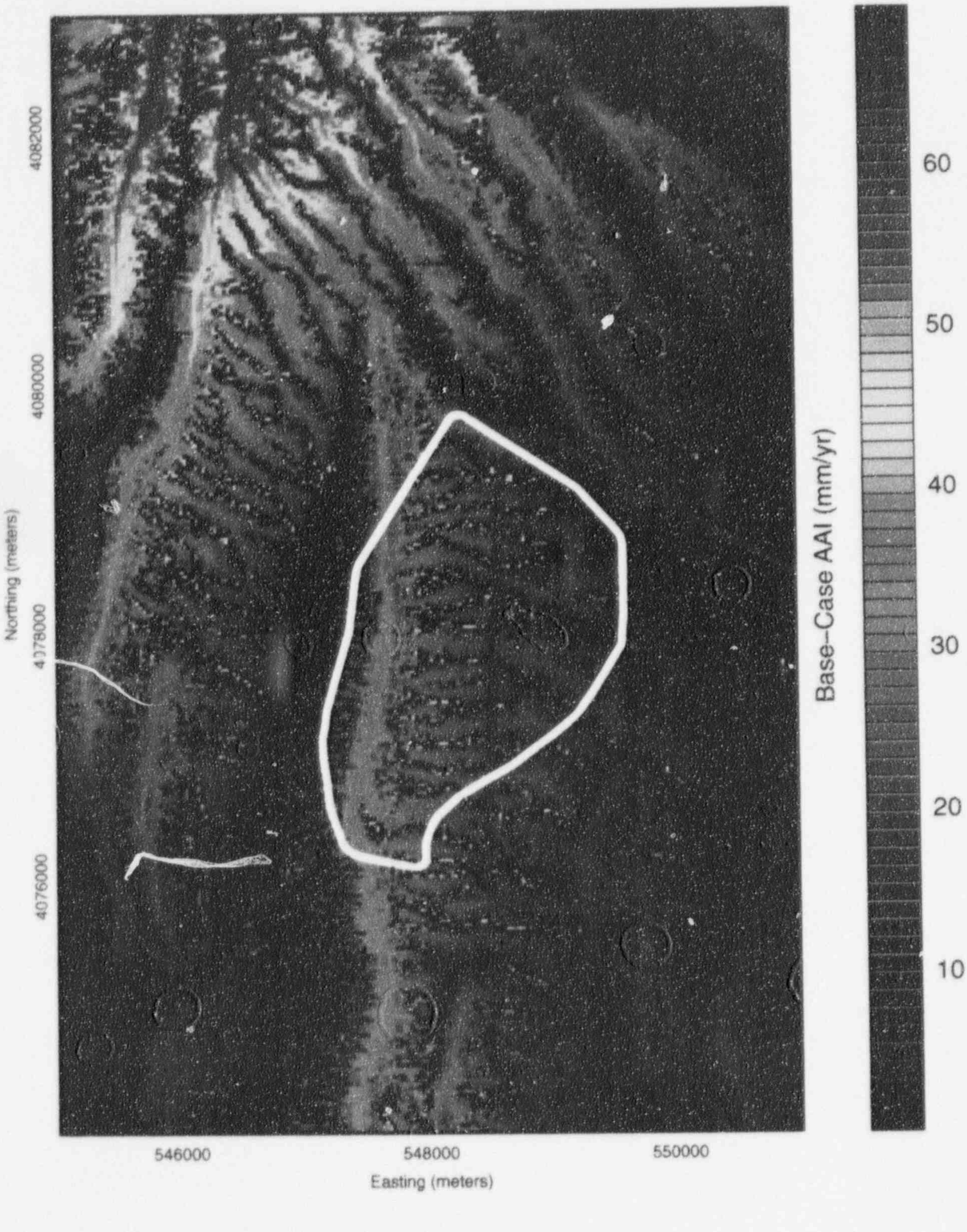

Figure 10-4. Example spatial distribution of AAI accounting for depth of alluvium, underlying bedrock, and meteorological effects

changing the base-case value for a single input parameter. Due to the high correlation between I_{D0} and C_f, sensitivity calculations always use an identical value for both parameters.

Values for the input parameters used to calculate sensitivity coefficients are shown in table 10-1. For cases where alternate input parameter values were used to examine sensitivity coefficient variability, the alternate input values are shown as well as the resulting relative change in areal average AAI. Sensitivity coefficients estimated using the perturbations in table 10-1 are shown in table 10-2. The sensitivity coefficients are for the entire region; the calculated areal average AAI values within the 12 km^2 area centered on the repository footprint are generally within 25 percent of the regional values, so that sensitivity coefficients are quite similar.

As can be seen from table 10-1, changing AAP and AAT individually by amounts that might be expected in a pluvial period results in relative increases in areal average AAI of 3.1 and 2.0 for the base-case set of hydraulic properties. For comparison, simultaneously changing both factors by the amount shown in the table results in a relative increase of 4.9.

Several generalizations can be made by examining the sensitivity coefficients presented in table 10-2:

- Areal average AAI is quite sensitive to systematic variation in AAP and AAT.
- Colluvium/fracture system parameters cause the next largest response, with porosity causing larger variation than I_{D0}.
- Deep-alluvium hydraulic properties cause relatively small variation in areal average AAI due to the small contribution of alluvium to the overall AAI.
- Sizable variation in local AAI within PTn outcrop areas has little impact on areal average AAI due to the small outcrop area.
- As the total AAI contributed by a zone decreases, the sensitivity of areal average AAI to the zonal parameters also decreases.

10.3.4 Progress Toward Development of a Distributed Watershed Model of Solitario Canyon

The low matrix permeability and the general absence of through-cutting fractures in the PTn unit suggest that this hydrostratigraphic unit may act to limit deep percolation reaching the repository horizon. Fast flow paths from the surface to the repository are probably only found coincident with faults such as the Bow Ridge, Sundance, and Ghost Dance that completely transect the PTn and along which hydrostratigraphic units are offset. The reach of Solitario Canyon wash that extends from Little Prow in the north to Plug Hill to the south generally lies below the PTn unit but above and updip from the repository horizon. It has been postulated that focused infiltration (subissue ii) and deep percolation (subissue iii) may occur during extended periods of flow in Solitario Canyon or under conditions where runoff has ceased but water remains ponded in pools or embayments. Although runoff events in Solitario Canyon may be infrequent under present climatic conditions, pluvial conditions will undoubtedly recur during the next 10^5 yr (see section 10.3.1.1) and runoff events may be more frequent and more sustained.

Table 10-1. Parameter values used for sensitivity coefficient estimation

PARAMETER	BASE CASE			ALTERNATE BASE VALUE			
	Low	Reference	High	Low	Reference	High	Rel. AAI
Alluvium k (cm^2)	10^{-8}	10^{-7}	10^{-6}	10^{-7}	10^{-6}	10^{-5}	0.966
Alluvium m	0.1	0.2	0.3	—	—	—	—
Alluvium P_0 ($\times 10^3$ Pa)	1	2	5	—	—	—	—
Alluvium porosity ε_a	0.1	0.2	0.5	—	—	—	—
AAP fraction in PTn	0.0	0.1	0.2	—	—	—	—
I_{DO} and C_I	0.5	0.7	0.9	0.4	0.6	0.8	1.13
Colluvium porosity ε_c	0.1	0.2	0.3	0.05	0.1	0.15	2.2
Multiplier for depth b	0.5	1	2	0.25	0.5	1	1.7
AAP multiplier	0.67	1	1.5	1	1.5	2.25	3.1
AAT shift (°C)	−3	+3	+3	−6	+3	0	2.0

In areas where alluvial depths exceed 25 to 50 cm, detailed numerical simulations have shown that few wetting pulses are able to reach the fractured tuff units before being dissipated by evaporation (section 10.3.3). These detailed infiltration simulations for YM, however do not yet account for the effects of ponding and flow concentration through overland flow. Accordingly, a study was initiated to simulate rainfall-runoff processes in Solitario Canyon to determine the magnitude and duration of runoff producing storms and locations within the watershed where ponding and channel flow was likely to occur.

The distributed watershed model KINEROS (**KIN**ematic runoff and **EROS**ion model) (Woolhiser et al., 1990) was selected as the simulator primarily because it was developed and tested on small watersheds in the arid to semi-arid southwestern United States. The fundamental conceptual model underlying KINEROS assumes that the watershed can be approximated by a cascading network of 1D planar overland flow segments, 1D interception channels, and ponds or detention storage elements. Rainfall excess is computed by subtracting two components from the input rainfall pulse: (i) specified depth of rainfall intercepted by vegetation or other surface condition and (ii) infiltration, as computed by the Smith and Parlange (1978) approximate solution to the Richards equation. KINEROS then uses the kinematic wave equation to route rainfall excess over both the planar overland flow segments and through interception channels. For overland flow, the user may specify either the Manning resistance equation, a laminar flow resistance equation, or the Chezy law. The same options exist for channel segments that may be specified to have either a circular or a trapezoidal cross section. Surface detention is simulated by coupling the conservation equation with a power law depth-outflow relationship that represents a weir or other uncontrolled backwater producing outflow structure. The erosion modeling capability of KINEROS was not used in this study and is not described.

Table 10-2. Relative change in AAI used to calculate base-case sensitivity coefficients and the AAI sensitivity coefficient values for the base case and cases resulting from systematically changing parameters

PARAMETER	RELATIVE AAI PERTURBATION		SENSITIVITY COEFFICIENT						
			Base Case	ALTERNATE BASE VALUE					
	Low	High		k	I_{D0} and C_I	ε_c	b	AAP	AAT
k	1.11	0.965	−0.014	−0.005	−0.013	−0.007	−0.008	−0.014	−0.008
m	0.967	1.24	+0.271	+0.089	+0.239	+0.126	+0.156	+0.339	+0.186
P_0	1.20	0.961	−0.121	−0.040	−0.106	−0.056	−0.070	−0.152	−0.083
ε_a	1.05	0.975	−0.077	−0.025	−0.067	−0.035	−0.044	−0.096	−0.053
PTn	0.966	1.03	+0.034	+0.035	+0.030	+0.016	+0.019	+0.011	+0.017
I_{D0} and C_I	1.27	0.749	−0.914	−0.947	−0.683	−0.348	−0.261	−1.12	−1.19
ε_c	2.16	0.556	−1.60	−1.66	−1.40	−1.06	−0.99	−1.63	−1.39
b	1.73	0.463	−0.848	−0.878	−0.700	−0.441	−0.585	−0.499	−0.470
AAP	0.289	3.05	+3.33	+3.31	+3.43	+3.38	+2.47	+2.63	+2.44
AAT	2.04	0.609	−0.715	−0.731	−0.760	−0.814	−0.441	−0.442	−1.14

Initial KINEROS simulations were conducted for the small 1.23 km^2 subwatershed in the extreme northern end of Solitario Canyon near Little Prow to determine whether the model was capable of providing the required information on channel recharge. The subwatershed was divided into 28 plane elements with mean length 162 m and 12 channel reaches with mean length 326 m. Channel and overland flow segments had slopes that ranged from 0.08 to 0.21; the mean slope was 0.128. Based on observations made during a reconnaissance level field study, channel cross sections were approximated by trapezoids with one-to-one sideslopes and widths ranging from 0.3 to 4 m. The Manning resistance equation was used for both overland flow planes, channel segments. Manning's ***n*** was 0.101 for the overland flow planes and 0.0165 for the channels. Field reconnaissance conducted after the simulations were completed revealed there is substantial vegetation in channel bottoms and Manning's ***n*** should probably be greater than 0.0165.

In the absence of field measurements of saturated hydraulic conductivity under imbibition, estimates of K_s for the overland flow planes were based on the results of rainfall simulator studies conducted at Mercury, Nevada (12.7 mm/hr). For the channel bottom, soil texture data were used to develop a K_s estimate of 61 mm/hr. Other parameters used in the infiltration equation include (i) net capillary drive G (80 mm for overland flow planes, 63 mm for channels; both derived from rainfall simulator data); (ii) porosity (0.34 for overland flow planes, 0.44 for channels); (iii) rock fraction (set to 0 because K_s and G were derived from rainfall simulator data); (iv) microtopography factor, which affects the effective area of infiltration after rainfall ceases (20 mm); (v) maximum saturation (0.94 for overland flow planes, and 0.95 for channels); and (vi) initial soil saturation, which was varied depending on the month during which a shower occurred.

To adequately capture the dynamic response of a small watershed, rainfall intensity data must have a temporal resolution of at least 5 min. Yet there are no recording precipitation gages in Solitario Canyon to provide these data. Hourly precipitation data are available from the Beatty, Nevada, meteorologic station, but it is difficult to disaggregate hourly data. An alternate approach was used wherein two 100-yr sequences of daily precipitation were synthesized using the USCLIMAT model. Each shower in the second 100-yr synthetic sequence, having a rainfall total that exceeded 12.7 mm (0.5 in.), was disaggregated using a method described by Woolhiser and Osborn (1985) and Woolhiser and Econopouly (1986). Showers were sorted by increasing total precipitation and two showers were selected from each of the following percentile ranges: (i) greater than 95 percent, (ii) 70 to 80 percent, and (iii) 50 to 55 percent. Statistics for each of the six selected storms are listed in table 10-3.

The six simulated storms were used for determining the sensitivity of the volume of water infiltrated into the channels of the Little Prow watershed to variations in hydraulic and infiltration parameters. Dimensionless sensitivity coefficients were generally larger for the least intense runoff producing storm (storm 6) than for the most intense runoff producing storm (storm 2), a reflection of the extreme sensitivity of the runoff process when runoff is a small percentage of rainfall. Varying the saturated hydraulic conductivity under imbibition for both channels and overland flow planes had the greatest effect on channel infiltration. Manning's n on the overland flow planes had little effect on channel infiltration, while increasing n in the channels increases the flow depth and wetted area for infiltration. Channel infiltration is highly sensitive to the microtopography parameter for overland flow planes for small storms because a small or zero value for the parameter causes much of the water in storage on the surface when rainfall ceases to be infiltrated on the upland areas before it can reach the channel system.

Table 10-3. Statistics of simulated storms

Storm Number	Depth (mm)	Duration (min)	Average Intensity (mm/hr)
1	52.0	317	9.84
2	40.6	83	29.3
3	21.6	74	17.5
4	20.8	91	13.7
5	17.5	100	10.7
6	17.5	74	14.2

Subwatershed modeling conducted to date indicates that KINEROS is a reasonable tool for estimating channel recharge in Solitario Canyon, provided that error bands can be established. Actual estimates of channel infiltration in Solitario Canyon will not be provided until better estimates for the key hydraulic and infiltration parameters are obtained. Based on the absence of local rainfall data with high enough temporal resolution, simulation of daily rainfall coupled with disaggregation into showers and shower intensity patterns appears to be the only method that can be used to provide the required precipitation data. Because channel infiltration is highly sensitive to rainfall, the synthetic rainfall sequences must be compared to regional depth-duration statistics. In addition, the spatial distribution of rainfall during a storm may also be important for a watershed the size of Solitario Canyon (approximately 10 km^2).

10.4 ASSESSMENT OF PROGRESS TOWARD MEETING OBJECTIVES

Efforts during FY96 have been focused on three of the six subissues identified in the USFIC KTI. In addition, some effort was devoted to assessing ambient flow conditions in the saturated zone. Efforts at improving estimates of AAI and developing an understanding of the processes that may lead to the development and transient behavior of perched water bodies at YM will facilitate evaluation of the DOE assertion that seepage into the drifts will be low. Of the five hypotheses developed by DOE to test this assertion, the three hypotheses that are directly or indirectly addressed by these efforts are: (i) flux that percolates through the repository horizon is substantially less than net infiltration, (ii) rapid fracture flow occurs only within a limited volume of the repository block at any specific time, and (iii) the effect of climate change on seepage can be bounded.

Within this KTI, no general sensitivity analysis was conducted to evaluate the importance of each area of investigation to the overall performance of the repository. There is already ample evidence from TSPAs conducted both by the NRC and the DOE that the performance of the repository is highly sensitive to changes in infiltration and seepage. However, sensitivity analyses were integral parts of the two technical investigations described in sections 10.3.3 and 10.3.4 that addressed shallow infiltration. These sensitivity analyses were conducted primarily to determine which model parameters had the greatest effect on estimates of shallow infiltration.

Progress toward resolution on the effects of climate change on the ambient hydrogeologic regime at YM and on the range of shallow infiltration under current climatic conditions was described in

section 10.3.1. Analytical and empirical methods for determining ambient hydrogeologic conditions in the vicinity of the repository drift and in the saturated zone from beneath YM to the Amargosa Farms region have not yet been fully developed. It is anticipated that continued analyses of the ^{36}Cl data from the ESF coupled with the development of detailed, drift scale unsaturated flow models will help to bound estimates of seepage into the repository. Understanding of the saturated flow regime beneath YM and its effect on radionuclide dilution will primarily be gained from developing more detailed 3D flow and transport models. During FY97 it is anticipated that the regional-scale flow and transport model developed by DOE as part of the NTS environmental restoration program will be finished and the modeling results will greatly improve understanding of transport and mixing within the YM saturated zone. Results of tracer tests now being conducted at the C-well complex will further improve understanding of transport in the saturated zone.

- Significant progress was made toward resolving technical issues at YM. A draft issue resolution status report on climate change, future precipitation, and water table rise was prepared. Estimates of average annual precipitation under current climatic conditions developed by the NRC and the CNWRA using numerical models are similar in magnitude and areal distribution to estimates developed by the DOE from measured data.

- A quantitative method was developed for bounding the range of climatic and hydrostratigraphic conditions that are necessary for perched water bodies to develop beneath YM. ^{14}C data from boreholes at YM were used to constrain estimates of recharge rates and durations required to develop and sustain perched water bodies for an idealized YM.

- Estimates of average annual shallow infiltration at YM were developed using BREATH, a 1D two-phase, non-isothermal flow code. The effect of factors such as the thickness of alluvial cover, material properties, and hill slope orientation, on average annual shallow infiltration was assessed for each 30-m square pixel in the YM vicinity. From these analyses, maps were prepared that depict the estimated spatial distribution of AAI. Sensitivities of AAI to variations in material properties and climatic factors were calculated. Studies have been initiated to assess the effect of ponding during rainfall-runoff events in Solitario Canyon on local infiltration rates.

10.5 INTEGRATION WITH OTHER KEY TECHNICAL ISSUES

The USFIC KTI has provided general information on the regional saturated flow system to the KTI on Radionuclide Transport. Estimates of shallow infiltration developed in this KTI were supplied to the KTI on Total System Performance and Integration for the audit review of TSPA-95 (TRW Environmental Safety System, Inc., 1995). Boundary conditions from the unsaturated flow model used in the perched water study were provided to the KTI on Thermal Effects on Flow for simulating the effect of repository heating on the development of local perched water bodies above the repository horizon. Interaction with the KTI on Structural Deformation and Seismicity (SDS) has focused on assessing the effect of the geologic structure and the regional contemporary *in situ* stress field in the YM area on saturated zone flow. In addition, information from the GFM developed within the SDS KTI was used in developing the hydrostratigraphic cross sections used in the perched water study.

10.6 REFERENCES

Ababou, R., and A.C. Bagtzoglou. 1993. *BIGFLOW: A Numerical Code for Simulating Flow in Variably Saturated, Heterogeneous Geologic Media (Theory and User's Manual—Version 1.1)*. NUREG/CR-6028. Washington, DC: Nuclear Regulatory Commission.

Beaumont, C., P. Fullsack, and J. Hamilton. 1992. Erosional control of active compressional orogens. K.R. McClay, ed. *Thrust Tectonics*. London, UK: Chapman & Hall.

Bish, D.L., and S.J. Chipera. 1989. *Revised Mineralogic Summary of Yucca Mountain, Nevada*. LA-11497-MS. Los Alamos, NM: Los Alamos National Laboratory.

Burger, P., and K. Scofield. 1994. Perched water at Yucca Mountain and their implications on the Exploratory Studies Facility. *EOS, Transactions, American Geophysical Union* 75(44): 250.

Craig, R.W., and R.L. Reed. 1991. *Geohydrology of Rocks Penetrated by Test Well USW H-6, Yucca Mountain, Nye County, Nevada*. U.S. Geological Survey Water Resources Investigations Report 89-4025. Denver, CO: U.S. Geological Survey.

Czarnecki, J.B. 1985. *Simulated Effects of Increased Recharge on the Ground-Water Flow System of Yucca Mountain and Vicinity, Nevada–California*. U.S. Geological Survey Water Resources Investigations Report 84-4344. Denver, CO: U.S. Geological Survey.

Fabryka-Martin, J.T., P.R. Dixon, S. Levy, B. Liu, H.J. Turin, and A.V. Wolfsberg. 1996. *Systematic Sampling for Chlorine-36 in the Exploratory Studies Facility*. LA-CST-TIP-96-001. Los Alamos, NM: Los Alamos National Laboratory.

Flint, L.E., and A.L. Flint. 1990. *Preliminary Permeability and Water-Retention Data for Nonwelded and Bedded Tuff Samples, Yucca Mountain Area, Nye County, Nevada*. U.S. Geological Survey Open-File Report 90-569. Denver, CO: U.S. Geological Survey.

Flint, A.L., and L.E. Flint, 1994. Spatial distribution of potential near surface moisture flux at Yucca Mountain. *Proceedings of the Fifth Annual High-Level Radioactive Waste Management Conference*. La Grange Park, IL: American Nuclear Society: 2,352–2,358.

Flint, L.E., and A.L. Flint. 1995. *Shallow Infiltration Processes at Yucca Mountain, Nevada—Neutron Logging Data 1984–93*. U.S. Geological Survey Water Resources Investigations Report 95-4035. Denver, CO: U.S. Geological Survey.

Freeze, A.R., and J.A. Cherry, 1979. *Groundwater*. Englewood Cliffs, NJ: Prentice-Hall.

Iman, R.L., and M.J. Shortencarier. 1984. *A FORTRAN 77 Program and User's Guide for the Generation of Latin Hypercube and Random Samples for Use with Computer Models*. SAND83-2365. Albuquerque, NM: Sandia National Laboratories.

Loscot, C.L., and D.P. Hammermeister. 1992. *Geohydrologic Data from Test Holes UE-25 UZ#4 and UE-25 UZ#5, Yucca Mountain Area, Nye County, Nevada.* U.S. Geological Survey Open-File Report 90-369. Denver, CO: U.S. Geological Survey.

National Academy of Sciences. 1992. *Groundwater at Yucca Mountain: How High Can It Rise?* Report by the Panel on Coupled Hydrologic/Tectonic/Hydrothermal Systems at Yucca Mountain, Board on Radioactive Waste Management. Washington, DC: National Academy Press.

National Climatic Data Center. 1984 to 1994. *WBAN Hourly Surface Observations.* Asheville, NC: National Oceanic and Atmospheric Administration.

National Research Council. 1995. *Technical Bores for Yucca Mountain Standards, Board on Radioactive Waste Management.* National Research Council of the National Academy of Sciences. Washington, DC: National Academy Press.

Nuclear Regulatory Commission. 1992. *Initial Demonstration of the NRC's Capability to Conduct a Performance Assessment for a High-Level Waste Repository.* NUREG-1327. Washington, DC: Nuclear Regulatory Commission.

Nuclear Regulatory Commission. 1995a. *Disposal of High-Level Radioactive Wastes in Geologic Repositories.* Code of Federal Regulations, Title 10, Part 60. Washington, DC: U.S. Government Printing Office.

Nuclear Regulatory Commission. 1995b. *NRC Iterative Performance Assessment Phase 2: Development of Capabilities for Review of a Performance Assessment for a High-Level Waste Repository.* NUREG-1464. Washington, DC: Nuclear Regulatory Commission.

Pearson, F.J., and A.H. Truesdell. 1978. Tritium in the water of Yellowstone National Park. *Short Papers of the 4th International Conference on Geochronology, Cosmochronology, Isotope Geology.* R.E. Zartman, ed. U.S. Geological Survey Open-File Report 78-701. Denver, CO: U.S. Geological Survey: 327–329.

Quade, J., M.D. Mufflin, W.L. Pratt, W. McCoy, and L. Burckle. 1995. Fossil spring deposits in the southern Great Basin and their implications for changes in water-table levels near Yucca Mountain, Nevada, during Quaternary time. *Geological Society of America Bulletin* 107(2): 213–230.

Russell, C., J. Hess, and S. Tyler. 1987. Hydrogeologic investigations of flow in fractured tuffs, Rainier Mesa, Nevada Test Site. D.D. Evans and T.J. Nicholson, eds. *Flow and Transport Through Unsaturated Fractured Rock.* Geophysical Monograph 42. Washington, DC: American Geophysical Union: 43–50.

Sandia National Laboratories. 1992. *TSPA 1991: An Initial Total-System Performance Assessment for Yucca Mountain.* SAND91-2795. Albuquerque, NM: Sandia National Laboratories.

Schenker, A.R., D.C. Guerin, T.H. Robey, C.A. Rautman, and R.W. Barnard. 1995. *Stochastic Hydrogeologic Units and Hydrogeologic Properties Development for Total-System Performance Assessments*. SAND94-0244. Albuquerque, NM: Sandia National Laboratories.

Scott, R.B., and J. Bonk. 1984. *Preliminary Geologic Map (1:12,000 scale) of Yucca Mountain, Nye County, Nevada, With Geologic Cross Sections*. U.S. Geological Survey Open-File Report 84-494. Denver, CO: U.S. Geological Survey.

Smith, R.E., and J.-Y. Parlange. 1978. A parameter-efficient hydrologic infiltration model. *Water Resources Research* 14(3): 533–538.

Spaulding, W.G. 1985. *Vegetation and Climates of the Last 45,000 Years in the Vicinity of the Nevada Test Site, South-Central Nevada*. U.S. Geological Survey Professional Paper 1329. Washington, DC: U.S. Government Printing Office.

Stirewalt, G., B. Henderson, and S. Young. 1994. *A Preliminary Three-Dimensional Geological Framework Model for Yucca Mountain, Nevada: Report to Accompany Model Transfer to the Nuclear Regulatory Commission*. CNWRA 94-023. San Antonio, TX: Center for Nuclear Regulatory Analyses.

Stirewalt, G.L., and D.B. Henderson. 1995. A preliminary three-dimensional geological framework model for Yucca Mountain. *Proceedings of the Sixth International Conference on High-Level Radioactive Waste Management*. La Grange Park, IL: American Nuclear Society: 116–118.

Stothoff, S.A. 1995. *BREATH Version 1.1—Coupled Flow and Energy Transport in Porous Media: Simulator Description and User Guide*. NUREG/CR 6333. Washington, DC: Nuclear Regulatory Commission.

Stothoff, S.A., and A.C. Bagtzoglou. 1996. Subregional Hydrogeologic Flow and Transport Processes. *NRC High-Level Radioactive Waste Research at CNWRA, July—December 1995*. B. Sagar, ed. CNWRA 95-02S. San Antonio, TX: Center for Nuclear Waste Regulatory Analyses: 9-1 through 9-20.

Stothoff, S.A., H.M. Castellaw, and A.C. Bagtzoglou. 1995. Estimation of Spatial Distribution of Recharge Factors at Yucca Mountain. *NRC High-Level Radioactive Waste Research at CNWRA, January–June 1995*. B. Sagar, ed. CNWRA 95-01S. San Antonio, TX: Center for Nuclear Waste Regulatory Analyses: 9-5 through 9-12.

Sykes, J.F., J.L. Wilson, and R.W. Andrews. 1985. Sensitivity analysis for steady state groundwater flow using adjoint operators. *Water Resources Research* 21(3): 359–371.

Thordarson, W. 1965. *Perched Ground Water in Zeolitized-Bedded Tuff, Rainier Mesa and Vicinity, Nevada Test Site, Nevada*. U.S. Geological Survey Open-File Report TEI-862. Washington, DC: U.S. Geological Survey.

TRW Environmental Safety System, Inc. 1995. *Total System Performance Assessment—1995: An Evaluation of the Potential Yucca Mountain Repository*. B00000000-01717-2200-00136. Las Vegas, NV: TRW Environmental Safety Systems, Inc.

Tyler, S.W., J.B. Chapman, S.H. Conrad, and D. Hammermeister. 1995. Paleoclimatic response of a deep vadose zone in southern Nevada, USA, as inferred from soil water tracers. *Application of Tracers in Arid Zone Hydrology* 232: 351–361.

U.S. Department of Energy. 1988. *Site Characterization Plan, Yucca Mountain Site, Nevada Research and Development Area, Nevada*. Volume II, Part A. Oak Ridge, TN: U.S. Department of Energy.

U.S. Geological Survey. 1981. *Subsurface-Water Flow and Solute Transport—Federal Glossary of Selected Terms*. Subsurface-Water Glossary Working Group, Ground-Water Subcommittee, Interagency Advisory Committee on Water Data. Washington, DC: U.S. Geological Survey.

Wang, J.S.Y., N.G.W. Cook, H.A. Wollenberg, C.L. Carnahan, I. Javandel, and C.F. Tsang. 1993. Geohydrologic data and models of Rainier Mesa and their implications to Yucca Mountain. *Proceedings of the Fourth International Conference on High-Level Radioactive Waste Management*. La Grange Park, IL: American Nuclear Society: 675–680.

Whelan, J.F., and J.S. Stuckless. 1992. Paleohydrologic implications of the stable isotopic composition of secondary calcite within the Tertiary volcanic rocks of Yucca Mountain, Nevada. *Proceedings of the Third International Conference on High-Level Radioactive Waste Management*. La Grange Park, IL: American Nuclear Society: 1,572–1,581.

Whitfield, M.S., C.M. Cope, and C.L. Loscot. 1993. *Borehole and Geohydrologic Data for Test Hole USW UZ-6, Yucca Mountain Area, Nye County, Nevada*. U.S. Geological Survey Open-File Report 92-28. Denver, CO: U.S. Geological Survey.

Winograd, I.J., T.B. Coplen, J.M. Landwehr, A.C. Riggs, K.R. Ludwig, B.J. Szabo, P.T. Kolesar, and K.M. Revesz. 1992. Continuous 500,000-Year Climate Record from Vein Calcite in Devil's Hole, Nevada. *Science* 258: 255–260.

Wilson, M.L., J.H. Gauthier, R.W. Barnard, G.E. Barr, H.A. Dockery, E. Dunn, R.R. Eaton, D.C. Guerin, N. Lu, M.J. Martinez, R. Nilson, C.A. Rautman, T.H. Robey, B. Ross, E.E. Ryder, A.R. Schenker, S.A. Shannon, L.H. Skinner, W.G. Halsey, J.D. Gansemer, L.C. Lewis, A.D. Lamont, I.R. Triay, A. Meijer, and D.E. Morris. 1994. *Total-System Performance Assessment for Yucca Mountain—SNL Second Iteration (TSPA-1993)*. SAND93-2675. Albuquerque, NM: Sandia National Laboratories.

Woolhiser, D.A., and H.B. Osborn. 1985. Stochastic daily precipitation models. 2: A comparison of distributions of amounts. *Water Resources Research* 18(5): 1,461–1,468.

Woolhiser, D.A., and T.E. Econopouly. 1986. Stochastic characterization of rainfall events. *Proceedings of the Sixth Annual AGU Front Range Branch Hydrology Days, Ft. Collins, CO*. Washington, DC: American Geophysical Union.

Woolhiser, D.A., R.E. Smith, and D.C. Goodrich. 1990. *KINEROS, A Kinematic Runoff and Erosion Model: Documentation and User Manual*. ARS-77. Washington, DC: United States Department of Agriculture, Agricultural Research Service.

Yang, I.C. 1992. Flow and transport through unsaturated rock—data from two test holes, Yucca Mountain, Nevada. *Proceedings of the Third International Conference on High-Level Radioactive Waste Management*. La Grange Park, IL: American Nuclear Society: 732–737.

Yang, I.C., A.K. Turner, T.M. Sayre, and P. Montazer. 1988. *Triaxial-Compression Extraction of Pore Water from Unsaturated Tuff, Yucca Mountain, Nevada*. U.S. Geological Survey Water Resources Investigations Report USGS-WRI-88-4189. Denver, CO: U.S. Geological Survey.

Yang, I.C., G.W. Rattray, and P. Yu, 1996. *Interpretations of Chemical and Isotopic Data from Boreholes in the Unsaturated Zone at Yucca Mountain, Nevada*. U.S. Geological Survey Water Resources Investigations Report 96-4058. Denver, CO: U.S. Geological Survey.

11 RADIONUCLIDE TRANSPORT

Primary Authors: D.R. Turner, R.T. Pabalan, J.W. Bradbury, D.A. Pickett, and W.M. Murphy

Technical Contributors: M.G. Almendarez, F.P. Bertetti, J.W. Bradbury, A.M. Hoh, R.H. Martin, W.M. Murphy, R.T. Pabalan, E.C. Pearcy, D.A. Pickett, J.D. Prikryl, and D.R. Turner

Key Technical Issue Co-Leads: E.C. Pearcy (CNWRA) and J.W. Bradbury (NRC)

11.1 INTRODUCTION

A fundamental concern in evaluating the suitability of Yucca Mountain (YM), Nevada as a potential repository for high-level radioactive waste (HLW) is the possibility of radionuclide transport through the subsurface from the proposed repository to the accessible environment. Dose calculations of the type recommended by the National Academy of Sciences (NAS) (National Academy of Sciences, 1995) ultimately require an estimate of concentrations of different radionuclides in aqueous, gas, and/or solid phases that occur along the exposure pathway. These concentrations will vary as a function of space and time depending on the processes that control the rate of radionuclide transport through the subsurface and the effects of changes in system chemistry and hydrology. Therefore, processes that control the reduction (or increase) of radionuclide concentration in the groundwater need to be studied in any evaluation of proposed repository performance.

The Radionuclide Transport Key Technical Issue (KTI) is concerned with the processes that may affect radionuclide transport from the proposed repository to the accessible environment. A number of processes, such as sorption, matrix diffusion, dispersion, mineral precipitation, radioactive decay, and dilution may serve to reduce radionuclide concentration during transport, ultimately leading to a reduction in potential dose to man. This is especially true for the longer time periods recommended by NAS (National Academy of Sciences, 1995). On the other hand, existence of fast transport paths can keep the concentration relatively higher. An understanding of the geochemical processes that influence radionuclide transport may be used to offset uncertainties in hydrologic models of the YM system (Simmons et al., 1995). Not understanding the degree to which these processes are affected by changes in system chemistry/hydrology makes it difficult to reasonably bound radionuclide transport. In the U.S. Department of Energy (DOE) Waste Containment and Isolation Strategy (WCIS),[1] matrix diffusion, sorption, and dilution are mentioned as key site attributes that need to be tested in any suitability demonstration for a proposed repository at YM. The attributes include three hypotheses related to matrix diffusion, sorption, and dilution: (i) reduction of radionuclide concentration by depletion and dispersion during radionuclide transport (Hypothesis 10), (ii) a flux in the saturated zone that is much greater than the flux contacting the waste (Hypothesis 11), and (iii) strong mixing within the saturated zone that leads to a dilution of a radionuclide-bearing aqueous phase (Hypothesis 12).

---

[1]U.S. Department of Energy. 1996. *Highlights of the U.S. Department of Energy's Updated Waste Containment and Isolation Strategy for the Yucca Mountain Site.* DOE Concurrence Draft. July 1996. Washington, DC: U.S. Department of Energy.

The Nuclear Regulatory Commission (NRC) and Center for Nuclear Waste Regulatory Analyses (CNWRA) have identified subissues to cover data and analysis needs to address the effects of radionuclide transport on overall repository performance:

- Identifying which radionuclides require some form of retardation to meet performance requirements at YM.

- Evaluating geochemical and hydrological controls on radionuclide transport and the potential for dilution at YM, corresponding to DOE WCIS Hypotheses 11 and 12.

- Evaluating conceptual models and mathematical approaches to modeling radionuclide retardation at YM, corresponding to DOE WCIS Hypothesis 10.

- Evaluating the sensitivity of the overall performance of the proposed repository to ranges in parameters controlling radionuclide transport.

The following sections present technical work accomplished during fiscal year (FY) 1996. Work includes evaluation of DOE flow and transport conceptual models using both site specific and natural analog data. Experimental data and models are presented for constraining radionuclide sorption coefficients. Progress in developing geographic information system (GIS) coverages for existing hydrochemical data is also presented. These activities have been designed to establish a basis for subsequent review and evaluation of DOE submittals. It is important to note that some of the information necessary for answering these questions is also needed to address other KTIs. For example, hydrostratigraphy and hydraulic properties are necessary for both the Radionuclide Transport and Unsaturated and Saturated Flow Under Isothermal Conditions KTIs.

11.2 OBJECTIVES AND SCOPE OF WORK

The work under this KTI is intended to lead to resolution of these subissues through the use of quantitative models in evaluating the effects of transport and dilution processes on repository performance under geochemical and hydrologic conditions specific to YM. The complex geochemical and hydrological conditions at YM make it difficult to establish reasonable boundary and initial conditions for modeling of transport processes. The system heterogeneity makes it especially difficult to determine bounding values for radionuclide transport given the possible changes through space and time in key parameters such as pH. Sensitivity analyses can provide some insight as to which parameters have the greatest effect on repository performance, and identify those areas of the KTI that can use bounding calculations in performance assessment (PA).

Both the NRC and the DOE have attempted to include the effects of geochemistry on radionuclide transport in PA calculations (e.g., Wilson et al., 1994; TRW Environmental Safety Systems, Inc., 1995; Wescott et al., 1995). However, there remains sufficient uncertainty in both the hydrological and the transport models used in these efforts that continued study of radionuclide transport is warranted. Therefore, the NRC has elected to conduct a detailed review of a vertical slice of the overall DOE program in the area of radionuclide transport.

FY96 activities for the Radionuclide Transport KTI were designed to:

- Seek resolution with the DOE on data used for neptunium (Np) sorption coefficients (K_d). This is related to DOE WCIS Hypothesis 10. PA calculations in DOE Total System Performance Assessment (TSPA) include retardation for all radionuclides in the unsaturated and saturated zones. Preliminary sensitivity analyses (TRW Environmental Safety Systems, Inc., 1995) have identified Np sorption as an important parameter in repository performance. The NRC/CNWRA and the DOE experimental data for Np sorption may be similar enough to allow agreement on the likely magnitude and conservative estimates of sorption coefficients for Np at YM. Ultimately, this type of information will be combined with stratigraphy, flowpath information, and saturation data to address Np transport in the subsurface.

- Provide a basis for critical evaluation of conceptual models of flow and transport used by the DOE in TSPA calculations. This is related to DOE WCIS Hypotheses 10 and 11.

- Identify critical radionuclides for which retardation is likely to be necessary for performance requirements to be met. This is related to DOE WCIS Hypothesis 10. An evaluation of key radionuclides has already been done by the DOE (Kerrisk, 1985) and the NRC/CNWRA (Jarzemba and Pickett, 1995) under the existing Environmental Protection Agency (EPA) regulations based on inventory and initial geochemical considerations. Because of the NAS recommendations for a new EPA standard, identifying key radionuclides will require input from the KTI on TSPA and Integration and the Support Development of the EPA Standard KTI.

- Identify, acquire, and evaluate available hydrochemical data to bound flow and the potential for dilution and mixing within the YM system. This is related to DOE WCIS Hypotheses 11 and 12. The DOE on-line databases will be searched for electronic forms of site specific data to supplement existing GIS databases at the CNWRA. The search of DOE data will focus on concentrations of geochemical tracers. The tracer information can be used to evaluate the extent of mixing between aquifers in the YM region and perhaps establish boundary conditions for flow models being developed in the Isothermal Flow KTI.

11.3 SIGNIFICANT TECHNICAL ACCOMPLISHMENTS

11.3.1 Chlorine-36 at the Yucca Mountain Site and Evaluation of Conceptual Models

It is important to evaluate DOE conceptual models of flow and transport using, to the extent possible, available site specific data (DOE WCIS Hypotheses 10 and 11). Radionuclide transport in groundwater of the unsaturated zone at YM is demonstrated by analyses of natural and bomb-pulse ^{36}Cl. A review was conducted of a Los Alamos National Laboratory (LANL) report released in April 1996 (Fabryka-Martin et al., 1996) on studies of ^{36}Cl extracted from rock samples collected in the Experimental Studies Facility (ESF). The data appear to have been collected with care and data quality seems to be high. The data set reveals a fairly coherent pattern of relatively low values of $^{36}Cl/Cl < 1{,}500\times10^{-15}$ all along the ESF. The prevailing interpretation of these data is that they represent natural cosmogenic ^{36}Cl and imply maximum groundwater travel times ranging from 50,000 to 550,000 yr. In addition, five zones

ranging in width from a single sample to a discontinuous zone spanning 130 m have elevated $^{36}Cl/Cl$ ratios to $3{,}800\times10^{-15}$. These high ratios in the rock are reasonably interpreted to indicate some component of bomb-pulse ^{36}Cl generated within the last 50 yr. All these samples with elevated $^{36}Cl/Cl$ were collected from features such as fault gouge, joints, or fractures. Four of the five elevated $^{36}Cl/Cl$ zones were located in zones in the vicinity of projections from surface expressions of mapped faults, but only one of these four was collected from a fault. Collectively the elevated $^{36}Cl/Cl$ data demonstrate short ^{36}Cl transport times (less than 50 yr) from the ground surface to the depth of the ESF (280 m). An estimate of mass of ^{36}Cl transported through these rapid paths is not available at this time. Surface infiltration in fault zones and rapid groundwater flow in various (but not all) fractures is also indicated. The $^{36}Cl/Cl$ data indicate the importance of through-going fractures in radionuclide transport; if it is determined that significant mass can be transported though fast paths from the repository to the groundwater table, then DOE conceptual models should be designed to take into account the importance of fracture transport.

11.3.2 Using Uranium Transport at Peña Blanca Natural Analog to Constrain Radionuclide Transport

Technical activities related to this effort were centered on two fronts: interpretation of uranium transport at the Nopal I uranium deposit at the Peña Blanca natural analog site, and followup laboratory analyses of samples from Nopal I. The journal article was submitted to the NRC and is intended for publication in the journal *Applied Geochemistry* (Pickett et al., 1996).[2] The article made use of data and analyses initiated under the former Geochemical Analogs Research Project and continued under the Radionuclide Transport KTI. A summary of the results from this study and their relationship to subissue resolution is presented below.

Data from Nopal I have been used to identify key processes and bound parameters in hydrologically unsaturated tuffs. Understanding which processes are most critical in radionuclide transport in a field-scale site is an important step in developing conceptual transport models appropriate to hydrologic and geochemical conditions at YM. This effort focuses on bounding conceptual models of radionuclide transport, the third subissue of this KTI, and addresses DOE WCIS Hypothesis 10.

Pickett et al. (1996)[3] used uranium-series isotopic data from rocks surrounding the Nopal I deposit to deduce information on the salient features of uranium (U) transport behavior at the analog site. Geologic, geochemical, and hydrologic features of Nopal I that make it an appropriate analog for the proposed HLW repository at YM have been detailed elsewhere (Pearcy et al., 1994). Uranium-series analyses provide information on the relative distribution of natural radionuclides as a function of time. At the Nopal I site, radioactive disequilibria among three nuclides in the ^{238}U chain (^{230}Th, ^{234}U, and ^{238}U) in tuffs and fracture-filling materials surrounding the U ore deposit reveal a complex, multistage, history of U mobility over the past few hundred thousand years. Apparent episodicity in U transport behavior may have implications for attempts to model long-term radionuclide transport at the proposed repository.

---

[2]Pickett, D.A., J.D. Prikryl, W.M. Murphy, and E.C. Pearcy. 1996. Uranium-series disequilibrium investigation of radionuclide mobility at the Nopal I uranium deposit, Peña Blanca District, Mexico. *Applied Geochemistry*. In press.

[3]*Ibid.*

Uranium distributions around the deposit (Pearcy et al., 1995; Pickett et al., 1996)[4] demonstrate an apparent horizontal component of transport (i.e., assuming a vertically aligned ore body) on the scale of tens of meters in hundreds of thousands of years; the vertical component is likely to have been greater. Concentrations of U in solids filling discrete fractures are higher relative to the surrounding, generally fractured, tuff. This implies that discrete fractures may have accommodated more U transport than the bulk rock. Uranium was transported the greatest distances from the ore deposit along mappable mesofractures. While calculations have suggested that the microfracture network surrounding one such mesofracture contains about five times the amount of U as the mesofracture itself (Pearcy et al., 1995), the generally microfractured tuff is not apparently itself a conduit for distal transport. Furthermore, among the matrix traverses (i.e., those through generally fractured tuff rather than along mapped mesofractures), correlations between outcrop-scale fracture density and U concentration gradients suggest greater transport in more fractured tuff. The majority of both solids from mineralized fractures and samples representative of the bulk rock exhibit ^{230}Th-^{234}U-^{238}U disequilibria relationships requiring a multistage U transport history (Pickett et al., 1996).[5] In particular, while $^{234}U/^{238}U$ ratios greater than unity imply addition of water-mobilized U within the past few hundred thousand years, $^{230}Th/^{234}U$ ratios significantly greater than unity require a subsequent U removal event (Osmond and Ivanovich, 1992). The history of U mobility at the Nopal I site, as suggested by the U-series data, is (i) removal of U from the deposit and transport and addition of U to rocks outside the deposit; (ii) a period of at least 200,000 yr following or accompanying U transport; and (iii) partial U removal from rocks outside the deposit (figure 11-1). Patterns of activity ratio variations with distance, as well as local deviations from the patterns, imply smaller-scale episodic behavior superimposed on this overall pattern. Sequential extraction experiments on Fe oxide-rich fracture infillings reveal distinct histories for different phases/sites within the rocks. Most notably, uranium-series distributions demonstrate that U sequestered in secondary phases, chiefly Fe oxides and oxyhydroxides, is incorporated into the minerals over time through either coprecipitation or dissolution/reprecipitation.

The key results of this study and implications for KTI resolution are three-fold. First, radionuclide mobility at the Nopal I site and, by analogy, YM is sensitive to changes in geochemical and hydrologic conditions. U transport behavior at Nopal I has been complex and episodic over the past few hundred thousand years, with significant recorded U transport events at least as young as 9,000 yr. The period recorded by the uranium-series features of the rocks has been dominated by oxidizing hydrochemical conditions; this is supported by caliche ages as old at 54 ka (Pearcy et al., 1995) and by preliminary U/Pb ages of around 3 Ma on uranophane. Nevertheless, significant (and possibly cyclic) shifts in the mobility of U have been possible. At Nopal I it has not yet been determined what caused these shifts, but environmental variations due to climate change may be important. The most important effect of climate change would be on the flux of water through the unsaturated zone, and the episodicity of transport at Nopal I suggests that such changes can alter transport. Because of the strong analogy between conditions at Nopal I and YM, the demonstrated timing, episodicity, and complexity of transport at Peña Blanca suggest that such conditions can be expected at YM and are likely to be important to radionuclide transport at the proposed repository. To what extent repository performance will be affected remains to be determined. This study suggests that key parameters (e.g., K_d) in modeling transport behavior at YM

---

[4]Pickett, D.A., J.D. Prikryl, W.M. Murphy, and E.C. Pearcy. 1996. Uranium-series disequilibrium investigation of radionuclide mobility at the Nopal I uranium deposit, Peña Blanca District, Mexico. *Applied Geochemistry*. Submitted to NRC.

[5]*Ibid.*

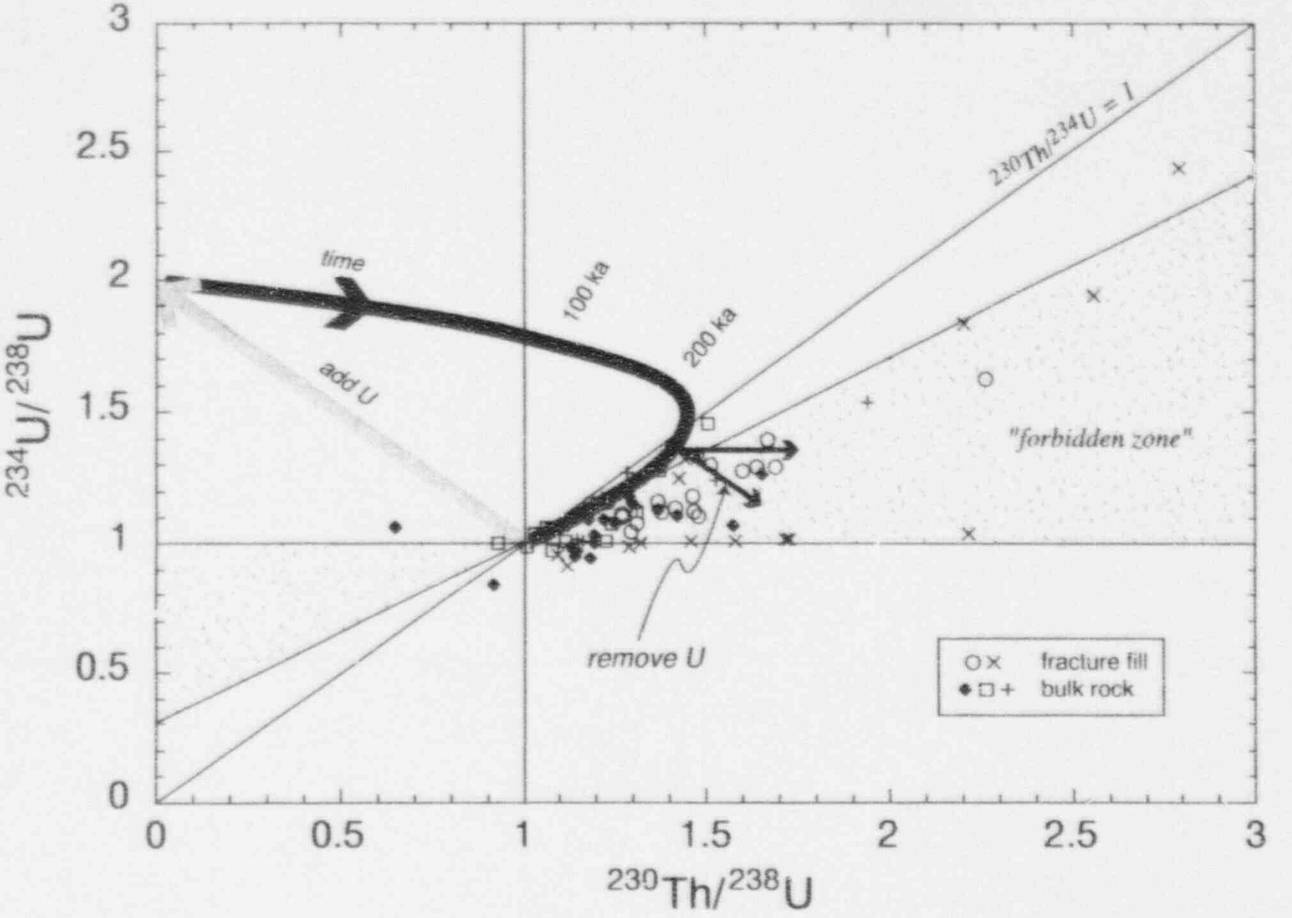

Figure 11-1. $^{234}U/^{238}U$ versus $^{230}Th/^{238}U$ plot of Nopal I traverse bulk rock samples, with preferred model for evolution. Symbols denote separate traverses away from the ore deposit. The crosses and circles represent samples of minerals filling mesofractures; the other symbols are for samples from traverses through generally microfractured tuff. Note the different axis scales. The model assumes an initial rock at or near secular equilibrium (i.e., both ratios equal to one) to which high-$^{234}U/^{238}U$ aqueous U is added, followed by significant time evolution (note time labels on curve), and finally by partial U removal with or without U isotope fractionation. Clearly, not all rocks would have followed the same path, and U addition and removal likely occurred in a more continuous or episodic manner. The "forbidden zone" reflects combinations of the two activity ratios that require multistage histories.

should have sufficiently broad bounds to account for such potential variations in geochemistry. Second, with respect to distance, fracture transport is dominant over matrix tuff transport and hydrology. The importance of transport along fracture pathways at YM has been demonstrated by ^{36}Cl evidence for rapid transport (Fabryka-Martin et al., 1996). For the unsaturated zone at Nopal I, this is supported by observation of rapid near-surface water infiltration following storms. Finally, incorporation of aqueous U into fracture filling minerals suggests that sorption is not fully a reversible process. In constructing process-level models, it is important to consider other geochemical processes such as mineral growth or dissolution that may affect potential radionuclide remobilization. Furthermore, distribution of U among minerals at Nopal I may be useful in assessing K_d's used in PA at YM, at least in a relative sense.

New laboratory analyses of Nopal I samples have been centered on the use of gamma spectrometry for more rapid, non-labor-intensive, non-destructive analysis of decay-series radionuclides. Many analyses were conducted and detailed study of data reduction procedures are planned to allow maximum utility of the gamma spectra. In addition to ease of analysis compared to alpha spectrometry, these data provide information on mobilization and transport at Nopal I of other radionuclides of potential interest to PA of the proposed HLW repository at YM, including ^{226}Ra, ^{231}Pa, ^{227}Ac, and ^{210}Pb.

11.3.3 Geochemical Parameters Controlling Radionuclide Sorption

Under the current DOE WCIS, Hypothesis 10 calls for reduction in radionuclide concentration through depletion and dispersion. Testing this hypothesis requires a means of constraining processes that contribute to the depletion and retardation of radionuclide transport. An important mechanism for retarding the migration of radionuclides such as Np, U, and Pu is sorption onto minerals present along groundwater flow paths. A quantitative understanding of actinide sorption behavior is complicated by the possible dependence of sorption on geochemical parameters, including aqueous solution properties (e.g., pH, ionic strength, radionuclide concentration, complexing ligands) and sorptive phase characteristics (e.g., composition, surface area, sorption site density, surface charge). The dependence of sorption on various parameters makes it difficult to describe and predict actinide retardation and transport in geochemical systems of variable and composite mineralogic composition and changing aqueous speciation, but it is possible to determine reasonable bounds.

Batch experiments were conducted at the CNWRA to investigate the sorption of U(6+) and Np(5+) on the minerals quartz, clinoptilolite, montmorillonite, and α-alumina over wide ranges of experimental conditions. These minerals were selected because their mineralogic and surface characteristics, that could potentially influence radionuclide sorption behavior, are distinct from each other. In addition, quartz, clinoptilolite, and montmorillonite are abundant mineral phases at the proposed HLW repository at YM. The experiments were designed to evaluate the possible effect on radionuclide sorption of pH, radionuclide concentration, radionuclide aqueous speciation, ionic strength, and solid-mass to solution-volume ratio (M/V). Results of these experiments, as well as data from published literature, were used in determining what various geochemical parameters are key to understanding radionuclide sorption behavior. The data were also used to develop and parameterize surface complexation models for describing and predicting radionuclide sorption onto mineral substrates. The results of these interpretations were

summarized in two peer-reviewed articles (Pabalan et al., 1997;[6] Bertetti et al., 1997[7]) submitted to the NRC and intended for publication by Academic Press as part of the book *Metals in Geomedia: Sorption Processes and Model Applications* (E. Jenne, ed.).

The results of selected sets of experiments are plotted in figures 11-2 to 11-10 as a function of pH. Although radionuclide sorption data are typically plotted in terms of percent sorbed, a useful representation is as a distribution coefficient, K_d, that may be defined as

$$K_d \text{ (ml/g)} = \frac{\text{equilibrium amount sorbed}}{\text{equilibrium amount in solution}} \times \left(\frac{V}{M}\right) \quad (11\text{-}1)$$

where V is the volume of experimental solution (ml) and M is the mass of solid (g). The use of K_d provides a means of normalizing sorption results with respect to the sorbent concentration (or M/V ratio) and of taking into account the decrease in solution concentration of the radionuclide due to sorption.

Uranium(6+) Sorption

As an example of the importance of geochemical conditions on sorption behavior, figure 11-2 shows data on U(6+) sorption on common minerals as a function of pH taken from both the literature and from the CNWRA experiments. Data in the figure demonstrate that U(6+) sorption on these minerals is strongly affected by solution pH. Although the minerals used in the experiments have different mineralogic and surface properties, U(6+) sorption on these minerals is similar with respect to dependence on pH. In all cases, U sorption is at a maximum at near neutral pH (~6.0 to ~6.8) and decreases sharply towards more acidic or more alkaline conditions. Differences in experimental conditions (e.g., pH, PCO_2, surface area), however, can lead to large differences in K_d, as shown by the silica sorption data presented in figure 11-2.

Pabalan et al. (1997)[8] showed that there is a close correspondence between the pH dependence of U(6+) sorption and the predominance field of the U(6+) hydroxy aqueous complexes. U(6+) sorption occurs in the pH range where the U(6+) hydroxy complexes are important. At low pH values where the uranyl cation UO_2^{2+} is predominant, U(6+) sorption is typically weak for common minerals, except for those cation exchangers such as montmorillonite and clinoptilolite where U(6+) sorption through an ion exchange mechanism can be important. Aqueous carbonate complexation plays an important role in reducing radionuclide sorption at higher pH (Pabalan et al., 1997).[9] For example, at higher PCO_2, the

---

[6]Pabalan, R.T., D.R. Turner, F.P. Bertetti, and J.D. Prikryl. 1997. Uranium(VI) sorption onto selected mineral surfaces: Key geochemical parameters. *Metals in Geomedia: Sorption Processes and Model Applications*. E. Jenne, ed. New York, NY: Academic Press. In Press.

[7]Bertetti, F.P., R.T. Pabalan, and M.G. Almendarez. 1997. Studies of neptunium(V) sorption on quartz, clinoptilolite, montmorillonite, and α–alumina. *Metals in Geomedia: Sorption Processes and Model Applications*. E. Jenne, ed. New York, NY: Academic Press. In Press.

[8]Pabalan, R.T., D.R. Turner, F.P. Bertetti, and J.D. Prikryl. 1997. Uranium(VI) sorption onto selected mineral surfaces: Key geochemical parameters. *Metals in Geomedia: Sorption Processes and Model Applications*. E. Jenne, ed. New York, NY: Academic Press. In Press.

[9]*Ibid.*

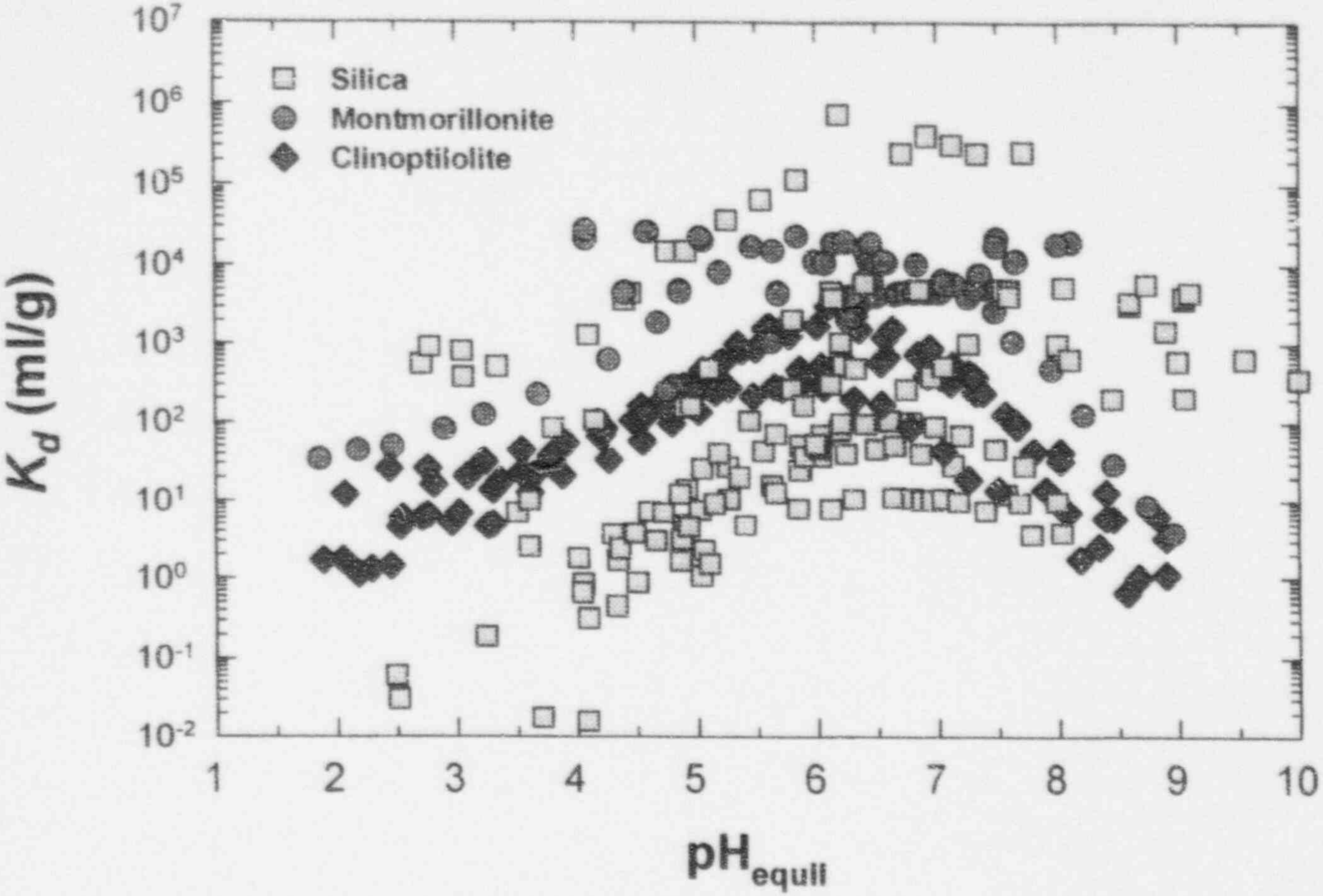

Figure 11-2. Uranium(6+) sorption (expressed as K_d in ml/g) on common rock-forming minerals. Results are taken from literature (Zachara and McKinley, 1993; McKinley et al., 1995) and from batch experiments conducted at the CNWRA for a range in geochemical conditions (ΣU, PCO_2, M/V). Note the similarities among the different minerals in strong pH dependence of U(6+) sorption behavior, and the wide range in K_d observed for a given mineral.

predominance field of the mononuclear U(6+) aqueous hydroxy species $[UO_2(OH)_x^{2-x}]$ becomes reduced in a manner similar to the reduction in U(6+) sorption envelope (i.e., the maximum is lowered and the high pH side is shifted to lower pH). This is due to the increased importance of the U(6+) aqueous carbonate complexes at higher PCO_2.

For the U(6+)-H_2O-CO_2-mineral systems considered, K_d decreases with increasing initial U concentration particularly in the intermediate pH range (Pabalan et al., 1997).[10] The effect is greater at higher initial U concentrations due to the nonlinearity of the sorption isotherm except at low U concentrations. The K_d, which is the slope of the isotherm at a fixed U solution concentration, is larger at lower solution concentrations and approaches a constant value at low enough solution concentrations where the isotherm is linear. In addition to the CNWRA results, decreasing sorption with increasing initial U concentration has also been observed for the U(6+)-ferrihydrite system (Waite et al., 1994). In the presence of excess sorption sites, the nonlinear trend in sorption with increasing U concentration may also be influenced by the formation of polynuclear aqueous complexes (O'Day, 1994). Likewise, the decrease in the proportion of sorbed U(6+) associated with an increase in initial U concentration has been used as evidence against formation of polynuclear U(6+) surface complexes (Waite et al., 1994). Experimental results also indicate that solution ionic strength has little influence on U(6+) sorption, at least over the range in ionic strengths considered here (Pabalan et al., 1997)[11] and where the ion exchange sorption mechanism is negligible.

Changes in sorption behavior for a given mineral as a function of solid-mass to solution-volume (M/V) ratio can appear to be significant when data are plotted in a typical manner of percent U sorbed versus pH (Pabalan et al., 1997)[12] (figure 11-3a). The apparent M/V effect, however, is mostly eliminated if the results are plotted in terms of K_d, a ratio of equilibrium concentrations in the solid versus in solution (figure 11-3b), although there is significant uncertainty in the data at both high and low pH. Plotting data in terms of K_d instead of percent U sorbed makes comparison of different sets of experimental data easier (figure 11-4).

Based on expert elicitation, DOE PA calculations use probability density functions for U sorption coefficients that range from 0 to 30 ml/g (TRW Environmental Safety Systems, Inc., 1995), but there is no clear link to the effects of geochemical conditions on U sorption. Based on CNWRA experiments, U(6+) sorption on quartz, α-alumina, clinoptilolite, and montmorillonite expressed in terms of K_d is similar with respect to pH dependence. However, the K_d values for the different minerals vary over three orders of magnitude. This variation is an artifact of representing sorption data using K_d, which normalizes the amount of U(6+) sorbed to the sorbent mass and not to the number of available sorption sites. Surface areas measured by gas adsorption (e.g., N_2-BET) methods are a relative index of the number of sorption sites on the mineral surface (Davis and Kent, 1990). Thus, it is more useful to represent sorption data normalized to the specific surface area of the mineral sorbent. Figure 11-5 presents the results of the CNWRA batch experiments on U(6+) sorption on quartz, α-alumina, clinoptilolite, and montmorillonite shown previously in figure 11-4 and replotted in terms of K_a (ml/m^2), where K_a is K_d normalized to the

---

[10]Pabalan, R.T., D.R. Turner, F.P. Bertetti, and J.D. Prikryl. 1997. Uranium(VI) sorption onto selected mineral surfaces: Key geochemical parameters. *Metals in Geomedia: Sorption Processes and Model Applications*. E. Jenne, ed. New York, NY: Academic Press. In Press.

[11]*Ibid.*

[12]*Ibid.*

a)

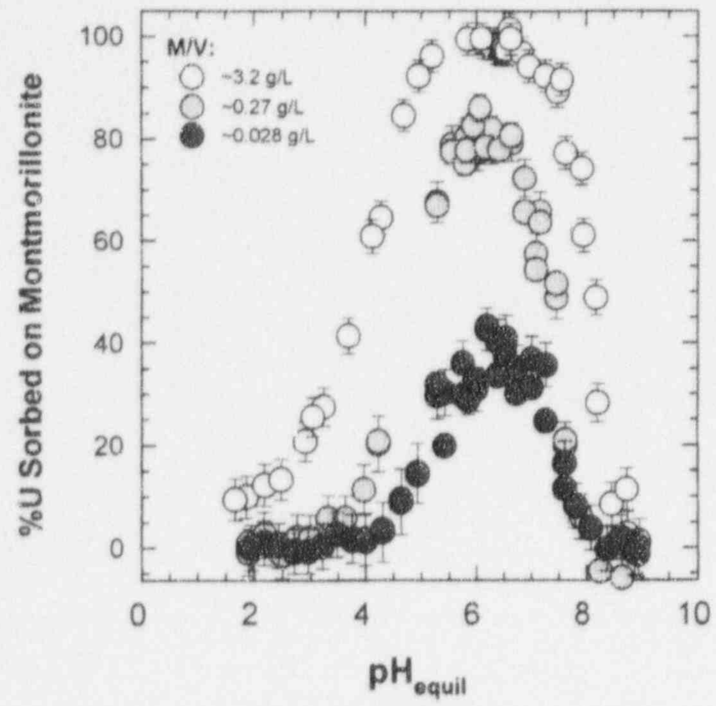

b)

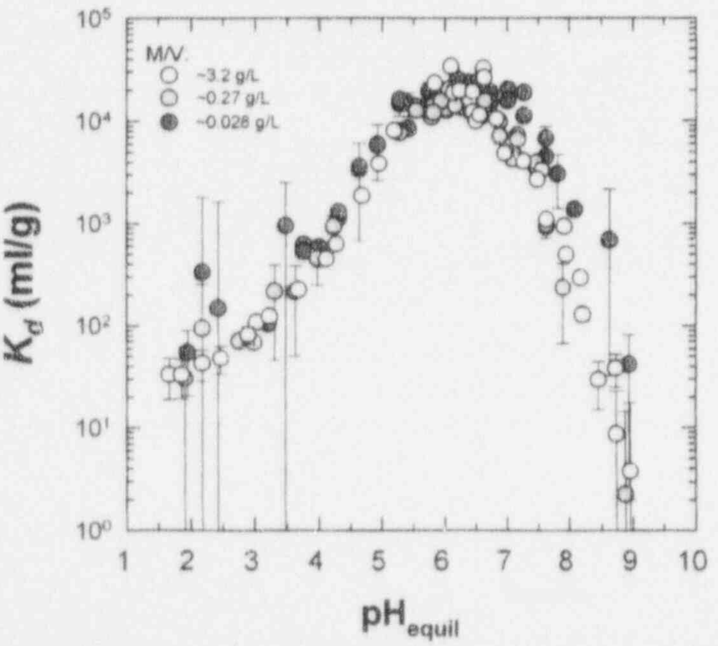

Figure 11-3. a) Uranium(6+) sorption on montmorillonite as a function of M/V expressed as percent U(6+) sorbed versus pH. Note the increasing percent sorbed with increasing M/V. b) Uranium(6+) sorption on montmorillonite as a function of M/V expressed as K_d versus pH. The effect of M/V is largely removed.

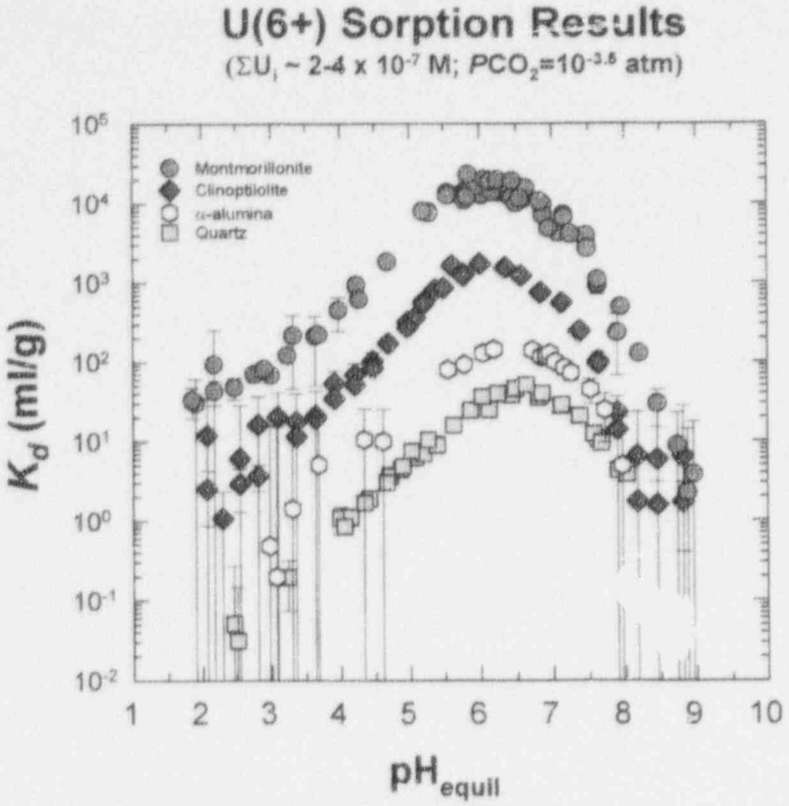

Figure 11-4. CNWRA experimental results for U(6+) sorption on montmorillonite, clinoptilolite, α-alumina, and quartz expressed as K_d

mineral's N_2-BET specific surface area (S_a in m^2/g) (i.e., $K_a=K_d/S_a$). The S_a used in the normalization are 0.03, 97, 0.23, and 10.1 m^2/g for quartz, montmorillonite, α-alumina, and clinoptilolite, respectively. Surface area normalized sorption data for clinoptilolite and montmorillonite are indistinguishable, whereas surface area normalized sorption data for quartz and α-alumina are almost coincident (figure 11-5). The α-alumina K_a are lower than those of quartz due to the higher initial U concentration of the α-alumina experiments.

The results plotted in figure 11-5 appear to indicate that quartz and α-alumina sorb more U(6+) per unit area than either clinoptilolite or montmorillonite. However, surface areas determined by N_2-BET methods most likely overestimate the amount of sorption sites on layered silicates such as montmorillonite and zeolitic minerals such as clinoptilolite. For example, it is believed that surface complex formation of U(6+) on montmorillonite occurs on the hydroxylated edge sites of the mineral (Zachara and McKinley, 1993). Wanner et al. (1994) estimated that only about 10 percent of the N_2-BET measured S_a is accounted for by the crystallite edges of montmorillonite. Assuming that the "effective" surface area ($S_{a'}$) for montmorillonite and clinoptilolite is equivalent to 10 percent of the measured S_a, sorption data for montmorillonite and clinoptilolite can be recast in terms of $K_{a'}$, where $K_{a'}=K_d/S_{a'}$. For nonlayered and nonporous minerals such as quartz and α-alumina, $K_a=K_{a'}$. Figure 11-6 plots $K_{a'}$ values for quartz, clinoptilolite, and montmorillonite. As shown in the figure, U(6+) sorption on these minerals, which have distinct mineralogic and surface properties, is essentially equivalent when recast in terms of $K_{a'}$.

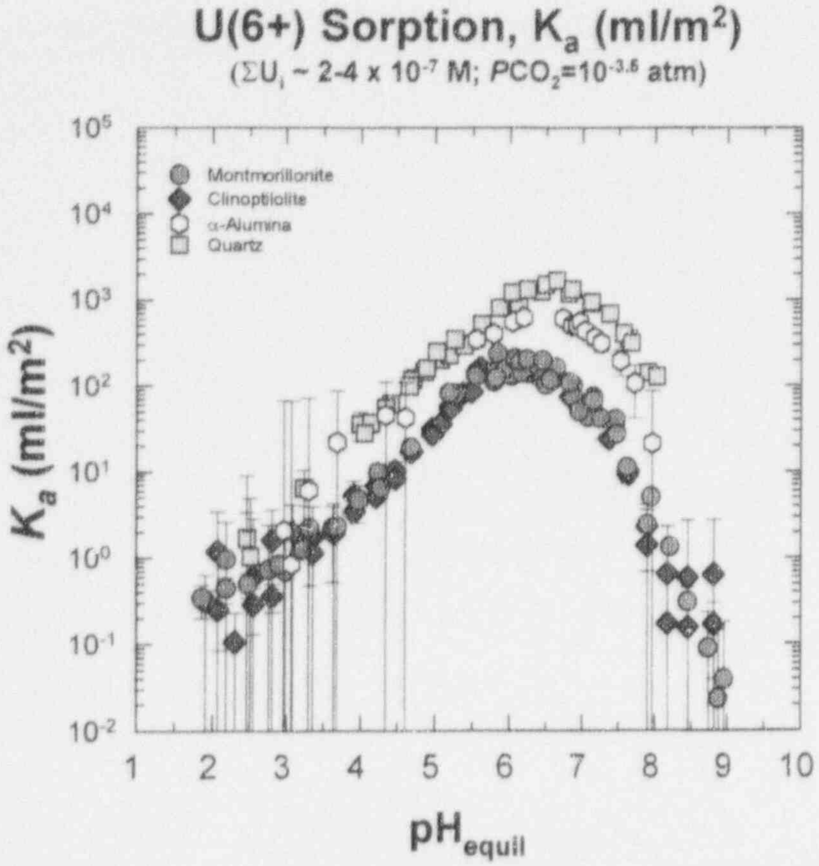

Figure 11-5. U(6+) sorption results shown previously in figure 11-4 and normalized to the measured N_2-BET surface area (S_a). Note similarity in U(6+) sorption on quartz and α-alumina and in U(6+) sorption on clinoptilolite and montmorillonite.

To test the usefulness of normalization to effective surface area as a relative measure of sorption effectiveness, Pabalan et al. (1997)[13] compiled literature data on U(6+)-sorption for $TiO_2 \cdot xH_2O$, montmorillonite, amorphous SiO_2, and kaolinite and recast them in terms of K_a versus pH. The literature data showed good agreement with the CNWRA results for K_a versus pH. Good correspondence between the K_a for different minerals and different experimental sets, indicates that S_a and K_a may be useful parameters for comparing and estimating U(6+) sorption on various sorbents.

In all U(6+)-H_2O-CO_2-mineral systems examined by Pabalan et al. (1997),[14] the experimental results show an unambiguous link between the aqueous speciation of U(6+) and its sorption behavior. Uranium(6+) sorption is most affected by geochemical parameters that influence the formation of U(6+)-hydroxy complexes in the aqueous phase. Geochemical conditions such as low pH and carbonate

[13]Pabalan, R.T., D.R. Turner, F.P. Bertetti, and J.D. Prikryl. 1997. Uranium(VI) sorption onto selected mineral surfaces: Key geochemical parameters. *Metals in Geomedia: Sorption Processes and Model Applications*. E. Jenne, ed. New York, NY: Academic Press. In Press.

[14]*Ibid.*

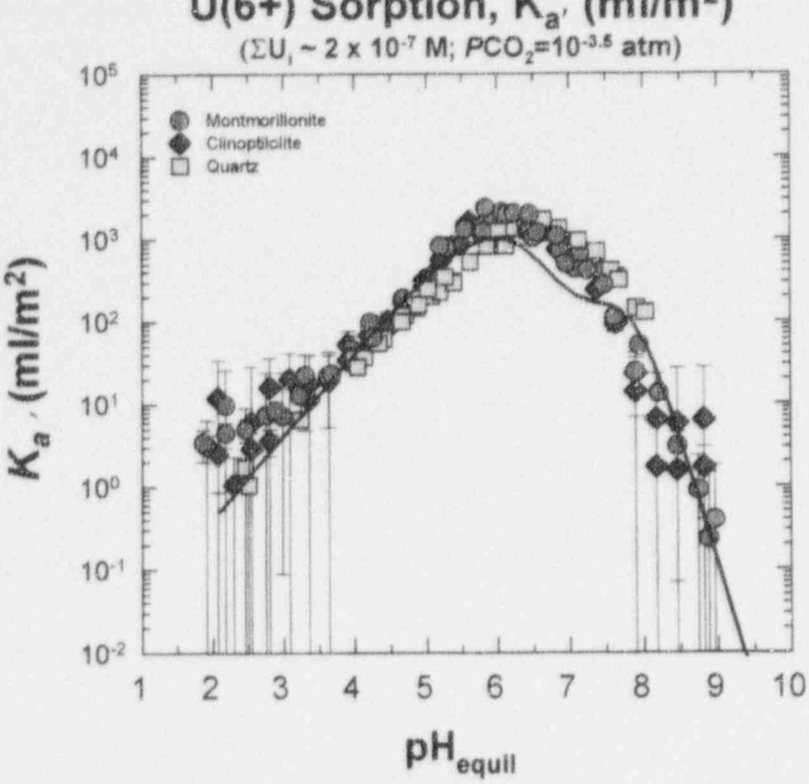

Figure 11-6. U(6+) sorption results shown previously in figure 11-4 and normalized to the effective surface area ($S_{a'}$). $S_{a'}$ was assumed to be 10 percent of measured N_2-BET surface area for montmorillonite and clinoptilolite. Note similarity in pH dependence and $K_{a'}$ for all minerals. The solid line shows the calculated pH dependence of mononuclear aqueous uranyl-hydroxy [$UO_2(OH)_x^{2-x}$] complexes for $\Sigma U = 2.1 \times 10^{-7}$ M, 0.1 m $NaNO_3$, $PCO_2 = 10^{-3.5}$ atm (see text for discussion).

complex formation that inhibit the formation of U(6+)-hydroxy complexes suppress U(6+) sorption. The similarity in the pH-dependence of U(6+) sorption on quartz, α-alumina, clinoptilolite, montmorillonite, amorphous silica, kaolinite, and titanium oxide suggests that U(6+) sorption is not sensitive to the surface charge characteristics of the sorbent as compared to the effect of changing the total number of available sites. The experimental and modeling results demonstrate that changing M/V has little influence on U(6+) K_d, except at very low M/V ratios. Ionic strength effects are minimal for surface complexation reactions, although these effects can be important if ion exchange is the predominant sorption mechanism and ionic strength effects on the activity of aqueous complexes can indirectly influence sorption behavior.

Np(5+) Sorption

Neptunium-237 has been identified as a radionuclide of concern with respect to disposal of HLW, especially at longer time frames (~10,000 yr) (Wilson et al., 1994; TRW Environmental Safety Systems, Inc., 1995; Wescott et al., 1995), because of its long half-life (2.14×10^6 yr), suspected high radiotoxicity, and reportedly low sorption characteristics. For example, DOE TSPA calculations (TRW Environmental Safety Systems, Inc., 1995) uses sorption coefficients for Np that range for 0 to 15 ml/g based on expert elicitation, while Rogers and Meijer (1993) report that for Np, K_d = 0.65 ± 0.15 for devitrified tuff (figure 11-7). Numerous uncertainties remain with respect to the magnitude of Np sorption

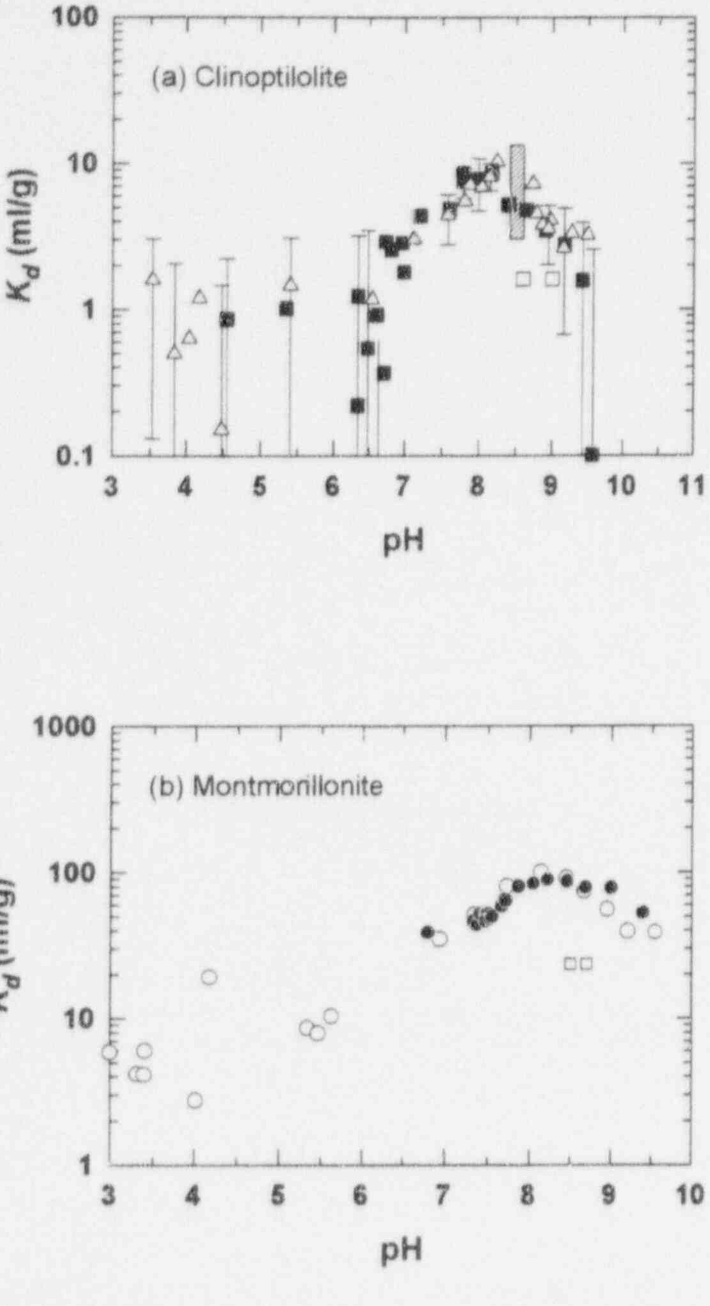

Figure 11-7. Sorption of Np(5+) on (a) clinoptilolite and (b) montmorillonite under conditions in equilibrium with atmospheric PCO_2 and with initial Np(5+) concentration of 1×10^{-6} M. Square and triangle symbols in (a) represent data from experiments with a matrix of 0.1 and 0.01 M $NaNO_3$, respectively. Open and closed circles in (b) represent data from forward and reverse experiments, respectively. For comparison, DOE data (Rogers and Meijer, 1993; Triay et al., 1993) are plotted in (a) for Np(5+) sorption onto clinoptilolite and clinoptilolite-rich tuff (open square symbols and hatched box, respectively), and in (b) for Np(5+) sorption onto montmorillonite (square symbols).

under the oxidizing conditions and in bicarbonate-rich groundwaters relevant to the proposed HLW repository at YM. For example, reported K_ds for Np sorption on quartz vary significantly and are dependent on the initial Np concentration, mineral impurities present, and activity of CO_2 (e.g., Nakayama et al., 1988; Triay et al., 1993).

Using experimental procedures developed for U(6+) sorption, Bertetti et al. (1997)[15] reported the results of experiments conducted at the CNWRA to investigate Np(5+) sorption on quartz, clinoptilolite, montmorillonite, and α-alumina (figure 11-8). Like U(6+), Np(5+) sorption is similar on different minerals with respect to pH dependence. In the presence of CO_2 (figure 11-7), Np(5+) sorption reaches a maximum and decreases toward lower or higher pH. The Np(5+) sorption maximum is typically at a higher pH (~8 to 8.5 in the presence of CO_2) and typically much lower (i.e., K_d is lower) than for U(6+) sorption.

At a given pH, the Np(5+) K_d for the different minerals vary by over two orders of magnitude. As with U(6+), when normalized with respect to surface area, the differences between minerals are reduced when Np(5+) sorption is expressed as K_a (figure 11-9). Differences are also evident between sorption on nonlayered and nonporous minerals quartz and α-alumina compared to sorption on clinoptilolite and montmorillonite. Similar to U(6+) sorption, K_a data appear to indicate that quartz and α-alumina sorb more Np(5+) per unit area than clinoptilolite and montmorillonite (figure 11-9). When normalized to an "effective" surface area as discussed previously, however, Np(5+) sorption expressed as $K_{a'}$, on these minerals is essentially equivalent (figure 11-10). The apparent scatter of data points at low pH is a result of larger uncertainties in the experimental data at low sorption values.

Neptunium(5+) aqueous speciation is dominated by NpO_2^+ at pH below seven in the absence of CO_2. However, near pH~7, Np hydrolysis becomes significant and the amount of the Np(5+) hydroxy species $NpO_2OH^0(aq)$ increases with increasing pH throughout the pH range under study. This increase in stability of Np(5+) aqueous hydroxy complex is mimicked by an increase in Np(5+) sorption with increasing pH under CO_2-free conditions (figure 11-10). Under atmospheric PCO_2 conditions, the stability of the neutral hydroxy species reaches a maximum near pH 8.5 and decreases with further increases in pH. Although the neutral hydroxy complex does not become a predominant species in an Np(5+)-H_2O-CO_2 solution, a comparison of Np(5+) sorption data and aqueous speciation indicates that the pH dependence of the stability of the $NpO_2OH^0(aq)$ species is distinctly similar to the pH dependence of Np(5+) (Bertetti et al., 1997).[16]

The pH dependent trends in observed U(6+) and Np(5+) sorption behavior are similar for many common minerals, including clinoptilolite, quartz, α-alumina, montmorillonite, iron oxyhydroxide, and kaolinite even though these minerals have different mineralogic and surface charge characteristics. This similarity suggests that actinide sorption is not sensitive to the surface charge properties of the sorbent as compared to the effect of changes in the surface area or number of sorption sites. On the other hand, actinide sorption is strongly dependent on pH. For conditions where solutions are at low PCO_2 or CO_2-free conditions, sorption increases with increasing pH over the entire pH range studied. For experiments

---

[15]Bertetti, F.P., R.T. Pabalan, and M.G. Almendarez. 1997. Studies of neptunium(V) sorption on quartz, clinoptilolite, montmorillonite, and α–alumina. *Metals in Geomedia: Sorption Processes and Model Applications*. E. Jenne, ed. New York, NY: Academic Press. In Press.

[16]*Ibid.*

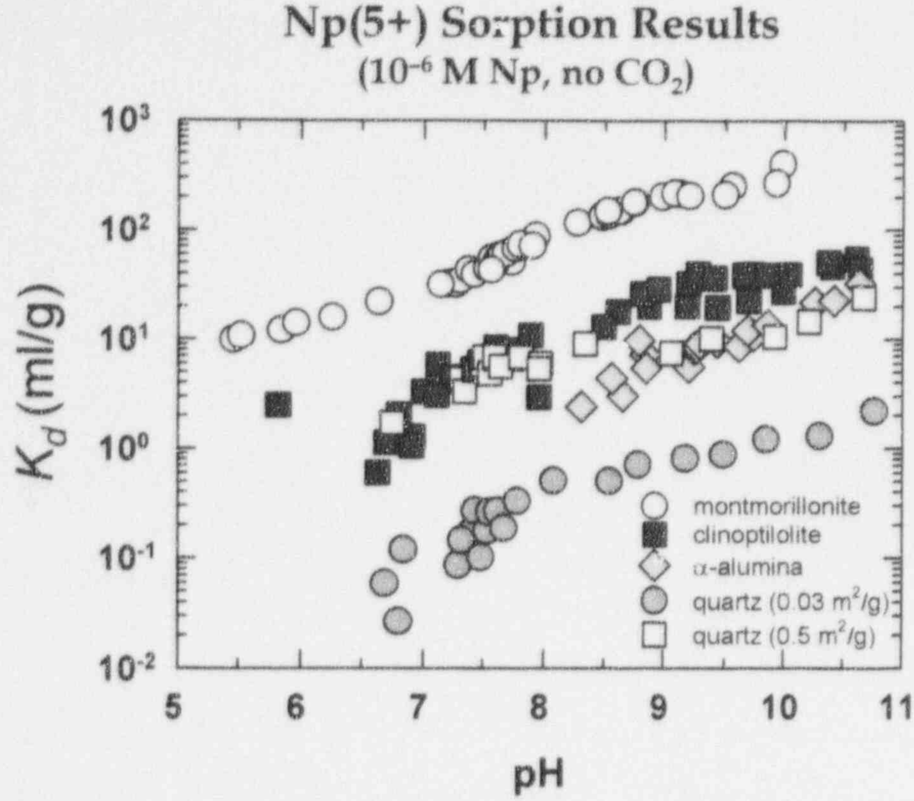

Figure 11-8. CNWRA experimental results for Np(5+) sorption on montmorillonite, clinoptilolite, α-alumina, and quartz expressed as K_d

with solutions in equilibrium with atmospheric PCO_2, a distinct sorption maximum is observed for all minerals. The data also suggest that the magnitude of actinide sorption is the same for different minerals if normalized to the number of available sites using an "effective" surface area.

Observations of data from Bertetti et al. (1997)[17] and Pabalan et al. (1997)[18] indicate a common pattern for actinide sorption that is related to the formation of hydroxy complexes in solution. This pattern suggests that modeling approaches that are capable of accounting for changes in solution chemistry (e.g., surface complexation models) are required for successful description and prediction of sorption of U, Np and other actinides on mineral surfaces over wide ranges of geochemical conditions. The methodology developed here provides a basis for evaluating conceptual models, sorption coefficient bounding limits, and probability distribution functions used by DOE in radionuclide transport calculations.

---

[17]*Ibid.*

[18]Pabalan, R.T., D.R. Turner, F.P. Bertetti, and J.D. Prikryl. 1997. Uranium(VI) sorption onto selected mineral surfaces: Key geochemical parameters. *Metals in Geomedia: Sorption Processes and Model Applications*. E. Jenne, ed. New York, NY: Academic Press. In Press.

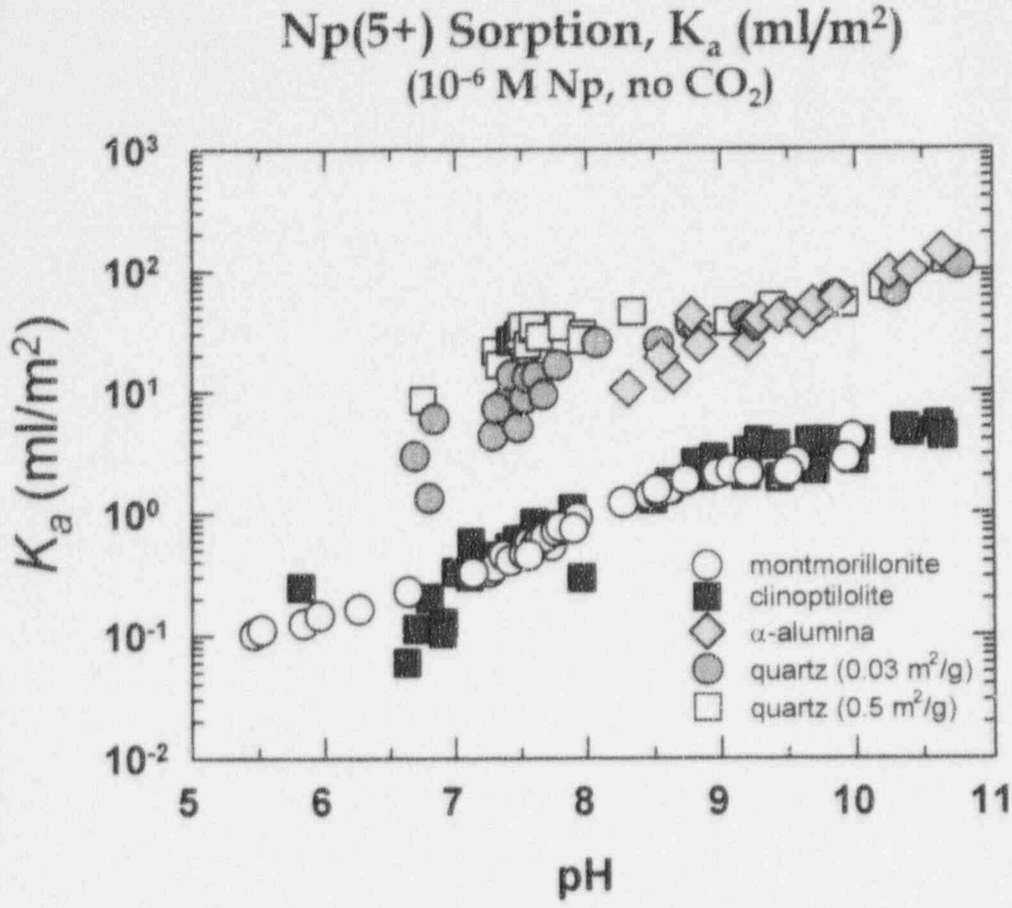

Figure 11-9. Np(5+) sorption results shown previously in figure 11-7, and normalized to the measured N_2-BET surface area (S_a). Note similarity in Np(5+) sorption on quartz and α-alumina and in Np(5+) sorption on clinoptilolite and montmorillonite.

11.3.4 Evaluating Saturated Zone Mixing Using Existing Hydrochemical Data

A key assumption in the DOE WCIS (Hypothesis 12) with regard to radionuclide transport is the dilution of radionuclide contaminated water upon mixing with the regional groundwater flow system. To address issues related to mixing at the YM site, geochemical information such as water chemistry and mineralogy can be used to provide constraining values for dilution factors used in PA. To allow for effective use, analysis, and interpretation, these data should be evaluated, compiled, and logged in a GIS database that can be related to the geologic, hydrologic, and geographic framework of the YM area. This approach is a necessary part of developing an understanding of the regional groundwater flow system at YM. The effort also serves as a baseline to extend both conceptual models of the current system and predictions of the future performance of the proposed repository.

Under the Radionuclide Transport KTI, the Structural and Seismicity KTI, and the Igneous Activity KTI, geologic and hydrologic GIS coverages including surface geology, structure, and hydrostratigraphy are being developed at the CNWRA for YM and the surrounding regions using the

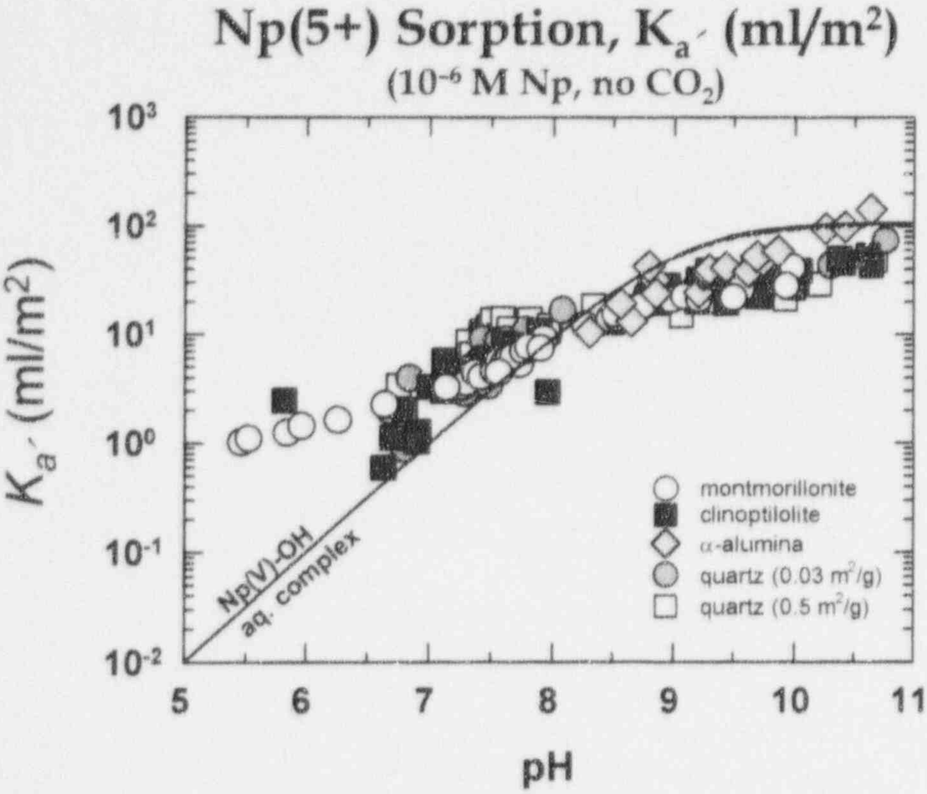

Figure 11-10. Np(5+) sorption results shown previously in figure 11-7 and normalized to the effective surface area ($S_{a'}$). $S_{a'}$ was assumed to be 10 percent of measured N_2-BET surface area for montmorillonite and clinoptilolite. Note similarity in pH dependence and $K_{a'}$ for all minerals. The solid line shows the calculated pH dependence of aqueous neptunyl-hydroxy (NpO_2OH^0) complex for $\Sigma Np=1\times10^{-6}$ M, 0.1 m $NaNO_3$, no CO_2 (see text for discussion).

Arc/Info (Version 6.1) software package. A similar hydrochemical database would augment and benefit from these coverages and enable aspects of these databases to be incorporated in conceptual models of hydrologic flow. In this manner, the geographic location of specific samples can be traced and associated data supplied. The PC-based GIS software package ArcView (Version 2.0b) provides a convenient means of displaying and combining different Arc/Info coverages and creating different coverages by importing spatially distributed hydrochemical and geochemical data. The display and analytical capabilities associated with the ArcView software provides a means of handling large datasets, with identification of hydrochemical signatures for different aquifers and trend analyses providing a strong basis for bounding conceptual models of the regional hydrologic flow system at YM. The ability to consider hydrochemical information in a geologic, structural, and hydrostratigraphic framework will allow more effective assessment of complex and interactive systems and processes.

Baseline geology and structure are essential in developing conceptual models of the hydrologic flow system in the YM region. Digital Arc/Info coverages were developed by the U.S. Geological Survey (USGS) at an original scale of 1:250,000 (D'Agnese et al., 1995). In greater detail, Frizzell and Shulters (1990) compiled a map of the surface geology at the Nevada Test Site (NTS) at an original scale of

1:100,000. This map has been digitized in Arc/Info and converted to ArcView GIS shapefile format at the CNWRA.

Based on the hydrostratigraphy, Winograd and Thordarson (1975) identified six aquifers and five aquitards within the YM region. From the bottom of the hydrostratigraphic section these hydrogeologic units are

- Lower clastic aquitard of Precambrian to Lower Cambrian quartzite, shale, and siltstone
- Lower carbonate aquifer of middle Cambrian to Devonian limestone and dolomite
- Upper clastic aquitard of Devonian to Mississippian argillite and quartzite
- Upper carbonate aquifer of Pennsylvanian to Permian limestone
- Local aquitards of Cretaceous granitic stocks, dikes and sills
- Tuff aquitard of Oligocene to middle Miocene interbedded, nonwelded to welded tuffs
- Lava-flow aquitard of upper Miocene lava flow and interflow breccia
- Bedded tuff aquifer of upper Miocene ash-fall and reworked tuff
- Welded tuff aquifer of upper Miocene to middle Pliocene nonwelded to densely welded tuffs
- Lava flow aquifer composed of upper Pliocene basaltic and rhyolitic flows
- Valley fill aquifer of upper Pliocene to Holocene alluvial, fluvial, and lacustrine deposits.

Winograd and Thordarson (1975) note that the surface and subsurface extent of the principal hydrogeologic units vary from basin to basin due to the complex structural and erosional history of the rocks. According to Winograd and Thordarson (1975), the interbasin flow of groundwater is not significantly influenced by the topographic boundaries of the individual basins but rather by the presence and relative positions of the lower carbonate aquifer and the upper and lower clastic aquitards. Figure 11-11 divides the geology of Frizzell and Shulters (1990) into the hydrostratigraphic units of Winograd and Thordarson (1975). For clarity, and due to the different nomenclature adopted by Frizzell and Shulters (1990), the Tertiary units have been divided here into a single aquifer and a single aquitard.

To use hydrochemistry as a means to constrain fluid flow and mixing, it is necessary to develop chemical fingerprints of water in different aquifers. Winograd and Thordarson (1975) also identified five distinct hydrochemical facies in the regional groundwater system:

- Ca-Mg-HCO_3 facies typical of waters discharged from perched springs and regional springs in the carbonate units
- Na-K-HCO_3 facies typical of waters in the tuff aquifer
- Ca-Mg-Na-HCO_3 facies typical of waters in east-central Amargosa Desert and Ash Meadows
- Na-SO_4-HCO_3 sodium sulfate bicarbonate facies typical of waters discharged at Furnace Creek Wash and Nevares Springs in Death Valley
- a playa facies high in Total Dissolved Solids (TDS), typical of waters discharged by evapotranspiration at Franklin Lake Playa (Alkali Flat).

Waters sampled from the lower carbonate aquifer at the NTS are of the calcium magnesium sodium bicarbonate type which lead Winograd and Thordarson (1975) to infer downward flow of water from the tuffaceous units into the Paleozoic carbonate aquifer.

The water facies of Winograd and Thordarson (1975) are based on a relatively small dataset of hydrochemical analyses. An additional, more comprehensive source of water chemistry data is found in the USGS report of Perfect et al. (1995). This report includes spreadsheet files with major and minor

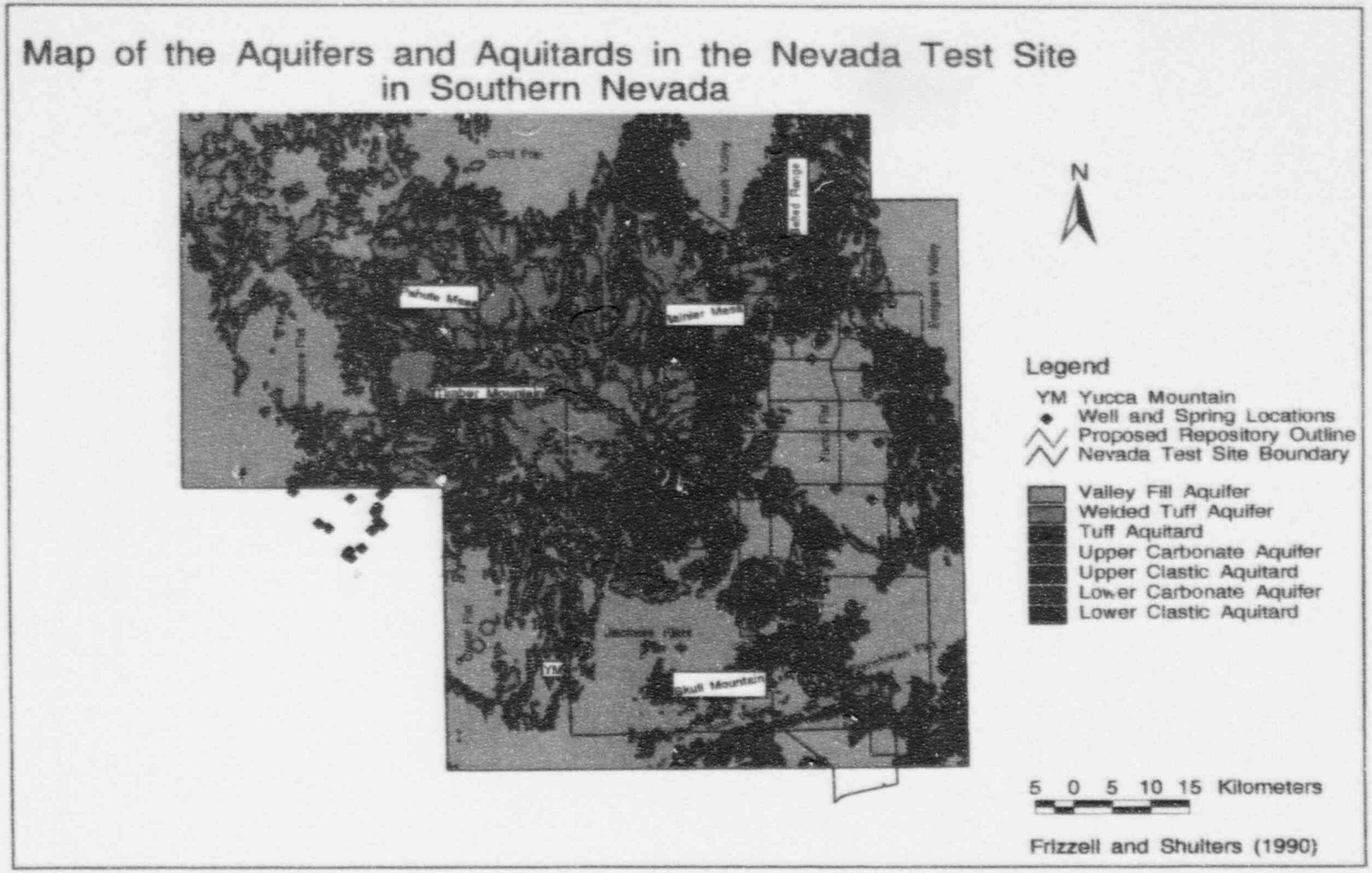

Figure 11-11. Geology coverage generated using ArcView (Version 2.0b) based on the geologic map of Frizzell and Shulters (1990) (original scale of 1:100,000). The units of Frizzell and Shulters (1990) were assigned to the hydrostratigraphic framework of Winograd and Thordarson (1975) and an additional coverage has been developed that includes the sample locations for charge-balanced water chemistry analyses from Perfect et al. (1995).

element analyses compiled over several decades for the region surrounding YM. One file contains the raw data for more than 4,700 wells and springs from USGS and the DOE reports and the USGS National Water Information Service database. A second file included with the report contains data that have been edited to remove duplicate entries, make the data chemically consistent, and calculate whether or note the reported analysis is charge balanced. The editing philosophy used by Perfect et al. (1995) is described in the report. Based on this editing, the number of charged balanced analyses reduces to about 1,800 although this reduced database still includes multiple analyses taken over an extended time at a single sampling point. Figure 11-11 shows the locations of those wells and springs where balanced hydrochemical analyses are available. Some of the hydrochemical data of Perfect et al. (1995) lie outside the current geologic coverage as shown in figure 11-11, particularly in Oasis and Amargosa Valleys. Additional geologic coverages (e.g., D'Agnese et al., 1995) are becoming available, however, to expand the area covered by CNWRA GIS database. These analyses can be used with a geochemical equilibrium code such as MINTEQA2 (Allison et al., 1991) to calculate water saturation with respect to different minerals such as calcite and gypsum. These saturation levels can provide an additional signature to identify different aquifer waters, and can also provide some information regarding groundwater evolution along flow paths.

Using only a GIS database cannot limit all types of uncertainties in PA modeling, such as uncertainties in mathematical models. A GIS database for hydrochemical information can, however, provide the best means for developing conceptual models of fluid flow and mixing, and one of the only means of calibrating, baselining, and validating a numerical model. The hydrochemical information can be used in either a qualitative sense such as defining regional or local trends in groundwater flow or quantitatively in geochemical modeling (Murphy and Pabalan, 1994). Relevant regional scale groundwater patterns can be analyzed by first using hydrochemical facies information and tracers to delineate plausible flow paths, and then using conservative tracers and isotopic data to constrain mixing between end-member solutions. The ability to tie the data to a geographic and geologic framework specific to the YM site is an important aspect of making the most out of the available data. As more data become available, it may also be possible to develop three-dimensional (3D) representations of the information, further increasing the value of the database.

11.3.5 Development of Preferred Pathway Model

Prior to the discovery of recent water at depth in the unsaturated zone at YM [e.g., Fabryka-Martin et al. (1996) using ^{36}Cl, Yang et al. (1996) using tritium, and ^{14}C], it was generally held that due to the high matrix potential, any water in fractures would be drawn quickly into the matrix. The preferred conceptual model (TRW Environmental Safety Systems, Inc., 1995) had water flowing through the matrix except in those rare situations where high infiltration rates caused saturated conditions. Having accepted the concept of matrix flow as predominant flow mechanism, it was reasonable to then consider chemical interactions between the aqueous species and the solid through which the solution flowed. Batch sorption experiments were used to simulate the interaction between dissolved radionuclides and the solid matrix. The sorption coefficients from those experiments were converted to retardation factors used in PA models simulating the waste isolation characteristics of a geologic repository (e.g., TRW Environmental Safety Systems, Inc., 1995). If transport of radionuclides is not predominantly through the matrix, then a K_d approach to retardation based on matrix sorption only is not conservative.

The latest DOE total system performance analysis (TRW Environmental Safety Systems, Inc., 1995) used a Monte Carlo approach in which K_ds were selected from distributions generated by expert elicitation (Wilson et al., 1994). In addition to this abstraction, the TSPA modeled individual flow paths

composed of part matrix and part fracture. The proportion of the path in each regime was based on a distribution, again generated by expert elicitiation (TRW Environmental Safety Systems, Inc., 1995; Chapter 7). The level of abstraction in the TSPA-95 made the comparison to site-specific characteristics difficult.

With the discovery of bomb-pulse water at the proposed repository horizon, investigators at LANL (Los Alamos National Laboratory) have begun sensitivity analyses to determine if alternative conceptual models or adjustments to parameter ranges using existing conceptual models are necessary to explain recent observations (Fabryka-Martin et al., 1996). In their analyses, LANL investigators chose to look at the effects of varying infiltration, fracture density, fracture aperture, and van Genuchten parameters through the nonwelded Paintbrush tuff that overlies the Topopah Spring tuff. They concluded it was not necessary to abandon the existing conceptual model, but found that the lower infiltration rates were inconsistent with the bomb-pulse observations. The code used in the analysis was FEHM, a dual continuum model, that simulated one-dimensional steady-state conditions.

To test whether the current conceptual model of radionuclide transport proposed by the DOE is conservative, the Radionuclide Transport KTI team is developing an alternative conceptual model of flow and transport in the unsaturated zone. Both models will be evaluated using site-specific data to determine if alternative conceptualizations supported by the same site data could result in significant differences in radionuclide mobility.

Alternative Conceptual Model

The Topopah Spring tuff was chosen as the repository horizon because of its well-drained character. It is proposed that portions of the flow system in the unsaturated zone at YM, like the Topopah Spring, can be approximated by a 3D network of fractures represented as intersecting disks of various sizes and orientations. Previous studies (Long et al., 1985; Dverstorp et al., 1992) have modeled flow in these features when they are totally filled with water or under unsaturated conditions (Rasmussen, 1987). In the current model, the fractures are partially filled with water analogous to a plumbing system that contains traps.

The rate of flow in fractures is considered to be so much greater than that in the matrix, as a first approximation, flow in the matrix can be disregarded. Geochemical evidence of fluid collected from the unsaturated zone and from perched water bodies presented by Yang et al. (1996) is consistent with a model where little interaction occurs between the fractures and matrix. The fact that perched water exists at YM is further evidence for relatively fast and substantial flow in fractures and relatively slow imbibition into the matrix (Striffler et al., 1996). Otherwise, drill holes would not fill with water during the time-scale of observation (months to years). Evidence suggests there are several examples of perched water or at least wet portions of the drillholes in and around YM (Striffler et al., 1996).

The flow of water in this system is envisioned to be intermittent in response to the sporadic rainfall events that occur in the desert. The water flows as rivulets, similar to flow on a smooth surface such as glass, down a single disk-shaped fracture and fills the bottom of the fracture to the level where the fracture intersects another disk-shaped fracture. At this point water flows into the second fracture trickling down to fill the bottom of it (figure 11-12). This process continues to the third, fourth, and more fractures, until the amount of water added to the system equals the capacity of these "traps" first filled to hold water.

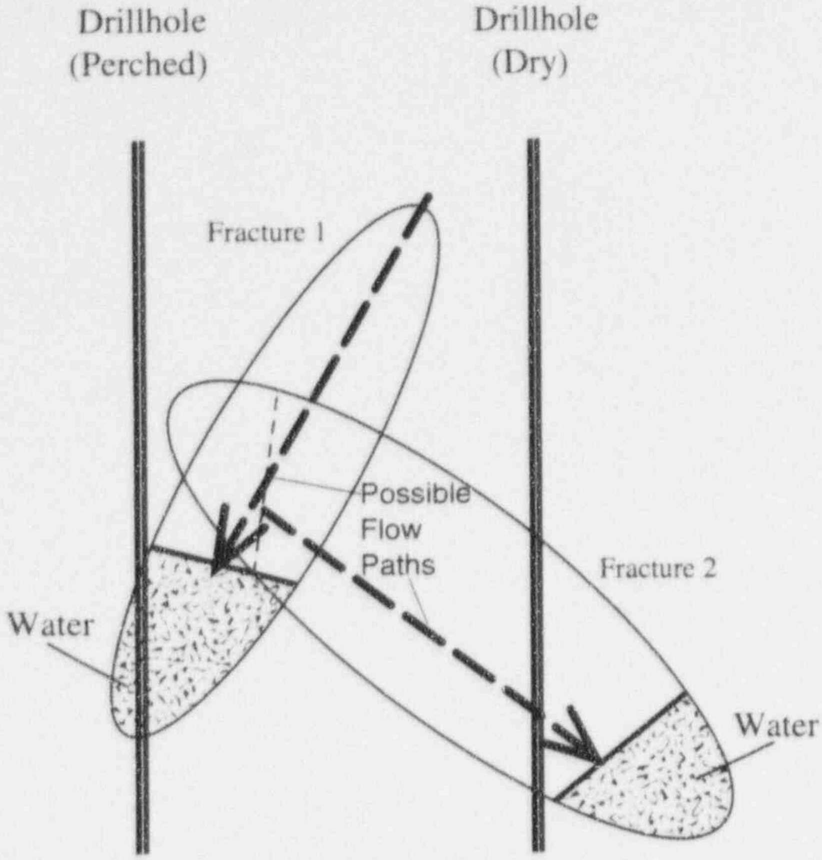

Figure 11-12. Schematic diagram of a conceptual model for flow through intersecting fracture planes

This flow system can also be envisioned as a series of buckets of various sizes. Pouring water in the first bucket fills it to its capacity at which point water spills over into the next and so on. To make the model more realistic, the buckets are "leaky" allowing the water to move into the matrix (figure 11-13). Consequently, in the time between rainfall events, the buckets lose water to the matrix at different rates depending on the hydraulic conductivity of the matrix and the head of each bucket. (Note that Darcy's law applies only to the individual fractures. In the series of fractures, the head in one fracture does not influence the head in the next.) The longer the time between rainfall events, the greater the capacity of the buckets to hold new water from the next event.

Each bucket is considered a reaction vessel, where processes such as sorption/desorption, precipitation/dissolution, and dilution occur. By considering the surface area contacted by the water, the length of time the water is in contact with the fracture surface and the hydraulic conductivity of the matrix, it is possible to estimate the rock to water ratio for each fracture with its surrounding matrix. Geochemical modeling, which requires masses of reactants to be input, is particularly amenable to this conceptual model.

Besides duration between rainfall events, the amount of rain in each event can affect the distribution of groundwaters of various ages. For example, the intersection of two disks may be toward the top of the disk first to fill. If sometime in the distant past a large rainfall event occurred, water could have filled the first disk and flowed into the second. Subsequent rainfall events might not have been so

"Leaky Bucket" Model

Figure 11-13. Schematic diagram of conceptual model of fracture controlled flow system with diffusion of water into the matrix.

extreme, in which case, new water would not be added to the second disk. As a result, the ages of water in the fractured system need not be a function of depth. There are examples of reversals of groundwater ages with depth at YM. This is interpreted to be lateral flow, possibly via fractures (Liu et al., 1995).

By generating various 3D fracture systems with different characterization parameters and then determining the effects on flow and transport, one may be able to identify those parameters most important in site characterization activities for modeling the repository performance. The types of fracture parameters necessary to model repository performance could include parameters such as fracture intersection length, intersection orientation, difference in height between fracture intersection and bottom of fracture, etc. Likewise, the effects on flow and transport are to be determined, but they could include possible age distribution of water in fracture systems containing traps or perched water, channeling in fracture systems resulting in more direct pathways to the groundwater table, and rock to water ratios important to geochemical modeling.

It should be noted that these simulated fracture systems can be compared with site data. For example, Sweetkind et al. (1996)[19] describe the fracture character of the Paintbrush Tuff nonwelded

[19]Sweetkind, D.S., E.R. Verbeek, J.K. Geslin, and T.C. Moyer. 1996. Fracture Character of the Paintbrush Tuff Nonwelded Hydrologic Unit, Yucca Mountain, Nevada (Draft Report).

hydrologic unit. This study provides information on fracture density, orientation, length, intersection, and aperture.

Another important aspect that can be addressed when one considers the flow system, not as an equivalent porous medium, but as a system of pipes, is the flux through the unsaturated zone. If it is assumed that fractures are necessary for perched water, then the intersection of the wet portion of a fracture or fractures can be assumed to constitute a perched water body, and one can determine the flux into the fracture by assuming as a first approximation flux into the matrix equals flux into the fracture. By determining the hydraulic conductivity of the matrix in the lab, the head of water at the fracture borehole intersection, and the volume of water in the fracture from a pump test, one can determine the flux into the matrix. Results of this calculation could then be considered in light of age determinations of the groundwater in the fracture/perched zone. Inconsistency in the flux calculation and age could be used to adjust assumptions (e.g., fracture flux≠matrix flux or when a trap is flushed, new water pushes the old water to the next trap).

Past arguments against discrete fracture models stated they were too computationally intensive for ready inclusion in a system code PA. However, the system code picks numerous pathways, models the flow and transport along those pathways, and then adds the contributions from all (TRW Environmental Safety Systems, Inc., 1995). This is not different from the modeling envisioned using the 3D disk-shaped fracture model proposed here. The advantage of this model is that it does not require steady-state conditions and is not computationally intensive. Furthermore, fracture properties presented as distributions for each rock unit are being collected at the site and are amenable to inclusion in Monte Carlo simulations. Finally, the geochemistry of the system, where water sits in traps for various periods of time, is well described by batch tests in the lab.

11.3.6 Conclusions

The technical objectives of the Radionuclide Transport KTI have been designed to address DOE WCIS Hypotheses 10, 11, and 12. The conceptual model necessary to describe uranium transport at Nopal I requires large, throughgoing fractures to control transport over large spatial scales. This conceptualization is consistent with the importance of fractures in providing fast flow and transport paths for relatively young waters, as indicated by YM-specific $^{36}Cl/Cl$ ratios. In addition, a hydrologic conceptual model has been developed that attempts to take into account the interactions between fractures and provide a framework for future geochemical modeling. Evaluation of conceptual models of transport used by DOE is a critical part of testing DOE WCIS hypotheses on radionuclide transport (Hypothesis 10) and dilution (Hypothesis 11). DOE and NRC PA transport calculations should continue to be designed to address the importance of fracture transport. Work undertaken as part of the Radionuclide Transport KTI has also identified similarities in Np and U sorption behavior between a number of minerals (quartz, montmorillonite, clinoptilolite) that are abundant at YM. When sorption coefficients are normalized to effective mineral surface area, sorption behavior is demonstrated to be strongly affected by changes in pH and PCO_2, but relatively insensitive to mineral substrate and changes in solid-mass to solution-volume ratios. This suggests the possibility of developing sorption response curves for PA that are a function of key geochemical parameters (e.g., pH and PCO_2) and provide support for chemically reasonable limits on sorption coefficients. The results from the sorption experiments will be used to assess sorption coefficients for U and Np used by DOE in PA calculations. Work conducted under the Radionuclide Transport KTI has also begun the process of assembling existing hydrochemical data in a geographic framework to constrain flowpaths and mixing in the saturated zone (DOE WCIS Hypothesis 12).

11.4 ASSESSMENT OF PROGRESS TOWARD MEETING OBJECTIVES

The four subissues identified in the Implementation Plan for the Radionuclide Transport KTI develop broad areas covering data and analysis needs to address the effects of radionuclide transport on overall repository performance. The research undertaken during FY96 moved toward addressing several of these subissues.

- Review of current DOE research in ^{36}Cl has provided a basis for critical evaluation of conceptual models of groundwater flow at YM that may be used by the DOE in future PA calculations and viability assessments (DOE WCIS Hypothesis 10).

- Transport studies conducted on samples from the Nopal I U deposit, Peña Blanca district, Mexico, have provided constraints on hydrologic and geochemical controls on radionuclide transport under hydrologically unsaturated conditions in fractured tuff. U transport at Nopal I is controlled by oxidizing hydrochemical conditions and radionuclide mobility at YM may similarly depend upon transient hydrological conditions. Research also identified the importance of considering radionuclide transport through fractures in unsaturated tuffs. This is consistent with a growing consensus that fractures will provide fast pathways for hydrologic flow and transport through the unsaturated zone at YM. Incorporation of aqueous U into fracture minerals at Nopal I suggests that retardation is not a simple reversible process. This work has helped establish a basis from which to critically evaluate conceptual models that may be used by DOE in future PA calculations and viability assessments (DOE WCIS Hypothesis 10).

- NRC/CNWRA research focused on identifying the sensitivity of radionuclide sorption (K_d) to different geochemical parameters based on the CNWRA experimental results and sorption results reported in the available literature. The results of this research are simplified approaches to data interpretation and sorption modeling for U and Np. Establishing a methodology to account for the effects of key geochemical parameters on radionuclide sorption coefficients is an important means for evaluating conceptual models, bounding limits, and probability distribution functions used by DOE in radionuclide transport calculations (DOE WCIS Hypothesis 10).

- Available hydrochemical data are being combined into a GIS coverage and tied to coverages of geology and structure. This will enable hydrochemical information to provide boundaries to flow and the potential for dilution within the YM system. The hydrochemical data will also provide a potential means for calculating sorption as a function of water chemistry and groundwater evolution through rock-water interaction along the flow paths. Accounts have been established with the DOE Automated Technical Data Tracking System that has been searched for additional site-specific data related to retardation. This has provided an important step in using existing data to constrain regional groundwater flow and saturated zone mixing (DOE WCIS Hypothesis 12).

Subissues pertaining to the sensitivity of overall performance of the repository to variations in parameters controlling radionuclide transport and the identification of radionuclides requiring some form of retardation to meet performance requirements were not addressed during this FY. Activities designed to address these issues are planned for FY97 under the TSPA and Integration KTI.

11.5 INTEGRATION WITH OTHER KEY TECHNICAL ISSUES

The Radionuclide Transport KTI has relied on GIS information provided by the KTIs on Structural Deformation and Seismicity and Igneous Activity to develop hydrochemical coverages for saturated zone dilution analysis. Information on the regional flow system from the KTI on Unsaturated and Saturated Flow Under Isothermal Conditions was used to identify general flow trends. Sensitivity analyses using sorption models and conceptual transport models will be used to support a sorption module for the TSPA and Integration KTI. The Radionuclide Transport KTI will not be supported by CNWRA for FY97, and therefore no changes in inputs or outputs have been identified.

11.6 REFERENCES

Allison, J.D., D.S. Brown, and K.J. Novo-Gradac. 1991. *MINTEQA2/PRODEFA2. A Geochemical Assessment Model for Environmental Systems: Version 3.0 User's Manual.* EPA/600/3-91/021. Athens, GA: Environmental Protection Agency.

Davis, J.A., and D.B. Kent. 1990. Surface complexation modeling in aqueous geochemistry. *Reviews in Mineralogy: Volume 23. Mineral-Water Interface Geochemistry.* M.F. Hochella, Jr., and A.F. White, eds. Washington, DC: Mineralogical Society of America: 23: 177–260.

D'Agnese, F.A., C.C. Faunt, and A.K. Turner. 1995. *Preliminary Digital Geologic Maps of the Mariposa, Kingman, Trona, and Death Valley Sheets, California.* U.S. Geological Survey Open-File Report 94-318. Denver, CO: U.S. Geological Survey.

Dverstorp, B., J. Andersson, and W. Nordqvist. 1992. Discrete fracture network interpretation of field tracer migration in sparsely fractured rock. *Water Resources Research* 28: 2,327–2,343.

Fabryka-Martin, J.T, P.R. Dixon, S. Levy, B. Liu, H.J. Turin, and A.V. Wolfsberg. 1996. *Summary Report of Chlorine-36 Studies: Systematic Sampling for Chlorine-36 in the Exploratory Studies Facility.* LA-UR-96-1384. Los Alamos, NM: Los Alamos National Laboratory.

Frizzell, V.A., Jr., and J. Shulters. 1990. *Geologic Map of the Nevada Test Site, Southern Nevada.* U.S. Geological Survey Miscellaneous Investigations Series, Map I-2046. Denver, CO: U.S. Geological Survey.

Jarzemba, M.S., and D.A. Pickett. 1995. *An Evaluation of the Important Radionuclides for Performance Assessment.* Letter Report to the Nuclear Regulatory Commission. San Antonio, TX: Center for Nuclear Waste Regulatory Analyses.

Kerrisk, J.F. 1985. *An Assessment of the Important Radionuclides in Nuclear Waste.* LA-10414-MS. Los Alamos, NM: Los Alamos National Laboratory.

Liu, B., J. Fabryka-Martin, A. Wolfsberg, and B. Robinson. 1995. Significance of apparent discrepancies in water ages derived from atmospheric radionuclides at Yucca Mountain, Nevada. *Proceedings of the Water Resources at Risk Conference, May 14–18, 1995.* Denver, CO: American Institute of Hydrology: NH-52 – NH-62.

Long, J.C.S., P. Gilmour, and P.A. Witherspoon. 1985. A model for steady fluid flow in random three-dimensional networks of disc-shaped fractures. *Water Resources Research* 21: 1,105–1,115.

McKinley, J.P., J.M. Zachara, S.C. Smith, and G.D. Turner. 1995. The influence of hydrolysis and multiple site-binding reactions on adsorption of U(VI) to montmorillonite. *Clays and Clay Minerals* 43: 586–598.

Murphy, W.M., and R.T. Pabalan. 1994. *Geochemical Investigations Related to the Yucca Mountain Environment and Potential Nuclear Waste Repository*. NUREG/CR-6288. Washington, DC: Nuclear Regulatory Commission.

Nakayama, S., H. Arimoto, N. Yamada, H. Moriyama, and K. Higashi. 1988. Column experiments on migration behaviour of neptunium(V). *Radiochimica Acta* 52/53: 179–182.

National Academy of Sciences. 1995. *Technical Bases for Yucca Mountain Standards*. Committee on Technical Bases for Yucca Mountain Standards, Board on Radioactive Waste Management, National Research Council of the National Academy of Sciences. Washington, DC: National Academy Press.

O'Day, P.A. 1994. Free energies of adsorption of divalent metal ions on quartz. *GSA Abstracts with Programs 1994 Annual Meeting*. Boulder, CO: Geological Society of America: A-111.

Osmond, J.K., and M. Ivanovich. 1992. Uranium-series mobilization and surface hydrology. *Uranium-Series Disequilibrium: Applications to Earth, Marine, and Environmental Sciences*. M. Ivanovic and R.S. Harmon, ed. Oxford, England: Clarendon Press.

Pearcy, E.C., J.D. Prikryl, W.M. Murphy, and B.W. Leslie. 1994. Alteration of uraninite from the Nopal I deposit, Peña Blanca District, Chihuahua, Mexico, compared to degradation of spent nuclear fuel in the proposed U.S. high-level nuclear waste repository at Yucca Mountain, Nevada. *Applied Geochemistry* 9: 713–732.

Pearcy, E.C., J.D. Prikryl, and B.W. Leslie. 1995. Uranium transport through fractured silicic tuff and relative retention in areas with distinct fracture characteristics. *Applied Geochemistry* 10: 685–704.

Perfect, D.L., C.C. Faunt, W.C. Steinkampf, and A.K. Turner. 1995. *Hydrochemical Data Base for the Death Valley Region, California and Nevada*. U.S. Geological Survey Open-File Report 94-305. Denver, CO: U.S. Geological Survey.

Rasmussen, T. 1987. Computer simulation model of steady fluid flow and solute transport through three-dimensional networks of variably saturated, discrete fractures. D.D. Evans and T.J. Nicholson, eds. *Flow and Transport Through Unsaturated Fractured Rock*. Geophysical Monograph 42: American Geophysical Union: 107–114.

Rogers, P.S.Z., and A. Meijer. 1993. Dependence of radionuclide sorption on sample grinding, surface area, and water composition. *Proceedings of the Fourth Annual International Conference on High Level Radioactive Waste Management*. La Grange Park, IL: American Nuclear Society: 1,509–1,516.

Simmons, A.M., S.T. Nelson, P.L. Cloke, T.R. Crump, C.J. Duffy, W.E. Glassley, Z.E. Peterman, M.D. Siegel, D. Stahl, W.C. Steinkampf, and B.E. Viani. 1995. *The Critical Role of Geochemistry in the Program Approach*. Las Vegas, NV: U.S. Department of Energy.

Striffler, P., G.M. O'Brien, T. Oliver, and P. Burger. 1996. *Perched Water Characteristics and Occurrences, Yucca Mountain, Nevada* (Draft Report). Denver, CO: U.S. Geological Survey.

Triay, I.R., B.A. Robinson, R.M. Lopez, A.J. Mitchell, and C.M. Overly. 1993. Neptunium retardation with tuffs and groundwaters from Yucca Mountain. *Proceedings of the Fourth Annual International Conference on High-Level Radioactive Waste Management*. La Grange Park, IL: American Nuclear Society: 1,504–1,508.

TRW Environmental Safety Systems, Inc. 1995. *Total System Performance Assessment — 1995: An Evaluation of the Potential Yucca Mountain Repository*. B00000000-01717-220-00136. Las Vegas, NV: TRW Environmental Safety Systems, Inc.

Waite. T.D., J.A. Davis, T.E. Payne, G.A. Waychunas, and N. Xu. 1994. Uranium(VI) adsorption to ferrihydrite: Application of a surface complexation model. *Geochimicha et Cosmochimica Acta* 58: 5,465–5,478.

Wanner, H., Y. Albinsson, O. Karnl, E. Wieland, P. Wersin, and L. Charlet. 1994. The acid/base chemistry of montmorillonite. *Radiochimica Acta* 66/67: 733–738.

Wescott, R.G., M.P. Lee, N.A. Eisenberg, and T.J. McCartin. 1995. *NRC Iterative Performance Assessment Phase 2: Development of Capabilities for Review of a Performance Assessment for a High-Level Waste Repository*. NUREG-1464. Washington, DC: Nuclear Regulatory Commission.

Wilson, M.L., J.H. Gauthier, R.W. Barnard, G.E. Barr, H.A. Dockery, E. Dunn, R.R. Eaton, D.C. Guerin, N. Lu, M.J. Martinez, R. Nilson, C.A. Rautman, T.H. Robey, B. Ross, E.E. Ryder, A.R. Schenker, S.A. Shannon, L.H. Skinner, W.G. Halsey, J.D. Gansemer, L.C. Lewis, A.D. Lamont, I.R. Triay, A. Meijer, and D.E. Morris. 1994. *Total System Performance Assessment for Yucca Mountain—SNL Second Iteration (TSPA-1993) Volume 2*. SAND93-2675. Albuquerque, NM: Sandia National Laboratories.

Winograd, I.J., and W. Thordarson. 1975. *Hydrogeologic and Hydrochemical Framework, South-Central Great Basin, Nevada-California with Special Reference to the Nevada Test Site*. U.S. Geological Survey Professional Paper 712-C. Washington, DC: U.S. Geological Survey.

Yang, I.C., G.W. Rattray, and P. Yu. 1996. *Interpretations of Chemical and Isotopic Data from Boreholes in the Unsaturated Zone at Yucca Mountain, Nevada*. U.S. Geological Survey Water Resources Investigations Report 96-4058. Denver, CO: U.S. Geological Survey.

Zachara, J. M., and J.P. McKinley. 1993. Influence of hydrolysis on the sorption of metal cations by smectites: Importance of edge coordination reactions. *Aquatic Science* 55: 250–261.

NRC FORM 335 (2-89) NRCM 1102, 3201, 3202

U.S. NUCLEAR REGULATORY COMMISSION

BIBLIOGRAPHIC DATA SHEET

(See instructions on the reverse)

1. REPORT NUMBER (Assigned by NRC, Add Vol., Supp., Rev., and Addendum Numbers, if any.)

NUREG/CR-6513, No. 1

2. TITLE AND SUBTITLE

NRC High-Level Radioactive Waste Management Program Annual Progress Report: Fiscal Year 1996

3. DATE REPORT PUBLISHED

MONTH	YEAR
January	1997

4. FIN OR GRANT NUMBER

D1035

5. AUTHOR(S)

Budhi Sagar (editor)

6. TYPE OF REPORT

Technical

7. PERIOD COVERED (Inclusive Dates)

8. PERFORMING ORGANIZATION - NAME AND ADDRESS *(If NRC, provide Division, Office or Region, U.S. Nuclear Regulatory Commission, and mailing address; if contractor, provide name and mailing address.)*

Center for Nuclear Waste Regulatory Analyses
6220 Culebra Road
San Antonio, Texas 78228-0510

9. SPONSORING ORGANIZATION - NAME AND ADDRESS *(If NRC, type "Same as above"; if contractor, provide NRC Division, Office or Region, U.S. Nuclear Regulatory Commission, and mailing address.)*

Division of Waste Management
Office of Nuclear Material Safety and Safeguards

10. SUPPLEMENTARY NOTES

11. ABSTRACT *(200 words or less)*

This annual status report for fiscal year 1996 documents technical work performed on ten key technical issues (KTIs) that are most important to performance of the proposed geologic repository at Yucca Mountain. This report was prepared jointly by the staff of the Nuclear Regulatory Commission (NRC) Division of Waste Management and the Center for Nuclear Waste Regulatory Analyses. The programmatic aspects of restructuring the NRC repository program in terms of KTIs is discussed and a brief summary of work accomplished is provided in Chapter 1. The other ten chapters provide a comprehensive summary of the work in each KTI. Discussions on probability of future volcanic activity and its consequences, impacts of structural deformation and seismicity, the nature of the near-field environment and its effects on container life and source term, flow and transport including effects of thermal loading, aspects of repository design, estimates of system performance, and activities related to the U.S. Environmental Protection Agency standard are provided.

12. KEY WORDS/DESCRIPTORS *(List words or phrases that will assist researchers in locating the report.)*

EPA Standard
High-level waste
Near-field environment
Performance assessment
Repository design
Seismicity
Source term
Structural deformation
Thermal loading
Volcanic activity
Yucca Mountain

13. AVAILABILITY STATEMENT

Unlimited

14. SECURITY CLASSIFICATION

(This Page) Unclassified

(This Report) Unclassified

15. NUMBER OF PAGES

16. PRICE

ISBN 0-16-048981-4

90000

9 780160 489815

UNITED STATES
NUCLEAR REGULATORY COMMISSION
WASHINGTON, DC 20555-0001

OFFICIAL BUSINESS
PENALTY FOR PRIVATE USE, $300

US NRC-OADM 1 1AN1CHIWA1WF1
DIV FOIA & PUBLICATIONS SVCS
TPS-PDR-NUREG
2WFN-6E7
WASHINGTON DC 20555

SPECIAL STANDARD MAIL
POSTAGE AND FEES PAID
USNRC
PERMIT NO. G-67